Determining SNPs and demographic variables that impact level one fingerprint pattern

by Andrew Walton

Thesis submitted in fulfilment of the requirements for the degree of

Doctor of Philosophy

under the supervision of Dr Sebastien Moret, Dr Dennis McNevin and Dr Mark Barash

University of Technology Sydney
Faculty of Science

April 2022

Certificate of original authorship

I, Andrew Walton declare that this thesis, is submitted in fulfilment of the requirements for the award of Doctor of Philosophy, in the Faculty of Science at the University of Technology Sydney.

This thesis is wholly my own work unless otherwise referenced or acknowledged. In addition, I certify that all information sources and literature used are indicated in the thesis.

This document has not been submitted for qualifications at any other academic institution.

This research is supported by the Australian Government Research Training Program.

Signature: Production Note:
Signature removed prior to publication.

Date: 2/4/2022

Abstract

The current forensic use of fingerprints is for identification purposes and requires a reference sample for comparison to any unknown fingermark. Features of individual ridges can be used for identification however in combination they create overall level one fingerprint patterns (arches, loops and whorls). Past studies have indicated that some fingerprint characteristics such as level one pattern may occur at higher frequencies in some biogeographical ancestries (BGAs) and ridge density (the number of ridges within a defined area) may be used to determine the sex of an individual. The frequency at which these patterns and their subclassifications occur is largely unknown in the Australian population as there have been no modern studies utilising statistical analysis. Fingerprint experts would benefit from the publication of this information as it is the first step in building a statistical model that may add probabilities to their opinions on pattern rarity in a court setting. Previously, they may only rely upon their own observations from their experience and studies based on overseas populations.

This research aimed to represent the level one fingerprint pattern and ridge density frequencies of the diverse Australian population. This also provided the opportunity to assess the association of pattern and ridge density with BGA, sex, hands, fingers, and genetic markers. By assessing these associations, a new avenue of investigative potential could be unlocked from fingerprint evidence. For fingermarks that do not return a match it may be possible to predict which hand or finger the mark came from (provided it is not a full set), the ancestry, sex, or genotype of the depositor.

A total of 828 volunteers, 515 people from Sydney donated their fingerprints, DNA and self-declared BGA through a questionnaire and 313 people from Melbourne provided fingerprints with self-declared BGA information. The fingerprints in Sydney were collected via fingerprint scanner and those from Melbourne were provided as ink on card. The fingerprints were then classified using the National Crime Information Center (NCIC) classification system. Goodness of fit tests, multinomial logistic regression and general estimating equations were utilised for association of ancestry, sex, hands, and fingers with the pattern and ridge densities. Associations between fingerprint patterns and genetic markers were investigated for five genetic models.

The goodness of fit and multinomial logistic regression analyses revealed several patterns occurring at significantly higher and lower frequencies than expected for all independent variables. The general estimating equations also showed significant differences amongst ridge densities (radial, ulnar, and proximal positions) for all independent variables. A further

investigation was made into the useability of ridge density in fingerprints of unknown finger or hand. Results showed that proximal and ulnar positions produced dissimilar results to right and left positions, indicating this characteristic would be limited in its usefulness in forensic casework.

In people of European and Middle Eastern biogeographical ancestry over 60 SNPs were significantly associated with fingerprint patterns and ridge densities and four genetic loci were amongst the hundreds of genetic markers that were not quite significant. The four loci included two distinct areas on chromosome six, an area on chromosome one and an area on chromosome 11. Several genetic markers were novel, and several replicated those found in previous studies. The hypothesis that non-coding regions and epigenetic regulation are causative of fingerprint development was tentatively supported. These results provide strong evidence that frequencies of level one fingerprint pattern and ridge density differ between ancestral populations and sex and occur with different frequencies amongst fingers and between hands. Genetic markers may be identified in the future with diverse and increased sample sizes and through DNA phenotyping the prediction of an individual's fingerprints may be possible, allowing the interrogation of a fingerprint database even if there are no physical fingerprints.

This research met the original aims to assess the association of pattern and ridge density with BGA, sex, hands, fingers, and genetic markers in the diverse Australian population. Many results were novel and created potential leads for future investigation. The use of this research by practitioners however would be premature as larger BGA groups are needed for both pattern to BGA and pattern to SNP association studies.

Acknowledgements

To,

The volunteers

My supervisors

My friends

My family

The University of Technology Sydney

New South Wales Police Force

Victoria Police

The Department of Home Affairs

Thank you for all the support, without you this research would not have been completed over the last five years.

Table of contents

Terms and abbreviations

BGA	Biogeographical Ancestry
SNP	Single Nucleotide Polymorphism
USA	United States of America
NCIC	National Crime Information Center
DNA	Deoxyribonucleic Acid
EVC	Externally Visible Characteristic
NCIDD	National Criminal Investigation DNA Database
ARC	Absolute Ridge Count
LOD	Logarithm Of Differentiation
QTL	Quantitative Trait Locus
ROES	Ridges Off the End Syndrome
PCA	Principal Component Analysis
FISWG	Facial Identification Scientific Working Group
FBI	United States Federal Bureau of Investigation
MLR	Multinomial Logistic Regression
GLM	Generalised Linear Model
GEE	General Estimating Equation
qPCR	Quantitative Polymerase Chain Reaction
HWE	Hardy-Weinberg Equilibrium
AIC	Akaike Information Criterion
CHR	Chromosome
BP	Base Pair
LL	Left Little finger
RL	Right Little finger
LR	Left Ring finger

RR	Right Ring finger
LM	Left Middle finger
RM	Right Middle finger
LI	Left Index finger
RI	Right Index finger
LT	Left Thumb finger
RT	Right Thumb finger
EMT	Epithelial Mesenchymal Transition

List of figures

List of tables

Research communication

Publications

Walton AD, Moret S, Gunn P, Barash M. Comment on “Linkage analysis of a model quantitative trait in humans: Finger ridge count shows significant multivariate linkage to 5q14. 1” by Medland *et al.*,“Common Genetic Variants Influence Whorls in Fingerprint Patterns” by Ho *et al.* and “Hot on the Trail of Genes that Shape Our Fingerprints” by Walsh *et al.* Forensic Science International: Genetics. 2018.

Walton A, Moret S, Barash M, Gunn P. (2019). "The frequency of fingerprint patterns separated by ancestry and sex in a general population from Sydney, Australia." Australian Journal of Forensic Sciences: 1-6.

Presentations

ANZFSS 24th International Symposium – September 14th, 2018, Perth – “The frequency of fingerprint patterns separated by ancestry and sex in a general population from Sydney, Australia” – Walton A, Moret S, Barash M, Gunn P.

NSWPF Fingerprint Expert Conference – December 11th, 2019, Parramatta – “Determining the effect of ancestry and sex on fingerprint patterns” – Walton A, Moret S, Barash M, Gunn P.

Chapter 1 – INTRODUCTION TO FINGERPRINT DEVELOPMENT AND DNA FOUNDATIONS

1. Introduction to fingerprint development and DNA foundations

1.1. Foetal fingerprint development

The process of ridge formation has been studied extensively in the 20th century. From the information gathered the pad regression model for fingerprint development has been established [1-9]. By understanding how ridge formation occurs, the scientific principles behind the permanence and unpredictability of fingerprints can be explained. However, how these ridges form patterns is still in question.

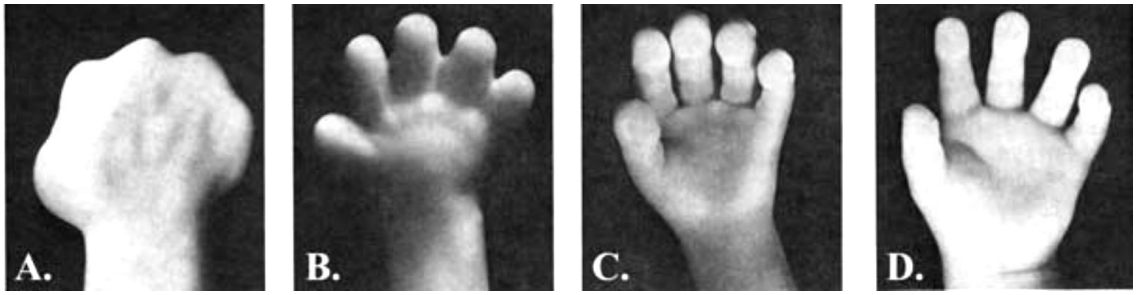

Figure 1: Growth of the hand between weeks five and eight of gestation **[1]**

(a) The hand forms from a paddle like shape. (b) Fingers then begin to project. (c) Fingers continue to lengthen and develop volar pads. (d) Fingers are fully formed meanwhile volar pads regress.

The friction ridges develop between 10 to 16 weeks *in utero* following the formation of the hand around the fifth to sixth week and the projection of fingers approximately during the seventh to eight week of gestation [2, 10]. The hands develop from a paddle like shape, the fingers then protrude and the volar pads become prominent before beginning to regress at 10 weeks gestation [1].

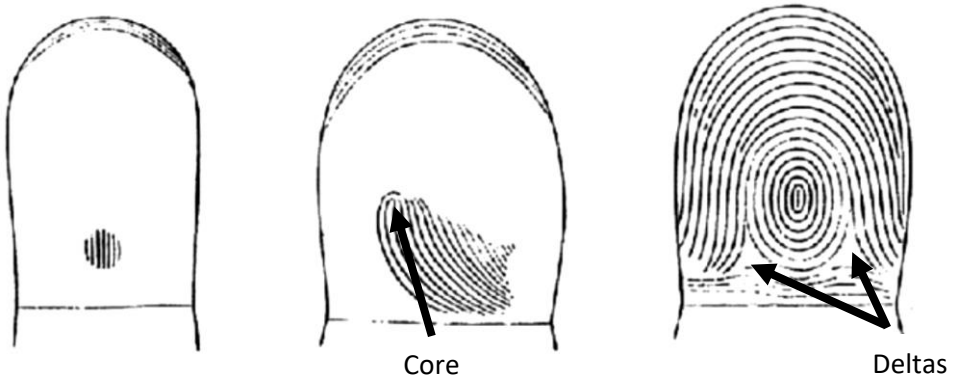

Figure 2: Radiating development of friction ridge pattern **[2]**

The development of friction ridges begins at the core of the level one pattern in addition to the tip of the finger. The ridges then develop by radiating outwards from these positions before populating the delta.

Friction ridges develop into patterns that can be classified. It is known that friction ridge patterns develop from focal points near the tip of the finger and in the core (centre) of the pattern. The

ridges then radiate from these points until the delta, an area where the ridges form a triangle, is the last area to develop (Figure 2) [2]. What is not known is how particular patterns develop, and there are competing hypotheses for this. Bonnevie [4] theorised that the arrangement of peripheral nerves determined the friction ridge patterns; if a nerve developed on the radial side of the finger it would produce a delta on the same side and consequently, an ulnar loop – a type of level one pattern. Conversely, Mulvihill and Smith [7] suggested pattern formations are determined by the ratio of volar pad height to width *in utero*. Bonnevie's theory was criticised by Penrose and Ohara [3] who believed the nerves may be involved in cell proliferation to produce ridges but not ridge pattern; ridge development has even occurred in experiments where innervation was prevented [8, 9]. Penrose's own theory, "the Penrose hypothesis" stated that friction ridges followed the curvature of the foetal skin at the time of ridge development [3]. "The Penrose hypothesis" was also endorsed by Mardia *et al.* [5] who extended work completed by Smith [6]. Mardia *et al.* [5] and Smith [6] analytically showed how particular patterns could be formed under the Penrose hypothesis, making it the most well rounded theory proposed at the time.

A decade following the study by Mardia *et al.* [5], Wertheim and Maceo [1] published a review article concluding that volar pad symmetry majorly affects pattern formation among a sea of other forces. Other features such as ridge count are determined by volar pad size and the minutiae, small details within the overall fingerprint pattern, are altered by localised tensions and compressions [1].

In 2005, Kucken & Newell [2] carried out an investigation in order to create the most comprehensive model of friction ridge development. Their proposal points the reason for fingerprint pattern development at buckling instability in the basal cell layer of the foetal epidermis; this buckling is said to originate in the basal cell layer and caused by the geometry and timing of regression of volar pads [2]. The geometry and timing of the regression of the volar pads are believed to be in turn governed by genetic factors [2].

As Wertheim and Maceo [1] mentioned, there are other forces that play their part in fingerprint pattern development such as pressures from the chorion that affects little finger and thumbprints alongside bone morphology however these are minor or play most of their part in the minutiae detail [11, 12].

Eccrine sweat glands, such as those found in the friction ridge skin may also have a minor role in ridge development given that ridges are comprised of individual pore units containing eccrine sweat glands. Ridges are composed of numerous aligned pore units which each contain a pore,

the opening on the skin where sweat glands reach the surface (Figure 3) [10]. Supporting this theory is the reoccurring symptom of hypohidrosis in abnormal friction ridge skin [13-15].

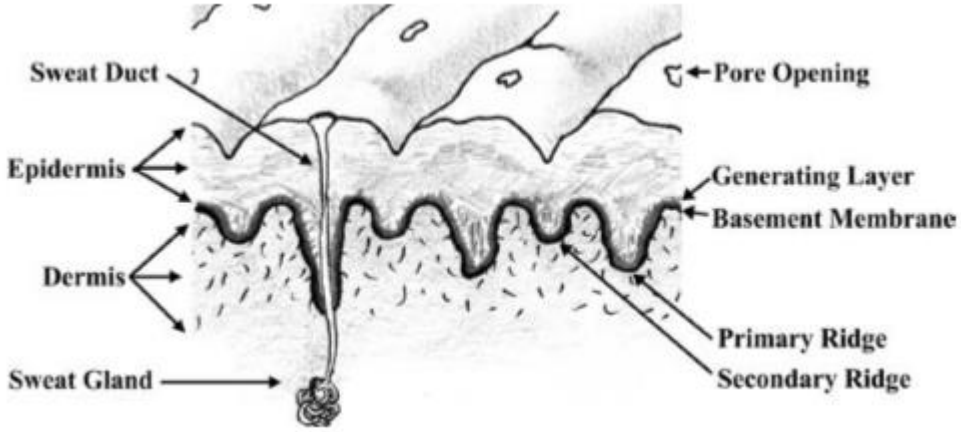

Figure 3: Pore units containing individual sweat glands create the epidermal ridges **[1]**

Individual pore units link together to create the friction ridges that together create the ridge patterns. Each pore unit contains a pore opening that is the exit of a sweat gland which originates in the dermis. Excretions from these eccrine glands as well as substances that have been collected on the skin are the reason fingerprints may be left on surfaces.

If fingerprint patterns are largely genetically regulated it may be possible to indicate a likelihood of an individual's ancestry or sex based on pattern statistics from various populations. It may also be possible to construct an individual's fingerprints from their DNA if enough associated markers are uncovered.

1.2. Characteristics of fingerprints

In 1686 Marcello Malpighi, noted the shared characteristics of spirals, loops and ridges in fingerprints among humans and was credited as the first to document the various level one patterns of fingerprints [16, 17]. It would not be for another 70 years that fingerprint pattern would be used for identification purposes by Sir William J. Herschel in British India [16, 17].

1.2.1. Fingerprint patterns

Level one

As the scientists that pioneered the research and introduction of fingerprints to law enforcement noted, fingerprints can be largely classified into three general patterns that are

termed "level one" detail (Figure 4)[10]. A single finger has one of these patterns though an individual's set of ten fingerprints may contain many different level one patterns.

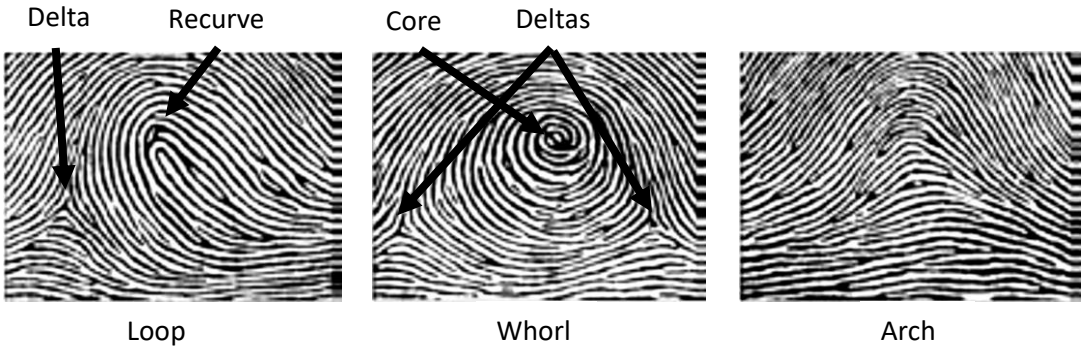

Figure 4: Three general patterns of level one fingerprint **[10]**

The loop, whorl and arch are the three most general level one fingerprint patterns. The loop features a recurve/core and one delta; the whorl a complete rotation and two deltas; and the arch patterns feature no delta or recurve. Each of these patterns has sub-categories to discriminate variations further.

The three general patterns can then be further classified into sub-categories [18]. In order to distinguish the patterns, the presence or absence of two main features, a core and delta, must be ascertained [18-20]. A core is defined simply as the centre of the dermal pattern area and is often where a ridge doubles back, "looping" on itself, whereas the delta of a fingerprint is the point where there is a triangulation of ridges [18, 19, 21]. The three general level one patterns can be described as:

1. Loop – The ridges that form loops flow from both sides of the finger however the distinguishing feature is at least one ridge returns to the side of the finger that it began; through the "looping" of the dermal ridges it creates a "recurve" or "core", and "delta" [18, 19, 21]. Loops are also the most common pattern and account for 60-65% of fingerprints in the USA population [20]. There are two sub-groups under the loop category:
    - Ulnar – subcategory of the loop pattern where the loop runs in the direction of the little finger (the ulna bone side of the arm)(Figure 5)[18, 20, 21]
    - Radial – subcategory of the loop pattern where the loop runs in the direction of the thumb (the radius bone side of the arm)(Figure 6)[18, 20, 21]

    The ulnar loop is much more common than the radial loop comprising of approximately 90-95% of all loops, with the radial loop being the remaining 5-10% [20, 22].

Figure 5: An example of an ulnar loop from the ring finger on the left hand

Figure 6: An example of a radial loop from the index finger on the left hand

2. Whorl – Present as 30-35% of fingerprints in the USA population [20], whorls are formed by complex spiral, oval or circular patterns with at least one ridge making a complete circuit. The category also possesses two deltas on either side of the fingerprint [18, 19]. The whorl category can be split in four sub-categories:
    - Plain – the basic whorl pattern where one ridge completes a full spiral, circle or oval while two deltas are present. In order to be classified a plain whorl an imaginary line between the two deltas must touch or intersect at least one ridge that is part of the inner rotation (Figure 7)[18, 20, 21].
    - Central Pocket Loop – combines both the features of loops and whorls. This pattern is distinguished by at least one ridge completing a full revolution and the placement of the two deltas; one on the edge of the pattern and one approximately in the centre of the fingerprint (Figure 8)[18, 20, 21].
    - Double Loop – consists of two loop formations that seem to spiral around each other. Along with the two loops formations are two deltas and "shoulders". Shoulders are where the ridge that forms the loop curves back around (Figure 9)[18, 20, 21].
    - Accidental – a mixed pattern consisting of two or more patterns excluding the plain arch. The accidental pattern may have two or more deltas and may conform to some requirements of other patterns but does not conform to other definitions exactly (Figure 10)[18, 20, 21].

    The plain whorl is the most common whorl subcategory comprising of approximately 70-75% of all whorls. The central pocket loop whorl and double loop whorl occur at very similar rates, around 10-15% of all whorls. The accidental whorl is a very rare pattern that usually occurs at approximately 1-3% of all whorls [20, 22].

Figure 7: An example of a plain whorl on the right thumb

Figure 8: An example of a central pocket loop whorl on the right middle finger

Figure 9: An example of a double loop whorl on the ring finger of the right hand

Figure 10: An example of an accidental loop whorl on the left thumb

3. Arch – The arch is the most simple of patterns and accounts for 5-15% of fingerprints in the USA population [20]. The ridges enter the fingerprint area on one side before rising in the centre slightly and exiting on the other side of the print; the highest point of the rise is called the "crest" [18, 21]. There are two types of arch patterns that can be distinguished:
    - Plain – this pattern is often referred to as the absence of pattern as there is no delta, whorl or core created by a loop. The ridges flow smoothly without any form of re-curve or whorl from one side to the other creating a crest (Figure 11)[18, 20, 21].
    - Tented – similar to the plain arch in there is no delta or core, however the difference is in the flow of the ridges. Whereas in the plain arch, the ridges flow smoothly from one side to the other, in the crest of the tented pattern, ridges do not flow through, instead stopping or starting, often producing short ridges (Figure 12) [18, 20, 21].

    The plain arch pattern is slightly more common than the tented arch pattern. The plain arch comprises of 55-60% of all arches and the tented arch comprises of the remaining 40-45%.

Figure 11: An example of a plain arch located on the left thumb

Figure 12: An example of a tented arch located on the left middle finger

Fingerprints are restricted to these three general pattern categories due to the regression timing and geometry of the volar pads *in utero*. This developmental timing is genetically based [10, 21] and supported by Machado *et al.* [11] and Temaj *et al.* [23] which showed that twins and siblings have more similar fingerprints than two random people from the population. These studies also demonstrated fingerprints had a high level of heritability, therefore indicating level one patterns are inherited both directly and indirectly from parent to offspring.

Level two

There are numerous small details that can be observed in individual's ridge patterns, these are called "minutiae" [10]. Minutiae are identifying features as they occur in diverse combination due to environmental pressures and growth factors while the fingerprints are in development [10]. Minutiae can also be referred to as "level two" detail, a continuation of the nomenclature from the level one general patterns [10]. Level two detail varies in shape, size, alignment and the fusion to other ridges; these variables combine to make ridges that may be very short, so short they may be a single dot, they may split or end abruptly too [19, 24]. There are two basic types of minutiae, these are:

1. Bifurcations – when a single friction ridge splits into two [10, 19]
2. Ridge endings – the sudden end of a friction ridge [10, 19]

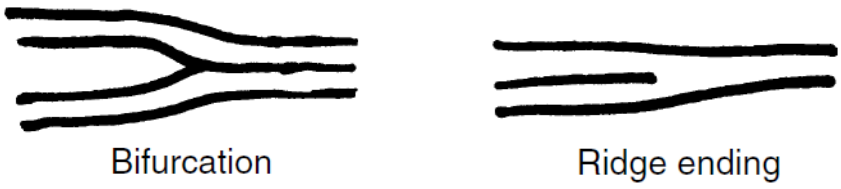

Figure 13: Bifurcations and ridge endings – two basic types of minutiae **[19]**

The minutiae in level two friction ridge details make an individual's fingerprint identifying. The most simplistic variations are the bifurcation and ridge ending.

The two basic types of minutiae can vary or interact to form even more complex formations. Variations of bifurcations include hook or spurs which diverge and shortly end and bridges which split from a ridge and then merge with another continuing ridge without interruption [19, 24]. Additionally, double bifurcations, trifurcations and opposed bifurcations can occur [19]. Ridge crossings are another bifurcation related feature except no ridges are produced or terminated, they simply cross (resembling an "X") and continue the flow on the level one pattern [19]. Lakes or enclosures could also be said to relate to both bifurcations and ridge endings as one ridge splits to form two ridges then reform as one, creating a ring like feature [19]. Ridge endings can also occur when two ridges join to form one, this is evident in opposed bifurcations [19]. The island feature is a variation of the dot minutiae and is also known as a short ridge; this feature appears and then abruptly ends within a short distance and is not attached to another continuing ridge [24].

Scars from skin damage or injuries can also fit under the umbrella term of "level two" detail [10]. These markings while modifying part of the original pattern make an individual's fingerprints more identifying [19]. However damage that alters the fingerprint permanently is quite rare as the injury is required to reach the basal layer of the skin [24]. When the basal layer is penetrated, the basal cells in the epidermis do not regenerate, thus leaving a permanent scar [24].

Some fingerprints may feature ridges that seem thin, fragmented or underdeveloped between other more pronounced normal ridges; these are termed incipient, secondary or subsidiary friction ridges [24]. These incipient ridges lack pores which normal ridges feature, this is due to the incipient ridges failing to reach full maturity in the developmental foetal stage [24]. It is not completely understood why some ridges may fully develop while others may not, but it is believed to be as a result of slight genetic alterations and uterine environmental influences in foetal development [1].

Level three

It should be noted that the particular formation of individual friction ridges can also be analysed, this detail is termed "level three" [10]. Of particular interest to investigators is the shape of each ridge and pore unit along with the position of the pore in relation to the ridges [10, 24].

While minutiae are important, and to a lesser extent level three detail, in analysing fingerprints forensically due to the ability to identify individuals from them, they are not being investigated in this study as it is widely agreed that genetics play a smaller role in the development of these features [10, 25, 26].

1.2.2. Methods of fingerprint classification

Fingerprint classification systems were developed before automated matching programs were introduced. They made searching for sets or a singular fingerprint match amongst a physical database much easier by following a systematic process. Modern classification systems were initiated by Juan Vucetich's *Dactiloscopía*, meaning finger description. Vucetich expanded Sir Francis Galton's previous three pattern classification method to four patterns. The four classifications of arch, whorl, internal loop, and external loop each had sub-categories. Where a fingerprint did not follow a standard pattern, the classification reverted to ridge counts between the core and delta [27]. Vucetich published this system in 1904 which allowed widespread classification and further refinement of the procedure. Simultaneously, Sir Edward Henry was developing his own classification system within British India also deriving from Galton's work. The Henry system is a logical method of categorising ten-print fingerprint records based on their general fingerprint pattern types. This used to reduce the complexity of completing one to many searches within a database and not used for individualisation. The method was adopted as the official criminal identification method within British India by 1987 and by 1900 within England too. Henry's system was adopted by English speaking countries and Vucetich's by Spanish speaking countries. The Henry classification system and several that were based upon it were used until the 1990's both manually and within the early automated fingerprint identification systems (AFIS). In some areas with legacy hardcopy fingerprint files it is still used, though new AFIS methods utilise distance between core and delta ridge flow classification approaches. The Henry and Vucetich classification systems are outlined in Appendix A and Appendix B.

NCIC classification system

The NCIC classification system was developed and used in the FBI's National Crime Information Center. It was based upon the Henry classification and designed to reduce errors in communication while also being convertible back to the Henry classification when needed. The method is based upon eight main pattern types, arches – plain and tented, loop – radial and ulnar, and whorls – plain, central pocket loop, double loop and accidental, additional categories are made for missing and scarred patterns (Table 1). The arches are not further sub-categorised however the loops are discriminated through ridge counting and the whorls through ridge tracing between the two deltas, designating them inner, meeting, or outer.

Table 1: NCIC classification system

Pattern type	**Sub-pattern**	**NCIC code**
Arch	Plain Arch	AA
	Tented Arch	TT
Loop	Radial Loop (≥51)	Actual ridge count plus 50
	Ulnar Loop (≥01)	Actual ridge count
Whorls		
Plain Whorl	Inner tracing	PI
	Meeting tracing	PM
	Outer tracing	PO
Central Pocket Loop	Inner tracing	CI
	Meeting tracing	CM
	Outer tracing	CO
Double Loop	Inner tracing	DI
	Meeting tracing	DM
	Outer tracing	DO
Accidental	Inner tracing	XI
	Meeting tracing	XM
	Outer tracing	XO
Other		
Missing		XX
Scarred		SR

The NCIC classification, when applied to a set of fingers is expressed in a line of 20 characters in the same order of fingers as the Henry classification (e.g., 10TT1462PI DMCI15TT11). Given there are no calculations to be equated and all fingers are given a code it is much simpler for the inexperienced or layman to follow.

1.2.3. Investigational information available from fingerprints

a. Pattern

The first studies investigating the relationship between fingerprint patterns, ancestry and sex was reported by Galton in 1892 [28] who was searching for unusual pattern to distinguish between English, Welsh, Basque, Jewish and African groups. Galton found no such pattern but

noted that statistics regarding standard patterns did show differences in large groups. In 1935, Cummins [29] made further investigations following an article written by a German anatomical doctor that stated ancestry could be determined by fingerprint observation. Results showed that there were in fact differences between populations from numerous countries though identification of ancestry could not be carried out.

Given there are differences between ancestries it may be possible that there are additional statistically discriminatory pattern differences relating to finger, hand asymmetry and sex dimorphism. The research in this thesis focusses on biogeographical ancestry (BGA), a concept that indicates an individual's origin based on geographical regions as opposed to race and ethnicity that are not biologically based.

b. Ridge Density

Ridge density is the measure of how many ridges are intersected by a line drawn diagonally through a defined area that is placed on the fingerprint.

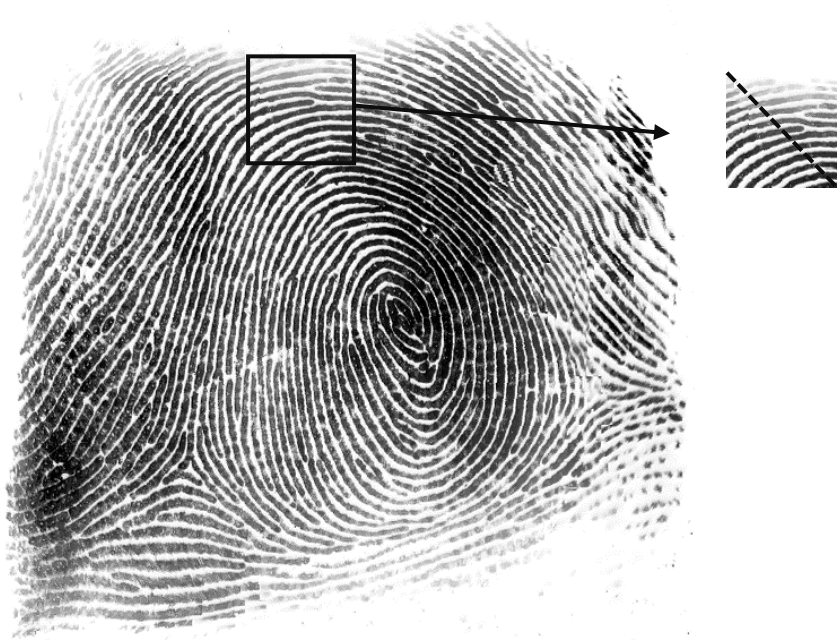

Figure 14: An example of the method used to calculate ridge density

A box is placed on the periphery of the fingerprint and the is area extracted, a line is drawn perpendicular to the flow of the friction ridges. The number of ridges this line crosses represents the fingerprint's ridge density.

In 1999, Acree [30] was the first to statistically investigate if ridge density was associated with sex, before this fingerprint examiners had only noted that females tended to have "fine" ridge detail and males more "coarse" [31, 32]. Using a population of 400 individuals, 200 males and 200 females, each comprising of 100 European and 100 African American individuals; results

showed women had significantly higher ridge density than men in both African American and European ancestry (F=81.96, $p < 001$). The European females were significantly different in ridge density to the African American females ($p < 0.05$) however the two male groups were not significantly different ($p > 0.05$). Further analysis using Bayes' theorem suggested 11 ridges/25mm^2 or less indicated male while 12 ridges/25mm^2 or more implied female.

Later studies assessed the ridge density of multiple locations on the fingerprint. The first of these was Gutiérrez-Redomero *et al.* [33]. This study investigated the density in the radial, ulnar and proximal areas of the fingerprint surrounding the main pattern. Using a population of 200 individuals results showed that women had significantly higher ridge density than men in both the radial ($p < 0.001$) and ulnar ($p < 0.001$) areas, however there was no difference in the proximal portion of the fingerprint. This was the first evidence that ridge density differs within the fingerprint.

While intra-fingerprint ridge density different would provide a challenge, it may be possible that in combination fingerprint patterns and ridge density could give an indication of ancestry and sex.

1.3. The uniqueness and evidential weight of fingerprints

Dr. J.C.A. Mayer in 1788 made the conclusion that no two individuals had the same arrangement of friction ridges [16, 17]. While similarities have been observed, no two fingerprints have ever been found to be the same. The inherent randomness from environmental pressures in the womb during development make it extremely unlikely that an identical fingerprint could be produced [1, 12].

The assertion that fingerprints are unique has come into question by lawyers, the first being United States v Byron Mitchell (July 13, 1999) following the Daubert hearing [34]. The defence raised questions concerning the admissibility of latent fingerprint identification evidence based on its validity. The defendant claimed there was no scientific basis for the assertion of individuality in matching fingerprints. The government presented several fingerprint experts to testify as to the uniqueness of fingerprints. The hearing resulted in the admissibility of fingerprint evidence being upheld and the challenge of the defence for the evidence to be excluded rejected.

The judge noted two factors in the decision:

1. Human friction ridges are unique and permanent through both the overall friction ridge skin and smaller ridge areas
2. Human friction ridge arrangements are unique and permanent

It is impossible to truly prove fingerprints are unique as all living person's fingerprints are unable to be collected in a centralised database for comparison; plus, the fingerprints of past people are unable to be assessed. Scientists have nevertheless tried to address this question through estimating the probability of exceedingly rare events and statistical modelling. An unpublished study prepared purely for court use analysed 50,000 images of fingerprints finding the probability of finding two people with an identical print was 1 in 10^{97} [35]. Subsequently using a subsection from the centre of a fingerprint found the likelihood of finding two people with an identical print was 1 in 10^{27}. This study however has been widely criticised, said to suffer from fundamental flaws in interpretation and reporting of methodology which severely underestimate the likelihood of a chance match [35, 36]. Going further, the critique of the unpublished study states that even if the statistical analysis was appropriate, the premise of the research ignores the fact that the same fingerprint rolled successively by the same individual will not be identical [35].

Instead of finding a definitive answer to uniqueness, research through probabilities and comparisons have indicated that fingerprints are perhaps more similar than previously thought. Initially assumptions were made that minutiae had random distribution however this was found to be incorrect [37]. Additionally, through the assessment of fingerprints of twins it has been found that the while fingerprints are sufficiently unique to distinguish between the siblings there was a small (statistically insignificant) decrease in identification accuracy [38]. Both these findings indicate to fingerprints not being as unique as previously thought.

Moving away from definitive statements, scientists have proposed breaking from the concepts of individualisation and uniqueness, arguing that biometric disciplines can live without these conclusions [39]. The courts have also followed this sentiment, dismissing uniqueness as irrelevant, preferring fundamental questioning of reliability of forensic practice [40]. With or without the concepts, the ongoing debate has led to a call for greater candour and fingerprint experts will need to express the strengths and limitations of their findings differently.

In the future perhaps the commonality of fingerprint patterns could be expressed and questioned alongside the reliability of fingerprint identification rather than the rarity of prints. The ability to provide weighting to fingerprint evidence was explored by Neumann *et al.* in 2012 [41]. The method focussed on minutiae (level two detail) and used a weighting function that

accounted for inter-operator variability and distortion of the finger pad. Results showed that the addition of more matching minutiae between fingerprints corresponded to the evidence carrying more weight with less bias to both prosecution and defence. Benefits of this process mean that if fingermarks are of poor quality they do not need to be rejected in absence of a categorical decision of match or no match. Instead, the information available could be used to produce a weighting and used as supportive evidence. Opposing this benefit is the negative of the calculation's complexity and results. The function used was termed a likelihood ratio however is dissimilar to the commonly referenced likelihood ratio used in Bayes' theorem. The complexity of the function and possible confusion over the common likelihood ratio term may greatly hinder the ability of lay people (jurors) to understand information provided to them in court, which has been proven to be common with the communication of DNA results [42].

An alternative to the weighting function approach has recently been published by Hendricks *et al.* [43]. An approximate Bayesian computation model supplemented by a receiver operating characteristic curve was used to create a model selection algorithm. The algorithm overcomes criticisms of the Neumann *et al.* [41] regarding the ability to submit the result into a Bayesian equation by being framed into a formal Bayesian framework. Results importantly showed consistency with the Neumann *et al.* paper [41] in that the probability of misleading evidence being biased towards the prosecution was very low when using over 7 corresponding minutiae and the probability of misleading evidence favouring the defence reduced dramatically with the addition of more corresponding minutiae. The authors note that while minutiae are taken into account by the model, level one fingerprint pattern also needs to be considered and the database from which the model is based has a significant effect on the calculated weighting.

This computational model has the potential to be used for other complex pattern analysis evidence such a shoe print, firearms and questioned documents. However given the Hendricks' approach to providing evidential weight is computationally based it is ultimately up to technology providers to develop programs that are easily incorporated into workflows and used by forensic examiners. Without this step the move away from categorical decisions (match or no match) of fingerprint examination may never occur.

1.4. Fingerprint genetics

The fact that a majority of fingerprints fall into three main categories despite their distinguishing nature, and the establishment that related people have more similar fingerprints than two random individuals' indicates there are genetic foundations for at least the level one ridge

pattern [38].The investigation of these foundations controlling fingerprints pre-dates modern DNA analysis methods. First studies focussed on Medelian genetic effects by studying the inheritance of level one pattern through numerous related individuals. These early studies indicated there was a genetic predisposition to fingerprint pattern however the view as to how this occurred was overly simplistic. With the development of accurate genotyping technologies and the uprise of genetic phenotyping the genetics behind fingerprints are once more at the forefront of research.

1.4.1. Inheritance of fingerprints

Early studies into fingerprint phylogeny were published towards the end of the 19th century however most if not all were published in German, a summary of these studies can be found in the report by Bonnevie [4]. Progress towards pinpointing the genetic basis of fingerprints for the most part began with an investigation in 1941 by Walker [44] following observations that twins had striking resemblances in palmar and plantar ridge patterns [45]. The conclusion of Walker's study [44] was that the phenotype of a radial loop on right index finger was recessively sex linked to the X chromosome. The findings were sound; however, the study only looked at the children of ten couples and no mention is made of how this group of individuals were selected. Additionally, given that it is now known that loop fingerprint patterns account for 60-65% of the population it is possible that this in fact happened by chance [20].

The findings of Walker's study [44] were disputed in several subsequent studies. Sarah Holt, a highly published scientist in the topic of dermal ridge genetics found no evidence of X-linked genes that present themselves in the phenotype of dermal ridges [46].

Sarah Holt of the Galton laboratory published numerous studies throughout the 50's and 60's looking at the inheritability of fingerprints; drawing from a database of fingerprints specifically focussed on total ridge count [25, 47-52]. Correlations were measured in r values; between 0.9 and 1.0 indicates a very high correlation, between 0.5 and 0.7 show moderate correlation, low correlation between 0.3 and 0.5, while below 0.3 indicates little to no correlation. Holt's 1952 study [25] looked into the bilateral asymmetry of fingerprints to get an insight as to the underlying cause. The results showed that the right hand is favoured in asymmetry to have a higher ridge count in both male and females (63.4% and 66.7% respectively) although correlation between the left and right hand were still very high (males, r = 0.94±0.01; females, r = 0.93±0.01). The average male and female distribution of ridge counts were found to be significantly different for both hands, however the measure of asymmetry (right hand ridge

count minus left hand ridge count) was found to be insignificant between the two sexes. When looking at related individuals it was found correlations for ridge count between siblings (sib) and parent-child were not significantly different to 0.5. Monozygotic twins had a correlation for both right and left hands of 0.92±0.02 and dizygotic twins a correlation of 0.43±0.10 for the right hand and 0.42±0.10 for the left hand. Therefore, asymmetry was found not to have a genetic basis, although Holt observed that the ridge count on each side of the body is inherited similarly to total ridge count, in an additive manor.

The follow up study in 1953 [48] confirmed the absence of significant correlation in the total ridge counts between sib-sib and most parent-child relationships (correlation coefficient not significantly different to 0.5). The only pair showing a correlation significantly different to 0.5 was the mother-daughter relationships (r = 0.68). The author explains that given the seven correlations tested and small sample numbers this may be by chance. However, the high association of total ridge count between monozygotic twins was also repeated. Additionally, inheritance of pattern-size measured by total ridge count was demonstrated, again with an additive effect. Holt also states that there were no environmental (maternal) effects observed.

Holt's 1955 study [49] investigated the total ridge count with an increased cohort of 1650 people, of which 825 were male and 825 female. Solidifying Holt's previous result from her 1952 study [25], the average total ridge count of males and females was again found to be significantly different by t-test.

Inheritance was again probed in the 1956 study [50] using a new set of data including 100 families with 104 sons and 91 daughters. The parent-child, mother-child and father-child correlations all proved to be not significantly different from 0.5. Added to previous familiar data the parent-child correlation remained near 0.5. Further categorisations of mother-son, mother-daughter, father-son, and father-daughter also showed correlation not significantly different to 0.5.

In 1957 another study was published by Holt [51] based on a new cohort of 254 sibships with 523 members; of those 254 were males and 269 females. The correlation between sib-sib partnerships for total ridge count confirmed previous results, being measured at 0.500±0.045, not significantly different from 0.5. When combined with the previous cohort, the correlation was measured at 0.501±0.038. On the same combined group, a new semi-weighted analysis of variance was also introduced which produced a similar r value of 0.488±0.039. Brother-brother correlation of total ridge count was also calculated at 0.530±0.066 and sister-sister association at 0.502±0.066.

Holt's 1960 study [52] differed slightly to the previous studies as the diversity in ridge count of an individual's ten fingers was calculated. The correlation of diversity between Parent-child, sib-pair and dizygotic twins were all approximately 0.25, meanwhile the ridge count diversity of monozygotic twins was highly correlated ($r = 0.73 \pm 0.06$). Holt's judgement on the diversity was that the ridge count from finger to finger has a genetic basis however there are considerable maternal influences during pre-natal development, a different stance to the one published in the 1953 study [48].

The recurring consensus from the Holt sequence of studies was that the passing of fingerprint characteristics between generations is governed by additive polygenic inheritance. This is supported by the continuous findings of slight association ($r \approx 0.5$) between related individuals.

The results of Walker's earlier study [44] were once again rejected in a 1976 study by Slatis and colleagues [53], they too found no evidence to support the sex-linked radial loops, index finger phenotype. Slatis *et al.* [53] utilised genetic family trees to show the inheritance of other ridge patterns. The subjects of the study were a relatively large (571) isolated Jewish population from the town of Habban, South Yemen. From the results, a theory of fingerprint genetics was produced; the basis was that all fingerprints are based on ulnar loops and that semidominant and dominant genes produce deviations from this. There were seven genes proposed:

1. A semidominant gene for whorl patterns on thumbs
2. A semidominant gene for whorls on the ring fingers
3. A dominant gene for arches on the thumbs
4. One or more dominant genes for arches on the fingers
5. A dominant gene for whorls on all fingers except the middle finger
6. A dominant gene for radial loops on the index fingers
7. A recessive gene for radial loops on the ring and little fingers

The theory produced from the Slatis study [53] lacked complexity, neglecting to include the likely intricacies surrounding the epistasis of genes – a phenomenon where one genes affect can be modified by numerous other genes; however, this was likely due to the Mendelian methodology employed in the study as DNA genotyping was in its early infancy and inadequate at the time.

1.4.2. Genetics of fingerprint pattern development in humans

The genetic architecture of fingerprints has only recently been further elucidated through studies using linkage analysis and genome wide association studies (GWAS). Medland and associates [54] performed a gene-wide association study with absolute ridge count (ARC – sum

of ridge counts for all fingers) using samples from 2,114 twin and singleton offspring from 922 twin families. Association is shown by logarithm of differentiation (LOD) which equates to a comparison between the chances of the test data occurring if the two variables are linked, to the chances of receiving the same test data by chance. The highest associated position is pinpointed through centimorgans (cM) which is a measure of distance along the genome that takes into consideration the recombination frequency.

The group's findings showed highest univariate linkage to be at 1q42.2 (250cM, LOD=2.04) and highest multivariate linkage located at 5q14.1 (95cM, LOD=3.34). The highest multivariate result was the only region in the genome to reach the empirical threshold; there were however four other regions that reached the lower suggestive threshold on the 5^{th}, 15^{th}, $16^{th,}$ and 17^{th} chromosomes. The highest univariate point was the only one to record a LOD above that of the suggestive threshold; falling just below the threshold were univariate results for 15q26.1 (95cM, LOD=1.52) and 7p15.3 (35cM, LOD=1.26). The univariate analysis, while having a lower LOD score, had a quantitative trait locus (QTL) that accounted for 21% of variation of ARC at the 1q42.2 region, while multivariate analysis in the same region revealed the QTL accounted for much less variation in the ARC, 7.7%, 12.7%, 10.0%, 13.8%, and 9.3% from thumb to little finger, respectively.

Ho *et al.* [55] continued the exploration using the same database as Medland *et al.* [54] from Queensland Institute of Medical Research (QIMR) in addition to a cohort from Avon Longitudinal Study of Parents and Children (ALSPAC). Instead of regions of DNA this study focussed on Single Nucleotide Polymorphisms (SNPs), which are single base variations in the DNA. Principal component analysis showed three distinct components amongst the level one pattern type: whorls on the middle three digits (Ring, middle and index fingers) on both hands, whorls on the thumbs and whorls on the little fingers. Univariate genome wide analyses were also conducted on both cohorts where meta-analytic p-values were calculated for each finger. For SNPs to be considered significant with the fingerprint pattern phenotype they were required to obtain a p-value $< 5 \times 10^{-8}$. Numerous SNPs reached the significance threshold including four in the ADAMTS9-AS2 gene for the whorl on left little finger (WL5 phenotype). SNPs located on chromosome 12 down stream of TBX3 and upstream of MED13L were significant for whorls on both the left are right ring fingers. The most highly associated SNP in this region was rs1863718 for the left and right index fingers. Additionally, significance association with the left index finger was found for a variant in the OLA1 gene. The p-values were replicated with much improved results in the ALSPAC data.

The for the whorl on left little finger was particularly fascinating as the propensity of whorls due to the variation decreasing from the little finger to the ring finger of both hands before attenuating in significance down to the thumbs. This is evidence of a morphogenetic field effect, a force that is epigenetically based that guides an organism's development as it grows into a head end and a tail end, and into a left side and a right side for most animals [56]. While highly significant the variant only accounted for 1.61% and 0.93% variation in pattern for the left and right thumbs, respectively.

The genes accommodating the significant variants, ADAMTS9-AS2 and OLA1 are known oncogenes down-regulated in glioma [57] and inhibit *in vitro* cell migration of breast cancer cells [58]. Interestingly, the TBX3 gene which was adjacent to significant SNPs in an intergenic region is known to be involved with ulnar mammary syndrome, a condition that presents itself in irregular ulnar bone development and asymmetry in the middle to little fingers [59]. This gives an indication via DNA that previous literature is correct in saying that limb development plays a role in fingerprint development [7].

1.4.3. Syndromes with known fingerprint pattern effects

There are numerous rare abnormalities that manifest themselves in the fingerprint phenotype or parts of the body that may affect fingerprints. One of the most significant diseases to affect the fingerprints is adermatoglyphia. The disease is classified by the absence of friction ridges on the fingertips, palmar and plantar surfaces, meaning an individual with the disease has no fingerprints [60]. The associated variation is inherited autosomal dominantly but it has only been documented in four extended families worldwide [60, 61]. Studies by Nousbeck *et al.* [60, 61] have tracked the disease to mutations that occur in a single conserved donor splice site adjacent to the 3' end of the non-coding exon within a skin specific, short isoform mutation of the SMARCAD1 gene. While these results seem to indicate the SMARCAD1 gene would have an influence in fingerprint development, Medland *et al.* [54] found no SNPs in the gene to be significantly associated (or even moderately associated (10^{-5})) with any particular pattern.

Basan syndrome has also been linked to the SMARCAD1 gene by Li *et al.* [13] after the analysis of the genomes of a unique Chinese family; possibly meaning this syndrome is a phenotypic variant to adermatoglyphia. Basan syndrome is similar in symptoms to adermatoglyphia however also features neonatal blisters and plentiful milia [14]. Most common indicators for Basan syndrome are abnormal fingerprints, either thick or thin skin, bent fingers due to tight skin and also hypohidrosis [13].

Ridges-off-the-end syndrome (ROES) and Nelson syndrome are additional conditions characterised by unusual friction ridge features. First described by David [62] in 1971, ROES presents itself through several ridge features, namely ridges running off the end of finger and toeprint patterns, a tendency towards radial patterns and a complete absence of arches, whorls, double loop whorls, central pocket loop whorls and composites. In both families where the condition was seen, it was inherited autosomal dominantly. ROES symptoms were again found in two more families by David [63] in 1973, in conjunction with the first family to display Nelson Syndrome where the characteristics present similarly to ROES loop patterns though are more pointed, closer to tented arches [63, 64]. A linkage study was carried out on members of the family exhibiting ROES symptoms which found a possible linkage of this trait to haptoglobin, a plasma glycoprotein that binds free haemoglobin [65]. In the same paper a low positive LOD score with the Duffy blood group locus was found for the individuals with Nelson syndrome [65]. The results of the linkage study however were far from conclusive due to the low number of participants.

Figure 15: An example of the main symptoms of Ridges Off the End Syndrome (ROES) **[57]**

Fingerprint patterns where ridges flow off the end of the finger are atypical, ordinarily ridges would loopback around to the side of the fingerprint they originated from.

Psoriasis among other debilitating dermatological conditions such as dermatitis and eczema has been recently linked to dermatoglyph defects [14]. Given that each of these conditions inflame the structure of the skin resulting in dry scaly skin, rashes and itching, this association is logical. Psoriasis itself is an inherited polygenic disease therefore epistasis with the genes or SNPs that develop fingerprints would be extremely hard to pinpoint [66]. Dogramaci *et al.* [66] looked into

whether psoriasis had an effect on friction ridge pattern, finding that ulnar loops were most common in both sexes, something that occurs in the normal population. Additionally, the study found that women's fingerprints were consistently more affected than men despite a prior Norwegian study not finding any sex-linked patterns of psoriatic inheritance [66, 67].

Perhaps the most unusual of fingerprint abnormalities occurs through chemotherapy [14, 68, 69]. The cancer drug Capecitabine (Xeloda), has been shown to remove fingerprints by inducing hand-foot syndrome [68]. Hand-foot syndrome is caused by disruption to the growth of the skin and small blood vessel. Symptoms include redness, swelling, burning sensations, tenderness to touch, tightness of skin and blistering on palms and soles of the feet [70]. This illustrates the importance of the cell migration process from lower layers of the skin.

Additionally, there have been numerous studies investigating the use of fingerprints as a biomarker for early detection of complex diseases; the intention being that if the disease can be diagnosed early, it can be treated more effectively and in a cost-efficient manner. Among the diseases found to be associated with pattern phenotype are gastrointestinal cancer [71], schizophrenia [72, 73], Down's Syndrome [74, 75] and parents of children with trisomy [76], K syndrome [77, 78], Turner's syndrome X [79], cervical cancer [80], type I diabetes [81], epilepsy [82] and oral cavity cancer [83].

Mixed results have been found regarding a fingerprint pattern biomarker and breast cancer [84-88]. Two earlier studies found association however three follow up studies failed to find such links. A systematic review of fingerprint biomarkers and hypertension was conducted by Wijerathne *et al.* [89]. The results point out that three thorough studies found no association while studies that happened to find a link had questions over their methodology.

While numerous diseases and conditions have been linked with fingerprints as a possible biomarker there are numerous recurring issues with these studies - small sample populations and unusual fingerprint phenotypes used pre-2005, including several studies using 6 or more whorls as an indicator. The usefulness of fingerprints as a diagnosis of disease has been doubtful and noted since at least 1983 [90].

1.4.4. Fingerprints from an evolutionary standpoint

Several other species have friction ridge skin including the chimpanzee which is the human's closest living relative, the marsupial Koala and several aquatic mammals [91, 92]. The Koala's fingerprints in particular are interesting as they bear a striking resemblance to those of humans,

an example of convergent evolution (Figure 16) [93, 94]. The reason for friction ridges to be present on the fingers, toes, palmar and plantar surfaces was largely agreed to be as the name suggests, to create friction for holding onto objects [94, 95]; however there has been conjecture where results showed that the ridges did not affect gripping ability [96]. Now the latest studies on the grip provided by human fingerprints have indicated it is due to the pores and eccrine sweat glands. The ridges, with the pores positioned along, them act as a microfluidic array which maintains optimal moisture levels by deforming and blocking the sweat pores [97, 98].

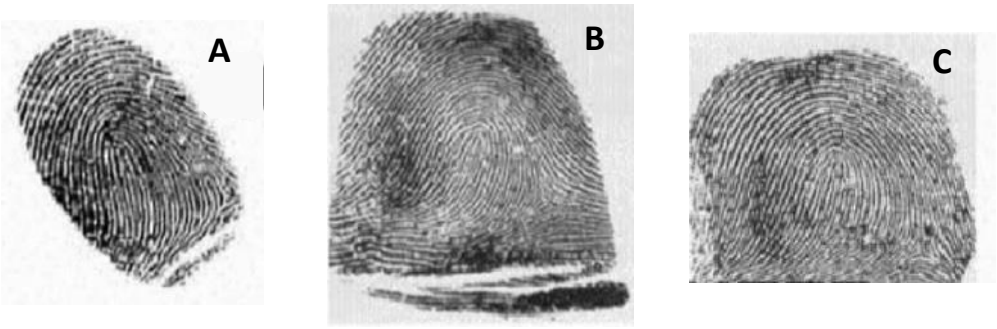

Figure 16: Similarities of fingerprints between species **[87]**

The fingerprints of several species are almost identical to the eye: (A) Koala, (B) Human and (C) Chimpanzee.

Over time, the study of dermal patterns has diversified to include forensic and anthropology applications.

1.5. Approach for targeting genes with influence on fingerprint phenotype

The identification of single nucleotide markers responsible for the development of fingerprint patterns can be approached using two different techniques:

Gene Wide Association Study (GWAS)

The approach involves genotyping millions of SNPs across the entire genome of thousands of individuals and analysing the data for potential statistically significant associations to the trait of interest [99, 100]. While being a powerful approach with proven results there is a requirement for large sample sizes to find significant associations spanning the entire genome. These requirements result in high costs rendering the approach out of reach for many studies, including this project.

Candidate gene approach

This approach does not require as large a sample size as the GWAS method as it is focussed on genotyping a limited number of markers rather than the entire genome. It can be performed by using one or more of the following steps:

- Identification of genes and subsequently selecting SNPs that have a known interaction or are involved in the development of the phenotype being investigated
- Identification of genotyping markers that are involved with disorders relating to the investigated phenotype. The phenotype may be one of many symptoms of the disorder. Examples of this are albinism, vitiligo and standard pigmentation [101, 102]. Genes that affect the fingerprints may also be involved in the development of standard variation in the phenotype.
- Selection of genotyping markers showing high population differentiation (High F_{st} values), particularly in or near genes involved in the development pathway of the selected phenotype. Given results of previous studies [22, 33, 103-105], indications are that some patterns occur in higher frequencies in different populations. It is hypothesised that expression of markers with high F_{st} values near or in genes controlling finger and skin development may be involved in the development of fingerprint pattern.

Based on the sample size, time, and cost limitations of this project it was determined that a candidate gene approach was the most appropriate. The chip will be selected based on this approach then the results will be assessed for SNPs associated with the fingerprint phenotype in a case-control design.

1.5.1. Fingerprint candidate SNPs and selection criteria

SNPs may be located within three areas: coding regions, non-coding regions or the intergenic regions. Thus, SNPs can be categorised by their location and effect on the transcription and translation from the DNA.

SNPs can be further categorised based on the phenotype they produce and the information that can be inferred from them. The combination of the effects of SNPs illustrated in Figure 17 and the information inferred from SNPs may help explain the differing fingerprint pattern frequencies between ancestries as they may have an impact on the function of genes directly or indirectly responsible for finger and skin development.

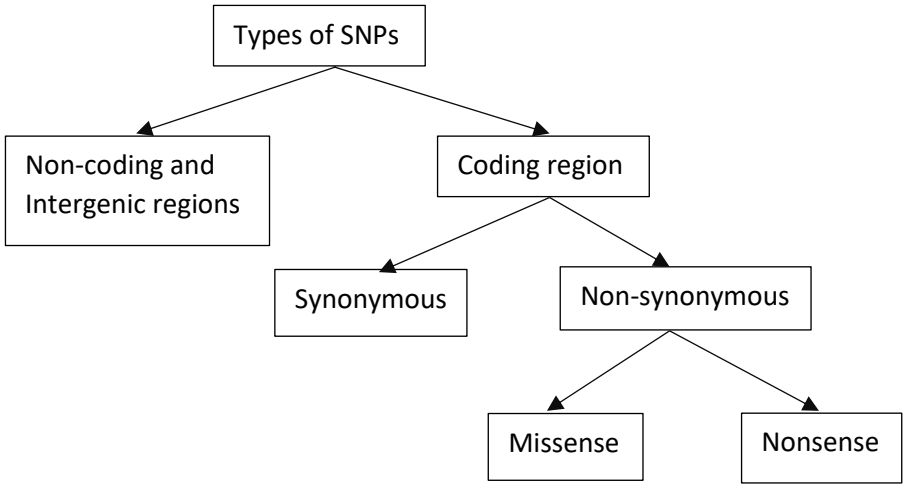

Figure 17: Types of SNPs based on their location and effect

SNPs can be categorised based on their location and effect on transcription and translation. Firstly, separated by region within the genome. Secondly, if they do (non-synonymous) or do not (synonymous) change the amino acid sequence of the protein and thirdly, depending on what amino acid they code for. If it is a premature stop codon it is a nonsense SNP and missense if it contributes to coding an incorrect amino acid.

a. Ancestry informative markers (AIMs)

Genetic differentiation occurs when two populations diverge and become sufficiently isolated to limit gene flow between them. Resulting from the gene flow limitation are SNP alleles that exhibit substantially different frequencies between the different populations; these are termed AIMs. Population variation can occur through a variety of evolutionary events and can be measured through both F_{st} and linkage disequilibrium (LD) based tests, with F_{st} being preferred for detection of ancient selective events.

The starting point for most of the worlds genetic variation outside Africa occurred due to a population bottleneck before a very rapid population growth and spread approximately 45,000 to 60,000 years ago [106]. The "serial founder effect" where small splinter groups create isolated populations reduced genetic variation but also allowed SNP mutations to be retained within the geographic regions [106]. Thus, F_{st} can reveal the effects of natural selection and variation for the last 60,000+ years, with the additional ability to investigate selection down to a single SNP. A study utilising the HapMap data has shown that negative and positive selection have contributed to the development of regional adaptions in humans [107]. These adaptations have primarily occurred at nonsynonymous and 5'-UTR polymorphisms [107].

b. Non-synonymous SNPs (nsSNPs) in coding regions

Polymorphisms within coding regions can be either synonymous or non-synonymous. Non-synonymous variants can change the protein structure derived from the DNA through missense, nonsense, and frameshift mutations whereas synonymous cannot. Using bioinformatic tools

nsSNPs can be predicted; a study by Burke *et al.* [108] analysed 5500 genes studies and found nearly 24000 SNPs that can alter protein sequences, possibly altering protein folding, function and the phenotypic expression of the gene. Such a significant fundamental effect may lead to disease or at the very least a normal altered phenotype.

Due to the redundancy of the genetic code, i.e. different codons coding for the same amino acid, synonymous SNPs are believed largely to not affect the folding or functions of proteins however recent studies have shown that these markers may in fact affect mRNA stability which may ultimately alter protein function leading to disease, a similar result to nsSNPs [109-111].

c. SNPs in splice sites

Alternative splicing is a complex process allowing a single gene to create multiple proteins which is regulated by numerous trans acting proteins binding to cis acting sites on the primary transcript. The diversity created through alternative splicing influences phenotypic variability and disease susceptibility in human populations; it has been demonstrated that up to 95% of genes are regulated through this mechanism [112, 113].

Since mutation in splice sites disrupts the splicing process, it can directly alter exon configuration. Due to this, SNPs within splice sites ultimately can have a larger effect on the protein structure than the previously mentioned non-synonymous SNPs.

d. SNPs in regulatory sites

DNA transcription is a key step in processing DNA into proteins that express the phenotype. Small regions of the DNA that regulate this process are promoters, enhancers, and silencers. Though the understanding of human transcriptome regulation sequences is limited, the importance of these is clear; any polymorphic variation may alter the level of protein expression and therefore play a significant role in affecting the phenotype.

e. TagSNPs

Around 335 million SNPs have been identified in the human genome across multiple populations; on average an individual has 3.3 million of these variations. Genotyping all these markers would be timely and costly, however it is known that SNPs located in close proximity are often inherited together as the area is said to be in high linkage disequilibrium (LD) [114]. By taking advantage of this tendency, a set of strongly associated SNPs (a haplotype) can be genotyped, reducing the number of SNPs required and providing more cost-effective information on genetic variation.

TagSNPs are selected based on the haplotype frequencies in the populations being genotyped. African populations are genetically more diverse (due to the “out of Africa” bottleneck) and have

smaller regions in high LD than European and Asian populations [114]. To date the HapMap project has identified approximately 3.2 million TagSNPs which are able to provide as much information as 10 million SNPs [115].

1.5.2. Forensic application of STRs, microhaplotypes and mitochondrial DNA

Autosomal short tandem repeats (STRs) are the gold standard for forensic DNA analysis and routine identification purposes. STRs, also known as microsatellites consist of repeats of 2-6 base pairs [116]. The forensic community focusses on tetranucleotide repeats as they produce less PCR artefacts than bi or tri-allelic repeats when amplified. The ability to use STRs as identifiers is due to the random nature of DNA polymerase slippage during DNA replication and the adding or subtraction of repetitions to the new DNA strand. The amplification of STR markers results in amplicons ranging from 100-500bp and mini-STRs have been developed for degraded DNA that result in amplicons ranging 51-211bp [117]. This technology uses capillary electrophoresis to provide a fast, robust, and accurate result by increasing sensitivity and reducing allele dropout. Commercial STR kits have been developed that provide multiplex reactions for 10-20 markers with as little as 0.5ng of DNA allowing the reanalysis of minute samples stored from unsolved crimes [118]. Developments have also been made in the software and statistical side of STR analysis which allowed the interpretation of DNA mixtures previously thought to be far too complex using probabilistic genotyping software combining biological modelling and mathematical processes to interpret a wide range of DNA profile permutations [119].

Capillary electrophoresis has now been superseded by Massively Parallel Sequencing that improves the throughput of samples and the ability to use the results for additional analysis such as DNA phenotyping [120, 121]. With this technological improvement has been the introduction of a relatively new DNA loci for individual identification, familial relationships and ancestry information called a microhaplotype [122]. A microhaplotype is defined as a locus with two or more SNPs within a short expanse of DNA, most often defined as 200bp [122]. Not only can these markers provide a wealth of information, they can be selected to avoid recombination hotspots which results in lower mutations rates than those of the STRs and can allow for DNA mixtures to be resolved unlike bi-allelic SNPs [123]. Microhaplotype panels have now been developed for use in forensic applications [124, 125] and a database of published marker and frequency data compiled [126] which will result in greater accessibility, accuracy and reliability of results.

Used in more niche areas, Y chromosome STR typing and mitochondrial sequencing of the HV1 and HV2 regions are also used [127, 128]. Y-STR typing is used where male-female mixed samples with low male contributions need to be resolved and for historical paternity or lineage testing [127]. Mitochondrial sequencing may be used to successfully deal with maternal ancestry cases and highly degraded DNA evidence such as those found in mass disaster scenarios or in desiccated tissues like hair and bones [128].

1.5.3. Forensically relevant SNP classes

a. Identity Testing SNPs

Markers used for identity testing are utilised just as STRs are currently. They are selected based on the SNP having high heterozygosity and low F_{st} values. It has been demonstrated that a panel of approximately 50 SNPs are comparable in discrimination to 13-15 STR loci multiplexes [129, 130]. Since these publications there are kits that utilise 24 STR loci which have higher discriminatory value, nevertheless the probability of any two individuals having an identical 50 SNP genotype is extremely low [130, 131].

SNP panels have been developed for forensic identification purposes on numerous platforms [132-134]. They are particularly useful in a forensic context as limited samples can be genotyped due to efficient multiplex reactions and optimised small amplicons; meaning more genetic data can be accumulated from the limited sample. The selection of platform largely depends on the number of samples needed to be genotyped plus the number of SNPs required to be interpreted. Although these panels are powerful in an identification context, they do not include SNPs that may be used to interpret phenotype and narrow a suspect pool or guide an investigation.

b. Lineage Informative SNPs

As the name suggests these are groups of tightly linked SNPs that act as haplotypes which may be used for kinship analyses in investigative genetic genealogy, missing person and mass disaster victim scenarios [135, 136]. As these markers have a low mutation rate, more stably inherited than STRs and occur as a haploblock they are ideal for lineage testing over several generations, similar to mitochondrial DNA [129].

Aside from the standard haploblocks, autosomal SNP haploblocks may also be used to track lineage. The autosomal haploblocks are also inherited together and provide a higher discrimination than singular SNPs within the block.

c. Ancestry Informative SNPs (AIMS)

AIMs are used to establish a probability of an individual originating from a determined geographical area or biogeographical ancestry (BGA) which is distinct from race or ethnicity as it is biologically based [137, 138]. SNPs within the AIM category are distributed with different allele frequencies amongst the world's population and therefore have high F_{st} and low heterozygosity values [138]. When typing these markers ancestry information may be revealed together with phenotypic traits of investigative value [138]. While AIMs are highly valuable they are only as reliable as the reference study population from which their F_{st} and heterozygosity values are sourced [137, 139]. As an example, specific BGA predictions are more difficult with Indigenous Australians as there have been a limited number of studies with many of these having small sample sizes. AIMs are also employed to detect population stratification in studies exploring risk factor indicators for various diseases allowing the development of more efficient treatments in the personalised medicine field [140].

d. Phenotype informative SNPs

These forensic DNA markers enable the prediction of the physical appearance of an individual [138]. As phenotype has an ancestry component phenotype informative SNPs overlap with AIMs [138]. The intention of these SNPs is to identify phenotypic characteristics such as pigmentation of hair, skin, and iris from a DNA sample for investigative purposes. These traits may also be inferred from AIMs however not with the same accuracy.

Pigmentation has been the trait most studied and published and as a research forensic assays have been developed for detecting hair and iris colour or both combined with ancestry [138, 141-143]. Research on additional traits such as height and weight are still ongoing but poorly understood at this stage [144]. However, with time and additional research there is hope for developing forensic arrays to predict these characteristics in the future.

1.5.4. Web-based bioinformatical resources for SNP selection

Freely available web-based resources have grown in numbers with the substantial progress of genetic studies in the last two decades. These resources are mostly free and provide a wide range of data on gene functions and interactions, SNP location and function, population data and statistical information. The information provided by these resources is plentiful given the size of the human genome, the number of polymorphisms and possible protein and genomic interactions. However, a recurring issue with these tools is that they are not updated frequently creating difficulties in candidate gene and SNP selection. An additional issue is that the tools often cease functioning after a period of time, which occurred in this study.

Two of the most comprehensive resources available are the GeneEpi toolbox and the dbSNP database. The GeneEpi toolbox was one of the first attempts to successfully systemise resources for candidate marker selection. This resource offers various workflow solutions for SNP selection and subsequent evaluation. The result is the identification of genetic variation which enables further study of physiological functions.

The dbSNP database is a subsection of a larger resource encompassing information on gene interaction, protein functions, taxonomy, and disease-related genetic information. The information within the SNP related dbSNP database represents an international central repository for single base nucleotide substitutions. Additional web resources used in this project are detailed in Chapter 2.

1.5.5. SNP chip platforms for targeted SNP genotyping

SNP arrays are used for the targeted genotyping of genetic markers and were originally designed for GWAS to study linkages between variations and diseases. Arrays allow the high throughput analysis of hundreds of thousands of SNPs for a single experiment and can be tailored for markers linked to different populations or diseases.

There are two main developers of the SNP microarrays, Affymetrix (Santa Clara, USA) and Illumina (San Diego, USA). Both chips use an oligonucleotide probe to which DNA attaches. The Affymetrix Axiom genotyping arrays are manufactured with *in situ* oligonucleotides which are 25 nucleotides in length, referred to as 25mers (Figure 18). The 25mers are attached to a glass or silicon slide at one end and are freely available to anneal to a specific sequence of DNA. The Axiom array uses multiple probes for each gene along with mismatched probes designed as controls for non-specific hybridisation. The probes are synthesized one base at a time in predefined locations meaning no barcodes system is needed for analysis. The structure reduces throughput as it allows for a single array to be processed at a time.

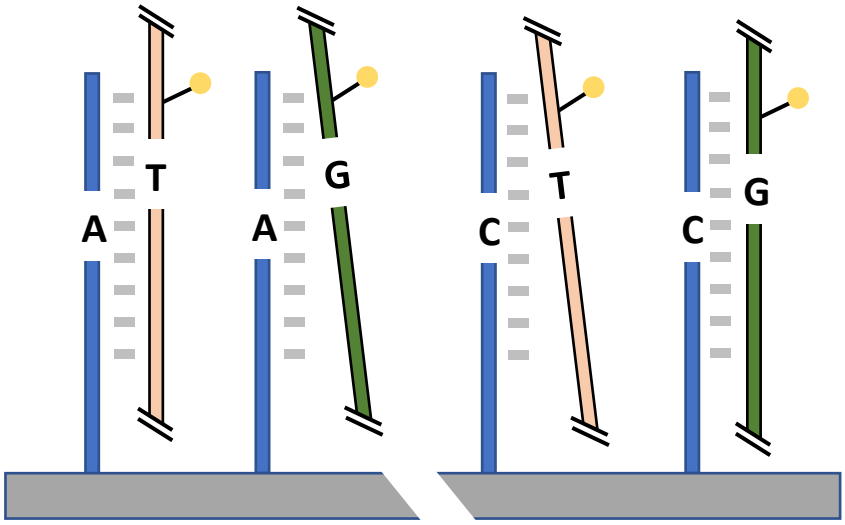

Figure 18: Diagram of the oligonucleotide SNP array principle

The Affymetrix Axiom SNP array utilises the oligonucleotide method. Oligonucleotides or 25mers are attached at one end to the silicon slide and the other end free to anneal to strand specific sequences of DNA. The probes are located in predefined locations on the surface and preferentially hybridise labelled complimentary target strands. While this diagram shows only one for simplicity, multiple allele-specific probes span the interrogated SNP. Allele abundance is quantified by intensities of labelled hybridised target strands.

Illumina BeadArrays utilise microscopic beads contained by microwells within fibre optic bundles or on a silicon slide (Figure 19). Each bead is impregnated with hundreds of thousands of copies of specific oligonucleotides that capture the targeted DNA within the assay. Different to the Axiom GeneChip the BeadArrays possess 30 copies of the same oligonucleotide, providing internal repetition which the Affymetrix offering lacks. The multiprobes are randomly distributed upon manufacture meaning a barcoding step is needed to catalogue the location of each hybridisation. This hybridisation can also occur in parallel with other steps due to multiple arrays being packaged on the same physical substrate.

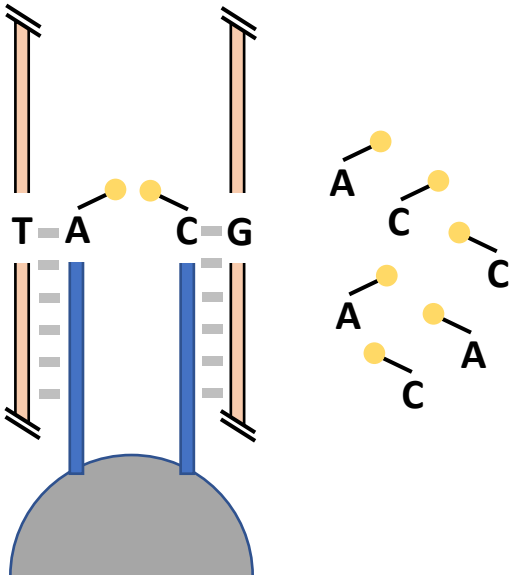

Figure 19: Diagram of the BeadArray principle

The bead array principle places microscopic beads into wells on a silicon slide. Each bead has numerous oligonucleotides impregnated which are complementary to the sequence adjacent to the targeted SNP. The probes hybridise with both parent strands in an allele non-specific manner. The hybridise target is used as a template to which a labelled nucleotide is added. By using different labelled nucleotides dual intensity quantification can be used to quantify allele abundance.

In comparisons between the two competing technologies they have been found to have similar genotyping accuracy and also similar accuracy for imputed SNPs for Asian samples [145]. Assessment of the available SNP arrays for use are detailed in Chapter 2.

1.6. Forensic Intelligence

Forensic intelligence utilises aggregated information from many cases to provide knowledge on criminal activity to inform decisions [146]. This knowledge may be leveraged in ways to support proactive and preventative law enforcement measures. There are three distinct types of intelligence: tactical, operational and strategic [147]. Tactical intelligence applies to front-line enforcement and is used on a case to case basis when deemed relevant [148, 149]. Operational intelligence assists in the planning of crime reduction and prevention techniques [148]. Strategic intelligence is proactive and draws on the understanding of pattern and behaviours to be future orientated [148, 149].

If databases of fingerprints could be utilised as more than just a reference for comparison associations could be made between patterns, ridge density, even minutiae to ancestry, sex, and DNA. These associations could initially make a sizeable impact as tactical intelligence and with

time and further data may morph to become future orientated as operation and strategic intelligence.

1.6.1. Locard's exchange principle

Locard's exchange principle is the basis of forensic science; it outlines the fundamental reasons why forensic science is possible. Named after the pioneer of forensic science, Dr. Edmond Locard, it has been translated and restated numerous times but perhaps stated best in English in Kirk, 1953 [150].

> *"Wherever he steps, whatever he touches, whatever he leaves, even unconsciously, will serve as a silent witness against him. Not only his fingerprints or his footprints, but his hair, the fibers from his clothes, the glass he breaks, the tool mark he leaves, the paint he scratches, the blood or semen he deposits or collects. All of these and more, bear mute witness against him. This is evidence that does not forget. It is not confused by the excitement of the moment. It is not absent because human witnesses are. It is factual evidence. Physical evidence cannot be wrong, it cannot perjure itself, it cannot be wholly absent. Only human failure to find it, study and understand it, can diminish its value." – Kirk, 1953*

This can be summarised predominantly into the statement "Every contact leaves a trace". Traces can be any material deposited from the contact of two surfaces in the physical world or a remnant of activity in the digital world, which often give an insight to the identity or acts of a perpetrator in a crime scene. As technology and knowledge has developed, more minute traces have been able to be detected. With that, latent, identifying biological traces and fingermarks have become invaluable due to their evidential value.

While STR DNA profiling and fingerprints have been considered the gold standard for identification in forensic science, the comparative nature of the method has always been a major limitation.

1.6.2. DNA phenotyping

Genome wide association studies (GWAS) have employed huge sample sizes and statistical analyses to uncover associations between genotype and phenotype with very high significance threshold. The phenotype may be fingerprints [54], facial morphology [151], pigmentation [152, 153] or illnesses such as breast cancer [154], prostate cancer [155] and Crohn's disease [156].

By identifying genetic markers associated with a disease or trait the phenotype can be predicted from the genotype [100]. Thus far research has mainly focussed on SNPs, single bases in the DNA, however recently there has been a push to look at STRs, short repeats of bases which have previously been thought to be "junk DNA" or inconsequential, but are now being identified as being significant in trait development [157, 158]. The uses for this information are far reaching, from forensic use to medical treatment and prevention which may cause issues with genetic privacy.

In a forensic context, DNA phenotyping (also known as molecular photo fitting) is the interpretation of genetic markers to provide a picture of an individual's externally visible characteristics (EVCs). EVCs include pigmentation of hair, skin and iris, in addition to facial metrics and fingerprints [143, 159]. The accuracy of prediction of traits is variable; eye colour has proven to be 94% accurate for predicting blue and brown eye colour in Europeans [160], hair pigmentation prediction accuracies are 69.5% for blond, 78.5% for brown, 80% for red and 87.5% for black hair colour on average [161] and the latest population specific skin colour area under the curve accuracies range from 0.75 to 1 for five different categories [162]. BGA prediction while not an EVC is also largely dependent on the admixture of BGA, quality of DNA sample and classifying algorithm used [163-165]. Facial metrics and fingerprint prediction are still in their infancy, with only a handful of single nucleotide polymorphisms associated in each case [55, 166].

For pigmentation, the research has moved from SNP discovery to amalgamating the SNPs into a multiplex assay for commercial use. Through a series of publications Walsh *et al.* [161, 167, 168] outlined the development of firstly the Irisplex kit used for the accurate prediction of eye colour and secondly the development of Hirisplex with 24 SNPs for the simultaneous prediction of hair and eye colour. The latest pigmentation multiplex assay is the HirisPlex-S that contains 41 SNPs for eye, hair and skin pigmentation [162]. The HirisPlex-S kit is the first kit that is forensically validated for skin pigmentation prediction. The kits were designed to work with extremely low amounts of DNA and returned full profiles with as little as 63 picograms [162].

SNP panels have also been developed to determine ancestry though each have limitations [169]. Numerous international efforts including the HapMap project [115], the 1000 genome project now known as the international genome sample resource [170], HGDP-CEPH Human Genome Diversity Cell Line Panel, the Simons Genome Diversity Project, Estonian Biocentre Human Genome Diversity Panel and the HUGO Pan Asian SNP database have determined the frequency of ancestry informative SNPs were over time and selected to discriminate between sufficiently

isolated populations. A panel with 128 markers was developed by Kosoy *et al.* [171] in 2009 and in 2014 a panel with a further 55 unique markers was produced by Kidd *et al.* [169]. These developmental panels have resulted in the recently available Precision ID Ancestry panel from Applied Biosystems. This panel targets 165 autosomal markers and can produce accurate ancestry prediction on DNA samples with as little as 30pg of DNA [172].

Statistical modelling software such as STRUCTURE can now also be used on genetic data to determine ancestry. This method analyses SNP genotypes in current populations and can assign individuals to ancestry clusters based on Bayesian likelihoods [173]. A comparison of five BGA classifiers (STRUCTURE, Bayesian weighted, Bayesian unweighted, GDA and MLR) showed that STRUCTURE had the best accuracy closely followed by the Bayesian approaches for all BGAs tested [163]. This high accuracy continued with only a minor drop when 90% of the original genotype was removed [163]. Although STRUCTURE is the most accurate modelling software, it is more complicated in method and not as versatile as the generic Bayesian approaches[163]. STRUCTURE is not able to be used for phenotype prediction because of underlying assumptions about Hardy-Weinberg equilibrium in ancestral clusters.

While DNA phenotyping has become a reality over the last decade there are still limitations, the most notable being age. Aging can change EVCs while stress, depression, sun exposure and chemical exposure (smoking) can all accelerate aging. Secondly, phenotyping cannot predict acquired characteristics such as scars, plastic surgery or alterations that are otherwise made to the appearance of a person. A final limitation that can be managed is the reference sample collections that are used for comparison and model training, particularly in the case of BGA and phenotype reporting in pigmentation. Phenotype is often self-reported and subjective. If an incorrect phenotype is reported it may cause incorrect associations with unknown samples. Efforts have been made to standardise colours into categories and new digital spectrophotometric technologies are now being introduced to increase objectivity in determining pigment-related colours [174, 175].

1.6.3. Phenotyping provides avenues for investigation

When DNA is deposited at a crime scene, it is genotyped and compared to a database of known profiles. In Australia, this is the National Criminal Investigation DNA Database (NCIDD) which is comprised of over 1.22 million profiles [176]. Without a match, investigations are often left at an impasse. The development of DNA phenotyping has allowed new avenues of investigation by utilising DNA that has no match to give an indication of what the suspect's BGA and EVCs are.

Private laboratories have leveraged these studies to offer a service to police to provide characteristics from a DNA profile. The most notable of these companies is Parabon Nanolabs which provide the Snapshot service. This service incorporates genetic genealogy, kinship inference and DNA phenotyping targeting skin, hair, and eye pigmentation alongside a confidence level for the presence of freckles. From the results of the DNA analysis a composite facial image is produced that can be altered by a forensic artist to show age progression, weight, or any acquired characteristics not available from the DNA.

There are several studies which have evaluated the methodology and results of the service which Parabon Nanolabs provides [177, 178]. The prediction of EVCs compared to self-reporting by volunteers has been upwards of 82% accurate for eye and hair pigmentation, 100% for skin pigmentation amongst Europeans and 92% amongst non-European. The sex and BGA predictions were all consistent with self-reporting [178]. The evaluation concluded that the majority of predictions on EVCs and BGA made with Snapshot were consistent with self-declarations from volunteers [178].

However, much controversy surrounds the facial composite produced alongside the phenotype data. Facial composites are images produced by forensic artists, either freehand or through computer programs [179]. They are often produced to represent a face memorised by a witness to a crime. In Parabon's case, facial composites are produced from associations between genetic markers and face morphology data. Greytak [177] explains that Parabon collected face morphology data and analysed a total of 21,450 quasi landmarks on each face. Principle component analysis (PCA) was then performed to reduce this data to points that represent the majority of variation in the faces [177]. From the reduced data a series of face shape phenotypes were produced which were corrected for sex and ancestry [177]. Wiley [178] notes that flaws in this process include the lack of anthropologically recognised facial points and the general lack of anthropological data. The facial composites are largely based on ancestry and sex, and then adjusted for genotypes that have strong associations with deviations from these class averages. They result in a resemblance to an individual, something that would not stand up to the rigors of a forensic facial comparison following the Facial Identification Scientific Working Group (FISWG) guidelines. When it is known that eyewitness reliability and recognition is flawed, a facial composite resemblance through class average characteristics may not be up to the required standard [159, 180-186].

1.6.4. Eyewitness unreliability

It has been established that false identifications resulting from eyewitness recall are a frequent occurrence however eyewitness testimony is often a deciding factor in legal cases. Eyewitness testimony has particularly been under fire from organisations such as The Innocence Project working to exonerate wrongly convicted individuals [187]. A study from 1981 by Clifford and Hollin [188] found average accuracy rates of only 27% for identifying an offender. A positive correlation between accuracy and offences of lower violence was also found in the study, something in line with Yerkes-Dodson law first noted in 1908 that states mental arousal increases performances to a point before declining [189].

From a 1985 study by Lindsay and Wells [190], it was shown that incorrect identifications may be made in up to 35% of cases depending on the viewing conditions. These results were developed further by looking at numerous variables that may affect a positive identification. It has been found over numerous studies that age of the viewer, disguise of the perpetrator, weapon visibility, instructions given to the viewer to elaborate and line-up instructions were detrimental to positive identifications [183, 184, 186].

An example of eyewitness unreliability and the strength of DNA phenotyping is the case of Derrick Todd Lee, otherwise known as the Baton Rouge serial killer [191]. Between the dates of August 1992 and March 2003 there was a serial rapist and murderer on the streets of Baton Rouge, Louisiana. The police had linked the crimes through matching DNA. As a result of United States Federal Bureau of Investigation (FBI) profiling and a confident eyewitness the police believe they were searching for a male of European ancestry. After a fruitless search and a fourth murder, the police performed a dragnet to obtain the DNA of approximately 1200 males of European ancestry. After all samples returned no matches, police turned to DNAPrint Genomics, a company whose flagship service was ancestry prediction, a relatively new science at the time. The ancestry results of the perpetrators DNA returned a result of 85% Sub-Saharan African and 15% Native American, something at complete odds with the eyewitness testimony. Two months after the ancestry prediction and a fifth victim, Derrick Todd Lee, a man who was initially overlooked due to one individual's misrecognition was taken into custody. This case demonstrates where DNA phenotyping can supplement an investigation and provide information that can be more heavily relied upon.

1.7. Project hypotheses and aims

Considering the proven benefits of predicting EVCs and BGA from the genotype, expanding this ability to additional biological characteristics would have profound benefits, particularly regarding fingerprints. An initial study by Ho *et al.* uncovered several SNPs linked to the increasing chance of possessing a plain whorl pattern on a finger [55]. By expanding the research to a wide range on fingerprint patterns it could be a technique useful for forensic investigations.

Although headway has been made on linking genetic markers to fingerprint pattern there is still a lack of understanding to the statistical distribution of these patterns among the population. Numerous studies have found both similar trends and conflicting results between different BGAs and sexes though rarely a direct comparison between BGA is made [22, 26, 29, 33, 90, 103-105, 192-217]. Ridge density too has been evaluated as a method of distinguishing between male and female fingerprints with inconsistent results [30, 33, 218-237]. By studying the fingerprint pattern distribution and ridge density on a multicultural Australian population for the first time, it will provide a direct comparison between BGAs and the sexes. Additionally, information regarding the rarity of patterns will be provided for fingerprint experts to rely upon when presenting as expert witnesses; beneficial as often they are asked about the rarity of a pattern to which they must use their experience and personal judgement.

This research has two main hypotheses: Indications of biodata (BGA, sex, hand, finger) can be extracted from fingermarks that do not return a biometric match through automated fingerprint identification systems based on the level one pattern and ridge density, and SNPs will be associated with level one fingerprint patterns.

To formulate extensive answers to these questions, the specific aims of this research are:

Aim 1: Assemble a repository of fingerprints and DNA samples from approximately 500 volunteers alongside sex and self-reported biogeographical data.

Aim 2: Identify any associations of fingerprint patterns with sex and BGA using goodness of fit tests and multinomial logistic regression (MLR) analysis.

Aim 3: Identify any difference in ridge density within sex or BGA groups using goodness of fit tests, general estimating equations (GEE) and generalised linear models (GLM).

Aim 4: Perform a small family study investigating the inheritance of fingerprint patterns.

Aim 5: Extract, quantify and genotype collected DNA and perform SNP association analysis utilising R packages (SNPassoc and qqman) plus generalised liner models to identify SNPs that influence fingerprint phenotype.

Chapter 2 outlines the method of collection, DNA extraction, quantification, and genotyping procedures. As well as the programs and statistical models selected to perform the analyses. The fingerprint information with then be assessed in chapter 3 using chi-squared ($\chi 2$) and MLR tests which will identify if any patterns are associated with BGA, sex, hand, and finger. Chapter 4 then assesses ridge density, another fingerprint characteristic, using GEE to determine its viability for use as a feature to sex classify prints. Chapter 4 also investigates how factors such as BGA, pattern, hand and finger all influence ridge density. Chapter 5 is a small family fingerprint case study that introduces the DNA underpinnings of fingerprints. The family is assessed using pedigree trees to determine if any traits are passed down as single loci traits in Mendelian inheritance models. Chapter 6 is the final research chapter which takes a deeper look into the DNA basis of fingerprint phenotypes using SNP association analysis, and chapter 7 outlines the conclusions that were made from this research, possible reasons for the trends that were seen and the future directions of these research topics.

Chapter 2 – MATERIALS AND METHODS

2. Materials and methods

2.1. Ethics approval

This project was conducted with ethics approval from the University of Technology Sydney Human Research Ethics Committee, project number 2015000296. The volunteers who participated were largely students or employees of the University of Technology Sydney. Participants were also recruited via news articles and emails asking for expressions of interest.

All volunteers completed an informed consent document before participation (Appendix C). The database of fingerprints taken electronically in Sydney were stored in a password protected file system on a dedicated computer. The volunteer questionnaires were stored within binders in a key-access room. DNA samples were stored in a locked -80^{o}C freezer.

2.2. Samples

Samples were provided on a voluntary basis from the Sydney population over a time of approximately 18 months. A total of 515 individual samples were collected with a form for self-reported ancestry and pigmentation information (Appendix D), three buccal swabs and fingerprint scans of all ten fingers.

An additional 324 samples collected from volunteers located in Melbourne were also used. The Melbourne data used a similar questionnaire to the Sydney data and ancestry was self-reported. The fingerprints were provided via rolled ink fingerprints on ten-print cards and no DNA data was provided. The Melbourne samples were collected according to the University of Canberra under ethics codes CEHR 11-119 and the extension, CEHR15-64.

To make the collection process as efficient and accessible as possible, an online booking system was used allowed volunteers to book an appointment at the best time to suit their needs. The online booking system also helped with the logistics of the sample collection process.

The volunteers were asked to self-report the ancestry of their maternal and paternal grandparents, with emphasis on BGA, not necessarily the country that the ancestor was born in.

The fingerprints were taken using a Futronic FS60 fingerprint scanner (Futronic Technology Co. Ltd., Hong Kong) using FS60 Demo software. The scanner was used on the “rolled” fingerprint setting and x4 magnification to make viewing easier. Each finger was scanned individually starting with the left little finger. The inside edge of each digit was placed on the scanner and rolled to the outside edge slowly.

If the finger was undetected by the scanner or produced a fingerprint that was not identifiable, with the volunteer's consent either a baby wipe was used to moisten the finger or sebaceous residue added by touching their face so that the individual ridges were visible. If the individual ridges were not distinct a facial tissue was used to dry or remove oil from the finger.

Care was taken as the rolling motion may cause stress on the wrist of the volunteer, which may cause issues especially if arthritic conditions are present. Additional caution was taken where volunteers had hyperhidrosis, allergies, or skin conditions such as eczema. The fingerprints of volunteers noted to have a skin condition were screened for fingerprint pattern failure as found by Haber *et al.* [14] and none were found to be devoid of pattern.

The DNA was collected via three Isohelix SK-5S DNA Buccal swabs (Cell Projects, Kent, UK). The volunteers were asked to rub the inside of their cheeks firmly with the swab for one minute with each swab. Once completed, the swab tips were separated from the shaft of the swab and placed into a labelled microcentrifuge tube. These samples were stored in a 0^{o}C freezer for temporary storage before being moved to a -80^{o}C freezer.

2.3. DNA extraction

DNA from the samples collected for this study was extracted from saliva using Isohelix BuccalPrep Plus DNA Isolation Kits (Cell Projects, Kent, UK). These kits were chosen for the ease of use and ability to produce relatively high DNA yields of high purity at a reasonable price. The extractions were processed with adaptations to the manufacture's recommended protocol to further increase yield [238]. Two out of three of the collected buccal swabs for each volunteer were used for extraction, the final swab was kept for additional studies.

2.4. DNA quantification

The quantification of the DNA was initially estimated by absorbance at 260nm using a NanoDrop One spectrophotometer (Thermo Scientific, Massachusetts, USA) with the standard manufacturer recommendations for DNA samples [239]. Further estimation was carried out using the Qubit dsDNA High Sensitivity Assay Kit and Qubit fluorometer (Life Technologies, Mulgrave, VIC, Australia) to prepare each sample for genotyping. The standard protocol supplied with the Qubit kit was followed for quantification [240]. As Qubit is not human specific the estimations can vary given the high amount of oral flora and bacteria in saliva samples. While

not as accurate as qPCR methods, this assay was used because an exact quantification of DNA was not necessary, and Qubit was sufficient at a lower cost.

2.5. Candidate genes and SNPs using bioinformatics resources and previous literature

A review of previous literature on the DNA basis of fingerprints was performed. This uncovered three studies: Medland *et al.* [54], Ho *et al.* [55] and Walsh *et al.* [166]. Ho *et al.* [55] and subsequent commentary of Walsh *et al.* [166] found association of whorl patterns with SNPs in the ADAMTS9-AS2, OLA1 and an area between the TBX3 and MED13L genes. These SNPs were rs1523452, rs2244503, rs796973 and rs17071864 within the ADAMTS9-AS2 gene, rs10201863 within the OLA1 gene and rs1863718 where significance peaked between the TBX3 and MED13L genes.

Medland *et al.* [54] investigated ridge density found significant multivariate linkage (individual finger ridge counts) at 5q14.1 on the genome through ring, index and middle finger ridge density. Univariate linkage (sum of individual finger ridge counts) was significant at 1q42.2. The 5q14.1 region is approximately 4.5 megabases long and the 1q42.2 region approximately 4.1 megabases long each containing numerous genes [241]. The genes within this region were assessed with the web resources below.

The following web resources were utilised for identification of genes that may play a role in how finger and skin development and by extension, fingerprint development. The compiled genes were then used to cross-reference genotyping arrays for the highest number of SNPs in common or in linkage disequilibrium.

Disease databases

- https://www.malacards.org/
- https://omim.org/
- https://www.ncbi.nlm.nih.gov/medgen/

Gene databases

- https://www.ncbi.nlm.nih.gov/snp/
- https://www.genecards.org/
- https://asia.ensembl.org/Homo_sapiens/Info/Index

Potentially functional SNP searches

- http://pfs.nus.edu.sg
- http://compbio.cs.queensu.ca/F-SNP/ - now not functional [242]
- https://snpinfo.niehs.nih.gov/

TagSNP investigation

- https://snpinfo.niehs.nih.gov/snpinfo/snptag.html

The search for genes was based on three criteria: Firstly, any that have had previous association from literature, secondly, genes that may cause disease where fingerprints are known to be affected and thirdly, genes where the function may play a direct or indirect role in fingerprint development and disease. This search resulted in a compilation of 215 genes. This search was intended to be very broad, with gene functions ranging from finger development to skin conditions and disease such as asthmas where studies indicated possible links to ridge patterns. Each of the 215 genes were examined via the potentially functionable SNP web resources listed above which returned 41,881 SNPs, many of which were duplicates due to the use of multiple resources. These were reduced to 23,438 once duplicates were removed.

2.6. SNP chip selection and DNA genotyping

The selection of a SNP chip to genotype the samples was hugely important given the trade-offs between price and the amount of SNP data that could be directly produced and inferred. The candidate SNP chips are listed in Table 2.

Table 2: Criteria for considered genotyping options

Array	**Qty DNA (ng)**	**DNA conc. (ng/µl)**	**DNA Purity (A_{260}/A_{280})**	**Sample vol. (µl)**	**Fixed SNPs**	**Custom SNPs**	**Price**
Illumina Infinium Exome-24 v1.0	>200	>100	>1.7	>20	243,345	400,000	US$78
Affymetrix Axiom Precision Medicine Genotyping Array	500	20	>1.8	>25	~900,000	-	AU$103
Illumina Infinium CoreExome-24 v1.1	1000	100	-	20	551,839	100,000	AU$124
Illumina Infinium Global Screening Array-24 v1.0	250	50	-	20	642,824	50,000	AU$50

Once the price and requirements were assessed, the candidate SNPs were cross-referenced with those analysed by the SNP arrays. TagSNPs were also considered when selecting the genotyping microarray. Using the TagSNP reference website listed above, the genotyping microarrays were screened for SNPs that inferred the genotype of others in genes identified as of interest through the candidate search. The Illumina Infinium Global Screening Array-24 v1.0 was selected as the array of choice due to price and amount of candidate SNPs targeted.

The samples were normalised 20 ng/µL in a 35µL total volume using TE buffer. Where the concentration was lower than required, a rotary evaporator was used to evaporate some liquid and thus increase concentration.

Following normalisation, samples were shipped for genotyping to the University of Newcastle, New South Wales, Australia. When loading each sample into the chip 10µL was used equating to 200ng of DNA. While this was slightly lower than the manufacturer recommendations of 250ng the results were still viable as the call rate for each sample (for all the markers) was on average 0.993991 (above 99%) while only 0.001106% markers produced no call. The rest of the genotyping procedure was performed as per manufacturer instructions [243].

2.7. Fingerprint classification

The fingerprint classification used was the NCIC classification system, discussed in detail in section 1.2.2. This system was chosen for its clarity and ability to distinguish eight different patterns, including the subcategories of arches, loops, and whorls. Further classification detail indicating inner, meeting, and outer ridge tracings between the two deltas in whorl patterns was completed for the Sydney data but not for the Melbourne data due to fingerprint quality and time constraints. The inner, meeting, and outer ridge tracing classifications of the Sydney dataset were not utilised in this study.

Fingerprints collected from the Sydney population were numbered 1 to 10 from left little finger to right little finger, classified and recording into a database within Microsoft Excel.

The fingerprints received from the Melbourne population were scanned to produce electronic copies then reclassified using the NCIC patterns to eliminate any inter-examiner variation.

2.8. Statistical analysis

The R programming language [244] in combination with R studio [245] and IBM SPSS Statistics 25 [246] were utilised to perform statistical analysis. Chi-squared tests (χ^2) [247] and Multinomial Logistic Regression (MLR) [248] were used for the association of fingerprint pattern the BGA, sex, hand, and finger. Previous studies have used χ^2 which is not an appropriate method as this assumes that a set of ten fingerprints are independent of one another. A comparison was made between the χ^2 and MLR results to identify differences the different approaches may produce. General Estimating Equations (GEE) [249] and Generalised Linear Models (GLM) [250] plus Shapiro-Wilk [251] and Kruskal-Wallis tests [252] were used for ridge density association to sex, BGA, pattern, hand, and finger. The GEE and GLM are two competing techniques, the GEE approach was selected for ongoing discussion of results given how the GEE accounts for random effects. Finally, the SNPassoc package [253] within R was sourced for analysis of SNP association with fingerprint pattern for five different genetic models. The output was then visualised within Manhattan plots using the qqman package [254].

Each statistical test and the parameters used are explained in further detail in each chapter they were employed to analyse data.

Chapter 3 – RARITY OF FINGERPRINT PATTERN AND ITS ASSOCIATION WITH BGA AND SEX

3. Rarity of fingerprint pattern and its association with BGA and sex

This chapter refers to aims 1 and 2 of this project which were:

Aim 1: Collect a database of fingerprints and DNA numbering approximately 500 volunteers alongside sex and self-reported biogeographical data.

Aim 2: Identify patterns associated with sex and BGA using multinomial logistic regression analysis.

Specifically, this chapter focusses on the results of the following steps and experiments

- Sample collection including fingerprints, DNA, and ancestry information
- Classification of the fingerprints
- Preliminary Chi-squared analysis of fingerprint pattern in relation to sex and BGA for comparison to MLR
- MLR of fingerprint pattern to sex and BGA, with hand and finger as additional variables

3.1. Introduction

When latent fingermarks are collected from crime scenes or when someone's fingerprints are collected, they are run against the automated fingerprint identification system (AFIS). Where there is a match from the system, a fingerprint examiner assesses the match to determine if the result is true. If the returned file is a true match an identification can be made. However, when there is no match found in the AFIS system this results in an investigative dead-end; meaning the fingerprint is left in the system to hopefully receive a match with a print enrolled in the future. A similar situation can occur with DNA samples, though recent sequencing techniques facilitate prediction of externally visible characteristics (EVCs). Perhaps a similar method can be used for fingerprint evidence. By calculating the frequency of patterns and the statistical association, likelihoods can be created for physical characteristics of the person who deposited the fingermarks. Possible characteristics include ancestry or sex in addition to finger and hand.

Calculating the statistical frequency of fingerprint patterns could potentially also be of benefit to fingerprint experts presenting as expert witnesses in court. Often, they are asked to give judgement on the rarity of a print which is usually based on opinion from their experience. This highlights a lack of research on the statistics of pattern frequency amongst populations. If the frequency of specific patterns could be provided, examiners could relay the information to add weight to any fingerprint evidence being presented.

3.2. Volunteers by categories

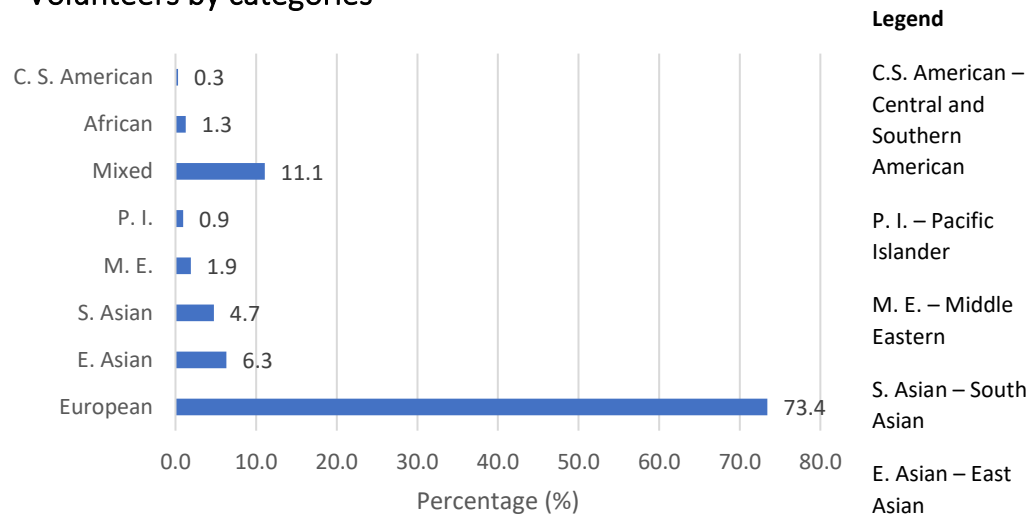

Figure 20: Biogeographical ancestry of volunteers (N=515) from Sydney

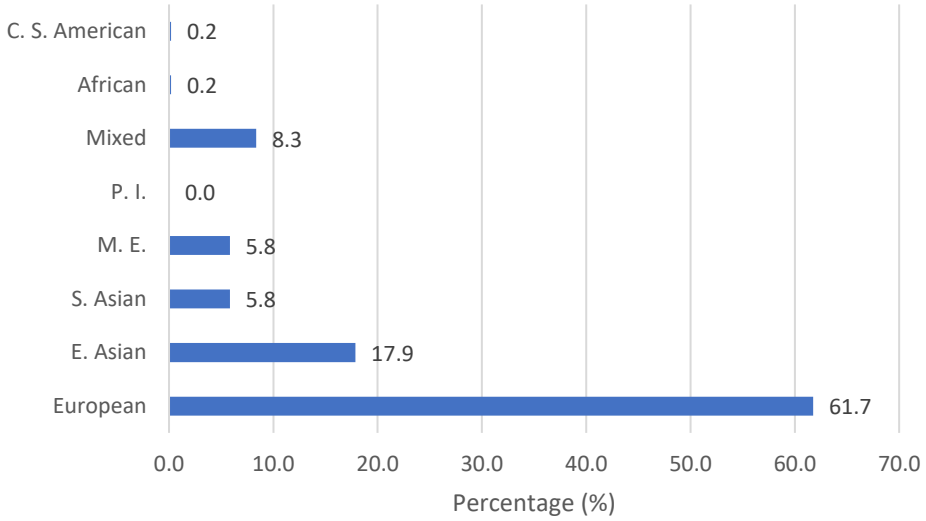

Figure 21: Biogeographical ancestry of volunteers (N=316) from Melbourne

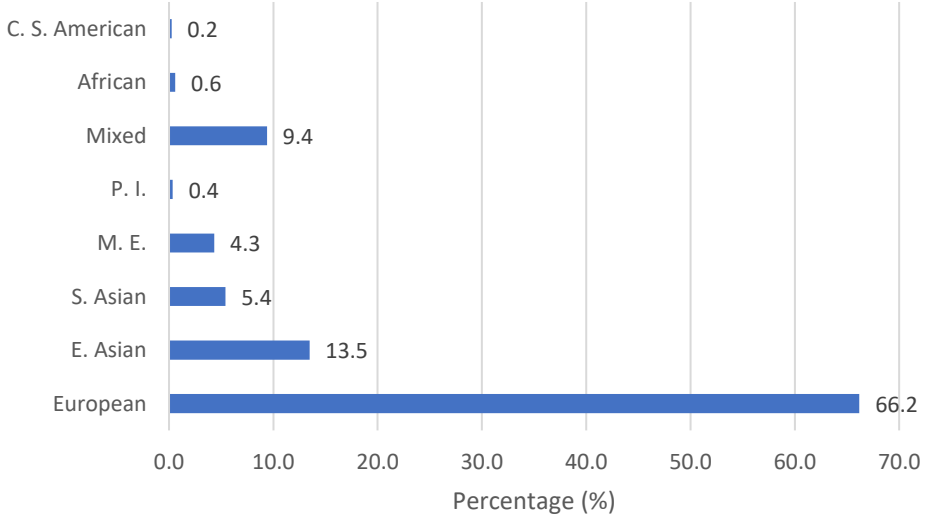

Figure 22: Combined biogeographical ancestry of volunteers (N=831) combined

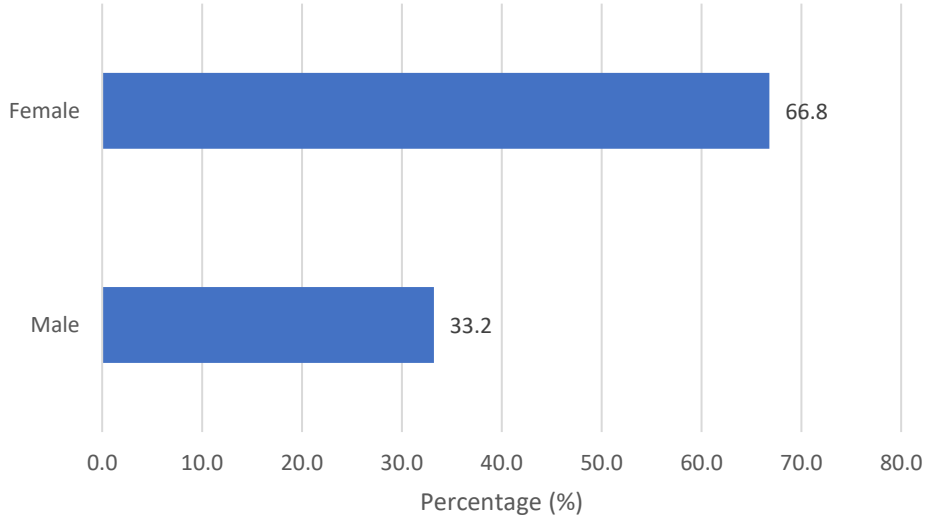

Figure 23: Sex of volunteers (N=515) from Sydney

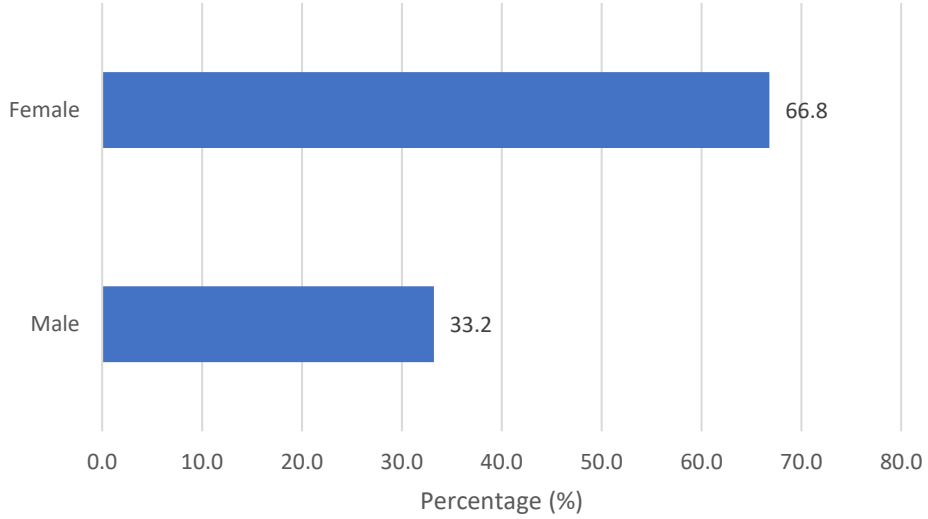

Figure 24: Sex of volunteers (N=318) from Melbourne

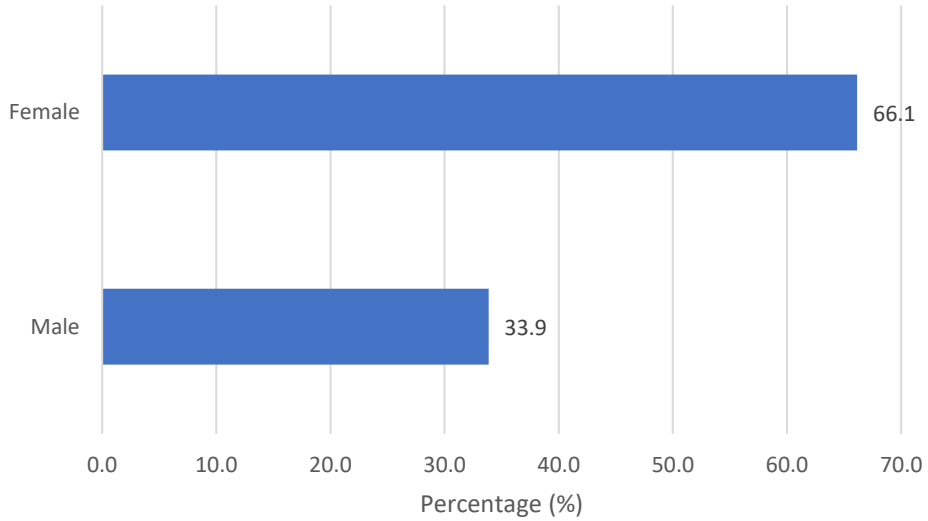

Figure 25: Combined sex of volunteers (N=833) combined

It is noted that some of the BGAs displayed in Figures 20-22 are represented by a single individual. This sample size means that statistical analysis and an overall observation of that BGA cannot be made. Only Middle Eastern, East Asian, South Asian and Europeans BGAs were used for statistical analysis. The mixed group, while large enough for statistical analysis contains a multitude of different BGAs and therefore cannot be used to infer the fingerprint characteristics of a single population. Should a statistical model be produced to indicate the BGA from which a set of fingerprints originated this mixed group fingerprint data could be of use.

3.3. Frequency distribution of pattern

The classified fingerprints of both the Sydney and Melbourne groups were catalogued, and the frequency tabulated to show the distribution of patterns within each subgroup of volunteers (Table 3 & Table 4). By presenting the frequency of the patterns in percentage form we can negate the effect of the unbalanced group numbers to show initial trends. The sex data table features all volunteers with a recorded sex of male or female and overlooks the effect that BGA may have on fingerprint patterns. We can see the male group have a lower percentage of arches than females and a lower percentage of loops than females. Conversely females have a higher percentage of whorls compared to males.

Table 3: Frequencies (%) of the three main fingerprint pattern groups in males and females

	N	Arch (%)	Loop (%)	Whorl (%)
Male	282	5.3	60.6	33.6
Female	551	6.7	65.3	27.5
Overall	833	6.0	62.9	30.6

The distribution of patterns was much less even between the ancestry groups than the two sexes (Table 4). Only volunteers of the Middle Eastern, East Asian, South Asian, and European BGAs are shown given their larger sample size. For the arch patterns, the European and Middle Eastern groups were clearly highest in percentage. Europeans also had the highest percentage for the loop patterns, this time followed by the South Asian group. The order of percentage changes again with the whorl pattern, the East Asian, Middle Eastern and South Asian ancestral groups were all clearly higher than the European group.

Table 4: Frequencies (%) of the three main fingerprint pattern groups in four BGA groups

	N	Arch (%)	Loop (%)	Whorl (%)
European	550	7.3	66.9	25.3
E. Asian	112	3.8	55.9	40.0
S. Asian	45	1.8	61.8	35.6
M.E.	36	7.2	53.6	39.2

One of the few papers to compare between ancestral groups was by Swofford [105]. Using a chi-squared test, disregarding what finger the pattern occurred on, results showed pattern was significantly associated with ancestry. Based on this result a frequency ranking for each pattern was created in African, European, Hispanic, and Asian populations. No geographical sub-classifications of the populations were detailed. For loops, African, European, and Hispanic were very similar while in Asian populations it occurred less; with the European loop pattern frequency being higher than the Asian group it is consistent with the results shown in Table 4. Whorls occurred most in Asian groups, followed by Hispanic, then African and European. A large difference between the whorl frequency percentage of Asian and European ancestries mirrors the results shown in Table 4. Arches were said to be of highest frequency in African populations, closely followed by Hispanic and Europeans. Asian populations were clearly the lowest in arch frequency which is congruent with the initial results of this study indicating they had lower frequencies than Europeans (Table 4).

A preliminary study by Walton *et al.* [22] of which data has been augmented in this thesis, revealed early trends in fingerprint patterns. It was seen in the cohort of 514 people from Sydney, Australia that women had a noticeably higher percentage of plain arches than males after utilising the chi-squared statistical method. For the rarer patterns (plain arch, tented arch, radial loop, central pocket loop whorl and double loop whorl), frequencies in Europeans were similar to those in Middle Eastern populations and frequencies in East Asian populations were similar to South Asians. However, these were reversed with the common pattern frequencies (ulnar loop and plain whorl); frequencies in Europeans were similar to those in South Asians and frequencies in Middle Eastern populations were similar to those in East Asians. This was the first time that ancestry association with more than three fingerprint classes had been examined.

Comparing these trends to the results of other studies is difficult given the demographic data is often not disclosed. Information on ancestry can only be indicated by the region in which the samples were collected, which is not reliable with newer studies given the multiculturalism of

many countries. Nevertheless, the overall percentages in Table 3 show roughly similar distribution of arches, loops, and whorls as the studies from Sweden and USA in Table 5.

Table 5: Frequencies (%) of fingerprint pattern groups in several studies within differing BGAs

Study	Frequency of Arches (%)	Frequency of loops (%)	Frequency of whorls (%)	Country	Sample size
Walton *et al.* [22] *	6.1	62.2	31.4	Sydney, Australia	514
De Jongh *et al.* [103]	4.9	62.2	32.9	Netherlands	2,452
Galton [28]	6.5	67.5	26.0	Unknown	500
Rignell [90]	7.0	63.9	28.2	Sweden	120,000
Champod *et al.* (FBI data) [255]	6.1	65.0	28.6	USA	17,951,192
Gutierrez [197]	5.3	67.3	27.5	Spain	200
Neggaz [192]	2.9	61.2	36.0	Oran, Algeria	228
* *The data in Walton et al. has been augmented in this study*					

The classification of pattern into three main groups is another limiting factor in drawing meaningful trends from this data. These main patterns contain distinctly different sub-patterns: Two different arches, two different loops and four different whorls. By grouping into fewer classes, the less frequent patterns such as radial loops and double loop whorls that may be more beneficial for stronger profiling are masked. In addition, if a frequency is being presented in court, the significance of a particular pattern may be wildly misrepresented.

Table 6 and Table 7 display frequencies of eight patterns from the NCIC classification system. By sub-dividing the three main patterns into smaller categories it can be seen there are large differences in frequency, most notably between the ulnar and radial loops. The female group has higher frequency of plain arches and ulnar loops. The male population has noticeably higher frequencies of plain whorls and double loop whorls. The percentage of tented arches, radial loops, central pocket loop whorls and accidental whorls are similar.

Table 6: Frequencies of fingerprint pattern groups between males and females

	Arches		Loops		Whorls				
	Plain arch	**Tented Arch**	**Ulnar loop**	**Radial loop**	**Plain whorl**	**Central pocket loop whorl**	**Double loop whorl**	**Accidental whorl**	**Missing/ Scarred**
Male (N=282)	2.1	3.2	57.0	3.6	25.6	3.4	4.2	0.5	0.5
Female (N=551)	3.9	2.8	61.3	4.0	20.7	3.7	2.8	0.3	0.4

Table 7: Frequencies of fingerprint pattern groups between four BGA groups

	Arches		Loops		Whorls				
	Plain arch	**Tented Arch**	**Ulnar loop**	**Radial loop**	**Plain whorl**	**Central pocket loop**	**Double loop whorl**	**Accidental whorl**	**Missing/ Scarred**
European (N=550)	3.8	3.4	62.4	4.5	18.5	3.6	2.9	0.3	0.5
E. Asian (N=112)	2.6	1.2	53.9	2.0	32.1	3.4	4.2	0.3	0.4
S. Asian (N=45)	0.7	1.1	59.6	2.2	26.9	3.6	4.9	0.2	0.9
M.E. (N=36)	4.4	2.8	50.8	2.8	32.8	5.3	0.8	0.3	0.0

Within the ancestral results there appears to be a distinct grouping trend between ancestries. For the common ulnar loop and plain whorl patterns the European and South Asian frequencies are noticeably different to the East Asian and Middle Eastern ancestries. The European and South Asian populations have higher ulnar loop rates and lower plain whorls rate, inverse to the East Asian and Middle Eastern cohorts. For the rarer patterns (plain arch, tented arch, radial loop, central pocket loop whorl and double loop whorl), a different grouping occurs. The European and Middle Eastern populations have more similar frequencies as opposed to the East Asians and South Asians. One exception to this general trend is the central pocket loop whorl frequencies which only appear markedly different in the Middle Eastern cohort.

Aside from general trends, the radial loop was clearly highest in frequency in the European cohort something noted by Swofford [105] and the accidental whorl occurs at largely the same frequency among all groups. Missing and scarred occurrences are also noted in the table however not considered in analysis as these are acquired characteristics.

3.4. Pattern distribution on the fingers

The distribution of fingerprint patterns per finger may also indicate or be a factor in indicating the ancestry or sex of an individual. The occurrence of patterns on each finger were calculated and are shown in Figure 26 below.

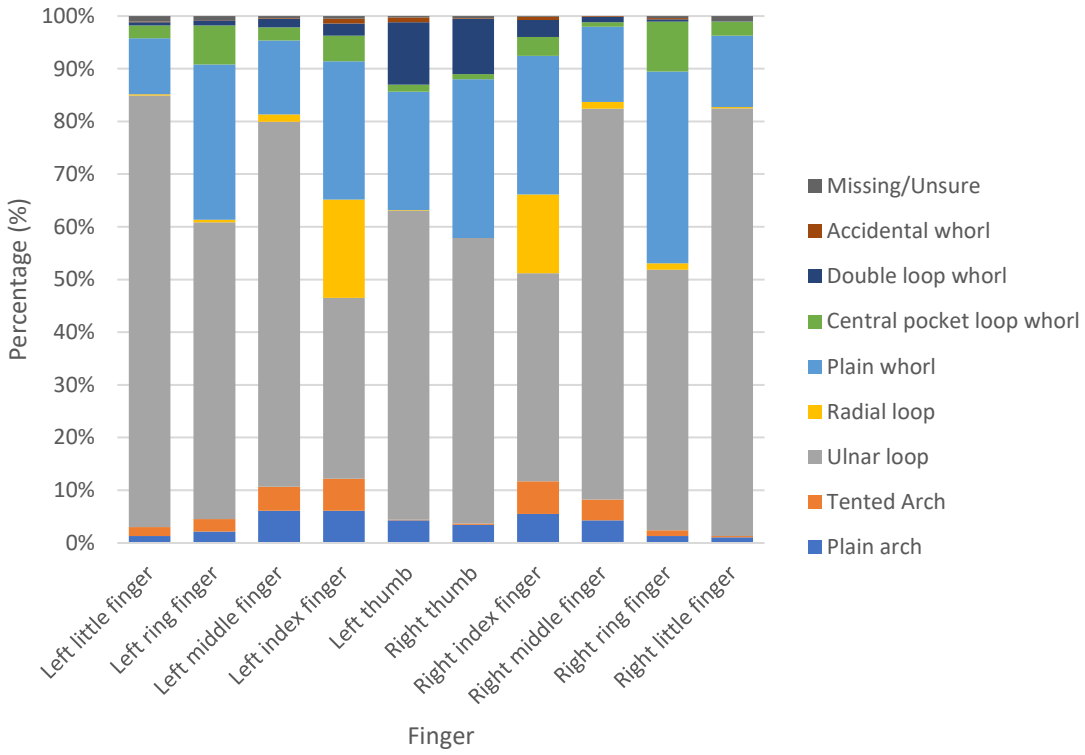

Figure 26: Occurrence of fingerprint patterns per finger

Radial loop

Immediately viewing the graph, the dramatic increase of radial loops on the two index fingers (4 and 7) is visible. This trend was noted very early in pattern frequency research when Walker [44] believed that the index finger has its own unique inheritance method due to the phenotype being so markedly different. Furthermore the trend has been noted in numerous modern studies investigating pattern distributions within Dutch, Swedish, Spanish, Algerian and American populations [90, 103, 192, 197, 255].

Double loop whorl

The increase of the double loop whorl frequency from less than one percent on the little fingers to over 10 percent on the thumbs is another evident trend. This trend has previously been noted in Sri Lankan and Dutch populations [103, 217]

Tented Arch

The frequency of the tented arch pattern increases from the little fingers (1 and 10) to the index fingers (4 and 7), though largely occurring on the middle and index fingers of both hands. The

pattern is however noticeably absent from both thumbs. To the authors knowledge this phenomenon has only been noted in the Dutch study by De Jongh *et al.* [103].

Central pocket loop whorl

The central pocket loop whorl has the highest frequency on the ring finger of both hands. The next highest frequency was on the index fingers of both hands, though the right hand was lower. The little finger and middle fingers on both hands have noticeably lower frequency as too were the thumbs.

The central pocket loop whorl pattern can often be difficult to classify as it appears as an intermediate between ulnar and radial loops, and plain whorls. It is therefore interesting that there is still a clear trend in the pattern distribution. On the fingers where the central pocket loop whorl has higher frequency it appears to come at the expense of ulnar loops.

Ulnar loop

The Ulnar loop is by far the most common pattern type on all fingers with the lowest frequency of 34.3% on finger four and the highest of 81.9% on finger one. Each hand follows a similar pattern with highest frequency on the two little fingers, dropping on the two ring fingers, higher on the middle fingers, lower again on the index finger and the higher again on the thumbs.

Plain whorl

The plain whorl is the second most common pattern after the ulnar loop, it similarly follows an undulating trend though inverse to the ulnar loop. The little fingers have the lowest frequency (10.6% and 13.5%) of all fingers, the ring fingers are highest on each hand with 29.4% and 36.4 % and the middle fingers lower. The index fingers and thumbs have similar frequencies though on the left hand the index finger has a higher frequency, while on the right hand the thumb has higher frequency.

Plain arch

The frequency of the plain arch increases from the little fingers to the index fingers where it slightly lowers in the thumbs. It is clear the increase occurs in coupled steps. The little fingers and ring fingers (1 and 10, 2 and 9) are lowest, the middle and index fingers (3 and 8, 4 and 9) are the highest, with the thumb's frequencies being positioned between these groupings.

Though qualitatively viewing the data shows obvious differences in pattern frequency statistical tool are needed to prove if these differences are significant. The increased frequency of radial loops on index fingers and double loop whorls on the thumbs has been noted numerous times there is still a lack of understanding or even a theory regarding the mechanism through which this can occur. In 1977, Babler noted a relationship where an increase in whorls appears to

correspond with a decrease in radial loops and secondly, an increased frequency of arches results in less radial loops [256]. Given the repetitive nature of the phenotype it indicates that there is either regulation of pattern per finger by DNA or some sort of physical control in the development of the foetus. The latest fingerprint development model by Kucken and Newell points to patterns being caused by basal layer buckling from geometry and regression timing of volar pads, which is in turn caused by genetics [2]. Though this does not resolve the issue of such an increase in frequency on a specific finger. A genetic study by Ho *et al.* [55] focussed on the occurrence of whorl patterns, the results showed SNPs that increased the frequency of whorls across the hand with a morphogenetic field effect, promising results for future research on other patterns.

3.5. Association of pattern using chi-squared (χ^2) with post-hoc analysis

The most common method of analysis in the string of publications on the topic of pattern frequency is χ^2 analysis. In these papers the test was used as a question of independence, i.e. "Is there a relationship between fingerprint pattern and sex or BGA?". To utilise this method there are several requirements for data; it must be random, mutually exclusive and drawn from independent variables with a large enough sample, meaning no more than 20% expected cell values should be less than five. A fisher's exact test can also be used in place of a χ^2 test. While the χ^2 test is an approximation the Fisher's exact test gives exact results. The exact test is usually utilised for small sample sizes where more than 20% of cells have expected frequencies of less than five though can be valid for any range of sample sizes. The largest detractor of Fisher's exact test and the reason it was not employed in this study was the required computing power and sample size of over 1000. With each added row or column, the number of calculations is exponentially increased making four by seven contingency tables unfeasible.

From the contingency table that expected and observed values have been calculated the χ^2 statistic can be calculated. The accidental whorl was omitted from the χ^2 analysis due to the low number of observations. A χ^2 test undertaken on the data between fingerprint pattern and sex rejected the null hypothesis of no association between fingerprint pattern and sex (p = 0.000, 6 degrees of freedom). A secondary χ^2 test rejected the null hypothesis of no association between fingerprint pattern and BGA (p = 0.000, 18 degrees of freedom). However, while there are two significant results with pattern associated with BGA and sex, the χ^2 test is known as an "omnibus test" meaning that the exact significant associations within the contingency tables cannot be identified. Therefore, post-hoc testing is required [257].

To perform post-hoc analysis the adjusted residuals must be calculated. The adjusted residuals are the difference between the observed counts and expected counts divided by an estimate of the standard error. The adjusted residuals for fingerprint pattern versus sex are shown in Table 8 and the adjusted residuals for pattern against BGA in Table 9. For the sex comparison, the largest difference from the expected value were for the plain whorl, plain arch, ulnar loop, and double loop whorl in descending order.

Table 8: Adjusted residuals of the chi-squared analysis for fingerprint pattern association with sex

	Plain arch	**Tented arch**	**Ulnar loop**	**Radial loop**	**Plain whorl**	**Central pocket loop**	**Double loop whorl**
Female	4.4	-1.2	3.7	0.9	-5.1	0.7	-3.3
Male	-4.4	1.2	-3.7	-0.9	5.1	-0.7	3.3

For the BGA comparison, the largest difference from the expected value were shown in the plain whorl pattern across East Asian, European, and Middle Eastern cohorts. The plain arch pattern was the most highly differentiated pattern for the South Asian ancestry though the plain whorl and tented arch patterns were comparable. The central pocket loop pattern showed the least difference from the expected value in the East Asian, European, and South Asian ancestries. Within the Middle Eastern population, the tented arch was the least differentiated.

Table 9: Adjusted residuals of the chi-squared analysis for fingerprint pattern association with BGA

	Plain arch	**Tented arch**	**Ulnar loop**	**Radial loop**	**Plain whorl**	**Central pocket loop**	**Double loop whorl**
E. Asian	-2.1	-3.6	-4.9	-3.6	9.1	-0.5	2.3
European	3.0	4.3	6.1	4.6	-11.4	-0.4	-1.8
S. Asian	-3.0	-2.7	-0.3	-1.9	2.8	-0.1	2.2
M. E.	0.7	0.1	-3.9	-1.2	5.1	1.7	-2.6

The adjusted residuals are then squared to give a χ^2 value for each individual cell. To produce a p-value the χ^2 values and degree of freedom are used to calculate the cumulative probability that a value from the χ^2distribution with nominated degrees of freedom will be greater than the squared adjusted residuals. For each residual analysis, the degrees of freedom are equal to one.

Finally, a correction to the threshold p-value must be made to mitigate against the multiple comparison problem. Because there are numerous comparisons being made in the post-hoc testing, it is possible that eventually a statistically significant association will occur by chance. For example, for a threshold p-value of 0.05, 1 in 20 tests will be significant by chance. By lowering the statistically significant threshold using a Bonferroni correction, the chance of this error can be drastically reduced.

To calculate the Bonferroni corrected p-value the standard p-value is divided by the number of comparisons being performed. In the sex to pattern comparison 0.05 is divided by 14 to give a significance threshold of 0.00357, all cells with a p-value below this are judged to have significant differentiation from the expected cell values. Using the same Bonferroni method though this time dividing by 28, the significance threshold for BGA to pattern is 0.00179.

The Bonferroni correction drastically reduces the chance of a type I error occurring however it may also be too conservative and increase the chance of a type II error.

Type I error = Rejecting the null hypothesis when it is true

Type II error = Accepting the null hypothesis when it is false

A sequential Bonferroni correction (Holm-Bonferroni) can therefore be used as a compromise that is not as stringent as the standard Bonferroni correction [258]. The sequential Bonferroni correction method involves ordering the individual p-values from most significant to least significant and assigning them a rank from 1 to *n* – 14 in the case of the sex data and 28 in the case of the ancestry data. The original p-value of 0.05 is then divided by *n* minus the rank plus one. This creates an individual threshold for each p-value ranging from the original Bonferroni threshold to the original p-value significance threshold of 0.05. The cells with significant results from the sequential Bonferroni correction can be seen coloured red and green in Table 10 and Table 11. There were two cells that achieved significance under the sequential Bonferroni correction and not under the original Bonferroni; the plain arch pattern for the European BGA and the plain arch for the South Asian BGA. There were no changes in significance for the sex data.

Given squaring the adjusted residuals effectively makes them an absolute value, this removes the context of the residual – whether it is positive or negative. After evaluating the individual cell p-values against the Bonferroni threshold the significant cells can be deduced to be significantly negatively or positively associated with sex or ancestry based on the negative or positive adjusted residuals. The positively associated residuals are coloured green, and the negatively associated residuals are coloured red. Thus, it can be said that plain arches and ulnar loops occur significantly more than expected in females while plain whorls and double loop whorls occur significantly less than expected in females. Conversely, plain whorls and double loop whorls occur significantly more than expected in males while plain arches and ulnar loops occur significantly less than expected in males.

Table 10: P-values calculated from each individual adjusted residual for sex against pattern

	Plain arch	**Tented arch**	**Ulnar loop**	**Radial loop**	**Plain whorl**	**Central pocket loop**	**Double loop whorl**
Female	0.00001	0.24277	0.00021	0.39259	0.00000	0.48164	0.00110
Male	0.00001	0.24277	0.00021	0.39259	0.00000	0.48164	0.00110

Individual p-values produced from the post-hoc process are shown in each cell. All cells that are coloured achieved a significant result ($p<0.05$). Green cells achieved a significant result with a positive adjusted residual and red cells achieved a significant result with a negative residual.

Regarding the BGA against pattern results, tented arches, ulnar loops, radial loops, and plain whorls occurred significantly less than expected in people of East Asian ancestry, though plain whorls occurred significantly more. The European ancestry showed the plain arch, tented arch, ulnar loop, and radial loop patterns occurred significantly more than expected while plain whorls occurred significantly less. The South Asian cohort showed significantly more plain arches than expected. The tented arch and plain whorl patterns were close to passing the sequential Bonferroni significance threshold however failed to do so. Middle Eastern ancestry showed significantly higher than expected occurrences of plain whorls whereas ulnar loops occurred significantly less.

Table 11: P-values calculated from each individual adjusted residual for BGA against pattern

	Plain arch	**Tented arch**	**Ulnar loop**	**Radial loop**	**Plain whorl**	**Central pocket loop**	**Double loop whorl**
E. Asian	0.03838	0.00037	0.00000	0.00026	0.00000	0.62904	0.02387
European	0.00260	0.00002	0.00000	0.00000	0.00000	0.70375	0.07112
S. Asian	0.00235	0.00714	0.77530	0.05785	0.00556	0.92995	0.02450
M. E	0.50020	0.88463	0.00008	0.24775	0.00000	0.09402	0.01023

Individual p-values produced from the post-hoc process are shown in each cell. All cells that are coloured achieved a significant result ($p<0.05$). Green cells achieved a significant result with a positive adjusted residual and red cells achieved a significant result with a negative residual.

The χ^2 test is a non-parametric statistical procedure that is extremely common for its ease of use and wide applicability. The post-hoc procedure that follows is more recent in development and has several alternate approaches in which it can be applied [259]. The method used in this study is performed with adjusted residuals and Bonferroni-Holm correction. As per Macdonald and Gardener's [260] method and findings this has been shown to be one of the most accurate methods for post-hoc analysis [257]. It is possible to employ standardised residuals paired with the Bonferroni adjustment though this makes the threshold too conservative [260].

Though performing a χ^2 test and post-hoc testing shows significance in association and non-association, there is a major flaw with the χ^2 approach that has been repeated in papers investigating fingerprint pattern occurrence. This technique assumes that all ten fingers are independent of one another, or more simply in effect each person has one fingerprint. For example, a European individual with ten plain whorl fingerprints would count as ten European individuals with a single plain whorl print, possibly over counting the occurrence of plain whorls in the European population.

3.6. Association of pattern using multinomial logistic regression (MLR)

Using a different approach, it is possible to overcome the major drawback of the χ^2 method. A multinomial logistic regression can be employed to predict a nominal dependent variable given multiple independent variables. A common use for an MLR is to analyse survey or marketing statistics such as preference for a type of drink based on age, sex, and location. This has been appropriated to examine fingerprint pattern based on finger, hand, sex and BGA.

The likelihood ratio test results of the MLR are shown in Table 12. This test determines if adding a variable makes the model predict the dependent variable better than the intercept only model.

When looking at the independent variables (hand, finger, sex and BGA), all have a significant effect ($p < 0.05$) on the dependent variable, fingerprint pattern.

Table 12: Multinomial logistic regression significance (p-value) analysing the effect of hand, finger sex and BGA on pattern

	Chi-squared	**Significance (p-value)**
Intercept	0.000	
Hand	19.139	0.008
Finger	1831.693	0.000
Sex	47.372	0.000
BGA	215.089	0.000

Table 12 suggests that all the independent variables have a statistically significant effect. The coefficients of the model can be individually assessed to determine which independent variable influences the selected dependent variable the most. The full results of the parameter estimates are shown in Appendix E.

As there were eight categories in the dependent variable there are seven sets of logistic regression coefficients (also called logits) and one reference category. The first logit represents the plain arch pattern comparison to the ulnar loop reference category. The ulnar loop was chosen as the reference category as it is the most common pattern and likely the least distinguishing between BGAs or sex in practice. The South Asian group was the BGA reference as only the plain arch was found to be significant after the χ^2 analysis and Holm-Bonferroni correction therefore it could act as a "baseline".

The coefficients (B) significant for the plain arch logit are the little fingers compared to thumbs, the thumbs with a p-value of 0.000, ring fingers compared to the thumbs with a p-value of 0.008 and index fingers compared to the thumbs with a p-value of 0.000. Given the coefficient (B) is negative for both little fingers and ring fingers it can be determined that an individual is more likely to have a plain arch relative to the ulnar loop frequency on those fingers. Since index fingers have a positive coefficient, an individual is more likely to have an ulnar loop over a plain arch on these fingers compared to the thumbs. More simply, the Exp(B) value can be examined, where this value is less than zero the phenotype is less likely to occur than the reference groups, when greater than one the phenotype is more likely to occur than the reference groups. Table 13 indicates the fingers that have a significant result for displaying plain arches compared to the ulnar loop pattern and thumb. Full results are in Appendix E, Table E1.

Table 13: Multiplier for presence of plain arch relative to ulnar loops compared to the thumbs

Finger	Significance (p-value)	Multiplier for presence of plain arch
Little fingers	0.000	0.24
Ring fingers	0.008	0.54
Index fingers	0.000	2.44

Females are also significantly different to males with a p-value of 0.000. With a positive coefficient, the probability of observing a plain arch rather than an ulnar loop is 1.69 times likely if the fingerprint is from a female rather than a male. This increased rate in females is supported by the largest study of fingerprint pattern distribution, which originates from the FBI database. The database comprises of 17,951,192 male donor ten-print cards and 4,313,521 female donor ten-print cards and statistical analysis showed the females tend to have higher rates of arches compared to men [255]. Numerous other studies have been undertaken on the American population and comparisons between the European American population and African American population have been investigated on multiple occasions [207, 208, 213]. Firstly, there was found to be differences within the male and female European American population ($p < 0.01$) and significantly different results between the males and females of the African American population [207, 213]. A further study on a population of African American individuals found that females had a higher frequency of arches, underlining the results of the FBI data and the current study's results [208]. Contrasting the numerous earlier links in European Americans between sex and pattern is a more recent study by Gutierrez *et al.* which focused on a Spanish cohort and found no association between sex and pattern [33].

A summation of these papers can be seen in Table 14. Of note are the several studies that had results that were inconsistent with the findings of this study. The author of this study interprets this to be due to a combination of factors including the age of studies and lack of statistical rigor, the size and randomness (unrelated individuals) of populations used, and the accuracy of the classification of the fingerprints.

Table 14: A summation of published results on the association of fingerprint patterns with sex

Study	Sex/ BGA	Association	Statistically tested	Supported by this study
Steinberg [213]	Female/ African	Arches	Yes	Yes – for plain arches
Stambouli *et al.* [104]	Male/ African	Whorls/ Radial loops	No	Yes – for plain whorls and double loops whorls No – for radial loops

Stambouli *et al.* [104]	Female/ African	Arches	No	Yes – for plain arches
Igbigbi & Msamati [200]	Male/ African	Whorls	Yes	Yes
Champod *et al.* (FBI data) [255]	Female/ -	Plain arches	Yes	Yes – for plain arches
Qazi *et al.* [208]	Female/ African	Arches	Yes	Yes – for plain arches
Gutierrez *et al.* [33]	-/ European	No	Yes	No
Cho [193]	Female/ Polynesian	Whorls	Yes	No
Veale & Adams [215]	Male/ Polynesian	Whorls	No	Yes – for plain whorls and double loop whorls
Veale & Adams [216]	Male/ Melanesian	Whorls	No	Yes – for plain whorls and double loop whorls
Rao [209]	Male/ Australian Aboriginal	Whorls	No	Yes – for plain whorls and double loop whorls
Cho [194]	–/ Polynesian	No	Yes	No
Cummins [195]	–/ Australian Aboriginal	No	No	No
Meier [204]	Females/ Melanesians	Arches	Yes	Yes – for plain arches
Singh [211]	–/ Australian Aboriginal	No – Intra-clan differences	Yes	No
Jaja & Igbigbi [202]	–/ African	No	No	No
Igbigbi & Msamati [199]	–/ African	No	No	No
Igbigbi & Msamati [201]	Both/ African	Yes – specific association not given	Yes	–
Igbigbi & Msamati [201]	Both/ African	Yes - Specific association not given	Yes	–
Gandahar & Reddy [196]	–/ South Asian	Yes – Specific association not given	Yes	–
Nithin *et al.* [205]	–/ South Asian	No	No	No
Wijerathne *et al.* [217]	Both/ South Asian	Males more whorls Females more ulnar loops	No	Yes – for plain whorls and double loop whorls

Significance was also seen in the BGA variable for plain arch. The European BGA was significant with a p-value of 0.007 and positive coefficient, as too were the Middle Easterners with a p-value of 0.004. Therefore the probability of observing a plain arch rather than an ulnar loop is 3.45 and 4.51 times likely if the fingerprint is from Europeans and Middle Easterners respectively rather than from people of South Asian ancestry. These likelihoods do not appear to have been published before. A Malaysian study by Heng *et al.* [198] studied individuals of Malay, Chinese and Indian descent, and arches account for 0.80%, 0.80% and 10.00% of all fingerprints for each respective group. From this they deduced the Indian population have a higher chance of plain arches, disagreeing with the current study's results where the South Asian population had the lowest frequency of plain arch. While the statement that Indian people had higher frequencies of plain arches fit the pattern percentage observations, there was no statistical analysis.

African populations studied previously show plain arches may occur in higher rates. The author of a study on Kenyan and Tanzanian populations stated that it is evident European populations can be differentiated from Sub-Saharan populations since Europeans have higher frequencies of arches and radial loops [201]. Both Kenyan and Tanzanian populations had ulnar loops as the most common pattern type, this was followed by whorls, then radial loops and arches [201]. Comparing this to the four groups in the study, the only one to have this order of commonality was the South Asian group whereas the people of European, East Asian, and Middle Eastern BGAs had arches more common than radial loops. The author's statement can be partly supported by the significantly higher rates of plain arch and radial loop in European cohort for the χ^2 and MLR tests.

However, based on other studies originating from Sub-Saharan Africa it appears the idea of separating Europeans and Sub-Saharan Africans by arch frequency does not hold true. Small tribes in Southern Nigeria have shown large variability from surrounding populations. From one study, the Anioma and Urhobo people in the Delta state of southern Nigeria exhibited over 17% and 14% of patterns as arches, more than double the rate seen in the European cohort of this study [261]. Couple this with the fact the two populations were found to themselves be significantly different ($p < 0.05$), any blanket statement regarding Sub-Saharan Africa does not hold up [261].

The tented arch logit coefficients are mostly significant. The multiplier of likelihood for fingers with significant result relative to the presence of loops compared to thumbs is shown in Table 15. The frequency of tented arches on the little fingers returned an insignificant result though close to threshold with a p-value of 0.059. Full results are in Appendix E, Table E1.

Table 15: Multiplier for presence of tented arch relative to ulnar loops compared to the thumbs

Finger	Significance (p-value)	Multiplier for presence of tented arch
Ring fingers	0.000	9.08
Middle fingers	0.000	16.7
Index fingers	0.000	48.5

These values are consistent with pattern distribution in Figure 26.

Additionally, significant differences were also found in the set of BGA coefficients. All BGAs were found to have positive coefficients relative to the South Asian reference group though only the European (p = 0.044) and Middle Eastern (p = 0.002) ancestral groups were significant. The probability of displaying a tented arch fingerprint rather than an ulnar loop is 5.00 times likely if the fingerprint is from a European and 5.64 times likely if the fingerprint is from a Middle Easterner rather than a South Asian. The χ^2 results showed the European tented arch frequency was higher and the East Asian frequency lower than expected, with the Middle Eastern and South Asian ancestries being insignificant. When looking at the adjusted residuals, the European and Middle Eastern ancestries were positive while the East Asian and South Asian groups were negative (Table 9). These indications align with the MLR results of Europeans and Middle Easterners having higher frequencies of tented arches. Comparing the tented arch results to previously published papers is difficult given its grouping under the general arch pattern, lack of statistical rigor within methodologies and different presentation of results. No previous study has presented results regarding the association of tented arches to hand, finger, sex or BGA.

The radial loop logit also contained numerous significant coefficients. The p-value of the hand coefficient is markedly higher with 0.266 in this logit compared to the previous two logits. Of the finger coefficients, ring fingers, middle fingers and index fingers are significant with positive coefficients while the little fingers are not significant relative to ulnar loops on thumbs in the South Asian reference population. The index fingers are extremely likely to display a radial loop (Table 16). Full results are in Appendix E, Table E2.

Table 16: Multiplier for presence of radial loops relative to ulnar loops compared to the thumbs

Finger	Significance (p-value)	Multiplier for presence of tented arch
Ring fingers	0.009	15.2
Middle fingers	0.006	16.3
Index fingers	0.000	398

The extremely high exponential coefficient for index fingers is supported by the distribution results in Figure 26 and Dutch, Swedish, Spanish, Algerian and American populations where the increased chance of radial loops on the index finger has previously been noted [90, 103, 192, 197, 255].

The female sex is not significantly more likely to have radial loops over the reference category than males. Similarly, the East Asian and Middle Eastern BGA coefficients are insignificant compared to the South Asian reference group. The only significant BGA coefficient was the European ancestry (p = 0.023) which resulted in the probability of observing a radial loop over an ulnar loop being 2.19 times likely if a fingerprint is from a European rather than a South Asian. From studies on North American populations, European Americans were seen to have a significantly higher number of loops compared to the African American population [207, 213]. Unfortunately given the lack of volunteers with African ancestry this difference could not be investigated in this study. However, the χ^2 result while not the most appropriate statistical test showed that ulnar loops may occur at higher rates in European populations.

Appendix E, Table E3 shows the parameter estimate results for whorl patterns from the MLR. The first logit is that of the Accidental whorl that only shows significance in little fingers and Middle fingers. The probability of observing an accidental whorl rather than an ulnar loop is 0.088 times likely if the fingerprint originated on the little finger and 0.201 times likely if the fingerprint originated from the middle finger rather than the thumb. In describing the accidental whorl, it is often said to be an irregular phenotype and a combination of one or more pattern. Therefore it is believed to be a malformation, different to the other patterns in that it does not have a genetic basis. This pattern has not been studied before and given the low frequency of this pattern it would be difficult to get representative results for the greater population. It should also be noted that patterns fall into this category when they do not conform to the other patterns in the classification system which may result in two very dissimilar accidental whorls.

Within the central pocket loop whorl logit there are two parameters that are significant: Ring fingers and index fingers both with p-values of 0.000 and positive coefficients. The exponential coefficient shows the probabilities of displaying a central pocket loop whorl rather than ulnar loop is 7.86 times likely on the ring finger compared to the thumb. This makes the central pocket loop whorl the third most common pattern on this finger; something that does not occur on any other finger. As the central pocket loop whorl pattern is an intermediate between a plan whorl and loop it is somewhat surprising that there is clear preference for the pattern on fingers. Since this pattern is normally grouped under the general term of “whorl” there is a lack of study on

this pattern. The probability of having a central pocket loop whorl rather than an ulnar loop is 5.72 times likely on the index fingers compared to thumbs. Again, index fingers show significance reiterating the huge variability of the index fingers by coinciding with high rates of radial loops.

The double loop whorl logit shows there is significant difference between all fingers, males and females, plus the Middle Eastern and European cohorts. The exponential coefficients and p-values of the little, ring, middle and index fingers are shown in Table 17. Full results are in Appendix E, Table E3.

Table 17: Multiplier for presence of double loops whorls relative to ulnar loops compared to the thumbs

Finger	**Significance (p-value)**	**Multiplier for presence of tented arch**
Little fingers	0.000	0.03
Ring fingers	0.000	0.05
Middle fingers	0.000	0.09
Index fingers	0.000	0.33

Given all the coefficients are negative and significant it is implied that thumbs are significantly associated with the double loop whorl pattern.

The p-value of the female sex variable is 0.000 with a negative coefficient. The exponential coefficient shows that the probability of displaying a double loop whorl rather than an ulnar loop fingerprint is 0.592 times likely if the print originated from a female rather than a male. Dimorphism between male and female fingerprint pattern frequency has been noted in numerous studies though also found to be absent in several studies. The result from the MLR showing higher frequency of double loop whorls over the reference group of ulnar loops in men has not been noted before.

The European BGA passed the significance threshold with a p-value of 0.030. The negative coefficient translated to the probability of having a double loop whorl rather than an ulnar loop fingerprint being 0.584 times likely if the print originated from a European rather than a South Asian. The Middle Easterners demonstrated a more significant difference with a p-value of 0.014. The exponential coefficient showed the probability of displaying a double loop whorl pattern on the fingerprint rather than an ulnar loop pattern was 0.211 times likely if the person was of Middle Eastern ancestry rather than South Asian ancestry. There is a lack of statistical data regarding the double loop whorl pattern due to the classification of fingerprints, barring the FBI dataset, lacking the discrimination between whorl patterns.

The final pattern logit is that of the plain whorl, where significance is shown in all groups of coefficients. The left hand shows significance with a p-value of 0.000 and a negative coefficient. The exponential coefficient determines the probability of having a plain whorl pattern rather than an ulnar loop pattern is 0.855 times likely if the fingerprint originated from the left hand rather than the right hand. Further investigating the plain whorl asymmetry phenomenon showed that there is a lack of support other than a paper by Heng *et al.* originating from Malaysia [198]. Significant asymmetry was also found in the whorl frequency between the left and right hands with it being higher on the latter. Additionally a large study of the Moroccan population found there was more asymmetry between males and females on the right hand [104]. Conversely, the paper by Swofford [105] which is the closest piece of research to the one being undertaken, found no evidence of pattern asymmetry using χ^2 tests. Plato [207] and Steinberg [213] found symmetry in patterns within the European American and African American males though there was asymmetry in the female populations [207, 213]. While there appears to be no statistical analysis of this statement the authors note a higher percentage of whorls on the ring finger, higher rates of ulnar loops on the index finger and lower frequencies of radial loops on the ring and index finger. Given there was asymmetry dimorphism viewed, it implies intra-volunteer asymmetry was present though this is not discussed. A collation of results regarding pattern frequency asymmetry can be found in Table 18.

Table 18: A summation of published results on the asymmetrical frequency of fingerprint patterns

Study	**Hand/ Sex/ BGA**	**Association**	**Statistically tested**	**Supported by this study**
Swofford [105]	–	No	Yes	No
Heng *et al.* [198]	Right/ Both/ East Asian	Whorls	Yes	Yes
Plato [207]	Left/ Male/ European	Loops	Yes	No (Radial loops)
Plato [207]	Right/ Male/ European	Whorls	Yes	Yes
Steinberg [213]	Left/ Female/ African	Arches	Yes	No
Steinberg [213]	Right/ Male/ African	Whorls	Yes	Yes

Within each hand, all finger coefficients are shown to be significant with a p-value of 0.000 the exponential coefficients of plain whorls per finger is shown in Table 19. Full results are in Appendix E, Table E3.

Table 19: Multiplier for presence of plain whorls relative to ulnar loops compared to the thumbs

Finger	**Significance (p-value)**	**Multiplier for presence of tented arch**
Little fingers	0.000	0.312
Ring fingers	0.000	1.43
Middle fingers	0.000	0.426
Index fingers	0.000	1.54

Females are also significant compared to males with a p-value of 0.000 and a negative coefficient. The probability of displaying a plain whorl instead of an ulnar loop in the fingerprint is 0.787 times likely if it originated from a female rather than a male. The statistically significant increased chance of plain whorls in men compared to women is something that has been clearly outlined in small populations from the pacific region. Two studies by Veale and Adam and one by Rao on Māori, Melanesian and Australian Aboriginal populations respectively showed sex dimorphism with males having a higher frequency of whorls [209, 215, 216]. In reverse, females have also been associated with higher frequencies of plain whorls. New Zealand-Samoan females showed whorls were of higher frequency over males and arches were mostly less than one percent of all patterns [193]. Additionally, smaller studies found no sex dimorphism in Polynesians and Australian Aboriginals though a higher frequency of arches was seen in Melanesians females [194, 195, 204, 211].

Similar alignments of high whorl percentage has been indicated in Moroccan males and a Native Zimbabwean population [104, 200]. Within the Zimbabwean population the most common pattern type was ulnar loops for both male and female, though the second most common for males was whorls and arches for females [200]. The author does state there are significant differences between the sexes for pattern frequency with a p-value < 0.05 however no data was published other than the percentages [200]. In parallel, a study on the Sinhalese Sri Lankan population [217] showed that males had a higher frequency of plain whorl and females a higher frequency of ulnar loop, though this differences equated to two percentage points with no statistical analysis [217].

Additionally, studies from the African continent have found both support and rejection of sex dimorphism. In a study of 390 subjects from southern Nigeria no sex dimorphism was found in the fingerprint patterns and the prevalence was in the following order from highest to lowest: Ulnar loops, whorls, arches and radial loops [202]. There are no statistics given regarding an association of pattern. The same protocol was conducted on Malawian, Zimbabwean, Kenyan and Tanzanians by the same author [199-201]. Similar to the Nigerian population, both Kenyan

and Tanzanian population had ulnar loops as the most common pattern type, this was followed by whorls, then radial loops and arches [201]. However, in the Kenyan and Tanzanian populations the author found there are significant differences between the sexes for pattern frequency ($p < 0.05$) though no data was published other than the percentages. Within the Malawian population no sex dimorphism was found in patterns; more notably arches were the predominant pattern in the population [199]. For females the second most common pattern was for the whorl pattern and for males, the radial loop [199]. Given previous studies on the frequency of the radial loop this is highly surprising and indicates that perhaps there was an issue with the classification of the fingerprints.

Finally, there have been several studies focussing on dimorphism within Indian and Sri Lankan populations. The earliest study from India in 2003 [196] found a significant difference between the sexes though a study from 2009 [205] did not. While the latter study by Nithin *et al.* [205] found no differences between the sexes, the publication lacks any statistical data. A separate study within the Muslim Indian community again found there to be no difference between the sexes ($p > 0.05$) [203].

The mechanism by which sex dimorphism in fingerprints could originate is unknown. A GWAS published by Ho *et al.* [55] found no evidence of sex-linked polymorphisms that effected the fingerprint phenotype that has previously been proposed [44]. Given the reoccurring nature of dimorphism results mixed with biogeographic differences, it may be hypothesised that in combination, sex hormones, or the genes that control them, and BGA associated markers may influence ontogenetic processes that occur *in utero* when the volar pads of forming and regressing which produces friction ridges. The differences when comparing the European American and African American population and the ongoing variance of sex dimorphism shows that there is a basis for differences between biogeographical ancestries.

Regarding plain whorl association to BGA, the East Asian category is significant with a p-value of 0.012 and a positive coefficient. Translating the coefficient exponentially shows possessing a plain whorl fingerprint instead of an ulnar loop print is 1.40 times likely in people of East Asian BGA compared to the South Asian reference group. The European ancestry was shown to be significantly less than the reference group with a p-value of 0.001, the probability of having a plain whorl rather than an ulnar loop was 0.670 times likely in Europeans compared to South Asians. The Middle Eastern ancestry too showed significance ($p = 0.009$) though with a positive coefficient. Looking at the exponential coefficient, the probability of displaying a plain whorl rather than an ulnar loop fingerprint is 1.55 times likely if the print came from people of Middle

Eastern ancestry rather than people of South Asian ancestry. This creates a definitive hierarchy of Middle Eastern > East Asian > South Asian > European in terms of plain whorl frequency.

Comparing to previously published papers, the associations of the plain whorl pattern are well supported. Plato and Wertelecki compared Europeans to Middle Eastern populations in a previous study which found higher occurrences of whorls and lower ulnar loop frequencies in the Middle Easterners [206]. The plain whorl result was repeated in this study which found Middle Easterners are statistically more likely to have a plain whorl than ulnar loop compared to the South Asian reference group and by extension the European group.

Evidence of whorls being associated with the East Asian population has been noted previously by Swofford in 2005 [105]. A comparison of BGA pattern percentages found Asian populations to have the most whorls over people of Hispanic, African, and European background. Given the lack of statistical rigor this result carried little weight and only coincided with anecdotal evidence of first responders that whorls appeared to occur at higher rates at scenes of Asian organised crime [262].

Few other studies regarding fingerprint frequency from Asian populations have been published. Several studies originating from Japan probe the theory that fingerprints of parents may indicate the chance of having a child with Down's Syndrome or Klinefelter's Syndrome [76, 78]. These studies find differences to the control group however the mechanism for trisomy is already known and the theory that fingerprints of the parents could predict this is a very tenuous link. The data presented in these studies is also difficult to adapt given the fingerprints are only classified as arches, radial loops, ulnar loops, and whorls plus tabulated as percentages per finger so an overall pattern percentage cannot be obtained.

Heng *et al.* [198] provides a more relevant insight into the frequency of fingerprint patterns in an Asian population. This study utilised 192 participants incorporating 96 from the university campus and 96 siblings. The fingerprints collected from the volunteers were classified into whorls, loops, arches, and composites. While the rate of whorls was said to be high in all groups, what rate was used as a reference is unclear. Tentative conclusions that the Chinese group had a higher ratio of whorls to loops followed by Malays then the Indian group were made. These trends align the those seen in the South Asian and East Asian groups within this study and the 2005 Swofford study [105]. Statistical results using the χ^2 test showed that there were significant differences in all ten fingers between the Malay, Chinese and Indian population within the overall cohort. The Indian population however had a greater difference in distribution pattern

to the Malay and Chinese groups which may be evidence of the greater anthropological divide between these ancestral groups.

While several useful results originated from this paper there are several flaws that make these results difficult to rely on. The recruiting of such a large group of siblings creates an issue where the results may be skewed from being truly representative of the greater Malaysian population or the ancestry minorities. The methodologies of how the χ^2 tests were performed are absent from the paper and as discussed earlier in this chapter the χ^2 test is not best suited to fingerprint data, therefore the conclusion that all ten fingers are significantly different between BGAs cannot be relied upon. Finally, the classification of the fingerprint patterns falls under serious question where the "composite" pattern represents 15.3%, 20.0% and 8.6% of Malay, Chinese and Indian patterns respectively; this is exceptionally large especially given arches only account for 0.8%, 0.8% and 10.0% for the same groups. These numbers are incompatible with those provided in Table 4 showing the pattern breakdown for each BGA in this study or those provided from other studies in Table 5.

Though Heng *et al.* [198] assesses South Asian individuals situated in Malaysia, small populations within India and Sri Lanka have also had their fingerprint patterns assessed [196, 203, 205, 217]. Two studies focussed on regions in the southwest of India with one paper from the central west specifically focussing of people from a small Muslim community. The study of the Muslim population used an expanded pattern classification method with high discrimination however the patterns used are not standard which makes comparison difficult. The two southwestern cohorts and the Sri Lankan group showed similar traits where the loops are higher in frequency than the whorls with the arches being the lowest. When comparing ancestry, the ratio of loops to whorls and arches is more similar to South Asian and East Asian results in this study than Pacific and African populations of unaffiliated research; a high number of loops, followed by whorls, then arches at about 5% [194, 201].

The African population is difficult to assess given the separation of the North African and Sub-Saharan population in combination with effects from colonialism. Nevertheless, two studies have been based in northern Africa, one focussed on the Moroccan population and another on the Algerian population. The Moroccan study [104] was comprehensive, sourcing 2000 sets of fingerprints, 1000 male and 1000 female. For the overall population, ulnar loops were the most common followed by whorls; for females' arches were third most prevalent followed by radial loops, however this was reversed for males. The Algerian study looked at several small ethnic groups within Algeria and found for all the frequency of pattern occurred in the following order:

Ulnar loop, whorl, arch, radial loop. Though one exception was seen in the Reguibates group (a tribe of Western Algeria) where there was a relatively high percentage of radial loops. Given the small sample sizes this may be by chance through selection, similarity through genetic closeness or a genuine difference. These North African frequencies appear similar in trend to those found in this study with European and Middle Eastern groups however again there are no statistics supporting the claims originating from the North African papers.

Moving across the Mediterranean, a 1996 study by Sokal *et al.* [212] studied the fingerprints from 74 groups spread across Europe to determine similarities between ethnic groups. This study ignored traditional pattern categorisation and used principal components analysis and simple structure rotation, to simplify the patterns to the first 20 axes to represent 74.2% covariation. Within the European population it was found that fingerprint phenotypes were largely homogenous with the outliers being Icelanders, Faroe Islanders, Indigenous Sami people, Orkney Islanders, Aaland Islanders and Tartars. Given that all except the Tartar groups live to the northwest of Finland, the exception of their phenotypes make sense. How the Tartar group has acquired similarities to these populations needs to be examined. An ethnic subset of the tartars – the Tats – are often noted to have Scandinavian features [263]. The largest of all the Tatar groups – the Volga Tartars – are descended from Turkic-influenced Eastern Finns, and range from Scandinavian to Mongol in appearance with some mitochondrial DNA likeness [264, 265]. This origin may lead to an explanation for their differing phenotype from the homogeneity of the rest of Europe and similarity with the Scandinavian groups. There is a lack of studies originating from Europe regarding fingerprint frequency. Thus far it appears the study of minutiae frequency is more common within this region [33, 197].

Some of earliest studies on fingerprint pattern frequency originate from within Australia. In 1951 a paper was published regarding the fingerprints of Arnhem Land Australian Aboriginals. The results by Harold Cummins found a greater frequency of whorls and lower frequency of arches and radial loops compared to previously studied populations [195]. Rao [209] and Singh [211] also analysed the fingerprints of Aboriginal populations from Western Australia and Mornington Island, Queensland respectively, finding similar results. Overall these results show similarities to the results of investigations into Pacific and South Asian populations, including this study [193, 194, 196, 203, 205, 215, 216].

There are consistent trends emanating from these scientific studies. European populations have higher number of arches and populations originating from the Pacific having higher frequency of whorls with low occurrences of arches. There have been several contrasting results from

studies of African populations possibly due to higher genetic diversity. South Asians appear to have a higher ratio of whorls to loops though loops are still more common. East Asians take this ratio further with an even higher frequency of whorls. A summation of the findings regarding the association of patterns and BGA can be seen in Table 20. Limiting conclusions and discussion, many studies simply relay percentages from even numbers of males and females without any statistical application. Similarly, for ancestry comparisons, little has been done to compare raw data, this leaves open that chance that statistical and fingerprint classification methodology has been applied differently and limits the comparisons able to be made between studies.

Table 20: A summation of published results on the association of fingerprint patterns with BGA

Study	**BGA**	**Association**	**Statistically tested**	**Supported by this study**
Swofford [105]	Asian	Plain Whorls	No	Yes
Heng *et al.* [198]	Asian (Chinese/ Malay)	Whorls	No	Yes – for plain whorls
Heng *et al.* [198]	South Asian (Indian)	Arches	No	No
Steinberg *et al.* [213]	European (USA)	Loops	Yes	Yes – for radial loops and ulnar loops (chi-squared result)
Plato & Wertelecki [206]	Middle Eastern	Whorls	No	Yes – for plain whorl
Gangadhar & Reddy [196]	South Asian (Indian)	–	No	Similar ratio of loops to whorls and arches
Nithin *et al.* [205]	South Asian (Indian)	–	No	Similar ratio of loops to whorls and arches
Wijerathne *et al.* [217]	South Asian (Sri Lankan)	–	No	Similar ratio of loops to whorls and arches
Cummins [195]	Australian Aboriginals	Whorls	No	–
Rao [209]	Australian Aboriginals	Whorls	No	–
Singh [211]	Australian Aboriginals	Whorls	No	–
Cho [193]	Polynesian	Whorls	Yes	–
Veale & Adams [215]	Polynesian	Whorl	No	–
Veale & Adams [216]	Melanesian	Whorl	No	–

3.7. Summarising the multinomial logistic regression results

As already stated, MLR results are consistent with pattern distribution in Figure 26. Results are very comparable between the MLR results and the adjusted residuals of χ^2. It appears that despite how the χ^2 test represents all fingers as independent and not as a set of ten may not have overtly altered the associations of patterns. This may be due to similarities within a set of ten fingerprints being a smaller factor than the randomness of pattern development.

The figures visualising the MLR results are outlined from this page onwards.

Plain arches, tented arches, radial loops, double loops whorls and plain whorls all had significant differences within the BGA coefficients. Central pocket loop whorls and accidental whorls did not to have significant differences (Figure 27).

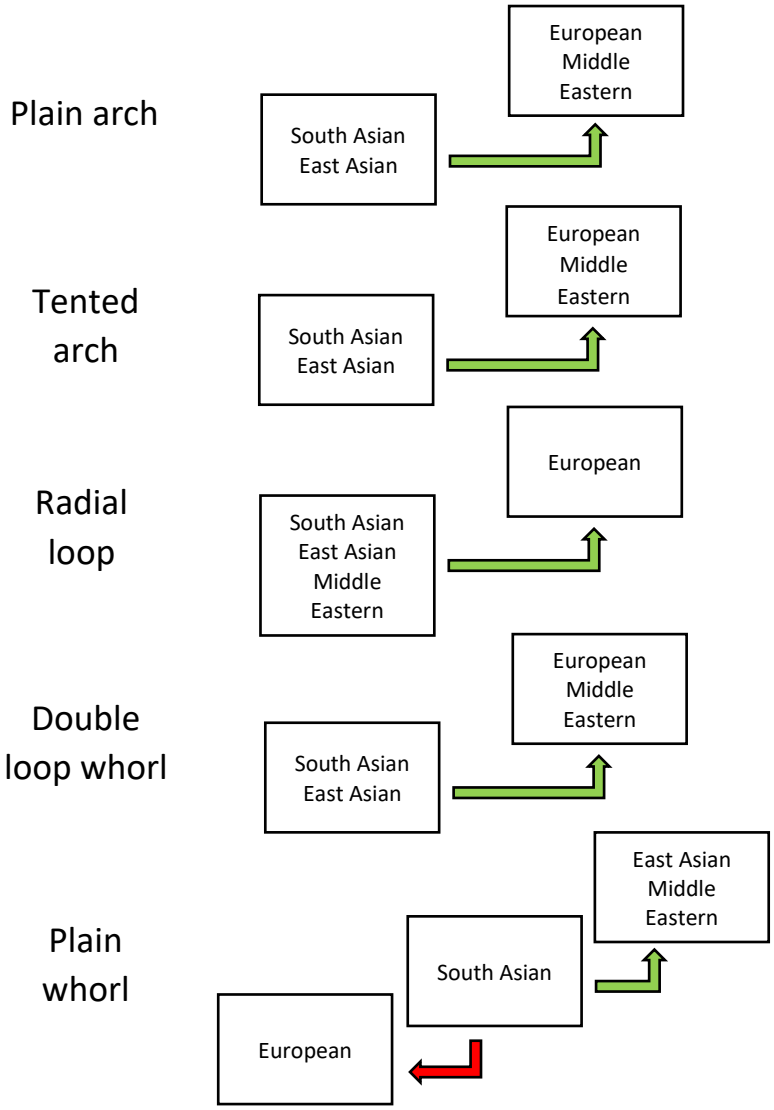

Figure 27: Summarised results of the MLR per pattern and BGA

BGAs that were significantly higher in pattern frequency than the South Asian reference group are indicated by green upward arrows. BGAs that were lower in pattern frequency than the South Asian reference group are indicated by red downward arrows. All pattern frequencies were calculated relative to the ulnar loop pattern.

The plain arch, double loop whorl and plain whorl are the only patterns to show sex dimorphism. It was shown that females are significantly less likely to have double loop whorls and plain whorls over ulnar loops compared to males and more likely to have plain arches (Figure 28).

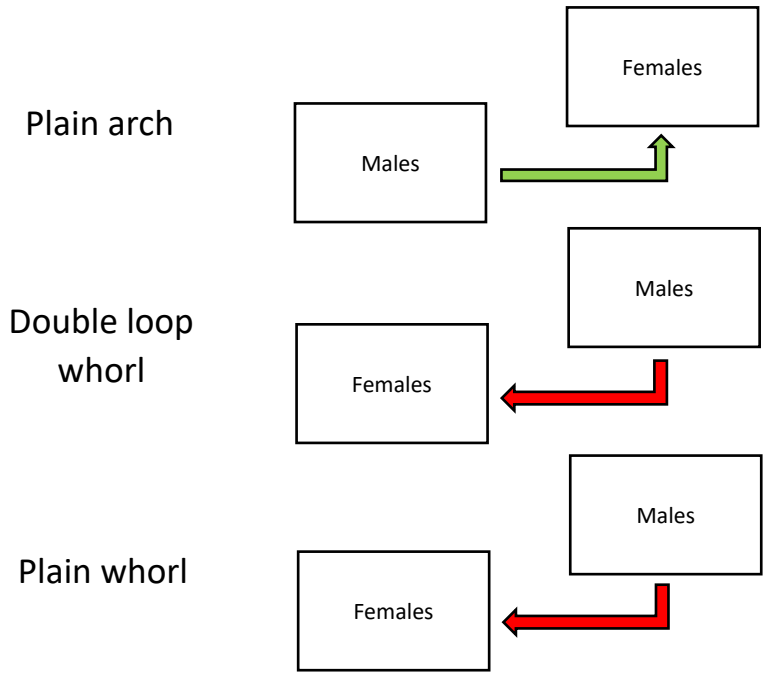

Figure 28: Summarised results of the MLR per pattern and sex

Where females had a significantly higher pattern frequency than the male reference group they are above and indicated by green upward arrows. Where the male reference group had a higher pattern frequency than females, they are above and have red downward arrows. All pattern frequencies were calculated relative to the ulnar loop pattern.

The likelihood of having plain whorls over ulnar loops is lower on the left hand than the right. No other pattern showed this asymmetry though plain arches were close to the significance threshold (Figure 29).

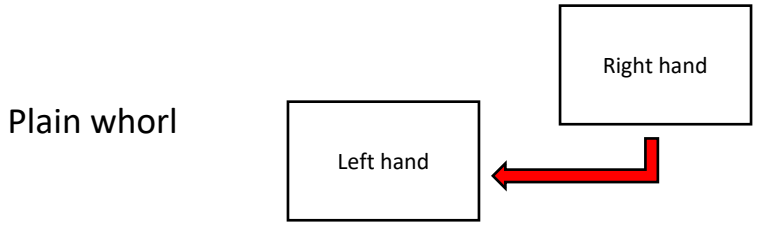

Figure 29: Summarised results of the MLR per pattern and hand

Where the right hand reference group had a higher pattern frequency than the left hand, they are above and have a downward arrow. All pattern frequencies were calculated relative to the ulnar loop pattern.

Finally, all patterns showed some significant frequency differences between fingers with reference to ulnar loop patterns and the thumbs (Figure 30).

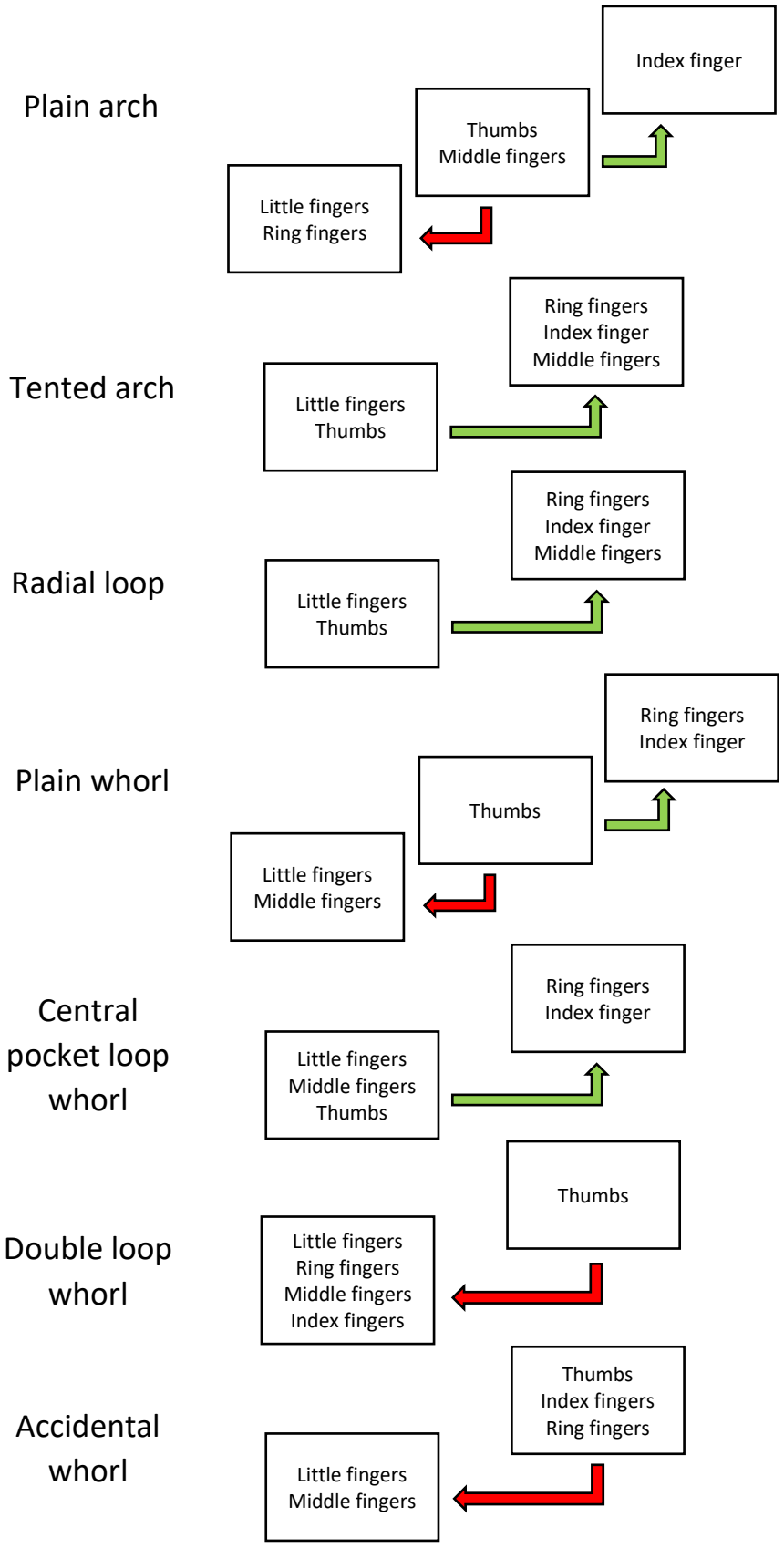

Figure 30: Summarised results of the MLR per pattern and finger

Where fingers had a significantly higher pattern frequency than the thumb reference group they are above and indicated by green upward arrows. Where the thumb reference group had a higher pattern frequency than the other fingers, they are above and have red downward arrows. All pattern frequencies were calculated relative to the ulnar loop pattern.

The results of the current study are limited by the size of the South Asian and Middle Eastern cohorts. As each contain 30 individuals this may not be representative of the greater population of these ancestries. Similarly regarding BGA, it was self-reported during the collection process; this can introduce errors within BGA groups where it is incorrectly reported. However, given the size of the European and East Asian cohorts, and the alignment of results to previous studies the author believes this to not be a significant issue. An additional limitation of this study is the lack of isolation of independent variables. For example, when assessing male and female groups, these groups contain individuals of all BGAs. Though this would be representative of the overall population, results may be skewed due to indications of varying sex dimorphism from previous studies. To completely remove the effect of BGA on the sex results this study would need to be repeated with a group of males and females from each BGA. This study did not have the sample size required to do this.

Recent advances to give latent fingerprint examiners pattern statistics ignore ancestry and sex. This advancement in fingerprint frequency research has found new and recurring interpersonal, sex and ancestry variabilities while providing a more comprehensive statistical result. Further research into pattern frequency and the data provided to fingerprint examiners should accommodate or at the minimum note that these irregularities do occur. It is anticipated that when results such as these have been replicated and proved reliable a frequency table or statistical model could be developed. Bayes' theorem is a possible method of doing this and is already used in presenting the probability of DNA results. If examiners were presented with a fingermark from an unknown finger, contextual information regarding its placement on an object or relative position to other fingermarks as part of a "slap" (multiple fingerprints from one hand deposited at the same time) is needed to indicate what finger the fingermark was deposited by. If the finger that deposited the mark is known the fingerprint examiners could utilise the multiplier of probability to adjust assumed prior probabilities or prior probabilities based on general population data input to the Bayes theorem equation. This also applies to other variables such as BGA and sex that can be corroborated by supporting evidence and be used to calculate a more appropriate posterior probability.

Chapter 4 – RIDGE DENSITY ASSOCIATION WITH BIOGEOGRAPHICAL ANCESTRY (BGA) AND SEX

4. Ridge density association with BGA and sex

The fingerprint pattern exhibited association to several variables, to further expand on the investigative value of fingerprint characteristics the density of friction ridges was assessed. Ridge density can be defined as the number of ridges that are located within a defined area of a fingerprint. The common method for determining ridge density is by selecting a 25mm^2 area and counting the ridges that intersect a line drawn diagonally across the area. This process can be completed in multiple areas of the fingerprint as is the case in this current study which focuses on the radial, ulnar and proximal positions, further explanation of this method is in section 4.3.

For clarity, it is important to note that ridge density and ridge count are not interchangeable terms. They are different characteristics and the terms have been confused in previous studies on the topic of ridge density. Ridge count refers to the number of ridges a line intersects between the core and delta of a fingerprint pattern. The arch patterns do not have a delta or core and thus are considered to not have a ridge count. The loop patterns have a core and one delta. The whorl patterns have a core and two deltas, meaning they have two ridge counts. Often the larger of the two is selected to be the ridge count of the whorl pattern. The concept of ridge count is demonstrated in Figure 31.

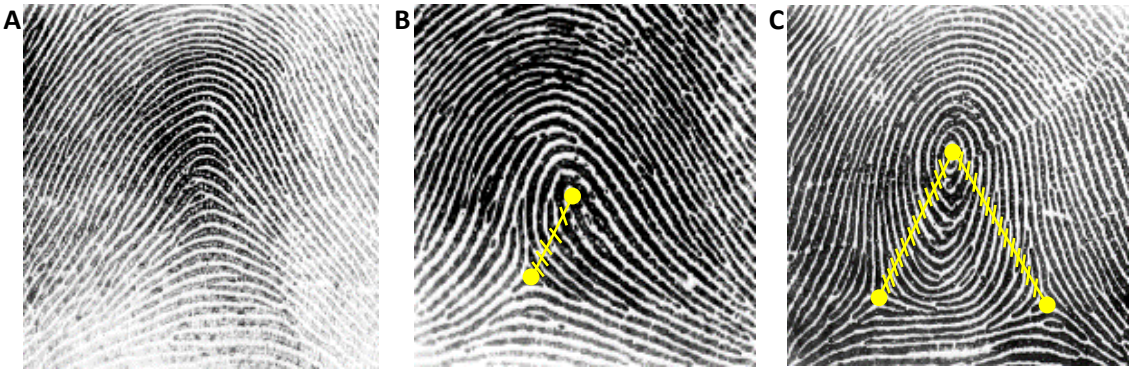

Figure 31: A demonstration in the concept of ridge count

Ridge count is determined by drawing a line from the core and the delta of a fingerprint and counting the number of friction ridges it intersects. The arch pattern (A) lacks a core or delta and has no ridge count. The loop pattern (B) has a core and one delta and a ridge count of 5. The whorl pattern (C) has a core and two deltas and ridge count of 13 as it is the higher count of the two.

The scope of this chapter covers aims 1 and 3 of this project which were:

Aim 1: Assemble a repository of fingerprints and DNA samples from approximately 500 volunteers alongside sex and self-reported biogeographical data.

Aim 3: Identify any difference in ridge density within sex or BGA groups using goodness of fit tests, general estimating equations (GEE) and generalised linear models (GLM).

Specifically, this chapter focusses on the results of the following steps and experiments:

- Sample collection including fingerprints, DNA, and ancestry information
- Classification of the fingerprints
- General Estimating Equation analysis of fingerprint ridge density to pattern, sex and BGA, with hand and finger as additional variables

4.1. Introduction

The development and width of epidermal ridges has been noted since the 19th century. In 1892 Francis Galton noted that the width of friction ridges on the feet were greater than on the hands, this one of the earliest recorded notes regarding level three ridge characteristics outside German publications [28].

In 1924, the work of A. F. Hecht investigated ridge widths by age and sex [266]. Translated from German and cited in Cummins *et al.* [31] the measurement of ridges of premature infants averaged 0.15mm, newborn infants had ridges averaging 0.18mm and 10 year old's had ridges 0.30-0.35mm in width. Between adults, women's ridges were between 0.40 and 0.50mm in width while adult men's ridges were 0.50mm in width. The width of the ridges directly translates to density when the valleys of the fingerprint are similarly narrow or broad and measurement is confined to a finite area. The measurements in Hecht and Cummins were calculated from inked fingerprints indirectly through the number of ridges crossed in a one-centimetre length (=1/no. of ridges). This means the width of the fingerprint' valleys were ignored, and the width of ridge doubled assuming a valley is the same width as a ridge. An additional variable that was not considered were the pressure applied when depositing the fingerprints.

Modern quantitative assessments of ridge density have only filtered through since the turn of the millennium. In 1999, Acree [30] was the first to statistically investigate if ridge density was associated with sex. Before this, fingerprint examiners had only noted that females tended to have "fine" ridge detail and males more "coarse" [31, 32]. Using a population of 400, results showed women had significantly higher ridge density than men in both African American and European ancestry ($p < 0.001$).

Gungadin [214] using a population of 500 individuals from southern India showed that males had significantly less dense ridges ($p < 0.001$) than females. Further studies of the Asian populations were completed by Nayak and colleagues [230] on 100 individuals of each sex from the Indian population and again, results showed a significantly higher ridge density for females.

Meanwhile the author also looked at populations from Malaysia and China finding similar results [231].

Acree, Gundagin and Nayak's studies produced similar trends when assessing sex as a ridge density variable, however the statistical analyses employed in the studies does not allow a difference in density to be quantified so a more in-depth comparison cannot be made.

The first study to move the analysis of ridge density from a single area on the fingerprint was Gutiérrez-Redomero *et al.* in 2008 [33]. This study investigated the density in the radial, ulnar and proximal areas of the fingerprint surrounding the main pattern while expanding to a new Spanish population where the now established trend had not yet been observed. Using a population of 200 individuals, results showed that women had significantly higher ridge density than men in both the radial ($p < 0.001$) and ulnar ($p < 0.001$) areas however there was no difference in the proximal portion of the fingerprint. A second study by Gutiérrez-Redomero [226] focusing on an Argentinian population again found women to have higher overall ridge densities than men.

A northern Indian population was studied in 2013 and found significant differences between male and females in all three measured positions on the fingerprint [228]. This was at odds with the studies performed by Gutiérrez-Redomero *et al.* [33]. The authors of the Indian paper do note however larger overlapping in ridge density between the male and female group in the proximal measurement area, more than the two distal areas. Additional smaller studies focussing on Turkish [232] and Filipino [237] populations showed trends consistent with other populations where women have higher ridge density in all areas to the men.

Moving to the African continent, studies on Sudanese [221], Kenyan and Tanzanian [201], and Nigerian [219] populations were conducted. The Sudanese results showed similar results to those before where all three regions measured were significantly higher in density in the female group ($p < 0.01$). The Nigerian [219] and Kenyan and Tanzanian [201] populations however produced different results to all studies previous. Both studies by different authors found ridge density in the proximal areas of the fingerprints to be higher in males than females. Standing against these results however are the different methodologies employed by the two studies and the miscommunication between the terms "ridge density" and "ridge count".

Finally, a study of note on Mauritians by Agnihotri *et al*. [220] continued the trend of women having significantly higher ridge densities than men. Statistical values of a set of 10 fingerprints were added together to give a discriminating value before assessing the likelihood of the prints being male or female. The authors used these likelihoods to predict the sex of the depositor with

a 92% success rate. This result shows the effectiveness of using the ridge density characteristic though it would not be practical for most casework given the requirements of a full set of fingerprints.

It is clear through numerous repetitions that females have higher ridge density than males. However, there is a severe lack of study regarding additional factors that may be influencing ridge density. Because of this it is unknown whether being male or female is the largest variable in ridge density. BGA, hand, inter and intra finger variations may all have a role in displaying more or less dense ridges. BGA is particularly of interest when Chapter 3 of this project found large variations in pattern within BGAs and fingers, and a review of studies on the topic of ridge density (summarised above) found different trends between continents. On top of these personal effects are the variations that may be induced when the fingerprint interacts with the physical world. The elasticity of friction ridge skin and the substrate which is interacted with may alter ridge density during deposition.

4.2. The effect of pressure on digital fingerprint scans

An immediate observation when approaching this study was that elasticity of the friction ridge skin may influence ridge density. Skin has been shown to deform, reduce the distance between ridges by 20% and affect fingerprint identification [267, 268]. A small experiment observing the effect of pressure in the rolled fingerprint scan process was undertaken. Three volunteers, aged 19, 24 and 26, two male and one female had their right thumb and right index fingerprint scanned. The fingerprint scanner was placed on kitchen scales and when rolling the finger four approximate downward pressures of 250, 500, 750 and 1000 grams were used. A square box measuring 25mm^2 was placed on the fingerprint in the upper right position, outside the main pattern area (Figure 32).

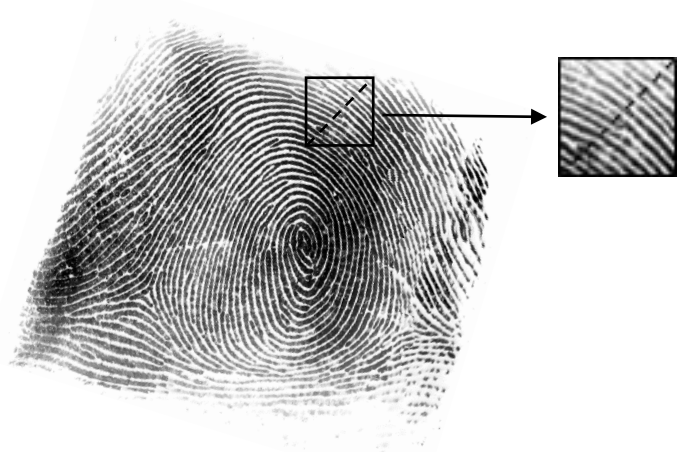

Figure 32: Location of ridge density box and direction of counting for the assessment of deposition pressure effect

The number of ridges that intersected a line from the top right of the box to the bottom left was documented; the results are shown in Table 21.

Table 21: Ridge density of fingers when applying increasing pressure

Volunteer	Finger	250g	500g	750g	1000g
1	Right thumb	9	9	9	9
	Right index	9	9	9	9
2	Right thumb	9	9	9	9
	Right index	10	10	10	10
3	Right thumb	10	11	11	11
	Right index	9	9	9	9
Ridge density - 25mm^2					

The ridge density has been shown to not alter drastically with deposition pressure of the rolled fingerprint. Only one change was seen amongst the six repetitions, that being the right thumb of volunteer three. After observing the fingerprint scans and given that there was no change with the five other repetitions it is likely this change is due to a difference in rotational alignment between fingerprints and a small difference in placement of the density area box. Ultimately, from this small investigation it appears that the downward pressure applied during rolled fingerprint deposition does not affect ridge density on a large enough scale to invalidate the results.

4.3. The semi-automated ridge count method

Automating the ridge counting process was considered a priority in this study as calculating it manually would have been too time demanding. Initial searches for programs or code that could complete this uncovered MATLAB code that was specifically designed for recognised fingerprint minutiae however was no longer functioning on updated MATLAB versions. MATLAB code that was designed to count rows of crop from aerial images was also considered however this was deemed too difficult to adapt to the smaller, lower resolution, monochrome fingerprint scans. Thus, a new process was developed for cropping regions of the fingerprint and automating the counting of the ridges.

Firstly, an automated process was created within Photoshop CC (Adobe, California, USA) to apply three 25mm^2 boxes as layers to each fingerprint. These boxes were then manually moved into ulnar, radial, and proximal positions according to the fingerprint's orientation (Figure 33).

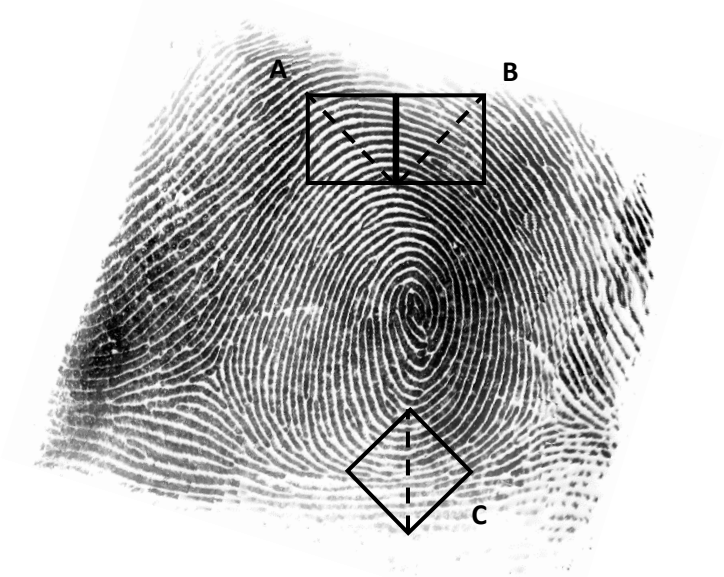

Figure 33: An example of (A) radial, (B) ulnar and (C) proximal positioning of ridge density boxes (25mm^2) with direction of counting indication by dashed lines

Another automated process was then created to crop the fingerprint to each of these boxes, thus creating three individual images from the one fingerprint. The individual images were sorted as per their position and saved in separate folders.

Moving to Wolfram Mathematica [269] (Wolfram Research, Illinois, USA), the fingerprint section images were analysed by a newly written code (Appendix F). The code assessed the image's pixels diagonally and perpendicular to the ridges. Each pixel was assigned an intensity value ranging from 0 (black) to 255 (white). This data was exported to Microsoft Excel.

Finally, the presence or absence of a ridge needed to be determined from the pixel colour value. Within excel thresholds could be set and manipulated to give the best ridge reading according to the quality of the fingerprint scans. Lighter images needed a lower threshold for the presence of a ridge than darker images. Additionally, to prevent incipient ridges skewing density results only ridges of more than two pixels were counted.

This process was used as manually counting the ridge density of all fingerprints in three positions was not feasible due to time constrains. However, it must be noted that the workflow was not infallible in its counting. Numerous patterns were of too poor quality to be reliably counted therefore many fingerprints ended up with no ridges or lower ridge count than if counted manually. Similarly, prints may have been assessed to have more ridges than if counted

manually. Both these scenarios mainly occurred mostly in the proximal area where the ridges were often less defined. The datasets also played a part in quality of results, with fingerprints from Melbourne being taken using ink it resulted in finer ridges which were more difficult to set a threshold for. The quality of the Melbourne fingerprints was also lower outside of the main pattern area, this occurred as there was no intention of using the prints for ridge density assessment when they were taken.

Where fingerprints recorded no ridges or lower ridge count from the Wolfram method (referred to on the previous page) they were assessed and if found to be of insufficient quality to be counted manually they were removed from ongoing analyses. A summary of the number of images excluded in shown in Table 22.

Table 22: The number of observations removed based on quality due to inability to measure ridge density

Dataset	**Sydney**			**Melbourne**		
Position	**Radial**	**Ulnar**	**Proximal**	**Radial**	**Ulnar**	**Proximal**
No. of observation removed	12	13	49	45	59	769
% of observations removed	0.23	0.25	0.95	1.41	1.85	24.18

The higher number of removed observations from the Melbourne dataset illustrates the issues outlined with pattern quality outlined previously. With all locations of the Sydney dataset having a removal rate of less than one percent there would be minimal impact any results. The Melbourne dataset had relatively low removal rates of less than two percent for the radial and ulnar location therefore it too is assessed as having a low impact on any results. However, the proximal area of the Melbourne dataset had a quarter of the images removed for being poor quality. This would undoubtably affect results by not giving a true representation of the population and perhaps skewing distribution. Skewing of data is particularly apparent when noting that if person's set of fingerprints were of poor quality, they were likely to have nearly all datapoints excluded due to poor quality.

4.4. Ridge density results and discussion

4.4.1. Mode, median and mean for sex and BGA ridge density per position

When condensed the individual ridge density scores create a normalised distribution. The mode, median and means of each demographic variable and data pool are summarised in Table 23 to

Table 28 below. The mode and median have been provided to illustrate where the peak of ridge density frequency distribution is positioned.

Table 23: Sex ridge density ulnar position

	Sydney		**Melbourne**	
	Male	**Female**	**Male**	**Female**
MODE	10	11	15	16
MEDIAN	10	11	15	16
MEAN	9.98	10.65	15.04	15.99
MEAN *	9.98	10.65	15.00	15.94
* Mean excludes readings under 4 ridges in Sydney group and under 8 in the Melbourne group				

Immediately when viewing the ridge density of the ulnar position in the Sydney and Melbourne data the difference in ridge density becomes apparent however trends can still be extracted. The mode and median values in both datasets are one higher for the females than males showing a slight separation of the two groups though also a large overlap. More representative of the delineated groups is each mean ridge density. The ridge density mean in both the Sydney and Melbourne data is higher in females than males. In the Sydney data females average an extra 0.67 of a ridge in the 25mm^2 area and in the Melbourne group the mean difference was 0.95. When removing outliers due to miscounting of poor quality fingerprints the average difference remains unchanged in the Sydney data and closes minutely to 0.94 in the Melbourne group.

Table 24: Sex ridge density radial position

	Sydney		**Melbourne**	
	Male	**Female**	**Male**	**Female**
MODE	9	10	15	16
MEDIAN	10	10	15	16
MEAN	9.68	10.38	14.99	16.04
MEAN *	9.68	10.38	14.97	16.02
* Mean excludes readings under 3 ridges in Sydney group and under 6 in the Melbourne group				

The radial position has a similar trend between the sexes in both groups (Table 24). The females have higher ridge density than the males. There is no change between the mean and the adjusted mean in the Sydney cohort which shows a mean 0.70 higher ridge density in females. Again, the Melbourne dataset has a larger difference in density between the sexes. Both mean

and adjusted mean show females to have a mean ridge density 1.05 higher than males. Comparing the radial position to the ulnar position, both sexes in the Sydney group have a lower mean density in the radial position. Similarly, the males in Melbourne have lower density in the radial position though dissimilarly Melburnian females have a higher mean ridge density in the radial position. The significance of these differences is explored in section 4.4.2.

Table 25: Sex ridge density proximal position

	Sydney		**Melbourne**	
	Male	**Female**	**Male**	**Female**
MODE	8	9	14	15
MEDIAN	8	9	14	14
MEAN	8.08	8.46	11.62	11.41
MEAN *	8.07	8.46	11.35	11.10
* Mean excludes readings under 4 ridges in Sydney group and under 6 in the Melbourne group				

The proximal position has a lower ridge density than both the radial and ulnar positions in both cohorts, though the same trends of females having higher ridge density is still seen (Table 25). Females have a mean ridge density that is 0.39 higher than males in the Sydney group. The first occurrence of an inverse trend between sexes is in the Melbourne cohort. The adjusted mean shows that males have a mean 0.25 higher ridge density than females. This result lacks reliability given nearly a quarter of all samples were removed due to their poor quality and results were likely skewed. A further indication of this is the mode of 15 ridges/25mm^2 in the Melburnian females opposed to the mode of 14 ridges/25mm^2 in the males.

Focussing on the BGA groups, the same reporting process for accessing the trends of ridge density was used.

Table 26: BGA ridge density ulnar position

	Sydney				**Melbourne**			
	European	**E. Asian**	**S. Asian**	**M.E.**	**European**	**E. Asian**	**S. Asian**	**M.E.**
MODE	10	11	9	10	16	17	16	16
MEDIAN	10	11	10	10	16	16	15	16
MEAN	10.38	10.79	9.98	10.35	15.70	15.99	14.81	15.83
MEAN *	10.38	10.79	9.98	10.35	15.65	15.98	14.67	15.83
* Mean excludes readings under 4 ridges in Sydney group and under 8 in the Melbourne group								

Investigating the order of the adjusted mean ridge densities immediately shows BGAs that are similarly highest and lowest relative to others (Table 26). The South Asian group is the lowest BGA of the four and the East Asian group the highest. Despite being on opposite ends of the

spectrum these two groups were separated by less than one ridge (0.81) in density in the Sydney dataset and a larger 1.31 ridges per 25mm^2 in the Melbourne dataset. Outside of this similar trend, the two datasets differ. In Sydney, the European BGA have the second highest density, 0.03 higher than Middle Easterners. Whereas in Melbourne, the Middle East BGA is 0.18 higher than Europeans.

Table 27: BGA ridge density radial position

	Sydney				**Melbourne**			
	European	**E. Asian**	**S. Asian**	**M. E.**	**European**	**E. Asian**	**S. Asian**	**M.E.**
MODE	10	11	9	10	16	16	15	16
MEDIAN	10	10	10	10	16	16	15	16
MEAN	10.13	10.40	9.82	10.00	15.72	16.00	14.81	15.70
MEAN *	10.13	10.40	9.82	10.00	15.69	15.99	14.73	15.70
* Mean excludes readings under 3 ridges in Sydney group and under 6 in the Melbourne group								

The trends observed in the ulnar position between BGAs is repeated in the radial position (Table 27). The East Asian group have the highest ridge density and the South Asian group the lowest; separated by 0.58 and 1.26 ridges in average ridge density in the Sydney and Melbourne datasets, respectively. The difference between the two ends of the spectrum is slightly lower in the radial position to the ulnar position. This also means the European and Middle East BGAs fall in the centre for ridge density. In the Sydney dataset the European group was once again second highest in density, 0.13 higher than those of Middle East ancestry. In Melbourne, Middle Easterners were 0.01 higher than Europeans in average ridge density.

All BGAs in the Sydney dataset had lower density in the radial position compared to the ulnar position. In Melbourne, the comparison was mixed with Europeans, East Asians and South Asians being slightly higher in density in the radial position and Middle Easterners being lower in density in the radial position.

Table 28: BGA ridge density proximal position

	Sydney				**Melbourne**			
	European	E. Asian	S. Asian	M. E.	European	E. Asian	S. Asian	M.E.
MODE	8	8.5	8	8	14.5	13	13	15
MEDIAN	8	9	8	8	14	13	13	12
MEAN	8.26	8.60	8.26	8.40	11.67	10.78	10.87	10.75
MEAN *	8.25	8.59	8.25	8.40	11.38	10.42	10.60	10.42
* Mean excludes readings under 4 ridges in Sydney group and under 6 in the Melbourne group								

The trend of East Asians being highest in ridge density and South Asians being lowest does not hold true in the proximal position (Table 28). The Sydney cohort has the lowest range of density seen in the three positions, a mean difference of 0.34 between the East Asian group that had the highest average ridge density and the European and South Asian groups that had the equal lowest. The most dissimilar trend is exhibited in the Melbourne proximal position, the same area where over 24% of samples were of poor quality and discarded. The European BGA had the highest average ridge density of 11.38 and the lowest average was shared between East Asian and Middle Eastern groups with an average ridge density of 10.42. This range of 0.96 is the smallest of all the positions in the Melbourne dataset, similarly to the Sydney dataset.

The difference between the Sydney and Melbourne datasets is an approximate constant of six ridges. Where this discrepancy was introduced is unclear. Though the author hypothesises that the two differing methods of fingerprint collection was to blame. The electronic fingerprint scanner may have scaled up the size of prints incongruent with what the manufacturers software indicates.

Compared to previous studies, the ridge density in the Melbourne group is relatively high, particularly in the ulnar and radial areas and the ridge density is unusually low in the Sydney group compared to previous studies (Table 29).

Table 29: A summary of the Bayesian probability outcomes for ridge density according to males and females

Study	**Ancestry**	**Male**	**Female**
Acree [30]	USA (European/African American)	≤11 P=0.74	≥12 P=0.66
Gungadin [236]	India	≤13 P=0.84	≥14 P=0.66
Gutiérrez-Redomero *et al.* [33]	Spain (European)	≤16 P=0.53	≥17 P=0.60
Nayak *et al.* [230]	India	≤12 P=0.90	≥13 P=0.77
Nayak *et al.* [231]	China	≤12 P=0.80	≥13 P=0.92
Nayak *et al.* [231]	Malaysia	≤11 P=0.99	≥13 P=0.66
Nithin [270]	India (South)	≤13 P=0.30	≥14 P=0.90
Abdullah *et al.* [218]	Malaysia (Northern)	≤12 P=0.99	≥14 P=0.86
Kapoor [227]	India (Central)	≤12 P=0.90	≥13 P=0.69

Several studies have assessed the ridge densities of populations using Bayes' Theorem.

$$P(A|B) = \frac{P(B|A).P(A)}{P(B)} \qquad Posterior = \frac{Likelihood \times Prior}{Marginal}$$

Posterior is the probability of "A" being true given "B" is true

Likelihood is the probability of "B" being true given "A" is true

Prior is the probability of "A" being true

Marginal is the probability of "B" being true

Posterior probability (P) for the proposition of a pattern originating from a male or female were produced and show varying selectivity with P ranging from 0.30 to 0.99. To calculate posterior probabilities using Bayes' theorem, the frequencies of a phenotype occurring in the population is needed to calculate the likelihood and marginalisation, while prior probabilities can be set as 50/50 in the absence of data. Where the effects of additional variables such as BGA are not understood the likelihood cannot be properly equated. The paper by Acree [30] illustrates this by using 200 male and 200 females fingerprint sets, each having 100 European American and 100 African American ancestry to determine frequencies of ridge density. The posterior odds results show a fingerprint of 11 ridges/25mm^2 has a large probability of being male though there is evidence of BGA influencing ridge density as the posterior odds differ between BGA, P=0.74 for European Americans and 0.61 for African Americans. If the whole population was determined to have the same likelihood for ridge density, then the posterior probability would differ.

4.4.2. General estimating equation analysis of ridge density

The ridge density results were analysed with both General estimating equation (GEE) and Generalised linear models (GLM) each method returned similar results however there are some key differences between the two approaches.

GEEs were first developed by Liang and Zeger [249] and are a method for modelling longitudinal or clustered data. The marginal model that is used calculates the mean response and ignores within-subject variance. This makes the GEE less affected by biases of random effects and useful to assess populations as a whole. GLMs are linear regression models for continuous response variable given continuous and/or categorical predictors. Developed by McCullagh and Nelder [250] this model requires that all the data points are independent given the covariates.

The GEE results were preferred given this approach accounts for biases of random effects. The model incorporates intra- and inter-subject variances to indicate population averaged effects of covariates to characteristics of interest and assumes data points are dependent within subjects and independent between subjects [271]. In this case the GEE is being used to identify how covariates such as the hand, finger, pattern, sex and BGA affect ridge density. Within SPSS the GEE was carried out using a Poisson loglinear model and an exchangeable structure of the working correlation matrix. The exchangeable structure specifies homogenous correlations between elements.

Analysis of ridge density per sex using general estimating equations

The trends evident in the mode, median and mean results are mirrored by the GEE results which are in Appendix G. All positions and cohorts, except Melbourne proximal showed significant difference between male and female with females having a higher ridge density. For females, the ulnar position recorded densities 6.9% and 4.8% higher in the Sydney and Melbourne cohorts, respectively. Similarly, females recorded ridge densities 7.4% higher than males in the radial location of the Sydney group; the Melbourne group showed females to have 5.8% higher ridge density in the same location. The proximal position showed significant sex dimorphism in the Sydney cohort only. Females again had higher density, this time by 4.8%. An explanation for the single cohort finding a significant different between the sexes in the proximal location is in the quality of fingerprints. The Sydney fingerprints were planned to be subjected to ridge density analysis prior to acquisition so extra care was taken when using the fingerprint scanner. Conversely, this use case was unknown to the collectors of the Melbourne fingerprints. Couple this with the use of ink to deposit the fingerprints and ridge detail in the proximal area can get lost easily. This then was compounded by the semi-automated ridge counting process that may have miscounted fine, faded, or missing ridges and skewed the results despite care being taken to eliminate unusually low ridge count scores.

Given numerous papers have found significant differences between the ridge density of males and females (Table 29) a working hypothesis has been formulated. An early study by Penrose and Loesch [272] and a more recent study by Kralik and Novotny [273] have hypothesised that this is due to the extra X chromosome in females. However, Penrose and Loesch also stated the reduction in density in males through wider valleys between ridges is linked to the Y chromosome. This has been supported by investigations showing low ridge density in people with XYY syndrome [273]. With GWAS studies finding limited association between patterns and the DNA it is believed these ridge density differences are due to the high testosterone levels

from the presence of the Y chromosome delaying the maturation of the fingerprint *in utero* [274].

Analysis of ridge density per BGA, pattern, finger and hand using general estimating equations

The focus of most ridge density studies is squarely on the effect of sex on ridge density. However, given the effect of BGA and sex on pattern it would be remiss to not assess further variables on ridge density. Despite the numerous investigations of ridge density in many different populations the effect of BGA on ridge density has been assessed a limited number of times. In 1999, Acree [30] studied a population from the United States of America consisting of African American and European American males and females. Ridge densities of participants ranged from 10.60–16.80 ridges/25mm^2 for Caucasian females and 9.70–16.00 ridges/25mm^{2}for African American females. Likewise, ridge density ranges were 7.90–14.70 ridges/25mm^2 for Caucasian males and 8.2–14.30 ridges/25mm^2 for African American males. ANOVA results show European background females were significantly different in ridge density to the African American females ($p < 0.05$) however the two male groups (European and African BGA) were not significantly different ($p > 0.05$).

Gutiérrez-Redomero et al, 2008 [33] subsequently compared results from the radial area (the only positioned measured in the older studies) to the results of Acree [30] and an Indian study by Gungadin [236]. Ridge density was shown to be higher in the Spanish population compared to the Indian and American populations, both those of African and European decent. The author notes that placing of the areas for density sampling could introduce variance in results though differences in the extent of 5 ridges on average between the Spanish population and the European American, African American, and Indian populations are largely unexpected even due to intrinsic differences between populations.

A further study by Gutiérrez-Redomero [226] comparing an Argentinean cohort with the previously studied Spanish group found that the men between groups did not differ significantly however the Argentinean and Spanish women differed significantly in density in the radial and ulnar areas of the fingerprint. Similarities between Argentinean and Spanish groups are not unexpected given the colonial past of Argentina. Overall, the Argentinian sample presented a higher mean ridge density than the Spanish sample for each area (radial, ulnar, and proximal) of each finger. The significant differences between the female groups clearly influencing the overall Argentinian comparison. The mechanism accounting this large dissimilarity in only females is unknown, though the positions of areas for density sampling are again indicated as a point of potential variance.

The ridge density trend is consistent between all three sampled positions in the Sydney cohort. The East Asian ridge density was found to be significantly higher than the reference group and by extension the other ancestries in all three locations of the Sydney dataset. The ulnar position was 6.5% higher in ridge density, the radial position 4.5% higher and the proximal position 3.0% higher. Asian populations having higher ridge density has not been observed as studies have only focussed on the differentiation between the sexes. The only comparison that can be made is the comparison of European to the American and Indian population from the studies by Acree [30] and Gungadin [236]. Those studies found no difference between populations which is similar to the current study which also found no statistically significant difference between the European and South Asian BGA.

The Melbourne group found varying significance between the three sampled positions and different trends to those shown in the Sydney population. In the ulnar position the European ancestry was 3.5% higher in ridge density overall than the South Asian reference group. The East Asian and Middle Eastern groups were insignificant compared to the same reference group. In the radial position, the East Asian and European ancestries were significantly higher in ridge density compared to South Asians, 4.7% and 4.4% higher, respectively. The Middle Eastern BGA was not significantly different to the South Asian ridge density. Finally, like the Melbourne ulnar position, the proximal position found Europeans to be higher in density compared to the other ancestries. The European group was found to have ridge density 5.8% higher. The results of the Melbourne group do not as easily correlate with previous studies as the Sydney cohort. The European cohort is consistently higher in ridge density across all sampled areas. As the European American population in Acree [30] was not significantly different to the African American population or the Indian population in the study by Gungadin [236] the only comparable results can be seen in the study on Spanish individuals by Gutiérrez-Redomero [33]. It has already been discussed that this population had remarkably high ridge density. Though fundamental differences within smaller European populations cannot be ruled out as it appears that it may be due to differences in methodology. The Melbourne and Sydney datasets used fingerprints from different substrates which resulted in a large difference in ridge density counts and this is perhaps representative of comparisons to the Spanish and Argentinian studies by Gutiérrez-Redomero *et al.* [33, 226]

Assessing the ridge density across three regions of the finger is important as partial fingerprints of the same finger may display different density values. It may also be a confounding factor in understanding the sex dimorphism of ridge density. Gutiérrez-Redomero *et al.* [33] established the three area sampling method and compared the density between regions. The radial, ulnar

and proximal areas within volunteers all showed significance. Both the radial and ulnar areas were significantly denser than the proximal area and the radial area was significantly higher in density than the ulnar area. Repeating this approach on Sub-Saharan populations Gutiérrez-Redomero *et al.* [225] found the radial and ulnar areas had significantly higher density than the proximal area. All three areas also correlated, meaning that if a person had high density in one it would be relatively high in the other. The radial and ulnar areas were not significantly different to each other and this result was repeated in an unrelated study of the Turkish population [232]. The results of these three studies align with the those produced from the Kruskal-Wallis test from the Sydney and Melbourne dataset where the two proximal positions are significantly different to the proximal position. When comparing the radial and ulnar positions the results of the Turkish study are similar to the Melbourne group which saw no different between the radial and ulnar positions. The Sydney population was similar to the results seen in the original study by Gutiérrez-Redomero *et al.* [33] where the radial and ulnar positions were significantly different.

The significant difference in Gutiérrez-Redomero *et al.* [33] and the Sydney population is hypothesised to be a reflection of the gestation environment with a small genetic component, consistent with the belief of how individual minutiae and the symmetry of level one patterns develop [275]. It is further theorised that the level one pattern may influence the ridge density, and therefore some populations show asymmetry between ulnar and radial ridge density and others do not.

Only studies by Gutiérrez-Redomero *et al.* [33, 225] consider the effect of level one pattern on the density. They found that pattern played no part in density in the radial and ulnar areas of the fingerprint though for whorls the proximal area has significantly more dense ridges than in loops in both Spanish and Sub-Saharan African populations. Comparing this to the results from Sydney and Melbourne populations an alternate trend is shown. In the Sydney and Melbourne groups the plain and tented arches along with the radial and ulnar loops all had significantly higher ridge density than the whorl patterns in the ulnar position. The radial position in the Sydney dataset finds differentiation of whorl patterns in the ulnar position. The plain whorl and double loop whorl were not only significantly less dense than the loops and arches but also the central pocket loop whorl and accidental whorl are significantly less dense. The radial position in the Melbourne dataset did not show the additional trend, only the tented arch and ulnar loop had a significantly higher ridge density in the radial position over the plain whorl reference category and all other whorls. In the proximal position the trend is reversed. In the Sydney cohort the four loop and arch patterns are all significantly less dense than the whorl patterns,

the same as both the Spanish and Sub-Saharan African populations. The trend in the Melbourne data was inconsistent in the proximal ridge density with only the ulnar loop having significantly less ridge density than the plain whorl reference category. An observation of the whorl patterns gives an insight to why there is a higher density in the proximal area. Below the core of the loop pattern the ridges "fan" out due to the valleys of the friction ridge skin getting wider. Also, outside the main whorl pattern, the valleys do the opposite and narrow which condenses the ridges, this is observed in Figure 34.

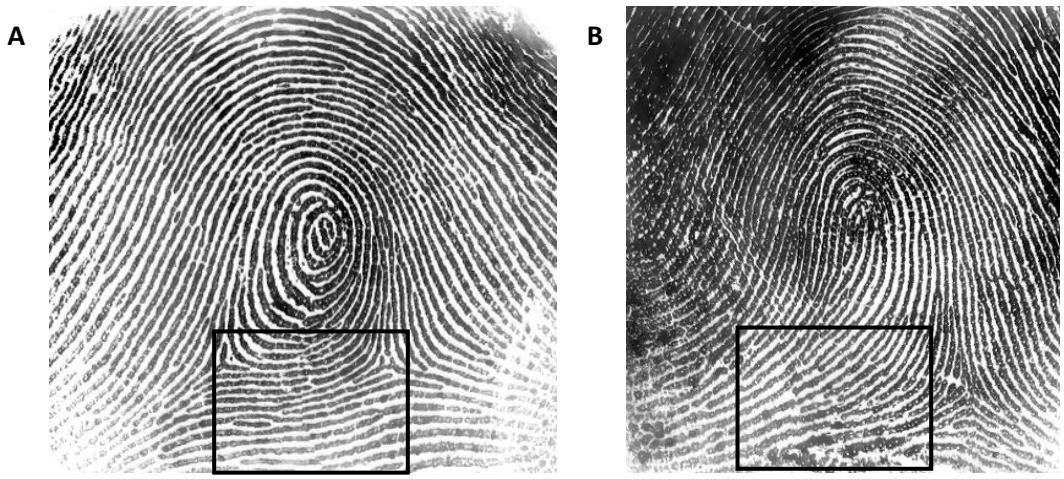

Figure 34: A demonstration in the variation of ridge density in the proximal position per pattern

A) An example of a whorl pattern where ridges are condensed below the central pattern area before getting less dense when moving in a further proximal direction
B) An example of a loop pattern where the ridges become less dense as the loop 'flares' on the opposite side of the pattern to the delta

Following on from fingerprint pattern, Gutiérrez-Redomero *et al.* [33] also assessed how the finger number affected ridge density. The Spanish population presented with the lowest density on the thumbs for the radial and ulnar areas while the ring fingers presented the highest. The proximal area differed with the thumbs having the highest density and the little fingers being the lowest. A study by Taduran *et al.* [237] on Filipino subjects following the Spanish paper also noted differences among fingers however a completely different trend was observed, different also to the one seen in this study. The thumbs had higher ridge density on the ulnar area while the four fingers had higher ridge density in the radial area. While no difference was seen in the proximal areas.

The results in the current study follow closely to those in the Spanish study and there were no trends observed in the current study that aligned with those seen in the Filipino study. The ulnar and radial positions in the Sydney cohort had significantly higher density on all fingers compared to the thumbs barring the ulnar and proximal position on the index finger. The Melbourne data

exhibited similarities to Gutiérrez-Redomero *et al.* [33] and the Sydney data in the ulnar position where the little finger and middle finger are significantly different to the thumb. However, the little finger had lower ridge density and the middle finger higher. The ring and index finger in the ulnar position for the Melbourne data were not significantly different to the thumb ridge density. The radial position in the Melbourne group was closer to the Spanish trend as the ring, middle and index fingers were all significantly higher in ridge density than the thumbs. However, the little finger was not significantly higher in ridge density. The proximal position shows a different trend between Sydney and Melbourne groups. The little, ring and middle fingers in the proximal positions are all significantly lower in ridge density than the thumbs, with the index not being significantly different in the Sydney dataset. The Melbourne group in the proximal area also saw ridge density on the index finger not being different to the thumbs, however so too was the ring finger. Similar results were seen between Melbourne ulnar and proximal positions as the little finger was lower and the middle finger higher in ridge density compared to the thumbs.

Moving to the hand variable, Gutiérrez-Redomero *et al.* have produced two papers on this, assessing two different populations. The 2008 study [33] on a Spanish population found overall ridge density to be higher on the left hand. Further breaking it down, the ridge density was significantly higher in the left hand over right hand in both sexes for the radial and ulnar areas ($p < 0.001$) but not the proximal area. The Gutiérrez-Redomero *et al.* study from 2013 [225] on an African population found an entirely different trend where the right hand had higher density on the ulnar side of the fingerprint while the left hand had higher density on the radial side. Either asymmetry trend did not correspond and were broader in observation than the current study. The only positions between the Sydney and Melbourne groups to show statistically significant hand asymmetry were the Sydney ulnar and Melbourne proximal positions. The ridge density of the left hand in the Sydney ulnar position was 1.034 times (3.4%) higher than the same position in the right and ridge density of the left hand in the Melbourne proximal position was 1.016 times (1.6%) higher. The highly variable nature of ridge density hand asymmetry between studies indicates that it is perhaps an effect of another variable. It is hypothesised that the fingerprint pattern coupled with the sample area positioning would cause variations large enough that could be observed to be significant, especially when the plain whorl pattern itself was seen to be asymmetrical in distribution in section 3.6.

It is a significant issue that only a few papers have considered finger, hand or fingerprint pattern in their analysis when assessing ridge density. Fingerprint pattern particularly can vary significantly between fingers as demonstrated in section 3.4. Given that there have been

indications that patterns are associated with sex and a similar trend of ridge density to pattern association, it is something that should be investigated further for ridge density to be a useful investigational biometric tool.

Further to the biographic and interpersonal variables, aging needs to be approached with caution as it is currently unknown if this changes an individual's own ridge density over time. Age was included as a variable in ridge density for the first time by Gutiérrez-Redomero *et al.* [224] with a population from northern Argentina. It was found for all ages above 12 years old females had a higher ridge density in radial, ulnar and proximal areas of the fingerprints. The author compared the results of individuals over 18 years of age to the results from the Spanish group in a previous study finding the ulnar and proximal areas, in both sexes the Mataco-Mataguayo population presented significantly higher RD than the Spanish population ($p < 0.05$). Age was similarly assessed with a Thai population finding similar trends where ridge density dropped with age from 14 to 24 years old and females had higher ridge density in all areas measured [235]. Unfortunately, these studies did not assess the changing of ridge density over time. The current study could not assess this either as participants were required to be over 18 years of age.

An additional complication that may influence the usage of ridge density that accompanies the many co-variables is how the fingermark was deposited. When using traditional ink methods, a mark is guaranteed to be of the original size however with new electronic fingerprint scanners it is possible that software may incorrectly scale the mark, significantly altering measurements. This was found to be an issue in this study due to having two cohorts, though trends could be compared.

4.4.3. Assessment of intra-finger ridge density using Kruskal-Wallis tests and pairwise comparison

Intra-finger differences in ridge density were investigated by first assessing the normality of the ridge density distributions. A Shapiro-Wilk test of the density for each position resulted in the rejection of the null hypothesis ($p < 0.05$) for all three positions, meaning each independent variable is not normally distributed (Table 30 and Table 31).

Table 30: Shapiro-Wilk test of normality with observations of skewness and kurtosis for the Sydney data

Position	Statistic	df	Significance (p-value)	Skewness		Kurtosis	
				Statistic	Standard Error	Statistic	Standard Error
Radial	0.967	4665	0.000	0.158	0.036	0.210	0.072
Ulnar	0.970	4666	0.000	0.119	0.036	0.117	0.072
Proximal	0.939	4635	0.000	0.062	0.036	0.074	0.072

Table 31: Shapiro-Wilk test of normality with observations of skewness and kurtosis for the Melbourne dataset

Position	Statistic	df	Significance (p-value)	Skewness		Kurtosis	
				Statistic	Standard Error	Statistic	Standard Error
Radial	0.972	2645	0.000	-0.387	0.048	0.885	0.095
Ulnar	0.977	2647	0.000	-0.294	0.048	0.592	0.095
Proximal	0.962	2049	0.000	-0.320	0.054	1.697	0.108

A skewness equalling zero indicates the distribution is perfectly symmetrical. A kurtosis value of zero means that the distribution is neither peaked ("leptokurtic") nor flattened ("platykurtic"). Therefore, the distribution of the Sydney ridge density data is relatively close to being normal however the extremely large dataset (10 readings per independent variable and volunteer) is producing a significant result. The Melbourne dataset on the other hand is skewed in the opposite direction by the lower ridge density counts and the kurtosis is much larger as there is a much sharper peak in distribution.

Due to the independent variable's non-normality a Kruskal-Wallis test was used instead of a one-way ANOVA. The null hypothesis that the distribution of ridge density is the same across each position of the finger was rejected ($p < 0.05$). Pairwise comparisons showed the specific differences between the positions (Table 32 and Table 33).

Table 32: Pairwise comparisons of the Kruskal-Wallis test for ridge density positions for the Sydney dataset

Comparison	Test Statistic	Standard Error	Standard Test Statistic	Significance (p-value)
Proximal -Radial	4205	82.4	51.1	0.000
Proximal – Ulnar	4767	82.4	57.9	0.000
Radial - Ulnar	-561.4	82.2	-6.83	0.000

Table 33: Pairwise comparisons of the Kruskal-Wallis test for ridge density positions for the Melbourne dataset

Comparison	Test Statistic	Standard Error	Standard Test Statistic	Significance (p-value)
Proximal -Radial	1050	61.8	17.0	0.000
Proximal – Ulnar	1079	61.8	17.5	0.000
Radial - Ulnar	28.69	57.7	0.497	0.619

The pairwise comparisons show that in both datasets the distal positions (radial and ulnar) are significantly different in ridge density to the proximal position. This was expected given the observation of a large difference in the mean. The Melbourne dataset showed no significant difference between the radial and ulnar positions, understandable given the proximity in which the samples were taken. However, this is countered by the fact the Melbourne fingerprints were of lesser quality for ridge density counts. The larger and higher quality fingerprints in the Sydney dataset mean that result was more reliable. The significant difference between the radial and ulnar positions in the Sydney dataset was not expected, this would therefore play a part when the hand or finger from which a fingermark was deposited fingermark is unknown. This demonstrated by comparing results of ulnar and loop positions against left and right positions.

4.4.4. Ridge density as radial and ulnar positions compared to left and right positions

Radial position is an anatomical location description meaning it is on the side of the finger towards the thumb. Ulnar position is the alternate location position on the outside towards the little finger. The radial and ulnar position are named due to the position of the similarly named radius and ulna bones [276]. When the hand or finger is not known, the ulnar or radial position cannot be defined as the position is mirrored per hand. Therefore, when a fingermark is located and the hand or finger from which it was deposited is not known, it is referred to as left or right position which are not mirrored. Right position is on the right side of all fingers and the left position is on the left side of all fingers.

The previous analysis and research completed on ridge density has utilised three measurement positions: ulnar, radial, and proximal. This is useful as it has shown that ridge density changes within a fingerprint. Intra-fingerprint differences therefore mean knowing the orientation of the fingermark is very important for accurate assessment of ridge density. This section reassesses ridge density using left and right positions and compares them to the results of the ulnar and radial positions. This was completed by substituting the right hand left position with the right hand right position before GEE analysis. The results are shown in Appendix H.

Starting with the hand variable the Sydney and Melbourne cohorts exhibited differences. For the Sydney group the left hand had significantly more dense ridges in left position than the right hand and the right hand had significantly more dense ridges in right position than the left hand. The Melbourne group exhibited no hand asymmetry in ridge density for left and right positions. This compared to the left hand ulnar position of the Sydney group having 3.35% higher ridge density than the right hand.

Comparing the ridge density of the fingers, the left positions of the Sydney group were all significantly higher on the fingers than the thumb, up to 10.5% higher on the ring fingers. The right positions of the Melbourne group exhibited an inconsistent trend where the little finger was significantly lower in ridge density than the thumb, the ring finger was not significantly different, the middle finger was significantly higher in ridge density and the index finger was insignificant to the thumb. The right positions in the Sydney cohort were significantly higher on the little finger, ring finger and middle finger over the thumb. The index finger was not significantly different to the thumb, different to the opposing left position. The Melbourne right position is similar to the Sydney right in the index finger was not significantly different to the thumb. The ring and middle fingers were significantly different, both approximately 5% higher than the thumb ridge density. Different to the Sydney cohort, in the Melbourne cohort the little finger is insignificant to the thumb in the right position.

The Sydney ulnar trend was similar to the Sydney right in that all the fingers bar the index finger were significantly higher in ridge density than the thumb with similar B values. The Sydney radial result had the same trend as the Sydney left position where all fingers were significantly higher than the thumb, again with similar B values. The opposite correspondence occurs in the Melbourne cohort. The Melbourne left position had a similar trend to the Melbourne ulnar where the little finger and middle finger are significantly different in ridge density to the thumb. The little finger was significant lower and the middle finger significantly higher in ridge density than the thumb. The Melbourne right position was similar in trend to the Melbourne radial as the ring and middle finger were significantly higher in ridge density than the thumb. The little finger was similarly not significantly different to the thumb. The main difference was the index finger which was significantly different in the radial position and not significantly different in the right position.

These results highlight how having fingermarks of unknown hand and finger can change the parameters that would be used to predict sex or another other variable. The number of factors

that impede reliable ridge density readings further add up to demonstrate unreliableness and that ridge density cannot infer information when a fingermark is from an unknown finger.

4.5. Summarising the general estimating equation results

The opposite correspondence of radial and ulnar to the right and left position originating from the intra-finger differences in the two proximal areas highlights big issues with classifying fingerprints from ridge density when information about the print is unknown. While ridge density is well understood to be affected by sex there are many more variables which have a significant effect.

The East Asian ridge density was found to be significantly higher than the reference group and by extension the other ancestries in all three locations of the Sydney dataset. Asian populations having higher ridge density has not been observed as studies have only focussed on the differentiation between the sexes. The Melbourne data for BGA was not congruent to the Sydney data and previous studies. In the ulnar position the European ancestry was higher in ridge density overall than the South Asian reference group. In the radial position, the East Asian and European ancestries were significantly higher in ridge density compared to South Asians. Finally, the proximal position found Europeans to be higher in density compared to the other ancestries. It is important to note that the quality of the Melbourne fingerprints was lower which resulted in many prints being excluded from the analysis.

Level one pattern had a large impact on ridge density in both the Sydney and Melbourne groups. The plain and tented arches along with the radial and ulnar loops all had significantly higher ridge density than the whorl patterns in the ulnar position. The radial position in the Sydney dataset found the plain whorl and double loop whorl were significantly less dense than the loops, arches, central pocket loop whorl and accidental whorl. The radial position in the Melbourne dataset did not show the same additional trend, only the tented arch and ulnar loop had a significantly higher ridge density in the radial position over the plain whorl reference category and all other whorls. In the proximal position the trends are reversed. In the Sydney cohort the four loop and arch patterns are all significantly less dense than the whorl patterns. In the Melbourne group the ulnar loop had significantly less ridge density than the plain whorl reference category.

On all finger the ulnar and radial positions in the Sydney cohort had significantly higher density compared to the thumbs barring the ulnar and proximal position on the index finger. In the Melbourne data the ulnar position showed the little finger had lower ridge density and the

middle finger higher than the reference group. In the radial position, the Melbourne group exhibited significantly higher ridge density on the ring, middle and index fingers compared to the thumbs. In the proximal area the Melbourne and Sydney groups varied the most. The little, ring and middle fingers in the proximal positions are all significantly lower in ridge density than the thumbs, with the index not being significantly different in the Sydney dataset. This compared to the Melbourne fingerprints where the little finger was lower and the middle finger higher in ridge density compared to the thumbs. All the other fingers were insignificant in their difference.

Finally, looking at the hands, the only positions between the Sydney and Melbourne groups to show statistically significant asymmetry were the Sydney ulnar and Melbourne proximal positions. Both being higher on the left hand.

Given the previous studies and their issues, plus the current observations and cross analysis, it is determined that the numerous variables would require a huge sample size and amount of time to decipher. Even then, the accuracy regarding ancestry prediction may be far too low due to overlapping distribution between the different groups. Only predictions based on the extreme upper and lower limits would be reliable, and it should be noted that when samples are large, any difference between means will be declared "statistically significant". As this study shows, the finger and hand show significant differences in the overall population. When these details are unknown from crime scene fingermark lifts and especially when quality is poor, they cannot be accounted for. The factors to overcome in crime scenes coupled with large overlaps in ridge density distribution make any intelligence gathering from ridge density an unviable approach in all but the most controlled environments. A model to classify the fingerprints or fingermarks per sex is currently not feasible.

Chapter 5 – INHERITANCE OF FINGERPRINT PATTERNS – A CASE STUDY

5. Inheritance of fingerprint patterns – A case study

Results from the previous chapters have elucidated the difference in frequency of pattern and ridge density between males, females and four BGA groups. This indicates there is a genetic component to fingerprint characteristics. This chapter analyses the genetics of fingerprints using an observational inheritance approach on two sides of a family each with four generations. Previous inheritance studies have focussed on fingerprint characteristics mainly in twins and parents, not over several generations. The fingerprint characteristics were also forensically unconventional with a suite of papers by Sarah Holt [25, 47-52] focussing on total ridge count. The total ridge count is calculated by adding the ridge count of all fingers together. The term ridge count was outlined in section 4, p81 as it is often confused with the term ridge density; simply, it is the number of ridges been the delta and core of a fingerprint pattern.

The scope of this chapter covers aim five of this project which was:

Aim 4: Perform a small family study investigating the inheritance of fingerprint patterns.

This will introduce the concept of DNA behind fingerprint pattern phenotypes and build upon a limited number of past papers from the 20th century by using a more discriminatory classification system. Of particular interest will be the rare patterns or unusual occurrences of pattern on fingers that were established in section 3.4.

5.1. Introduction

The hereditary nature of fingerprint phenotype has been a lightly studied topic of discussion and has been replaced by more complex DNA analysis studies. However, there is still area for development using more distinguishing and modern fingerprint classification systems. Previous studies have used a combination of simple whorl, loop, and arch patterns with C-, D- and hypothenar lines as classifiers for ancestral groups [277, 278]. This approach has produced positive results in distinguishing between closely related ethnic groups within Iran and more widely spread indigenous groups of the Americas. This approach is not forensically viable due to the need for a full handprint of high quality.

Prior to these studies were numerous publications assessing the hereditary nature of another fingerprint characteristics, total ridge count. Over eight years, seven papers were published by Holt focussing on distribution, asymmetry and inheritance from parent-sibling and sibling-sibling relationships [25, 48-52]. In this sequence of publications, the ridge count was used for both

loop and whorl patterns. The ridge count method was the same as the current study for loop patterns though all ten fingers were then added. The Holt studies counted ridges between both deltas and the core of whorl pattern then selected the largest count to represent the pattern, dissimilarly the current study did not assess ridge count for whorls patterns instead using ridge tracing between the two deltas.

The 1955 study of distribution examined the total ridge count only of 1650 people with a 50% male to female mix. Included in this are numerous examples of both complete and incomplete families as well as unrelated people. These relationships within the sampled population immediately make these results unrepresentative of a general population provided ridge density is found to be inherited. The author does note reasonably sized differences in the mean total ridge counts of males and females compared to other samples in earlier publications. Interestingly the males have a higher ridge density than females, adding this to males having lower ridge density implies males have overall larger patterns. Both males and females when graphed show negative skewing of the distribution of total ridge count, the author attributes this to a small number of genes having an “appreciable” effect as many additive genes would produce a normal distribution. The author also stated their work to differentiate the distribution in to three components representative of phenotypes from a pair of alleles was unsuccessful. This indicated to the author that at least three alleles or more than one locus were involved in the development of the total ridge count phenotype.

Holt also determined ridge counts on each side of the body to be inherited similarly to total ridge count, in an additive manner [25]. There was no indication asymmetry had its basis in genetics. Overall, it was found that approximately two-thirds of people have a higher total ridge count on the right hand while also having high correlation. Separate analyses on mono- and heterozygotic twins, sibling-sibling and parent-child correlation were completed and showed no significant difference or correlation.

Further examining inheritance of total ridge count as a whole Holt selected sibling – sibling and parent – child relationships [48]. By calculating the variance within and between relationships correlation can be found. The highly correlated total ridge counts indicated that pattern size (a larger total ridge count equates to larger pattern sizes) was inherited. Further support for this conclusion was found in monozygotic twins which were found to be more tightly correlated then heterozygotic twins. A second conclusion was that the phenotypes were not caused by any dominant allele. This statement aligns with the 1955 distribution study and is interpreted to mean that the theorised multiple alleles are additive in nature. Finally, the mother and father

correlation to children was assessed and there was found to be no significant difference between the two, thus environmental factors from the maternal environment were said to have no effect. All three of these conclusions were supported by additional studies using larger sample sizes [50, 51].

After examining total ridge count Holt examined the diversity of ridge counts from finger to finger [52]. The correlation coefficients between relatives were lower than total ridge count however still showed a hereditary basis; again, monozygotic and heterozygotic twins support this finding. Further assessing monozygotic twins shows a much lower correlation compared that found in total ridge count. The author interpreted there being a considerable environmental influence during early pre-natal development which is contrary to the conclusion made regarding environmental influence and total ridge count. These incongruent results between individual and total ridge count introduced some uncertainty and supported a counter argument by Weninger [279]. Weninger postulated that ridge counts of individual fingers are independent and therefore the concept of total ridge count and the results obtained from the numerous heritability studies were invalid.

In 1976, Slatis [53] published a study tracing fingerprint patterns (a different characteristic) down family trees. Two populations were studied, a group from Israel that formerly lived in an isolated Jewish Population in Southern Yemen and a control group of families not from Yemen. Each of their fingerprints were classified to be an arch, radial loop, ulnar loop, or whorl, utilising the three main pattern types in fingerprints. All the results from Holt's studies on ridge count indicated a lack of dominance however from Slatis' pattern results seven genes were proposed based on phenotype observation inheritance models. The proposals included many that were dominant in their theoretical effect.

The genes were:

1. A semidominant gene for whorls on thumbs
2. A semidominant gene for whorls on the ring finger
3. A dominant gene for arches on the thumbs and often other fingers
4. One or more dominant genes for arches on the fingers
5. A dominant gene for whorls on all fingers except for an ulnar loop on the middle finger
6. A dominant gene for radial loops on the index fingers, frequently associated with an arch on the middle fingers
7. A recessive gene for radial loops on the ring and little fingers

Slatis states that due to the inbred nature of the isolated Yemeni group if recessive traits were common, they would have likely been very clear observations in this study. The effects of the fourth proposal, one or more dominant genes for arches was not observed in the control group. In a representative population the genes may work independently or in epistasis.

A limitation to constructing a study based on phenotype observation inheritance models is phenotypic variability of genotypes which has been observed in monozygotic twins. The variability introduces some uncertainty into interpretation of results due to additional factors in phenotype development.

5.2. Classification

Expanding upon the study method by Slatis [53], the fingerprint classification used in the current study was the NCIC classification system, discussed in detail in section 1.2.2. This system was chosen for its clarity and ability to distinguish eight different patterns, including the subcategories of arches, loops, and whorls. Further classification indicating inner, meeting, and outer ridge tracings between the two deltas in whorl patterns was completed. By utilising subclassifications of the main three patterns and then further differentiating between nuances within those patterns, inheritance may be easier to pinpoint. Although ridge density would be a novel variation to assess alongside inheritance this was not viable in this case due to numerous individuals being under the age of 18. Due to their age the fingerprints would not be of an established size or provide a representative density.

5.3. Family structure and demography

The sample population consists of the extended relations on each side of one core family consisting of parents and three children. On the father's side of this core family are 24 individuals. The extended family on the mother's side of the core family numbers 13. In total 36 people were fingerprinted with 18 of these being male and 18 being female. All members of the family self-reported their ancestry to be European with the full family tree shown in Figure 35.

The fingerprints were of high quality due to no time pressure, the known intention of use and the Futronic FS60 fingerprint scanner (Futronic Technology Co. Ltd., Hong Kong). Only two fingerprints were unable to be fully classified due to scarring. The level one pattern of these prints was determined however the ridge count could not be assessed due to the position of the scars.

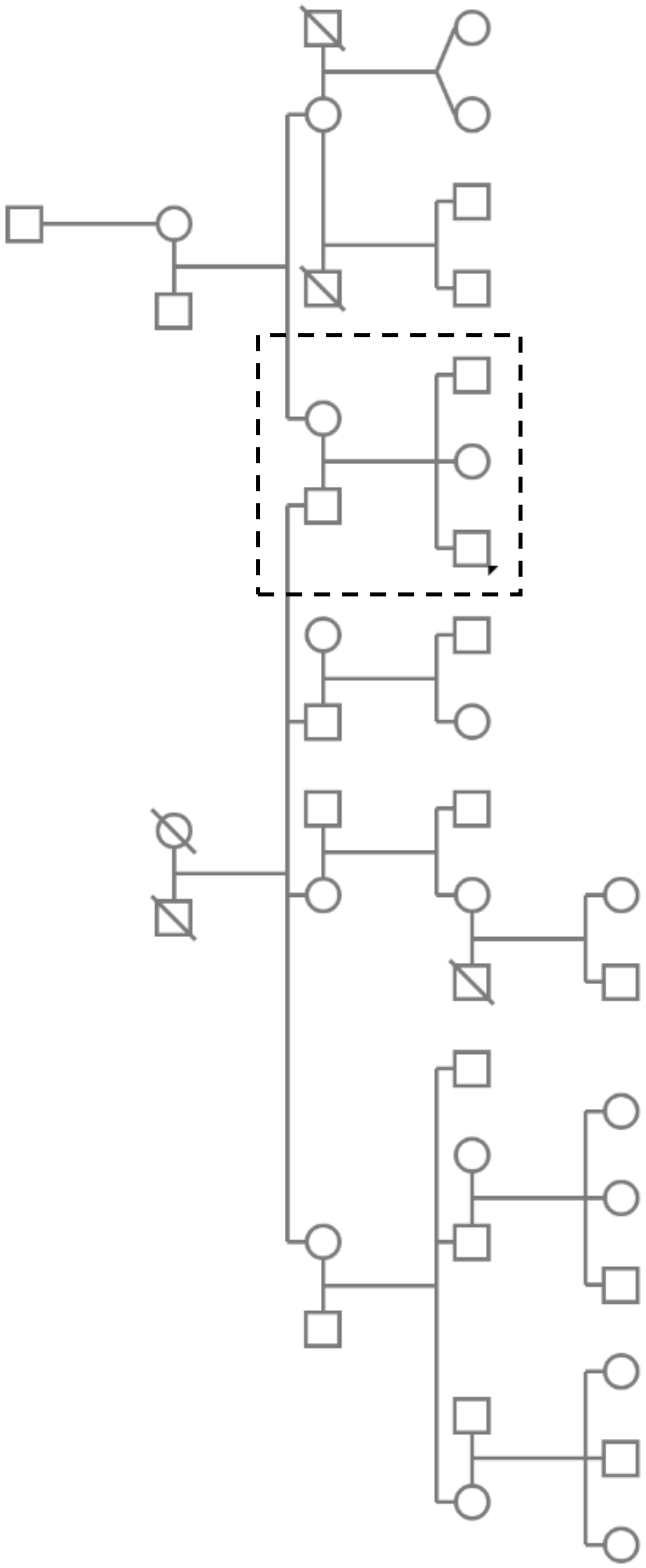

Figure 35: A diagram of the relationship between individuals fingerprinted for the inheritance case study

A circle is representative of a female and a square representative of a male. Individuals that are struck out were not included in the case study and the two individuals with a forked tree are heterozygotic twins. Thirty-six extended family members were sampled, the core family of five individuals is indicated by the dashed box. Outside of the core family the two sides will be referred to as the father's extended family and the mother extended family.

5.4. Pattern frequency, ridge count and ridge tracing

The fingerprint patterns of the sampled family members were classified and tabulated per finger. The results are illustrated in Figure 36 below. An immediately visible trend within the family is the homogeneity of pattern on the left hand. All fingers on the left hand have frequency of ulnar loops greater than 85%. The maximum occurrence of ulnar loop is on the left little finger and mirrored on the right little finger where one person exhibited a tented arch.

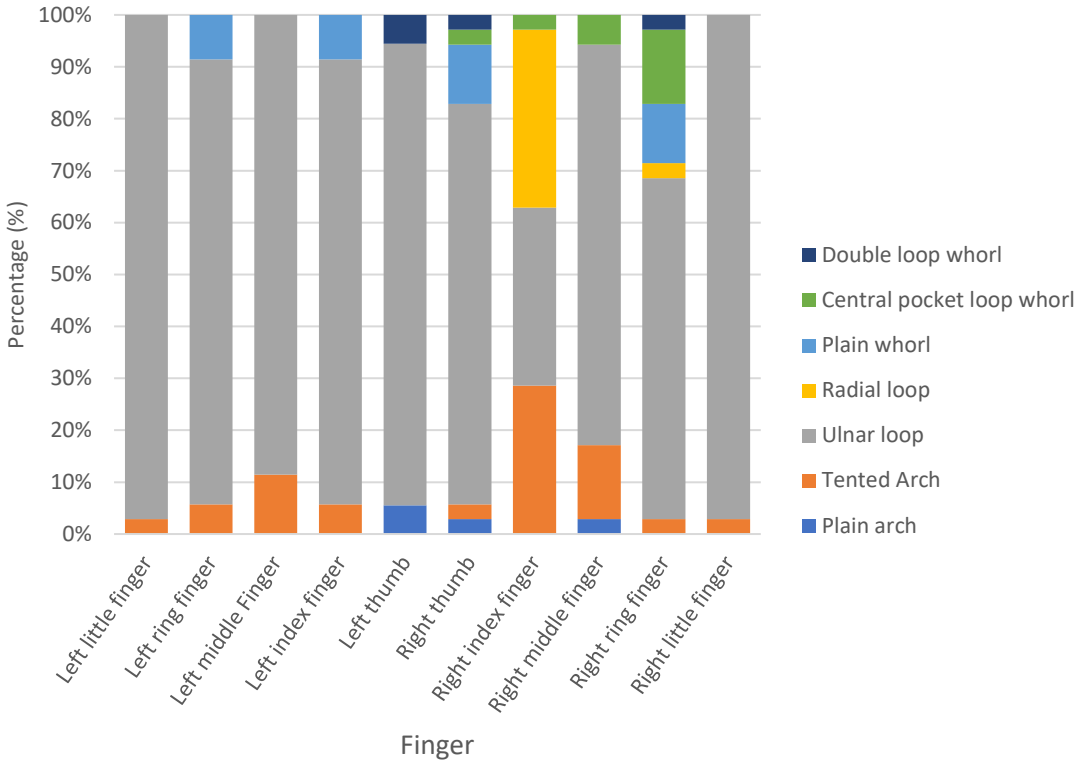

Figure 36: Distribution of level one fingerprint pattern within the two linked extended families

The variability of the right hand pattern contrasts the left hand strongly. There is an increase of tented arch frequency. Radial loops occur exclusively on the right hand and mostly on the right index finger. The occurrence of radial loops on index fingers is common, seen in the Melbourne and Sydney populations however the degree of asymmetry seen in the family is not. Of the occurrences of a radial loop on the right index finger four occurred in father's extended family, two occurred in the core family and four occurred on the mother's extended family.

The central pocket loop whorl also occurs exclusively on the right hand and mostly on the ring finger. Central pocket loop whorls having a higher frequency on the ring finger than any other was similarly seen in the Melbourne and Sydney populations but once again the degree of asymmetry was not.

A further dissimilarity to the general Sydney and Melbourne populations was the asymmetry of the tented arch frequency. There were eleven occurrences of a tented arch on the right index finger, eight occurred in the father's extended family, two within the core family and one in mother's extended family. Despite the larger extended family on the father's side there is a higher incidence that may indicate an inherited trait. Notably, in the family the tented arch is also the second most common pattern and occurs at least once on all fingers bar the left thumb. This can be accounted for by one female descendant within the core father's extended family which had a dramatically different set of fingerprints which accounted for several unique observations of plain arches and tented arches on each finger (Table 34).

Table 34: A female's distinct set of mirrored fingerprints within the family sample

Finger	**Left little**	**Left ring**	**Left middle**	**Left index**	**Left thumb**	**Right thumb**	**Right index**	**Right middle**	**Right ring**	**Right thumb**
Pattern	Tented Arch	Ulnar loop	Tented Arch	Tented Arch	Plain arch	Plain arch	Tented Arch	Tented Arch	Ulnar loop	Tented Arch

Comparing the frequency of each pattern in the family to the European BGA of the Melbourne and Sydney datasets, a very different frequency trend is seen (Figure 37).

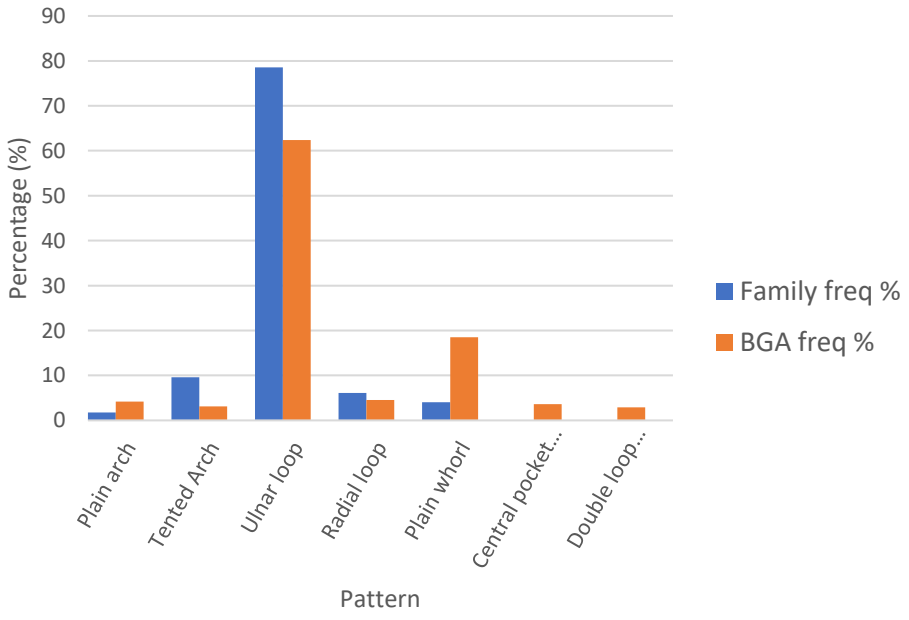

Figure 37: The percentage frequency of patterns in the extended family and the combined European BGA from Sydney and Melbourne

The ulnar loop pattern is clearly the most common fingerprint pattern in the family group and the European BGA. This was expected given the European ancestry of the family though the

difference still exceeds 10% of all patterns. More unexpected was the tented arch pattern being the second most common pattern in the family given it was sixth most common in people of the European BGA. The plain arch also showed dissimilar frequencies by being the less common arch pattern in the family and more common than tented arches in the European BGA.

Whorls also had distinct differences in frequencies. The double loop whorl occurred at 2.8% in the European population however was at 1.1%, less than half the rate in the family group. Visibly in Figure 37 the largest difference between the family and the European BGA was the frequency of plain whorls. The plain whorl was the second most common pattern in the European population of Sydney and Melbourne at more than 18% and within the family sample it was the fourth most common pattern at less than 4%. This 14% difference, the asymmetry in pattern distribution and the more subtle differences seen in the arch and ulnar loop frequencies heavily indicate that fingerprint phenotype has a hereditary factor.

Breaking the most common pattern into subcategories, the ridge count frequency of the overall family for ulnar loops is shown in Figure 38 below. The average ridge count is 12.7, the median is 13 and the mode is 14 meaning the distribution curve is slightly skewed to the right, or higher ridge counts. This same skew is observed in total ridge counts in groups of males and females in Britain [49].

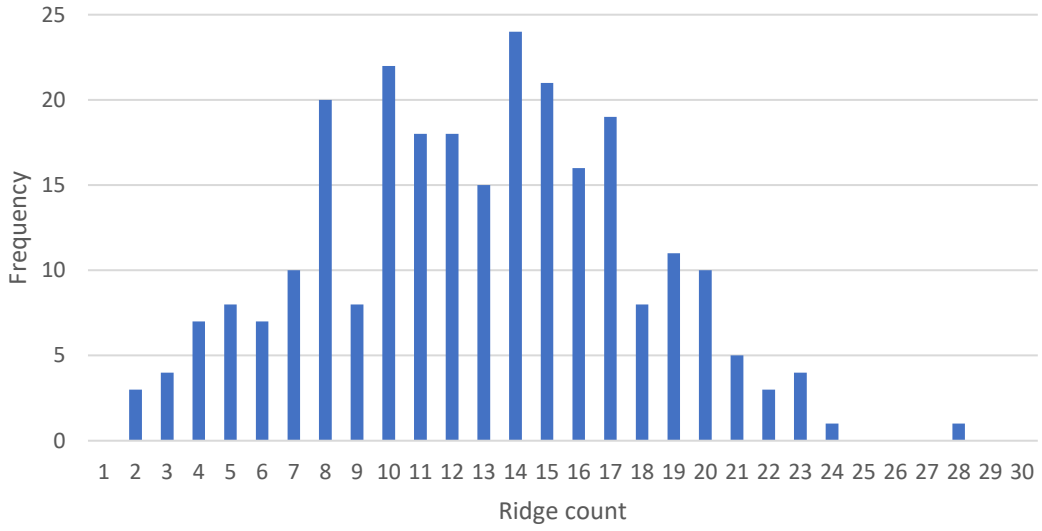

Figure 38: Ridge count frequency of the family sample

The family's ridge count data compares similarly to the Sydney dataset (Figure 39). The Sydney population has a mean ridge count of 13.2 with a standard deviation of 5.3. The median is a ridge count of 14 as is the mode. The lower mean coupled with the slightly higher mode and

median again shows a distribution curve that is minimally skewed to the right with a greater number of patterns with smaller ridge counts.

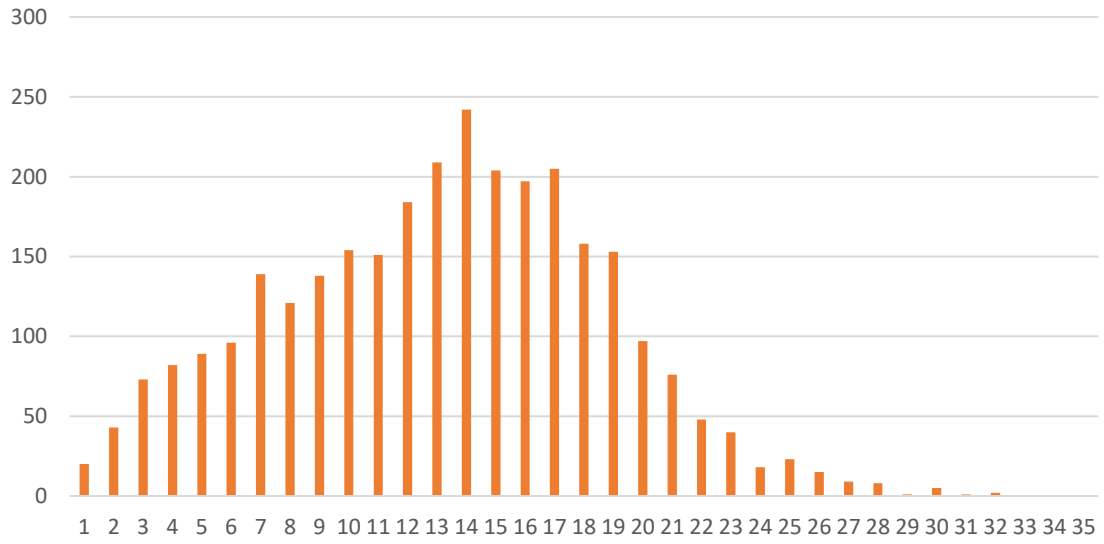

Figure 39: Ridge count frequency of the Sydney population

Breaking the ridge count into the three groups (mother's extended family, father's extended family and core family) within the larger family in Figure 40 we can see that the outliers from a normal distribution at ridge counts of 8 and 10 mainly come from the core family. The extreme occurrence of this ridge count may be an indication of inheritance.

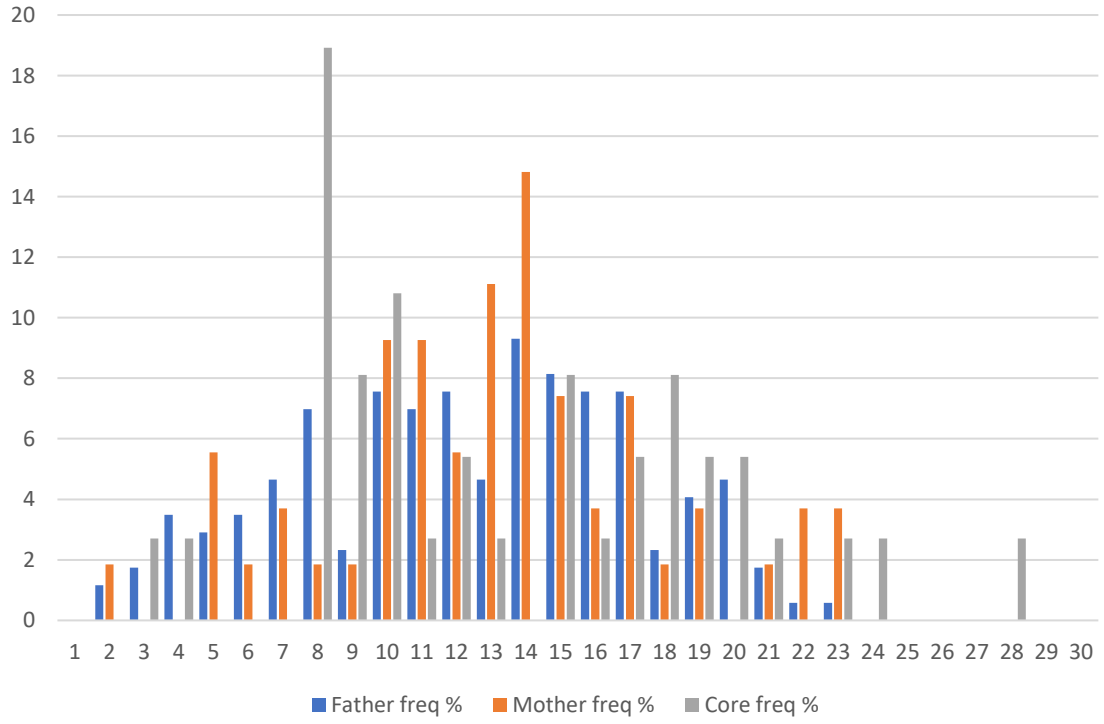

Figure 40: Family breakdown of ulnar loop ridge count

Just as loops can be differentiated by ridge count, whorls can be subcategorised as inner, meeting, and outer as part of the NCIC classification system. This can be done by tracing the first ridge originating from the radial side delta; if this ridge falls within three ridges of the ulnar side delta it is classified as "meeting", inside and outside fall internally and externally of the three-ridge threshold. An illustration of this is shown in Figure 41.

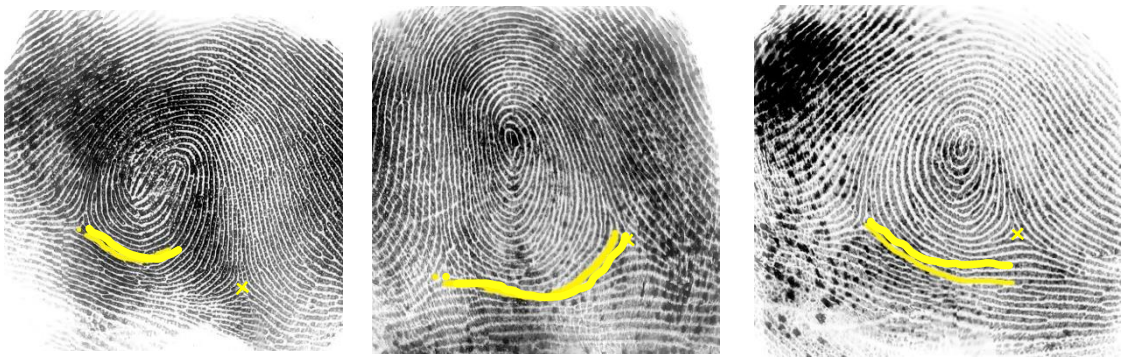

Figure 41: Examples of inner, meeting, and outer whorls on fingers of the left hand

The overall frequency shows that inner and outer ridge tracings between whorl pattern deltas are much more common than meeting patterns in the family (Figure 42). Given mirroring of fingerprint patterns on the fingers is commonly observed it was theorised that these minor characteristics may also be. Separating left and right hand observations, the meeting whorls occurrence is similar.

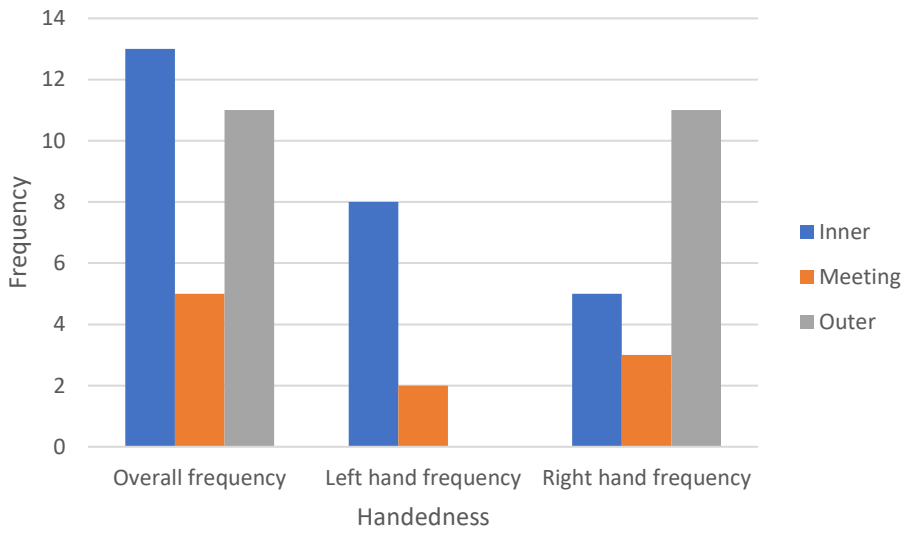

Figure 42: The frequency and locations of whorl pattern subclassifications in the family group

It must be noted the family sample is small especially given the low frequency of whorls within the families fingerprints however it compares favourably to the same data extracted from the

overall Sydney population. There is a higher frequency of inner whorls on the right hand compared to outer whorls on the left hand. The main difference is the further extreme nature of the asymmetry in outer traced whorl being on the right hand. This trend may occur due to two reasons: Mirroring of fingerprints also affects the characteristics within patterns or that whorls may have similarities to loops in that they are more common in one direction i.e. ulnar versus radial loops.

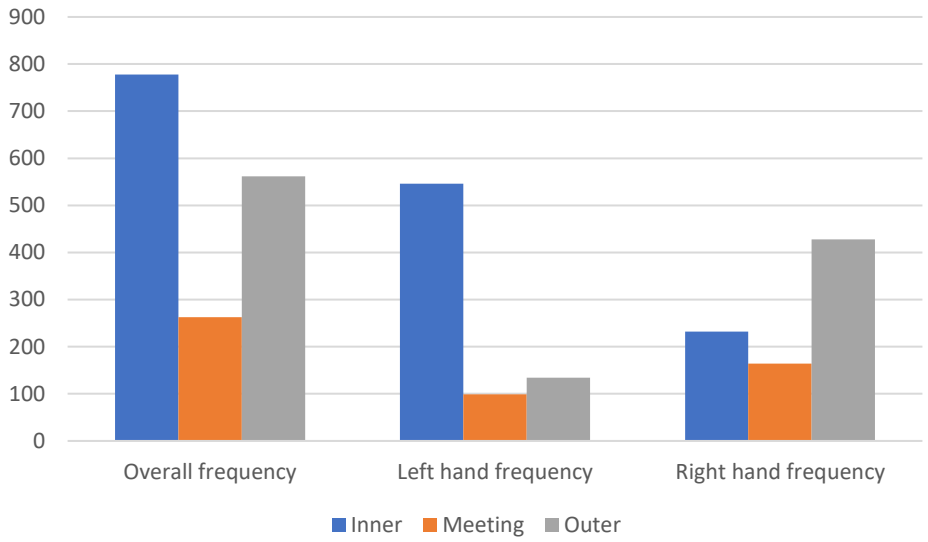

Figure 43: Frequency and location of whorl pattern subclassifications in the Sydney population

All characteristics from the overall pattern to subclassification of pattern show apparent deviation from the standard set by the overall population sample. It is possible these deviations are due to inheritance of traits, though due to the low sample size it would be troublesome to draw any definite conclusions.

5.5. Pattern inheritance

Radial loop on right index

The presence of a radial loop on the right index finger within the family is shown in Figure 44. Of the twelve occurrences, three occurred in spouses that went on to have children with those biologically linked to the family. Where a male with the phenotype had daughters, it was passed on 100% of the time. Interestingly, the heterozygotic twins did not have the same phenotype and the father's phenotype was unknown. If the 100% trend of the father passing on the phenotype to daughters was true both twins would have the radial loops on the right index finger. For the twins to have a different phenotype it must have come from the mother, which she does possess.

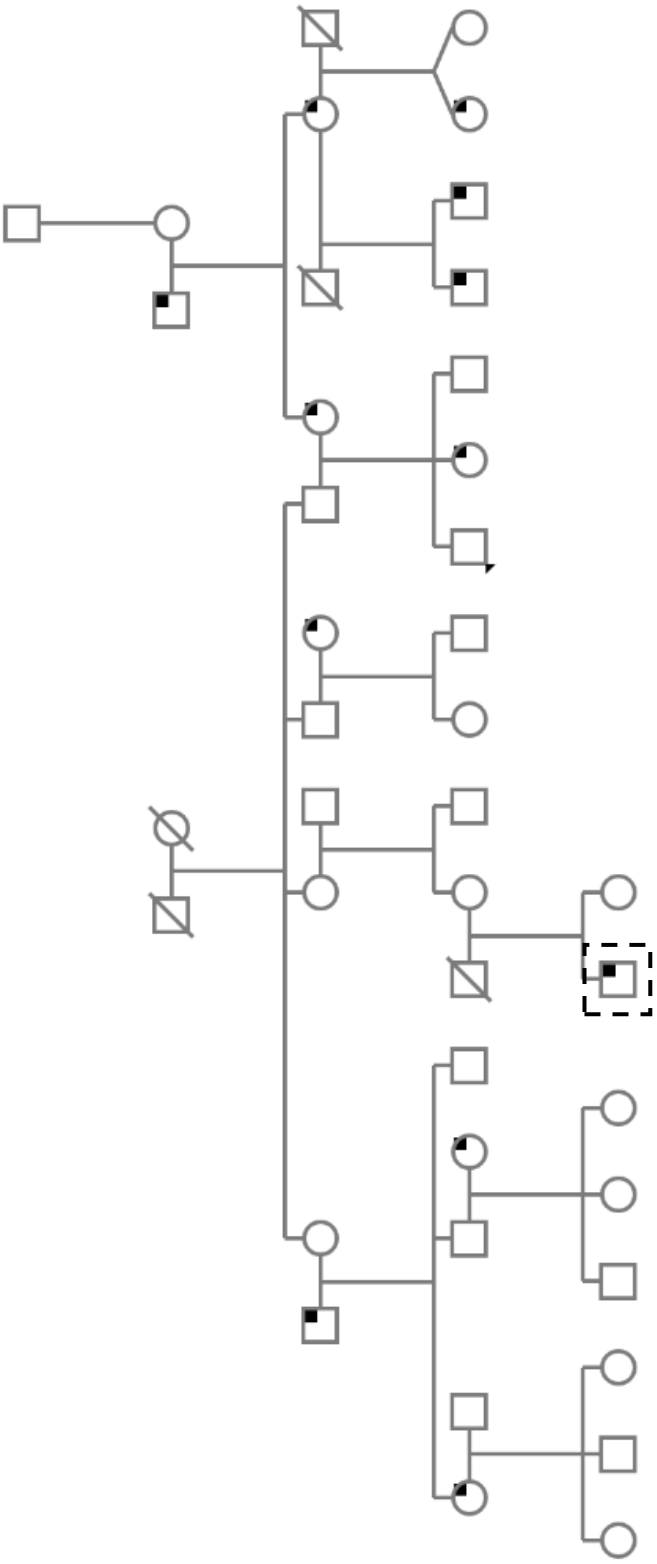

Figure 44: The presence of a radial loop on the right index finger

The inheritance pattern mostly appears to be an example of X chromosome linked dominance. This occurs where a father passes their trait via the X-chromosome given to his daughters and there is a 50% chance of the affected mother passing on the trait, this is illustrated in Table 35.

Table 35: An illustration of X-linked dominant inheritance

A)	**X**	**X**
X*	X*X	X*X
Y	XY	XY

B)	**X***	**X**
X	X*X	XX
Y	X*Y	XY

** indicates the presence of the trait*

A) Shows the method of inheritance for an X-linked dominant trait where the father is affected. The father passes the trait on to 100% of daughters and no sons.

B) Shows the method of inheritance for an X-linked dominant trait where the mother is affected. The mother passes the trait on to 50% of her daughters and 50% of her sons.

Contrary to an X-linked dominant trait is the affected male in the fourth generation of the core father's extended family (marked by a dashed box in Figure 44). His mother is unaffected, and his father's phenotype is unknown. In true X-linked dominant fashion it would not be possible for the son to inherit the trait from the father therefore the mother must be affected, which she is not. The idea of sex-linked inheritance of fingerprint patterns has been proposed before. Walker, 1941 [44] also assessed radial loops on the right index finger and uncovered examples of X-linked recessive inheritance. This study finds evidence against recessive inheritance within the core family where a radial loop occurred on the core mother's right index finger. According to X-linked recessive inheritance this would mean that both of her sons should have the same trait however both sons did not exhibit a radial loop on the right index finger.

Tented arch on right index

The presence of a tented arch on the right index finger in the family is shown in Figure 45. Of the 11 occurrences most occur in the fourth generations on each side of the family. Five of the occurrences are in females and six in males. The sparse nature of the phenotype would imply if there were any inheritance it is likely to occur recessively. It was already noted the heterozygotic twins had different patterns on the right index finger. One has a radial loop and the other a tented arch.

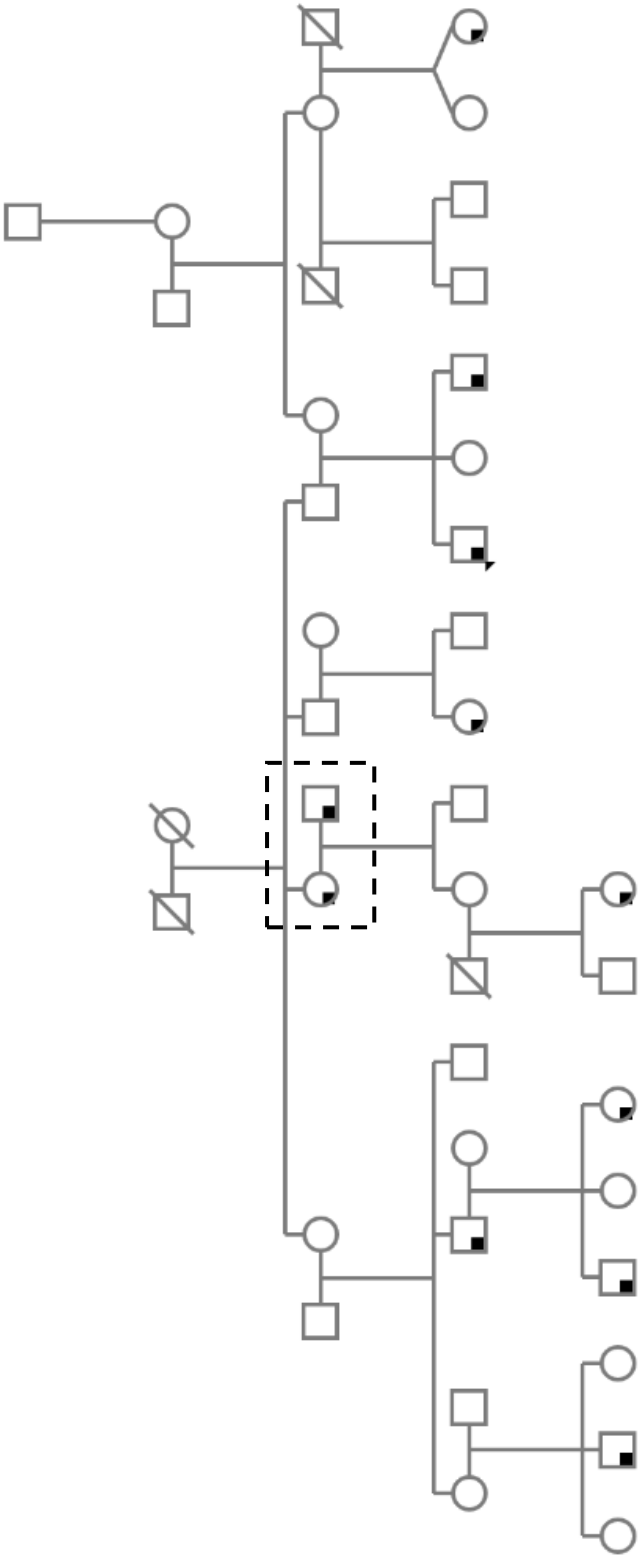

Figure 45: The presence of a tented arch on the right index finger

However, there are two occurrences of the phenotype that rule out recessive inheritance. In Figure 45 there is a couple (outlined by a dashed box) that both have the phenotype. If the inheritance of this trait was recessive both of their children must display it; neither were observed to display the phenotype.

A theory put forward is that there is a hierarchy of pattern dominance within the underlying genetics. The ulnar loop is clearly the most common pattern thus it makes sense that this is the most dominant pattern. This family is lacking in plain whorls, though in the greater population this would be the next most dominant pattern. Following this, given that one of the twins was the only sibling within that section of the family not to have a radial loop on the ring finger perhaps there is epistasis or additive effects of genes that create changeability between radial loops and tented arches.

Mirrored patterns and whorls

One of the phenotypes explored in Slatis *et al.* [53] was the mirroring of patterns between hands and fingers. The asymmetry of patterns in family members was already discussed in section 5.4, there was extreme homogeneity in pattern on the left hand. This meant only three individuals had mirrored patterns between hands. Mirroring between fingers (e.g., same pattern on both little fingers) was common however most of these occurrences were ulnar loop pairs. Because of the very high frequency of ulnar loops a method for inheritance cannot be computed from phenotype observation inheritance models.

The low frequency of plain whorls in the family compared to the greater population was also noted in section 5.4. Because of the low occurrence any model of inheritance is too sparse to interpret. A study from China in 2016 [280] analysed the inheritance of whorl patterns from parents to children in a Chinese population. The results showed that parents with a “moderate” number of whorls were likely to have children with a “high” number of whorls 26.5% of the time and children with “low” number of whorls 23.5% of the time, “which equated well to the theoretical value of 25%”. The result is interpreted to theorise that whorls are carried by a semi dominant allele where “AA” equals a high number of whorls, “Aa” equals a moderate number of whorls and “aa” equals a low number of whorls. This superficially could align with what was seen in the family, as perhaps both sides of the family carry the theoretical “low number of whorls” allele. All members in the family have two or less plain whorls on their ten fingers. If the classification for whorls was expanded to all subclassifications there would be three members that classify as having a moderate number of whorls.

Comparing the observed results of the family and Chinese study with Slatis *et al.* [53] is difficult. Slatis *et al.* proposed three different genes for whorls: a semidominant gene for whorls on thumbs, a semidominant gene for whorls on the ring finger and a dominant gene for whorls on all fingers except for an ulnar loop on the middle finger. These genes affect specific fingers whereas the Chinese proposal affects all fingers equally. Slatis' proposals align well with the frequencies of whorls on each finger in the Sydney and Melbourne populations however not in the family. Particularly a dominant gene for whorls on all fingers and an ulnar loop on the middle finger would result in this phenotype and mirroring being much more prevalent.

While the results of the 2016 Chinese study are supportive, there are concerns regarding the description of the classifications used. Patterns were classified in to two groups "regular whorl-shaped pattern" and "other". The method used to place patterns in the regular whorl shaped pattern group was not a standard procedure. The study then found that the number of whorls between spouses was significantly correlated which to this author implies whorl fingerprint patterns had an influence on the selection of a mate. It is important to note correlation does not equal causation and this conclusion which is included in the title undermines the research.

Ridge count of loops

As the ulnar loop pattern is common it is difficult to identify a method of inheritance other than it being the dominant trait. By breaking the pattern in to smaller categories using ridge counting a path of inheritance may be revealed. In the percentage frequency distribution (Figure 40) it was visualised that the core family had a disproportionate amount of ridge counts around 8-10. The ridge count of eight was seen seven times and of these, four occurrences were in the father of the core family; the other three occurred once in the spouse and two of the children. If we focus on the range from 8-10 then 38% of all ulnar loops in the core family fell in this range. In the father's extended family, it occurred in 17% of all ulnar loops and in the mother's extended family it occurred in 13% of all ulnar loops. Despite the much higher percentage for those counts the average ridge count in the core family was highest of each of the three family groups: 14 ridges against 13.1 average for the mother's extended family and an average of 12 for the father's extended family. This was due to only two ridge counts being lower the 8 in the core family.

The average ridge counts per person were calculated and displayed within the pedigree in Figure 46.

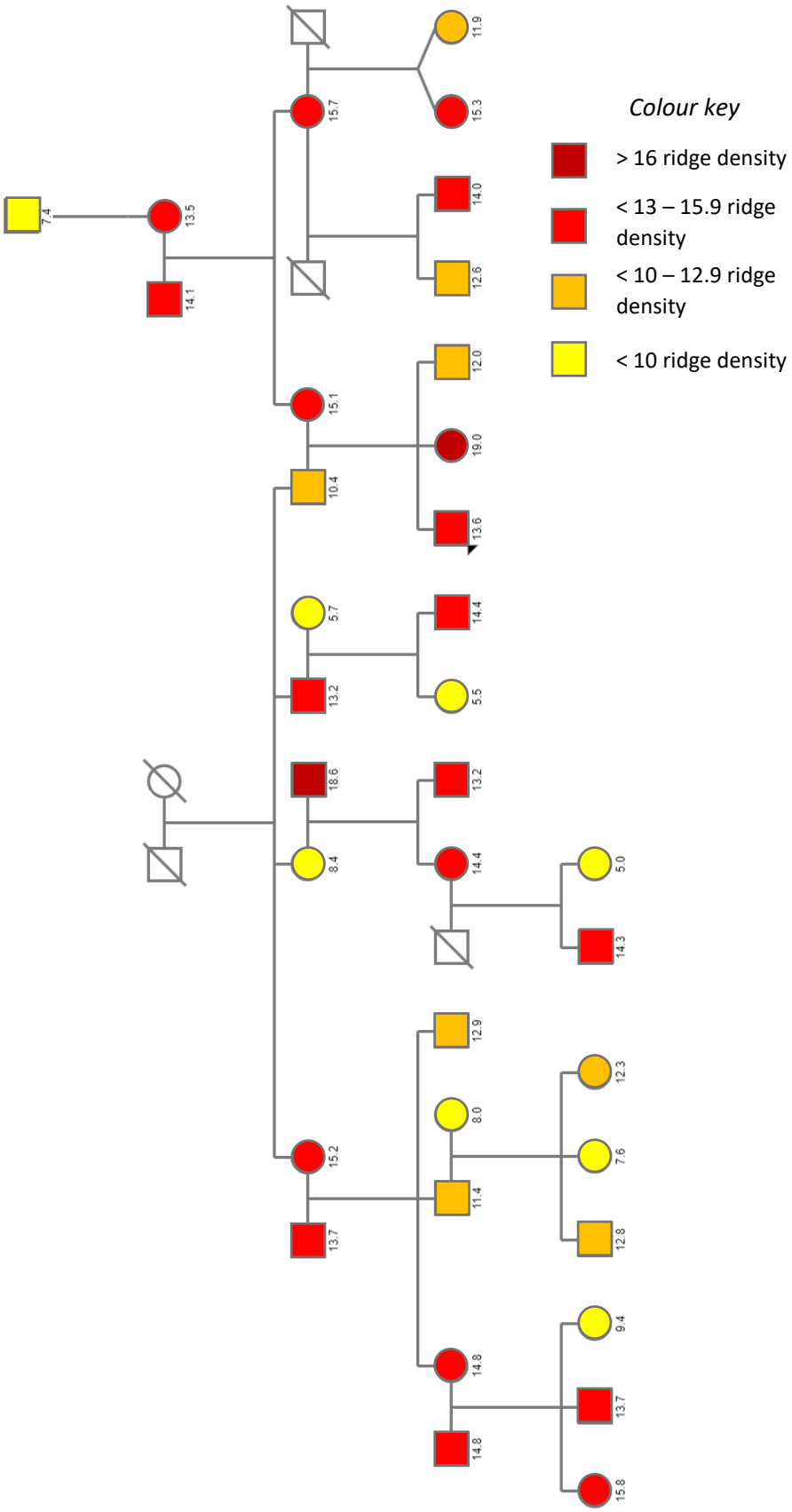

Figure 46: A family pedigree displaying the average ridge count of each person

A multiple linear regression analysis was used to examine whether there was any correlation between the average ridge count of children and parents (Table 36).

Table 36: Multiple linear regression results of correlation of average ridge density between children and parents

Model		Unstandardised Coefficients		Significance (p-value)	Collinearity Statistics	
		B	Standard Error		Tolerance	VIF
1	(Constant)	5.523	4.976	0.285		
	DAD_RC	0.204	0.300	0.506	0.980	1.020
	MUM_RC	0.387	0.193	0.064	0.980	1.020

This approach was limited by the small family size and was exacerbated by several parents not being fingerprinted. The output of the multiple linear regression showed that both mother's and father's ridge count were insignificant ($p > 0.05$) as predictors of the children's ridge count. The tolerance of each independent variable is 98% meaning that only 2% of variance can be covered by the other variable and the variance inflation factor is 1.02 for each independent variable suggesting low collinearity. Finally, the R^2 value of 0.22 indicates that 22% of the variation in the children's ridge count can be explained by the model containing the mother and father's ridge count (Table 37).

Table 37: Multiple linear regression results explaining the variation in children's ridge counts

Model	R	R Square	Adjusted R Square	Standard Error of the Estimate
1	0.466[a]	0.218	0.113	2.96941
a. Predictors: (Constant), MUM_RC, DAD_RC				

There does not appear to be any clear method of inheritance of ridge count when viewing the inheritance tree or when viewing the regression analysis results. It may be that overall pattern type is largely controlled by genetics while the ridge count along with minutiae are more controlled by the environmental pressures *in utero*, which is supported by the low R^2 score. Ultimately, examining such a complex trait with simple phenotype observations can only provide surface level information on inheritance. Gene-wide association studies on large populations are needed to provide any definitive answer on the inheritance of fingerprint characteristics.

Chapter 6 – SNP ASSOCIATION WITH FINGERPRINT PATTERNS

6. SNP association with fingerprint patterns

The previous chapter showed indications of inheritance of fingerprint patterns. However, there were some conflicting observations that did not align with predicted phenotypes. This chapter delves deeper into the relationship between fingerprint phenotype and the genotype by using a large-scale association approach. Previous publications have found fingerprints to be polygenic but also the genes are believed to be in epistasis [53-55].

The scope of this chapter covers aims one and four of this project, which were:

Aim 1: Assemble a repository of fingerprints and DNA samples from approximately 500 volunteers alongside sex and self-reported biogeographical data.

Aim 5: Extract, quantify and genotype collected DNA and perform SNP association analysis utilising R packages (SNPassoc and qqman) plus generalised liner models to identify SNPs that influence fingerprint phenotype.

Specifically, this chapter focusses on the results of the following steps and experiments:

- Sample collection including fingerprints, DNA, and ancestry information
- Classification of the fingerprints
- Association of the fingerprint phenotype to the genotype

6.1. Introduction

Single nucleotide polymorphisms (SNPs) are one of several common variations found within human DNA. SNP markers are typically bi-allelic base substitutions and occur approximately once every few hundred bases across the entire three billion base length human genome [281]. The HapMap project, a seven-year study which aimed to document common patterns of human genetic variation yielded approximately 3.2 million tag SNPs representing 25-35% of common variations across several populations [282]. A tag SNP is a SNP that is representative of several nucleotide markers. When one allele of a tag SNP is present or inherited, it implies the presence of many other alleles (haplotype) in nearby marker positions [115]. Utilising tag SNPs reduces the number of markers needed to be genotyped making investigations more cost and time efficient.

The “1000 Genomes Project”, launched in 2008, aimed to investigate the structural variations and SNPs in the genome (among other aims) to gain insight into the nature of genetic diversity

[283]. To date the study has genotyped over 15 million single nucleotide polymorphisms, 1 million short insertions and deletions, and 20,000 structural variants, most of which were novel [283].

Over recent years the use of SNPs in a forensic context has increased particularly in investigate genetic genealogy while still being a peripheral DNA technique [284]. The abundance, low mutation rate and short length of SNPs coupled with the development of highly accurate sequencing technology has made the markers useful for typing small and highly degraded forensic samples [285].

Additionally, ancestry and phenotypic prediction has changed forensic investigations markedly. Where traditional forensic methods use STRs, which provide a result for comparison to a reference sample, SNPs can be used to "paint a picture" of an individual's appearance. Through association studies phenotypes have been attributed to numerous SNPs, and the presence of particular alleles can indicate the DNA donor's ancestry or externally visible characteristics such as hair colour, eye colour and skin colour [143].

6.2. R packages – SNPassoc and qqman

'SNPassoc' [253, 286] is a specifically designed R programming package designed for use in large scale genotyping projects. The package facilitates data manipulation, exploratory data analysis of missing data and Hardy Weinberg Equilibrium (HWE), the graphical display of data and the assessment of gene wide genetic association of traits.

This package has been utilised in this study to simplify the process of carrying out a large-scale association study. SNPassoc can also run the permutations of multiple genetic models concurrently. Co-dominant, dominant, recessive, over-dominant and log-additive models are provided where there are relatively small datasets. For this study, given over 640,000 SNPs have been typed with the Illumina Infinium Global Screening Array-24 v1.0 (Table 2, p45), this was not an option as the association function was computationally limited. Two options are available to circumvent this issue. Firstly, the computing time can be reduced by parallelisation of the computation and secondly specifying which singular genetic model to compute. The parallelisation approach was taken using the "scanWGassociation" function from the GitHub version 2.0-2 of SNPassoc [287].

The package has an inbuilt function for producing Manhattan plots however when produced it was found to incorrectly order the chromosomes. The Manhattan plots were therefore

constructed for each genetic model using the "qqman" R package [254]. While not being as condensed, this package corrected the disordered chromosomes and allowed additional adjustments to be made to threshold lines and annotation of significant SNPs.

The code used is located in Appendix I.

6.3. Descriptive analysis

The genotyped group were all selected from the Sydney cohort where individuals self-reported their grandparent's ancestries. Unfortunately, due to limited funds not all the sampled individuals could be genotyped. The genotypes were therefore restricted mainly to individuals with self-declared European ancestry. Volunteers were placed into these categories based on the self-reporting of the grandparent's ancestries. Where all four grandparents were of the same ancestry an individual was classified as that ancestry. Where one to three grandparents are of the same ancestry an individual is classified as "mixed" ancestry. Within the genotyped sample of 207, 189 had European ancestry, 11 had mixed Middle Eastern and European ancestry, and seven had Middle Eastern ancestry. Of the 207 genotyped volunteers, 146 were female and 61 were male. While European and Middle Eastern ancestries were genotyped, it is theorised that pattern association to SNPs and alleles would occur in other ancestries though possibly to different SNPs. Population specific allele frequency and rare polymorphisms would result in the differing fingerprint pattern frequencies observed between populations.

After cleaning and manipulating the data into a usable format, the SNPassoc package was used to explore missing data and determine which SNPs were in Hardy-Weinberg Equilibrium.

6.3.1. Missing SNP data

There were 623,586 SNPs autosomal SNPs genotyped. Once polymorphisms that had no readings were removed there were 623,161 SNPs. The remaining data was plotted to visualise missing readings (Figure 47), when viewing the figure each point represents missing SNP data. There is significant drop out in two volunteers out of the 207 volunteers likely due to a low quality DNA sample. There was also two SNPs that have a significant percentage of missing readings that were removed from the analysis. Despite the missing readings a large proportion of the SNPs were still read.

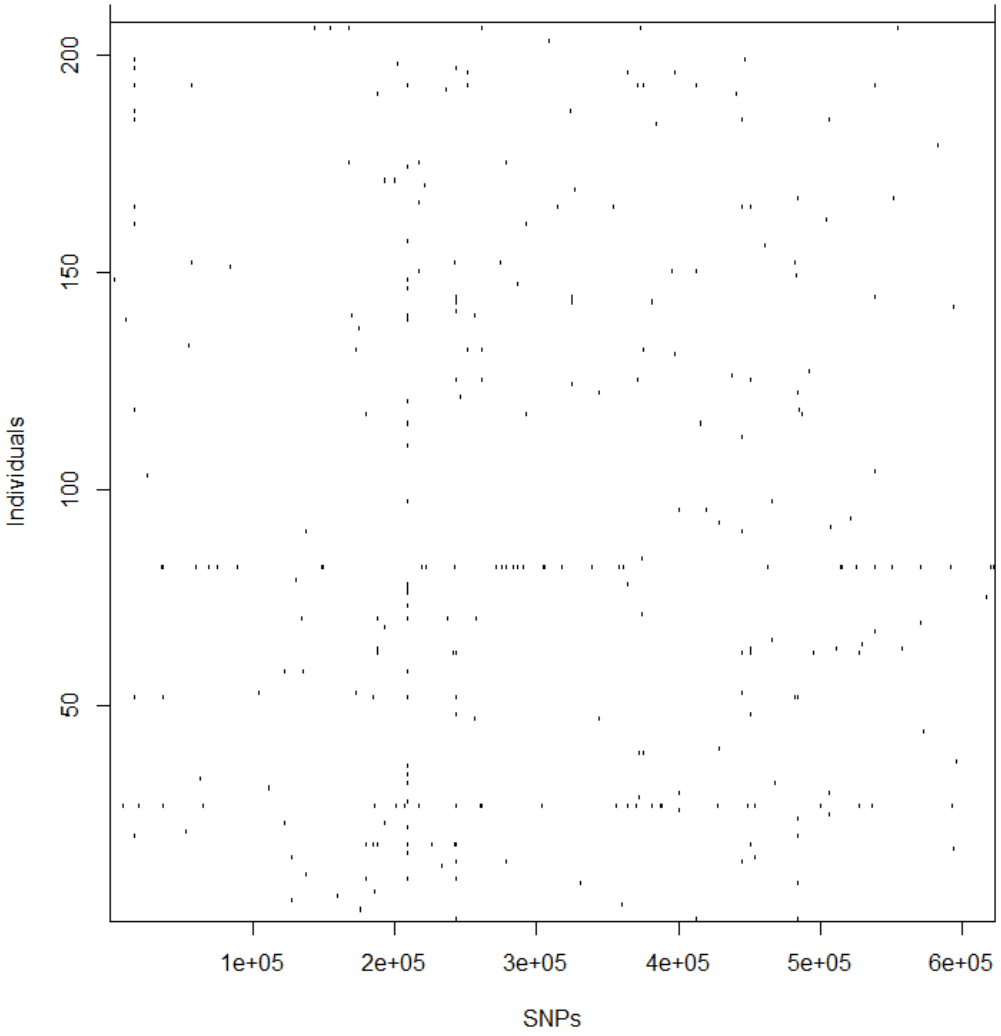

Figure 47: Missing SNP data from the genotyped samples

6.3.2. Hardy-Weinberg Equilibrium

Hardy-Weinberg equilibrium is a principle stating that allele and genotype frequencies within a population over multiple generations will remain constant if several assumptions are met. One prerequisite for the population to reach equilibrium is random mating. When a population is large enough, HWE can be approached.

HWE is rarely applied in reality as outside factors commonly disrupt equilibrium. Outside factors include non-random mating, mutations, natural selection, genetic drift, and gene flow. HWE is therefore best considered to be an idealised state with real populations deviating from the ideal. Checking HWE is also a method for quality control in large scale association studies where it is used to determine if a genotype can be a sequencing error, or to infer population structure. When ratios of the heterozygous and homozygous genotypes are significantly different to those predicted under HWE assumptions, it can be indicative of genotyping errors, population

structure or more rarely, association. If the genotypes are outside of the expected ratio, they can be excluded from the association study though a decision needs to be made on the threshold for exclusion.

HWE threshold settings can differ between the control group and the case group, and the SNP HWE were stratified accordingly. The case group displays the phenotype, and the control does not display the phenotype. These two groups are needed to demonstrate the effect a variable has on a dependent variable and to strengthen results. Often thresholds are less stringent in cases than those in controls. SNPs were required to be in HWE only in the control group, as the violation of the HWE law in cases can be indicative of true genetic association with the phenotype. SNPs were selected for association analysis using a fast exact test in the SNPassoc package. The threshold for selecting SNPs was a p-value greater than 0.001 for the null hypothesis of no deviation from HWE, as several SNPs are being tested and multiple comparisons are being made. After selecting SNPs adhering to HWE there were approximately 292,000 SNPs used for association analysis. This number varied by a few hundred as the stratification meant SNPs were in HWE for some phenotypes and not others.

6.4. Association of pattern

Each general fingerprint pattern (loop, whorl, and arch) was assessed for association for each finger. Pattern phenotypes of interest were also selected from the distribution of pattern outlined in section 3.4. The phenotypes were checked for association for multiple genetic models: dominant, codominant, overdominant, recessive and log-additive – definitions of each model given two SNP alleles A and B are below.

A *dominant* model is where one allele in a SNP is required for an increased risk of the phenotype. If B is the dominant phenotype allele, AB and BB will have the phenotype and AA will not.

A *recessive* model is where two copies of one allele in a SNP are required for increased risk of the phenotype. Therefore, if A is recessive AA will have the phenotype and AB and BB will not. The individual with the genotype AB is termed a "carrier".

An *overdominant* model is where the heterozygote phenotype lies outside of the typical phenotype range determined by either alternate homozygote genotypes (AA or BB).

A *codominant* model means that neither allele is recessive. An AA homozygote may have one phenotype and a BB homozygote another. A heterozygote (AB) may have a blend of both phenotypes. Similarities can sometimes be seen in SNP association results between the

codominant and recessive models as homozygotes with the same phenotype can fit both models.

A *log-additive* model is one where there is a dichotomous, quantitative phenotype. In the case control approach the investigated phenotype is a 1 and all others are 0. An additive effect occurs where an AB heterozygote has an *x*-fold increased risk of the phenotype, and the BB homozygote has a 2*x*-fold increased risk of the phenotype. There can also be additive alleles in polygenic traits where each add together to make the observed phenotype.

The association of pattern is limited by the number of whorls and arches in the genotyped population. Where there is a larger genotyped population more statistically significant SNPs can be found. A suggestive association threshold was set at 1.00×10^{-5}; this was a low default threshold in the SNPassoc package which was used due to the number of individuals genotyped. For significant association, a Bonferroni correction (=0.05/No. of SNPs) was used as multiple comparisons are being made. The number of SNPs changed slightly per phenotype due to HWE selection criteria however the threshold was always approximately 1.71×10^{-7}.

Thirty-nine different phenotypes were assessed for association. These were:

- “Eight or more loops”
- “Eight or more ulnar loops”
- “One or more radial loop”
- “Radial loops on both index fingers”
- “Eight or more whorls”
- “Whorls on both thumbs”
- “Whorls on both ring fingers”
- “One or more arches”
- “Arches on both index fingers”
- Loops, whorls, and arches for each single finger (30)

Within sections 6.4.1 and 6.4.2 only significant results, areas of adjacent SNPs of suggestive significance and erroneous results are shown and discussed. All SNPs that passed the suggestive and significance thresholds are tabulated in Appendix J and all Manhattan plots are in Appendix K.

6.4.1. Multiple finger phenotypes

Radial loops on both index fingers

The most striking distribution of pattern is the locations of radial loops on the index finger. Individuals that had a radial loop on both the left and right index finger were selected for phenotype association. This was one of the rarest phenotypes assessed with only 13 of the 207 individuals possessing it. The low frequency of this phenotype is an issue for association as it can make the potential for chance association to occur much higher. The log-additive model was the only model to have SNPs pass the Bonferroni significance threshold. Among the four other models, nine SNPs only passed the suggestive threshold (Appendix J). The significant SNPs for the log-additive model are displayed in Table 38 below.

Table 38: Significant SNPs for the log-additive model of radial loops on the index fingers

SNP	**p-value**
rs41269369	4.74×10^{-11}
rs7333557	2.09×10^{-8}
rs17068763	2.09×10^{-8}
rs75950241	3.50×10^{-8}
rs117116926	3.50×10^{-8}
rs76437304	1.18×10^{-7}
rs7650693	1.44×10^{-7}
rs16833596	1.44×10^{-7}

Viewing the Manhattan graph of the log-additive model for this phenotype, the proximity of the SNPs to one another can be seen; three of the SNPs overlay one another (Figure 48).

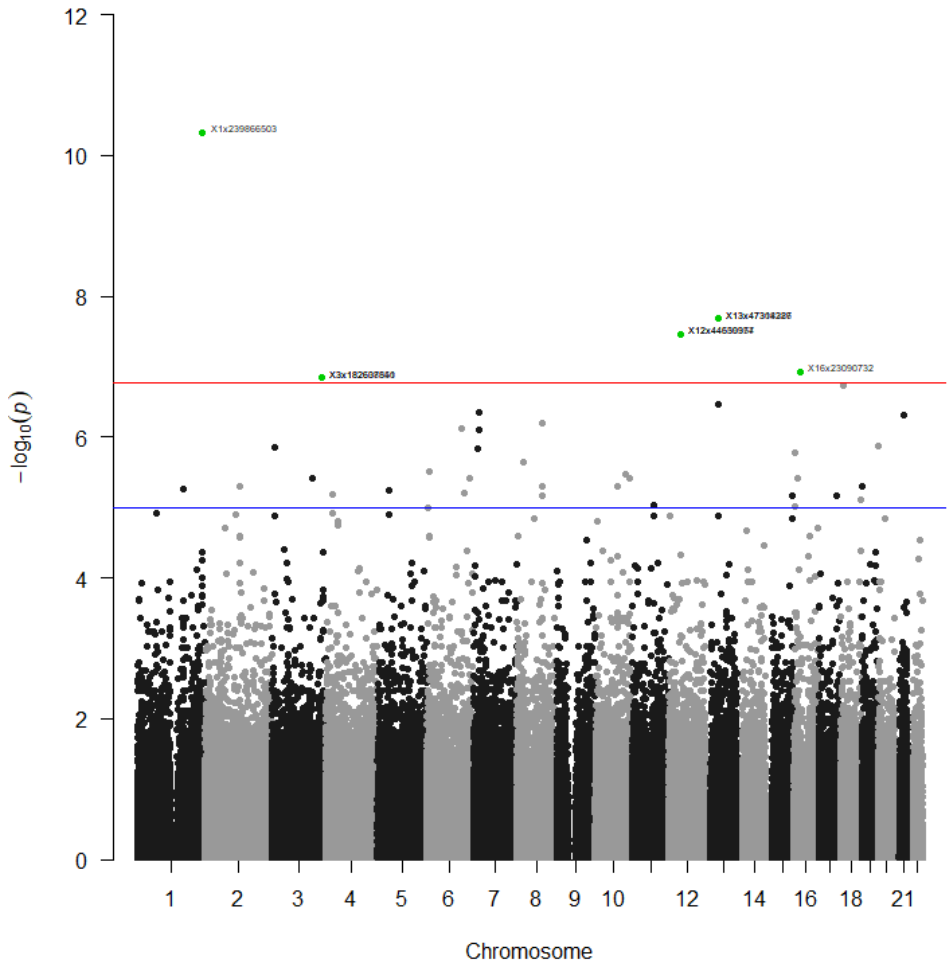

Figure 48: Log-additive model of SNP association to the radial loop on index fingers phenotype

The -log_{10} p-values for association of each individual SNP are plotted against the Y-axis and SNP location on the X-axis. Each mark represents a SNP however some are overlayed. This is evident in the eight significant SNPs where only five are visible as three are overlayed. The blue line represents the suggestive threshold of 1 x 10^{-5} and the black line represents the Bonferroni significance threshold of 1.71 x 10^{-7}. The SNPs are annotated with codes for their location in the genome – "X(chr)x(bp)".

When observing rs41269369 (X1x239866503) on chromosome one it can be seen how both the rarity of both the phenotype and the G allele make the SNP potentially appear significant by chance (Table 39). This occurs similarly in the other significant SNPs though in a less extreme manor. The log-additive model produced the most significant results as it appears the G allele could increase the likelihood of possessing radial loops on both index fingers.

Table 39: Genotypes and occurrence of the phenotype in rs41269369

Genotype	No radial loops on index'		Radial loops on index'	
	Frequency	Percentage	Frequency	Percentage
A/A	184	94.8%	6	46.2%
A/G	10	5.2%	6	46.2%
G/G	0	0.0%	1	7.7%

The assessment of association for each individual finger, particularly for the general loop patterns is less likely to be affected by low frequency as the ulnar loop is the most common pattern. Instead, the frequency of control cases, those without loops on the little fingers is an issue. Ideally, the case group (with the desired phenotype) and the control group are even.

Eight or more whorls

The first whorl phenotype assessed was eight or more whorls on an individual's fingers. This was exploratory in nature as there were 11 people out of the 207 with the phenotype, meaning the groups were uneven and more likely to produce chance significance. The results showed similarities to the radial loops on index fingers as the log-additive model had numerous SNPs pass the significance threshold. The overdominant and recessive models had no SNPs over the suggestive threshold. The dominant model showed rs1339062 (p = 4.45 x 10^{-8}) to be over the Bonferroni threshold and was shared by the codominant model (p = 3.15 x 10^{-7}). rs1339062 is clearly higher than the five SNPs that passed the suggestive threshold in the dominant model. The suggestive SNPs were on chromosome four, five and six. Assessing the significant SNP in more depth, the alleles (C, T) have a roughly even frequency and in the dominant model all people with more than eight whorls possessed the CC homozygote (Table 40).

Table 40: Distribution of the phenotype per genotype for rs1339062 in a dominant model

Genotype	**Less than 8 whorls**		**More than 8 whorls**	
	Frequency	**Percentage**	**Frequency**	**Percentage**
C/C	46	23.6%	11	100.0%
C/T-T/T	149	76.4	0	0.0%

Such uneven distribution of the phenotype amongst the three genotypes deserves further attention and analysis with a larger and more even dataset between the case and control groups. The log-additive model does not find rs1339062 significant, instead there are eight SNPs spread across the genome (Figure 49).

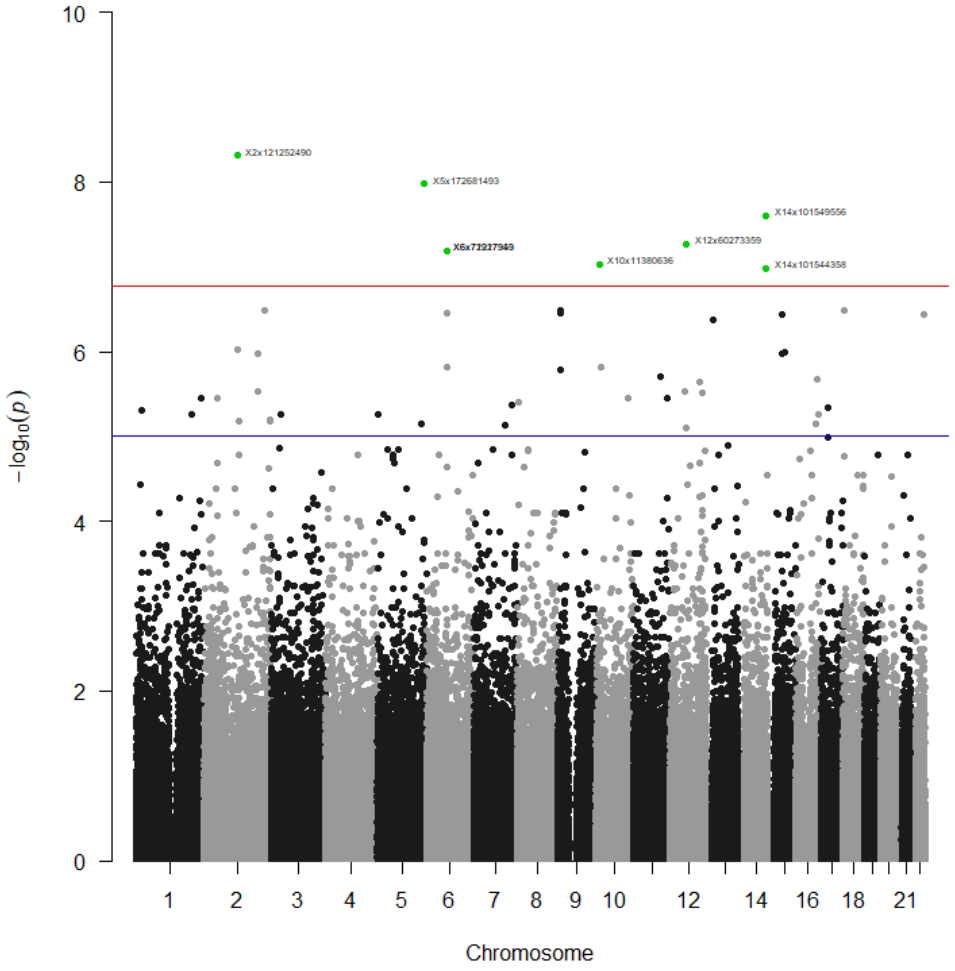

Figure 49: Manhattan plot of SNPs for the "eight or more whorl" phenotype for the log-additive model

The most significant of these is rs114125518 (p = 4.86 x 10^{-9}) however the genotypes are highly uneven in their in their frequency. The C allele occurs 408 times with the A allele occurring 6 times. The phenotype occurs in the singular AA homozygote and twice in four occurrences of the CA heterozygote and eight times in the 202 occurrences of the CC homozygote. Where the A allele is present the rates of the phenotype are higher, however it is much too rare with not enough phenotype observations to draw any strong conclusions. Similar observations are made though with less extreme allele frequency imbalances in the seven other significant SNPs under the log-additive model.

At least one arch

The arches phenotype is the most uncommon of the three general fingerprint patterns therefore chance association is more likely, particularly in the log-additive model as seen previously. To account for this the more common phenotype of displaying at least one arch was assessed. There were no SNPs that were over the Bonferroni significance threshold. The overdominant

model did not return any suggestive SNPs and the recessive model had one SNP, rs28506195 (p = 7.52 x 10^{-6}). The codominant model had four SNPs over the suggestive threshold, rs2443426 (p = 2.90 x 10^{-6}) and rs1447177 (p = 3.73 x 10^{-6}) both on chromosome 11 and, rs356969 (p = 8.60 x 10^{-6}) and rs259929 (p = 8.60 x 10^{-6}) both on chromosome 6 (Figure 42). Each of these SNPs were also found to be over the suggestive threshold for dominant, recessive and log-additive models.

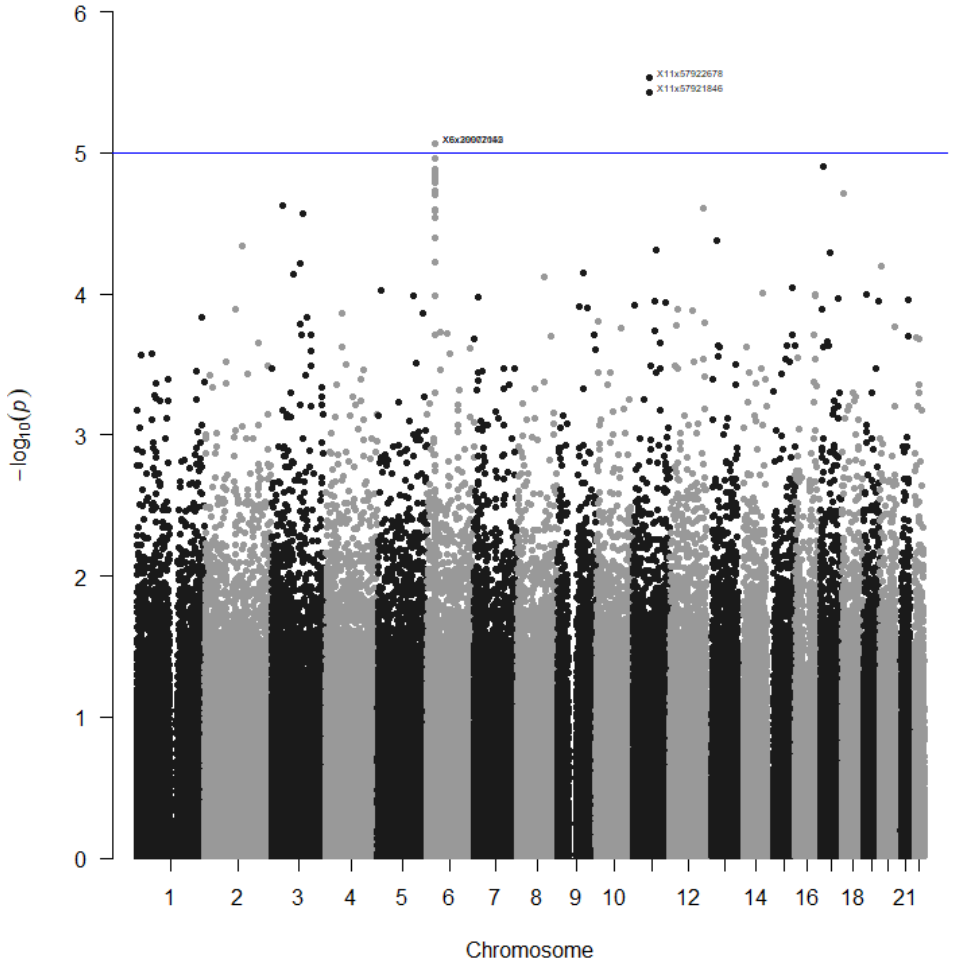

Figure 50: P-values suggesting association to phenotype of at least one arch pattern for the codominant model

Interestingly, a clustered area on chromosome 6 and two SNPs (not the same) from chromosome 11 over suggestive threshold were the same as results seen in the analysis on loops on the left thumb. When assessing the chromosome 11 SNPs independently the dominant model fits the data better than the codominant model, evident by the lower Akaike information criterion [288]. The lower AIC means the model strikes a greater balance between fitting and

over-fitting the dataset. In Table 41 and Table 42, the frequency of the phenotype per genotype for the dominant model is shown. Both SNPs shown an increased likelihood of displaying at least one arch on the fingers if the individual possesses the C allele.

Table 41: Frequency of the phenotype per genotype in the recessive model for rs2443426

Genotype	**No arches**		**One or more arches**	
	Frequency	**Percentage**	**Frequency**	**Percentage**
T/T	68	50.0%	11	15.5%
C/T-C/C	68	50.0%	60	84.5%

Table 42: Frequency of the phenotype per genotype in the recessive model for rs1447177

Genotype	**No arches**		**One or more arches**	
	Frequency	**Percentage**	**Frequency**	**Percentage**
A/A	68	50.0%	11	15.5%
C/A-C/C	68	50.0%	59	84.3%

While the two chromosome 11 SNPs have the lowest p-values, the SNPs of chromosome 6 also stand out. These SNPs are the peak of an area that have heightened association that centre around the 30,000,000 base position and span multiple genes at 6p22.1. This is the exact area which was of interest with loops on the left thumb though more concentrated to a narrower area. A more focussed view of the region is shown in Figure 51 which makes clear that not every SNP in the area has a heightened association.

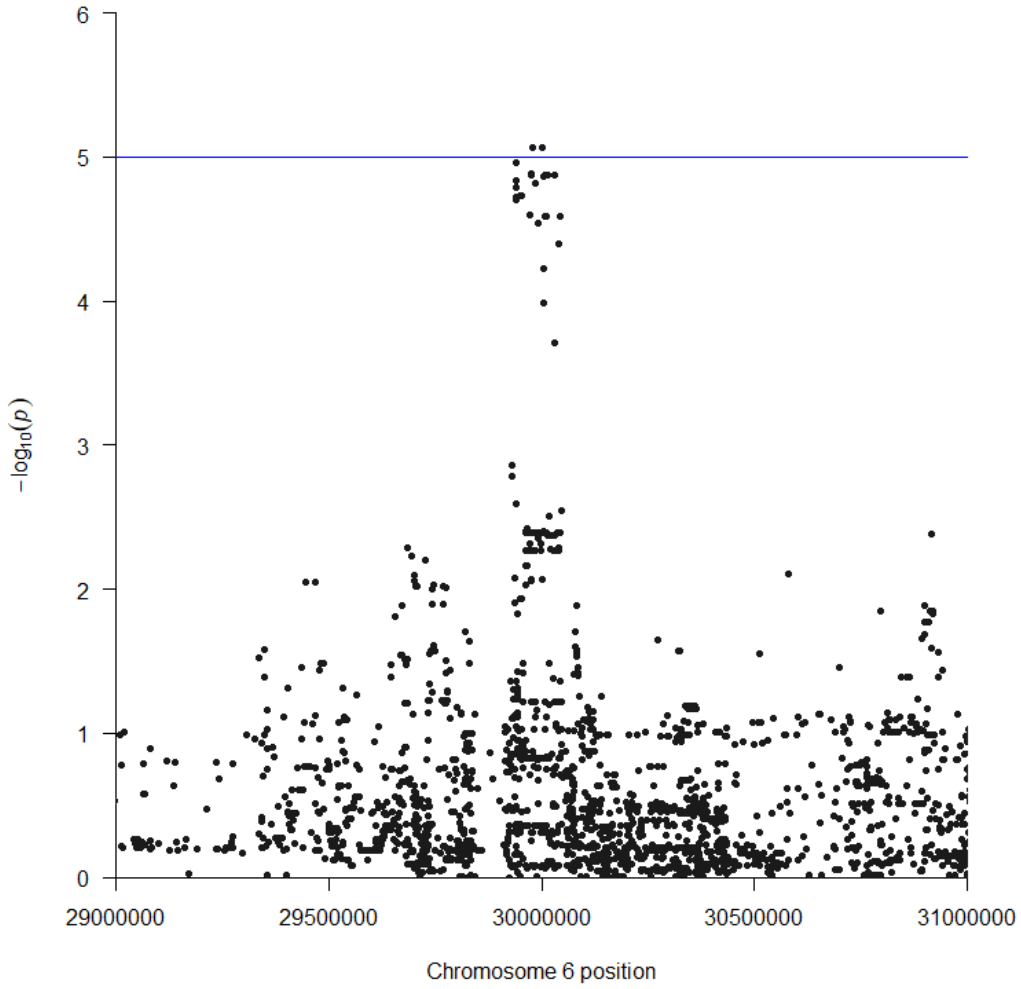

Figure 51: A subsection of chromosome six p-values suggesting association to phenotype of at least one arch pattern for the codominant model

The peaks on chromosome 6 occur at rs356969 (p = 8.60 x 10^{-6}) and rs259929 (p = 8.60 x 10^{-6}). These SNPs are both located in the ZNRD1ASP gene which has been linked to endometrial and cervical cancer plus differing white blood cell counts [289].

6.4.2. Single finger phenotypes

Thumbs

The only significant result on the thumbs is the display of arches on the left thumb. This phenotype occurred in 13 instances out of the 207 individuals. This is too low to produce a reliable result as chance correlation increases dramatically with smaller sample sizes. A common pattern was seen in the log-additive model where low frequency phenotypes were assessed. Numerous SNPs were observed passing the significant and suggestive thresholds (Figure 52).

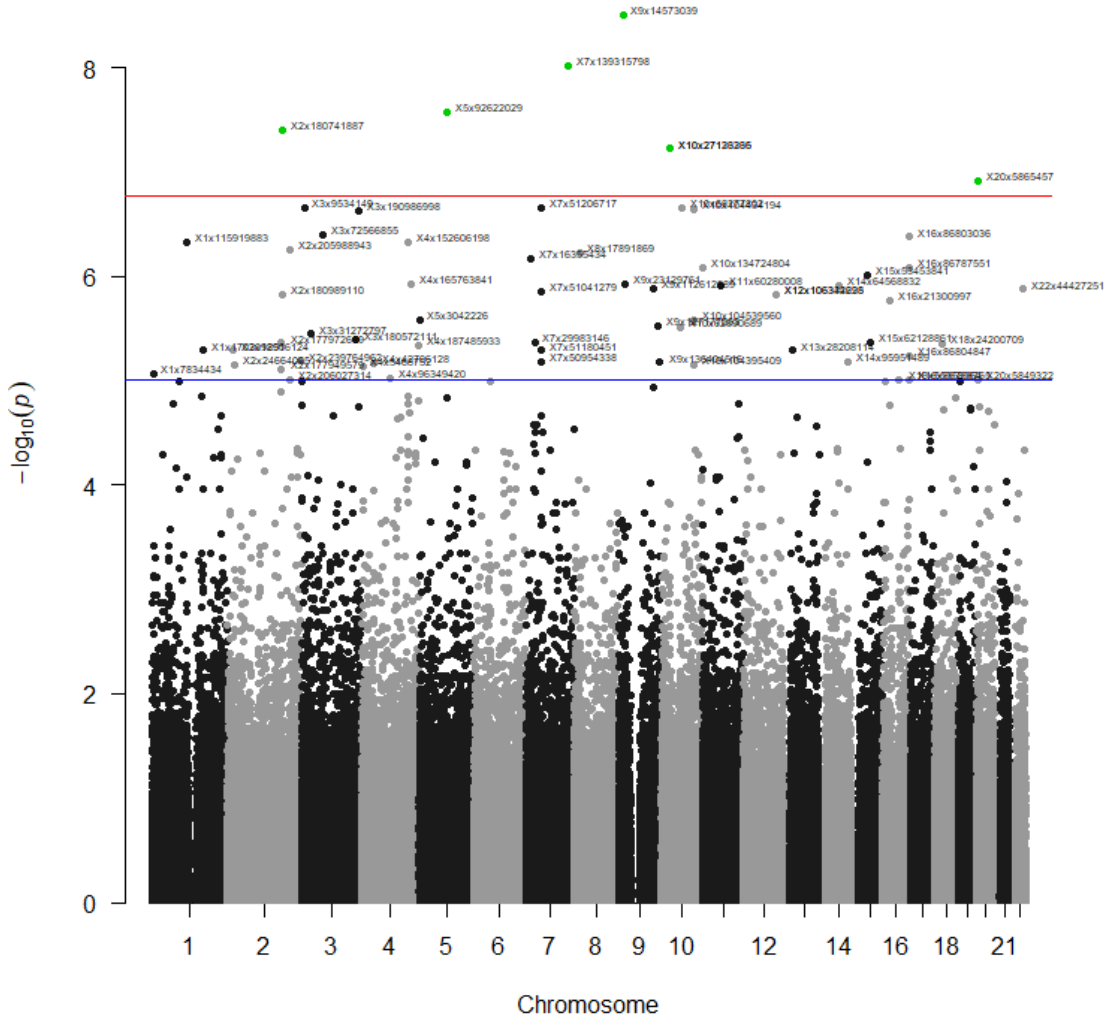

Figure 52: Manhattan plot of SNPs for arches on the left thumb for the log-additive model

The SNP with the lowest p-value is rs76586700 (X9x14573039) located on chromosome 9. Analysing the distribution of the genotype according to phenotype shows that the 12 examples of an arch on the left thumb occur in a higher ratio of people with the A allele (Table 43).

Table 43: Frequency of the phenotype per genotype for rs2891225 in the dominant model

Genotype	**Arch not on LT**		**Arch on LT**	
	Frequency	**Percentage**	**Frequency**	**Percentage**
G/G	176	90.3%	5	41.7%
G/A	19	9.7%	5	41.7%
A/A	0	0.0%	2	16.7%

There is an indication of a relationship between the A allele and arches on the left thumb. This is however undermined by low frequency of the phenotype and the highly uneven genotypes. The SNP is not reported to be located in a particular gene or have a known function or consequence, though is upstream of NFIB, a gene that is essential for brain development, and downstream of ZDHHC21, which catalyses the addition of palmitate onto various protein substrates. Palmitoylates in turn play a key role in epidermal homeostasis and hair follicle differentiation [290, 291].

Both the left (LT) and right thumb (RT) phenotypes produced no significant associations with the genotypes. However, both had areas where groups of SNPs had a noticeable decrease in p-value; the peaks of these areas passed the suggestive line. For the left thumb, this area was located on chromosome 6 and can be seen in Figure 53. The peak SNPs are rs35128564 ($p = 8.28 \times 10^{-6}$) and rs13193532 ($p = 8.59 \times 10^{-6}$), while the allele frequencies are uneven the number of elevated SNPs helps support the notion that this area may have legitimate association. This is in contrast to the SNPs with the smallest p-value on chromosome 11, rs55979208 ($p = 5.22 \times 10^{-6}$) and rs67485448 ($p = 9.33 \times 10^{-6}$) which while adjacent to one another are clear of any other SNPs in the chromosome. These are the same areas that were significant for “at least one arch pattern”.

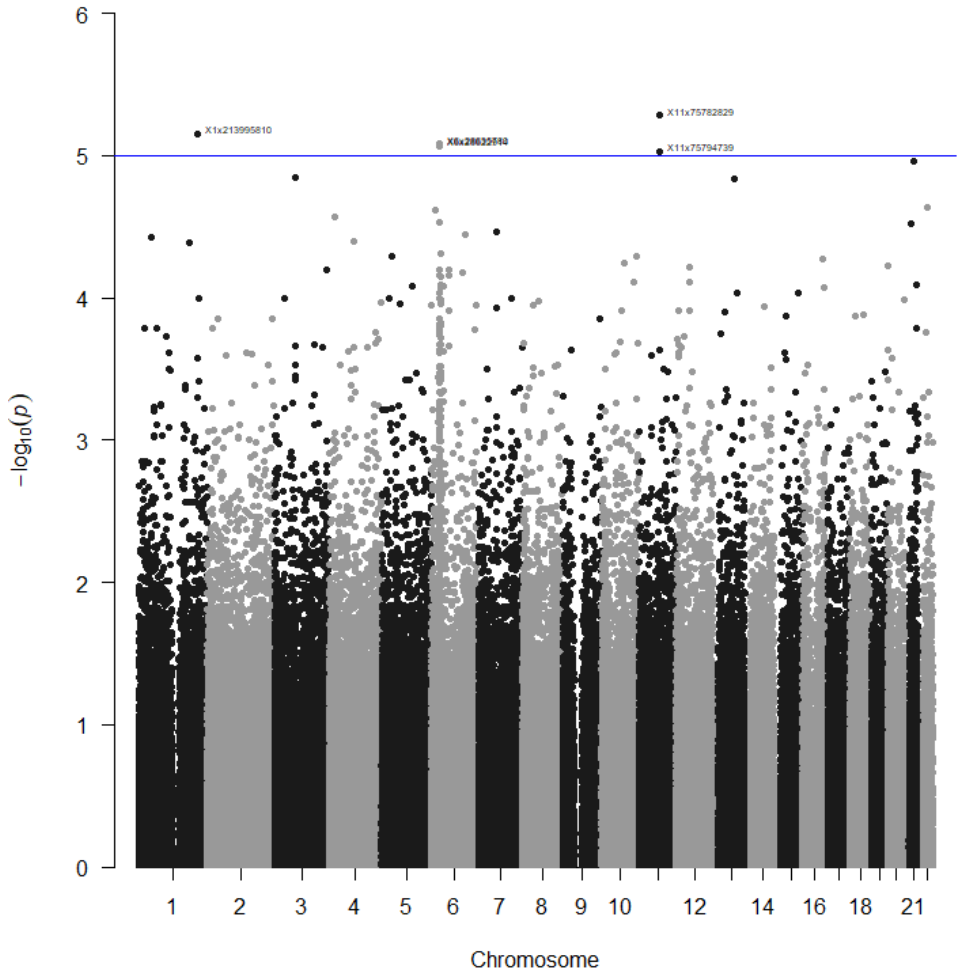

Figure 53: Manhattan plot of SNPs for loops on left thumb for the dominant model

Focussing on the area on chromosome 6 (Figure 54) shows that the two suggestive SNPs are located at the start of the raised area. This area is located between two tRNA genes in 6p22.1 which has been linked to schizophrenia and contains a several immunity genes. While this area has been linked to schizophrenia, a link between fingerprints and this disease has been investigated twice previously, with each study returning no relationship [72, 73].

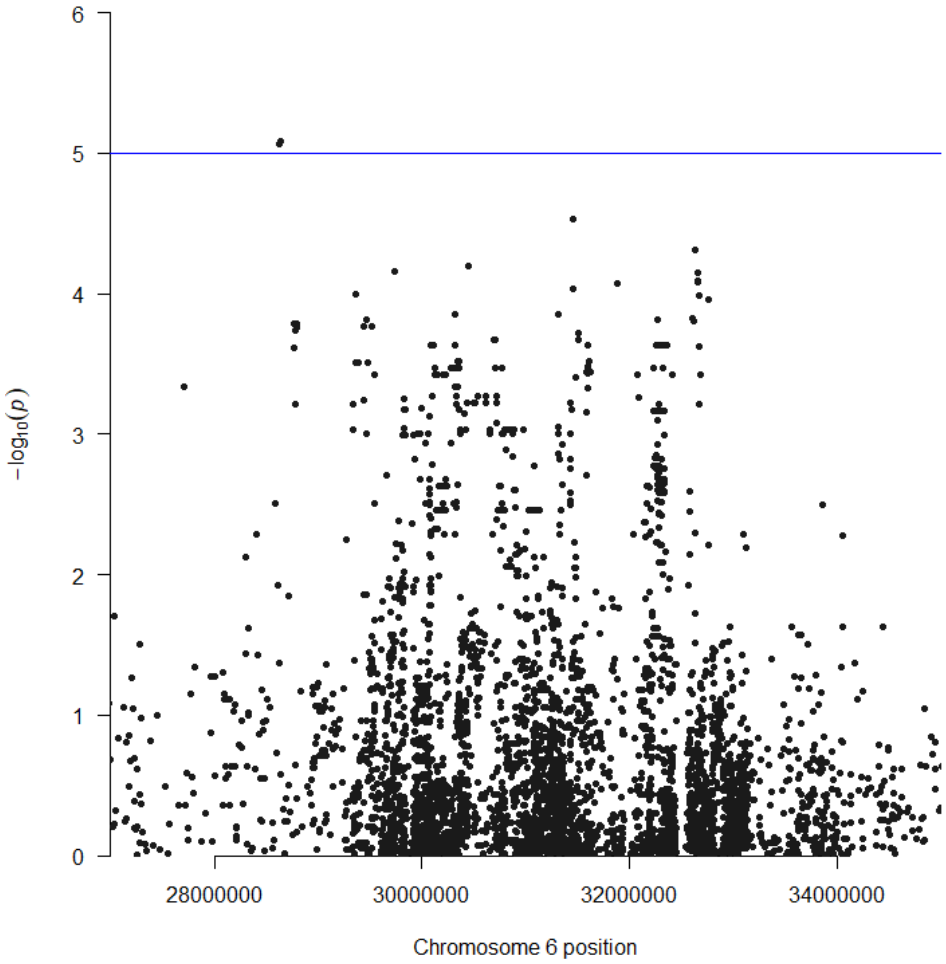

Figure 54: A subsection of chromosome 6 displaying an area of increased association for loops on the left thumb in the dominant model

Since patterns are mirrored in their frequency in the overall population it would be expected that the thumbs have similar areas of significance although that was not seen. The right thumb area of interest was on chromosome one (Figure 55). Compared to the area for the left thumb it is less dense, however it is differentiated from the surround "noise" much more clearly. There are three SNPs on chromosome one that meet the suggestive criteria, rs11579178 (p = 1.50 x 10^{-6}), rs2765524 (p = 2.92 x 10^{-6}) and rs61786785 (p = 9.91 x 10^{-6}), and one each on chromosome 4 and 12.

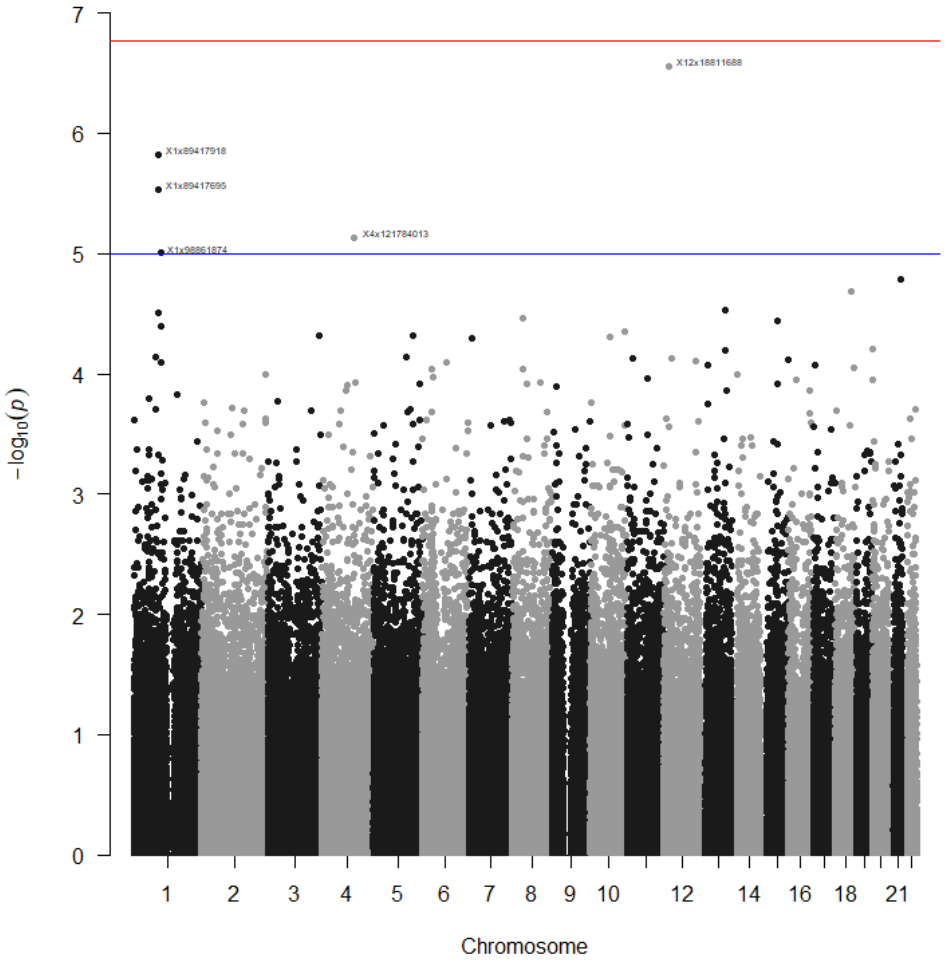

Figure 55: Manhattan plot of SNPs for the loops of the right thumb phenotype for the dominant model

rs668502 (p = 2.77 x 10^{-7}) on chromosome 12 was relatively close to the Bonferroni threshold with no adjacent SNPs showing similar p-values. Often these SNPs are seen to have extremely unbalanced allele frequencies though rs668502 has 37% of people with the AA homozygote, 50% with the heterozygote and 13% with the GG homozygote. When distributing the phenotype per the genotype in Table 44 it shows that the G allele appears to increase the likelihood of having a loop on the right thumb.

Table 44: Phenotype distribution per genotype for rs668502 for the dominant model

Genotype	No loop on RT		Loop on RT	
	Frequency	**Percentage**	**Frequency**	**Percentage**
A/A	52	56.5%	25	21.9%
A/G – G/G	40	43.5%	89	78.1%

Further analysing the area on chromosome one, two peaks were clarified from the one seen in Figure 55 when a subset of the area was plotted (Figure 56). The two separate peaks are located

at base position 89417918 (rs11579178) and 98861874 (rs61786785). They are in two different regions, being 1p22.2 and 1p21.3. Specifically, the first peak occurs in gene KYAT3 and the second between SNX7 and LINC01776. KYAT3 encodes an aminotransferase protein and has been found linked to blood pressure variations by GWAS studies[292].

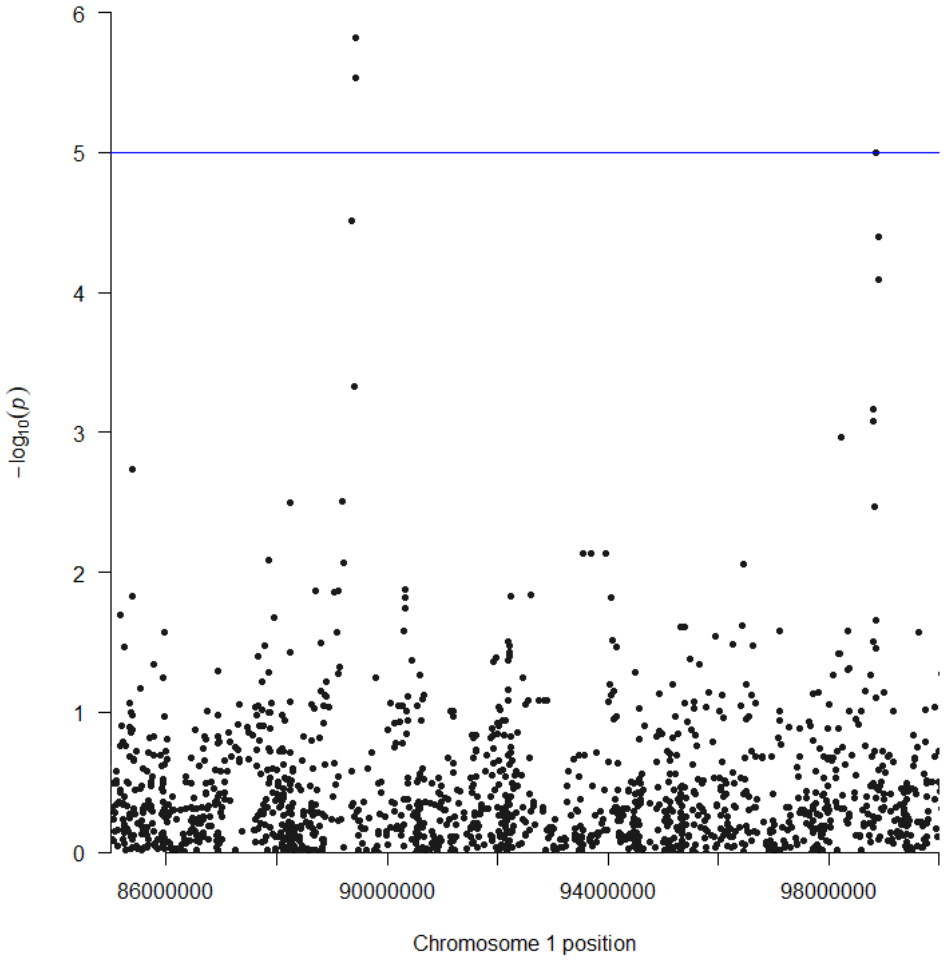

Figure 56: A subsection of chromosome one showing areas of chromosome 1 displaying an area of increased association for loops on the right thumb in the dominant model

The exact function of SNX7 is unknown though members of this gene family are involved intracellular tracking and are expressed most in the colon [293]. LINC01776 is a long intergenic non-protein coding RNA gene and has been linked to schizophrenia and cognitive ability [294]. On face value these functions appear not to be related to the development of fingerprints but nonetheless these genes should be tested for this phenotype with a larger population to see if the apparent significance of associating strengthens or decreases.

Index fingers

The left index finger had one significant SNP associated with arches, rs6871490 (X5x10861222, $p = 8.72 \times 10^{-9}$) in the log-additive model (Figure 57).

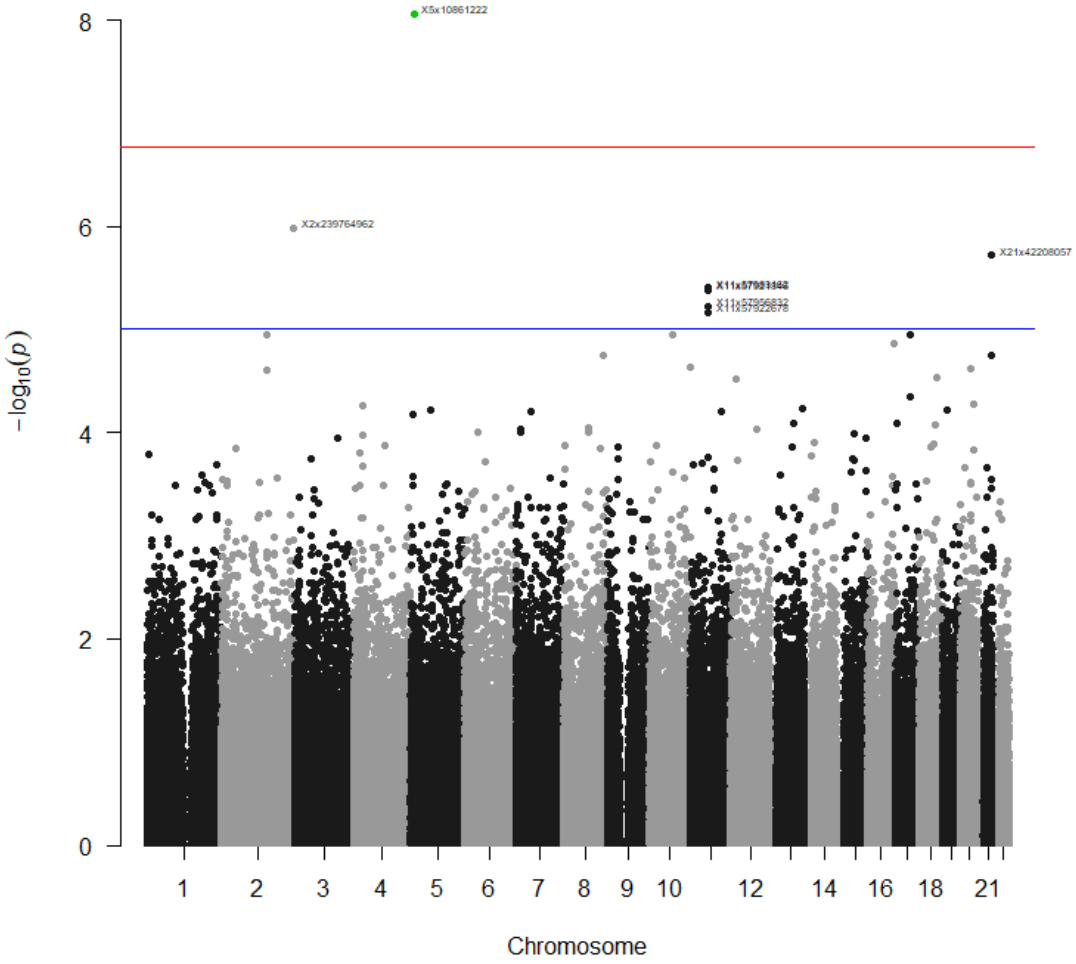

Figure 57: Manhattan plot of SNPs for arches on the left index finger for the log-additive model

This SNP is also suggestive in association for the dominant and codominant model however best fits the log-additive model, indicated by the lower AIC value. The singular analysis of the SNP and the phenotype distribution per genotype is shown in Table 45.

Table 45: Phenotype distribution per genotype for rs6871490 for the log-additive model

Genotype	No arches on LI		Arches on LI	
	Frequency	**Percentage**	**Frequency**	**Percentage**
A/A	147	87.5%	18	47.4%
A/C	20	11.9%	17	44.7%
C/C	1	0.6%	3	7.9%

With the addition of C alleles to the genotype the rate of arches on the finger increases to 75% of people with the CC genotype displaying the phenotype. The issue with this SNP is that there is only four data points for the CC homozygote genotype and 28 data points for the phenotype.

rs6871490 is located between two non-coding RNA genes. LOC105374654 and CTD-2154B17.1 both have undocumented functions however are thought to enhance expression of genes involved with white blood cells [295, 296].

Also, in the log-additive model are four adjacent SNPs on chromosome 11 that passed the suggestive threshold. rs7103026 is the highest of the four with a p-value of 3.97 x 10^{-6}. These are the same SNPs and area that was over the suggestive threshold when association was assessed for the "one or more arches" phenotype. Provided the association is genuine and not by chance this may mean that the area has a small association to arch patterns in general or the fingers with higher arch frequency skewed the association assessment of the 'one or more' phenotype.

The left index finger did not show any significantly associated SNPs for whorl patterns, instead there were multiple SNPs that reached the suggestive threshold. Of particular interest were three SNPs on chromosome 6 that were in close proximity and reached a peak of p = 2.82 x 10^{-7} for rs3761781 in the dominant model (Figure 58).

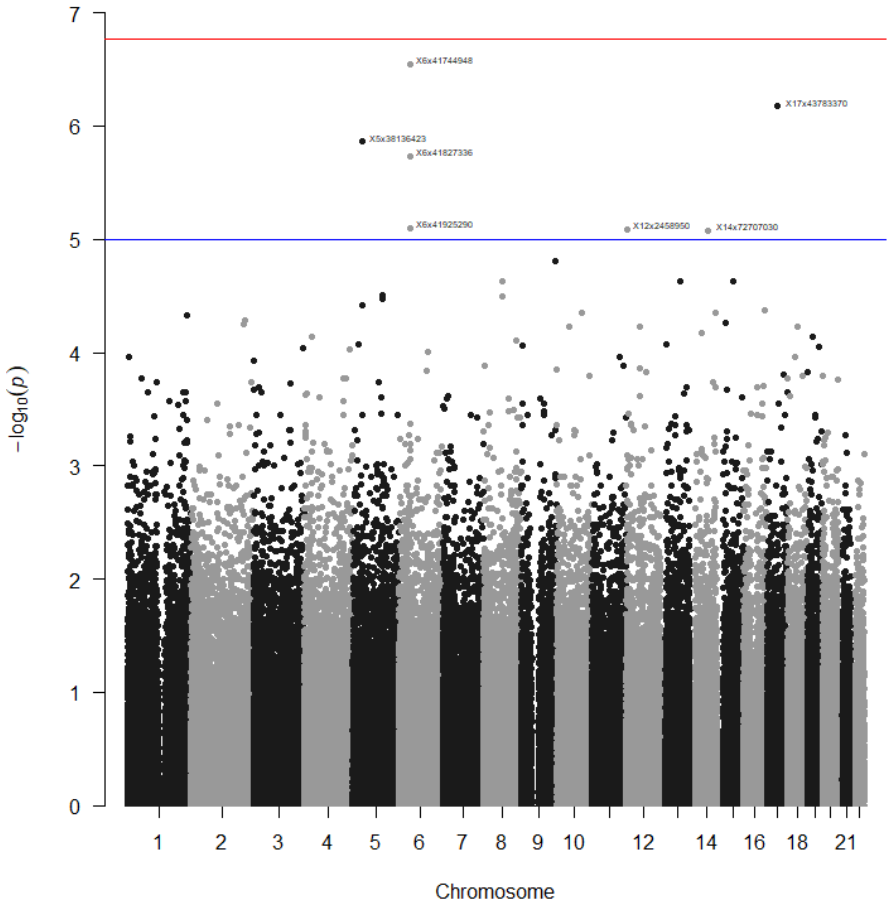

Figure 58: Manhattan plot of SNPs for whorls on the left index finger phenotype under the dominant model

Each of these SNPs show a greater rate of whorls in the more common homozygote genotype despite a large imbalance in the frequency of the genotypes. This is a potential area where additional significance may be found if the analyses were done with a large dataset. Though it must be noted that the study by Ho *et al.* [55] found no significance in this area for the left index finger.

rs3761781 and the adjacent SNPs are located within the FRS3 gene. The FRS3 gene is linked to Kallmann syndrome, characteristics of this syndrome include a lack of production of hormones that direct sex development. This is possibly an indicator for the cause of difference between males and females.

Middle fingers

More SNPs were found to be significant with whorls on the left middle finger. There were two SNPs on chromosome ten that passed the Bonferroni threshold and were best fit by the dominant model (Figure 59).

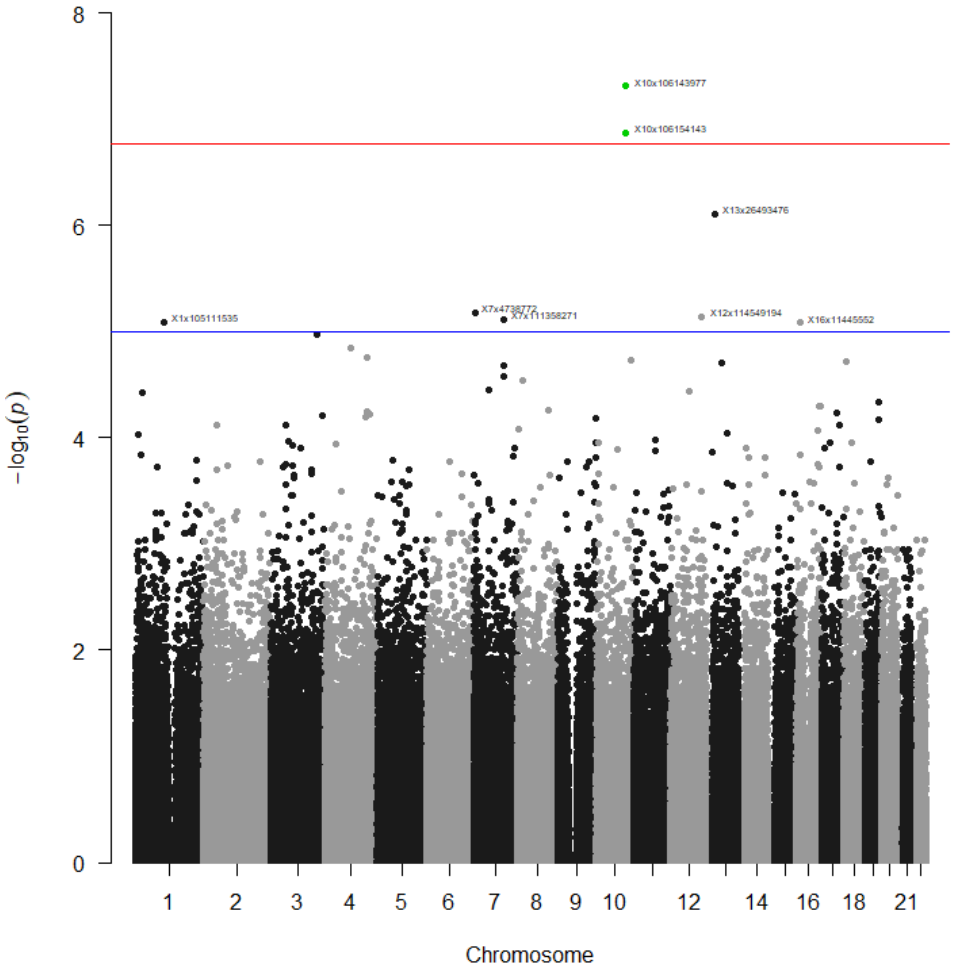

Figure 59: Manhattan plot of SNPs for whorls on the left middle finger for the dominant model

rs1109126 (X10x106143977, $p = 4.88 \times 10^{-8}$) and rs11192037 (X10x106154143, $p = 1.35 \times 10^{-7}$) are in close proximity with both located in 10q25.1, and both when examined show an increase of the phenotype in the heterozygote and the rarer frequency homozygote (Table 46 and Table 47).

Table 46: Phenotype distribution per genotype for rs1109126 for the dominant model

Genotype	No whorls on LM		Whorls on LM	
	Frequency	**Percentage**	**Frequency**	**Percentage**
A/A	120	69.0%	5	16.7%
A/G – G/G	54	31.0%	25	83.3%

Table 47: Phenotype distribution per genotype for rs11192037 for the dominant model

Genotype	No whorls on LM		Whorls on LM	
	Frequency	**Percentage**	**Frequency**	**Percentage**
A/A	125	70.6%	6	20.0%
A/C – C/C	52	29.4%	24	80.0%

These two SNPs were isolated from the rest of the chromosome as no other SNP in this location reached the suggestive threshold. The SNPs are located in the CFAP58 gene which has been associated with cutaneous malignant melanoma and spermatogenic failure [297]. Other SNPs that reached the suggestive threshold were spread sparsely across the autosome from chromosome one to 16.

There were no SNPs that were over the Bonferroni threshold for loops on the right middle finger, however over four models (codominant returned no suggestive SNPs) there were nine unique SNPs that were suggestive in nature. Of particular interest were three SNPs on chromosome 11, rs1791810 (X11x21168295, $p = 3.73 \times 10^{-6}$), rs59292470 (X11x11048650, $p = 4.10 \times 10^{-6}$) and rs1607098 (X11x21157762, $p = 7.04 \times 10^{-6}$) (Figure 60).

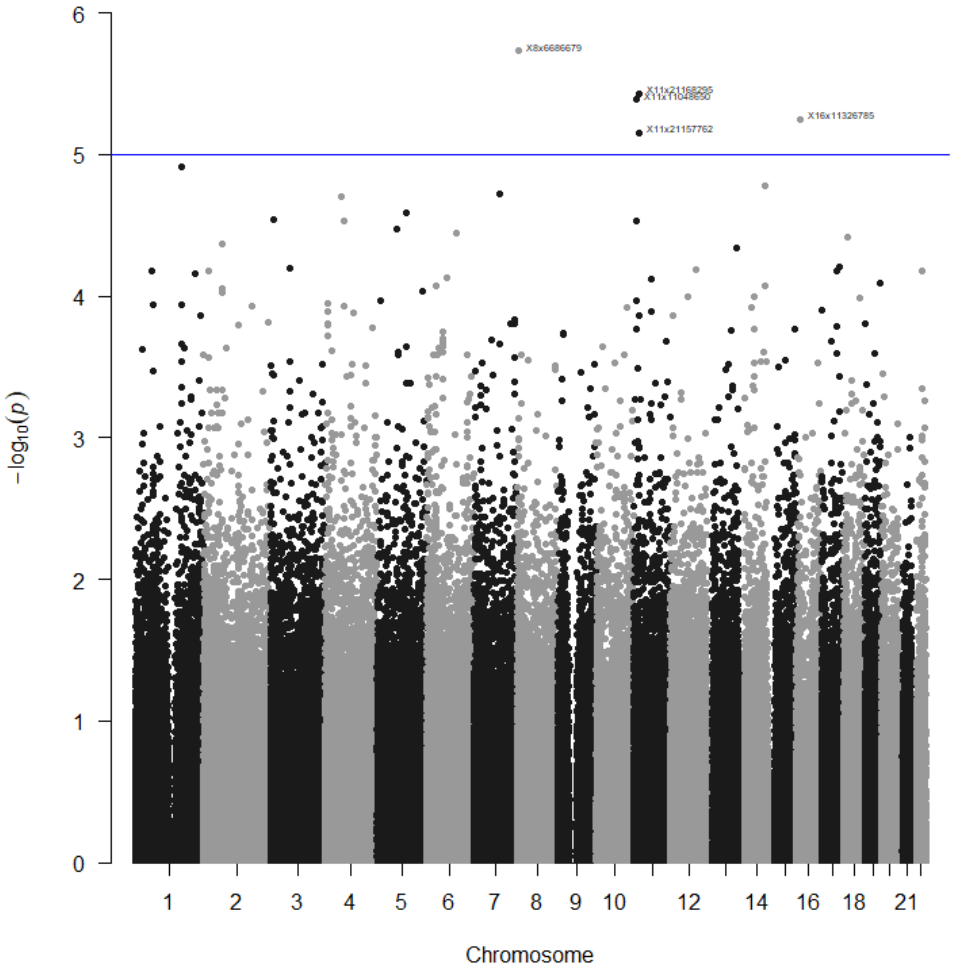

Figure 60: Manhattan plot of SNPs for loops on the right middle finger for the log-additive model

Examining the small area on chromosome 11 shows rs1791810 and rs1607098 display closeness and are at the top of a narrow area of lower p-values (Figure 61).

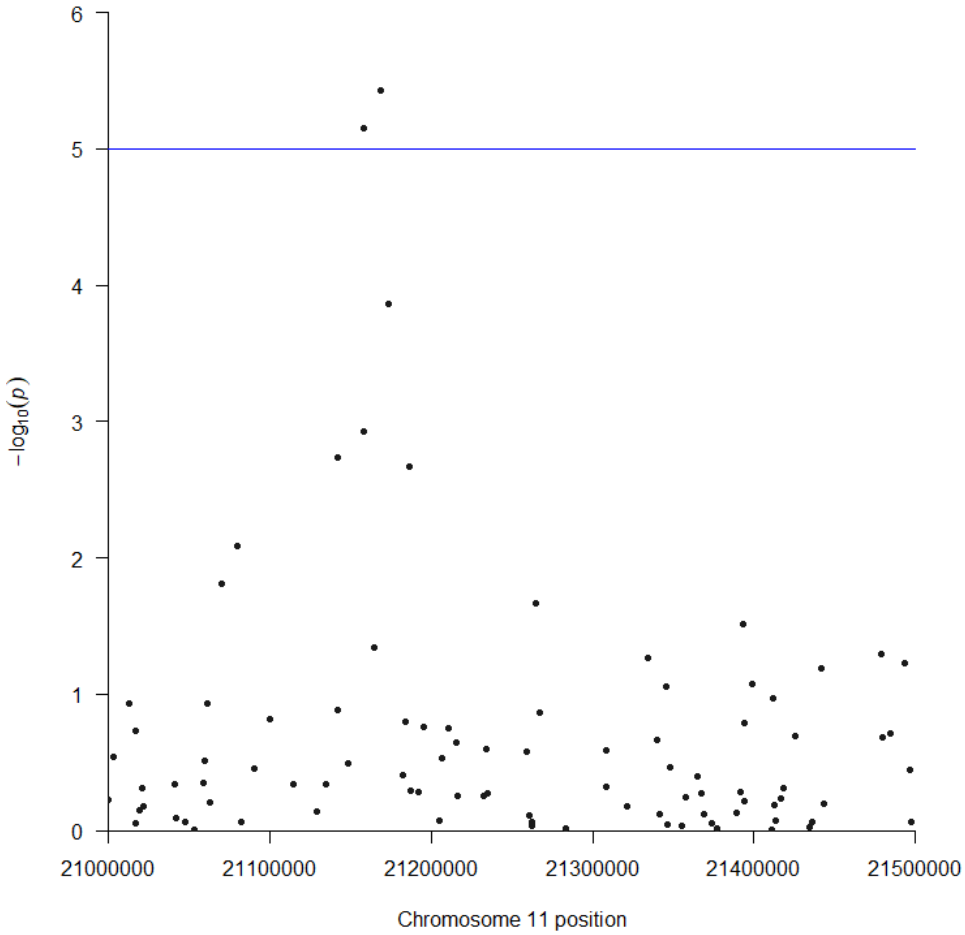

Figure 61: A subsection of chromosome 11 for loops on the right middle finger in a log-additive model

In most examples of the whorl pattern phenotype the cases are more numerous than the control leading to those opposite issue compared to the arch patterns. Table 48 and Table 49 show the distribution of the phenotype compared to the genotypes of both suggestive SNPs at the small peak. The frequencies show the likelihood of having the phenotype increase with the presence of the A allele and G allele in rs1791810 and rs1607098, respectively.

Table 48: Frequency of the phenotype per genotype for rs1791810

Genotype	**No loops on RM**		**Loops on RM**	
	Frequency	**Percentage**	**Frequency**	**Percentage**
A/A	14	27.5%	94	60.3%
A/G	27	52.9%	55	35.3%
G/G	10	19.6%	7	4.5%

Table 49: Frequency of the phenotype per genotype for rs1607098

Genotype	No loops on RM		Loops on RM	
	Frequency	**Percentage**	**Frequency**	**Percentage**
G/G	15	29.4%	94	60.3%
G/A	26	51.0%	55	35.3%
A/A	10	19.6%	7	4.5%

This area is within the NELL1 gene that encodes for a cytoplasmic protein which in turn may be involved in cell growth regulation and differentiation [298]. This gene has previously been associated with adverse metabolic responses and cardiomyopathy.

The highest suggestive SNP for loops on the right middle finger was located on chromosome 8. rs62498864 (X8x6686679, p = 1.85 x 10^{-6}) appears to be another SNP reaching the suggestive threshold by chance due to highly unbalanced allele frequencies. The T allele account for 85% of all the alleles in this locus, and the C allele the other 15%. This translates to the appearance that the T allele and the TT homozygote create an increased likelihood of an individual having a loop on the right middle finger.

Ring fingers

The left ring finger presenting loops returned one significant SNP, rs1465555 (X5x151289698, p = 1.49 x 10^{-7}) for the recessive model (Figure 62). This SNP was also suggestive for the codominant model. Given ulnar loops are the most abundant pattern overall and on the ring finger, a recessive cause is possible if the recessive allele is extremely common.

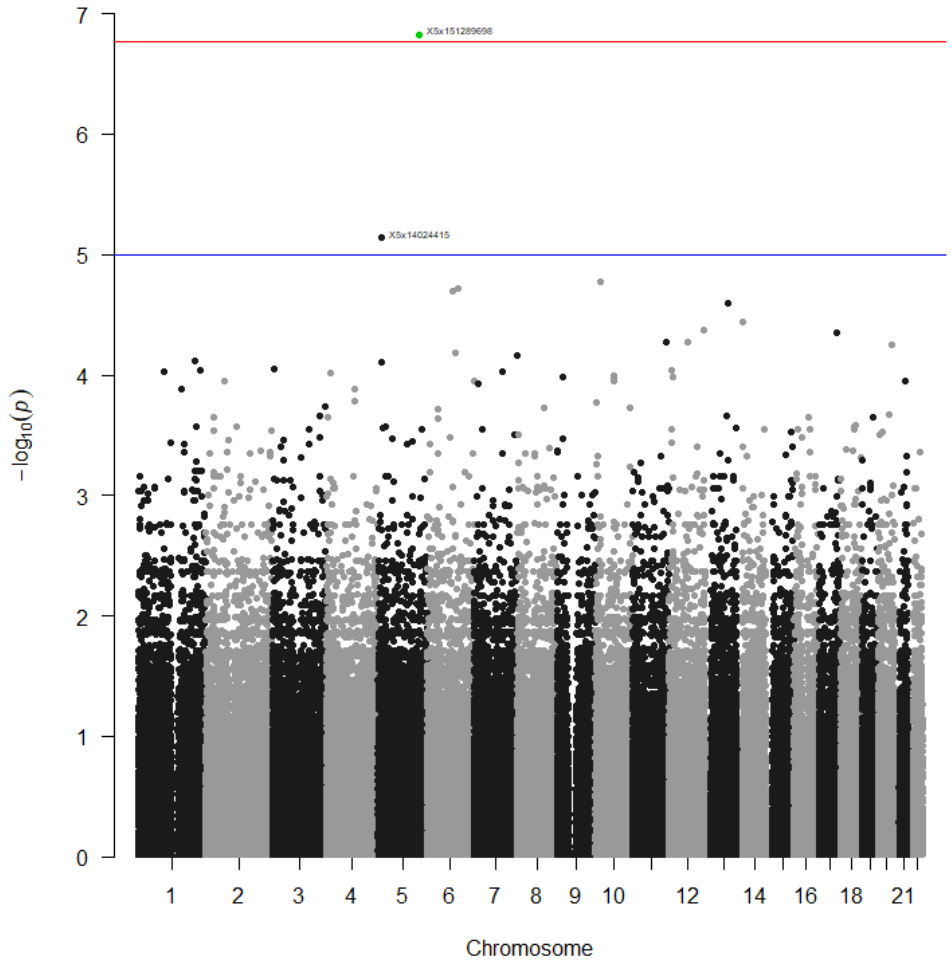

Figure 62: Manhattan plot of SNPs for loops on the left ring finger for the recessive model

All but one of 114 observations of the phenotype were associated with CC and CT genotypes. These genotypes accounted for 89% of the individuals meaning that the TT genotype had unusually low occurrences for the phenotype (Table 50). The TT genotype therefore appears to encode patterns other than a loop.

Table 50: Frequency of the phenotype per genotype for rs1465555 for the recessive model

Genotype	**No loops on LR**		**Loops on LR**	
	Frequency	**Percentage**	**Frequency**	**Percentage**
C/C – C/T	73	78.5%	113	99.1%
T/T	20	21.5%	1	0.9%

rs1465555 is within the GLRA1 gene which encodes a protein that forms part of receptor regulation synaptic inhibition of the central nervous system. As a result, this gene has been linked to several neurological disorders [299]. This means the possible link to friction ridge skin

is unclear. A second SNP, rs10462717 (X5x 14024415) on chromosome 5 passed the suggestive threshold in the recessive model however it was distanced from the significant SNP not adjacent. Nine other SNPs passed the suggestive threshold spread across the four other models. Three of these were located on chromosome 14 plus one each on chromosomes two, five, seven, 13, 17 and 18.

One SNP was found to be significantly associated with the whorl pattern on the left ring finger. rs1887263 (X13x23483716) is on chromosome 13 and was significant for the dominant (p = 8.63 x 10^{-8}) and overdominant (p = 4.22 x 10^{-8}) models while being close to the threshold in the codominant model. There were only five unique SNPs found to be above the suggestive threshold, one being the significant SNP. The data for rs1887263 is fit better by the overdominant model, indicated by the lower AIC score in the association analysis and the lower p-value, therefore the Manhattan plot of the overdominant model is shown in Figure 63.

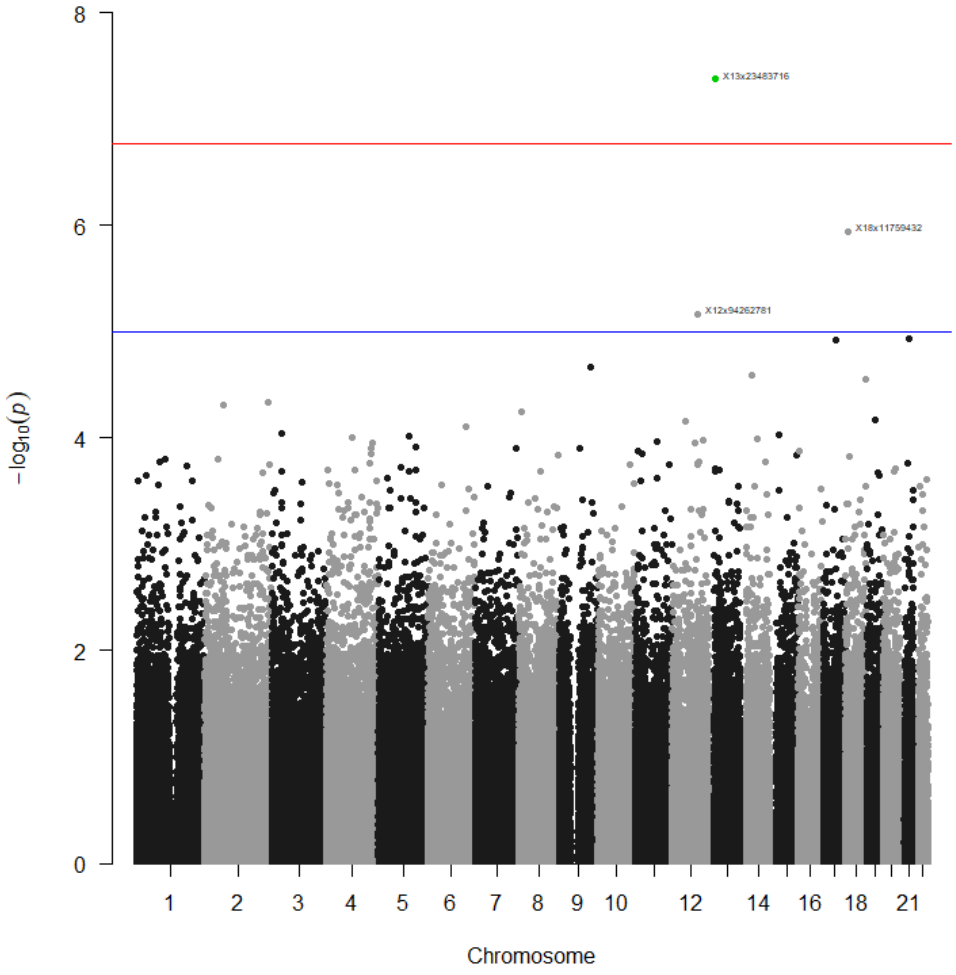

Figure 63: Manhattan plot of SNPs for whorls on the left ring finger for the overdominant model

The same assessment of allele imbalance and phenotype frequency as with the previous significant SNPs was completed and the results are shown in Table 51.

Table 51: Frequency of the phenotype per genotype for the overdominant model for rs1887263

Genotype	Whorls not on LR		Whorls on LR	
	Frequency	**Percentage**	**Frequency**	**Percentage**
G/G-A/A	74	56.1%	68	90.7%
G/A	58	43.9%	7	9.3

This data shows that the heterozygote has a lower rate of the whorl phenotype on the left ring finger. The much higher phenotype observation of 75 people out of the 207 plus the less uneven allele frequency leads there to be relatively more confidence in this result than other associations. rs1887263 is located at region 13q12.1 and in the LINC00621 gene which is a long intergenic non-protein coding RNA (lincRNA) [300]. lincRNA can act as regulators of protein coding gene expression.

Displaying an arch on the left ring (LR) finger is less common than all loop and whorl frequencies. Once again, the log-additive model returned numerous SNPs above the suggestive threshold and three were above the Bonferroni threshold (Figure 64). The highest of these was rs114920443 (X1x118497043, $p = 6.37 \times 10^{-9}$) on chromosome one.

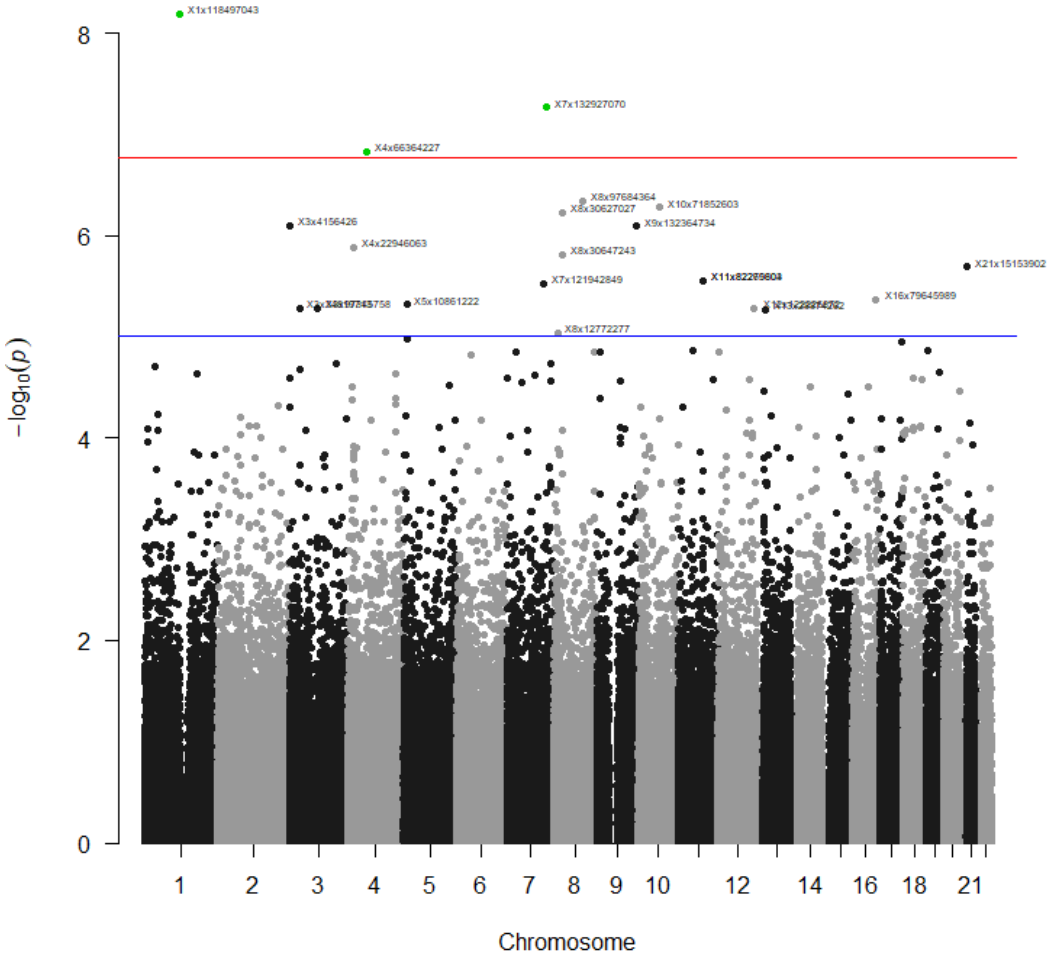

Figure 64: Manhattan plot of SNPs for arches on the left ring finger for the log-additive model

rs114920443 is located within the WDR3 gene. Genes within this family play a role in a variety of cellular processes. These include cell cycle progression, apoptosis, and gene regulation. WDR3 specifically has been associated with non-syndromic intellectual disability and blood cell characteristics [301].

Analysing the single SNP, the log-additive model slightly fits the data better than the dominant model. However, there is again extreme imbalance in the genotypes influencing the significance. The distribution of the phenotype is outlined in Table 52 below.

Table 52: Frequency of the phenotype per genotype for rs114920443

Genotype	Arch not on LR		Arch on LR	
	Frequency	Percentage	Frequency	Percentage
G/G	186	99.5%	13	76.5%
G/A	1	0.5%	3	17.6%
A/A	0	0.0%	1	5.9%

The phenotype is presented more with the presence of the A allele however there is only 5 data point on which to base this decision. This is a further example where association is implied but due to limitations on population size and genotype frequency the conclusions that can be made are limited.

The right ring (RR) finger saw the presence of 10 arches in the genotyped population. As observed with several other arch phenotypes this frequency is too low for any meaningful results. The log-additive model saw numerous SNPs pass the Bonferroni threshold (Figure 65) however it has been observed numerous times to be a side effect of low frequency phenotypes and imbalanced genotypes.

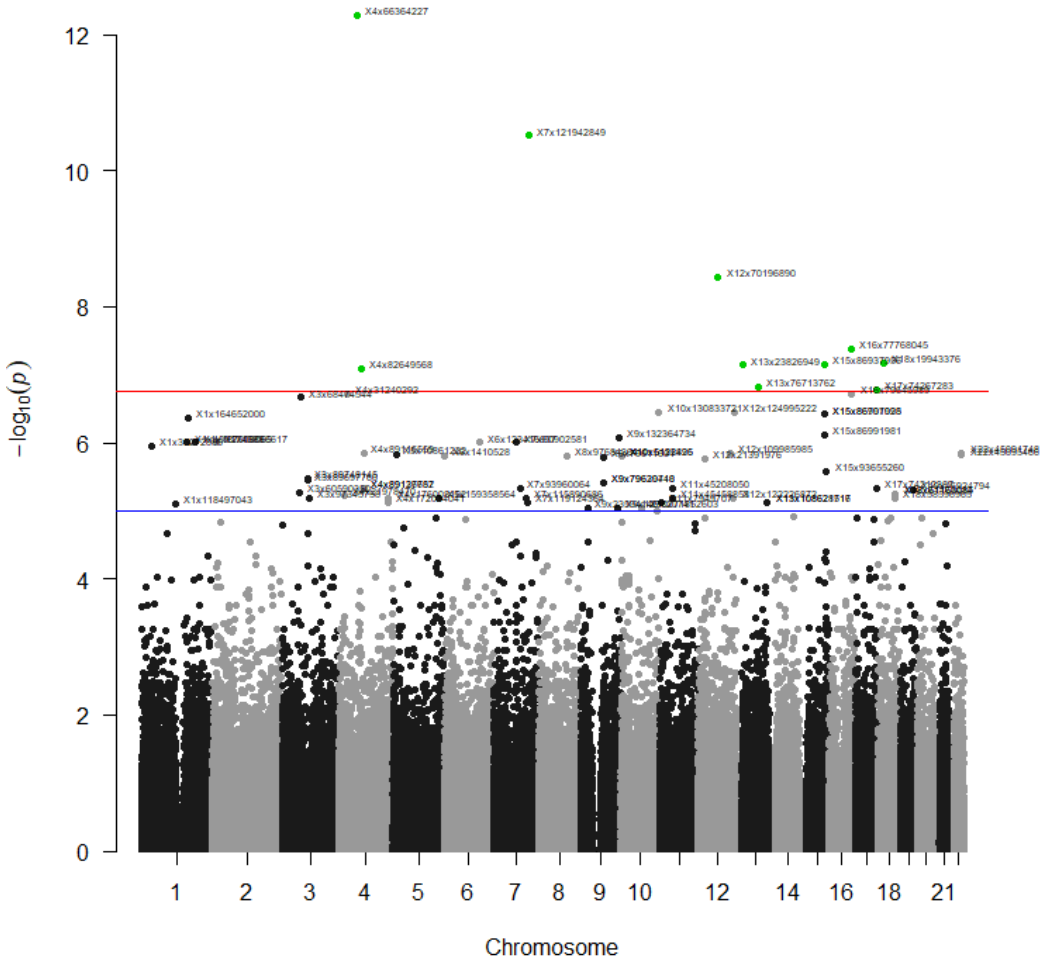

Figure 65: Manhattan plot of SNPs for arches on the right ring finger for the log-additive model

The highest significant SNP in the log-additive model was rs72641095 (X4x66364227, $p = 5.17 \times 10^{-13}$). This same SNP passed the significance threshold for association to arches on the left ring finger which increases the power of the result somewhat. It also indicates this SNP may have a

presiding effect over both ring fingers. rs72641095 is in the EPHA5 gene, it is another example involved in the development and function of the nervous system. Diseases associated with the gene are therefore neurodevelopmental disorders [302].

The frequency of the phenotype per genotype for rs72641095 is shown in Table 65.

Table 53: Frequency of the phenotype per genotype for rs72641095

Genotype	**Arch not on RR**		**Arch on RR**	
	Frequency	**Percentage**	**Frequency**	**Percentage**
G/G	192	97.5%	5	50.0%
G/T	5	2.5%%	4	40.0%
T/T	0	0.0%	1	10.0%

The distribution shows that with the addition of T alleles the incidence of an arch per individual moves from 2.5% with the GG genotype to 44% with the heterozygote and 100% with the TT homozygote. This addition and increase of likelihood are why the log-additive model fit the data.

An additional significant SNP was found linking arches to the right ring finger for the recessive model. rs889472 (X16x79645989) reached a p-value of 4.88×10^{-8} and is shown in Figure 66. This variant is located in LOC101928230 which is a ncRNA gene that has been linked to kidney disease.

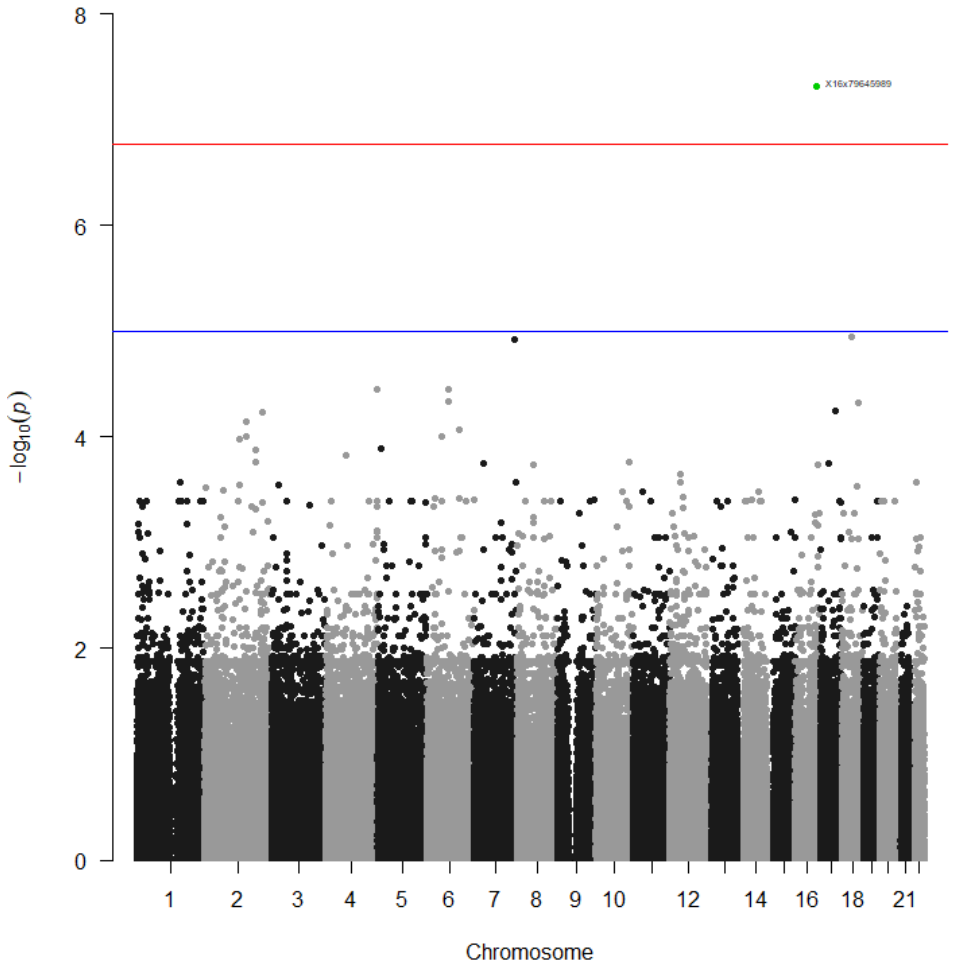

Figure 66: Manhattan plot of SNPs for arches on the right ring finger for the recessive model

Despite being identified through a different model it appears the same causes of significance (low frequency) are at play when viewing the distribution of the genotypes (Table 54).

Table 54: Frequency of the phenotype per genotype for rs889472 for the recessive model

Genotype	**No arch on RR**		**Arch on RR**	
	Frequency	**Percentage**	**Frequency**	**Percentage**
A/A – A/C	174	88.3%	1	10.0%
C/C	23	11.7%	9	90.0%

Of the 31 individuals with the CC genotype, nine displayed an arch on the right ring finger. The 175 people that did not carry the CC homozygote variant saw the phenotype occur once. Nevertheless, while there appears to be a link between the phenotype and genotype in both these SNPs, the genotype imbalance and low pattern frequency prevents a substantive conclusion on being made regarding the association.

Little fingers

The left little finger (LL) was assessed for association with presence of a loop. 171 of the 207 genotyped volunteers displayed this trait. There were several common SNPs between the five models; rs11805515 (X1x10767785, $p = 2.22 \times 10^{-8}$) was significant under the log-additive model (Figure 67) and suggestive under the dominant, codominant and overdominant models.

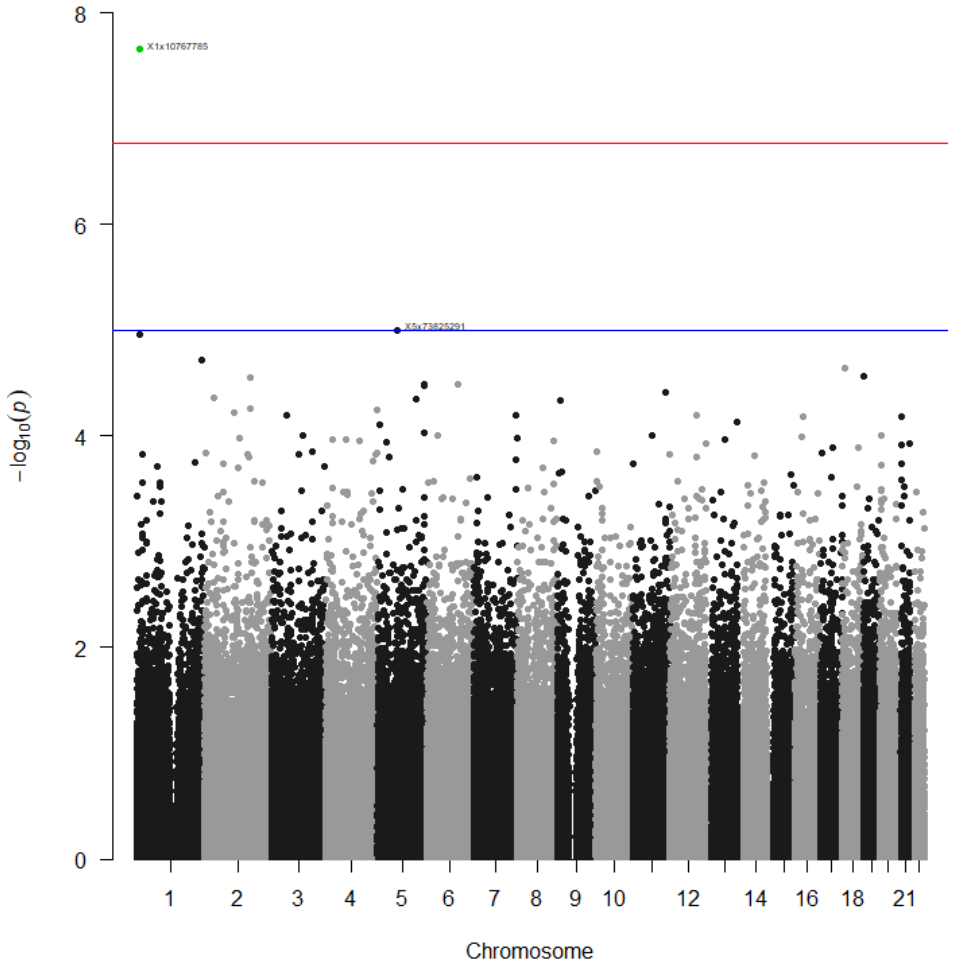

Figure 67: Manhattan plot of SNPs for loops on the left little finger for the log-additive model

All other SNPs for the models were suggestive and below the Bonferroni threshold, they included three SNPs from chromosome 13 and one each from chromosomes two, three, four and five. The lone significant SNP, rs11805515, was best fit by the log-additive model evident from the lowest p-value and supported by the AIC value. The SNP is highly uneven in allele frequency and genotype; 188 individuals were TT homozygote, 18 were TC heterozygote and one was CC homozygote. In Table 55, the distribution of the phenotype per the genotype is shown.

Table 55: Phenotype distribution per genotype for rs11805515

Genotype	No loop on LL		Loop on LL	
	Frequency	**Percentage**	**Frequency**	**Percentage**
T/T	24	66.7%	164	95.9%
T/C	11	30.6%	7	4.1%
C/C	1	2.8%	0	0.0%

The phenotype occurs in a much higher proportion in the TT genotype, 88% compared to the phenotype being present in 39% of the heterozygote and 0% of the CC genotype. The log-additive model fits this SNP well as the T allele appears to increase the likelihood of displaying a loop on the left little finger however the frequency of the rarer C allele is much too low to make a confident conclusion despite the significant result.

rs11805515 is located in the CASZ1 gene and encodes a transcription factor protein that may act as a tumour suppressor in neuroblastoma. A disease associated with the gene is dystonia, a movement disorder that causes muscles to contract involuntarily. SNPs in this gene have also been linked to blood pressure variation [303].

The left little (LL) finger whorl phenotype was assessed, which 26 of the 207 genotyped individuals displayed. This is the second lowest frequency of whorls on the fingers. One significant SNP was returned in the log-additive model located on chromosome 1, rs11805515 (X1x10767785p = 1.82×10^{-10}) and is shown in Figure 68.

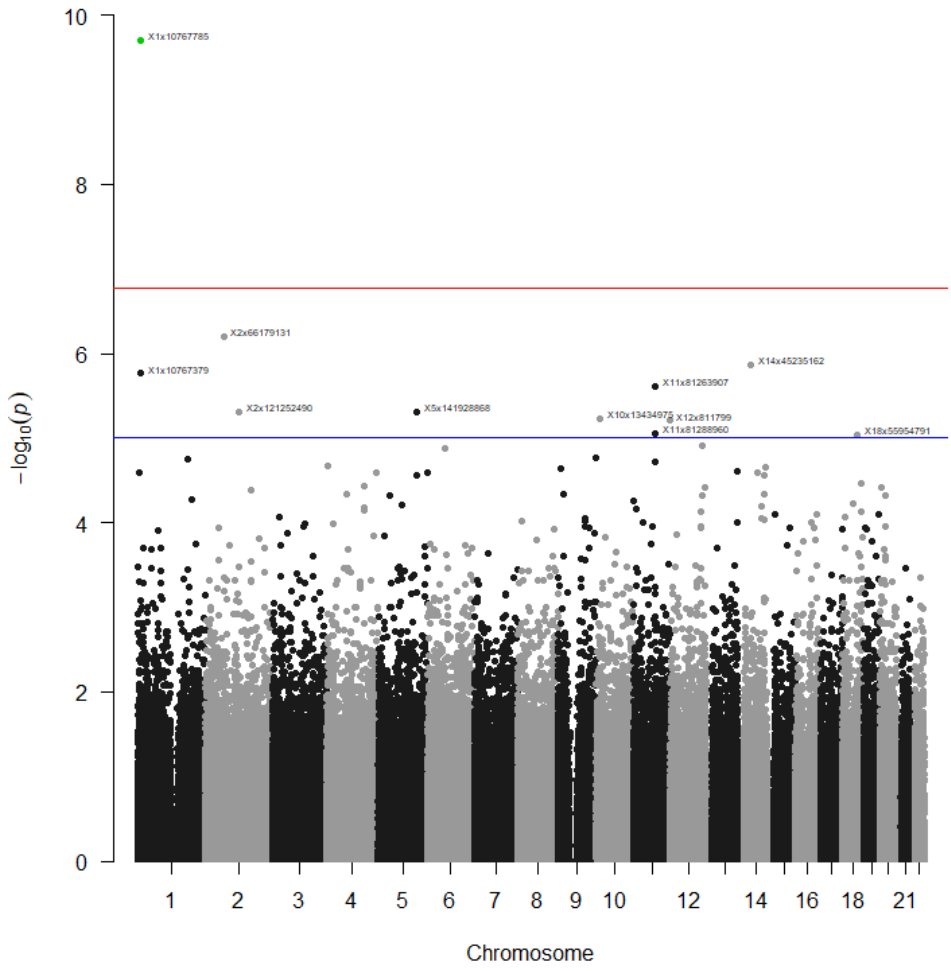

Figure 68: Manhattan plot of SNPs for whorls on the left little finger for the log-additive model

rs11805515 is the same SNP that was significant for loops on the left little finger. Over 90% of the genotyped group had the genotype TT and 9% having the heterozygote genotype. A single person had the CC homozygote genotype. Tabulating the phenotype per genotype (Table 56) it evident the heterozygote has a much higher rate of displaying the phenotype than the TT genotype which partially explains the low p-value.

Table 56: Frequency of the phenotype per genotype in the log-additive model for rs11805515

Genotype	**Whorls not on LL**		**Whorls on LL**	
	Frequency	**Percentage**	**Frequency**	**Percentage**
T/T	173	95.6%	15	57.7%
C/T	8	4.4%	10	38.5%
C/C	0	0.0%	1	3.8%

The p-value is further lowered by the one instance of the CC homozygote also displaying the phenotype. The results make it appear that the C allele is linked to an increase in the whorl phenotype whereas the T allele is linked to loops on the left little finger. However, it is likely the extremely uneven allele frequency and the low phenotype observations have exacerbated the significance of the SNP. Further analysis would need to be completed on a bigger population for rs11805515 to be considered to truly associated with the presence of a whorl on the left little finger. There were several other SNPs from the models that reached suggestive significance, none of which appeared to be a peak of an area of increased significance. These SNPs can be viewed in Appendix J.

The association of SNPs was sought to arches on the left little finger which was displayed in 9 volunteers. The log-additive model returned 14 SNPs above the Bonferroni threshold, common with low frequency phenotypes.

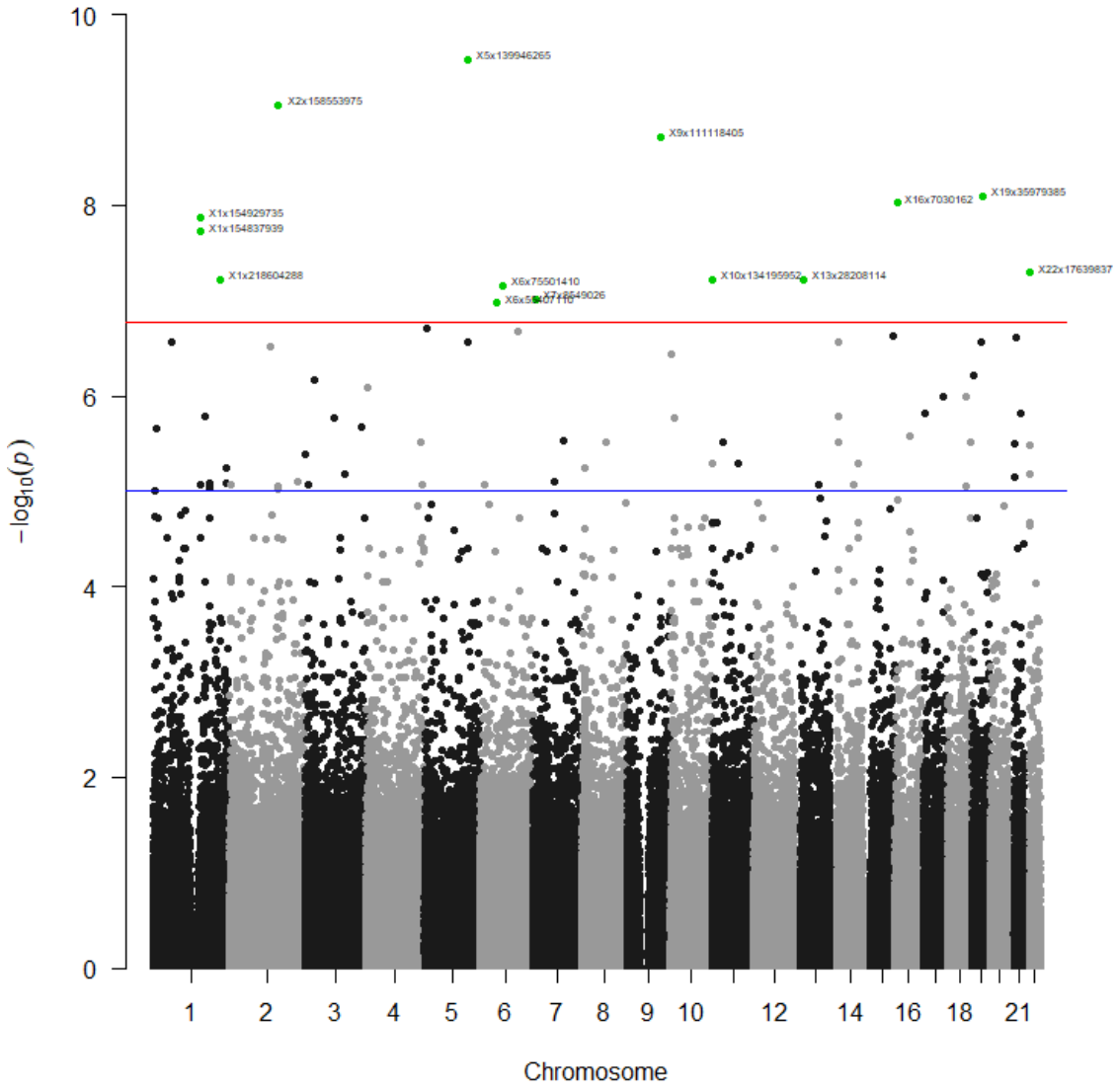

Figure 69: Manhattan plot of SNPs for arches on the left little finger for the log-additive model

The most significant of these SNPs was rs17524123 (X5x139946265, p = 2.88 x 10^{-10}) which is located in SLC35A4 gene which has been linked to Aminoaciduria and Hydranencephaly [304]. Out of the 207 volunteers, 205 of them possessed the AA genotype with 7 displaying the phenotype. The AG and AA genotypes both were possessed by singular individuals that also happened to display an arch on the left little finger. This is a prime example of how extreme allele frequency imbalances and low frequency phenotypes can skew results.

Another rare phenotype was arches on the right little (RL) finger which only four people exhibited. The typical result of this for the log-additive model was observed as numerous SNPs passed the Bonferroni threshold (Figure 70).

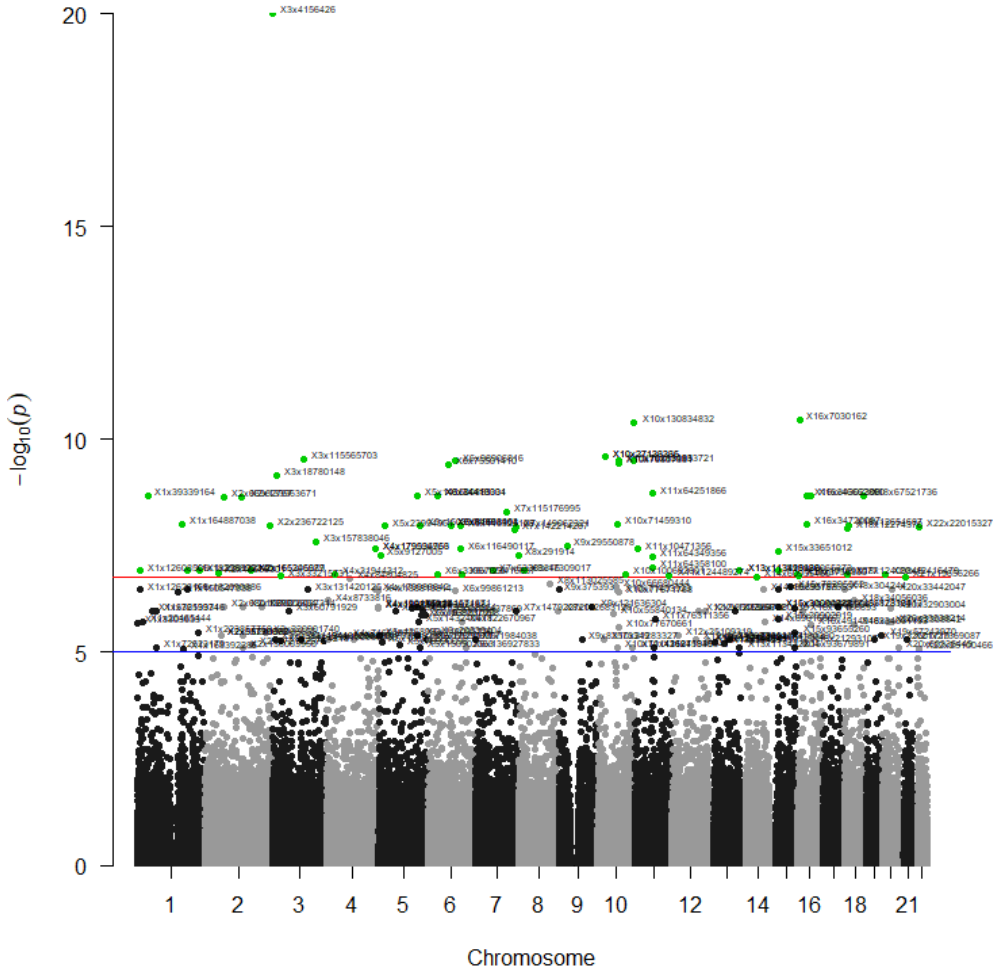

Figure 70: Manhattan plot of SNPs for arches on the right little finger in the log-additive model

One SNP was differentiated from the others, rs77698137 (X3x4156426, p = 6.70x10^{-21}) was the most significant SNP seen in all the association analyses completed. This outstanding result was produced by the distribution of the phenotype outlined in Table 57.

Table 57: Frequency of the phenotype per genotype for rs77698137

Genotype	Arch not on RL		Arch on RL	
	Frequency	**Percentage**	**Frequency**	**Percentage**
T/T	192	96.5%	0	0.0%
T/C	7	3.5%%	3	75.0%
C/C	0	0.0%	1	25.0%

Once again, the extreme imbalance of genotypes and low frequencies of the phenotype combined to produce an extremely low p-value. While the frequency of arches in the heterozygote and CC homozygote cannot be predicted, it can be noted that the TT homozygote is very unlikely to result in an arch of the right little finger.

The gene that rs77698137 is located in, SUMF1, encodes an enzyme that oxidises cysteine residues. Mutations in this gene have been showed to cause severe disorders such as Multiple Sulfatase Deficiency. This condition mainly affects the brain, skin and skeleton and can result in neurological issues, seizures, developmental delay and slow growth [305].

An additional distinct SNP that was further examined was rs6048024 (X20x22308842, $p = 2.59 \times 10^{-6}$). Located on chromosome 20, the SNP was above the suggestive threshold in the recessive model and at the top of what appeared to be a narrow peak in the Manhattan plot (Figure 71).

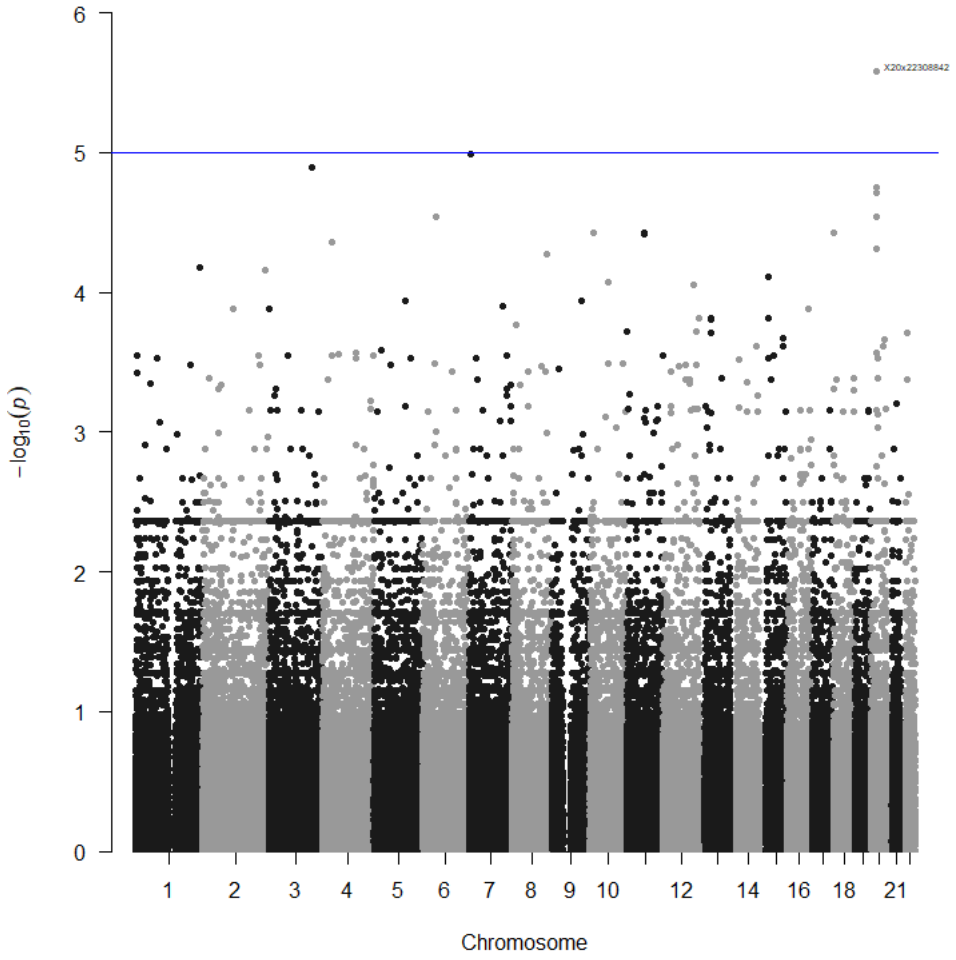

Figure 71: Manhattan plot of SNPs for arches on the right little finger in the recessive model

rs6048024 is located between the LINC01427 and LOC284788 genes. LINC01427 is a long intergenic non-coding RNA gene that has been linked to alopecia and facial morphology via GWAS. Furthermore, the lincRNA gene has been noted to be an a regulatory feature of keratinocytes [306]. LOC284788 is also a non-coding RNA gene and has been linked to the quantification of sex hormone binding globulin via GWAS. This test is used when investigating testosterone deficiency, another possible example of how male and female fingerprint characteristics may differ.

In the 15 instances of the TT genotype four displayed the phenotype; the CC and CT phenotypes accounted for 192 of the volunteers and the arch on the little finger was not observed once. For any meaningful association results to be returned a much larger genotyped population is required. The limiting factor is the extremely low frequency phenotype.

6.4.3. Summary

For all SNP results over the suggestive threshold per phenotype and model, see Appendix K. Genetic loci and trends between phenotypes and previous studies are outlined in this section.

Distilling the large amount of data and separating erroneous chance significance results is complicated as there are several factors involved. These factors were most clear in the log-additive models which displayed numerous significant and suggestive SNPs. Commonly, this would occur when phenotypes were rare, for example arches on each little finger. When these instances are paired with extremely unbalanced SNP genotypes only a few observations of the phenotype in the rare genotype can produce a significant result. Chance associations would be greatly reduced with a much larger set of genotypes such that all phenotypes and genotypes are adequately represented. It is important to note that these unbalanced SNPs were not removed through HWE checks as the control population was in HWE and the case group was not, which can be indicative of phenotypic effect. The method of HWE selection is outlined in section 6.3.2.

Despite the issues with the sample population there were several trends identified in the results. Significant and suggestive SNPs appeared commonly on chromosomes six and 11 for multiple fingers and phenotypes. There was a wide area of increased association on chromosome six and two SNPs on chromosome 11 for the loops on the left thumb phenotype. These same regions were identified as over the suggestive threshold in people with at least one arch pattern on their fingers. Chromosome six also harboured suggestive SNPs for the left thumb whorl. Having the same regions weakly associated with different phenotypes implies there may be a general underlying cause for fingerprint phenotypes on chromosome 6.

A similar trend was seen on both chromosome one and 12 with loops and whorl patterns on the same finger. On chromosome one, both loops and whorls on the left little finger were found to be significantly associated with rs11805515. On chromosome 12, rs1075177 was associated (suggestively) with the same phenotypes on the left middle finger. An argument against these associations is the lesser number of controls for the loop association models and the low frequencies of whorls on the little finger. However, given this trend occurred in two separate areas of the autosome and on different fingers, particularly one where loops and whorls are plentiful, there is a greater likelihood this is a genuine association.

Another SNP of note was rs1887263 which was found to be significantly associated with whorls on the left ring finger for both the dominant and overdominant models. This SNP was found to be suggestively associated with individuals that displayed whorls on both ring fingers. It is likely it was less significant for ring fingers as a pair due to individuals that did not have mirrored

fingerprints. Nevertheless, this is a strong result given its repetitive nature. Adding to the strength of result was that loops on the left ring finger was also suggestive in association to rs1887263. This trend was also observed for the right ring finger. rs4955637 which lies in the MECOM gene that is involved with cell differentiation was suggestive of an association for both loops and whorls to the right ring finger in both the codominant and overdominant models [307]. There are numerous examples of SNPs that appear to be specific to multiple fingerprint patterns perhaps highlighting the presence of some SNPs that specify not having a phenotype. rs4955637 is an example of a SNP where there is an association with not having arch patterns on the right ring finger.

Comparing these results to previous studies, Ho *et al.* [55] found strong association with the whorl pattern to the ADAMTS9-AS2 gene and specifically outlined four SNPs where association was highest. Three of these SNPs, rs2244503, rs17071864 and rs796973, were featured in the chosen SNP chip within this study. rs17071864 was removed from the dataset when selecting SNPs based on Hardy-Weinberg equilibrium and therefore was not assessed for association. Results of this study showed rs2244503 and rs796973 both did not reach the suggestive or Bonferroni threshold for association to any phenotype.

Additional areas of significance found by Ho *et al.* were downstream of TBX3 and upstream of MED13L with a peak association at rs1863718. In that study the SNP was significant for whorls on both the left and right ring finger. It was not genotyped in this study, however two nearby SNPs, rs1075177 and rs10161338 reached the suggestive threshold. rs1075177 was associated with loops and whorls on the left middle finger and rs10161338 with arches on the left middle finger.

A final area of significance found by Ho *et al.* peaked at rs10201863 in the OLA1 gene on chromosome two. This SNP was not assessed in this study as it was not present on the SNP chip. There were no SNPs with p-values below the suggestive threshold in that region. The closest was rs67757319, a significant SNP that was associated with arches on the left thumb for the log-additive model. However, this association is questionable due to the low frequencies of arches.

An earlier study by Medland *et al.* [54] examining finger ridge count (discussed in section 4) found significant multivariate linkage to the chromosome region 5q14.1 and significant univariate linkage at 1q42.2. Ridge count measures the size of a pattern between the core and delta as opposed to the shape. Nevertheless, it is a feature of a fingerprint that may be altered due to pattern as ridge density is. Of the SNPs that passed the suggestive threshold in this study, one was located at the 5q14.1 (rs62355044) region and another at the 1q42.2 region

(rs9793010). rs62355044 passed the suggestive threshold for association with arches on the right index finger and rs9793010 passed the suggestive threshold for whorls on the left ring finger. Neither SNP are documented as being within a gene and neither have been reported to be associated with function or abnormal phenotypes [308, 309]

There are two further studies linking fingerprints to the genome. Nousbeck *et al.* [60, 61] uncovered a mutation in the SMARCAD1 gene that causes adermatoglyphia, a disease where the sufferers do not display friction ridges on the skin. The earlier study mapped the disease phenotype to 4q22 and discovered a heterozygous mutation. The second identified three more heterozygous mutations within the SMARCAD1 gene. These mutations result in decreased stability of a short RNA isoform and a total of eight genes are differentially expressed [310]. Those eight genes all have roles in epidermal development, differentiation, and psoriasis. Within this study there were no SNPs that reached the suggestive threshold within the SMARCAD1 gene, or the region surrounding it. Adding to this result, there was a 30,000,000 bp gap encompassing this gene that had no suggestive or significant association.

Overall, there were no exact repetitions in association to previous studies, though there were similar trends where numerous suggestive SNPs were in areas that were previously linked with fingerprint pattern. A substantive conclusion however cannot be made upon these results, as a larger population is needed as well as specific individuals featuring rarer fingerprint phenotypes. This would increase the statistical significance of the associations.

It is important to note SNPs do not fully account for the variation in fingerprint phenotype, and it is likely there is also epigenetic regulation among other factors at play. This is supported by discoveries that only 7% of disease associated SNPs are located in protein coding regions [311]. ADAMTS9-AS2 (the associated gene discovered by Ho *et al.* [55]) is a long non-coding RNA and its regulation may be important in early embryonic development. Long non-coding RNAs (lncRNA) are involved in gene expression and generally found outside of the cell nucleus. In this study rs1887263 was significant for whorls and loops on the left ring finger. This SNP is in region 13q12.1 and specifically in the LINC00621 gene. Long intergenic non-coding RNAs (lincRNA) are slightly longer than lncRNAs and are specifically located in the nucleus where they contribute to cell differentiation. The finding of associations to these non-coding regions supports the hypothesis that epigenetic regulation is behind fingerprint development as suggested by Walsh *et al.* [166]

Chapter 7 – CONCLUSIONS AND FUTURE DIRECTIONS

7. Conclusions and future directions

7.1. Conclusions

This thesis aimed to investigate the factors that influence fingerprint pattern using a multifaceted statistical approach to find association to sex, ancestry, hand, finger, and SNPs.

This research originated from two main questions: Can indications of investigative information (BGA, sex, hand, finger) be extracted from fingermarks that do not return a biometric match through automated fingerprint identification systems and are SNPs associated with level one fingerprint patterns?

To address these questions five specific steps were taken:

1. Assemble a repository of fingerprints and DNA samples from approximately 500 volunteers alongside sex and self-reported biogeographical data.
2. Identify any associations of fingerprint patterns with sex and BGA using goodness of fit tests and multinomial logistic regression analysis.
3. Identify any difference in ridge density within sex or BGA groups using goodness of fit tests, general estimating equations and generalised linear models.
4. Perform a small family study investigating the inheritance of fingerprint patterns.
5. Extract, quantify and genotype collected DNA and perform SNP association analysis utilising R packages (SNPassoc and qqman) plus generalised liner models to identify SNPs that influence fingerprint phenotype.

The research has found that fingerprint patterns have different frequencies per ancestry, sex, hand, and finger. Ridge density differs mostly between sex with smaller differences between ancestries. SNPs were found to be significant for multiple phenotypes and multiple models. These results show superficial DNA underpinnings of fingerprint patterns and how the effects are expressed in different demographic variables.

7.1.1. Pattern association with BGA and sex

The fingerprints of the 831 volunteers were collected; BGA, sex, hand and fingers were all assessed as potential factors in fingerprint frequency and distribution. Chi-squared tests with post-hoc analysis and MLR were used in the statistical analysis. A comparison of the two statistical approaches showed that despite chi-squared tests considering each finger independent rather than a set of ten, results were comparable. With both tests showing similar

results, it is strong evidence that ancestry and sex are factors in fingerprint pattern development, and the hand and fingers significantly influence the distribution of fingerprint pattern.

Sex dimorphism was evident in plain arches, double loop whorls and plain whorls. Females had significantly less plain and double loop whorls and significantly more plain arches than males. These results are supported by studies on the FBI database and a study of African Americans where females displayed more arches [10, 206]. The increased rate of plain whorls and double loop whorls has been observed previously in Polynesian, Melanesian, Australian Aboriginal and South Asian populations [209, 215-217] however none of these studies used statistics to show significance, just observations in two even groups of males and females. In reverse, New Zealand-Samoan females showed whorls were of higher frequency over males and arches were mostly less than one percent of all patterns [193]. Some previous studies also saw no sex differences, these were performed on Spanish, Nigerian and Malawian populations, though only the Spanish study contained statistical analysis [197, 199, 202]. These differences in the sex comparisons are difficult to rely on given the lack of statistical rigor in most of the analyses however they possibly indicate that BGA has a larger effect than sex on fingerprint pattern. One theory for the difference between males and females varying within BGA is based on hormones. Testosterone, luteinizing hormone and oestrogen have all been shown to be factors in the development of the fingers and hand [312]. Additionally, this theory could also explain the significant asymmetry observed between the left and right hand. The left hand displayed plain whorls significantly less than the right and has been seen before in Asian, European and African populations, meaning it transcends ancestry [198, 207, 213]. In the hormones study they found the developmental effects to be asymmetrical on the finger length ratio trait even when accounting for sex, age and height [312]. This may indicate sex hormones play a minor role in fingerprint pattern development.

The MLR results for BGA showed plain and tented arches, plus double loop whorls to be higher in frequency in Europeans and Middle Easterners compared to South and East Asians. These were novel association not reported before in comparisons between these ancestries. Plain whorls were the most differentiated in frequency, East Asians and Middle Easterners had a significantly higher frequency and Europeans presented a significantly lower frequency compared to South Asians. The result of higher plain whorl frequency in East Asians and Middle Easterners was supported by studies on Chinese, Malaysian [105, 198] and other Middle Eastern groups [206] though again all of these studies lack any statistical data in the publication. There is also anecdotal evidence which aligned with this result from New South

Wales Police Force crime scene examiners that whorl patterns were observed in greater numbers when investigating Asian organised crime scenes [262]. Finally, Europeans were solely higher in radial loop frequency compared to the other ancestries which had only been demonstrated once previously with chi-squared test on a European American population [213].

The effect of BGA on fingerprint pattern shared many more similarities to previous papers than comparisons to sex. Simply, these BGA differences are more likely due to genetic variants, unlike the sex variation, and could be explained by genetic drift. When these BGAs are isolated, genetic variants may be naturally lost or fixed over time which results in some fingerprint patterns being more common than others. Alternatively, an insight may be gained from the function of fingerprints. Fingerprints are believed to have developed to create friction and therefore increase grip onto objects [94, 95]. This aligns with observations of koala and chimpanzee friction ridge skin which are an example of convergent evolution and are very similar to humans given the requirements and habitat of those animals [93, 94]. However, the most recent study has linked the grip provided by fingerprints to be due to the pores and eccrine sweat glands. The ridges, with the pores positioned along them act as a microfluidic array which maintains optimal moisture levels by deforming and blocking the sweat pores thereby increasing grip [97, 98]. This opens the possibility that different level one fingerprint patterns may be better at regulating moisture in different environments and climates. This has not been tested before but would create selection pressure and explain why patterns occur at different rates between BGAs.

A possible selection pressure however would not explain the many significant differences in pattern distribution compared to the thumbs. The plain arch occurred in higher frequencies on the index fingers and lower frequencies on the little and ring fingers. The tented arch was higher from ring to index finger in a linear increasing fashion; as too was the radial loop, though the frequency increased exponentially to the index fingers. Both the plain whorl and central pocket loop whorl were higher on ring and index fingers though lower on little and middle fingers compared to the thumbs. Double loops whorls were lower in frequency on all fingers relative to the thumbs and the accidental whorl was lower in frequency than the thumbs on little and index fingers. The most striking of these results and the only trait to have previously had its distribution documented was the radial loop on the index finger. This trait has previously been noted in Dutch, Swedish, Spanish, Algerian and American populations [90, 103, 192, 197, 255]. The highly specific location of this pattern means this finger is likely targeted by the factor that produces this pattern. Thus far genetic studies (including this one) have not uncovered variants linked to

this pattern likely due to the low frequency. Once enough individual's displaying radial loops on at least one index finger volunteer it is likely this trait will be linked to several genetic variants.

This subsection of this study was the first known analysis of fingerprint pattern frequency and distribution in the general Australian population and the first known study where ancestry association has been examined with loop, whorl and arch subclassification. Previous studies looked at only loops, whorls and arches and only used chi-squared analysis for assessing pattern frequency. Chi-squared analysis was used in this study for comparison; however, this approach has a flaw where it assumes the ten fingerprints to be independent. Therefore, this study is the first to apply multinomial logistic regression to this topic to overcome this issue. The results of this analysis quantify the association of fingerprint patterns to sex, BGA, hand and finger which could be used as a basis in the future for expert statements regarding the rarity of patterns in the future. At this stage predicting sex can be done but omits BGA as a factor. Predicting BGA from fingerprint patterns currently cannot be done accurately.

7.1.2. Ridge density links with BGA and sex

The fingerprints of the 831 participants (515 from Sydney, 316 from Melbourne) were subjected to the semi-automated ridge density workflow outlined in section 4.3. The refined ridge density data was then assessed using a GEE and Kruskal-Wallis test. The Sydney and Melbourne data were analysed separately as there was a large difference between the ridge density of the cohorts that was believed to be due to the digital fingerprint scanner scaling the size of the images incorrectly according to the software magnification setting. This highlights an incompatibility issue where multiple fingerprinting systems may be used across Australia which would greatly hinder using fingerprints characteristics in casework. A further complication would be knowing the orientation of a fingermark, this could only reliably be deduced when there are multiple deposited at the same time, termed "a slap". Nevertheless, this investigation supported previous studies that found females had significantly higher ridge densities than males and found several novel factors which proved to make distinguishing males and females through ridge density less accurate.

There were very few variables where all three sampled positions showed the same trends between the Sydney and Melbourne data. Only results where there were some congruencies between the datasets have enabled a conclusion. The most prominent explanation for differences between the two datasets is sampling error due to the lower number of individuals and poorer quality fingerprints in the Melbourne dataset. This could have been compounded by

Melbourne data exhibiting 5% more loops at the expense of whorls compared to the Sydney population since level one pattern was seen to cause significant differences. Selection pressure could not be attributed to the intra-city differences as it would imply a difference in environment that would mean a benefit to lower or high ridge density. Given fingerprints develop *in utero* it is highly unlikely the environmental differences between the cities are the deciding factor. Naturally produced genetic drift was also discounted given the lack of a bottleneck event or isolation between the two cities.

Genetic drift may explain differences amongst different populations though not between sexes as they are co-located and interbreeding. Sex differences were expected in all positions of the fingers. In the Sydney group females presented with significantly higher densities than males of 6.9%, 7.4% and 4.8% across the ulnar, radial, and proximal positions, respectively. The Melbourne group only had significantly higher densities in females compared to males in the ulnar (4.8%) and radial (5.8%) positions. The author interprets this difference to be a result of discarding 25% of proximal data points from the analysis of the Melbourne dataset due to poor quality which would induce a sampling error. Females having higher ridge density than males has been observed in numerous studies of populations on several continents [30, 33, 218, 227, 230, 231, 270]. The fundamental reasons for differences between the male and female's ridge density has been hypothesised from observation of features in sex-chromosome linked syndromes. Investigations have shown that people with XYY syndrome have lower ridge density than people without the syndrome [273]. It is believed that the high testosterone levels from the presence of the extra Y chromosome is delaying the maturation of the fingerprints *in utero* causing the lower ridge density [274].

Significant differences were seen between the radial and ulnar positions of the Sydney dataset. These differences are hypothesised to be due to how the fingerprint patterns form. The ulnar side of the fingerprints particularly on the thumb and little finger accumulate distinct variances in pattern and minutiae from pressure on the chorion *in utero* when the fingerprints are developing, this may also effect ridge density [1, 12]. However, variation in ridge density when rolling the finger during deposition due to the elasticity of the skin cannot be fully ruled out. This could explain the difference between the Melbourne and Sydney results as they were taken using different methods – Ink versus fingerprint scanner.

This research demonstrates that the are many more factors at play in ridge density than just sex. Previously, this was largely unknown as the studies focused mainly on sex. More studies are needed to analyse the variability of ridge density per BGA, level one patterns and fingers

specifically as these appear to be similarly large factors in ridge density as sex. To create a prediction model to classify fingerprints for casework would be premature at this stage.

7.1.3. Inheritance of fingerprint patterns

The inheritance of fingerprint patterns was initially explored using the fingerprints of an extended family on both sides of a core family of five. In total 36 individuals over four generation had their fingerprints scanned and classified using the NCIC classification system including the ridge counts of loops. This project was undertaken to investigate and visualise fingerprint characteristics in mendelian trait models.

The family exhibited an unusual frequency and distribution of patterns compared to the Melbourne and Sydney groups. Observed were low whorl frequencies and a higher ratio of tented arches to plain arches. The reason for the unusual frequency of patterns may be the same as in the greater population however more concentrated due to the inheritance of the variants that influence fingerprint phenotype.

Extreme asymmetry was also observed in radial loops and tented arches which were skewed to the right hand, specifically the index finger. This asymmetry also stretched to the ridge tracing of whorls. Outer traced whorls occurred exclusively on the right hand, dissimilar to the Sydney dataset where three-quarters of outer tracings occurred on the right hand. Again, this extreme result may be due to inheritance of the variants that cause magnification of the asymmetrical trait. Underlying this may be an imbalanced morphogenetic field effect where genes develop the left and right hands similarly and genes that develop each hand singularly. How the morphogenetic effect may develop fingerprints is explored in 7.1.4.

Pedigree charts visualised 12 occurrences of radial loops on the right index finger of which 11 adhered to X-linked dominant inheritance. One male son displayed the phenotype which was contrary to the inheritance model as his mother did not display the phenotype (The father was not fingerprinted). Ridge density inheritance was also assessed using a multinomial logistic regression. The results showed insignificant correlation of average ridge density between parents and children. Despite this, 22% of the variation in the children's ridge count was explained by the model containing the mother and father's average ridge count.

This topic of research adds additional support to the theory that fingerprints are polygenic and additive in their genetic development. The fingerprint phenotype is much too complex for this

method of assessment though it rules out single loci mendelian trait inheritance of fingerprint pattern and ridge count.

7.1.4. SNPs linked to fingerprint pattern

The SNP association analysis featured the genotypes and fingerprints of 207 individuals from the Sydney dataset. Over 620,000 SNPs were genotyped which were refined to more than 292,000 based on Hardy-Weinberg Equilibrium criteria. Previously a handful of SNPs have been linked to the whorl pattern, this project wanted to expand the scope to find links to other fingerprint patterns. The results contributed to this goal by identifying over 60 SNPs that passed the significance threshold (1.71×10^{-7}). Not all these markers are likely to be genuine associations despite the use of a Bonferroni correction. When low frequency genotypes were paired with rare phenotypes the likelihood of chance significance greatly increased, particularly in the log-additive model. A greater sample size would determine if these associations are strengthened or reduced.

Genes containing SNPs that were significant and exhibited genotypes the that were relatively balanced are detailed for their function.

LINC00621 located at 13q12.1 is a long intergenic non-protein coding RNA (lincRNA), there is little documented about the function of this gene however it appears to function like an oncogene. Studies have linked this gene to the enhancement of proliferation and invasion ability of bladder cancer and osteosarcoma cells. In bladder cancer LINC00621 regulates miR590 to increase expression of PHF14 which alters epithelial-mesenchymal transition (EMT) [313]. PHF14 has been linked to Floating harbour syndrome which among other more prominent developmental issues is characterised by finger abnormalities in some people [314]. In Osteosarcoma LINC00612 competes with miR214-5p and mediates EMT to increase the proliferation and invasion of the cancer cells [315]. EMT is naturally involved in embryogenesis and wound healing though can allow tumours to thrive when epithelial cells transform and gain mesenchymal characteristics to migrate easily to other tissues. EMT has been proposed as a therapeutic target for skin conditions such as ulcers, alopecia, melanoma, and squamous cell carcinoma [316]. While there is no direct link to the development of friction ridge skin, specifically whorls on the left ring finger, the regulatory functions controlling embryogenesis and epithelial cell proliferation indicate there could be a potential role in fingerprint development *in utero*.

The CFAP58 gene was significantly associated with whorls on the left middle finger. The gene is also expressed highly in testis and appears to be important in the development of spermatogenesis and cilia formation [317]. Functions of this gene have been linked to the increase in familial melanoma and glioma through the interaction with TRF1 and POT1 [297, 318]. When POT1 increases in transcriptional expression, carcinogenesis and tumour progression also increase. Additionally, CFAP58 has been linked to total blood protein levels which are used as a biomarker for disease [319].

Also involved with increased melanoma growth is FOXK1. This gene was significant for whorls on the left middle finger and is fundamentally a transcriptional regulator that regulates glucose metabolism and myogenic differentiation [320]. To function as an oncogene in melanoma, FOXK1 targets MMP9 in cooperation with other genes. By activating expression of MMP9 melanoma invasion and metastasis is promoted [321].

Conversely, CASZ1 is linked to tumour suppression and was significantly associated with loops on whorls on the left little finger. This gene encodes a transcription factor which regulates additional genes that control cell growth and developmental processes [303]. When CASZ1 is restored in neuroblastoma cells, cell differentiation and adhesion increase while migration and oncogenesis is suppressed [322]. This result highlights the importance of CASZ1 as a modulator in neural cell development. Variants in the gene have been associated with blood pressure variation however how this links to the development friction ridge skin and specifically loop patterns is unclear [303].

There is a definite theme of significant genes being important factors in tumour suppression and growth, specifically in epithelial and neural development. GLRA1 was significantly associated with loops on ring fingers and is involved with the function and regulation of the neurotransmission through the building of glycine receptors [299]. These protein receptors have specific sites where ligands bind to trigger signals that affect cell development and function. When there are mutations in GLRA1, Hyperekplexia is caused which is a disorder that triggers the affected individual to have an excessive startle reaction to unexpected external stimuli [323]. GLRA1 therefore has an important role in the normal function of the central nervous system.

SNPs that were found to have suggestive association display similar functional themes.

The 1p22.2 and 1p21.3 regions were found to have variants of suggestive association for loops on the right thumb. One variant was in KYAT3, a gene that catalyses transamination in the kynurenine pathway and may be involved in blood pressure irregularities [292]. KYAT3 is ubiquitous in its expression in the cytoplasm and has low cancer specificity [292]. The functional

pathways in which this gene is involved are integral to cell metabolism and have been highlighted as potential targets of cancer therapies [324]. The variant in 1p21.3 was located between SNX7 and LINC01776. SNX7 is a member of a gene family involved in intracellular transport though it has a differing structure to other genes in the family and its exact function is unknown. LINC01776 is a long intergenic non-protein coding RNA that also has no known function however it houses variants linked to schizophrenia via GWAS. Deletions on chromosome 1p21.3 have been seen as a cause of autism spectrum disorders and syndromic obesity indicating this area is a factor in neural function and development [325, 326]. More SNPs were found in areas linked to schizophrenia and grey matter reduction on 6p22.1 [327]. The peak suggestive association with loops on the left thumb was a variant (rs35128564) between TRA-AGC4-1 and TRA-CGC2-1, both tRNA anticodon genes [328, 329].

Returning to the cell growth regulation and differentiation theme, variants in NELL1 were suggestive in association to loops on the left middle finger. The gene encodes for a cytoplasmic protein which promotes osteoblast differentiation [298]. When the pathway is disrupted craniofacial development can be affected which results in craniosynostosis and synostosis [298]. Craniofacial development occurs between five to 10 weeks post-conception, this is the same time when fingers begin to form from paddles [2]. Therefore, it would be possible for these development processes to be simultaneously affected resulting in defined fingerprints by the 16^{th} week post conception [2].

Finally, FRS3 was identified as containing variants that were suggestive to having whorls on the left index finger. This gene encodes a substrate for the fibroblast growth factor receptor and is located in the peripheral plasma membrane [330]. This gene may influence fingerprint pattern through growth factor pathways and signalling though it may also a play a role through its cause of Kallmann syndrome [330]. Characteristics of this syndrome include a lack of production of certain hormones that direct sex development leading to delayed or absent puberty. If this gene were to influence sex hormones *in utero* this could explain some of the sex dimorphism seen in level one pattern and ridge density

There appears to be three main themes regarding the genes that suggestive and significant SNPs are located within. Long intergenic non-coding RNA such as LINC00621 may affect fingerprint patterns through protein coding gene regulation. Fingerprints may be regulated by protein coding genes (like NELL1) that control cell differentiation and development, and finally, genes such as FRS3 may affect fingerprints via regulation of development through hormones.

Ho *et al.* found variants in ADAMST9-AS2 and OLA1 plus a variant in an intergenic region adjacent to the TBX3 gene to be associated with whorl patterns. Variants in these genes were not found to be significant in the current study though the functions appear similar to variants that were. ADAMST9-AS2 and OLA1 are both oncogenes down-regulated in glioma and involved in the inhibition of migration of breast cancer cell lines [331, 332]. ADAMTS9-AS2 is a long non-coding RNA gene (lncRNA) similar to LINC00621 (lincRNA) since they are both non-coding RNA genes and can regulate gene expression, though lincRNAs have been distinguished from lncRNAs as they do not overlap coding loci. Also, lincRNA are usually found in the nucleus influencing cell differentiation whereas lncRNA are usually found outside the nucleus.

OLA1 is a protein coding gene, dissimilar to ADAMTS9-AS2 and LINC00621, but shares the same oncogene characteristic. This gene interacts with BRCA1 which is responsible for aggressive breast cancer and its overexpression is also evident in lung cancer [333]. OLA1 prevents cancer development by suppressing the GSK-3β/Snail/E-cadherin signalling pathway. This pathway is one of the main pathways promoting EMT (the same process LINC00621 regulates).

Finally, the TBX3 gene encodes transcription factors the regulate development processes. Specifically, TBX3 is a transcriptional repressor that is involved in the development of the tetrapod forelimb (arms in humans). Mutations in this gene have been determined to cause ulnar-mammary syndrome, symptoms of which are limb abnormalities, and poor apocrine gland and hair development [334]. The link between limb and fingerprints is logical given their proximal location. Apocrine glands and hair also somewhat linked to fingerprints through the skin however friction ridge skin (also known as thick skin) is the only hairless skin on the body, and the ridges of fingerprints align with the pores that are positioned above the eccrine glands not apocrine glands. Furthermore, TBX is another gene that effects EMT. Overexpression of TBX3 has been seen in melanoma, breast, lung, and bladder carcinomas. Specifically in breast cancers, TBX3 promotes tumour growth by upregulating SNAI2 (a transcription factor in the Snail pathway) and inducing EMT [335, 336]. The functions of this gene align with some findings in this study and also previous literature that hypothesised and found evidence for limb formation *in utero* influencing fingerprint development [7].

An additional hypothesis for fingerprint formation is the morphogenetic field effect which was seen in significant variants of ADAMTS9-AS9. The allele frequencies of rs1523452 showed the G allele was associated with a higher proportion of whorl patterns. This effect increased from the thumbs to the little fingers. Evidence of the morphogenetic field effect was not seen in this study, there were few SNPs that were significant on multiple fingers. Where SNPs were

significant or suggestive for multiple phenotypes it was located on the same finger (rs11805515, CASZ1).

It is hypothesised that EMT is involved with the morphogenetic field effect given the similar roles and effects. The ultimate example of morphogenetic fields is the differentiation of pre-embryonic cells into a head end and a tail end, and into a left side and a right side for most animals. Morphogenetic fields have also been identified as being important in wound healing and cancer suppression. The overarching control of this effect are signals that function distantly providing positional, polarity and growth cues [337]. The morphogenetic field has been shown to be controlled by biochemical and electromagnetic signals in embryonic development studies of brainless animals [338, 339]. In humans, anencephaly neonates (babies born missing parts of the brain and rudimentary brain stems) have relatively normal gross morphology indicating the cerebral structures of the brain do not have explicit control on morphogenesis [340]. Recent evidence has indicated that innervation is modulating tumour growth and disruption of the standard neural function may have wider ranging effects on morphology, particularly in early development [341]. This regulatory basis aligns with the significant CASZ1 and GLRA1 genes involved in the neural cell development and neurotransmission, and other suggestive genes and loci in this study linked to schizophrenia. Connecting the neural effect back to development and EMT are indications that people with schizophrenia have an increase and decrease in the rates of different cancers. These results have fuelled the theory that the genetic underpinnings of schizophrenia may have protective effects. However thus far studies have not been able to elucidate the true association from the confounding factors [342, 343].

While there were no exact comparisons between Ho *et al.* and this study. There was evidence supporting similar genetic pathways in cell development, tumour suppression and the function of the nervous system. This research uncovered new variants that may play a significant role in the development of the fingerprint phenotype. No single genetic variant was observed to solely encode for a specific fingerprint phenotype; therefore, it is understood variants in the genes work in an additive manor to influence the development of fingerprints.

7.2. Future directions

Genetic regulation in embryonic development is an extremely complex process. This study has found how fingerprint pattern frequency and ridge density changes per sex, ancestry, hand, and finger; plus investigated and uncovered several significant candidate markers that may be

responsible for fingerprint pattern phenotype. However, this study has not provided the most robust results possible with this study design due to cost and sample size.

The study of fingerprint pattern frequency was limited in this study by the size of the South Asian and Middle Eastern populations. Several ancestries such as Pacific Islander, African and Central and South American also had limited participants which meant they were excluded from statistical analysis. Indigenous Australians should also be included in any future investigations to provide a complete understanding of the various ancestries in the diverse Australian population. Once these ancestries have a sufficient fingerprint sample size a more wholistic view of pattern frequency could be formed which would reduce bias, important were this data to be relied upon for an expert statement on rarity. Increasing the sample size would also allow the isolation of independent variables. When assessing males and females, these groups contain individuals of all BGAs. This may mean that the sex dimorphism results may be skewed due to the greater effects of ancestry on pattern. It is especially a concern when two thirds of the fingerprinted sample were of European ancestry.

Further studies are required globally to confirm differences between BGA and pattern frequency. While there are several studies that have already reported frequencies there are serious flaws in many of the statistical approaches if there were any at all. Statistical analyses need to use a similar method to aid in meta-analyses of various populations. Once population pattern frequencies are reliably established, the effect of complex relationships such as the mixing of ancestries and the divergence of populations due emigration could be examined for a more comprehensive understanding.

In the assessment of fingerprint ridge density, the capture and computation could be further refined. Many of the fingerprints especially those made in ink were of too poor quality to apply the density measurement workflow. Furthermore, while digital fingerprint scans were of better quality there were obvious issues with scaling of the image. This study demonstrated there is too much uncertainty regarding ridge density, and it is unviable for classification in forensic casework. Moving forward there are two paths that could be taken. Variables in deposition could be examined more thoroughly before moving forward with classification research to test the validity. This may rule out the use of ridge density for classification all together. Alternatively and more complexly, deposition variables could be eliminated through a standardised approach of collecting fingerprints which may mean developing a process to regulate pressure and movement of the finger. Doing this would make the extraction of a ridge density value more accurate and reliable. Agnihotri *et al*. [220] classified sets of 10 fingerprints per sex with 92%

accuracy using ridge density. For this approach to work universally the prediction model needs to account BGA, pattern, finger, and hand, therefore studies need to be completed analysing these factors. At this step viability of classification would again need to be tested through a meta-analysis. Once a universal or Australian specific prediction model is developed, the model then would need to be tested by reintroducing variables linked to deposition. If a model upholds high accuracy after these many steps, only then could it be applied to fingermarks obtained through casework. When teamed with level one pattern this could create a comprehensive investigative tool for providing information where fingermarks do not return a match.

The genotyped sample size also needs to be expanded by a factor of ten. Gene wide association studies are best performed on extremely large datasets. Realistically, the sample size of 207 in this study is large enough for only a superficial analysis. Included in this expanded sample size needs to be specific people with rare fingerprint phenotypes. The increase in frequency of these phenotypes would also increase the statistical significance of the association results dramatically.

To determine where in the genome fingerprint phenotypes are modulated, full genome sequencing is required and epigenetic factors need to be considered. This would require considerable amounts of money, time and bioinformatic resources. Epigenetic factors can influence gene transcription and subsequent expression by DNA methylation, histone modifications and chromatin packaging without directly effecting the original DNA sequence. Additionally, enhancers of SNPs may also trans-regulate various factors which affect gene expression [344]. This is the type of regulation that may cause the development of phenotypic differences in monozygotic twins [345]. If we can associate SNPs and epigenetic factors with fingerprints (even fingerprints on specific fingers), then we may one day be able to predict someone's fingerprints from their DNA, allowing the interrogation of a fingerprint database even if we do not have physical fingerprints.

Studies investigating pattern frequency, ridge density and genetic markers all contribute to the understanding of fingerprint pattern phenotype. DNA has evolved as evidence from something that can provide only a match or no match, to a trace that has a comprehensive statistical basis. Furthermore, DNA can now provide wide-ranging information regarding the characteristics of the depositor through DNA phenotyping. DNA has developed relatively quickly in comparison to other forensic techniques. Fingerprints have been used forensically for much longer than DNA yet remained purely a trace for comparison and identification. With additional statistical and association research, fingerprints could ultimately also become a tool for investigative purposes.

The rarity of patterns for the presentation of expert evidence could be calculated, biographical information could be provided regarding the depositor and cross-analysis of DNA and fingerprints could occur.

APPENDICES

Appendices

Appendix A

Henry classification system

This is a peripheral text for understanding of the complexity of fingerprint classification systems other than the NCIC classification system that used in this study. This example also demonstrates why this system could not have been used in this study as pattern sub-types of arches, lops and whorls are not given separate classifications.

Given an individual's fingerprints are:

Table A1: An example set of fingerprints for Henry classification

Hand	Left					Right				
Finger	Little	Ring	Middle	Index	Thumb	Thumb	Index	Middle	Ring	Little
Finger number	10	9	8	7	6	1	2	3	4	5
Pattern	loop	loop	loop	arch	whorl	whorl	loop	loop	loop	arch

The following criteria need to be calculated:

Key – Ridge count of the first loop in the set of fingers starting from finger 1 to 10

Major – Value of ridge counts or ridge tracings of fingers 1 and 6

Primary – Often used singularly to catalogue fingerprints - Each finger is assigned a number, the right thumb being one and the right little finger being 5; for the left-hand thumb is designated 6 whereas the little finger is number 10. The finger is also assigned a numerical value if a whorl pattern is present. Fingers with an arch or loop pattern have a 0 value.

Table A2: Henry classification - Primary values

Hand	Left					Right				
Finger	Little	Ring	Middle	Index	Thumb	Thumb	Index	Middle	Ring	Little
Finger number	10	9	8	7	6	1	2	3	4	5
Value (if whorl)	1	1	2	2	4	16	16	8	8	4
Pattern	loop	loop	loop	arch	whorl	whorl	loop	loop	loop	arch
Value	0	0	0	0	4	16	0	0	0	0

To determine an individual's primary grouping ratio the following formula is applied to the finger values:

$$\frac{1 + (Sum\ of\ whorls, EVEN\ finger\ value)}{1 + (Sum\ of\ whorls, ODD\ finger\ value)} = Primary\ Grouping\ Ratio$$

Using the systematically assigned values from Table A3 above

$$\frac{1 + (4)}{1 + (16)} = \frac{5}{17}$$

This individual therefore belongs to the 5:17 primary group. If an individual were to have no whorls, their primary group would be 1:1. If an individual were to have whorls on all ten fingers, their primary group would be 32:32.

Secondary – Pattern type of fingers 2 and 7 (Radial loop – R, Ulnar loop – U, Whorl – W, Arch – A)

Sub-secondary – Value or ridge counts or tracing for fingers 2, 3 and 4 on the upper line and fingers 7, 8 and 9 on the bottom

Final – The ridge count of loops and/or whorls on the right and left little fingers. The count for the right finger is the numerator and the left finger the denominator. If the pattern is a whorl it is treated as an ulnar loop

Once calculated, the full Henry classification of the example set of fingerprints in Table A1 can be presented as follows:

Table A3: Henry classification - example

Key	Major	Primary	Secondary	Sub-secondary	Final
14	I	5	R	OOM	
	M	17	A	IOO	14

Appendix B

Vucetich classification system

This is a peripheral text for understanding of the complexity of fingerprint classification systems other than the NCIC classification system that used in this study. This example also demonstrates why this system could not have been used in this study as pattern sub-types of arches, lops and whorls are given complex designations which are difficult to express and translate back to a pattern type. Furthermore, resources in Australia heavily lean towards the Henry system making the Vucetich system more difficult to learn and use.

The Vucetich system uses primary and secondary classifications to represent the pattern of each finger. Just as the Henry classification system does, it begins with the right-hand thumb moving through to the left little finger.

Table B1: Primary classification of the Vucetich system

Pattern	Thumbs	Fingers
Arch	A	1
Internal loop	I	2
External loop	E	3
Whorl	V	4

The secondary classification specifies the sub-category of the level one fingerprint pattern. Where a loop pattern is of the normal flow description, the superscript defaults to the ridge count value.

Table B2: Secondary classification of the Vucetich system

Pattern	Superscript	Description		Ridge count spread	Superscript value
Arch	5	Vaulted/Normal		1-5	5
	6	Left inclined		6-10	10
	7	Right inclined		11-15	15
	8	Tent-shaped		16-20	20
	9	All others		Over 20	25
Internal loop	5,10, 15, 20 25	Normal flow			
	6	Invaded			
	7	Interrogatory			
	8	Hooked			
	9	All others			
External loop	Same as Internal loop				
Whorl	5	Normal			
	6	Sinuous			
	7	Ovoid			

	8	Hooked			
	9	All others			

Given an individual has the set of fingerprint patterns outlined in Table B3, a classification would appear as shown in Table B4.

Table B3: An example of fingerprint for Vucetich classification

Hand	Left					Right				
Finger	Little	Ring	Middle	Index	Thumb	Thumb	Index	Middle	Ring	Little
Finger number	10	9	8	7	6	1	2	3	4	5
Primary pattern	Internal loop	Internal loop	Internal loop	Arch	Whorl	Whorl	External loop	External loop	Internal loop	Arch
Secondary classification	Normal flow	Normal flow	Invaded	Vaulted/Normal	Normal	Ovoid	Normal flow	Normal flow	Normal flow	Right inclined

Within Table B4 the upper row represents the right hand and the bottom row the left. The first column are the thumbs and the final column the little fingers.

Table B4: Final Vucetich classification of a set of fingerprints

Hand	Thumb	Index	Middle	Ring	Little fingers
Right	$V^{(7)}$	$3^{(10)}$	$3^{(10)}$	$2^{(5)}$	$1^{(7)}$
Left	$V^{(5)}$	$1^{(5)}$	$2^{(6)}$	$2^{(5)}$	$2^{(5)}$

While simpler in terms of calculation compared to the Henry system, the Vucetich system provides a result that is more difficult for catalogue searches. The final Henry classification system distils the information into a more manageable primary group ratio.

Appendix C

Statement of consent presented to each volunteer

Participant ID:

UNIVERSITY OF TECHNOLOGY, SYDNEY
CRICOS Provider Code: 00099F

STATEMENT OF CONSENT

This information is required by the Ethics committee and stored separately from the rest of the data

I, (Name, please print) _____

agree to participate in this research project named: **Identification of single nucleotide polymorphisms (SNPs) involved in the determination of externally visible characteristics (EVCs), such as normal craniofacial morphology and pigmentation,** being conducted by Dr. Mark Barash, Centre for Forensic Sciences, Faculty of Science at the University of Technology Sydney, Room 04.05.315, Building 4, Thomas St, Broadway NSW 2007, Ph: 02 95141784.

I understand that the purpose of this study is to investigate the human genetics of the externally visible characteristics (EVCs), such as facial morphology, eye, skin and hair colour and hair pattern.
I have read the attached explanatory information.
I understand that this study will be of no direct benefit to me, not including a complimentary coffee voucher or/and a file with my 3D facial image.

I understand that my participation in this research may involve some discomfort due to the questions I would be asked (as per attached questionnaire) or as a result of my facial image being taken.
I understand that participation in this study is voluntary and that I am free to withdraw at any time without penalty or comment and without giving a reason. I am aware that I can contact Dr. Mark Barash if I have any concerns/questions about the research.

☐ I agree for a buccal swab sample to be taken.

☐ I agree for an image of my face to be taken.

☐ I agree for my fingerprints to be scanned

☐ I agree for my DNA sample to be used for other similar studies in the future.

☐ I agree to complete the questionnaire.

Please tick the appropriate boxes.

I understand that my confidentiality will be strictly preserved and my facial images will be used only to classify my facial features and pigmentation. I agree that the research data gathered from this project may be published in a form that does not identify me in any way.
I agree that Dr. Mark Barash or his representative has answered all my questions fully and clearly.

Signature of Participant _____ Date _____

Signature of Researcher/Delegate _____ Date _____

NOTE:
This study has been approved by the University of Technology, Sydney Human Research Ethics Committee HREC 2015000296. If you have any complaints or reservations about any aspect of your participation in this research which you cannot resolve with the researcher, you may contact the Ethics Committee through the Research Ethics Officer (ph: +61 2 9514 9772 Research.Ethics@uts.edu.au), and quote the UTS HREC reference number. Any complaint you make will be treated in confidence and investigated fully and you will be informed of the outcome.

Appendix D

UTS questionnaire for self-reported ancestry and phenotypic traits

UTS
UNIVERSITY OF TECHNOLOGY, SYDNEY
CRICOS Provider Code: 00099F

Participant ID:

Project title: Identification of single nucleotide polymorphisms (SNPs) involved in the determination of externally visible characteristics (EVCs), such as normal craniofacial morphology and pigmentation

Questionnaire

Gender: M / F
Age at the time of collection: _____ Time of sample donation ☐ AM ☐ PM

The form will be filled by the person collecting the samples.
If you have any questions regarding this form, please ask the researcher or email

Ancestry	Caucasian	E. Asian	S. Asian	Indigenous Australian	African	Other
Ethnicity Details (please note that the country of origin might be different to the Ethnical origin)	Paternal grandmother:		Paternal grandfather:			
	Maternal grandmother:		Maternal grandfather:			
Head measurements (mm)	**v-gn (max head height)**		**eu-eu (max head width)**		**g-op (max head length)**	
HAIR: natural colour & shade:	**RED**	Auburn	Orange	Carrot	Strawberry	
	BLONDE	Light Blonde	Dark Blonde			
	BROWN	Light Brown	Medium Brown	Dark Brown	Brown with red	
	BLACK	Light Black	Dark Black			
***Significant* hair colour change from child to adult?**			No		Yes	
			got much darker		got lighter	
Curliness	VERY CURLY	CURLY	WAVY		STRAIGHT	
Beard	Red	Blonde	Brown	Black	Mixture	
Eyebrows	Red	Blonde	Brown	Black	Mixture	
Grey Hair	Approximate age you commenced going grey?					
Baldness	Approximate age you commenced going bald?					
Was the hair loss	From the crown		From the forehead		Both	
EYES	**Eyelid**		single		double	
Colour & Shade	BLUE	Light Blue	Medium Blue		Dark Blue	
	GREEN	Light Green	Medium Green		Dark Green	
	GREY	Light Grey	Medium Grey		Dark Grey	
	HAZEL	Light Hazel	Medium Hazel		Dark Hazel	
	BROWN	Light Brown	Medium Brown		Dark Brown	
SKIN colour & freckling	**FAIR**	Extensive Freckling	Medium Freckling	Light Freckling	No Freckling	
	AVERAGE	Extensive Freckling	Medium Freckling	Light Freckling	No Freckling	
	DARK	**Olive**	**Light Brown**	**Dark Brown**	**Black**	
Ear lobes	attached		detached			
Height	Your height (cm or feet, inches)					
Weight	Your current weight (kg or pounds)					
Have you had any severe facial injuries or undergone facial surgery? If yes, please provide general details:						
Comments						

Appendix E

MLR results for arches, loops, and whorls

Table E1: Parameter estimates – arches – the effect of the independent variables on each dependent variable category

Pattern[a]		B	Standard Error	Wald	df	Significance (p-value)	Exp(B)	95% Confidence Interval for Exp(B)	
								Lower Bound	Upper Bound
ARCH - Plain	Intercept	-4.372	0.485	81.179	1	0.000			
	Left hand	0.242	0.126	3.722	1	0.054	1.274	0.996	1.630
	Right hand	0[b]			0				
	Little fingers	-1.412	0.263	28.856	1	0.000	0.244	0.146	0.408
	Ring fingers	-0.619	0.232	7.094	1	0.008	0.538	0.341	0.849
	Middle fingers	0.108	0.178	0.365	1	0.546	1.114	0.785	1.579
	Index fingers	0.890	0.176	25.455	1	0.000	2.435	1.723	3.440
	Thumbs	0[b]			0				
	Females	0.524	0.150	12.260	1	0.000	1.689	1.259	2.265
	Males	0[b]			0				
	E. Asian	0.934	0.491	3.616	1	0.057	2.544	0.972	6.658
	European	1.239	0.459	7.301	1	0.007	3.453	1.405	8.484
	M. E.	1.507	0.525	8.245	1	0.004	4.511	1.613	12.615
	S. Asian	0[b]			0				
ARCH - Tented	Intercept	-7.084	0.827	73.409	1	0.000			
	Left hand	0.231	0.150	2.379	1	0.123	1.260	0.939	1.689
	Right hand	0[b]			0				
	Little fingers	1.204	0.638	3.563	1	0.059	3.334	0.955	11.639
	Ring fingers	2.206	0.613	12.949	1	0.000	9.082	2.731	30.207
	Middle fingers	2.812	0.593	22.466	1	0.000	16.648	5.204	53.260
	Index fingers	3.882	0.589	43.390	1	0.000	48.544	15.291	154.111
	Thumbs	0[b]			0				
	Females	-0.276	0.154	3.228	1	0.072	0.759	0.562	1.025
	Males	0[b]			0				
	E. Asian	0.645	0.653	0.976	1	0.323	1.906	0.530	6.852
	European	1.611	0.589	7.481	1	0.006	5.006	1.579	15.875
	M. E.	1.731	0.670	6.665	1	0.010	5.644	1.517	21.001
	S. Asian	0[b]			0				

a. The reference category is: LOOP - Ulnar.

b. This parameter is set to zero because it is redundant.

Table E2: Parameter estimates – loops – the effect of the independent variables on each dependent variable category

Pattern[a]		B	Standard Error	Wald	df	Significance (p-value)	Exp(B)	95% Confidence Interval for Exp(B)	
								Lower Bound	Upper Bound
LOOP - Radial	Intercept	-7.524	1.060	50.404	1	0.000			
	Left hand	0.146	0.131	1.236	1	0.266	1.157	0.895	1.495
	Right hand	0[b]			0				
	Little fingers	0.766	1.156	0.439	1	0.508	2.150	0.223	20.710
	Ring fingers	2.724	1.036	6.912	1	0.009	15.248	2.000	116.235
	Middle fingers	2.796	1.026	7.430	1	0.006	16.381	2.194	122.313
	Index fingers	5.987	1.004	35.596	1	0.000	398.303	55.721	2847.163
	Thumbs	0[b]			0				
	Females	0.031	0.141	0.048	1	0.826	1.031	0.783	1.359
	Males	0[b]			0				
	E. Asian	0.030	0.404	0.006	1	0.940	1.031	0.467	2.278
	European	0.784	0.344	5.200	1	0.023	2.190	1.116	4.295
	M. E.	0.536	0.480	1.247	1	0.264	1.709	0.667	4.376
	S. Asian	0[b]			0				
a. The reference category is: LOOP - Ulnar.									
b. This parameter is set to zero because it is redundant.									

Table E3: Parameter estimates – whorls – the effect of the independent variables on each dependent variable category

Pattern[a]		B	Standard Error	Wald	df	Significance (p-value)	Exp(B)	95% Confidence Interval for Exp(B)	
								Lower Bound	Upper Bound
WHORL - Accidental	Intercept	-5.144	1.090	22.281	1	0.000			
	Left hand	0.377	0.394	0.917	1	0.338	1.458	0.674	3.155
	Right hand	0[b]			0				
	Little fingers	-2.431	1.062	5.242	1	0.022	0.088	0.011	0.705
	Ring fingers	-0.611	0.615	0.989	1	0.320	0.543	0.163	1.810
	Middle fingers	-1.603	0.792	4.096	1	0.043	0.201	0.043	0.951
	Index fingers	0.849	0.460	3.401	1	0.065	2.336	0.948	5.758
	Thumbs	0[b]			0				
	Females	-0.528	0.390	1.828	1	0.176	0.590	0.274	1.268
	Males	0[b]			0				
	E. Asian	0.399	1.160	0.118	1	0.731	1.491	0.153	14.489

	European	0.654	1.028	0.405	1	0.525	1.923	0.256	14.429
	M. E.	0.541	1.422	0.145	1	0.704	1.718	0.106	27.880
	S. Asian	0[b]			0				
WHORL - Central Pocket Loop	Intercept	-3.975	0.367	117.481	1	0.000			
	Left hand	0.108	0.128	0.709	1	0.400	1.114	0.867	1.430
	Right hand	0[b]			0				
	Little fingers	0.478	0.294	2.642	1	0.104	1.613	0.906	2.871
	Ring fingers	2.062	0.264	61.183	1	0.000	7.864	4.690	13.184
	Middle fingers	0.241	0.313	0.593	1	0.441	1.273	0.689	2.351
	Index fingers	1.744	0.279	39.123	1	0.000	5.720	3.312	9.880
	Thumbs	0[b]			0				
	Females	-0.009	0.136	0.005	1	0.946	0.991	0.759	1.294
	Males	0[b]			0				
	E. Asian	0.078	0.311	0.063	1	0.802	1.081	0.587	1.990
	European	-0.050	0.272	0.034	1	0.853	0.951	0.558	1.620
	M. E.	0.614	0.359	2.930	1	0.087	1.848	0.915	3.735
	S. Asian	0[b]			0				
WHORL - Double Loop	Intercept	-0.920	0.257	12.808	1	0.000			
	Left hand	0.028	0.140	0.039	1	0.843	1.028	0.782	1.351
	Right hand	0[b]			0				
	Little fingers	-3.671	0.419	76.932	1	0.000	0.025	0.011	0.058
	Ring fingers	-2.930	0.366	64.124	1	0.000	0.053	0.026	0.109
	Middle fingers	-2.392	0.247	93.431	1	0.000	0.091	0.056	0.149
	Index fingers	-1.100	0.193	32.496	1	0.000	0.333	0.228	0.486
	Thumbs	0[b]			0				
	Females	-0.525	0.141	13.789	1	0.000	0.592	0.449	0.781
	Males	0[b]			0				
	E. Asian	0.040	0.281	0.020	1	0.888	1.040	0.600	1.805
	European	-0.538	0.248	4.723	1	0.030	0.584	0.359	0.949
	M. E.	-1.556	0.632	6.066	1	0.014	0.211	0.061	0.728
	S. Asian	0[b]			0				
WHORL - Plain	Intercept	-0.394	0.134	8.635	1	0.003			
	Left hand	-0.162	0.061	7.113	1	0.008	0.850	0.755	0.958
	Right hand	0[b]			0				
	Little fingers	-1.166	0.104	125.208	1	0.000	0.312	0.254	0.382
	Ring fingers	0.355	0.086	17.076	1	0.000	1.427	1.205	1.688
	Middle fingers	-0.854	0.100	73.250	1	0.000	0.426	0.350	0.518
	Index fingers	0.434	0.092	22.141	1	0.000	1.543	1.288	1.849
	Thumbs	0[b]			0				

	Females	-0.239	0.063	14.270	1	0.000	0.787	0.696	0.891
	Males	0[b]			0				
	E. Asian	0.334	0.134	6.246	1	0.012	1.397	1.075	1.816
	European	-0.401	0.120	11.133	1	0.001	0.670	0.529	0.848
	M. E.	0.437	0.168	6.748	1	0.009	1.548	1.113	2.152
	S. Asian	0[b]			0				
a. The reference category is: LOOP - Ulnar.									
b. This parameter is set to zero because it is redundant.									

Appendix F

Wolfram Mathematica code for counting ridges

```
SetDirectory["D:\\file_name "]

images = FileNames["*.jpg"]

count = 1

Do[imagevar[count++]=Import[image],{image,images}]

PixelValue[ColorConvert[imagevar[1], "Grayscale"], {1,1}, "Byte"]

PixelValue[ColorConvert[imagevar[1], "Grayscale"],
{{57,1},{56,2},{55,3},{54,4},{53,5},{52,6},{51,7},{50,8},{49,9},{48,10},{47,11},{46,12},{45,13},{44,
14},{43,15},{42,16},{41,17},{40,18},{39,19},{38,20},{37,21},{36,22},{35,23},{34,24},{33,25},{32,2
6},{31,27},{30,28},{29,29},{28,30},{27,31},{26,32},{25,33},{24,34},{23,35},{22,36},{21,37},{20,38
},{19,39},{18,40},{17,41},{16,42},{15,43},{14,44},{13,45},{12,46},{11,47},{10,48},{9,49},{8,50},{7,
51},{6,52},{5,53},{4,54},{3,55},{2,56},{1,57}}, "Byte"]

table1 = Table[PixelValue[ColorConvert[imagevar[x], "Grayscale"],
{{57,1},{56,2},{55,3},{54,4},{53,5},{52,6},{51,7},{50,8},{49,9},{48,10},{47,11},{46,12},{45,13},{44,
14},{43,15},{42,16},{41,17},{40,18},{39,19},{38,20},{37,21},{36,22},{35,23},{34,24},{33,25},{32,2
6},{31,27},{30,28},{29,29},{28,30},{27,31},{26,32},{25,33},{24,34},{23,35},{22,36},{21,37},{20,38
},{19,39},{18,40},{17,41},{16,42},{15,43},{14,44},{13,45},{12,46},{11,47},{10,48},{9,49},{8,50},{7,
51},{6,52},{5,53},{4,54},{3,55},{2,56},{1,57}}, "Byte"],{x,1,5552}]

table1//TableForm

Export["table1.csv", table1]
```

Appendix G

Ridge density GEE results for the ulnar, radial, and proximal positions

Table G1: GEE results of ulnar position ridge density in the Sydney cohort

Parameter	B	Standard Error	95% Wald Confidence Interval		Hypothesis Test		
			Lower	Upper	Wald Chi-Square	df	Significance (p-value)
(Intercept)	2.187	0.0172	2.153	2.221	16097.191	1	0.000
Left hand	0.033	0.0043	0.024	0.041	57.243	1	0.000
Right hand	0						
Little fingers	0.044	0.0067	0.031	0.057	42.516	1	0.000
Ring fingers	0.090	0.0067	0.077	0.103	183.255	1	0.000
Middle fingers	0.075	0.0061	0.063	0.087	149.845	1	0.000
Index fingers	0.010	0.0064	-0.003	0.022	2.269	1	0.132
Thumbs	0.000						
ARCH – Plain	0.052	0.0150	0.023	0.081	12.024	1	0.001
ARCH – Tented	0.086	0.0131	0.060	0.111	42.434	1	0.000
LOOP – Radial	0.038	0.0114	0.016	0.061	11.335	1	0.001
LOOP – Ulnar	0.038	0.0057	0.027	0.049	45.053	1	0.000
WHORL - Accidental	-0.012	0.0379	-0.086	0.062	0.104	1	0.747
WHORL - Central Pocket Loop	0.016	0.0100	-0.004	0.035	2.449	1	0.118
WHORL - Double Loop	0.003	0.0118	-0.020	0.026	0.057	1	0.812
WHORL – Plain	0						
Females	0.067	0.0089	0.049	0.084	55.959	1	0.000
Males	0						
E. Asian	0.065	0.0181	0.030	0.101	12.924	1	0.000
European	0.017	0.0166	-0.150	0.050	1.068	1	0.301
M. E.	0.017	0.0242	-0.030	0.064	0.492	1	0.483
S. Asian	0						
(Scale)	1						
Dependent Variable: RD Model: (Intercept), Sex, BGA, Pattern, Hand, Finger							
a. Set to zero because this parameter is redundant.							

Table G2: GEE results of ulnar position ridge density in the Melbourne cohort

Parameter	B	Standard Error	95% Wald Confidence Interval		Hypothesis Test		
			Lower	Upper	Wald Chi-Square	df	Significance (p-value)
(Intercept)	2.696	0.0150	2.666	2.725	32426.740	1	0.000
Left hand	-0.005	0.0054	-0.015	0.006	0.826	1	0.363
Right hand	0[a]						
Little fingers	-0.047	0.0071	-0.061	-0.033	43.430	1	0.000
Ring fingers	-0.002	0.0071	-0.016	0.012	0.085	1	0.771
Middle fingers	0.021	0.0068	0.008	0.035	10.037	1	0.002
Index fingers	-0.009	0.0080	-0.025	0.007	1.191	1	0.275
Thumbs	0[a]						
ARCH – Plain	0.045	0.0166	0.012	0.077	7.308	1	0.007
ARCH – Tented	0.040	0.0179	0.005	0.075	5.115	1	0.024
LOOP – Radial	0.041	0.0134	0.015	0.067	9.558	1	0.002
LOOP – Ulnar	0.021	0.0073	0.007	0.036	8.597	1	0.003
WHORL - Accidental	-0.035	0.0838	-0.199	0.130	0.170	1	0.680

WHORL - Central Pocket Loop	-0.002	0.0216	-0.045	0.040	0.010	1	0.920
WHORL - Double Loop	0.006	0.0141	-0.022	0.034	0.180	1	0.671
WHORL – Plain	0[a]						
Females	0.047	0.0093	0.029	0.065	25.553	1	0.000
Males	0[a]						
E. Asian	0.038	0.0210	-0.003	0.080	3.314	1	0.069
European	0.034	0.0125	0.009	0.058	7.214	1	0.007
[BGA=M. E.]	0.028	0.0279	-0.027	0.082	0.975	1	0.323
S. Asian	0[a]						
(Scale)	1						
Dependent Variable: RD Model: (Intercept), Hand, Finger, Pattern, Sex, BGA							
a. Set to zero because this parameter is redundant.							

Table G3: GEE results of radial position ridge density in the Sydney cohort

Parameter	B	Standard Error	95% Wald Confidence Interval		Hypothesis Test		
			Lower	Upper	Wald Chi-Square	df	Significance (p-value)
(Intercept)	2.166	0.0176	2.132	2.201	15079.170	1	0.000
Left hand	-0.002	0.0045	-0.011	0.006	0.278	1	0.598
Right hand	0[a]						
Little fingers	0.074	0.0072	0.060	0.089	106.196	1	0.000
Ring fingers	0.096	0.0072	0.081	0.110	175.003	1	0.000
Middle fingers	0.085	0.0067	0.072	0.098	161.907	1	0.000
Index fingers	0.034	0.0070	0.020	0.048	23.602	1	0.000
Thumbs	0[a]						
ARCH – Plain	0.081	0.0139	0.054	0.108	33.938	1	0.000
ARCH – Tented	0.065	0.0133	0.039	0.091	23.974	1	0.000
LOOP – Radial	0.040	0.0127	0.015	0.064	9.808	1	0.002
LOOP – Ulnar	0.046	0.0060	0.034	0.057	58.431	1	0.000
WHORL - Accidental	0.064	0.0253	0.015	0.114	6.426	1	0.011
WHORL - Central Pocket Loop	0.027	0.0097	0.008	0.046	7.844	1	0.005
WHORL - Double Loop	-0.004	0.0128	-0.029	0.021	0.087	1	0.768
WHORL – Plain	0[a]						
Females	0.071	0.0077	0.056	0.087	86.163	1	0.000
Males	0[a]						
E. Asian	0.045	0.0174	0.011	0.079	6.781	1	0.009
European	0.008	0.0167	-0.025	0.041	0.224	1	0.636
M. E.	-0.001	0.0225	-0.045	0.043	0.002	1	0.961
S. Asian	0[a]						
(Scale)	1						
Dependent Variable: RD Model: (Intercept), Sex, BGA, Pattern, Hand, Finger							
a. Set to zero because this parameter is redundant.							

Table G4: GEE results of radial position ridge density in the Melbourne cohort

Parameter	B	Standard Error	95% Wald Confidence Interval		Hypothesis Test		
			Lower	Upper	Wald Chi-Square	df	Significance (p-value)
(Intercept)	2.653	0.0200	2.614	2.692	17541.228	1	0.000

Left hand	-0.006	0.0051	-0.016	0.004	1.519	1	0.218
Right hand	0[a]						
Little fingers	-0.008	0.0080	-0.024	0.008	1.034	1	0.309
Ring fingers	0.039	0.0076	0.024	0.054	26.815	1	0.000
Middle fingers	0.047	0.0073	0.033	0.061	42.096	1	0.000
Index fingers	0.032	0.0084	0.016	0.049	14.981	1	0.000
Thumbs	0[a]						
ARCH – Plain	0.028	0.0151	-0.002	0.057	3.403	1	0.065
ARCH – Tented	0.040	0.0139	0.013	0.068	8.431	1	0.004
LOOP – Radial	0.013	0.0150	-0.017	0.042	0.728	1	0.394
LOOP – Ulnar	0.026	0.0077	0.010	0.041	11.057	1	0.001
WHORL - Accidental	-0.121	0.0640	-0.246	0.005	3.543	1	0.060
WHORL - Central Pocket Loop	0.009	0.0172	-0.024	0.043	0.286	1	0.593
WHORL - Double Loop	0.006	0.0161	-0.026	0.037	0.128	1	0.721
WHORL – Plain	0[a]						
Females	0.056	0.0100	0.036	0.076	31.068	1	0.000
Males	0[a]						
E. Asian	0.046	0.0224	0.002	0.090	4.197	1	0.040
European	0.043	0.0188	0.006	0.080	5.235	1	0.022
M. E.	0.025	0.0305	-0.035	0.084	0.645	1	0.422
S. Asian	0[a]						
(Scale)	1						
Dependent Variable: RD Model: (Intercept), Hand, Finger, Pattern, Sex, BGA							
a. Set to zero because this parameter is redundant.							

Table G5: GEE results of proximal position ridge density in the Sydney cohort

Parameter	B	Standard Error	95% Wald Confidence Interval		Hypothesis Test		
			Lower	Upper	Wald Chi-Square	df	Significance (p-value)
(Intercept)	2.135	0.0144	2.107	2.163	21864.951	1	0.000
Left hand	0.003	0.0040	-0.005	0.011	0.588	1	0.443
Right hand	0[a]						
Little fingers	-0.038	0.0064	-0.050	-0.025	35.305	1	0.000
Ring fingers	-0.032	0.0057	-0.043	-0.021	32.164	1	0.000
Middle fingers	-0.024	0.0061	-0.036	-0.013	16.253	1	0.000
Index fingers	-0.004	0.0058	-0.015	0.008	0.385	1	0.535
Thumbs	0[a]						
ARCH – Plain	-0.034	0.0120	-0.057	-0.010	7.921	1	0.005
ARCH – Tented	-0.051	0.0136	-0.077	-0.024	13.719	1	0.000
LOOP – Radial	-0.045	0.0114	-0.067	-0.022	15.311	1	0.000
LOOP – Ulnar	-0.036	0.0054	-0.047	-0.026	45.012	1	0.000
WHORL - Accidental	0.022	0.0169	-0.011	0.055	1.756	1	0.185
WHORL - Central Pocket Loop	-0.002	0.0108	-0.023	0.019	0.030	1	0.862
WHORL - Double Loop	-0.022	0.0115	-0.045	9.558E-05	3.809	1	0.051
WHORL – Plain	0[a]						
Females	0.047	0.0071	0.033	0.061	44.053	1	0.000
Males	0[a]						
E. Asian	0.030	0.0151	0.000	0.060	3.948	1	0.047
European	0.000	0.0138	-0.027	0.027	0.001	1	0.976
M. E.	0.000	0.0177	-0.035	0.034	0.001	1	0.980
S. Asian	0[a]						
(Scale)	1						

Dependent Variable: RD Model: (Intercept), Hand, Finger, Pattern, Sex, BGA
a. Set to zero because this parameter is redundant.

Table G6: GEE results of proximal position ridge density in the Melbourne cohort

Parameter	B	Standard Error	95% Wald Confidence Interval		Hypothesis Test		
			Lower	Upper	Wald Chi-Square	df	Significance (p-value)
(Intercept)	2.635	0.0224	2.591	2.679	13829.855	1	0.000
Left hand	0.016	0.0070	0.003	0.030	5.553	1	0.018
Right hand	0[a]						
Little fingers	-0.031	0.0107	-0.052	-0.010	8.503	1	0.004
Ring fingers	0.007	0.0106	-0.014	0.028	0.450	1	0.502
Middle fingers	0.024	0.0093	0.006	0.042	6.706	1	0.010
Index fingers	0.017	0.0105	-0.004	0.037	2.475	1	0.116
Thumbs	0[a]						
ARCH – Plain	-0.010	0.0142	-0.038	0.017	0.538	1	0.463
ARCH – Tented	-0.013	0.0316	-0.075	0.049	0.178	1	0.673
LOOP – Radial	-0.005	0.0172	-0.039	0.029	0.080	1	0.778
LOOP – Ulnar	-0.020	0.0093	-0.038	-0.001	4.455	1	0.035
WHORL - Accidental	-0.075	0.1126	-0.295	0.146	0.442	1	0.506
WHORL - Central Pocket Loop	-0.014	0.0166	-0.047	0.018	0.756	1	0.384
WHORL - Double Loop	-0.010	0.0248	-0.059	0.038	0.170	1	0.680
WHORL – Plain	0[a]						
Females	0.016	0.0105	-0.005	0.036	2.257	1	0.133
Males	0[a]						
E. Asian	0.018	0.0227	-0.027	0.062	0.617	1	0.432
European	0.056	0.0191	0.018	0.093	8.450	1	0.004
M. E.	-0.040	0.0549	-0.148	0.068	0.530	1	0.467
S. Asian	0[a]						
(Scale)	1						
Dependent Variable: RD Model: (Intercept), Hand, Finger, Pattern, Sex, BGA							
a. Set to zero because this parameter is redundant.							

Appendix H

Ridge density GEE results for left and right finger position

Table H1: GEE results of left position ridge density in the Sydney cohort

Parameter	B	Standard Error	95% Wald Confidence Interval		Hypothesis Test		
			Lower	Upper	Wald Chi-Square	df	Significance (p-value)
(Intercept)	2.168	0.0169	2.135	2.201	16483.987	1	0.000
Left hand	0.042	0.0043	0.034	0.051	95.249	1	0.000
Right hand	0[a]						
Little fingers	0.072	0.0063	0.059	0.084	130.562	1	0.000
Ring fingers	0.100	0.0066	0.087	0.113	230.168	1	0.000
Middle fingers	0.083	0.0065	0.071	0.096	164.413	1	0.000
Index fingers	0.035	0.0064	0.023	0.048	30.243	1	0.000
Thumbs	0[a]						
ARCH – Plain	0.046	0.0149	0.017	0.075	9.513	1	0.002
ARCH – Tented	0.064	0.0126	0.040	0.089	26.035	1	0.000
LOOP – Radial	0.029	0.0114	0.006	0.051	6.382	1	0.012
LOOP – Ulnar	0.034	0.0056	0.023	0.045	37.115	1	0.000
WHORL - Accidental	0.003	0.0277	-0.051	0.058	0.014	1	0.904
WHORL - Central Pocket Loop	0.013	0.0103	-0.007	0.033	1.600	1	0.206
WHORL - Double Loop	0.004	0.0120	-0.020	0.027	0.105	1	0.745
WHORL – Plain	0[a]						
Females	0.070	0.0080	0.054	0.086	76.383	1	0.000
Males	0[a]						
E. Asian	0.053	0.0172	0.019	0.087	9.508	1	0.002
European	0.016	0.0163	-0.016	0.048	0.981	1	0.322
M. E.	0.018	0.0241	-0.029	0.065	0.540	1	0.463
S. Asian	0[a]						
(Scale)	1						
Dependent Variable: RD Model: (Intercept), Hand, Finger, Pattern, Sex, BGA							
a. Set to zero because this parameter is redundant.							

Table H2: GEE results of left position ridge density in the Melbourne cohort

Parameter	B	Standard Error	95% Wald Confidence Interval		Hypothesis Test		
			Lower	Upper	Wald Chi-Square	df	Significance (p-value)
(Intercept)	2.676	0.0189	2.639	2.713	19986.959	1	0.000
Left hand	-0.007	0.0050	-0.017	0.003	1.915	1	0.166
Right hand	0[a]						
Little fingers	-0.055	0.0071	-0.069	-0.041	59.102	1	0.000
Ring fingers	-0.010	0.0069	-0.023	0.004	2.020	1	0.155
Middle fingers	0.021	0.0067	0.008	0.034	9.614	1	0.002
Index fingers	0.010	0.0074	-0.005	0.024	1.696	1	0.193
Thumbs	0[a]						
ARCH – Plain	0.042	0.0181	0.007	0.078	5.420	1	0.020
ARCH – Tented	0.044	0.0173	0.010	0.078	6.466	1	0.011
LOOP – Radial	0.027	0.0132	0.002	0.053	4.317	1	0.038
LOOP – Ulnar	0.025	0.0070	0.011	0.038	12.395	1	0.000
WHORL - Accidental	-0.048	0.0920	-0.229	0.132	0.277	1	0.599
WHORL - Central Pocket Loop	0.005	0.0176	-0.029	0.040	0.095	1	0.757
WHORL - Double Loop	-0.012	0.0167	-0.045	0.021	0.498	1	0.481
WHORL – Plain	0[a]						
Females	0.054	0.0094	0.035	0.072	32.685	1	0.000
Males	0[a]						

E. Asian	0.048	0.0228	0.003	0.093	4.430	1	0.035
European	0.051	0.0179	0.016	0.086	8.236	1	0.004
M. E.	0.019	0.0300	-0.039	0.078	0.419	1	0.518
S. Asian	0[a]						
(Scale)	1						
Dependent Variable: RD Model: (Intercept), Hand, Finger, Pattern, Sex, BGA							
a. Set to zero because this parameter is redundant.							

Table H3: GEE results of right position ridge density in the Sydney cohort

Parameter	B	Standard Error	95% Wald Confidence Interval		Hypothesis Test		
			Lower	Upper	Wald Chi-Square	df	Significance (p-value)
(Intercept)	2.185	0.0160	2.154	2.217	18742.692	1	0.000
Left hand	-0.012	0.0048	-0.022	-0.003	6.731	1	0.009
Right hand	0[a]						
Little fingers	0.046	0.0071	0.032	0.060	42.811	1	0.000
Ring fingers	0.086	0.0067	0.072	0.099	161.757	1	0.000
Middle fingers	0.076	0.0066	0.063	0.088	131.988	1	0.000
Index fingers	0.008	0.0067	-0.006	0.021	1.292	1	0.256
Thumbs	0[a]						
ARCH – Plain	0.089	0.0152	0.059	0.119	34.105	1	0.000
ARCH – Tented	0.088	0.0138	0.061	0.116	40.778	1	0.000
LOOP – Radial	0.050	0.0123	0.026	0.074	16.897	1	0.000
LOOP – Ulnar	0.050	0.0058	0.039	0.062	76.562	1	0.000
WHORL - Accidental	0.051	0.0363	-0.020	0.122	1.964	1	0.161
WHORL - Central Pocket Loop	0.031	0.0103	0.011	0.051	9.196	1	0.002
WHORL - Double Loop	-0.004	0.0125	-0.029	0.020	0.130	1	0.718
WHORL – Plain	0[a]						
Females	0.068	0.0085	0.051	0.084	62.981	1	0.000
Males	0[a]						
E. Asian	0.058	0.0161	0.027	0.090	13.150	1	0.000
European	0.009	0.0148	-0.020	0.038	0.360	1	0.548
M. E.	-0.002	0.0208	-0.043	0.039	0.007	1	0.933
S. Asian	0[a]						
(Scale)	1						
Dependent Variable: RD Model: (Intercept), Hand, Finger, Pattern, Sex, BGA							
a. Set to zero because this parameter is redundant.							

Table H4: GEE results of right position ridge density in the Melbourne cohort

Parameter	B	Standard Error	95% Wald Confidence Interval		Hypothesis Test		
			Lower	Upper	Wald Chi-Square	df	Significance (p-value)
(Intercept)	2.673	0.0155	2.642	2.703	29594.089	1	0.000
Left hand	-0.006	0.0059	-0.017	0.006	0.949	1	0.330
Right hand	0[a]						
Little fingers	0.002	0.0086	-0.015	0.018	0.039	1	0.843
Ring fingers	0.047	0.0083	0.031	0.063	32.230	1	0.000
Middle fingers	0.049	0.0073	0.035	0.064	45.446	1	0.000
Index fingers	0.010	0.0087	-0.007	0.027	1.415	1	0.234
Thumbs	0[a]						
ARCH – Plain	0.025	0.0137	-0.002	0.052	3.387	1	0.066

ARCH – Tented	0.038	0.0170	0.005	0.072	5.009	1	0.025
LOOP – Radial	0.026	0.0160	-0.006	0.057	2.612	1	0.106
LOOP – Ulnar	0.022	0.0084	0.006	0.039	6.854	1	0.009
WHORL - Accidental	-0.104	0.0546	-0.211	0.003	3.608	1	0.057
WHORL - Central Pocket Loop	0.006	0.0198	-0.033	0.045	0.087	1	0.769
WHORL - Double Loop	0.027	0.0149	-0.003	0.056	3.212	1	0.073
WHORL – Plain	0[a]						
Females	0.049	0.0100	0.029	0.068	23.558	1	0.000
Males	0[a]						
E. Asian	0.037	0.0189	0.000	0.074	3.927	1	0.048
European	0.024	0.0132	-0.001	0.050	3.413	1	0.065
M. E.	0.033	0.0283	-0.022	0.089	1.376	1	0.241
S. Asian	0[a]						
(Scale)	1						
Dependent Variable: RD Model: (Intercept), Hand, Finger, Pattern, Sex, BGA							
a. Set to zero because this parameter is redundant.							

Appendix I

R code – SNPassoc and qqman packages

```
#import packages
library(SNPassoc)
library(graphics)
library(data.table)
library(janitor)
library(ggplot2)

  #set directory
  setwd("C:/file_path")
  getwd()

  #read all chromosomes - change per phenotype binary file and pattern to RD
  d1<-read.csv("Chr1.csv", header=T, sep=",")
  d2<-read.csv("Chr2.csv", header=T, sep=",")
  d3<-read.csv("Chr3.csv", header=T, sep=",")
  d4<-read.csv("Chr4.csv", header=T, sep=",")
  d5<-read.csv("Chr5.csv", header=T, sep=",")
  d6<-read.csv("Chr6.csv", header=T, sep=",")
  d7<-read.csv("Chr7.csv", header=T, sep=",")
  d8<-read.csv("Chr8.csv", header=T, sep=",")
  d9<-read.csv("Chr9.csv", header=T, sep=",")
  d10<-read.csv("Chr10.csv", header=T, sep=",")
  d11<-read.csv("Chr11.csv", header=T, sep=",")
  d12<-read.csv("Chr12.csv", header=T, sep=",")
  d13<-read.csv("Chr13.csv", header=T, sep=",")
  d14<-read.csv("Chr14.csv", header=T, sep=",")
  d15<-read.csv("Chr15.csv", header=T, sep=",")
  d16<-read.csv("Chr16.csv", header=T, sep=",")
  d17<-read.csv("Chr17.csv", header=T, sep=",")
  d18<-read.csv("Chr18.csv", header=T, sep=",")
  d19<-read.csv("Chr19.csv", header=T, sep=",")
  d20<-read.csv("Chr20.csv", header=T, sep=",")
  d21<-read.csv("Chr21.csv", header=T, sep=",")
  d22<-read.csv("Chr22.csv", header=T, sep=",")

  #combine all chr
  aSNPs<-
rbind(d1,d2,d3,d4,d5,d6,d7,d8,d9,d10,d11,d12,d13,d14,d15,d16,d17,d18,d19,d20,d21
,d22)

  #transpose
  t(aSNPs)
  aSNPst<-t(aSNPs)
  aSNPst[1:10,1:14]

  #convert matrix back to data frame
  aSNPst.df<-as.data.frame((aSNPst))
  aSNPst.df[1:10,1:21]
```

```
        #Make first row header and remove duplicate
        colnames(aSNPst.df)<-aSNPst.df[1,]
        aSNPst.df=aSNPst.df[-1,]
        #remove blank columns
        aSNPst.df.nb <- aSNPst.df[colSums(aSNPst.df != '') > 0]
        #print
        aSNPst.df.nb[1:10,1:21]

        #remove unneeded dataframes to clear memory
        rm(d1,d2,d3,d4,d5,d6,d7)
        rm(d8,d9,d10,d11,d12,d13)
        rm(d14,d15,d16,d17,d18,d19,d20,d21,d22)
        rm(aSNPs, aSNPst, aSNPst.df)

#DATAFRAME READY FOR ANALYSIS
#DESCRIPTIVE ANALYSIS
#adjust dataframe - select column SNPs start in - Long running
aSNPst.df.nb.s<-setupSNP(data=aSNPst.df.nb, colSNPs =4:ncol(aSNPst.df.nb), sep="")

#Plot missing data - Optional
plotMissing(aSNPst.df.nb.s, print.labels.SNPs = FALSE)

#HWE
#stratify HWE by control - adjust for association phenotype col name
hwe2 <- tableHWE(aSNPst.df.nb.s, RDU)
snpNHWE <- hwe2[,1]>0.05 & hwe2[,2]<0.05
rownames(hwe2)[snpNHWE]
hwe2[snpNHWE,]

#SNPS not in HWE are removed
snps.ok <- rownames(hwe2)[hwe2[,2]>=0.001]
pos <- which(colnames(aSNPst.df.nb.s)%in%snps.ok, useNames = FALSE)
aSNPst.df.nb.s <- setupSNP(aSNPst.df.nb, pos, sep="")


#Multi SNP analysis - adjust for association phenotype col name
ans.fast <- scanWGassociation(Phenotype_column_name, aSNPst.df.nb.s)
print(ans.fast)


        #SIngle SNP view
        head(aSNPst.df.nb.s$SNP_name)
        class(aSNPst.df.nb.s$SNP_name)
        summary(aSNPst.df.nb.s$SNP_name)
        plot(aSNPst.df.nb.s$SNP_name, type=pie)
        #Single SNP analysis
        association(Phenotype_column_name ~ SNP, data=aSNPst.df.nb.s)

#MANHATTAN PLOT
        # Load the library
        library(qqman)
        library(dplyr)
```

```
        library(tidyr)

        # Make the Manhattan plot on the ans.fast dataset
        #remove uneeded large dataframes
        rm(hwe, hwe2, snpNHWE, snps.ok, pos, aSNPst.df.nb)

        #remove hyphen from logadditive
        colnames(ans.fast)[6] <- "logadditive"

#repeat from here for all models
#keep column to plot – e.g. which model to show Manhattan graph
keeps <- c("dominant")
df = ans.fast[keeps]
#remove scientific notation
options(scipen = 999)

#make rownames a column
df <- data.frame(SNP = row.names(df), df)
rownames(df) <- c()

#turn SNP dummy names to location names to chr and pos columns
df$Split = df$SNP
col_order <- c("SNP","Split","dominant")
df <- df[,col_order]
df = df %>% separate(Split,
        c("Chr","Pos"), sep = 'x')

#remove rows with NA
df <- na.omit(df)

#check data type
sapply(df, mode)
df$Pos = as.numeric(as.character(df$Pos))
df$Chr = gsub("X","", df$Chr)
df$Chr = as.numeric(as.character(df$Chr))
#change col name
df = df %>% mutate_at(vars(dominant), funs(round(., 10)))

#check for NAs - change col name
which(is.na(df$dominant))
which(is.na(df$Pos))
which(is.na(df$Chr))

HighlightedSNPs <- df[df$dominant <0.0000001711, ]
Select <- HighlightedSNPs[,1]

#Change column names
colnames(df)[2] <- "CHR"
colnames(df)[3] <- "BP"
colnames(df)[4] <- "P"

#Produce Manhattan graph – change model, adjust threshold lines and annotated threshold
```

```
manhattan(df, chr="CHR", bp="BP", p="dominant", genomewideline = -log10(0.0000001711),
annotatePval = 0.00001, annotateTop = FALSE, highlight = Select)
#For Manhattan of subset of chromosome – select chromosome and bp location
manhattan(subset(df, CHR == 11), xlim = c(21000000,21500000))
```

Appendix J

A list of all significant and suggestive SNPs

Note: Within the "closest gene" column if one gene is listed the SNP is within that gene. If multiple genes are listed with a "+" the SNP is located within overlapping genes. If there are multiple genes listed with a "/" the SNP is located between the two genes.

Table J1: A list of SNPs that passed the significant threshold per phenotype for the association models

Pattern	Finger	Hand	Significant					
			Model	**SNP**	**CHR**	**BP**	**Closest gene**	**p-value**
Loops	Radial loops on both index fingers		Log-additive	rs41269369	1	239866503	CHRM3	4.74E-11
			Log-additive	rs7333557	13	47308287	LRCH1	2.09E-08
			Log-additive	rs17068763	13	47314326	LRCH1	2.09E-08
			Log-additive	rs75950241	12	44539357	TMEM117	3.50E-08
			Log-additive	rs117116926	12	44650974	TMEM117	3.50E-08
			Log-additive	rs76437304	16	23090732	USP31	1.18E-07
			Log-additive	rs7650693	3	182608551	ATP11B	1.44E-07
			Log-additive	rs16833596	3	182637840	ATP11B	1.44E-07
	Little finger	Left	Log-additive	rs11805515	1	10767785	CASZ1	2.22E-08
	Ring finger	Left	Recessive	rs1465555	5	151289698	GLRA1	1.49E-07
Whorls	8+ whorls		Log-additive	rs114125518	2	121252490	LINC01101 / LOC105373585	4.86E-09
			Log-additive	rs3132144	5	172681493	NKX2-5 / LOC105377731	1.06E-08
			Log-additive	rs78114274	14	101549556	LOC105370670 / LINC02285	2.50E-08
			Dominant	rs1339062	1	18978482	PAX7	4.45E-08
			Log-additive	rs73117589	12	60273359	LOC100996696 / LOC107984481	5.35E-08
			Log-additive	rs13193439	6	71917349	RNU6-411P / LOC100132834	6.47E-08
			Log-additive	rs13196838	6	72227953	LOC105377853 / LOC100131890	6.47E-08
			Log-additive	rs117064346	10	11380636	CELF2-AS1	9.41E-08
			Log-additive	rs73355019	14	101544358	LOC105370670	1.04E-07
	Little finger	Left	Log-additive	rs11805515	1	10767785	CASZ1	1.82E-10
	Ring finger	Left	Overdominant	rs1887263	13	23483716	LINC00621	4.22E-08
			Dominant	rs1887263	13	23483716	LINC00621	8.63E-08
	Middle finger	Left	Log-additive	rs75218590	7	4738772	FOXK1	2.70E-08
			Dominant	rs1109126	10	106143977	CFAP58	4.88E-08
			Dominant	rs11192037	10	106154143	CFAP58	1.35E-07
Arches	Little finger	Left	Log-additive	rs17524123	5	139946265	SLC35A4	2.88E-10
			Log-additive	rs1377909	2	158553975	ACVR1C / LOC105373713	8.59E-10
			Log-additive	rs10119809	9	111118405	LOC105376214	1.90E-09
			Log-additive	rs17638234	19	35979385	KRTDAP	8.04E-09

			Log-additive	rs71374924	16	7030162	RBFOX1	9.52E-09
			Log-additive	rs189767206	1	154929735	PYGO2 + PBXIP1	1.34E-08
			Log-additive	rs116839452	1	154837939	KCNN3	1.89E-08
			Log-additive	rs79822985	22	17639837	HDHD5 + HDHD5-AS1	5.12E-08
			Log-additive	rs10482787	1	218604288	TGFB2	5.97E-08
			Log-additive	rs77164781	10	134195952	LRRC27 / PWWP2B	5.97E-08
			Log-additive	rs1323968	13	28208114	POLR1D	5.97E-08
			Log-additive	rs11962416	6	75501410	LOC105377858	7.05E-08
			Log-additive	rs76855160	7	8549026	NXPH1	9.73E-08
			Log-additive	rs41271324	6	55407110	HMGCLL1	1.06E-07
		Right	Log-additive	rs77698137	3	4156426	SUMF1	6.70E-21
			Log-additive	+83 more				
	Ring finger	Left	Log-additive	rs114920443	1	118497043	WDR3 + SPAG17	6.37E-09
			Log-additive	rs7778404	7	132927070	ST13P7 / EXOC4	5.44E-08
			Log-additive	rs72641095	4	66364227	EPHA5	1.48E-07
		Right	Log-additive	rs72641095	4	66364227	EPHA5	5.17E-13
			Log-additive	rs117528546	7	121942849	FEZF1 + FEZF1-AS1	3.08E-11
			Log-additive	rs116844269	12	70196890	RAB3IP	3.63E-09
			Log-additive	rs79802709	16	77768045	NUDT7	4.10E-08
			Recessive	rs889472	16	79645989	LOC101928230	4.88E-08
			Log-additive	rs117117998	18	19943376	LOC105372019 / CTAGE1	6.63E-08
			Log-additive	rs28674959	15	86937956	AGBL1	7.11E-08
			Log-additive	rs77593524	13	23826949	SGCG	7.22E-08
			Log-additive	rs79460180	4	82649568	LOC107986215	8.06E-08
			Log-additive	rs2249577	13	76713762	RN7SL571P / LOC105370262	1.52E-07
			Log-additive	rs1045166	17	74267283	UBALD2 + QRICH2	1.66E-07
	Index finger	Left	Log-additive	rs6871490	5	10861222	CTD-2154B17.1 / LOC105374654	8.72E-09
	Thumb	Left	Log-additive	rs76586700	9	14573039	NFIB / ZDHHC21	3.05E-09
			Log-additive	rs76469528	7	139315798	HIPK2	9.56E-09
			Log-additive	rs78059854	5	92622029	POLD2P1 / NR2F1-AS1	2.69E-08
			Log-additive	rs67757319	2	180741887	ZNF385B / CWC22	4.01E-08
			Log-additive	rs72629733	10	27126235	ABI1	6.00E-08
			Log-additive	rs17816804	10	27133366	ABI1	6.00E-08
			Log-additive	rs77803466	20	5865457	SHLD1 / RNU1-55P	1.23E-07

Table J2: A list of SNPs that passed the suggestive threshold per phenotype for the association models

Pattern	Finger	Hand	Suggestive					
			Model	**SNP**	**CHR**	**BP**	**Closest gene**	**p-value**
Loops	8+ loops		Recessive	rs11001272	10	76823164	DUPD1	7.40E-07
			Overdominant	rs710116	5	172141057	LOC107986479 / LOC101928093	7.76E-07
			Recessive	rs10740447	10	76821925	DUPD1	9.04E-07
			Codominant	rs710116	5	172141057	LOC107986479 / LOC101928093	1.48E-06
			Codominant	rs11001272	10	76823164	DUPD1	2.66E-06
			Dominant	rs710116	5	172141057	LOC107986479 / LOC101928093	2.67E-06
			Dominant	rs342177	12	63097348	PPM1H	2.91E-06
			Overdominant	rs3800274	6	151759192	RMND1	3.66E-06
			Codominant	rs10740447	10	76821925	DUPD1	3.67E-06
			Overdominant	rs57997075	6	1773378	GMDS	7.07E-06
			Dominant	rs6414386	3	157312876	SLC66A1L	8.68E-06
			Dominant	rs7223727	17	15243264	TEKT3	8.72E-06
			Log-additive	rs6571922	14	22053675	ACTR3P1	9.62E-06
	8+ ulnar loops		Dominant	rs9850392	3	6011404	LOC102723596	3.01E-06
			Log-additive	rs76410636	17	77852945	CBX4 / LINC01979	4.08E-06
			Dominant	rs342177	12	63097348	PPM1H	4.85E-06
			Recessive	rs994308	20	6603622	CASC20 / LINC01713	6.59E-06
			Log-additive	rs6801077	3	11031922	SLC6A11 / SLC6A1	7.02E-06
			Dominant	rs1812388	3	5911337	LOC105376941 / LOC102723596	9.10E-06
			Overdominant	rs939317	3	184045799	EIF4G1	9.30E-06
			Dominant	rs10470296	3	194667692	LOC107986173 / LOC105374294	9.71E-06
			Recessive	rs12691693	2	145255210	ZEB2	9.71E-06
	1+ radial loop		Overdominant	rs10933693	3	194767164	LOC105374295 / XXYLT1	2.19E-06
			Overdominant	rs1861452	12	13909730	GRIN2B	2.58E-06
			Dominant	rs10933693	3	194767164	LOC105374295 / XXYLT1	2.95E-06
			Recessive	rs2875967	8	61428280	RAB2A	4.24E-06
			Log-additive	rs7470425	9	38747064	FAM240B / LOC105376043	4.40E-06
			Dominant	rs7235169	18	71402735	LOC105372190 / RN7SL401P	5.14E-06
			Dominant	rs583827	20	10046537	SNAP25-AS1	5.16E-06
			Dominant	rs7470425	9	38747064	FAM240B / LOC105376043	5.42E-06
			Codominant	rs4078332	16	65169117	LOC105371314	5.61E-06

			Recessive	rs2331195	22	26335966	MYO18B	5.62E-06
			Dominant	rs6784911	3	79412192	ROBO1	6.54E-06
			Dominant	rs10142427	14	99673324	BCL11B	9.15E-06
			Dominant	rs1934113	9	23079926	LOC107987055	9.82E-06
	Radial loops on both index fingers		Overdominant	rs28759032	8	69047334	PREX2	4.93E-07
			Recessive	rs212666	7	18738911	HDAC9	2.32E-06
			Codominant	rs28759032	8	69047334	PREX2	3.22E-06
			Codominant	rs212666	7	18738911	HDAC9	4.38E-06
			Dominant	rs41269369	1	239866503	CHRM3	5.04E-06
			Dominant	rs4089701	18	2451449	LOC105371961 / METTL4	5.33E-06
			Overdominant	rs17764136	5	126988749	CTXN3 + LOC105379164	7.36E-06
			Dominant	rs1178118	7	18751998	HDAC9	8.82E-06
			Overdominant	rs8023214	14	69117512	RAD51B	9.68E-06
			Log-additive	+ 50 more				
	Little finger	Left	Dominant	rs11805515	1	10767785	CASZ1	1.92E-06
			Recessive	rs61951477	13	69322850	RN7SL761P / LINC00550	2.91E-06
			Overdominant	rs2160835	3	177735032	LOC105374234	4.66E-06
			Dominant	rs4884495	13	64143037	LINC00376 / LOC105370237	5.45E-06
			Recessive	rs11691023	2	113339719	POLR1B / LOC101927330	6.43E-06
			Codominant	rs61951477	13	69322850	RN7SL761P / LINC00550	6.79E-06
			Codominant	rs11805515	1	10767785	CASZ1	7.40E-06
			Dominant	rs10434319	4	189798780	LOC101930028 / LOC105377611	8.19E-06
			Overdominant	rs11805515	1	10767785	CASZ1	9.82E-06
			Log-additive	rs115327059	5	73825291	LINC01331	9.95E-06
		Right	Log-additive	rs1012499	8	83150776	LOC105375930 / HNRNPA1P4	1.83E-06
			Recessive	rs17172181	7	43283115	HECW1	2.12E-06
			Log-additive	rs17172181	7	43283115	HECW1	3.07E-06
			Recessive	rs62165687	2	79010826	LOC105374819 / LOC105374821	3.28E-06
			Codominant	rs17172181	7	43283115	HECW1	3.96E-06
			Recessive	rs7041847	9	4287466	GLIS3	5.45E-06
			Recessive	rs7020673	9	4291747	GLIS3	5.45E-06
			Log-additive	rs11059451	12	128531217	LINC02441 / LOC105370071	6.47E-06
			Dominant	rs10179297	2	7460260	LOC107985846	7.32E-06
			Recessive	rs2026465	10	19791144	MALRD1	8.15E-06
			Dominant	rs12762955	10	1078782	IDI2-AS1	8.19E-06
			Overdominant	rs7773233	6	162851519	PRKN	8.28E-06

			Recessive	rs1927520	13	27449015	GPR12 / FGFR1OP2P1	8.95E-06
			Log-additive	rs1339062	1	18978482	PAX7	9.15E-06
			Dominant	rs4278886	2	238522744	LOC105373958 / LRRFIP1	9.49E-06
			Log-additive	rs76090611	3	56174002	ERC2	9.91E-06
	Ring finger	Left	Dominant	rs17856536	17	45917605	SCRN2	2.06E-07
			Overdominant	rs17856536	17	45917605	SCRN2	4.21E-07
			Overdominant	rs10483508	14	40541386	LOC105370461 / LOC105370464	7.67E-07
			Codominant	rs1465555	5	151289698	GLRA1	9.30E-07
			Dominant	rs10483508	14	40541386	LOC105370461 / LOC105370464	9.57E-07
			Codominant	rs17856536	17	45917605	SCRN2	1.39E-06
			Overdominant	rs1887263	13	23483716	LINC00621	2.65E-06
			Codominant	rs10483508	14	40541386	LOC105370461 / LOC105370464	2.94E-06
			Overdominant	rs2242644	14	80286694	NRXN3	6.28E-06
			Dominant	rs117876804	14	87835590	LINC02296	7.06E-06
			Recessive	rs10462717	5	14024415	DNAH5 / TRIO	7.30E-06
			Dominant	rs6973868	7	146759484	CNTNAP2	8.22E-06
			Codominant	rs2242644	14	80286694	NRXN3	8.55E-06
			Codominant	rs1887263	13	23483716	LINC00621	8.66E-06
			Log-additive	rs1439745	2	210025481	CRYGFP / PKP4P1	9.64E-06
			Overdominant	rs9947295	18	11759432	GNAL	9.75E-06
		Right	Overdominant	rs4955637	3	168815099	MECOM	7.14E-07
			Dominant	rs11754813	6	42690514	PRPH2	1.57E-06
			Codominant	rs7951915	11	81259119	LINC02720 / MTCO3P25	2.89E-06
			Codominant	rs4955637	3	168815099	MECOM	4.02E-06
			Log-additive	rs11754813	6	42690514	PRPH2	4.06E-06
			Recessive	rs3780164	9	36958582	PAX5	4.32E-06
			Overdominant	rs7951915	11	81259119	LINC02720 / MTCO3P25	5.01E-06
			Overdominant	rs12551916	9	82603402	LINC01507 + LOC105376099	5.32E-06
			Dominant	rs2580189	13	50806640	DLEU1	5.69E-06
			Recessive	rs12539745	7	21809630	DNAH11	5.69E-06
			Codominant	rs11754813	6	42690514	PRPH2	6.47E-06
			Codominant	rs6127985	20	55824760	BMP7	7.65E-06
	Middle finger	Left	Recessive	rs2324154	4	24027226	PPARGC1A	6.29E-07
			Dominant	rs17585205	5	89028204	LINC02161	1.24E-06
			Overdominant	rs17585205	5	89028204	LINC02161	1.32E-06
			Overdominant	rs11192037	10	106154143	CFAP58	2.29E-06
			Recessive	rs6694034	1	202003987	ELF3 / LOC105371684	2.58E-06

			Log-additive	rs1075177	12	114549194	LOC105369995	3.54E-06
			Codominant	rs2324154	4	24027226	PPARGC1A	3.83E-06
			Log-additive	rs6497844	16	10350625	LOC105371078 / ATF7IP2	3.83E-06
			Codominant	rs77411613	7	147355378	CNTNAP2	4.22E-06
			Overdominant	rs77411613	7	147355378	CNTNAP2	4.37E-06
			Dominant	rs979043	2	67566281	LINC01828 / ETAA1	5.01E-06
			Codominant	rs17585205	5	89028204	LINC02161	5.70E-06
			Overdominant	rs995140	5	121633067	LOC100505841 / SNCAIP	5.87E-06
			Overdominant	rs7786720	7	106642123	PIK3CG / PRKAR2B	6.07E-06
			Overdominant	rs1109126	10	106143977	CFAP58	6.44E-06
			Recessive	rs13264030	8	82706253	CHMP4C / SNX16	6.55E-06
			Codominant	rs6497844	16	10350625	LOC105371078 / ATF7IP2	6.78E-06
			Dominant	rs923259	11	11521053	GALNT18	7.82E-06
			Log-additive	rs17585205	5	89028204	LINC02161	8.24E-06
			Dominant	rs13249845	8	103586800	ODF1 / POU5F1P2	8.73E-06
			Codominant	rs6694034	1	202003987	ELF3 / LOC105371684	8.91E-06
			Dominant	rs1075177	12	114549194	LOC105369995	9.83E-06
		Right	Log-additive	rs62498864	8	6686679	XKR5	1.85E-06
			Log-additive	rs1791810	11	21168295	NELL1	3.73E-06
			Log-additive	rs59292470	11	11048650	LOC105379882 / LINC02752	4.10E-06
			Log-additive	rs193756	16	11326785	LOC107984859 / HNRNPCP4	5.67E-06
			Log-additive	rs1607098	11	21157762	NELL1	7.04E-06
			Overdominant	rs1417056	6	164852232	LOC105379712 / LOC107986667	7.36E-06
			Recessive	rs17791096	3	5093858	LOC105376934 / RNF10P1	7.36E-06
			Recessive	rs1515367	3	134592440	EPHB1 + LOC105374121	8.80E-06
			Dominant	rs11850320	14	54920423	CNIH1 / GMFB	9.66E-06
	Index finger	Left	Codominant	rs2430822	8	140610241	COL22A1 / KCNK9	5.08E-07
			Overdominant	rs55946098	11	81070178	LINC02720 / MTCO3P25	7.74E-07
			Log-additive	rs17491493	7	70022011	AUTS2	8.61E-07
			Overdominant	rs7247922	19	53815965	LOC107987270 / VN1R6P	1.70E-06
			Dominant	rs6114780	20	24557888	SYNDIG1	2.30E-06
			Overdominant	rs6114780	20	24557888	SYNDIG1	2.73E-06

			Codominant	rs55946098	11	81070178	LINC02720 / MTCO3P25	3.35E-06
			Recessive	rs6010620	20	62309839	RTEL1 + RTEL1-TNFRSF6B	3.89E-06
			Overdominant	rs2299219	7	86417845	GRM3 + LOC105375382	4.27E-06
			Overdominant	rs11644456	16	84301001	RNA5SP433 / WFDC1	4.78E-06
			Overdominant	rs60701297	21	33292708	HUNK	5.67E-06
			Codominant	rs60701297	21	33292708	HUNK	7.27E-06
			Dominant	rs17491493	7	70022011	AUTS2	8.21E-06
			Dominant	rs2430822	8	140610241	COL22A1 / KCNK9	8.82E-06
			Log-additive	rs2430822	8	140610241	COL22A1 / KCNK9	9.15E-06
			Overdominant	rs671503	11	35879671	TRIM44 / KRT18P14	9.39E-06
			Overdominant	rs10792563	11	81142678	LINC02720 / MTCO3P25	9.87E-06
			Codominant	rs7247922	19	53815965	LOC107987270 / VN1R6P	9.97E-06
		Right	Recessive	rs10759642	9	116121058	BSPRY	7.36E-07
			Codominant	rs10759642	9	116121058	BSPRY	2.51E-06
			Codominant	rs17239735	15	57769899	CGNL1	3.05E-06
			Recessive	rs2447376	8	140534479	COL22A1 / KCNK9	6.01E-06
			Log-additive	rs2468677	8	140519517	COL22A1 / KCNK9	6.59E-06
			Overdominant	rs1600277	5	101095318	LOC105379102	7.08E-06
			Dominant	rs72748753	5	22803278	CDH12	7.09E-06
			Recessive	rs2468677	8	140519517	COL22A1 / KCNK9	7.13E-06
			Recessive	rs12675573	8	8483293	RN7SL178P / LOC105379225	7.66E-06
			Codominant	rs2468677	8	140519517	COL22A1 / KCNK9	9.92E-06
	Thumbs	Left	Overdominant	rs111948736	1	213995810	PROX1-AS1 + LOC105372912	1.05E-06
			Log-additive	rs67485448	11	75794739	UVRAG	3.94E-06
			Dominant	rs55979208	11	75782829	UVRAG	5.22E-06
			Recessive	rs7226983	18	27232815	LOC105372045 / MIR302F	5.22E-06
			Codominant	rs111948736	1	213995810	PROX1-AS1 + LOC105372912	6.31E-06
			Dominant	rs111948736	1	213995810	PROX1-AS1 + LOC105372912	7.00E-06
			Recessive	rs4268102	8	108408409	ANGPT1	7.48E-06
			Dominant	rs35128564	6	28635780	TRA-AGC4-1 / TRA-CGC2-1	8.28E-06
			Dominant	rs13193532	6	28622914	LINC00533	8.59E-06

			Dominant	rs67485448	11	75794739	UVRAG	9.33E-06
			Recessive	rs3770535	2	216838699	MREG	9.98E-06
		Right	Dominant	rs668502	12	18811688	PIK3C2G + PLCZ1	2.77E-07
			Dominant	rs11579178	1	89417918	KYAT3	1.50E-06
			Codominant	rs668502	12	18811688	PIK3C2G + PLCZ1	1.67E-06
			Dominant	rs2765524	1	89417695	KYAT3	2.92E-06
			Overdominant	rs1450476	4	121784013	PRDM5	3.54E-06
			Overdominant	rs7191587	16	26970674	LINC02195 / LOC105371153	4.15E-06
			Overdominant	rs9480199	6	156082954	LOC105378069 / LOC105378072	7.27E-06
			Dominant	rs1450476	4	121784013	PRDM5	7.33E-06
			Codominant	rs11579178	1	89417918	KYAT3	8.04E-06
			Log-additive	rs11579178	1	89417918	KYAT3	8.15E-06
			Dominant	rs61786785	1	98861874	LINC01776 / SNX7	9.91E-06
Whorls	8+ whorls		Codominant	rs1339062	1	18978482	PAX7	3.15E-07
			Dominant	rs1563605	6	70345513	ADGRB3 / LMBRD1	4.77E-06
			Dominant	rs17005759	4	83446505	TMEM150C	6.04E-06
			Dominant	rs4693454	4	83448764	TMEM150C	6.04E-06
			Dominant	rs980223	6	70269974	ADGRB3 / LMBRD1	6.97E-06
			Dominant	rs3132144	5	172681493	NKX2-5 / LOC105377731	7.02E-06
			Log-additive	+62 more				
	Whorls on both ring fingers		Recessive	rs7951915	11	81259119	LINC02720 / MTCO3P25	5.18E-07
			Log-additive	rs1600350	3	151739498	LOC107986047 / LOC101928166	8.67E-07
			Codominant	rs7951915	11	81259119	LINC02720 / MTCO3P25	1.29E-06
			Dominant	rs11754813	6	42690514	PRPH2	1.99E-06
			Dominant	rs1887263	13	23483716	LINC00621	3.27E-06
			Recessive	rs6427047	1	166914258	ILDR2 + MAEL	3.44E-06
			Overdominant	rs78270802	21	45340041	AGPAT3	3.64E-06
			Overdominant	rs1887263	13	23483716	LINC00621	5.71E-06
			Overdominant	rs7820620	8	136203934	RPL23AP56 / LINC01591	5.88E-06
			Dominant	rs1600350	3	151739498	LOC107986047 / LOC101928166	6.96E-06
			Codominant	rs1600350	3	151739498	LOC107986047 / LOC101928166	7.09E-06
			Codominant	rs7820620	8	136203934	RPL23AP56 / LINC01591	7.15E-06
			Overdominant	rs2979245	8	8939373	ERI1	7.66E-06

			Log-additive	rs7143120	14	95163142	LOC100288028 / RPSAP4	7.91E-06
			Dominant	rs12386983	8	70661988	SLCO5A1	9.12E-06
			Log-additive	rs2723362	3	151676322	LOC107986047	9.12E-06
	Whorls on both thumbs		Dominant	rs2472811	6	14783210	LOC107986572 / LOC105374944	7.77E-06
			Dominant	rs964411	16	69541877	CYB5B / LOC105371325	8.35E-06
			Codominant	rs2303815	19	374016	THEG	9.64E-06
	Little finger	Left	Dominant	rs11805515	1	10767785	CASZ1	3.44E-07
			Log-additive	rs7569665	2	66179131	LOC105369168	6.22E-07
			Overdominant	rs12739189	1	2757537	TTC34 / ACTRT2	7.97E-07
			Codominant	rs11805515	1	10767785	CASZ1	1.29E-06
			Log-additive	rs74790980	14	45235162	LINC02302	1.36E-06
			Recessive	rs517992	18	65964621	LINC01912 / AKR1B10P2	1.37E-06
			Log-additive	rs4845952	1	10767379	CASZ1	1.72E-06
			Dominant	rs12518455	5	85330526	LOC105379063 / PTP4A1P4	1.86E-06
			Log-additive	rs12272883	11	81263907	MTND4P36	2.42E-06
			Codominant	rs12739189	1	2757537	TTC34 / ACTRT2	2.46E-06
			Overdominant	rs11805515	1	10767785	CASZ1	2.56E-06
			Log-additive	rs33961	5	141928868	SPRY4-AS1 / RPS12P10	4.88E-06
			Log-additive	rs114125518	2	121252490	LINC01101 / LOC105373585	4.90E-06
			Dominant	rs4845952	1	10767379	CASZ1	5.43E-06
			Overdominant	rs6563564	13	38201657	POSTN / TRPC4	5.76E-06
			Log-additive	rs1414397	10	13434975	LOC105376419	5.90E-06
			Overdominant	rs4648384	1	2756621	TTC34 / ACTRT2	6.10E-06
			Log-additive	rs66876903	12	811799	LINC02455 + LOC101929432	6.19E-06
			Codominant	rs517992	18	65964621	LINC01912 / AKR1B10P2	7.59E-06
			Log-additive	rs10897844	11	81288960	MTCYBP25 / MIR4300HG	8.73E-06
			Log-additive	rs7243360	18	55954791	NEDD4L	9.05E-06
			Overdominant	rs17548053	4	171234457	LINC01612 / LINC02512	9.37E-06
		Right	Log-additive	rs11059451	12	128531217	LINC02441 / LOC105370071	2.95E-07
			Log-additive	rs76090611	3	56174002	ERC2	5.87E-07
			Dominant	rs4278886	2	238522744	LOC105373958 / LRRFIP1	1.49E-06
			Log-additive	rs6139282	20	4045738	RPL21P2 / SMOX	1.97E-06
			Log-additive	rs74994650	1	48536674	LINC02794	1.99E-06
			Log-additive	rs28665982	19	54584651	TARM1	2.18E-06

			Log-additive	rs10144417	14	67826910	ATP6V1D + EIF2S1	2.21E-06
			Log-additive	rs10139585	14	67860119	PLEK2	2.21E-06
			Log-additive	rs3818468	14	67862371	PLEK2	2.21E-06
			Recessive	rs1927520	13	27449015	GPR12 / FGFR1OP2P1	2.71E-06
			Overdominant	rs7773233	6	162851519	PRKN	3.01E-06
			Log-additive	rs1012499	8	83150776	LOC105375930 / HNRNPA1P4	3.18E-06
			Log-additive	rs28528982	21	47470831	LOC105372842 / PSMA6P3	3.33E-06
			Dominant	rs7773233	6	162851519	PRKN	3.50E-06
			Log-additive	rs33961	5	141928868	SPRY4-AS1 / RPS12P10	3.62E-06
			Log-additive	rs72847592	11	2876768	KCNQ1-AS1	3.69E-06
			Overdominant	rs17422727	6	32259923	TSBP1 + LOC105379657 + LOC101929163	4.56E-06
			Overdominant	rs17201917	6	32235757	LOC101929163	4.88E-06
			Dominant	rs12978500	19	406934	C2CD4C	4.97E-06
			Log-additive	rs78943498	1	53132517	SHISAL2A	5.82E-06
			Log-additive	rs79711188	13	46251180	COX4I1P2 / LINC01055	5.86E-06
			Overdominant	rs995904	3	65273669	LOC107986094	6.44E-06
			Log-additive	rs1369926	16	63276158	LOC105371308	6.48E-06
			Codominant	rs12857403	13	22865609	LINC00540 / LOC107984599	7.49E-06
			Log-additive	rs118180670	13	81039096	RNU6-61P / HNRNPA1P31	7.67E-06
			Overdominant	rs737438	8	134386337	LOC105375771	7.83E-06
			Codominant	rs1927520	13	27449015	GPR12 / FGFR1OP2P1	8.00E-06
			Codominant	rs4278886	2	238522744	LOC105373958 / LRRFIP1	8.28E-06
			Log-additive	rs7627890	3	73532069	PDZRN3	8.51E-06
			Dominant	rs11059451	12	128531217	LINC02441 / LOC105370071	9.90E-06
	Ring finger	Left	Codominant	rs1887263	13	23483716	LINC00621	2.28E-07
			Overdominant	rs9947295	18	11759432	GNAL	1.15E-06
			Dominant	rs9947295	18	11759432	GNAL	2.87E-06
			Dominant	rs55855959	12	94262781	CRADD	4.01E-06
			Dominant	rs564352	21	44749141	LINC00322	5.21E-06
			Log-additive	rs1887263	13	23483716	LINC00621	6.35E-06
			Dominant	rs17856536	17	45917605	SCRN2	6.89E-06
			Overdominant	rs55855959	12	94262781	CRADD	6.89E-06
			Codominant	rs9947295	18	11759432	GNAL	7.19E-06
		Right	Overdominant	rs4955637	3	168815099	MECOM	9.20E-07

			Recessive	rs7951915	11	81259119	LINC02720 / MTCO3P25	1.78E-06
			Log-additive	rs899239	16	56321119	GNAO1	3.51E-06
			Recessive	rs12952341	17	4385503	SPNS3	3.51E-06
			Overdominant	rs7081094	10	24670973	KIAA1217	3.90E-06
			Codominant	rs7951915	11	81259119	LINC02720 / MTCO3P25	4.58E-06
			Overdominant	rs12551916	9	82603402	LINC01507 + LOC105376099	4.79E-06
			Overdominant	rs10816959	9	113046742	LOC107987114 / TXNDC8	4.82E-06
			Codominant	rs4955637	3	168815099	MECOM	5.55E-06
			Overdominant	rs7896427	10	24674934	KIAA1217	9.92E-06
	Middle finger	Left	Overdominant	rs11192037	10	106154143	CFAP58	1.77E-07
			Codominant	rs1109126	10	106143977	CFAP58	2.23E-07
			Overdominant	rs1109126	10	106143977	CFAP58	3.49E-07
			Codominant	rs11192037	10	106154143	CFAP58	4.10E-07
			Dominant	rs306416	13	26493476	ATP8A2	7.81E-07
			Log-additive	rs12172730	1	105111535	FTLP17 / LOC105378880	9.06E-07
			Overdominant	rs12705794	7	111358271	IMMP2L / DOCK4	1.74E-06
			Recessive	rs11691023	2	113339719	POLR1B / LOC101927330	1.87E-06
			Log-additive	rs73117589	12	60273359	LOC100996696 / LOC107984481	2.86E-06
			Log-additive	rs7894450	10	62626977	CDK1 / RHOBTB1	3.41E-06
			Log-additive	rs115066744	3	83671916	LOC105377183 / LOC105377186	3.57E-06
			Codominant	rs306416	13	26493476	ATP8A2	3.79E-06
			Overdominant	rs17372441	3	152203657	MBNL1 / LOC105374163	3.82E-06
			Log-additive	rs116261393	3	83682335	LOC105377183 / LOC105377186	3.83E-06
			Log-additive	rs114040757	3	83966303	LOC105377187 / SRRM1P2	4.12E-06
			Overdominant	rs1549555	1	80858466	HMGB1P18 / HNRNPA1P64	4.68E-06
			Overdominant	rs6979050	7	111392415	DOCK4	4.77E-06
			Overdominant	rs13232211	7	111396632	DOCK4	4.77E-06
			Overdominant	rs9947295	18	11759432	GNAL	5.20E-06
			Log-additive	rs1109126	10	106143977	CFAP58	5.35E-06
			Codominant	rs11691023	2	113339719	POLR1B / LOC101927330	5.71E-06
			Dominant	rs75218590	7	4738772	FOXK1	6.70E-06
			Log-additive	rs79640667	12	49358392	ARF3 / WNT10B	7.20E-06
			Dominant	rs1075177	12	114549194	LOC105369995	7.27E-06

			Codominant	rs2410600	8	18922390	PSD3	7.38E-06
			Dominant	rs12705794	7	111358271	IMMP2L / DOCK4	7.63E-06
			Recessive	rs10799899	1	163073502	RGS4 / RGS5	7.83E-06
			Codominant	rs12705794	7	111358271	IMMP2L / DOCK4	7.97E-06
			Dominant	rs12172730	1	105111535	FTLP17 / LOC105378880	8.21E-06
			Dominant	rs1541702	16	11445552	RMI2 + LOC105371082	8.28E-06
			Log-additive	rs2410600	8	18922390	PSD3	9.27E-06
			Log-additive	rs12148472	15	79231478	CTSH	9.61E-06
			Overdominant	rs62267721	3	87542296	KRT8P25 / APOOP2	9.76E-06
		Right	Log-additive	rs9295984	6	31317697	LOC112267902 / HLA-B	1.06E-06
			Log-additive	rs62318874	4	72746136	GC / NPFFR2	1.37E-06
			Dominant	rs1423049	19	8935418	ZNF558	1.85E-06
			Log-additive	rs112107763	9	27037553	IFT74	1.99E-06
			Log-additive	rs13073493	3	176696111	LINC01209 / MTND5P15	2.01E-06
			Log-additive	rs1378796	3	157131788	VEPH1	2.04E-06
			Log-additive	rs144446174	11	6250837	FAM160A2	3.26E-06
			Overdominant	rs62430555	6	141636468	RPS18P10 / LOC105378029	3.46E-06
			Codominant	rs1423049	19	8935418	ZNF558	4.17E-06
			Log-additive	rs114097755	2	151854956	LINC02612 / LOC105373686	4.25E-06
			Log-additive	rs61249839	4	13269756	LOC105374494	4.78E-06
			Codominant	rs2254778	8	129157468	PVT1 / MIR1208	5.03E-06
			Overdominant	rs2254778	8	129157468	PVT1 / MIR1208	5.49E-06
			Codominant	rs2648840	8	129163424	MIR1208 / RN7SKP226	6.30E-06
			Overdominant	rs2648840	8	129163424	MIR1208 / RN7SKP226	6.81E-06
			Codominant	rs2648834	8	129171496	MIR1208 / RN7SKP226	7.05E-06
			Overdominant	rs2648834	8	129171496	MIR1208 / RN7SKP226	7.51E-06
			Overdominant	rs184389536	8	20942324	LINC02153 / LOC101929172	9.71E-06
			Log-additive	rs17239489	19	54276241	SEPTIN7P8	9.74E-06
	Index finger	Left	Dominant	rs3761781	6	41744948	FRS3	2.82E-07
			Overdominant	rs3761781	6	41744948	FRS3	3.06E-07
			Overdominant	rs6503444	17	43783370	LINC02210-CRHR1	3.36E-07
			Dominant	rs6503444	17	43783370	LINC02210-CRHR1	6.69E-07

			Log-additive	rs7737797	5	38136423	LINC02107	1.05E-06
			Codominant	rs3761781	6	41744948	FRS3	1.17E-06
			Dominant	rs7737797	5	38136423	LINC02107	1.37E-06
			Codominant	rs6503444	17	43783370	LINC02210-CRHR1	1.72E-06
			Dominant	rs61466555	6	41827336	USP49	1.85E-06
			Overdominant	rs1573408	18	32000277	NOL4 / DTNA	2.12E-06
			Log-additive	rs73035417	12	2458950	CACNA1C	3.11E-06
			Overdominant	rs7737797	5	38136423	LINC02107	4.25E-06
			Recessive	rs12289558	11	7727872	OVCH2 + LOC105376533	4.80E-06
			Recessive	rs888345	8	140646990	KCNK9	5.34E-06
			Overdominant	rs913693	13	77274819	LOC105370266 / LOC105370265	5.99E-06
			Log-additive	rs9793010	1	232295535	LOC105373171 / RN7SL299P	6.12E-06
			Codominant	rs7737797	5	38136423	LINC02107	7.25E-06
			Dominant	rs11970772	6	41925290	CCND3	8.00E-06
			Dominant	rs73035417	12	2458950	CACNA1C	8.22E-06
			Dominant	rs79084750	14	72707030	RGS6	8.31E-06
		Right	Overdominant	rs1280961	1	10980242	LOC105376735	5.05E-06
			Dominant	rs1280961	1	10980242	LOC105376735	5.80E-06
			Overdominant	rs3798713	6	11008622	ELOVL2	8.29E-06
	Thumbs	Left	Overdominant	rs914178	21	42582187	BACE2	2.30E-07
			Overdominant	rs737287	21	42581703	BACE2	1.23E-06
			Codominant	rs914178	21	42582187	BACE2	1.46E-06
			Overdominant	rs12199067	6	114762507	LOC107986638	2.17E-06
			Log-additive	rs4859906	4	78987285	FRAS1 + LOC107986293	2.21E-06
			Log-additive	rs873455	4	78989939	FRAS1 + LOC107986293	2.31E-06
			Log-additive	rs873453	4	78990145	FRAS1 + LOC107986293	2.31E-06
			Dominant	rs17062872	13	75084789	LOC107987191 / LINC00347	2.60E-06
			Dominant	rs12199067	6	114762507	LOC107986638	4.51E-06
			Dominant	rs873455	4	78989939	FRAS1 + LOC107986293	5.29E-06
			Dominant	rs873453	4	78990145	FRAS1 + LOC107986293	5.29E-06
			Codominant	rs737287	21	42581703	BACE2	6.93E-06
			Overdominant	rs9814536	3	73669348	PDZRN3	7.05E-06
			Dominant	rs35128564	6	28635780	TRA-AGC4-1 / TRA-CGC2-1	7.36E-06
			Overdominant	rs1605857	2	102177233	LOC105373514	7.48E-06
			Dominant	rs4859906	4	78987285	FRAS1 + LOC107986293	7.63E-06

			Dominant	rs13193532	6	28622914	LINC00533	7.94E-06
			Overdominant	rs10457277	6	114711584	LOC107986638	8.15E-06
			Overdominant	rs17062872	13	75084789	LOC107987191 / LINC00347	8.66E-06
			Recessive	rs12386464	4	30450095	LOC100130674 / PCDH7	8.66E-06
		Right	Dominant	rs668502	12	18811688	PIK3C2G + PLCZ1	1.98E-06
			Overdominant	rs2832408	21	30973268	GRIK1 + GRIK1-AS2	4.21E-06
			Overdominant	rs7085830	10	70999492	HKDC1	4.25E-06
			Recessive	rs10806425	6	90926612	BACH2	5.37E-06
			Overdominant	rs8098602	18	59058792	CDH20	7.01E-06
			Dominant	rs7097812	10	31995560	MACORIS	8.14E-06
			Codominant	rs2832408	21	30973268	GRIK1 + GRIK1-AS2	8.36E-06
			Recessive	rs11809495	1	165592722	TRK-CTT13-1 / MGST3	8.47E-06
			Recessive	rs6690679	1	165597321	TRK-CTT13-1 / MGST3	8.47E-06
			Overdominant	rs28584831	4	77813649	RPL26P17 / SOWAHB	8.75E-06
			Recessive	rs2999572	7	25590299	LOC105375196 / LOC646588	8.75E-06
Arches	1+ Arches		Dominant	rs2443426	11	57922678	OR9Q1	4.44E-07
			Dominant	rs1447177	11	57921846	OR9Q1	6.14E-07
			Codominant	rs2443426	11	57922678	OR9Q1	2.90E-06
			Codominant	rs1447177	11	57921846	OR9Q1	3.73E-06
			Log-additive	rs11872163	18	4582624	LOC105371968 / PPIAP14	4.47E-06
			Dominant	rs26354	3	42416670	LYZL4	5.35E-06
			Recessive	rs28506195	12	122012243	KDM2B	7.52E-06
			Codominant	rs356969	6	29977145	HLA-J + ZNRD1ASP + LOC107987448	8.60E-06
			Codominant	rs259929	6	30002052	ZNRD1ASP	8.60E-06
			Log-additive	rs1447177	11	57921846	OR9Q1	9.92E-06
	Arches on both index fingers		Dominant	rs12981450	19	57515110	MIMT1 / RPL7AP69	4.09E-06
			Overdominant	rs62024966	16	19735625	IQCK	6.71E-06
			Overdominant	rs299231	18	20315343	LOC101927571	7.47E-06
			Overdominant	rs998107	17	53587193	LOC101927367 / LOC105371833	7.96E-06
			Dominant	rs9520439	13	108079534	FAM155A	9.03E-06
			Overdominant	rs17239735	15	57769899	CGNL1	9.67E-06
			Overdominant	rs12981450	19	57515110	MIMT1 / RPL7AP69	9.79E-06

			Log-additive	+27 more				
	Little fingers	Left	Dominant	rs199793	20	22287303	LINC01427 / LOC284788	3.09E-06
			Recessive	rs902629	10	134038715	STK32C	4.39E-06
			Recessive	rs9959506	18	61177410	SERPINB5 / SERPINB12	4.39E-06
			Dominant	rs10969885	9	30840471	RPS26P2 / FTLP4	5.64E-06
			Codominant	rs12591771	15	97775695	LINC02253	7.38E-06
			Recessive	rs113469967	19	3940025	NMRK2	8.14E-06
			Dominant	rs12591771	15	97775695	LINC02253	8.66E-06
			Recessive	rs61608020	2	222056900	LOC107985988 / EPHA4	9.60E-06
			Dominant	rs11260946	1	18499884	IGSF21 / IGSF21-AS1	9.95E-06
			Log-additive	+85 more				
		Right	Dominant	rs77698137	3	4156426	SUMF1	5.99E-07
			Codominant	rs77698137	3	4156426	SUMF1	1.29E-06
			Recessive	rs6048024	20	22308842	LINC01427 / LOC284788	2.59E-06
			Log-additive	+200 more				
	Ring fingers	Left	Overdominant	rs10969885	9	30840471	RPS26P2 / FTLP4	6.00E-07
			Overdominant	rs7778404	7	132927070	ST13P7 / EXOC4	1.81E-06
			Dominant	rs10516632	4	117830724	LOC107986306	2.10E-06
			Dominant	rs729756	2	77940273	TRP-AGG5-1 / LOC101927967	2.30E-06
			Codominant	rs10969885	9	30840471	RPS26P2 / FTLP4	2.39E-06
			Dominant	rs1521973	2	79096243	LOC105374821 / RNU6-827P	2.96E-06
			Overdominant	rs12145301	1	74170796	LINC02238	2.96E-06
			Dominant	rs7778404	7	132927070	ST13P7 / EXOC4	3.04E-06
			Overdominant	rs74819480	7	3208899	LOC100129603 / SDK1-AS1	4.86E-06
			Dominant	rs17647989	2	79089793	LOC105374821 / RNU6-827P	5.77E-06
			Overdominant	rs2876687	6	25212558	RNY5P5 / LOC100533655	6.80E-06
			Dominant	rs1748012	1	17682100	PADI4	7.44E-06
			Dominant	rs10105118	8	30627027	UBXN8 / PPP2CB	7.84E-06
			Dominant	rs1635564	1	17683526	PADI4	7.99E-06
			Overdominant	rs1521973	2	79096243	LOC105374821 / RNU6-827P	7.99E-06
			Log-additive	+26 more				
		Right	Codominant	rs889472	16	79645989	LOC101928230	1.96E-07

			Overdominant	rs79802709	16	77768045	NUDT7	4.29E-06
			Dominant	rs17225596	12	70106835	BEST3 / LOC101928002	4.57E-06
			Dominant	rs79802709	16	77768045	NUDT7	6.10E-06
			Dominant	rs10761495	10	62171796	ANK3	7.36E-06
			Overdominant	rs2249577	13	76713762	RN7SL571P / LOC105370262	8.24E-06
			Dominant	rs72641095	4	66364227	EPHA5	9.35E-06
			Log-additive	+80 more				
	Middle fingers	Left	Codominant	rs10161338	12	115865303	LOC105370003	3.42E-07
			Log-additive	rs9900985	17	9179849	STX8	9.30E-07
			Log-additive	rs9915637	17	9181459	STX8	9.30E-07
			Codominant	rs7800857	7	152707641	ACTR3B	1.71E-06
			Log-additive	rs2186692	11	82269603	LOC105369410 / RPS28P7	1.80E-06
			Log-additive	rs77000724	11	82275804	LOC105369410 / RPS28P7	1.80E-06
			Dominant	rs9900985	17	9179849	STX8	1.82E-06
			Codominant	rs9900985	17	9179849	STX8	1.94E-06
			Log-additive	rs72630775	7	37429415	ELMO1	2.86E-06
			Log-additive	rs79790201	13	23742653	SGCG	4.26E-06
			Dominant	rs9915637	17	9181459	STX8	4.46E-06
			Log-additive	rs7800857	7	152707641	ACTR3B	4.46E-06
			Overdominant	rs10161338	12	115865303	LOC105370003	4.87E-06
			Dominant	rs11124734	2	40331887	SLC8A1-AS1 + SLC8A1	5.63E-06
			Log-additive	rs73256230	8	68678303	CPA6 / NDUSF5P6	6.04E-06
			Log-additive	rs34037363	3	48821036	PRKAR2A	6.96E-06
			Log-additive	rs11706052	3	49064110	IMPDH2	6.96E-06
			Log-additive	rs11873518	18	47503415	MYO5B	8.15E-06
			Dominant	rs12645126	4	3480718	DOK7	8.26E-06
			Dominant	rs9554857	13	102850867	FGF14	8.67E-06
			Dominant	rs874536	18	8333852	PTPRM	9.43E-06
		Right	Log-additive	rs806944	17	51358687	MTCO1P40 / LOC645163	6.33E-07
			Log-additive	rs34521506	17	6090906	LOC105371508	8.93E-07
			Log-additive	rs806922	17	51375411	MTCO1P40 / LOC645163	1.28E-06
			Log-additive	rs4803715	19	44998078	ZNF180	1.39E-06
			Log-additive	rs2717784	7	148146833	LOC392145 / RPL32P17	1.69E-06
			Dominant	rs34521506	17	6090906	LOC105371508	2.06E-06
			Log-additive	rs118160703	13	63075856	SQSTM1P1 / LOC105370232	2.28E-06
			Log-additive	rs77229893	14	34641963	LOC102724945	2.46E-06

			Log-additive	rs4801896	19	52312466	FPR3 / ZNF577	2.74E-06
			Log-additive	rs76256723	15	93655260	LOC101927025	2.80E-06
			Overdominant	rs34521506	17	6090906	LOC105371508	5.03E-06
			Log-additive	rs74619562	15	93664857	LOC101927025	5.16E-06
			Log-additive	rs75550483	5	37756046	WDR70 / GDNF	5.48E-06
			Overdominant	rs4801896	19	52312466	FPR3 / ZNF577	5.83E-06
			Recessive	rs16870149	4	20857804	KCNIP4	6.12E-06
			Log-additive	rs2363074	12	94224637	CRADD	6.32E-06
			Codominant	rs832094	3	97772846	OR5BM1P / OR5AC1	6.48E-06
			Overdominant	rs7692027	4	182287004	LINC02500 / LOC107986205	7.21E-06
			Log-additive	rs16863526	3	188407531	LPP	7.69E-06
			Dominant	rs1598120	3	82694000	LINC02008 / CYP51A1P1	8.84E-06
			Dominant	rs4801896	19	52312466	FPR3 / ZNF577	9.35E-06
	Index fingers	Left	Codominant	rs6871490	5	10861222	CTD-2154B17.1 / LOC105374654	9.63E-07
			Dominant	rs6871490	5	10861222	CTD-2154B17.1 / LOC105374654	9.63E-07
			Log-additive	rs140705160	2	239764962	TWIST2	1.03E-06
			Overdominant	rs10483427	14	33600978	NPAS3	1.15E-06
			Log-additive	rs932241	21	42208057	DSCAM	1.92E-06
			Log-additive	rs7103026	11	57983162	OR1S1	3.97E-06
			Log-additive	rs1447177	11	57921846	OR9Q1	4.21E-06
			Recessive	rs932241	21	42208057	DSCAM	5.35E-06
			Log-additive	rs1376486	11	57956832	OR9Q2	5.99E-06
			Codominant	rs932241	21	42208057	DSCAM	6.55E-06
			Log-additive	rs2443426	11	57922678	OR9Q1	6.75E-06
			Overdominant	rs1105032	3	70330440	MDFIC2	7.06E-06
			Codominant	rs10483427	14	33600978	NPAS3	7.19E-06
			Dominant	rs10483427	14	33600978	NPAS3	7.19E-06
			Overdominant	rs2803433	9	78940026	PCSK5	7.95E-06
			Overdominant	rs905122	12	130308990	TMEM132D	8.99E-06
			Dominant	rs2123465	2	152320118	RIF1	2.53E-05
			Dominant	rs7103026	11	57983162	OR1S1	2.75E-05
			Dominant	rs2240090	7	51096974	COBL	3.44E-05
			Dominant	rs2432955	2	152331999	RIF1	3.68E-05
		Right	Dominant	rs12981450	19	57515110	MIMT1 / RPL7AP69	7.85E-07
			Overdominant	rs12981450	19	57515110	MIMT1 / RPL7AP69	7.91E-07
			Log-additive	rs79572612	12	106334225	LOC105369960 / ST13P3	9.21E-07
			Log-additive	rs75786813	12	106342698	LOC105369960 / ST13P3	9.21E-07

			Log-additive	rs12981450	19	57515110	MIMT1 / RPL7AP69	1.21E-06
			Overdominant	rs1155206	4	141777368	TBC1D9 / RNF150	1.45E-06
			Overdominant	rs200906086	1	85657703	SYDE2	1.54E-06
			Dominant	rs200906086	1	85657703	SYDE2	2.47E-06
			Codominant	rs12981450	19	57515110	MIMT1 / RPL7AP69	3.45E-06
			Codominant	rs1155206	4	141777368	TBC1D9 / RNF150	5.65E-06
			Codominant	rs200906086	1	85657703	SYDE2	5.83E-06
			Log-additive	rs62355044	5	25638622	LINC02211 / RNU6-374P	5.99E-06
			Log-additive	rs1005631	17	55733373	MSI2	6.26E-06
			Log-additive	rs9865803	3	150237962	TSC22D2 / SERP1	6.30E-06
			Codominant	rs12518421	5	38137906	LINC02107	6.38E-06
			Log-additive	rs17143451	7	20921103	LINC01162	7.38E-06
			Overdominant	rs1447598	3	135345493	LOC105374122 / LOC105374123	8.27E-06
	Thumbs	Left	Overdominant	rs6059016	20	31600217	BPIFB2	5.80E-06
			Dominant	rs2891225	14	33345632	AKAP6 / NPAS3	6.87E-06
			Dominant	rs4982729	14	23576611	LMLN2 / CEBPE	7.30E-06
			Overdominant	rs1914204	11	83566115	DLG2	9.71E-06
			Overdominant	rs260880	12	22942130	LOC107984516 / LOC101928441	9.71E-06
			Log-additive	+76 more				
		Right	Log-additive	rs76469528	7	139315798	HIPK2	9.56E-09
			Log-additive	rs77135199	1	53653934	LOC105378724	2.50E-08
			Log-additive	rs72738028	1	198635853	PTPRC	2.50E-08
			Log-additive	rs6936025	6	47224903	TNFRSF21	4.40E-08
			Log-additive	rs72629733	10	27126235	ABI1	6.00E-08
			Log-additive	rs17816804	10	27133366	ABI1	6.00E-08
			Log-additive	rs730854	21	39749486	ERG	7.16E-08
			Log-additive	rs925821	3	2788576	CNTN4	1.37E-07
			Dominant	rs2808707	9	87558294	NTRK2	4.01E-07
			Codominant	rs2808707	9	87558294	NTRK2	2.64E-06
			Overdominant	rs28434715	11	69713973	LOC107984368 / ANO1	9.56E-06
			Log-additive	+57 more				

Appendix K

Manhattan plots for each variable and model

Eight or more loops

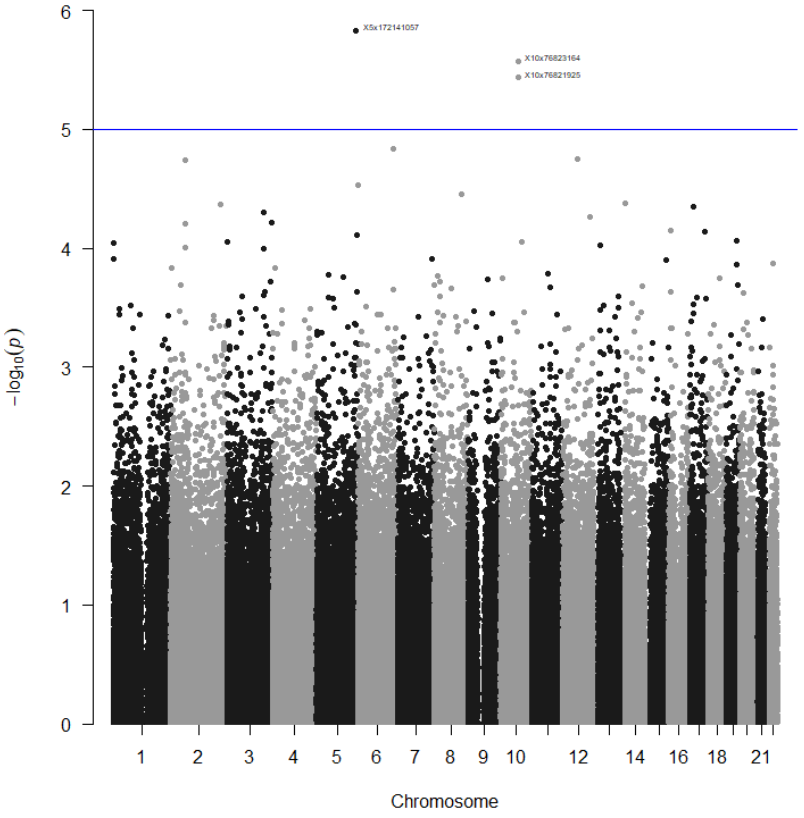

Figure K1: Manhattan plot of SNPs for "eight or more loops" for the codominant model

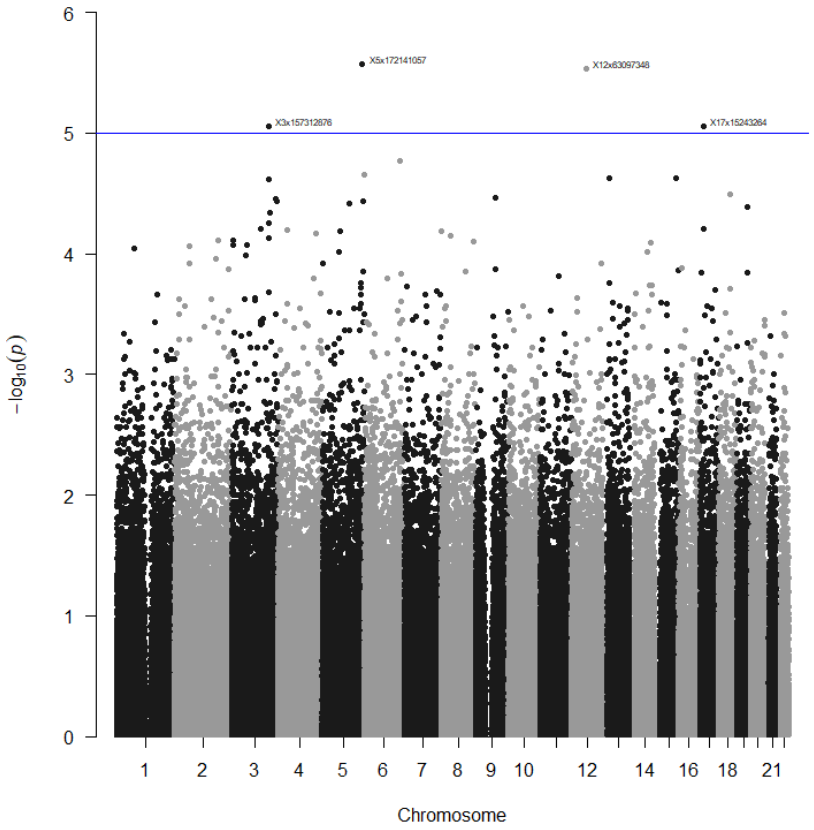

Figure K2: Manhattan plot of SNPs for "eight or more loops" for the dominant model

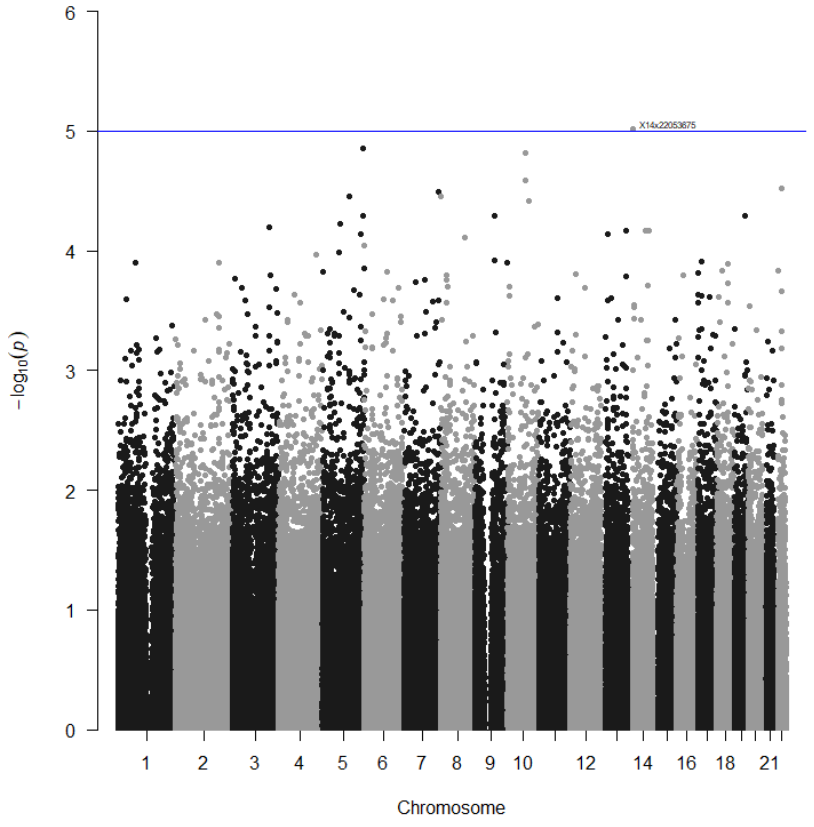

Figure K3: Manhattan plot of SNPs for "eight or more loops" for the log-additive model

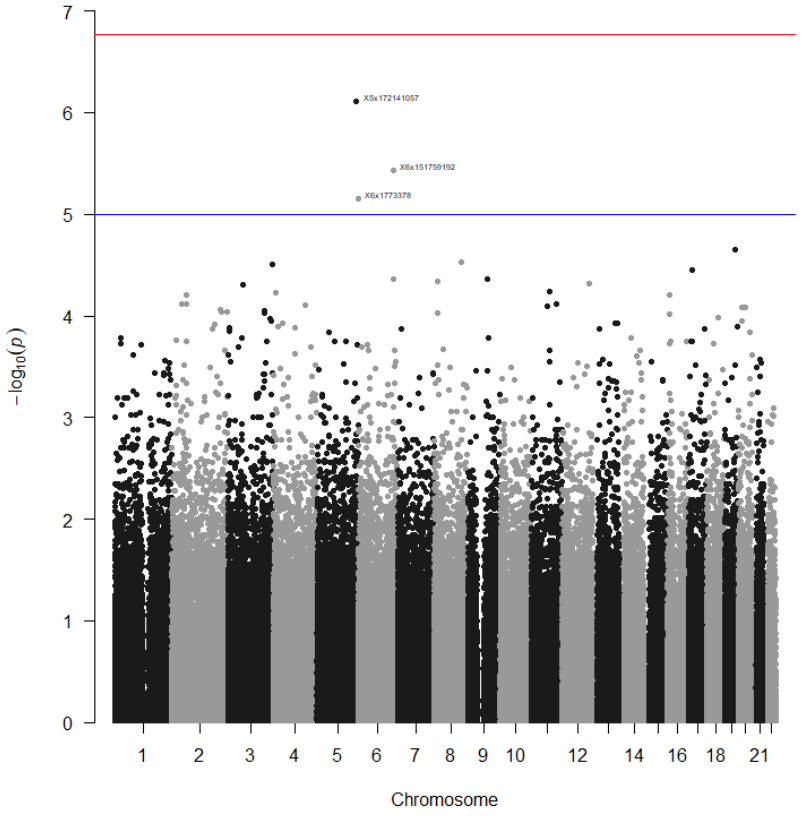

Figure K4: Manhattan plot of SNPs for "eight or more loops" for the overdominant model

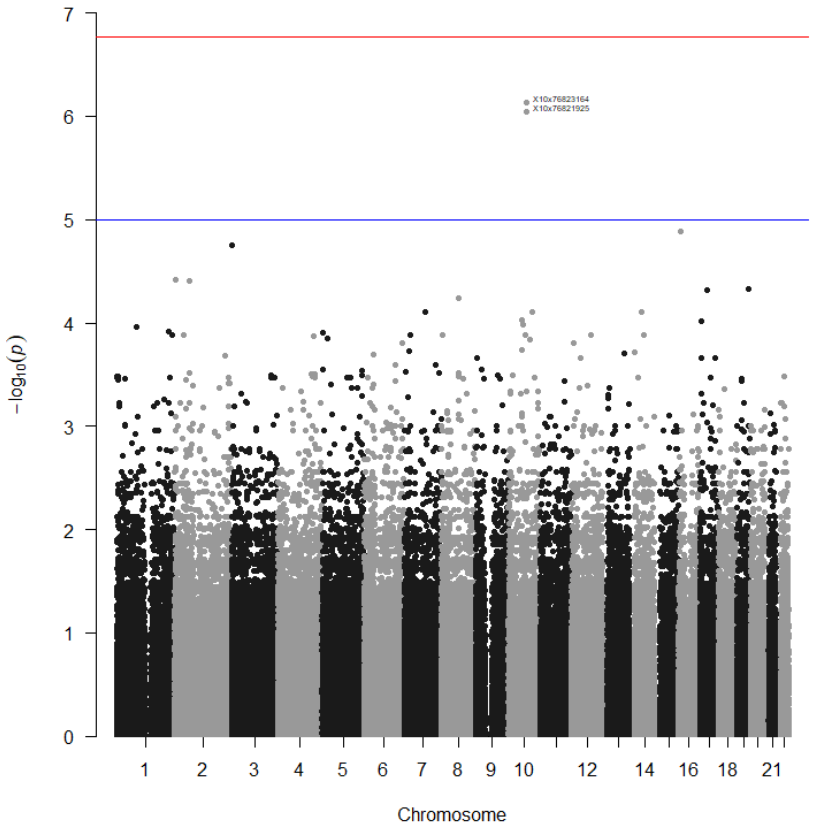

Figure K5: Manhattan plot of SNPs for "eight or more loops" for the recessive model

Eight or more ulnar loops

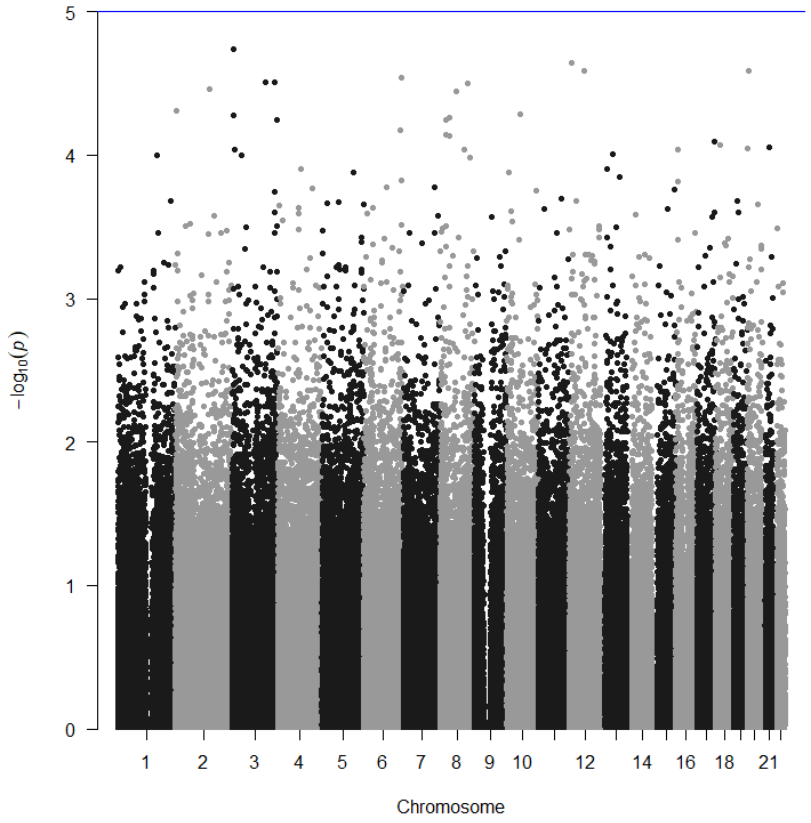

Figure K6: Manhattan plot of SNPs for "eight or more ulnar loops" for the codominant model

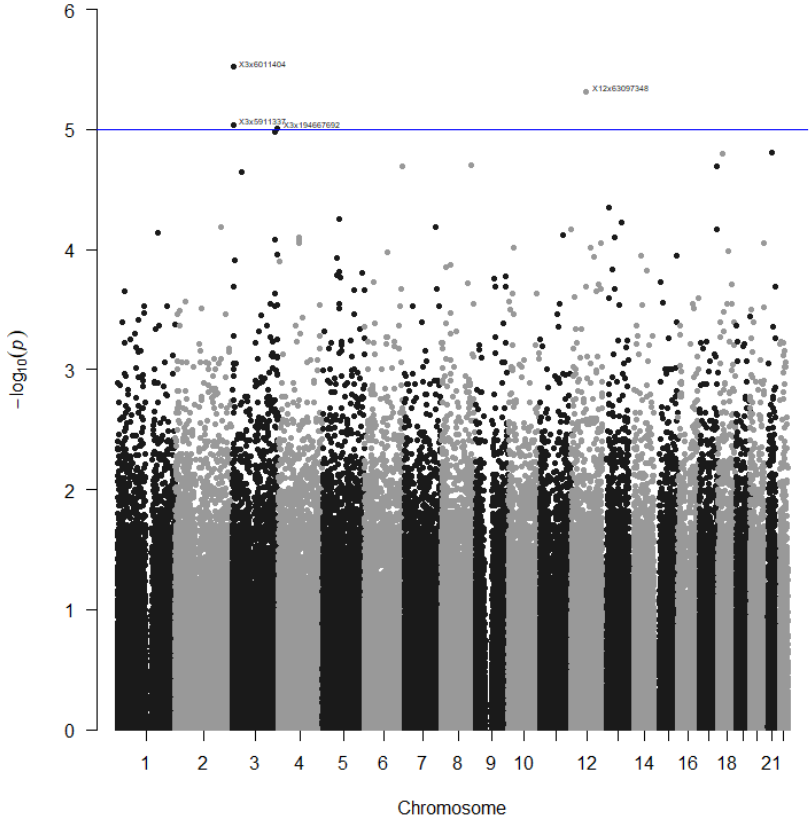

Figure K7: Manhattan plot of SNPs for "eight or more ulnar loops" for the dominant model

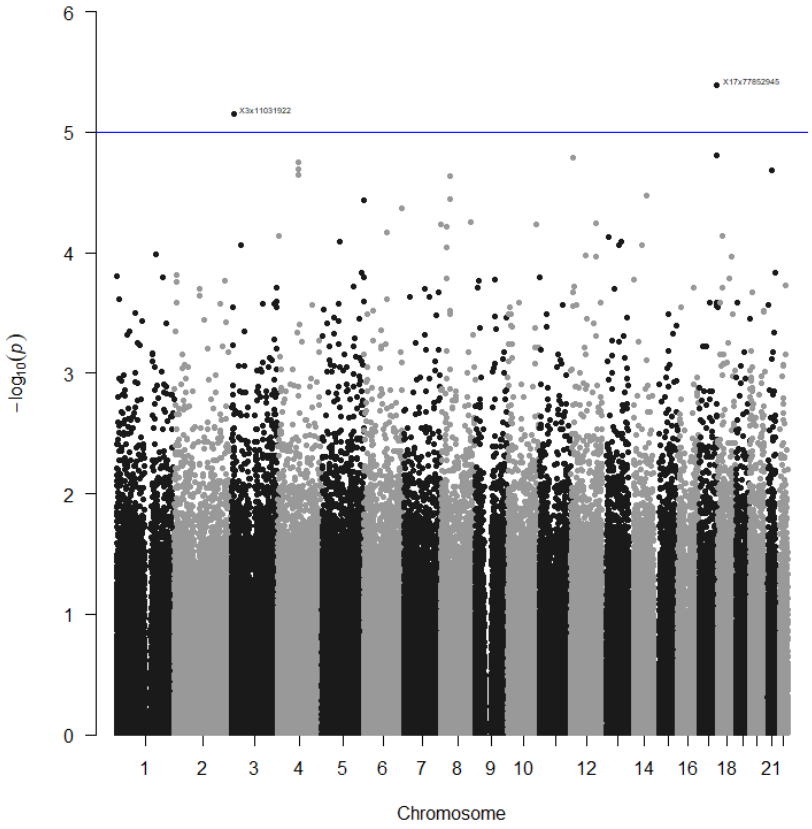

Figure K8: Manhattan plot of SNPs for "eight or more ulnar loops" for the log-additive model

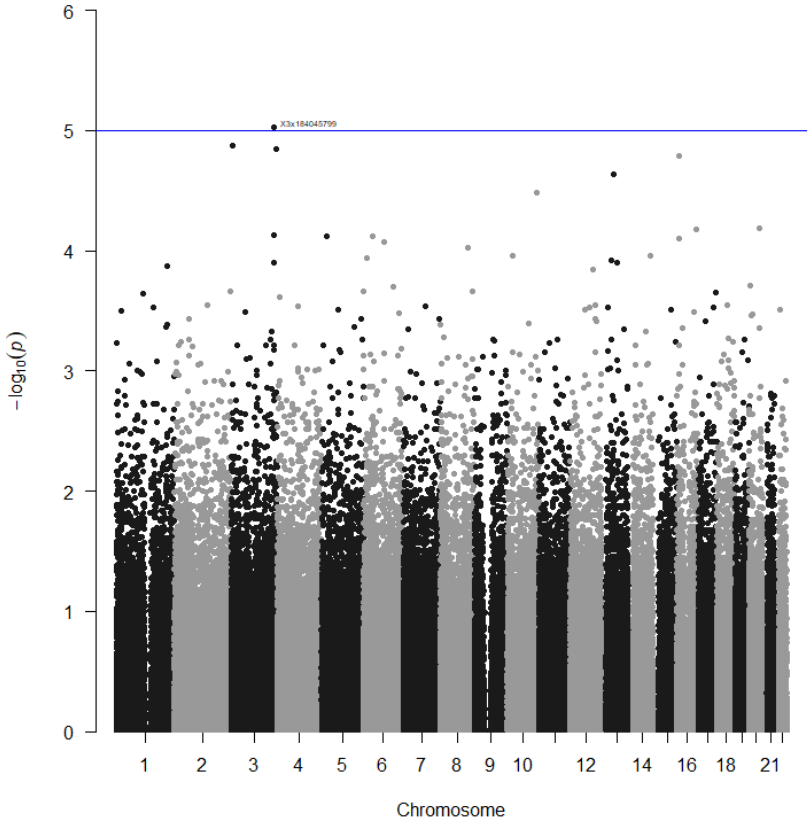

Figure K9: Manhattan plot of SNPs for "eight or more ulnar loops" for the overdominant model

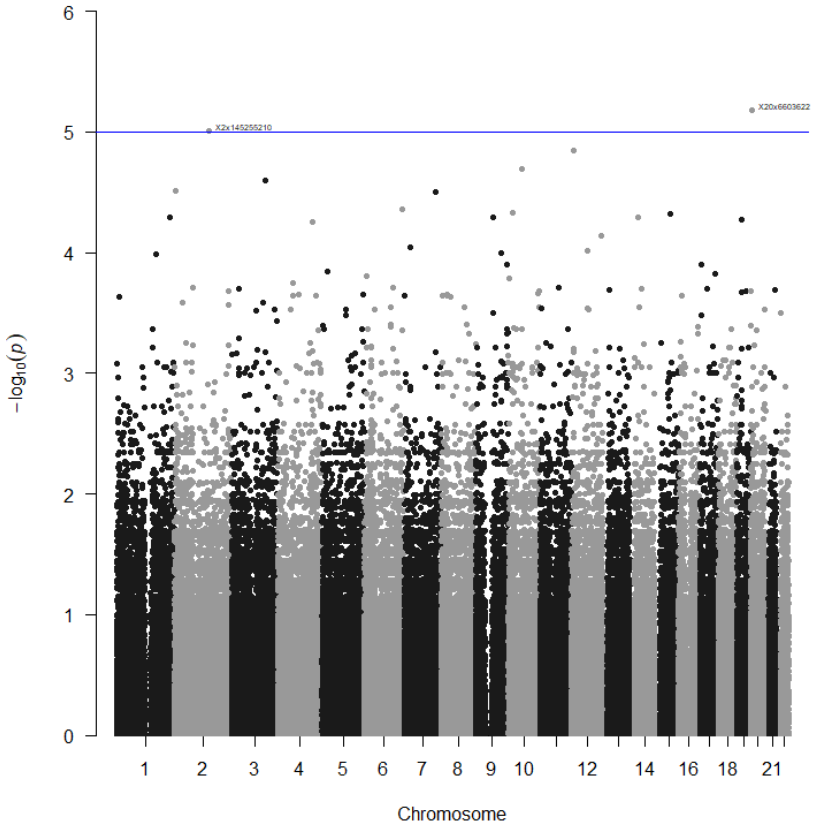

Figure K10: Manhattan plot of SNPs for "eight or more ulnar loops" for the recessive model

One or more radial loop

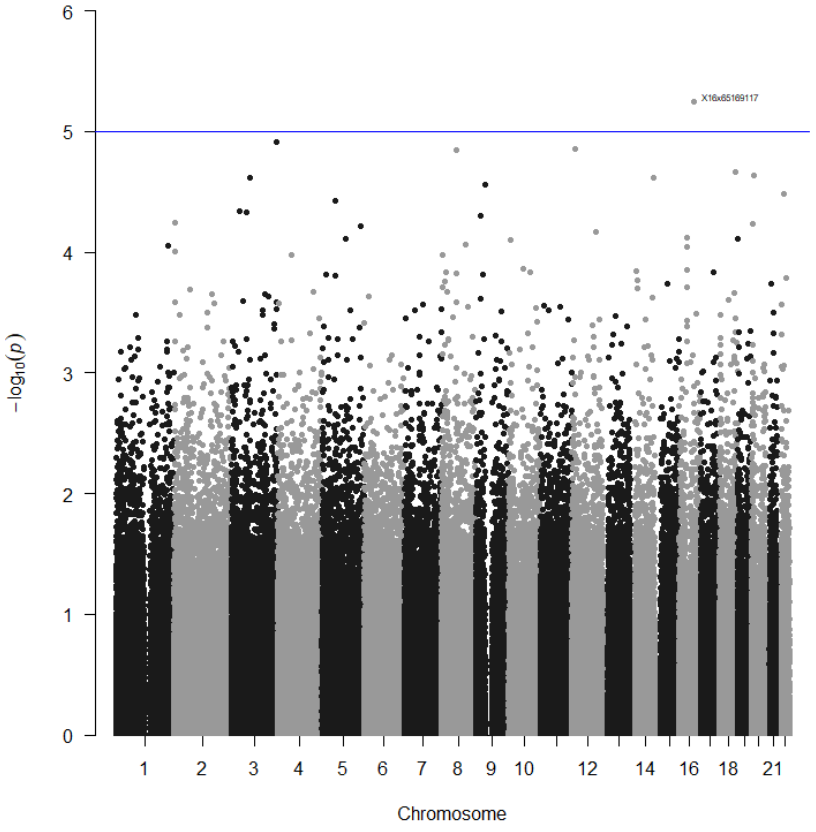

Figure K11: Manhattan plot of SNPs for "one or more radial loops" for the codominant model

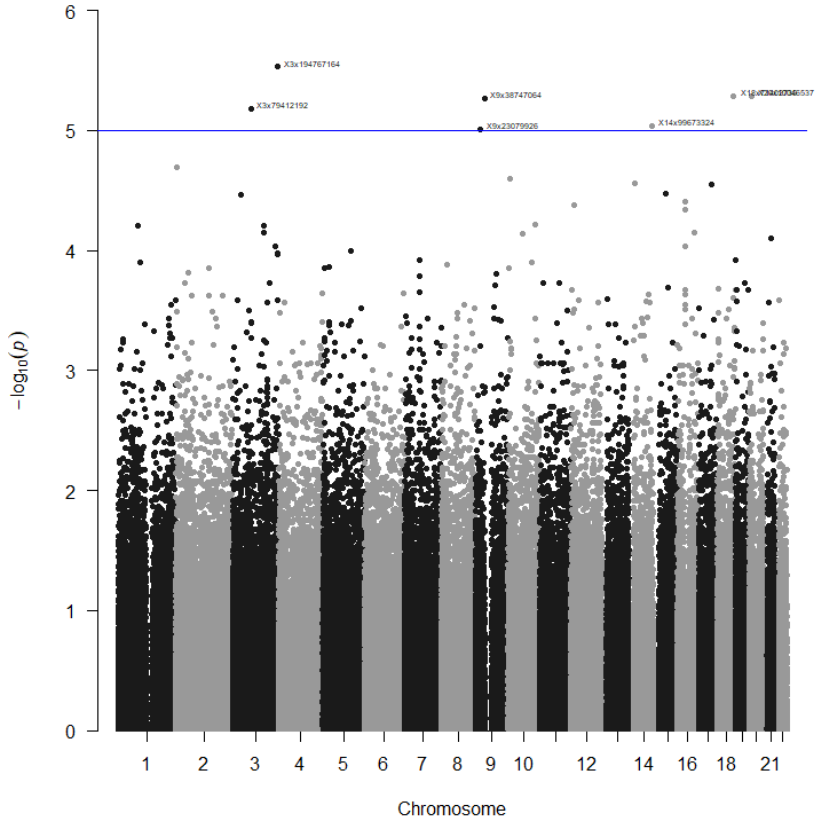

Figure K12: Manhattan plot of SNPs for "one or more radial loops" for the dominant model

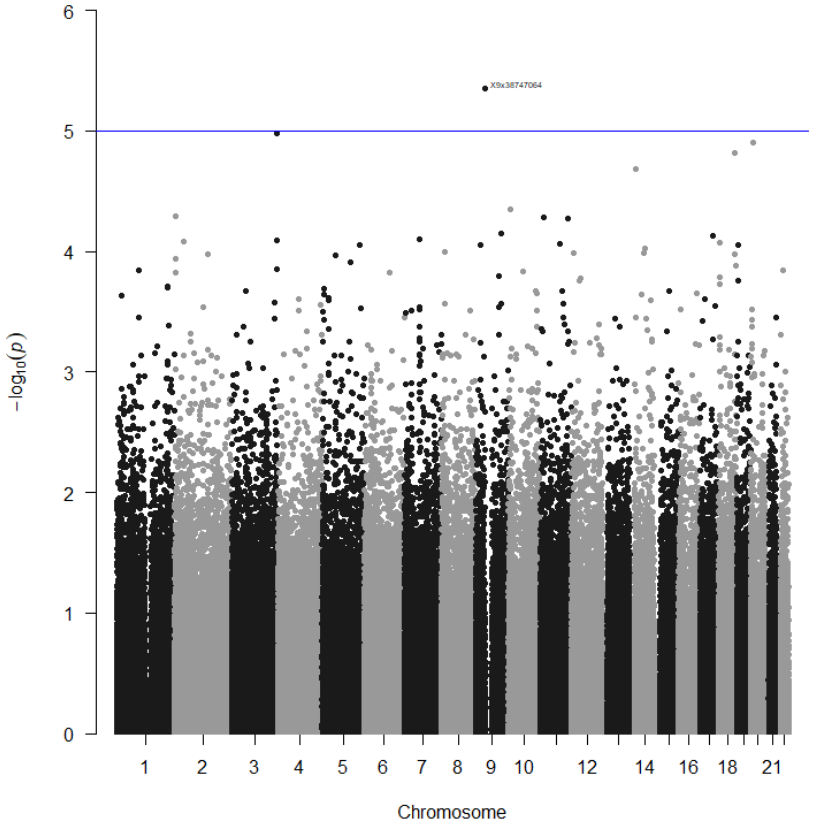

Figure K13: Manhattan plot of SNPs for "one or more radial loops" for the log-additive model

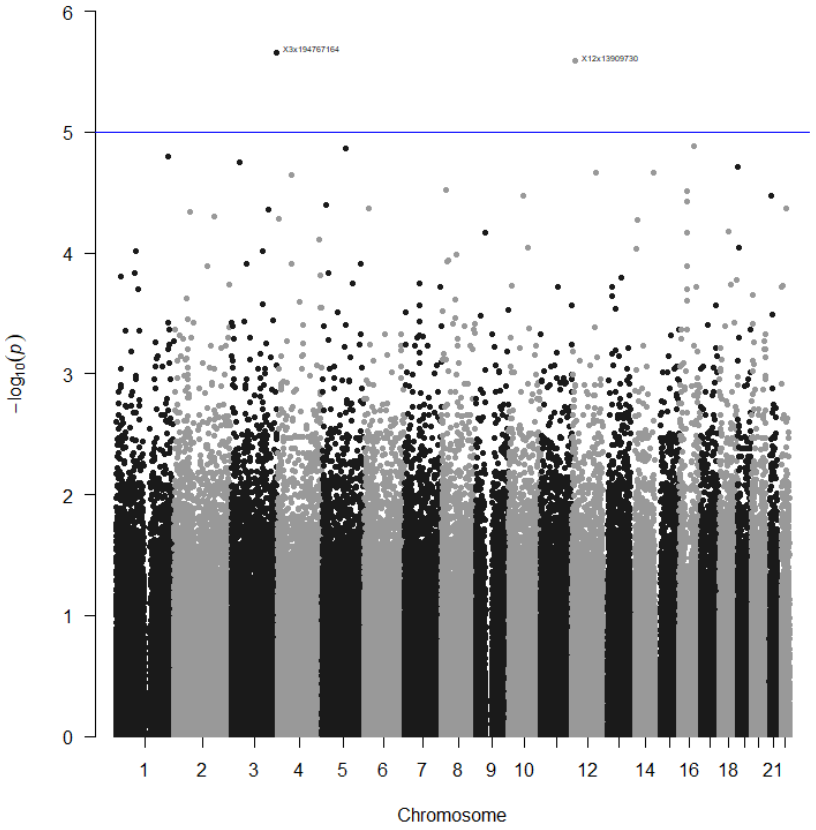

Figure K14: Manhattan plot of SNPs for "one or more radial loops" for the overdominant model

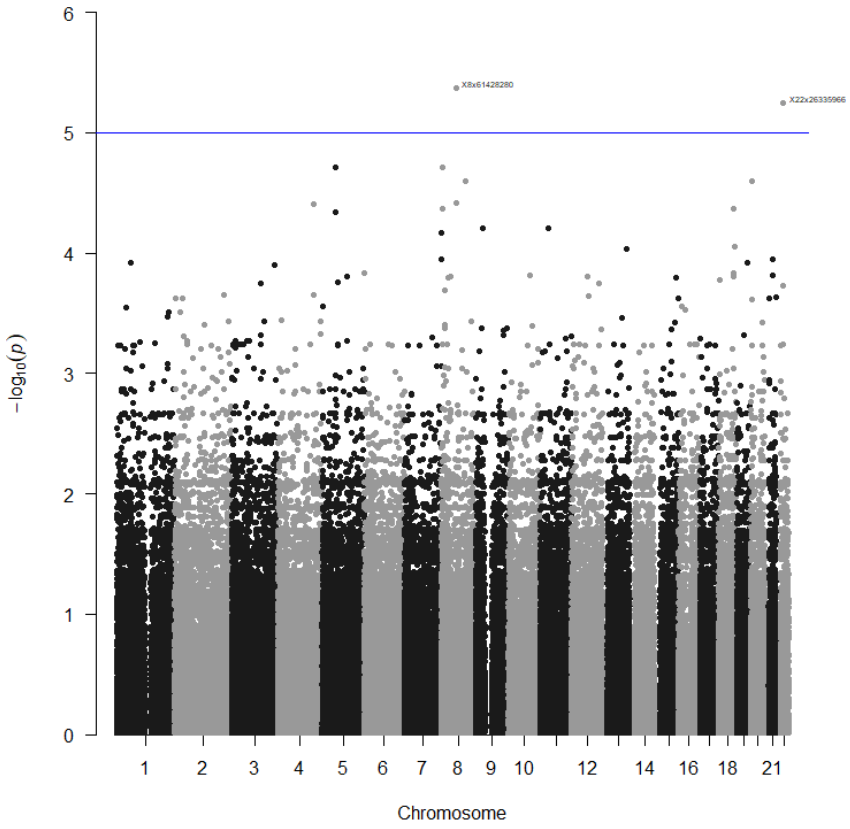

Figure K14: Manhattan plot of SNPs for "one or more radial loops" for the recessive model

Radial loops on both index fingers

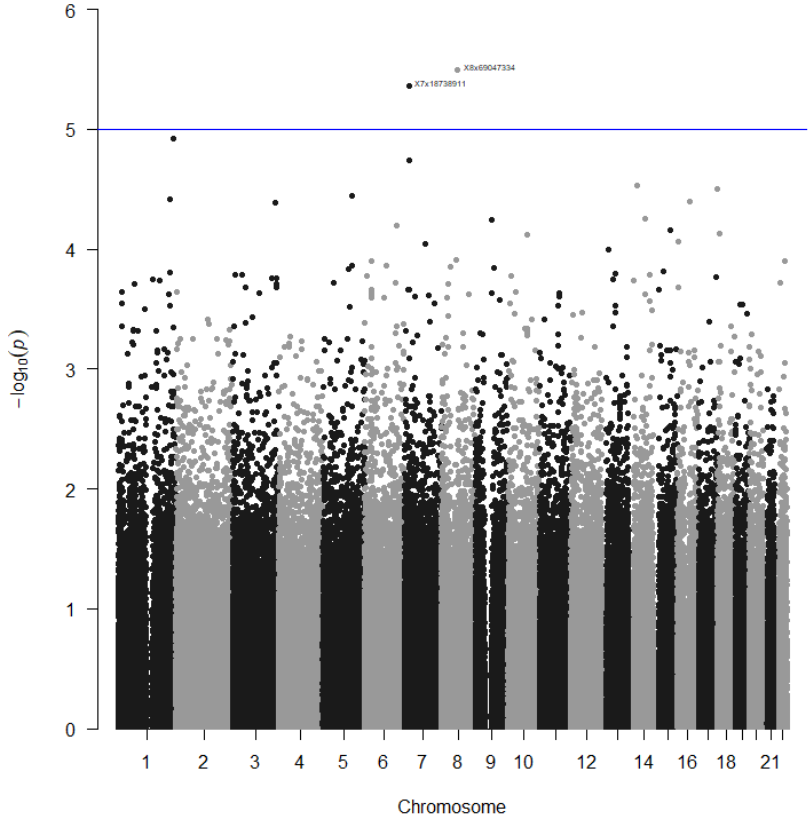

Figure K16: Manhattan plot of SNPs for "radial loops on both index fingers" for the codominant model

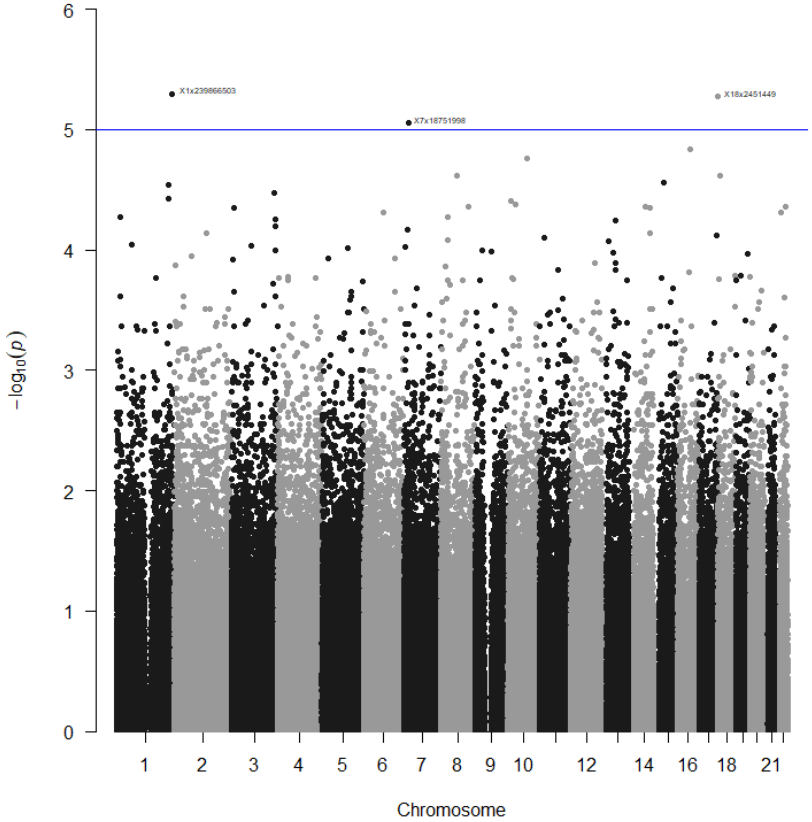

Figure K17: Manhattan plot of SNPs for "radial loops on both index fingers" for the dominant model

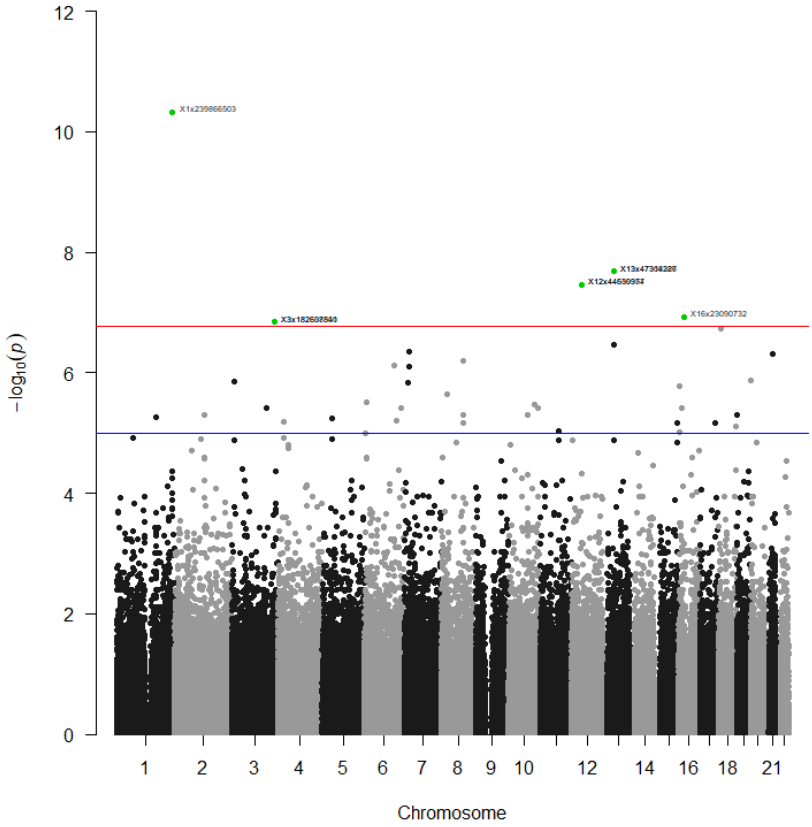

Figure K18: Manhattan plot of SNPs for "radial loops on both index fingers" for the log-additive model

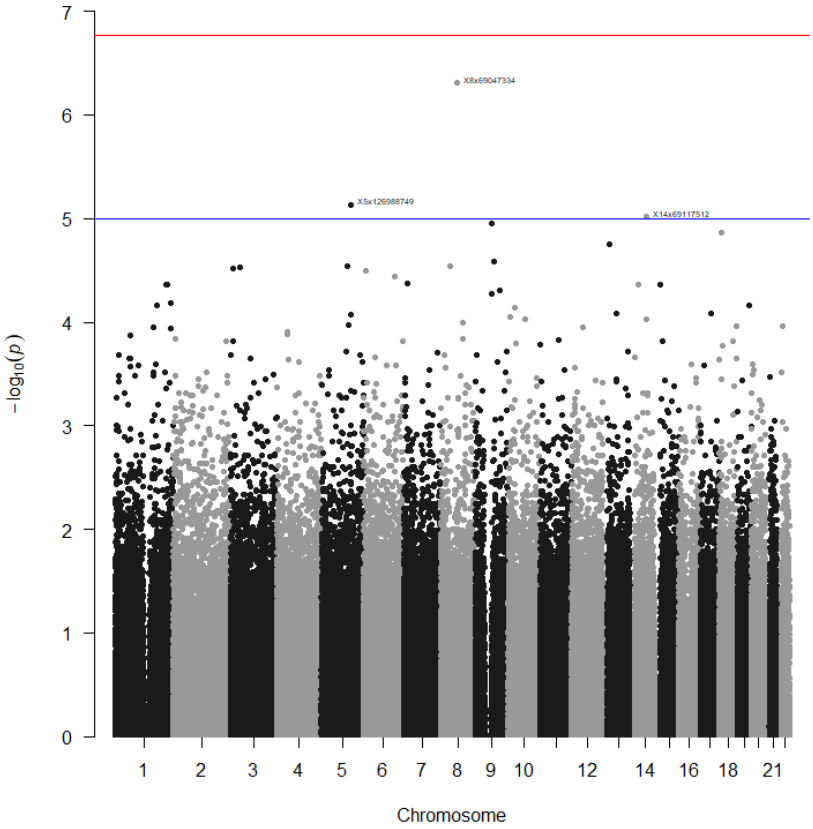

Figure K19: Manhattan plot of SNPs for "radial loops on both index fingers" for the overdominant model

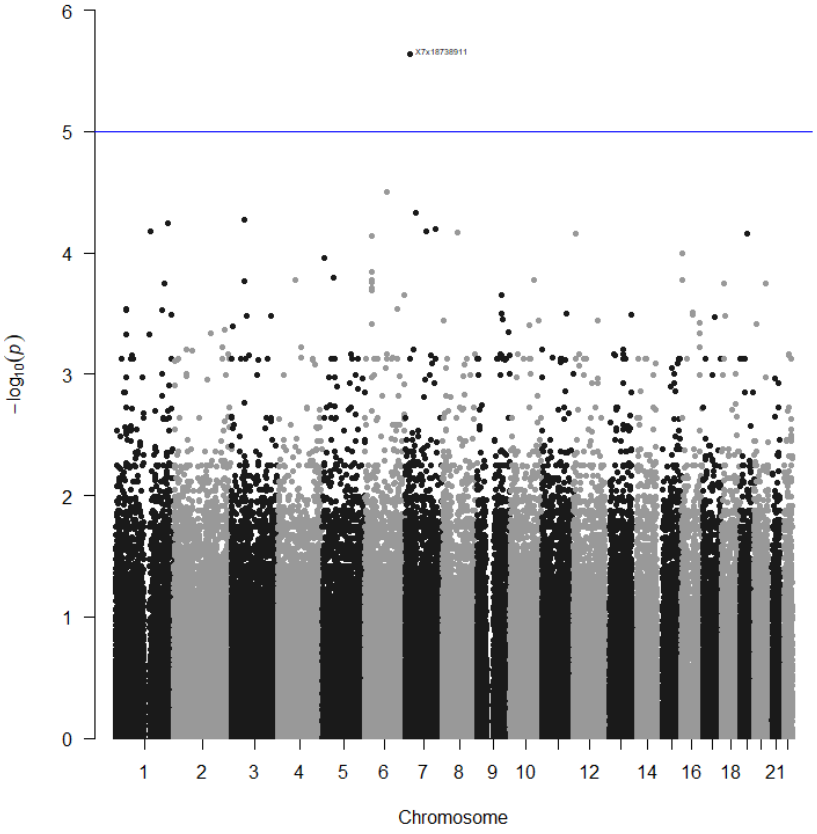

Figure K20: Manhattan plot of SNPs for "radial loops on both index fingers" for the recessive model

Eight or more whorls

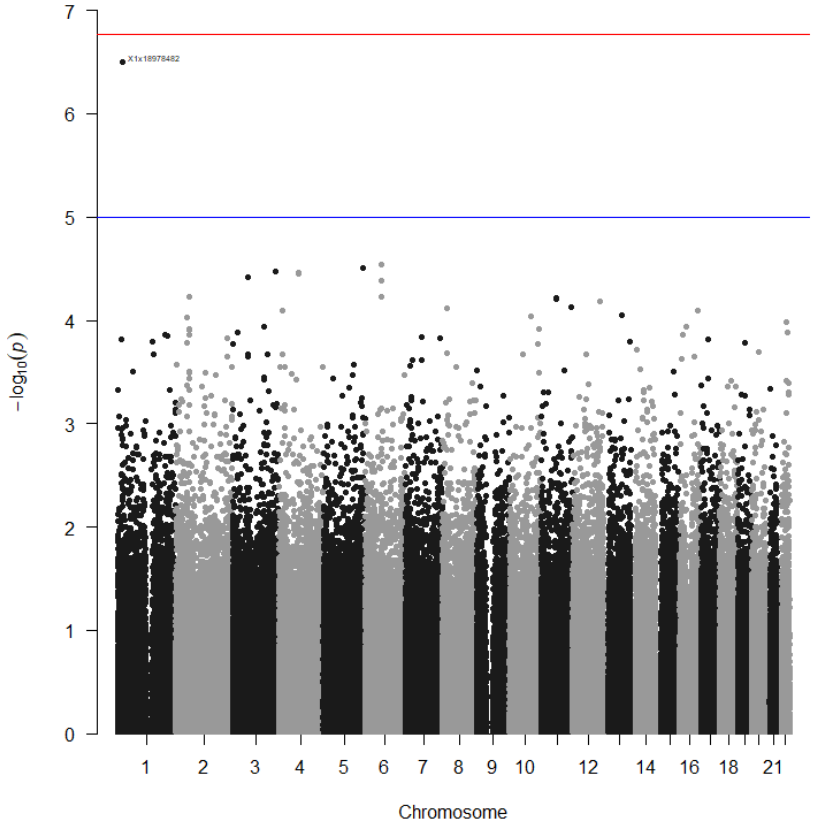

Figure K21: Manhattan plot of SNPs for "eight or more whorls" for the codominant model

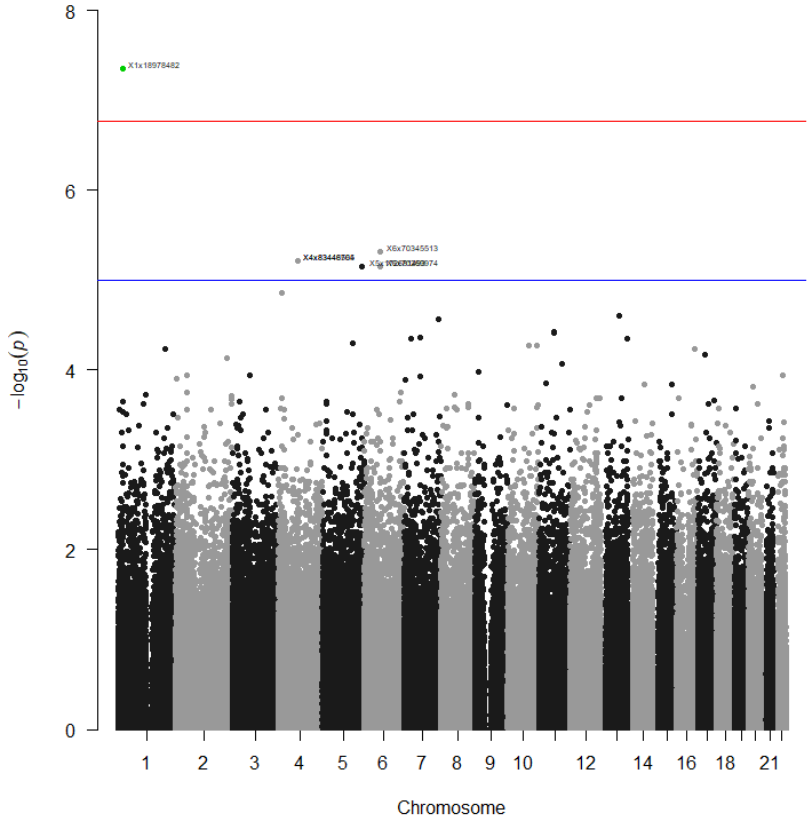

Figure K22: Manhattan plot of SNPs for "eight or more whorls" for the dominant model

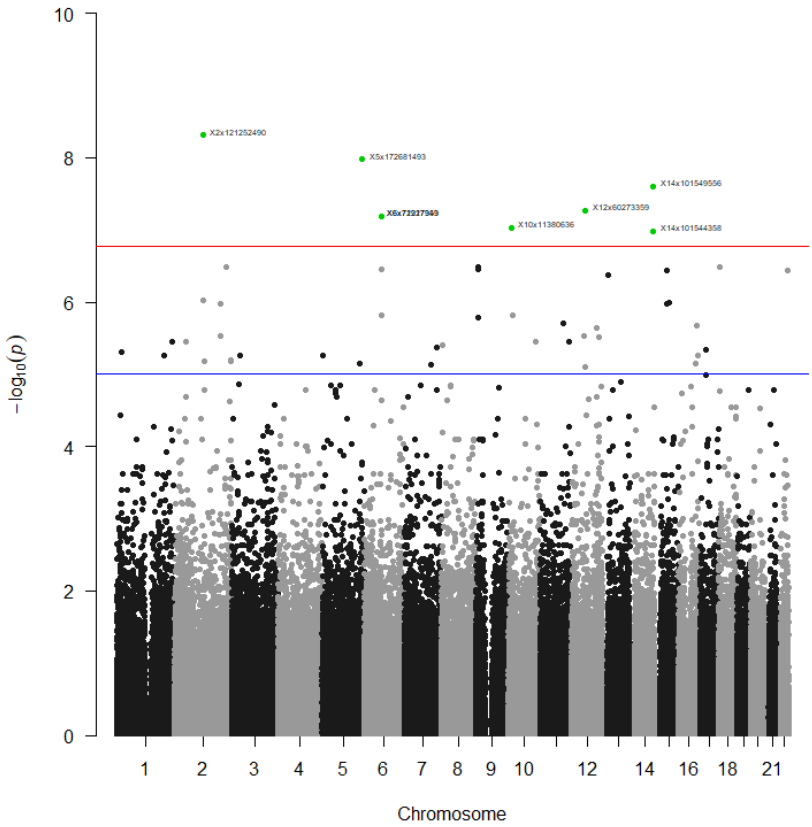

Figure K23: Manhattan plot of SNPs for "eight or more whorls" for the log-additive model

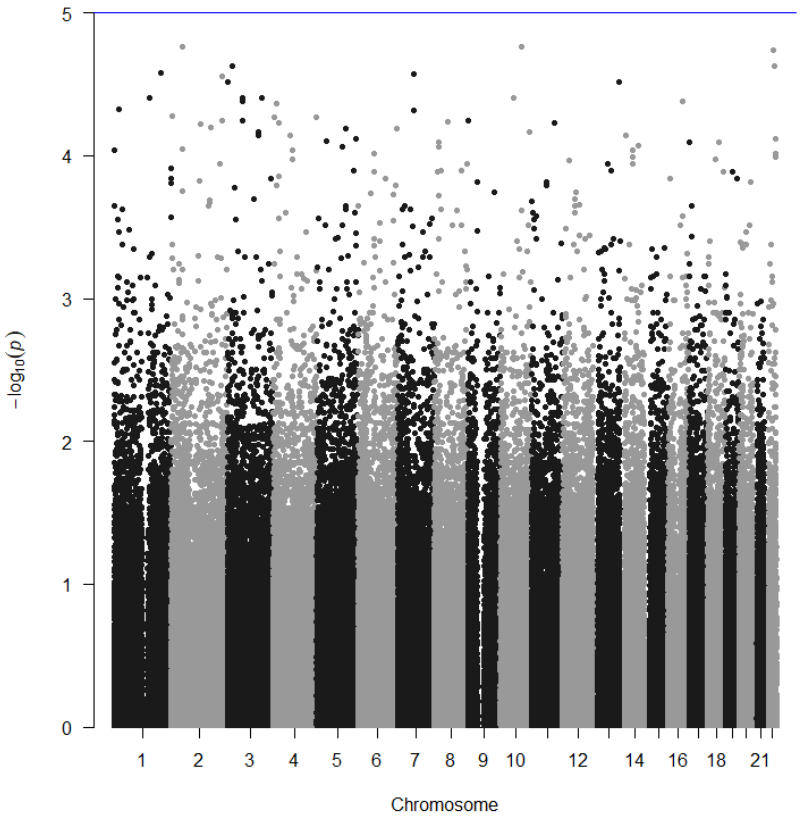

Figure K24: Manhattan plot of SNPs for "eight or more whorls" for the overdominant model

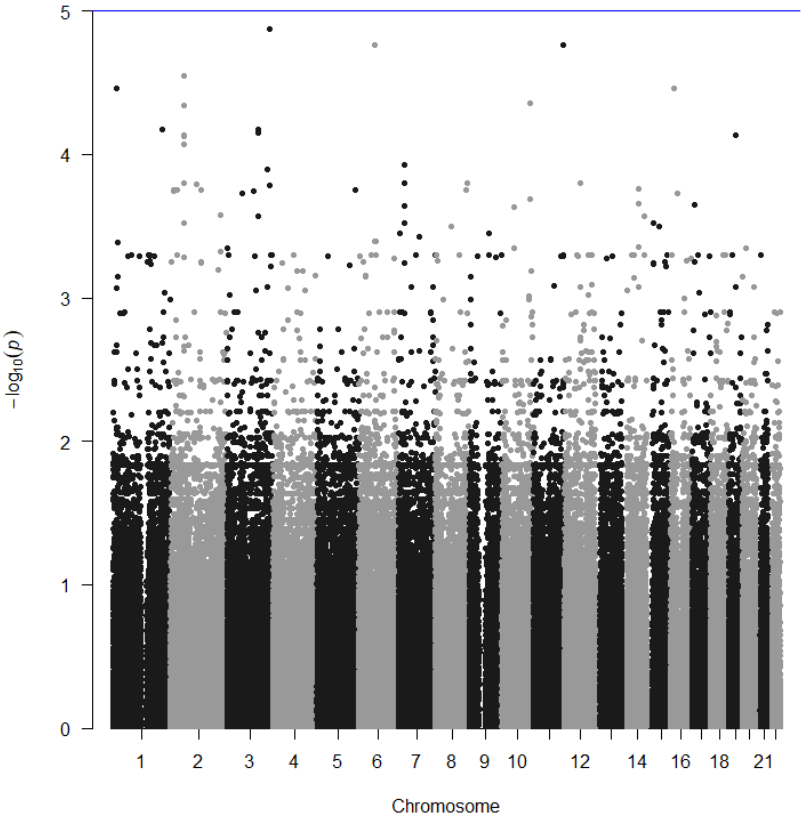

Figure K25: Manhattan plot of SNPs for "eight or more whorls" for the recessive model

Whorls on both thumbs

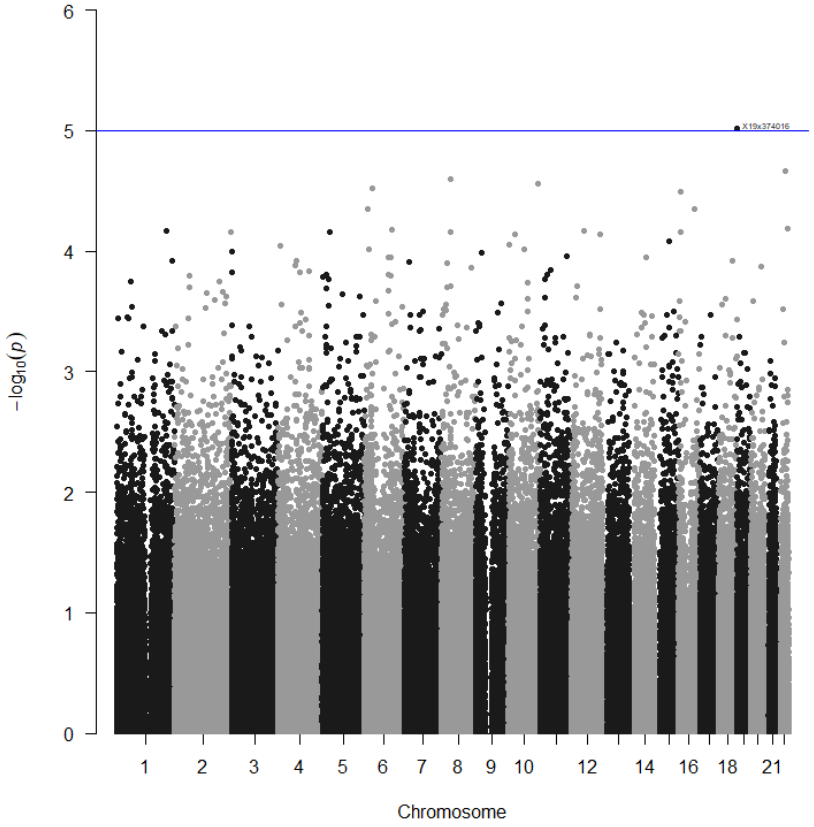

Figure K26: Manhattan plot of SNPs for "whorls on both thumbs" for the codominant model

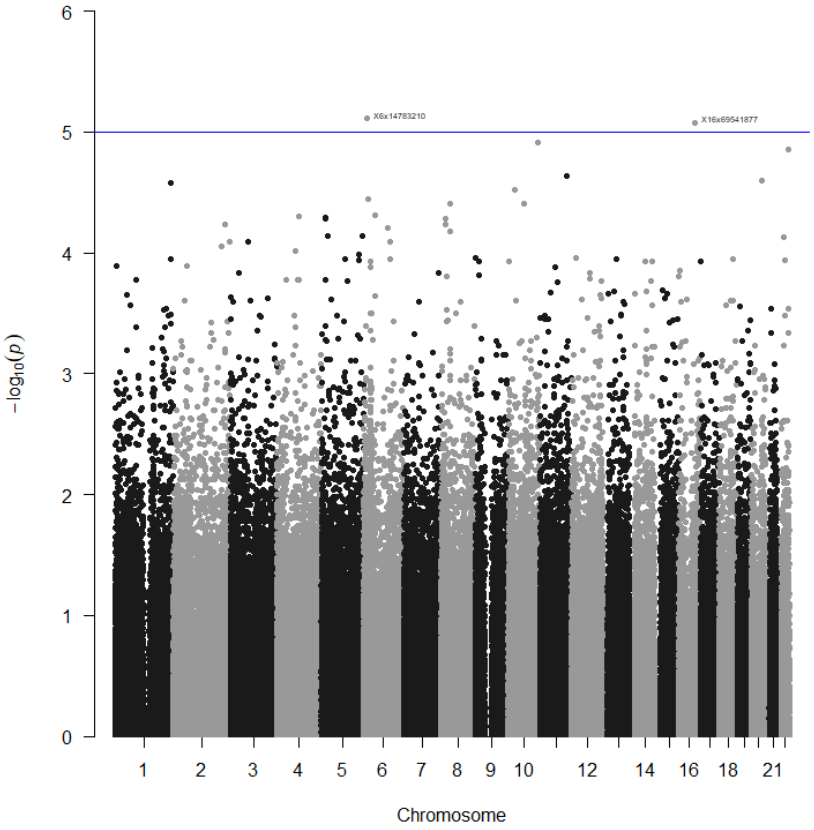

Figure K27: Manhattan plot of SNPs for "whorls on both thumbs" for the dominant model

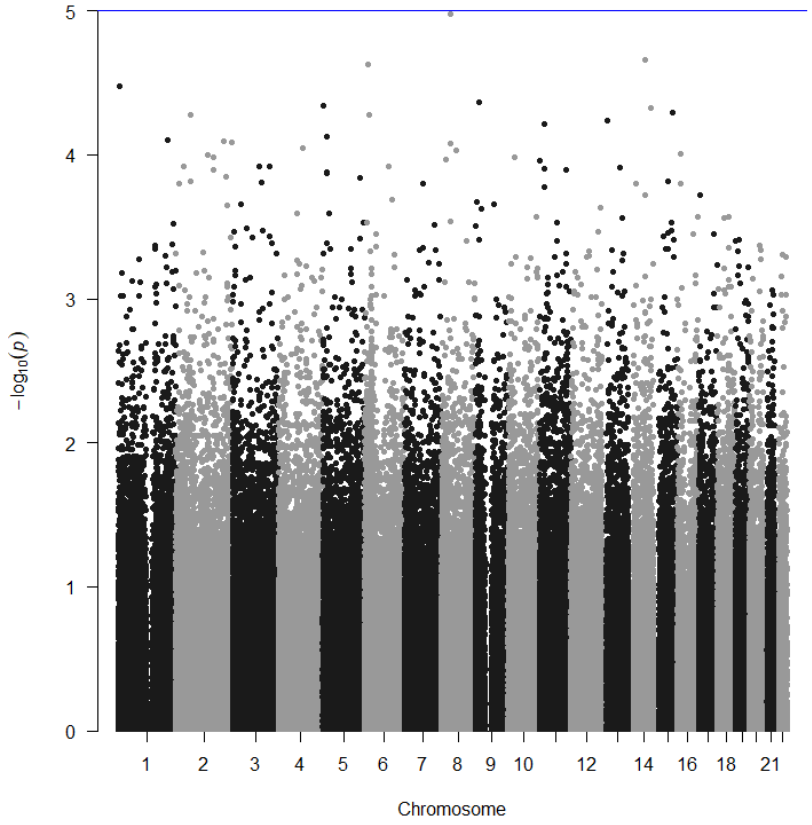

Figure K28: Manhattan plot of SNPs for "whorls on both thumbs" for the log-additive model

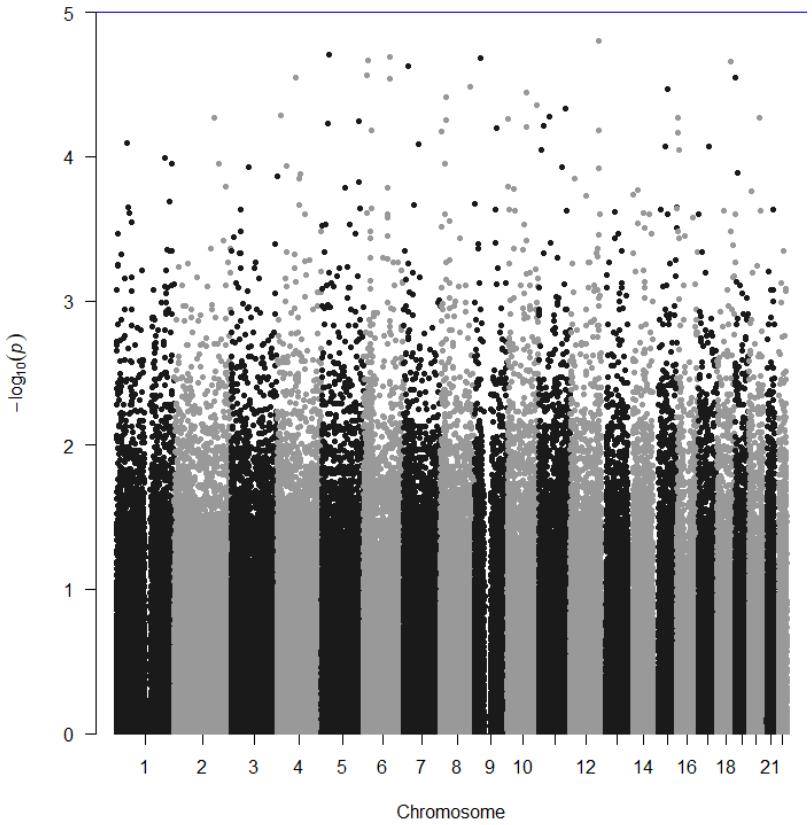

Figure K29: Manhattan plot of SNPs for "whorls on both thumbs" for the overdominant model

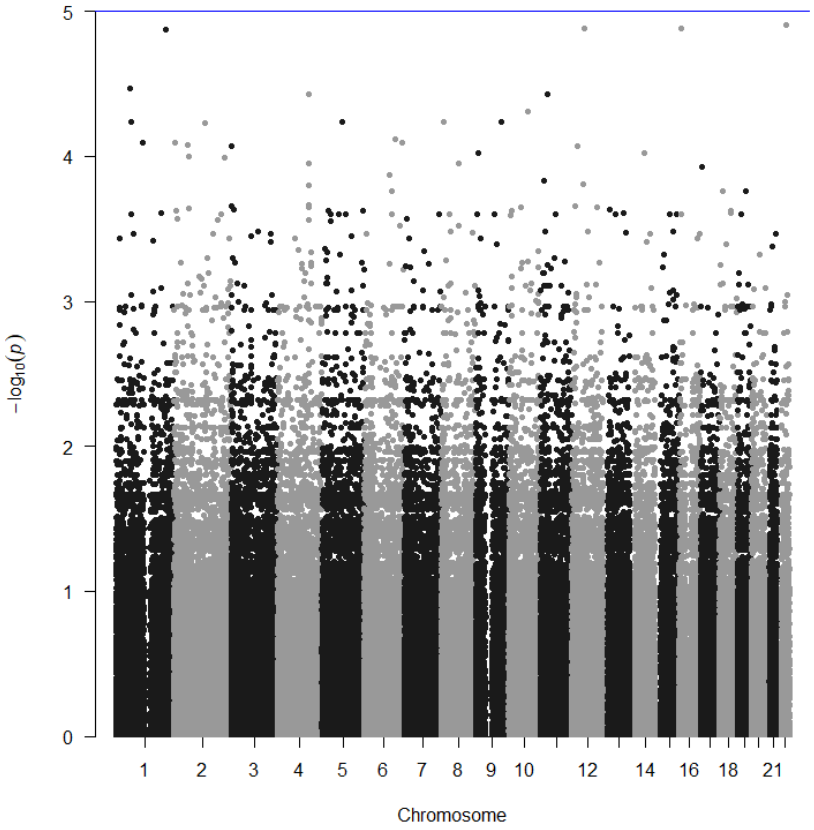

Figure K30: Manhattan plot of SNPs for "whorls on both thumbs" for the recessive model

Whorls on both ring fingers

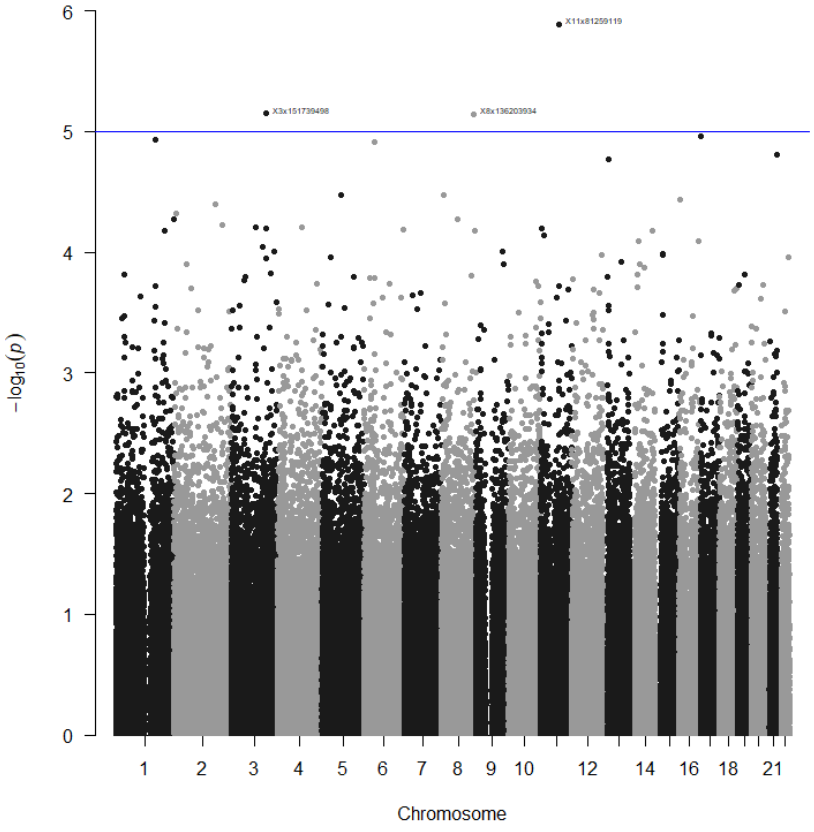

Figure K31: Manhattan plot of SNPs for "whorls on both ring fingers" for the codominant model

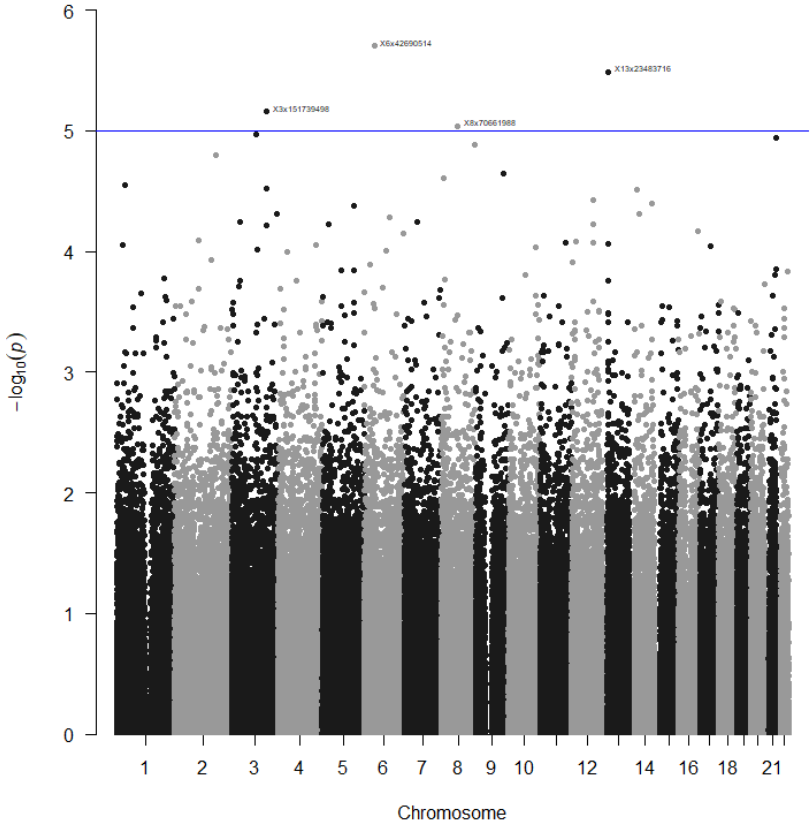

Figure K32: Manhattan plot of SNPs for "whorls on both ring fingers" for the dominant model

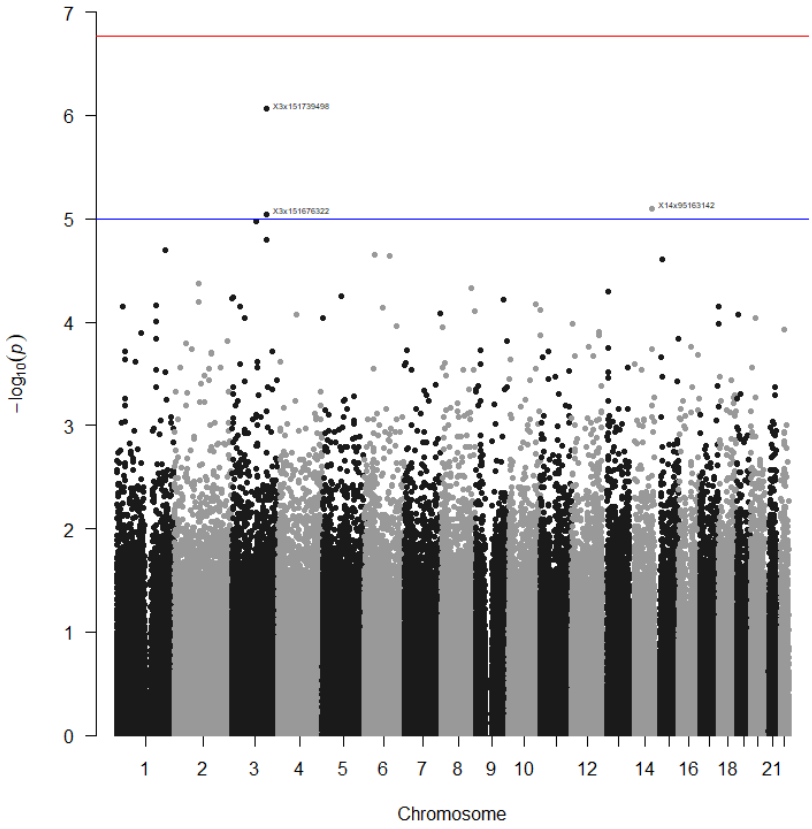

Figure K33: Manhattan plot of SNPs for "whorls on both ring fingers" for the log-additive model

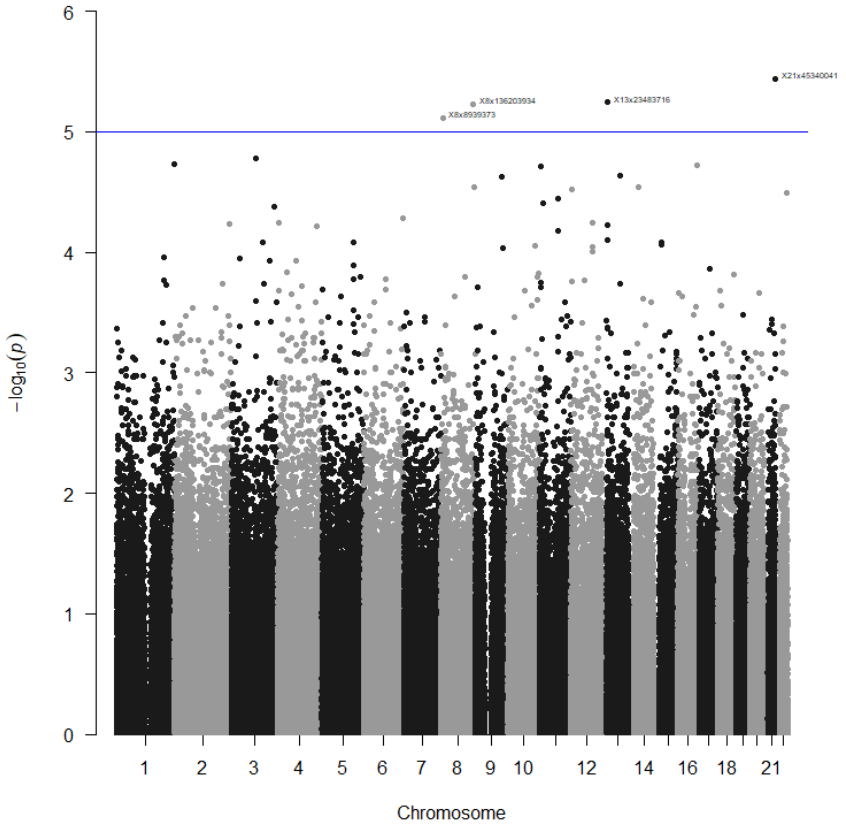

Figure K34: Manhattan plot of SNPs for "whorls on both ring fingers" for the overdominant model

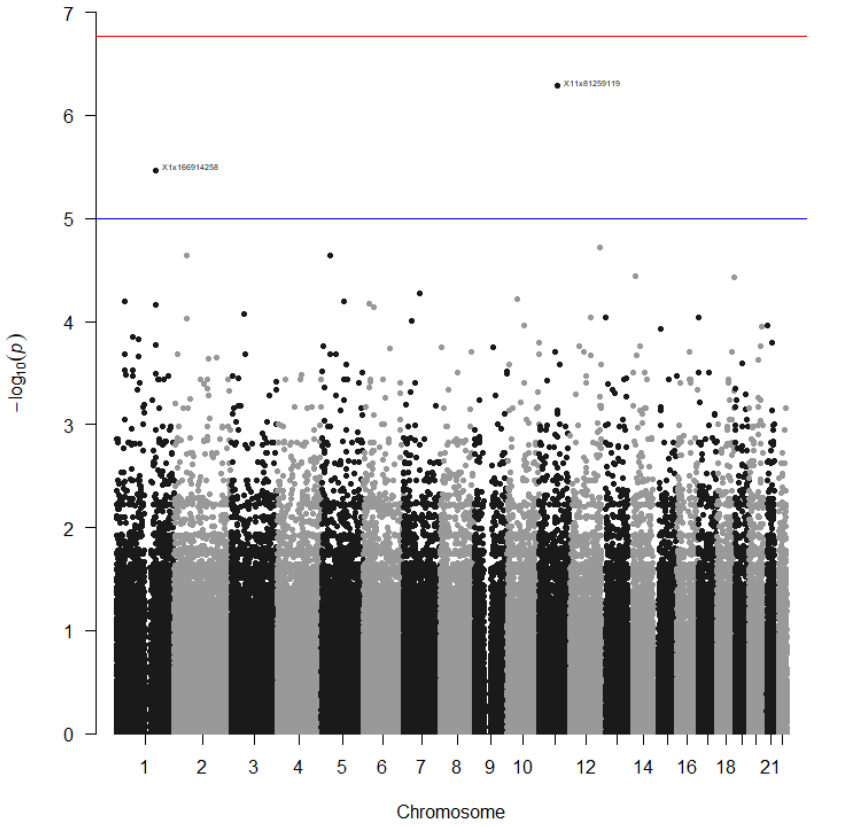

Figure K35: Manhattan plot of SNPs for "whorls on both ring fingers" for the recessive model

One or more arches

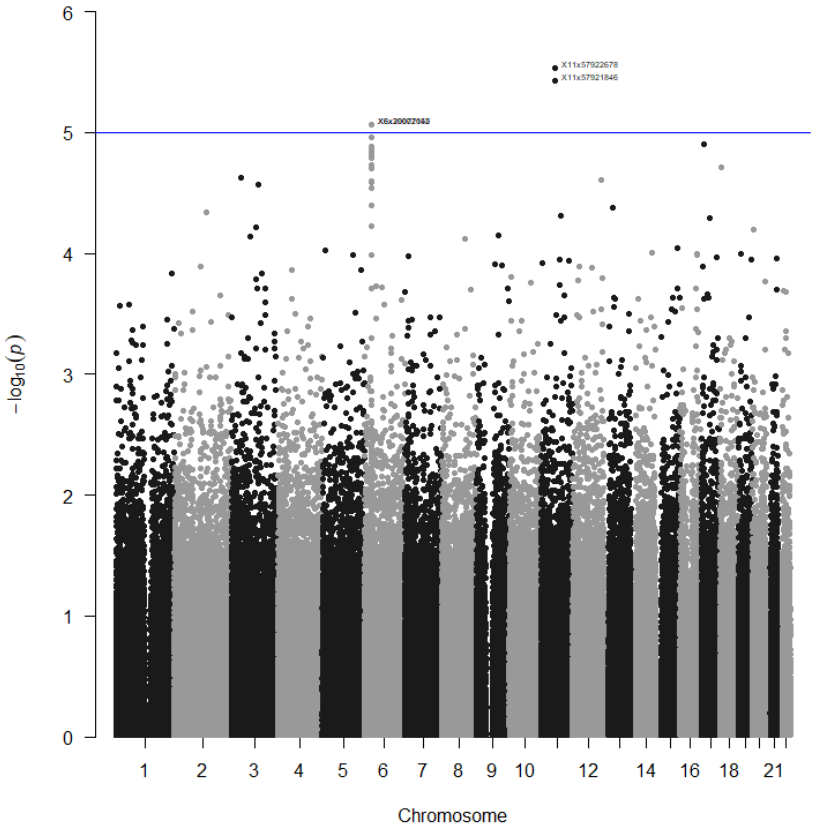

Figure K36: Manhattan plot of SNPs for "one or more arches" for the codominant model

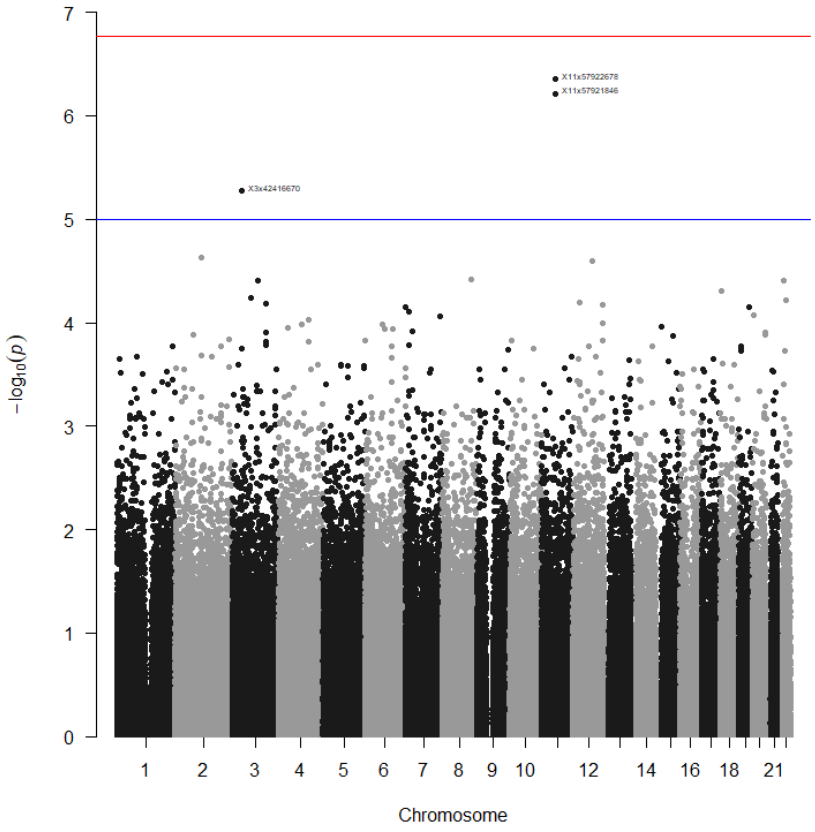

Figure K37: Manhattan plot of SNPs for "one or more arches" for the dominant model

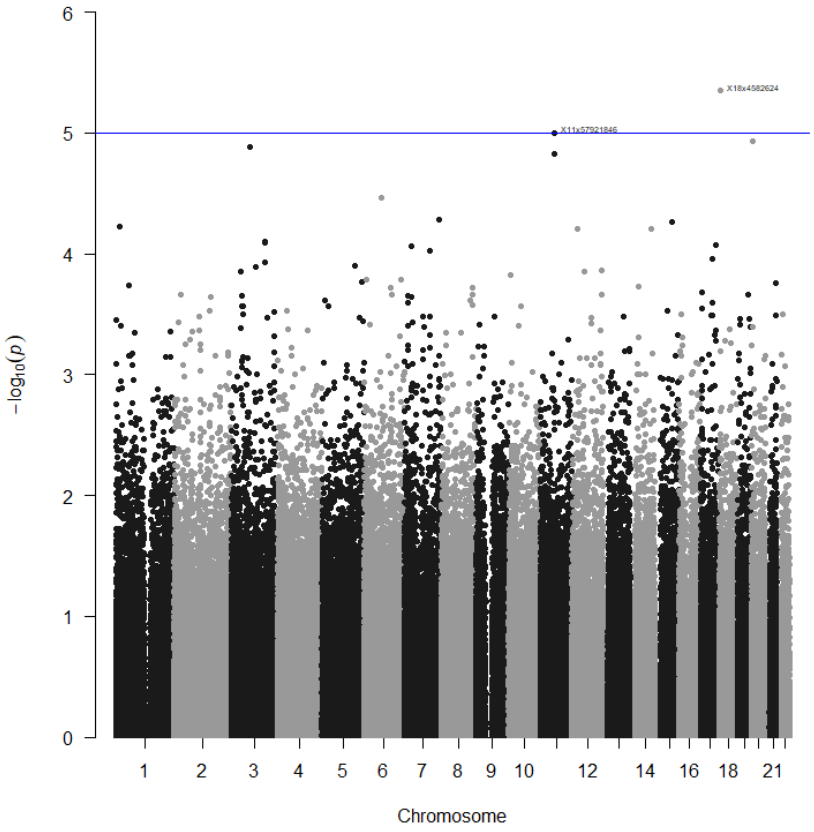

Figure K38: Manhattan plot of SNPs for "one or more arches" for the log-additive model

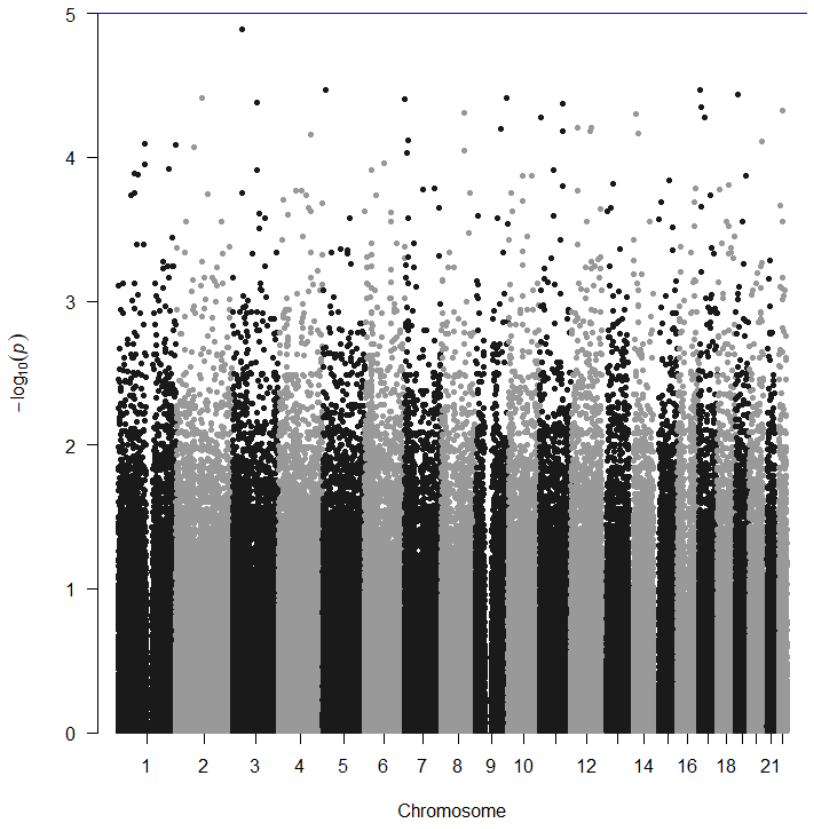

Figure K39: Manhattan plot of SNPs for "one or more arches" for the overdominant model

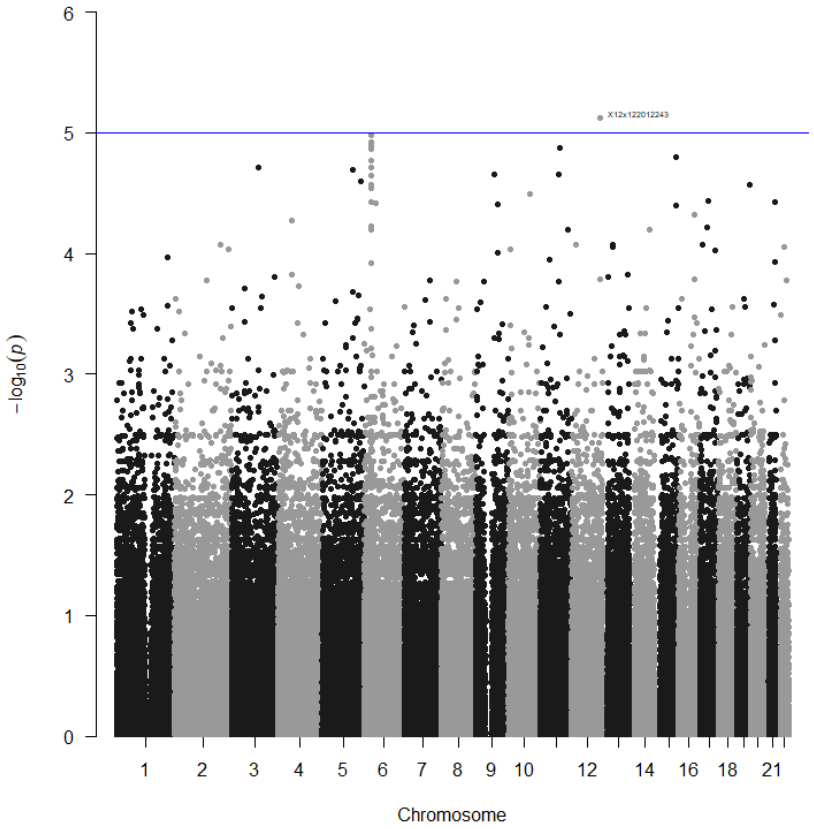

Figure K40: Manhattan plot of SNPs for "one or more arches" for the recessive model

Arches on both index fingers

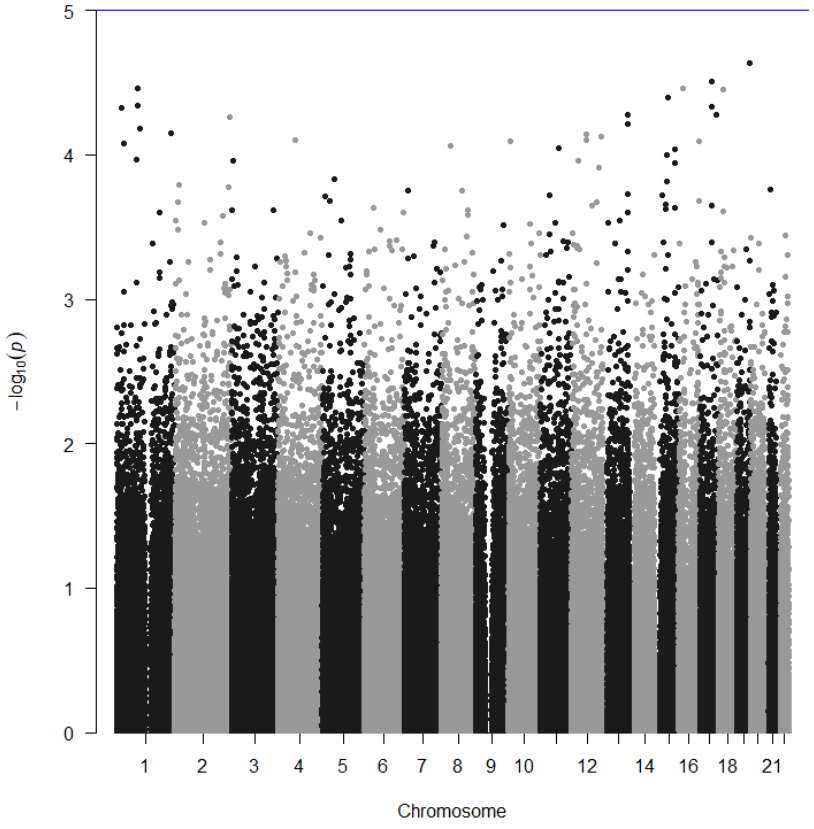

Figure K41: Manhattan plot of SNPs for "arches on the index fingers" for the codominant model

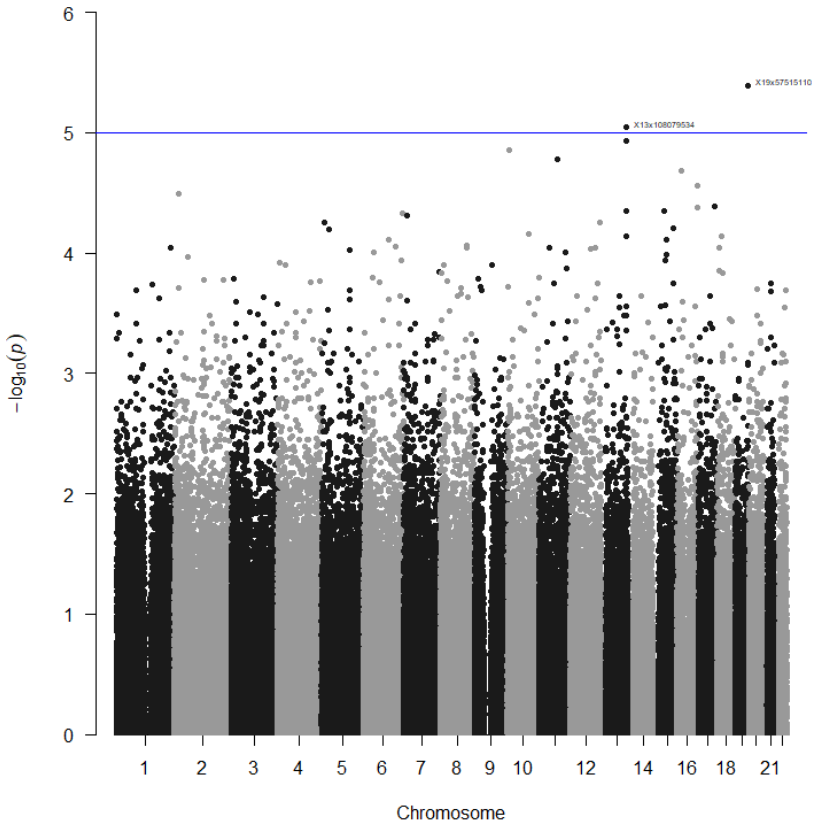

Figure K42: Manhattan plot of SNPs for "arches on the index fingers" for the dominant model

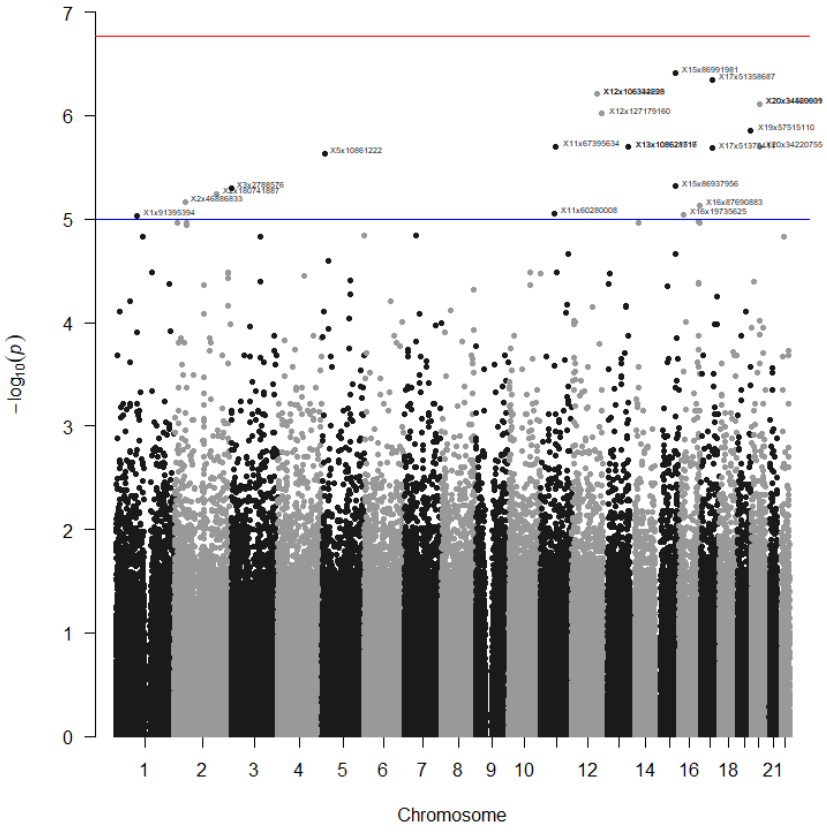

Figure K43: Manhattan plot of SNPs for "arches on the index fingers" for the log-additive model

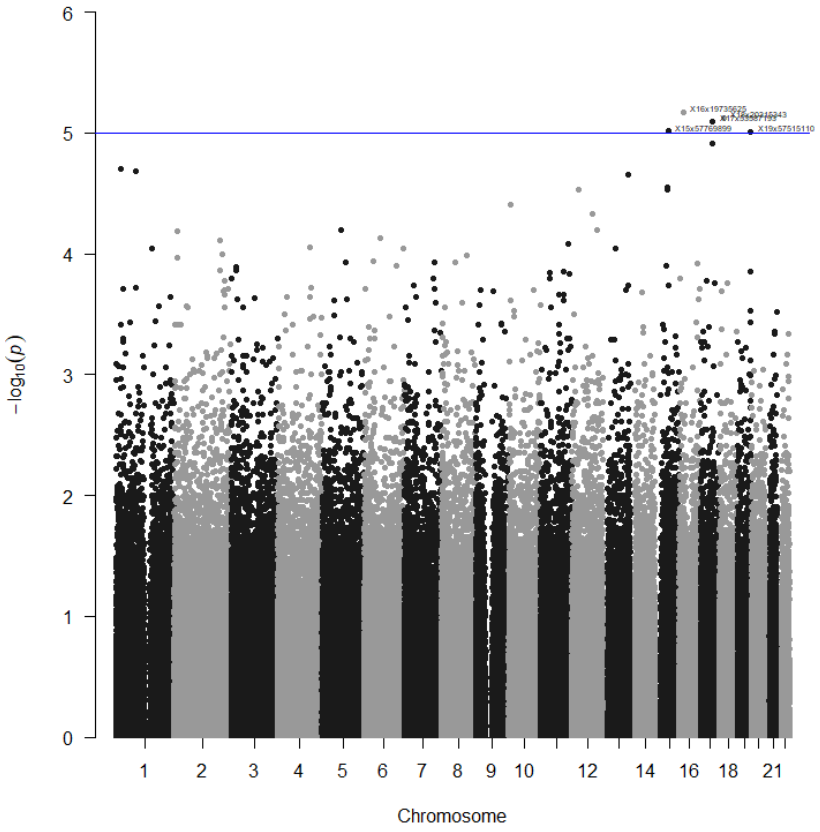

Figure K44: Manhattan plot of SNPs for "arches on the index fingers" for the overdominant model

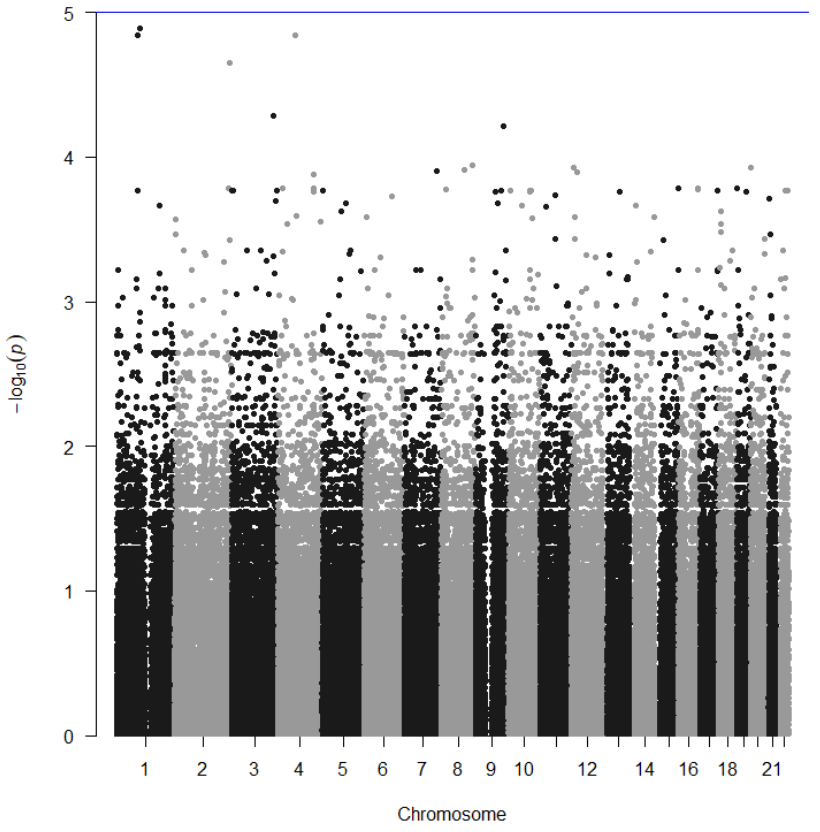

Figure K45: Manhattan plot of SNPs for "arches on the index fingers" for the recessive model

Loops on the left little finger

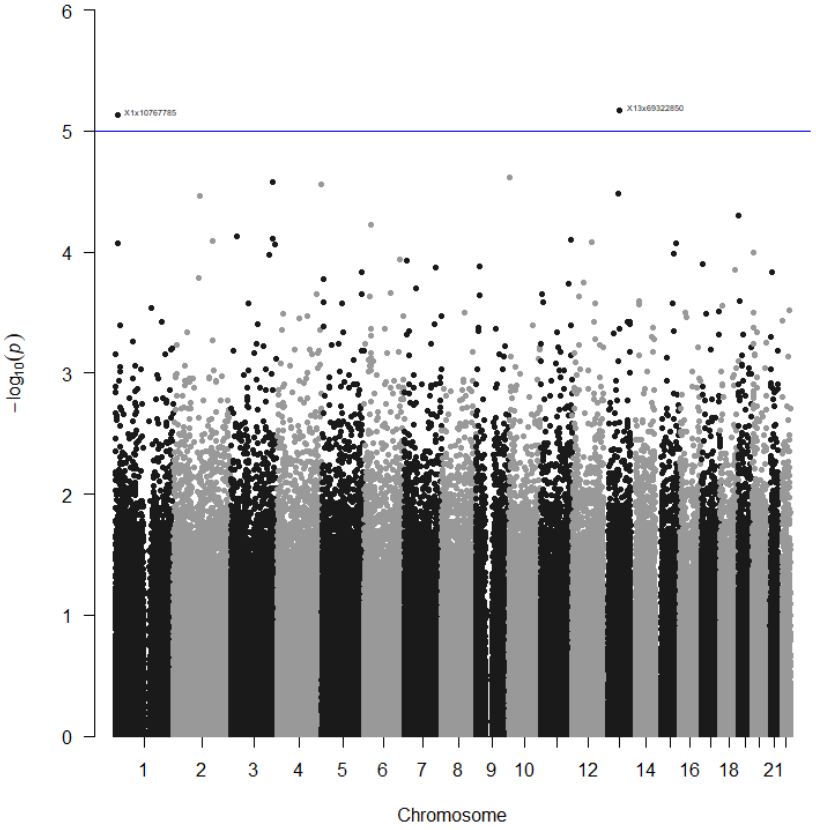

Figure K46: Manhattan plot of SNPs for loops on the left little finger for the codominant model

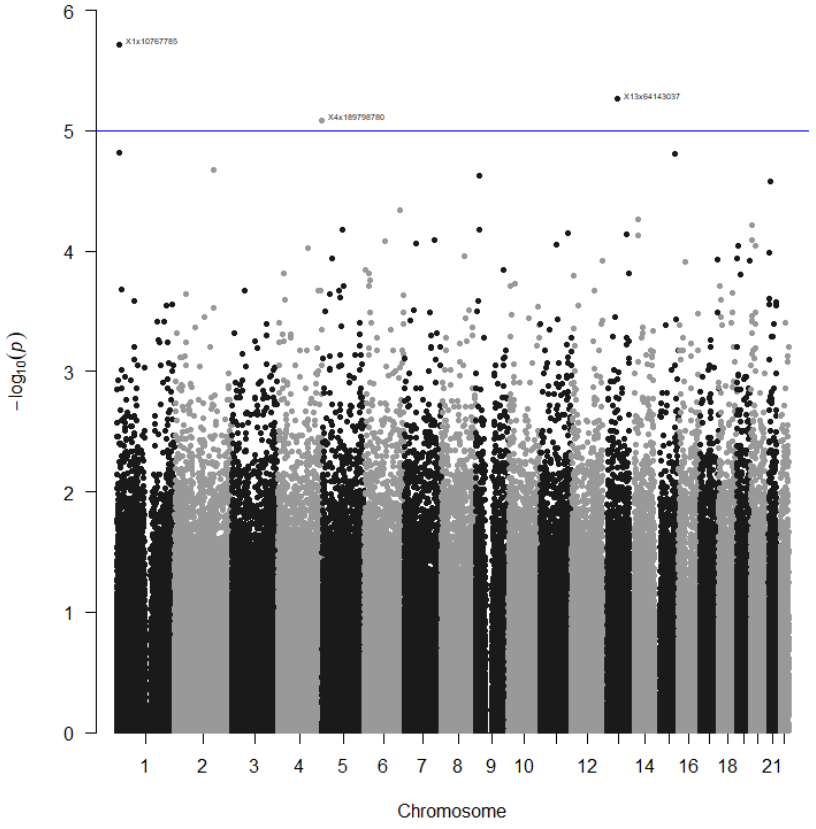

Figure K47: Manhattan plot of SNPs for loops on the left little finger for the dominant model

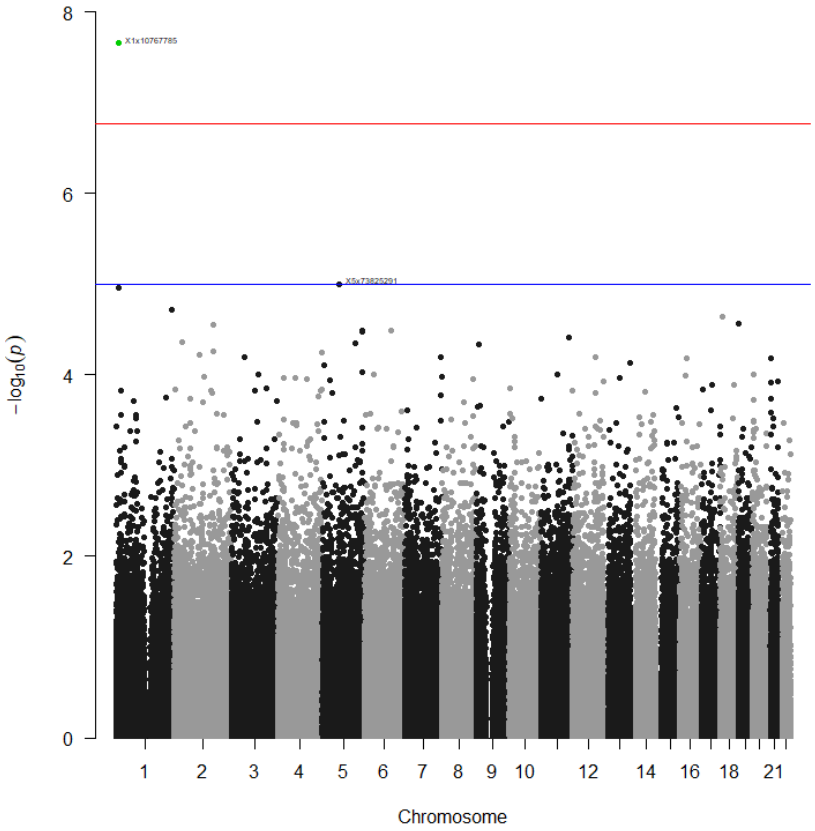

Figure K48: Manhattan plot of SNPs for loops on the left little finger for the log-additive model

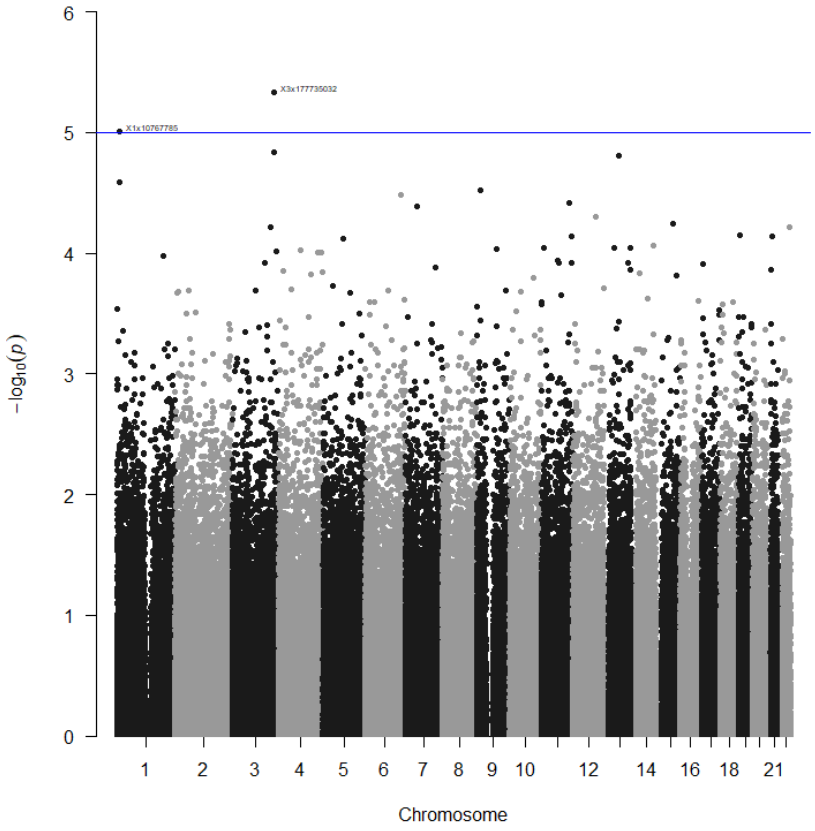

Figure K49: Manhattan plot of SNPs for loops on the left little finger for the overdominant model

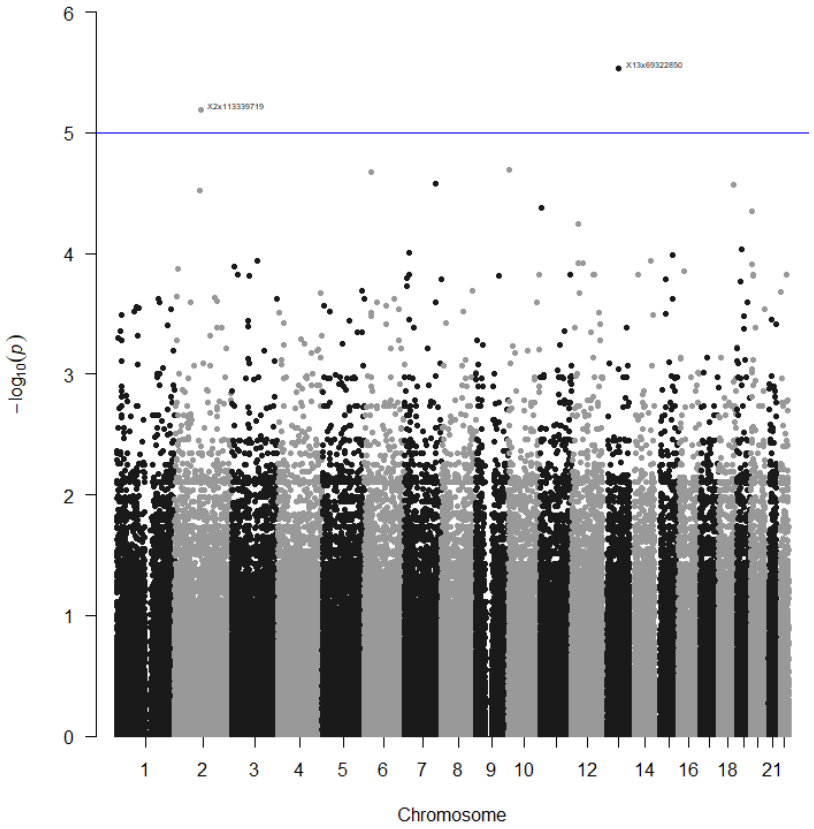

Figure K50: Manhattan plot of SNPs for loops on the left little finger for the recessive model

Loops on the right little finger

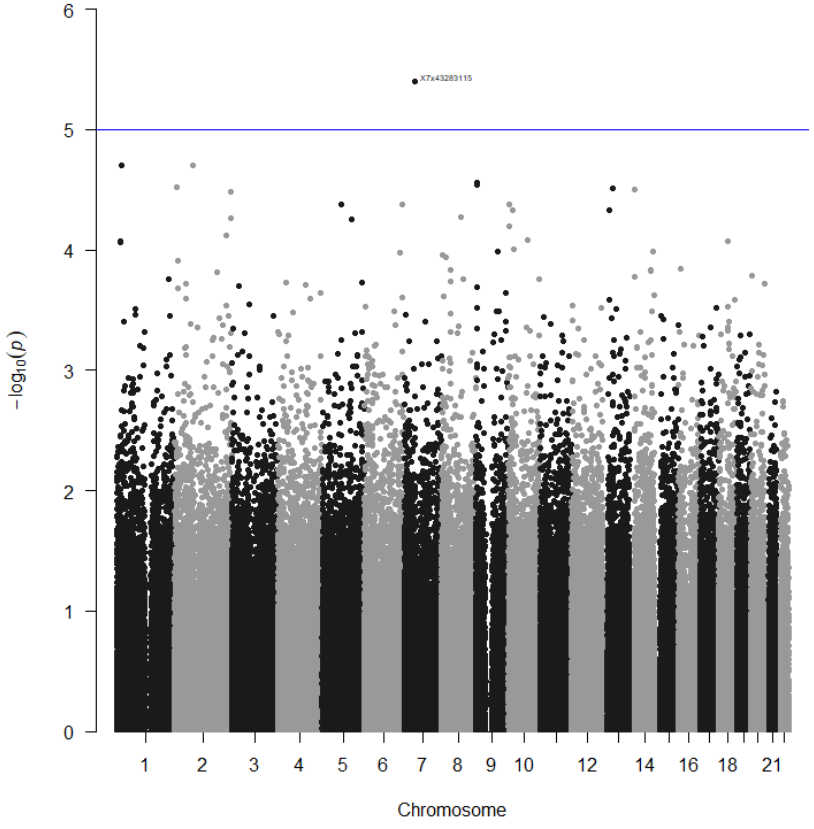

Figure K51: Manhattan plot of SNPs for loops on the right little finger for the codominant model

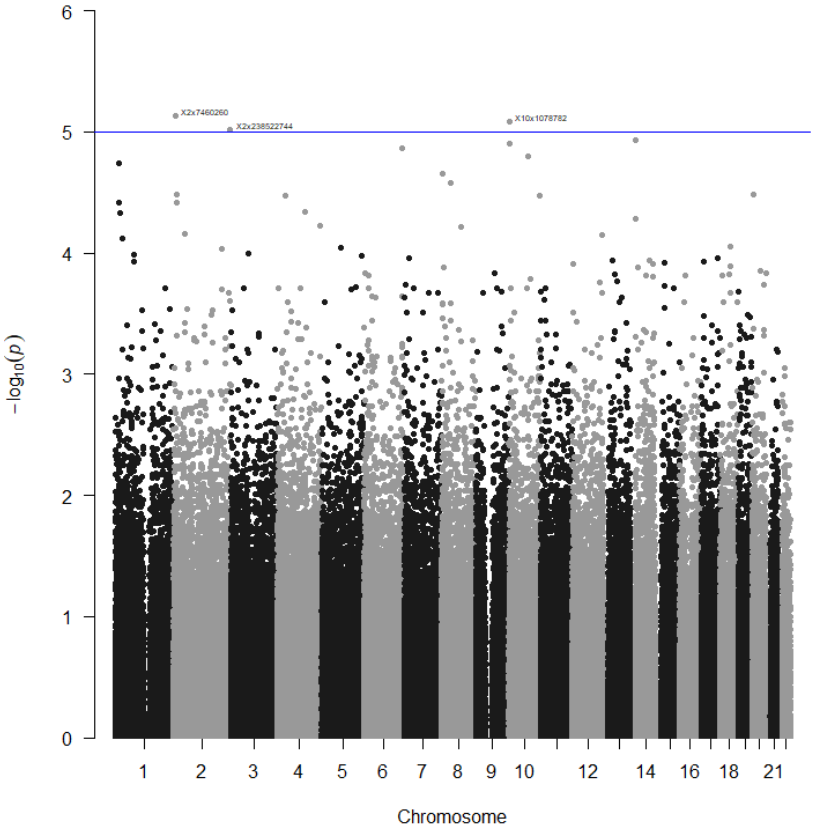

Figure K52: Manhattan plot of SNPs for loops on the right little finger for the dominant model

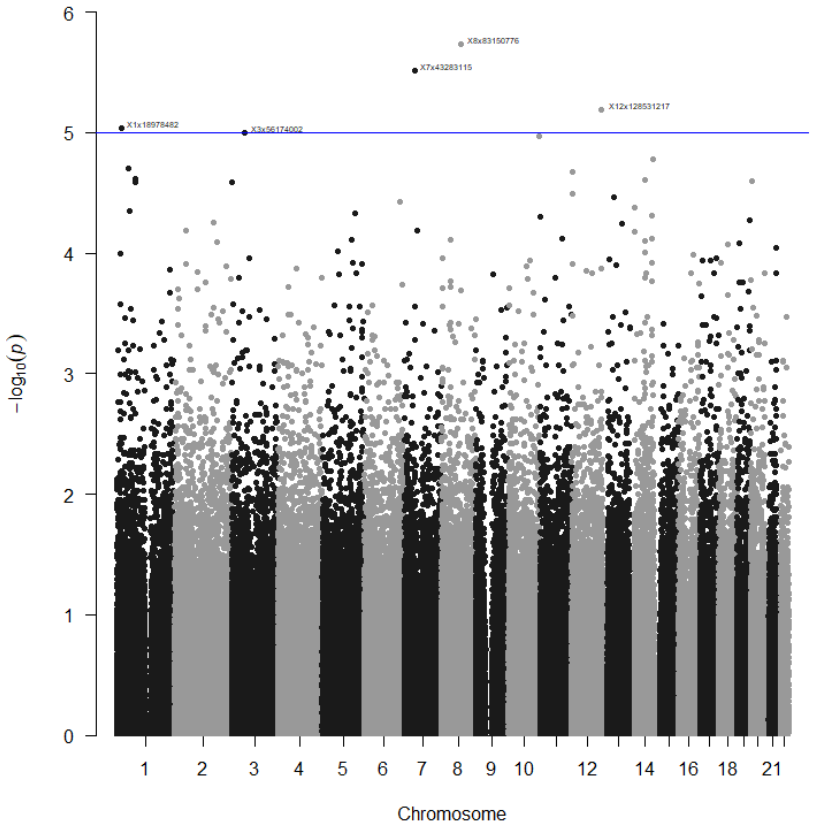

Figure K53: Manhattan plot of SNPs for loops on the right little finger for the log-additive model

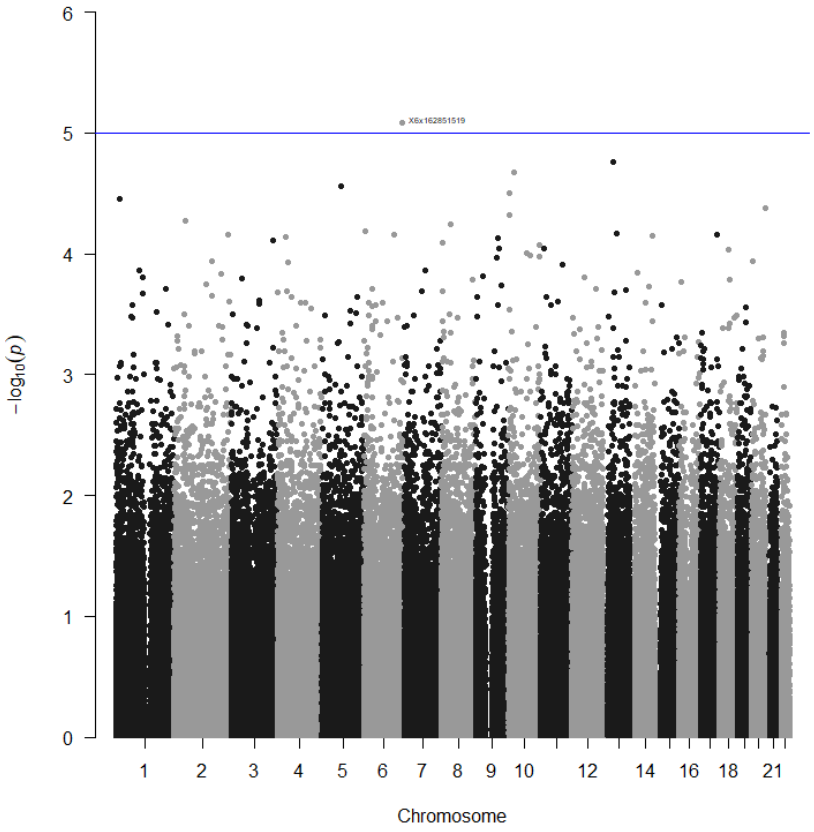

Figure K54: Manhattan plot of SNPs for loops on the right little finger for the overdominant model

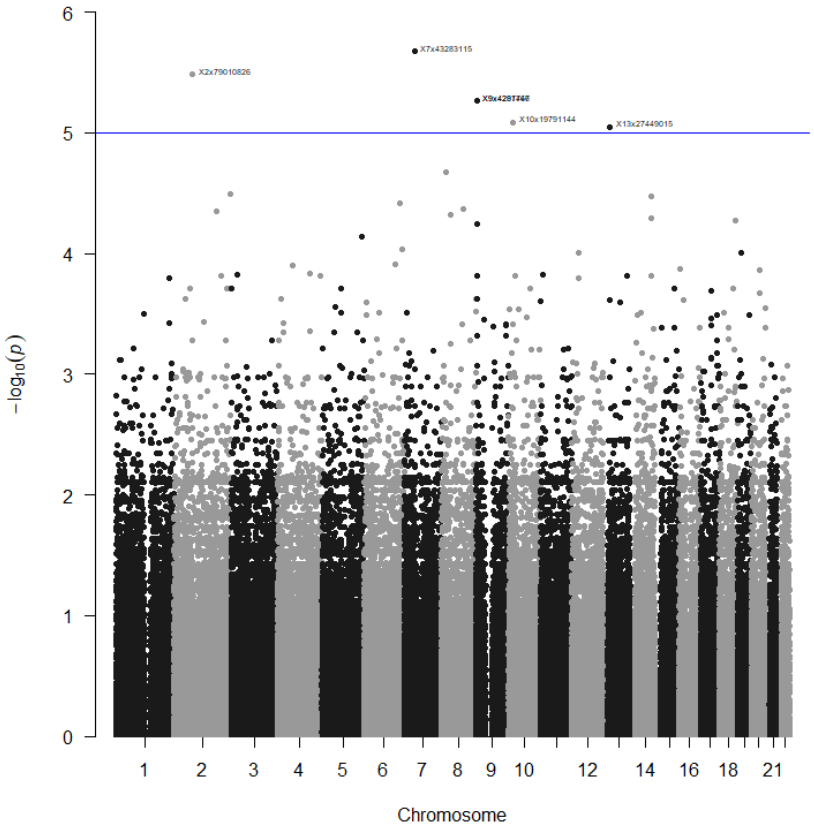

Figure K55: Manhattan plot of SNPs for loops on the right little finger for the recessive model

Loops on the left ring finger

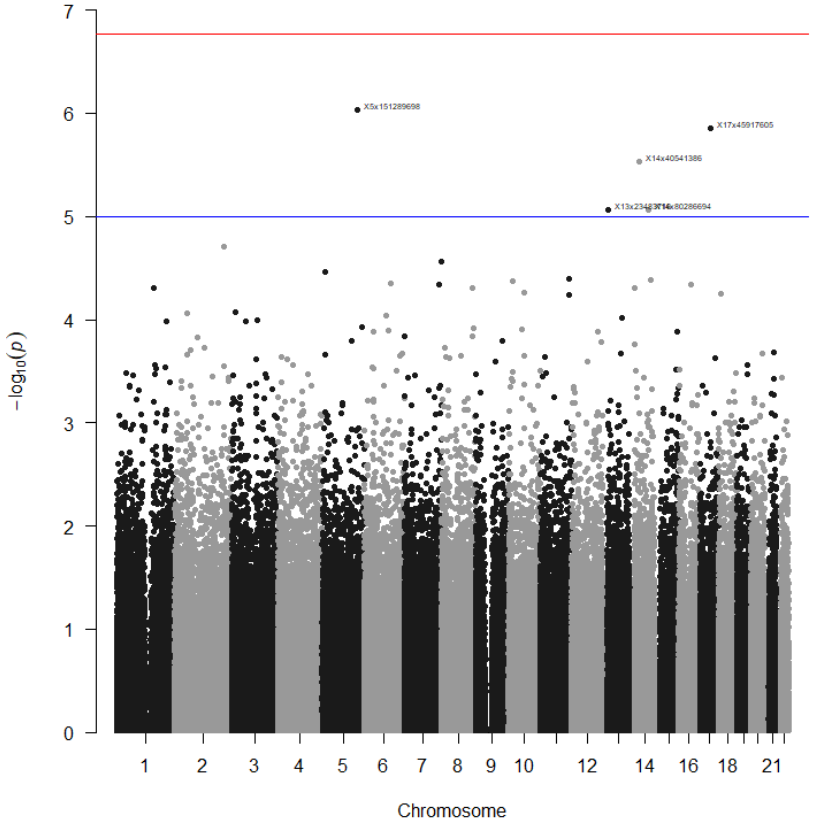

Figure K56: Manhattan plot of SNPs for loops on the left ring finger for the codominant model

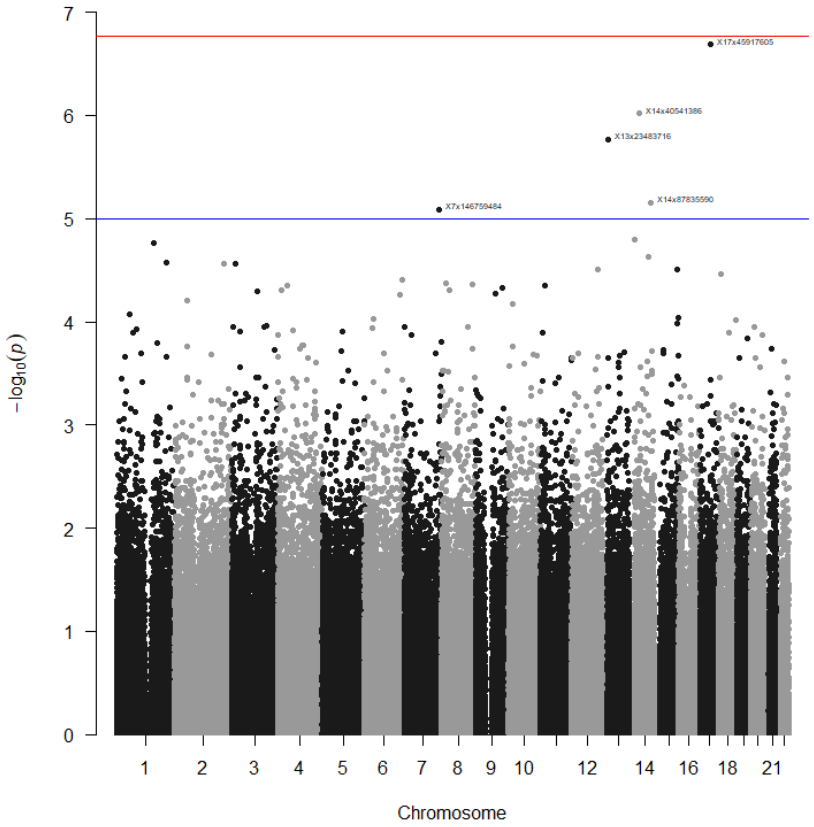

Figure K57: Manhattan plot of SNPs for loops on the left ring finger for the dominant model

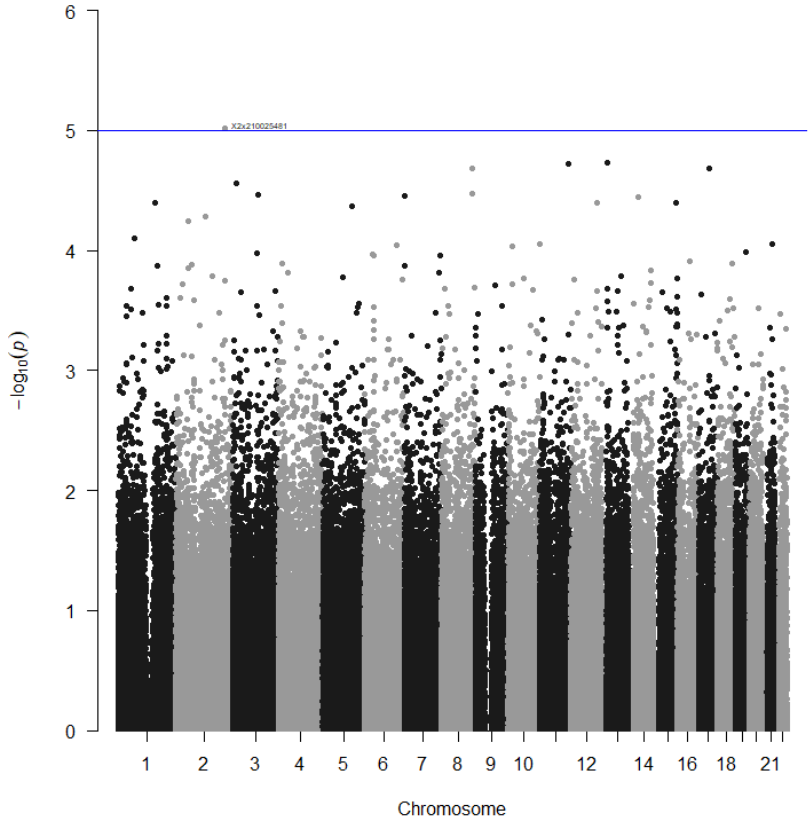

Figure K58: Manhattan plot of SNPs for loops on the left ring finger for the log-additive model

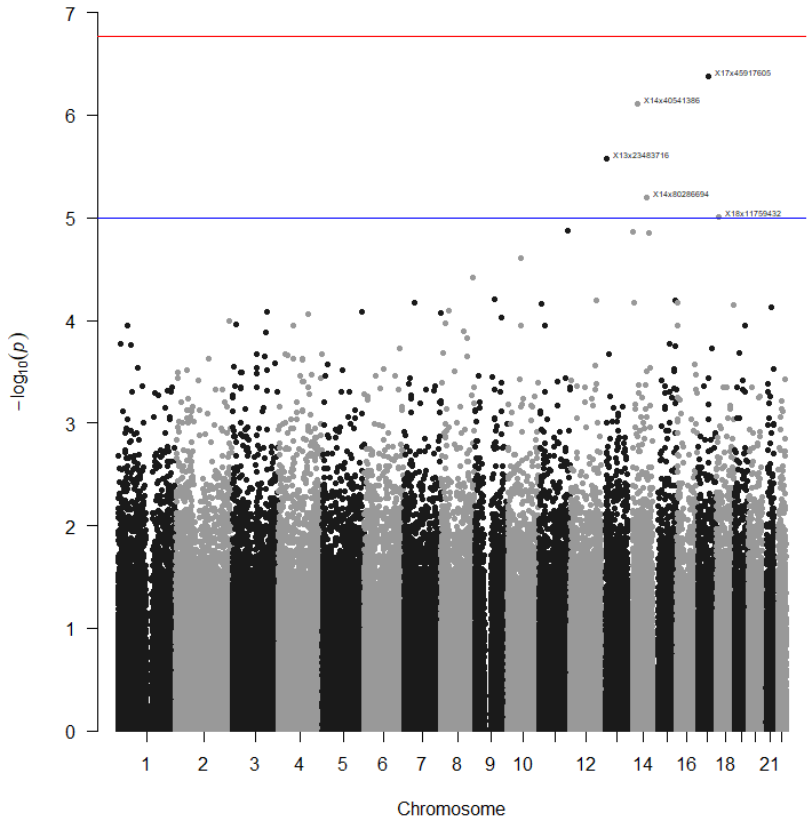

Figure K59: Manhattan plot of SNPs for loops on the left ring finger for the overdominant model

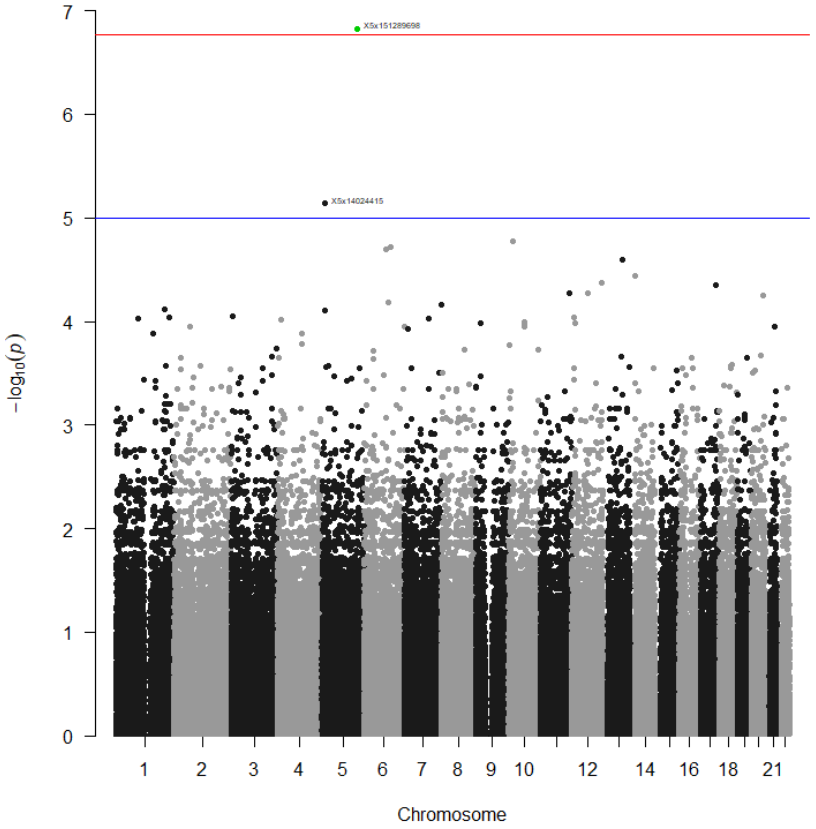

Figure K60: Manhattan plot of SNPs for loops on the left ring finger for the recessive model

Loops on the right ring finger

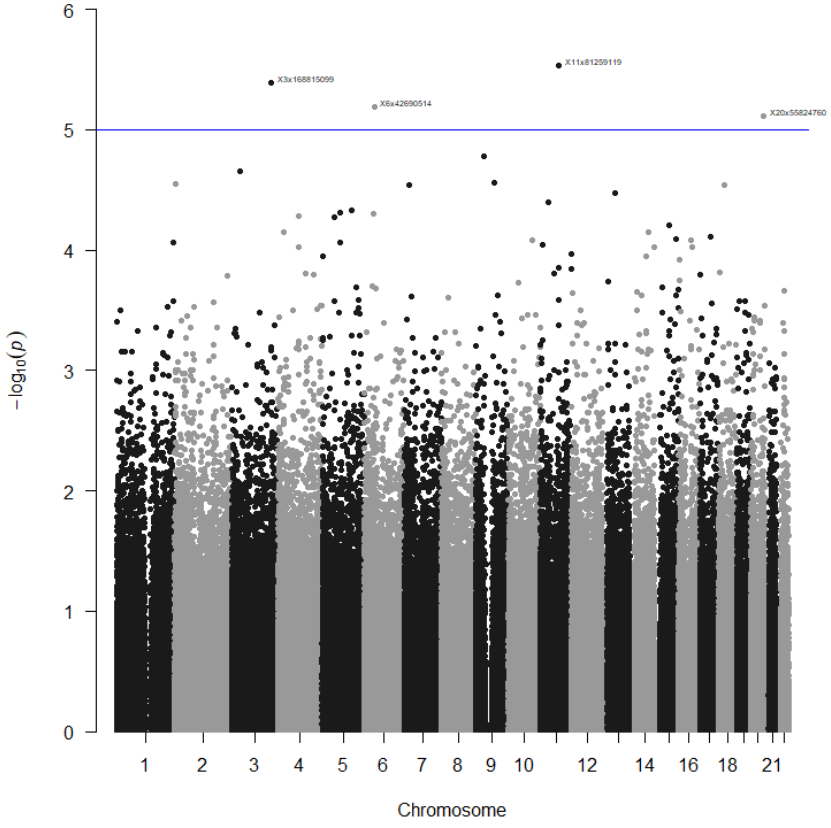

Figure K61: Manhattan plot of SNPs for loops on the right ring finger for the codominant model

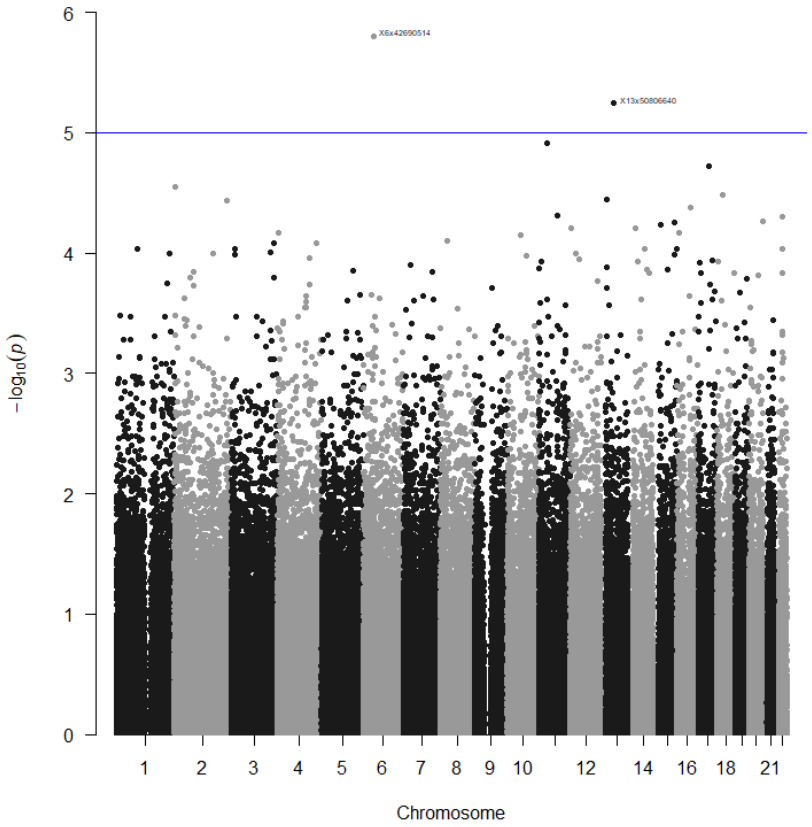

Figure K62: Manhattan plot of SNPs for loops on the right ring finger for the dominant model

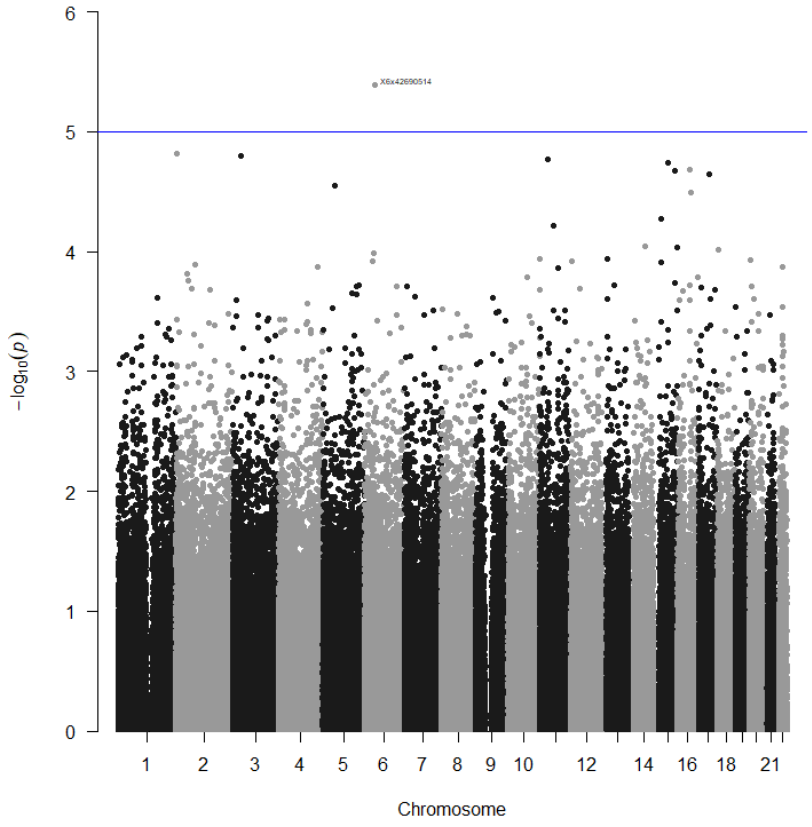

Figure K63: Manhattan plot of SNPs for loops on the right ring finger for the log-additive model

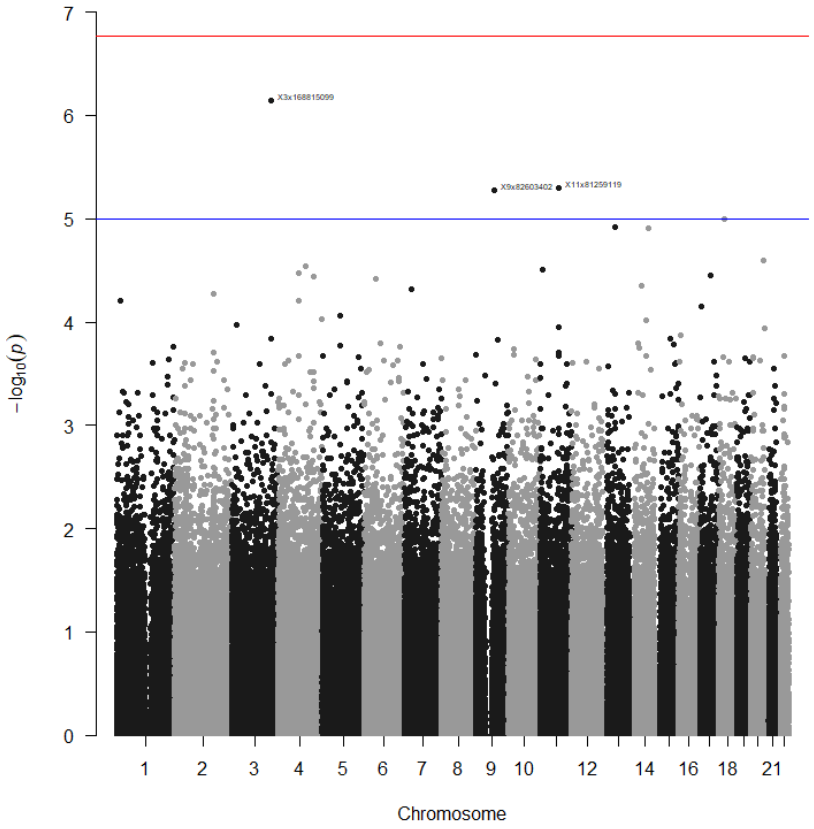

Figure K64: Manhattan plot of SNPs for loops on the right ring finger for the overdominant model

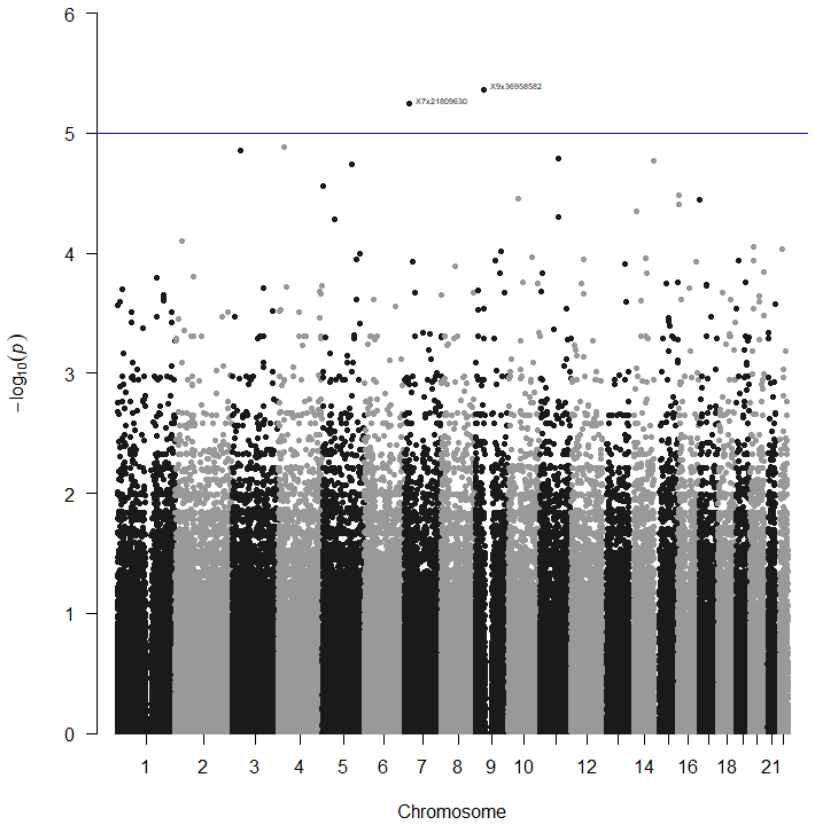

Figure K65: Manhattan plot of SNPs for loops on the right ring finger for the recessive model

Loops on the left middle finger

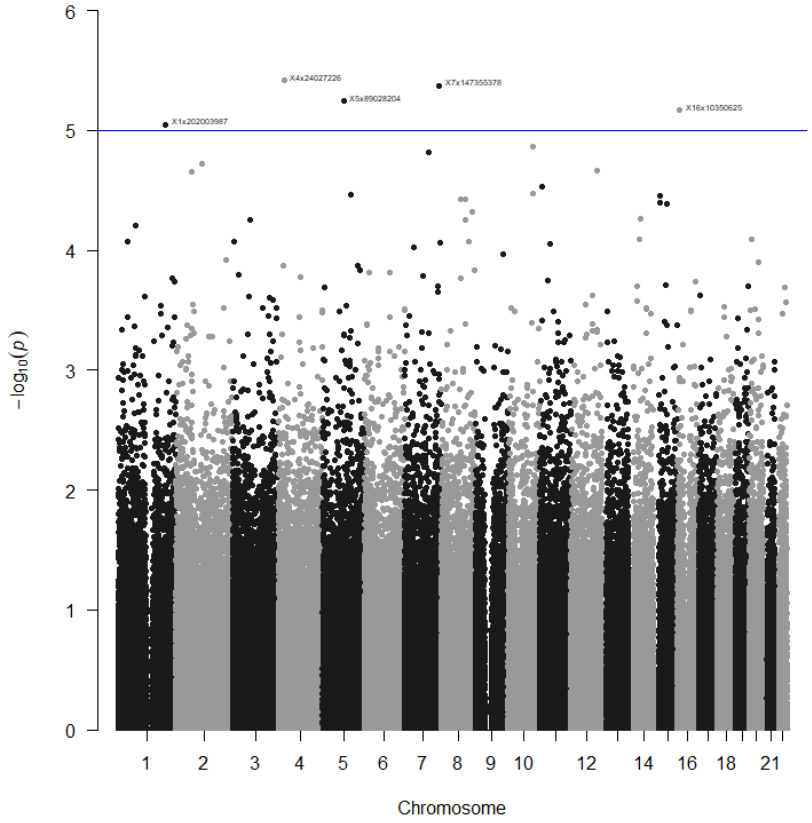

Figure K66: Manhattan plot of SNPs for loops on the left middle finger for the codominant model

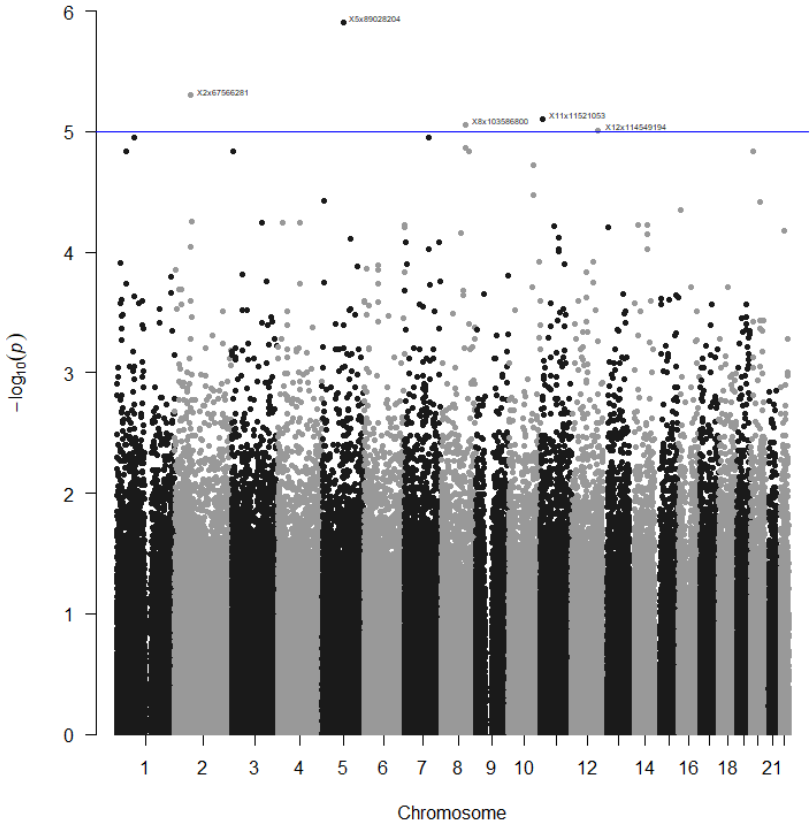

Figure K67: Manhattan plot of SNPs for loops on the left middle finger for the dominant model

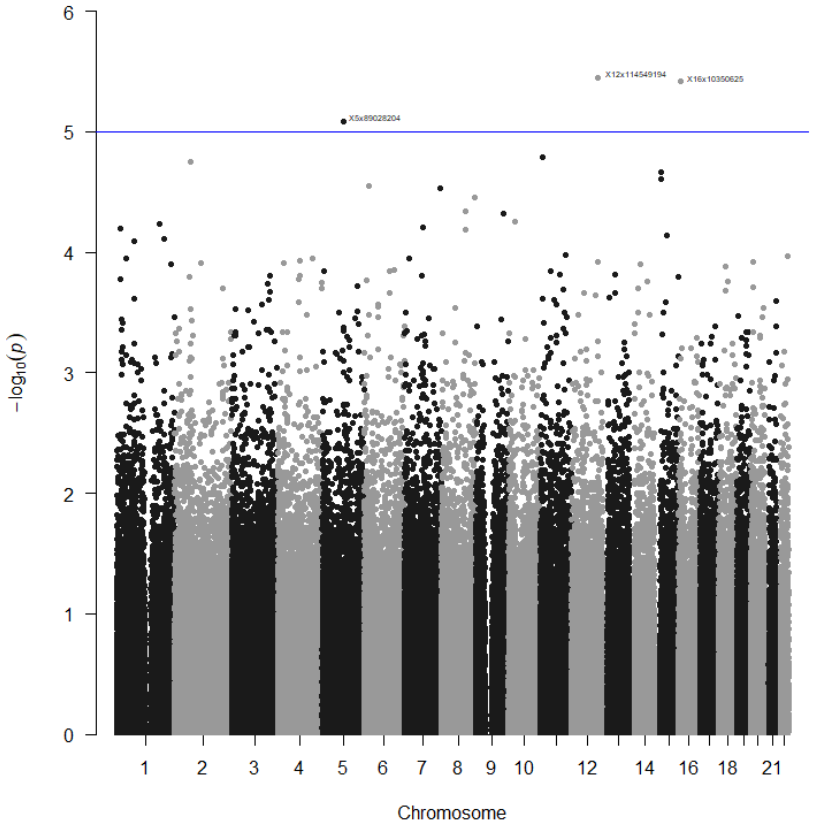

Figure K68: Manhattan plot of SNPs for loops on the left middle finger for the log-additive model

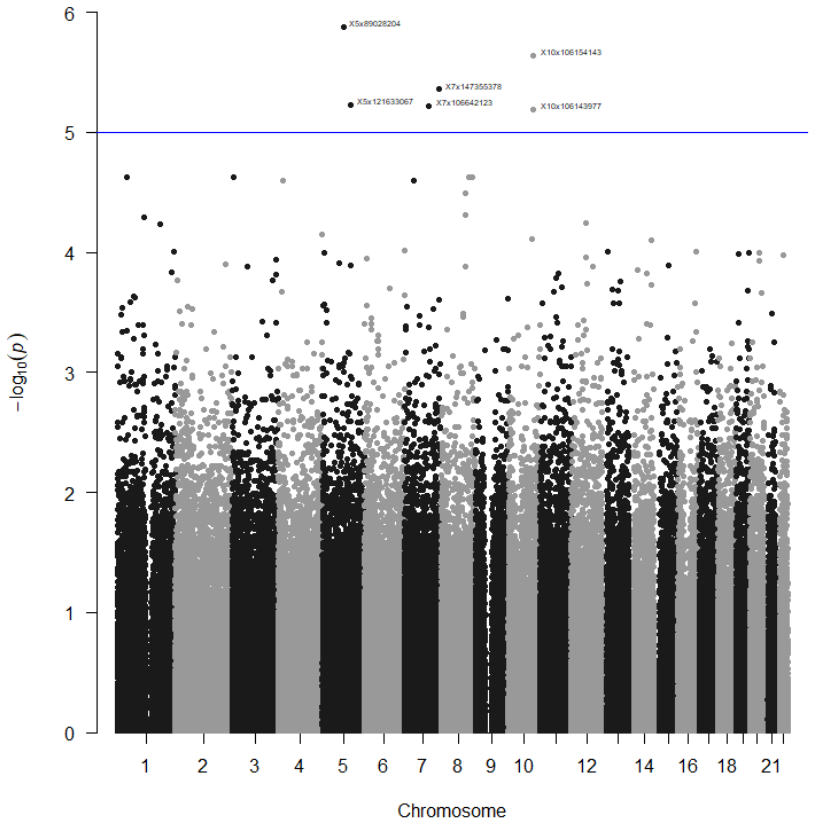

Figure K69: Manhattan plot of SNPs for loops on the left middle finger for the overdominant model

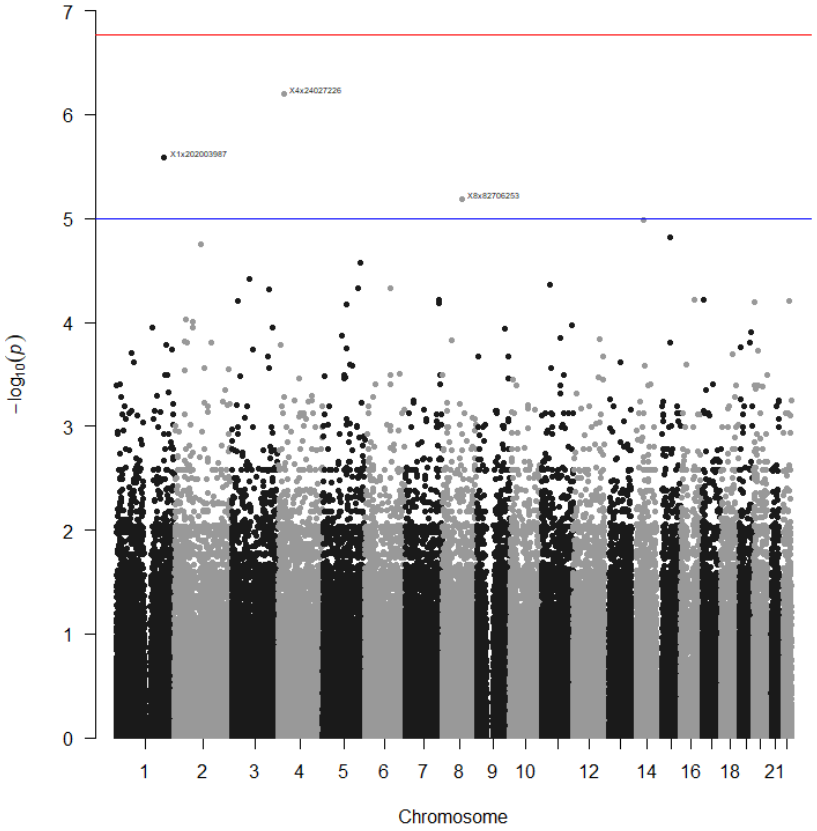

Figure K70: Manhattan plot of SNPs for loops on the left middle finger for the recessive model

Loops on the right middle finger

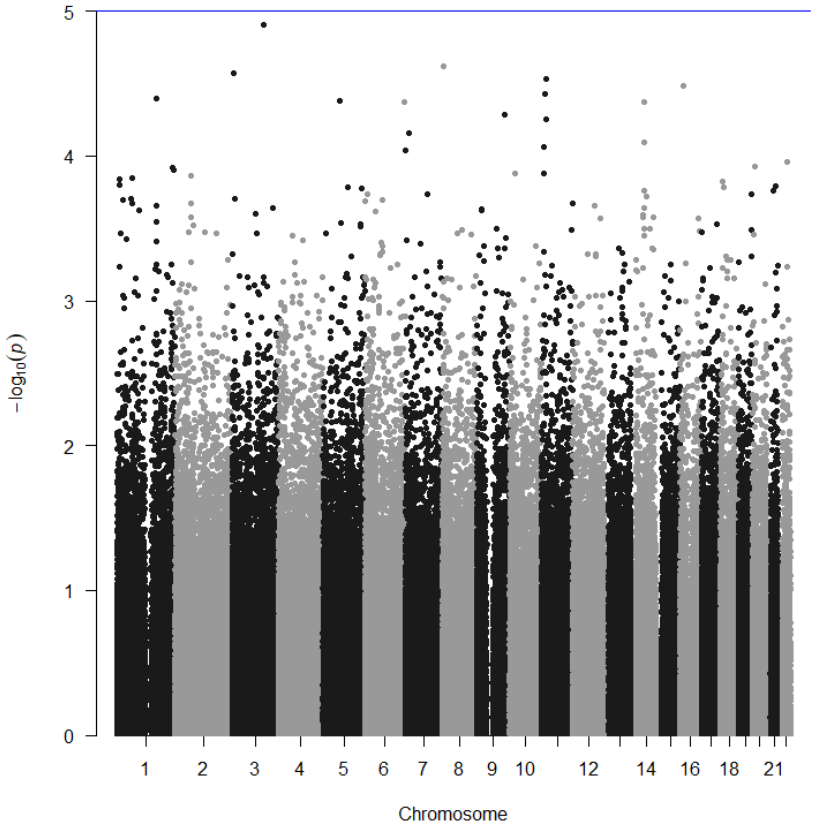

Figure K71: Manhattan plot of SNPs for loops on the right middle finger for the codominant model

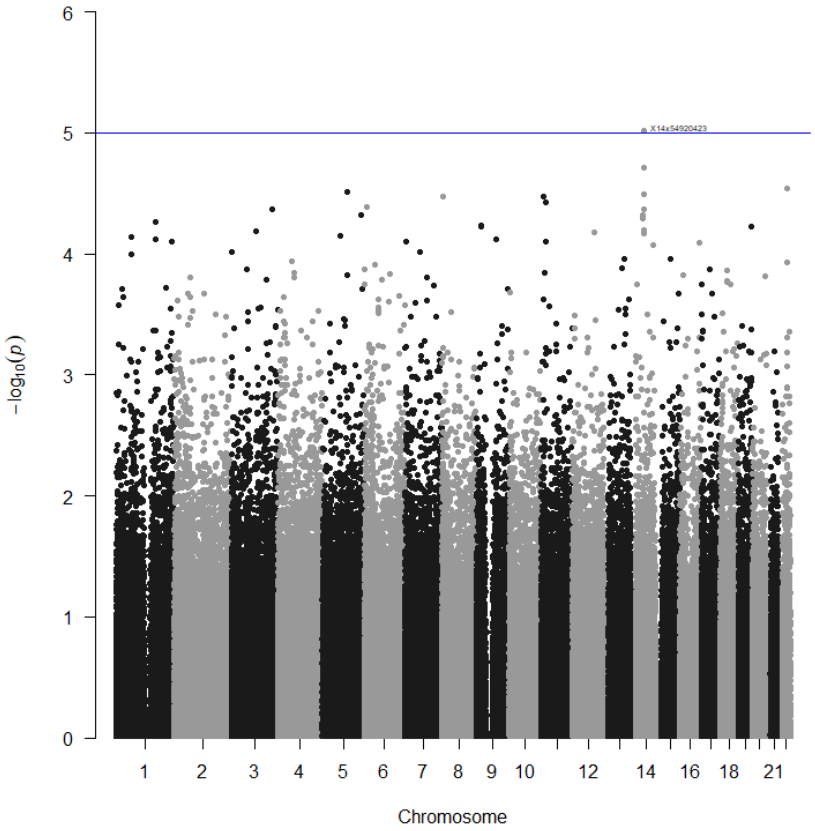

Figure K72: Manhattan plot of SNPs for loops on the right middle finger for the dominant model

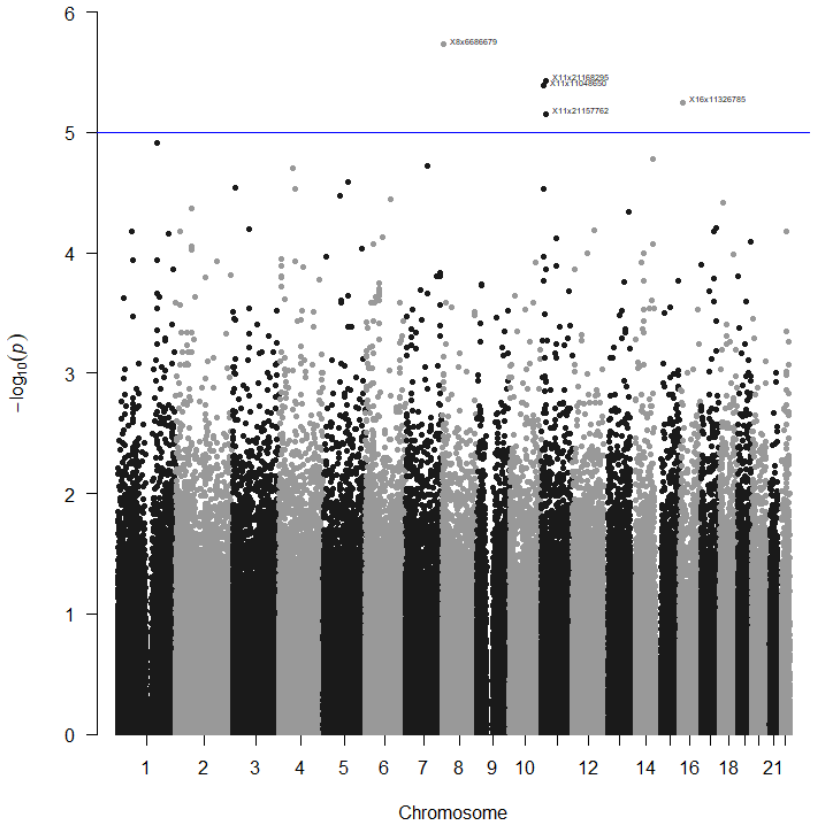

Figure K73: Manhattan plot of SNPs for loops on the right middle finger for the log-additive model

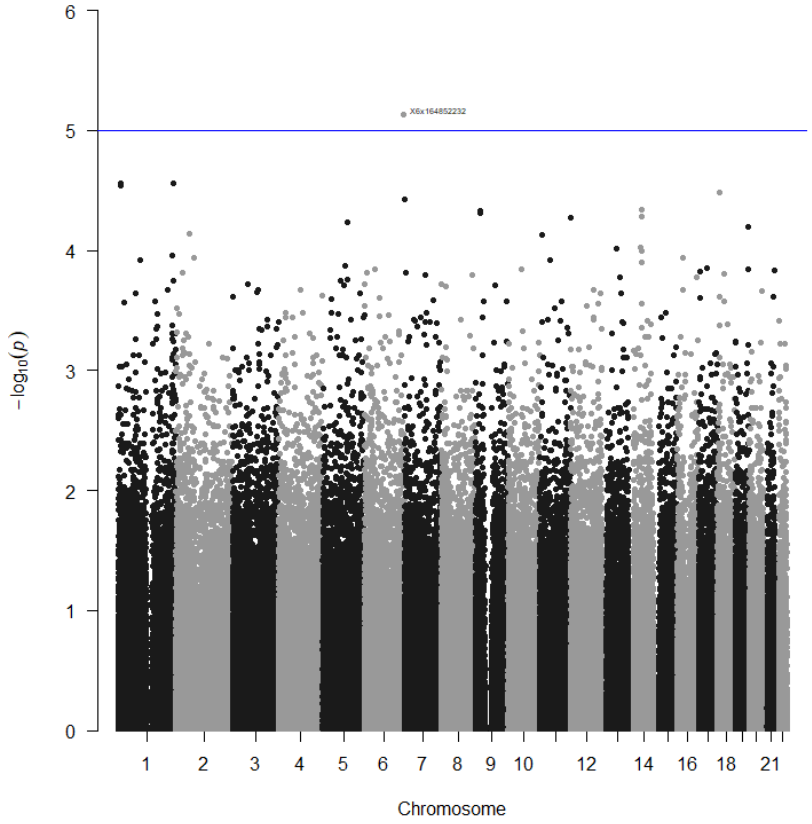

Figure K74: Manhattan plot of SNPs for loops on the right middle finger for the overdominant model

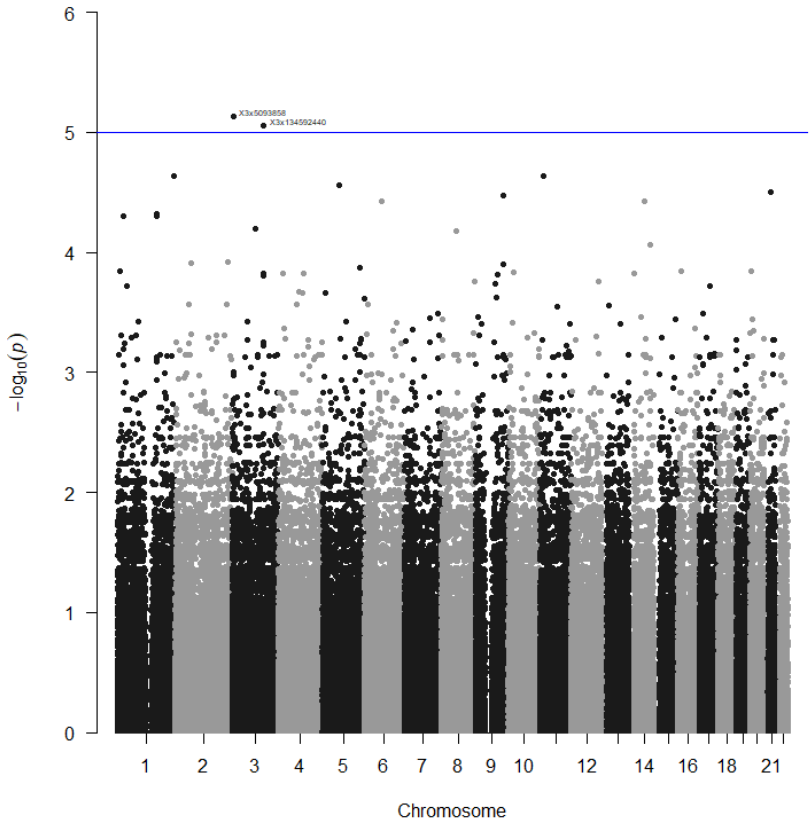

Figure K75: Manhattan plot of SNPs for loops on the right middle finger for the recessive model

Loops on the left index finger

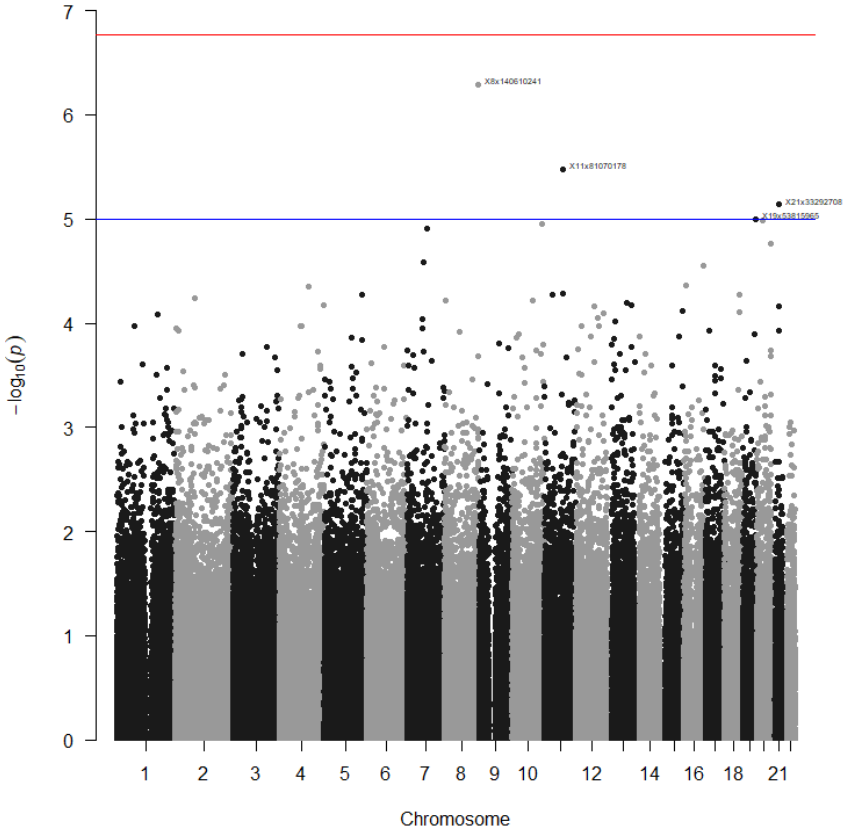

Figure K76: Manhattan plot of SNPs for loops on the left index finger for the codominant model

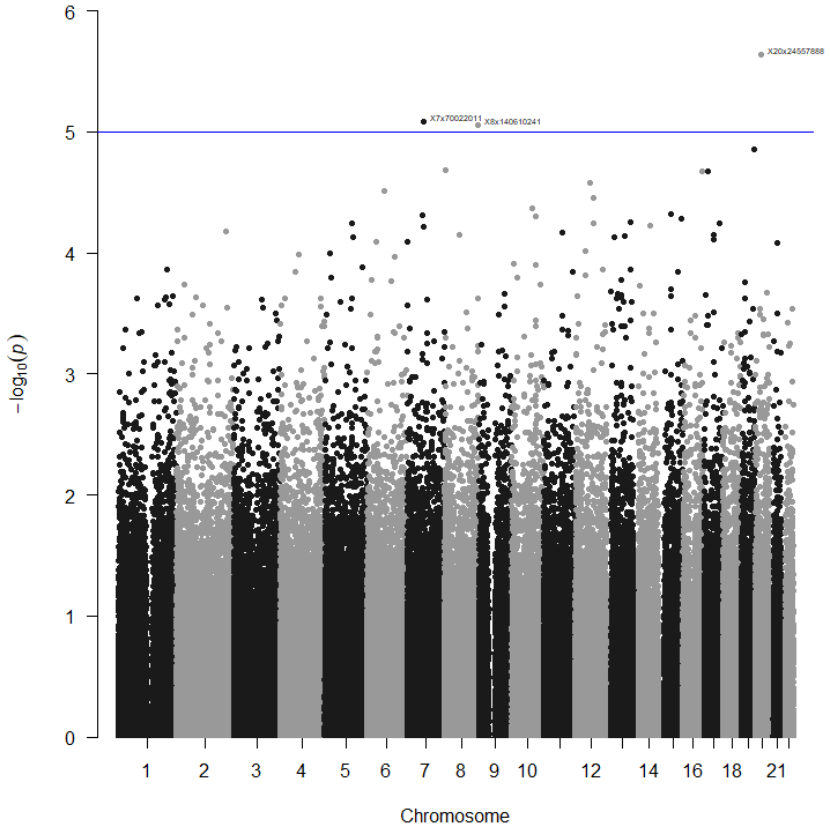

Figure K77: Manhattan plot of SNPs for loops on the left index finger for the dominant model

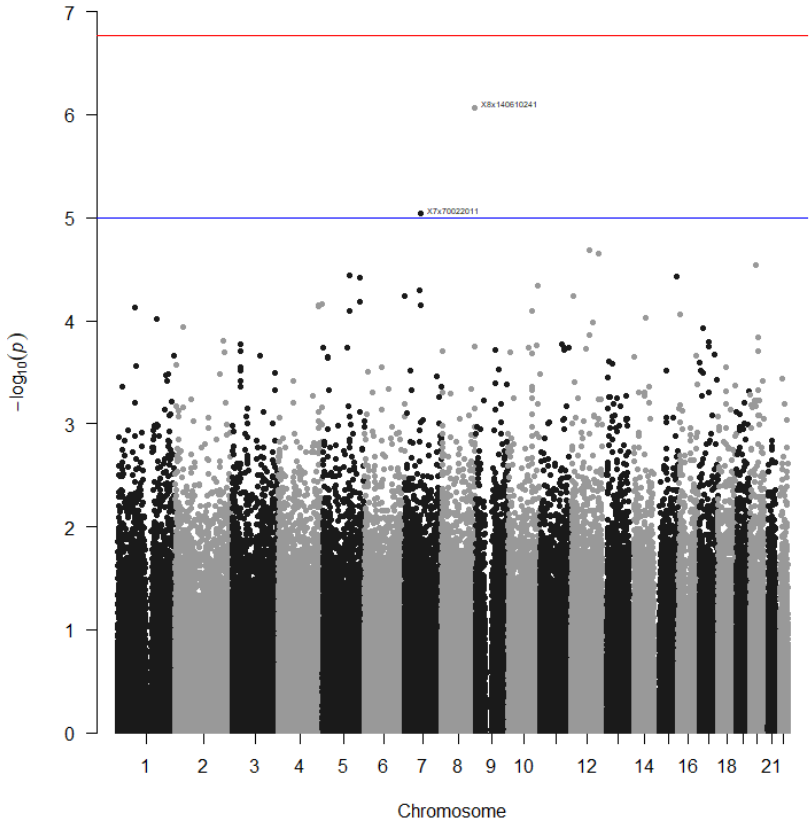

Figure K78: Manhattan plot of SNPs for loops on the left index finger for the log-additive model

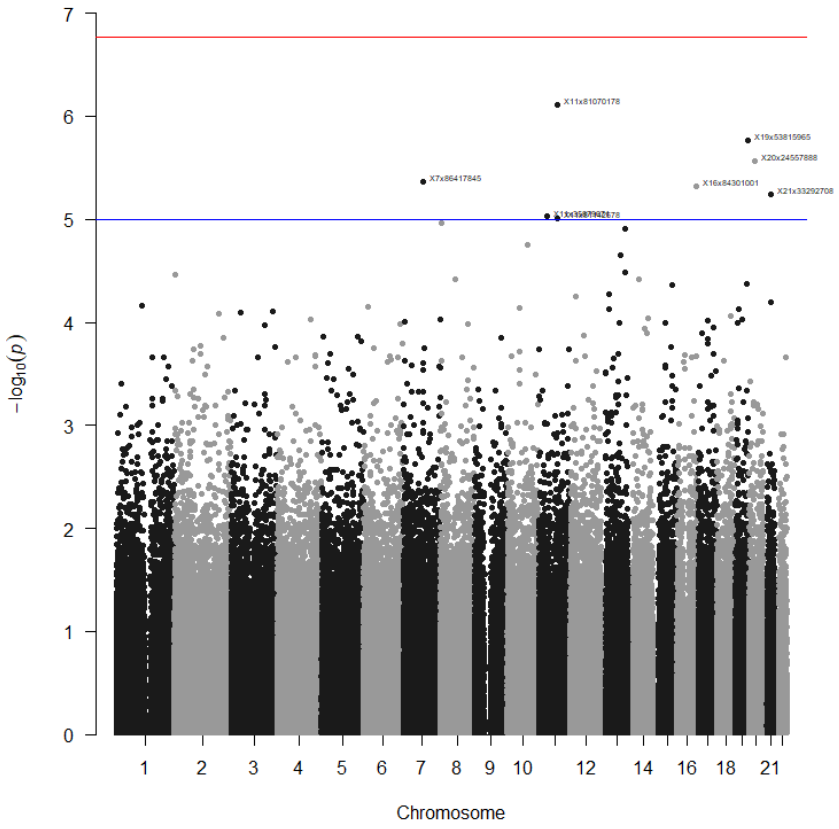

Figure K79: Manhattan plot of SNPs for loops on the left index finger for the overdominant model

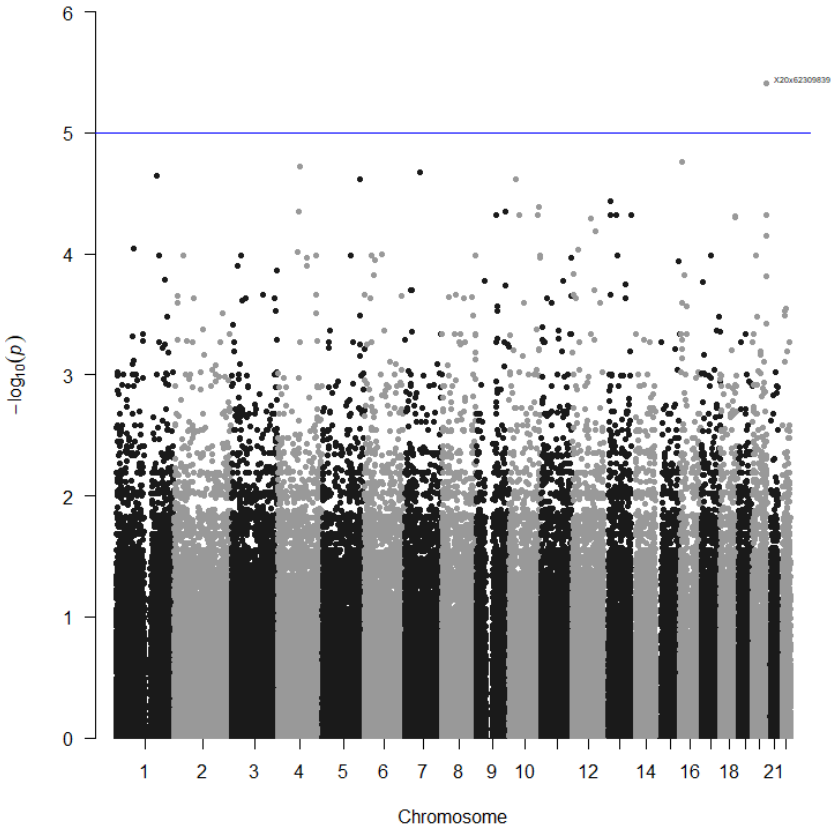

Figure K80: Manhattan plot of SNPs for loops on the left index finger for the recessive model

Loops on the right index finger

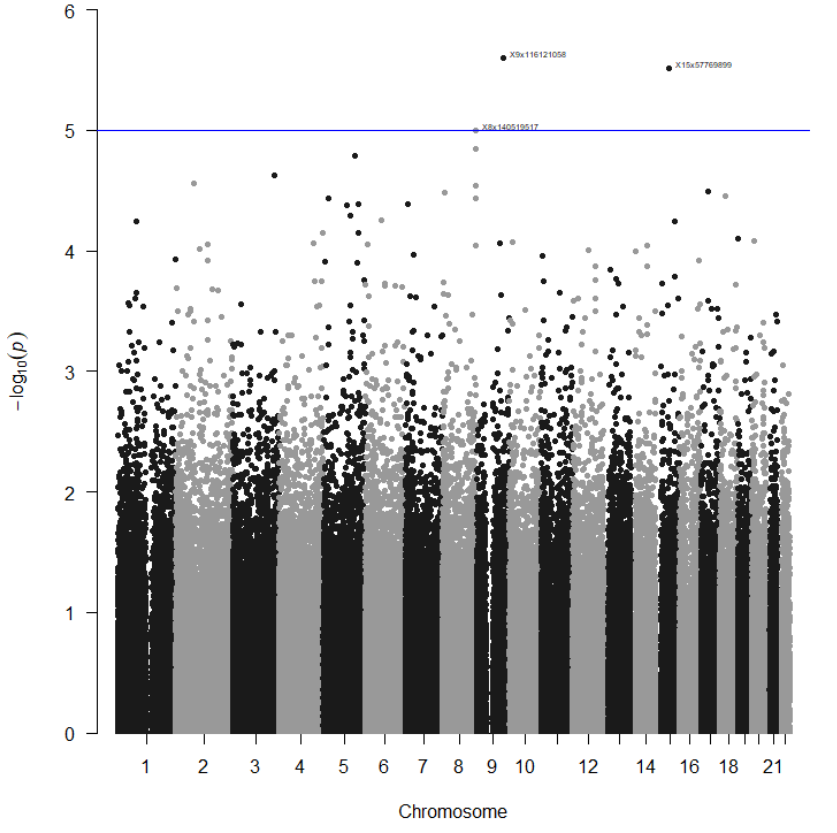

Figure K81: Manhattan plot of SNPs for loops on the right index finger for the codominant model

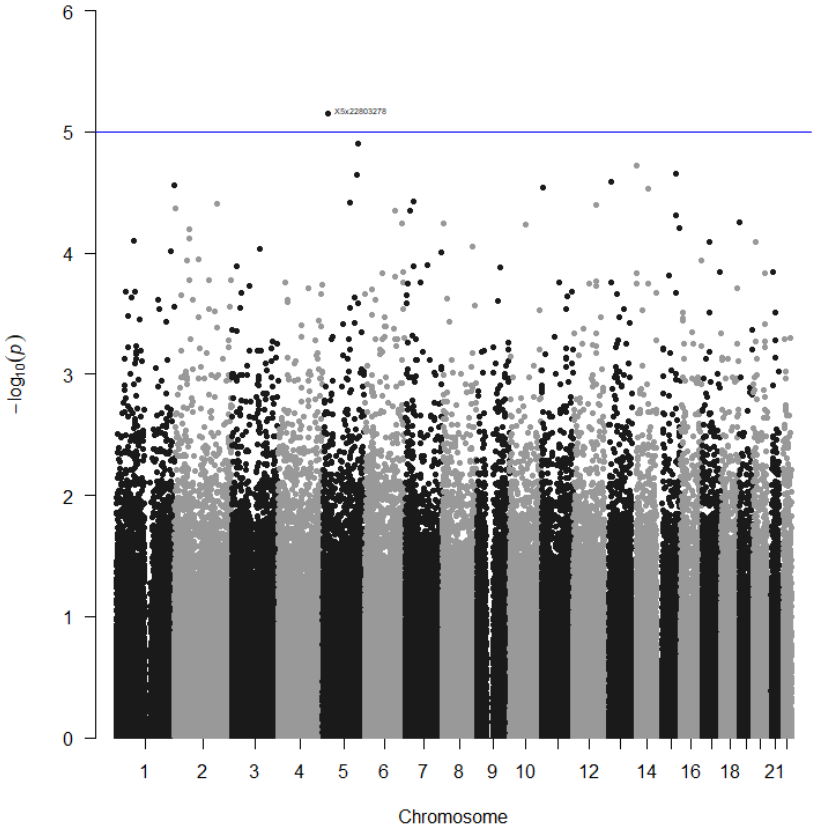

Figure K82: Manhattan plot of SNPs for loops on the right index finger for the dominant model

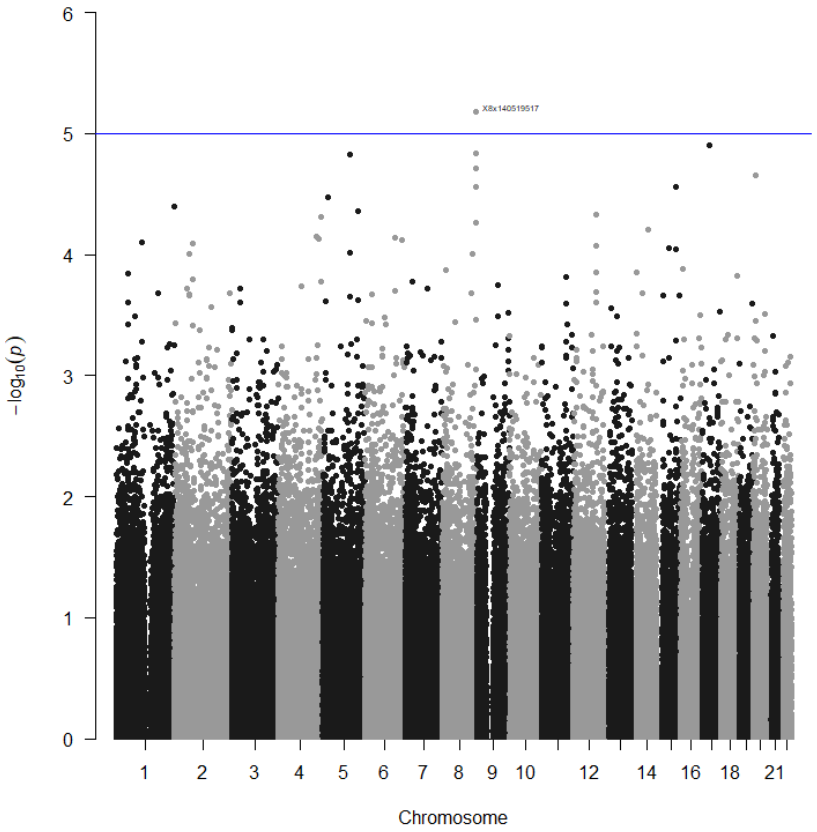

Figure K83: Manhattan plot of SNPs for loops on the right index finger for the log-additive model

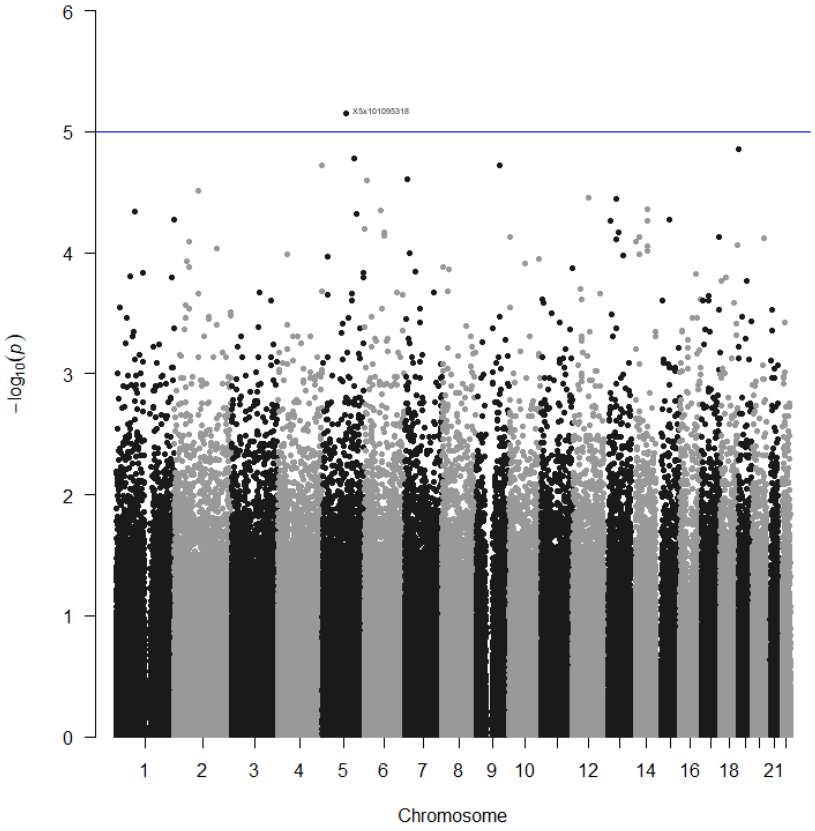

Figure K84: Manhattan plot of SNPs for loops on the right index finger for the overdominant model

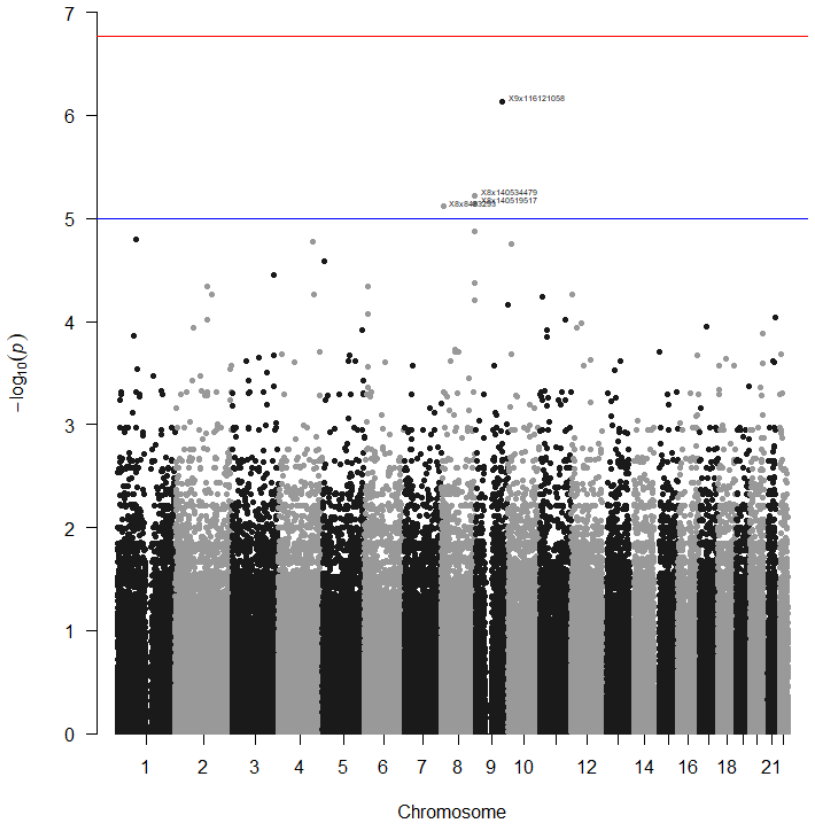

Figure K85: Manhattan plot of SNPs for loops on the right index finger for the recessive model

Loops on the left thumb

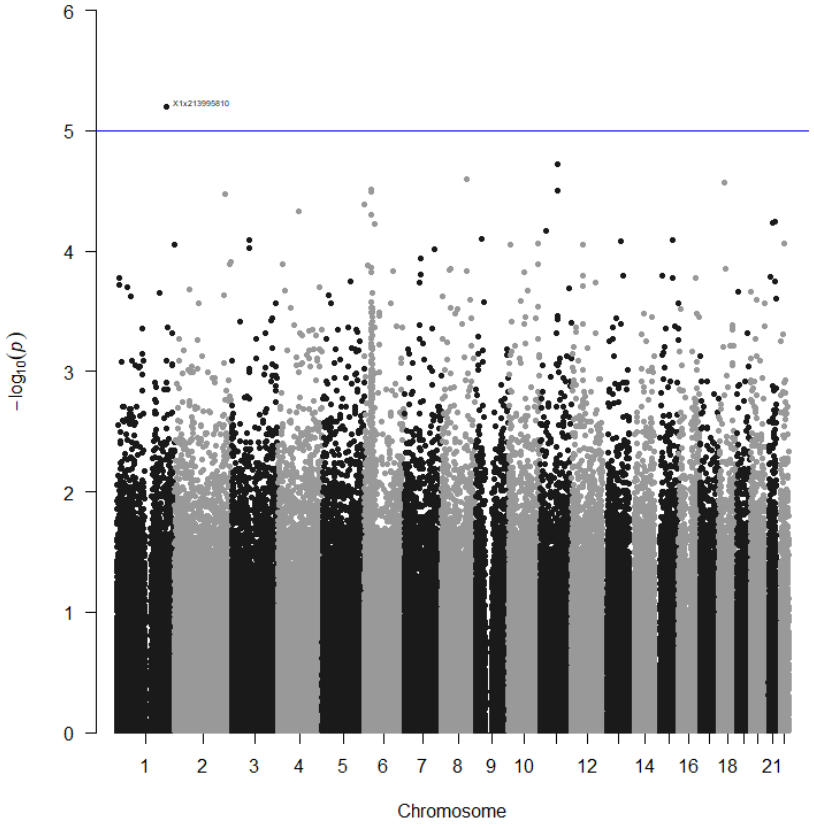

Figure K86: Manhattan plot of SNPs for loops on the left thumb for the codominant model

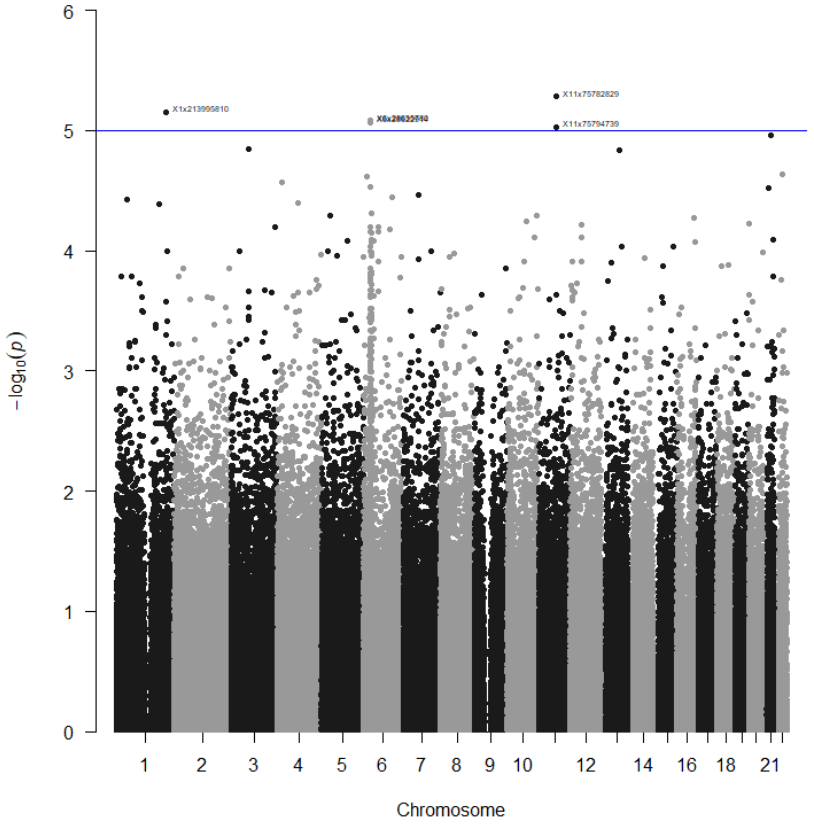

Figure K87: Manhattan plot of SNPs for loops on the left thumb for the dominant model

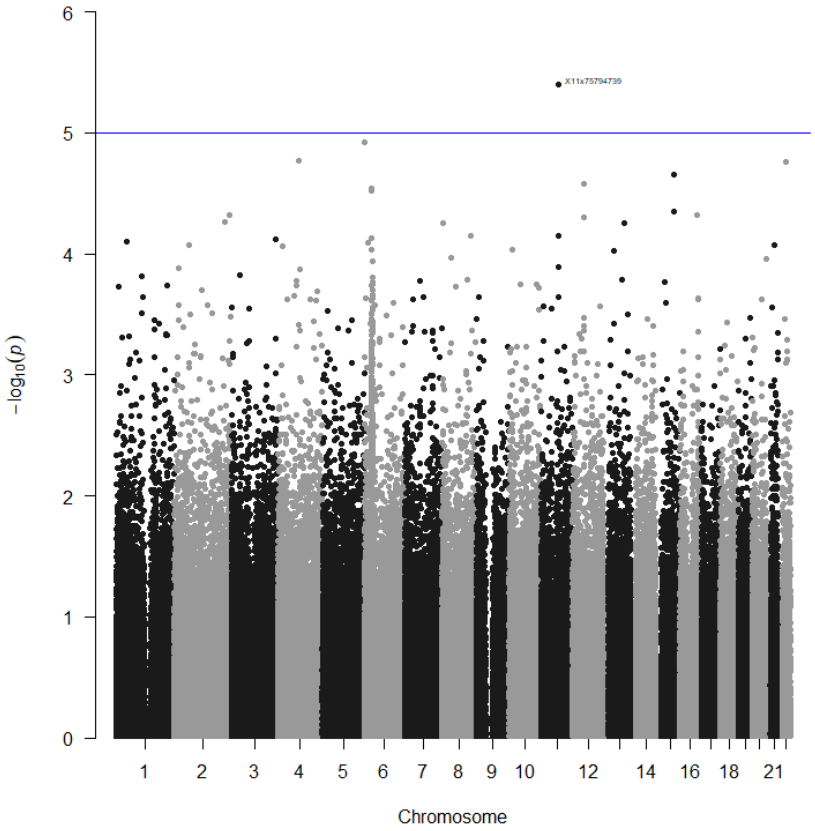

Figure K88: Manhattan plot of SNPs for loops on the left thumb for the log-additive model

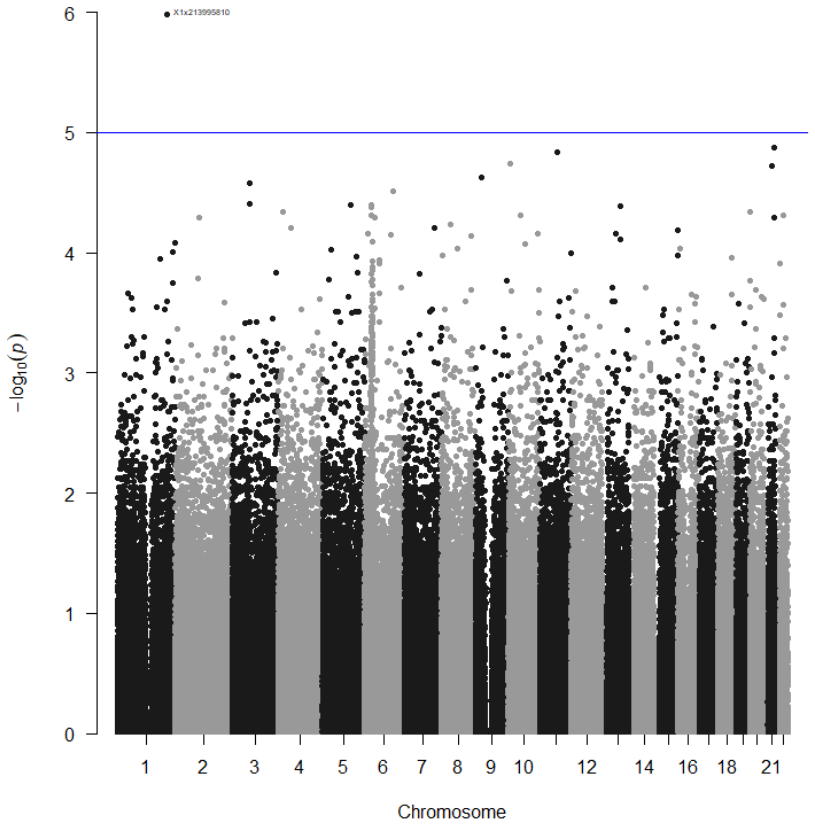

Figure K89: Manhattan plot of SNPs for loops on the left thumb for the overdominant model

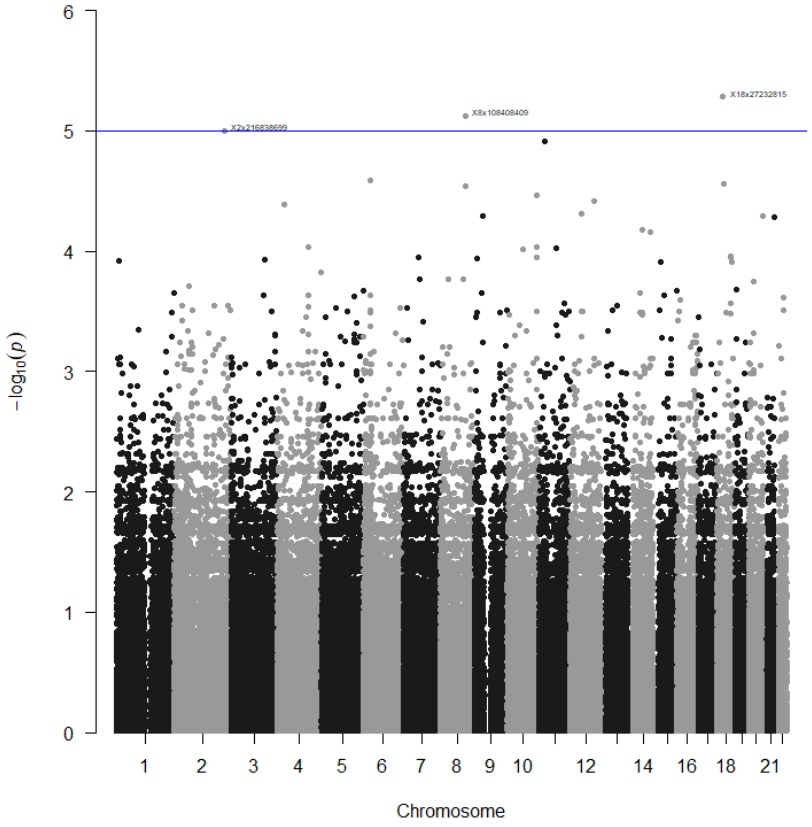

Figure K90: Manhattan plot of SNPs for loops on the left thumb for the recessive model

Loops on the right thumb

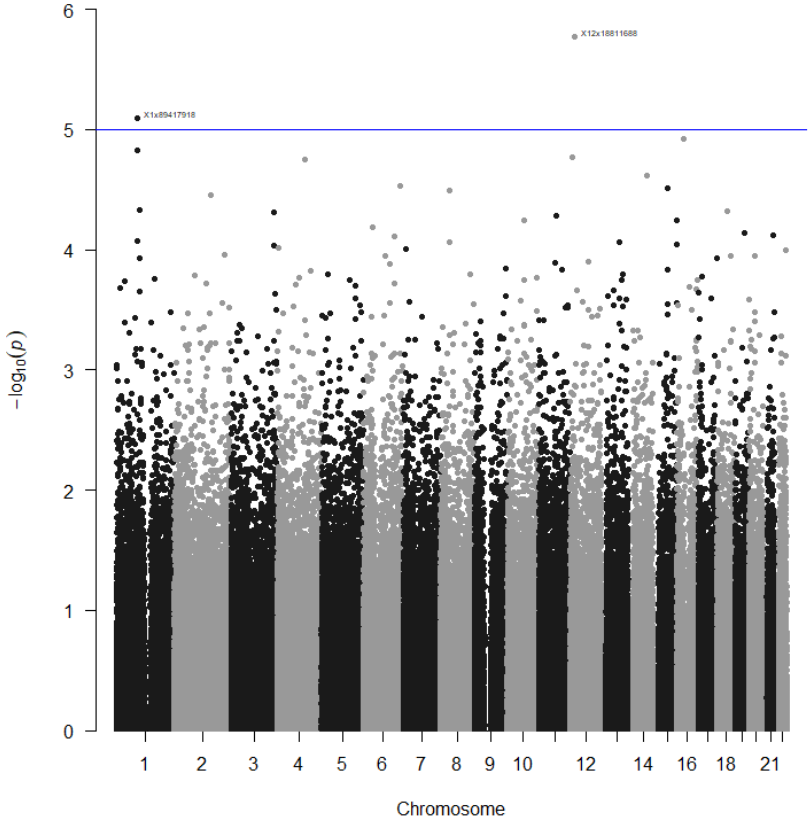

Figure K91: Manhattan plot of SNPs for loops on the right thumb for the codominant model

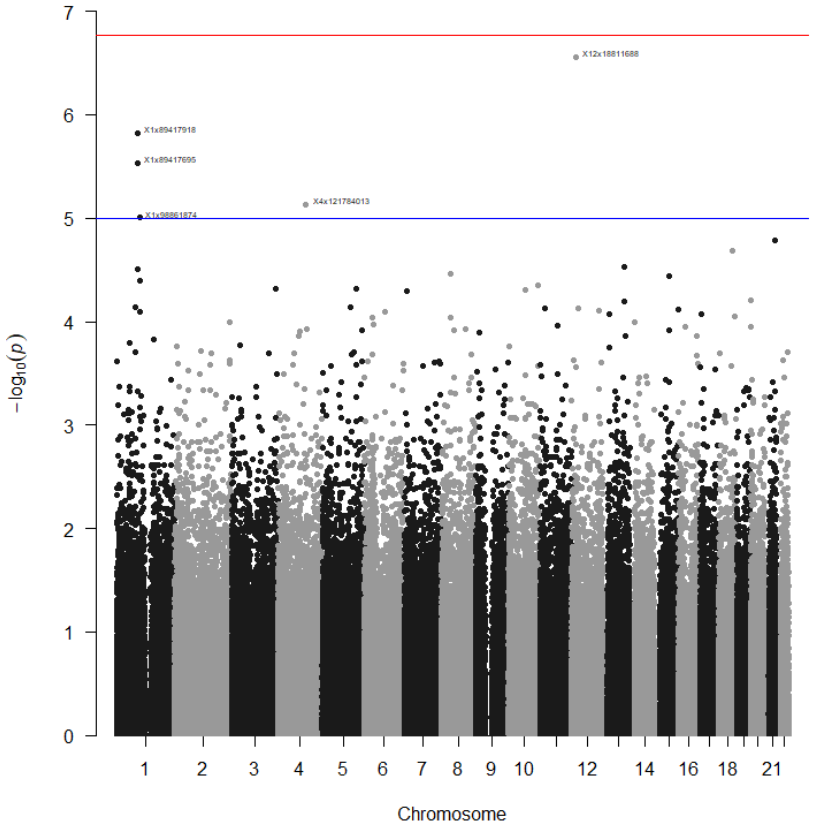

Figure K92: Manhattan plot of SNPs for loops on the right thumb for the dominant model

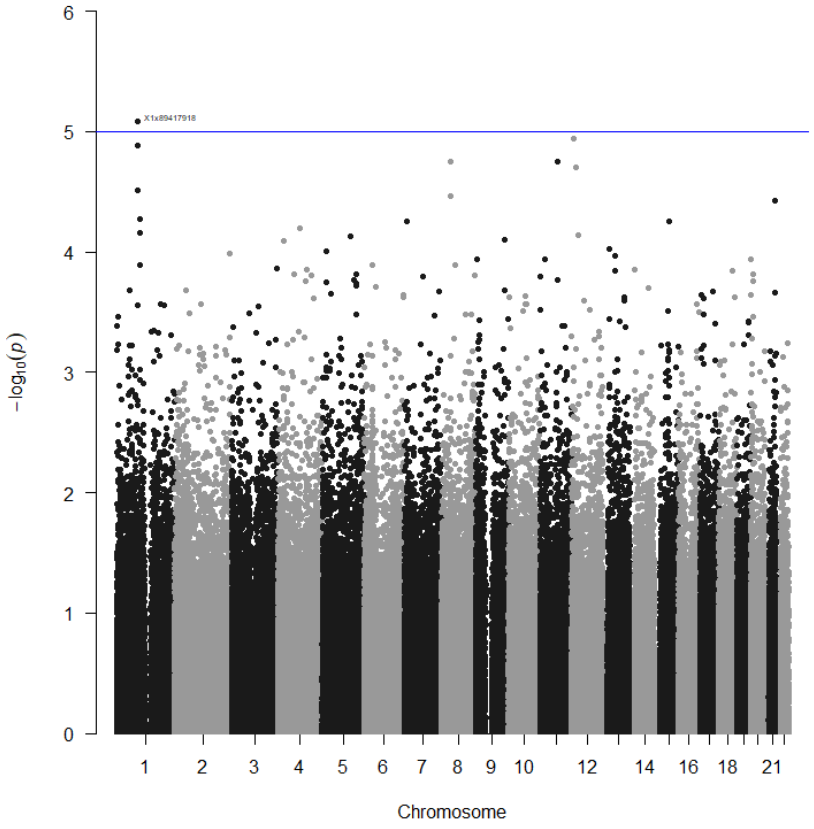

Figure K93: Manhattan plot of SNPs for loops on the right thumb for the log-additive model

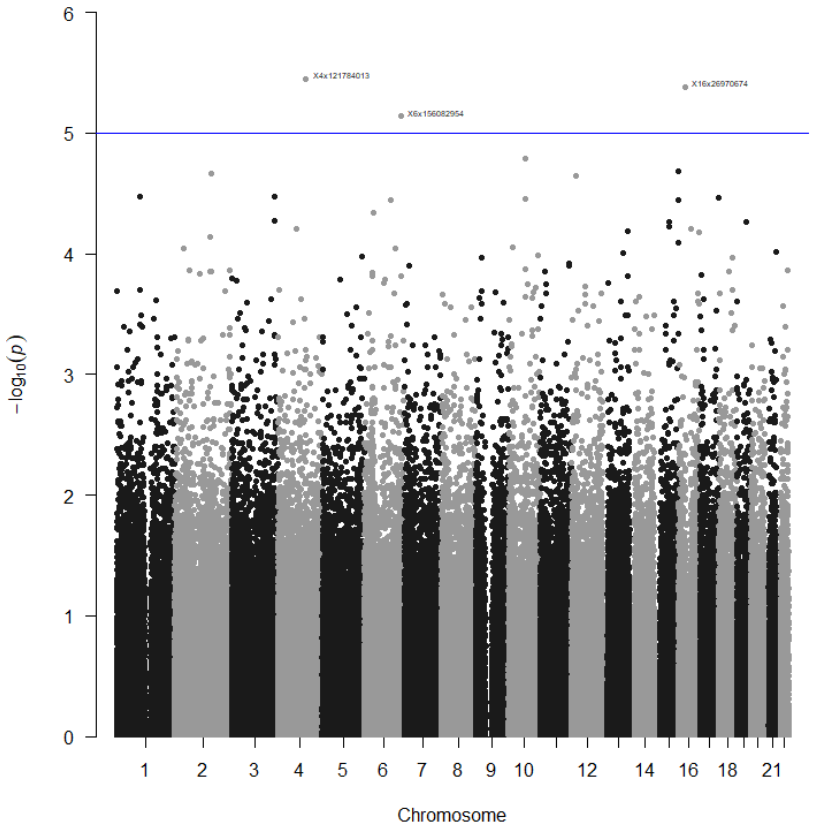

Figure K94: Manhattan plot of SNPs for loops on the right thumb for the overdominant model

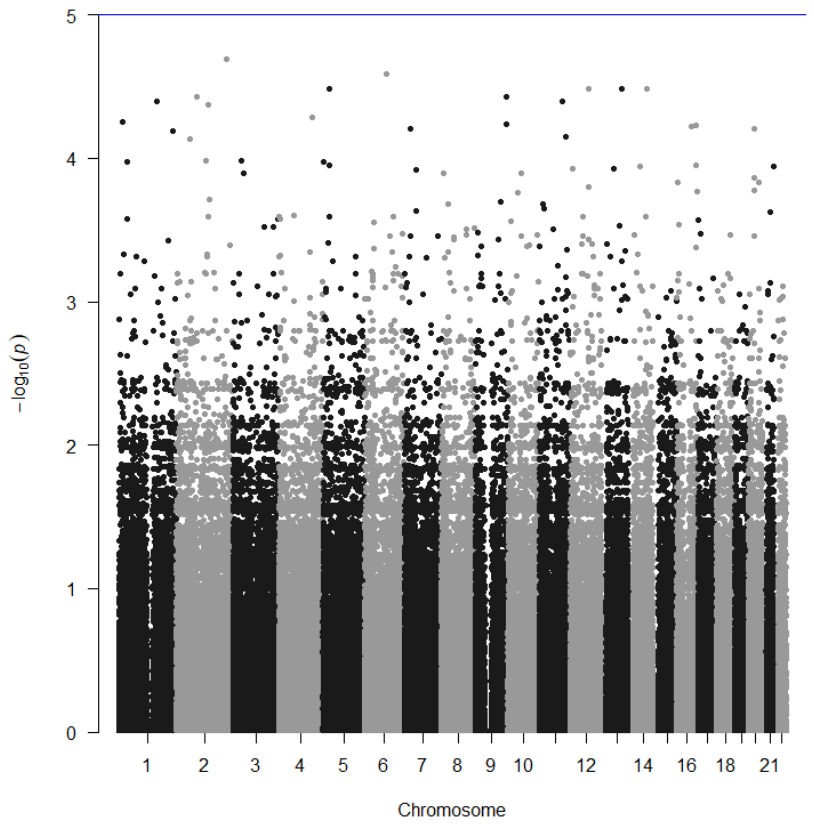

Figure K95: Manhattan plot of SNPs for loops on the right thumb for the recessive model

Whorls on the left little finger

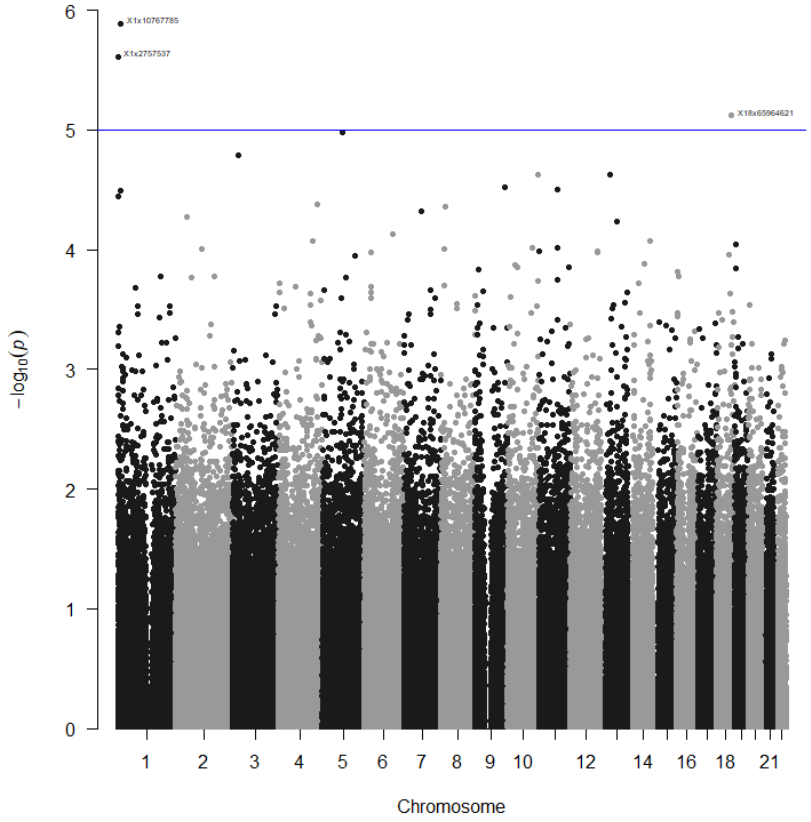

Figure K96: Manhattan plot of SNPs for whorls on the left little finger for the codominant model

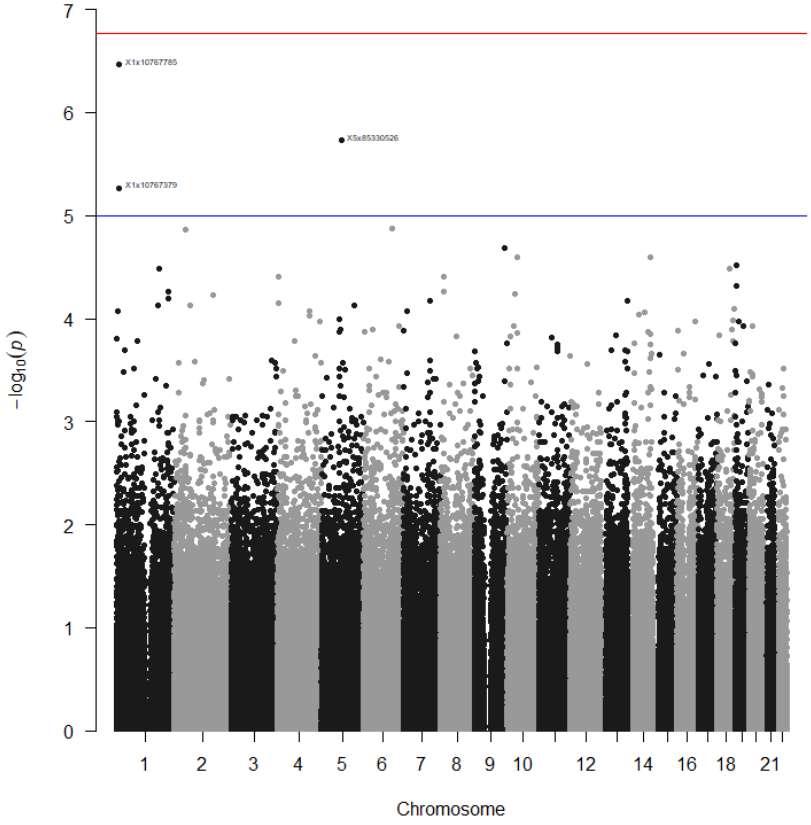

Figure K97: Manhattan plot of SNPs for whorls on the left little finger for the dominant model

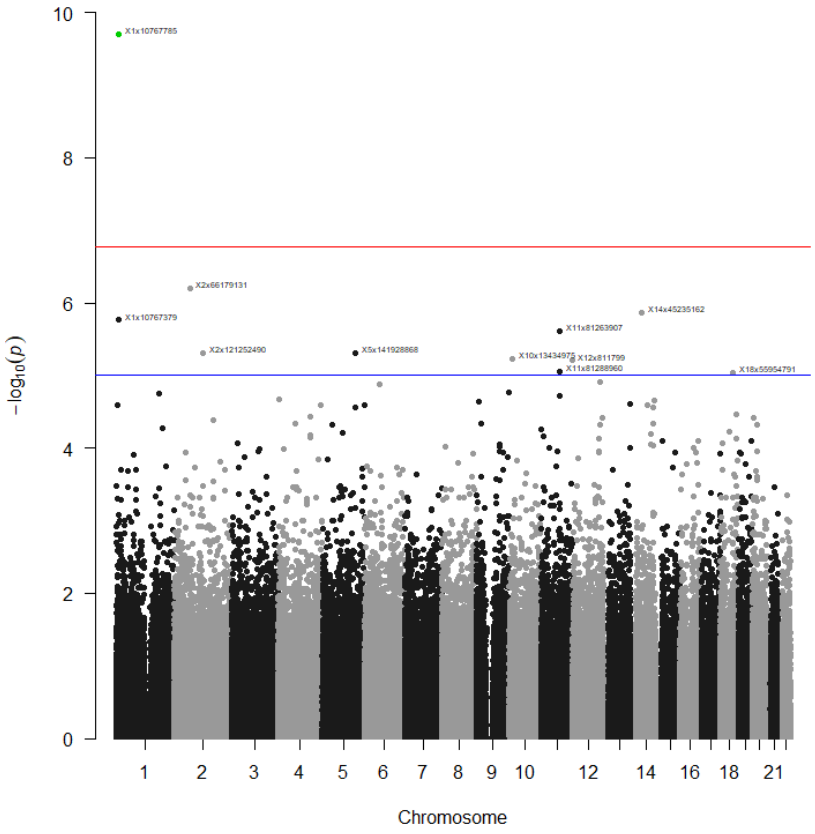

Figure K98: Manhattan plot of SNPs for whorls on the left little finger for the log-additive model

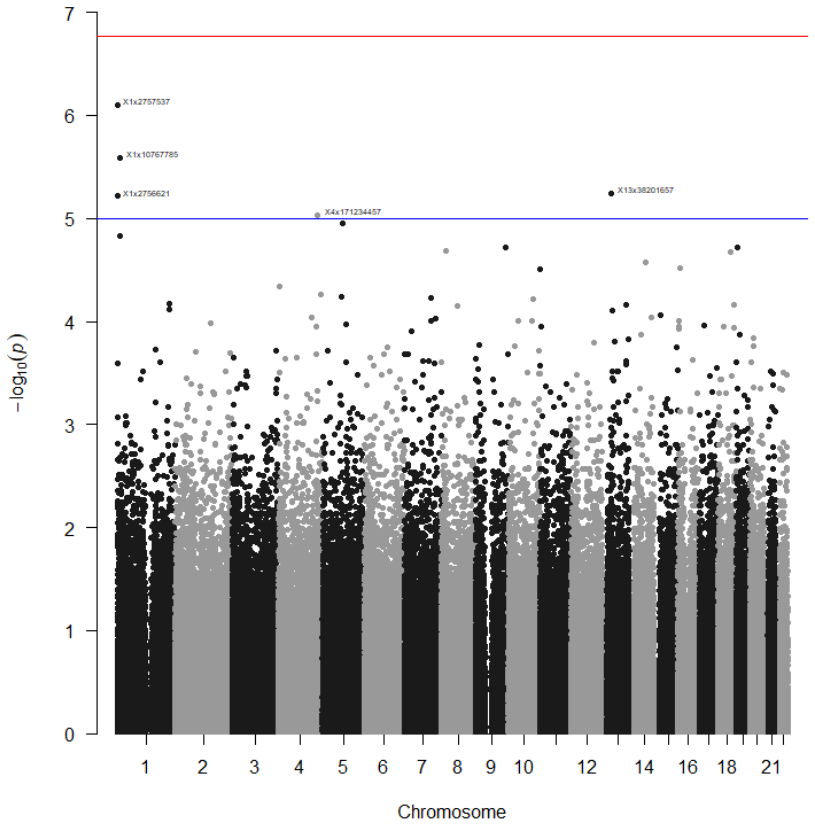

Figure K99: Manhattan plot of SNPs for whorls on the left little finger for the overdominant model

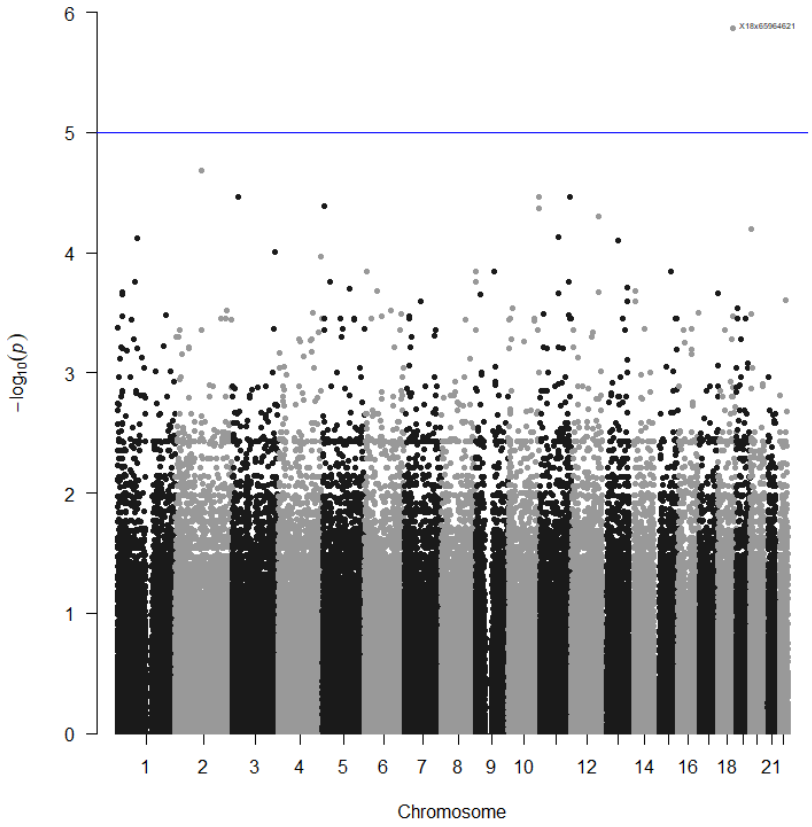

Figure K100: Manhattan plot of SNPs for whorls on the left little finger for the recessive model

Whorls on the right little finger

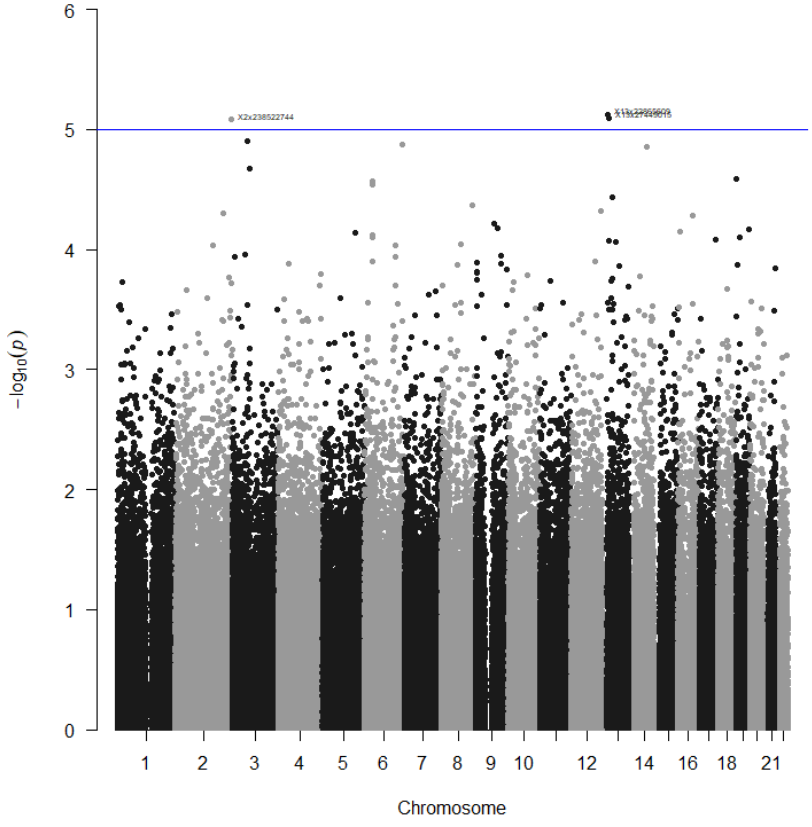

Figure K101: Manhattan plot of SNPs for whorls on the right little finger for the codominant model

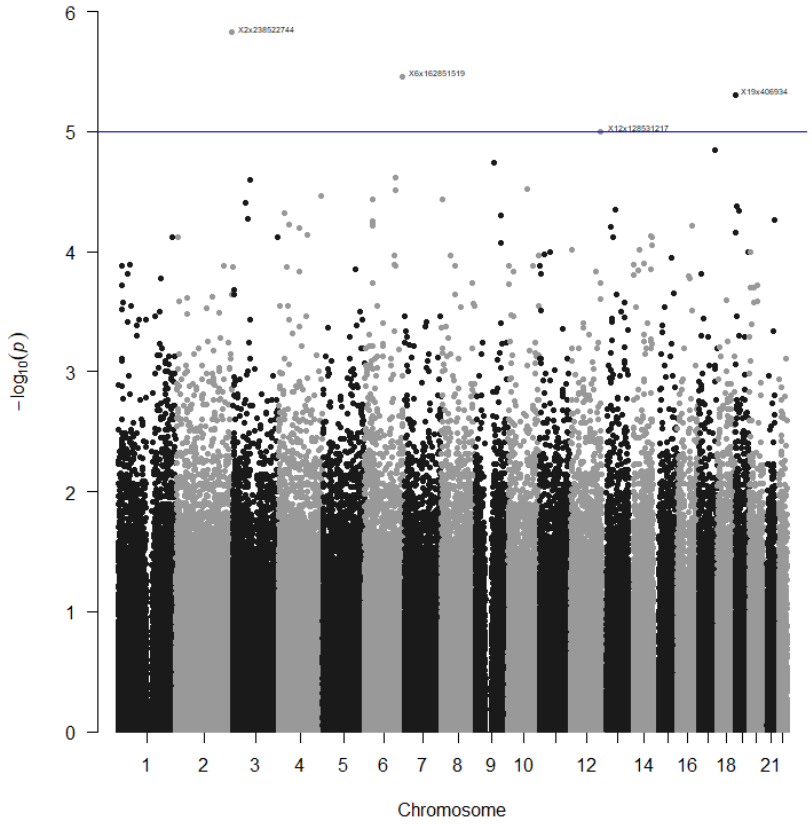

Figure K102: Manhattan plot of SNPs for whorls on the right little finger for the dominant model

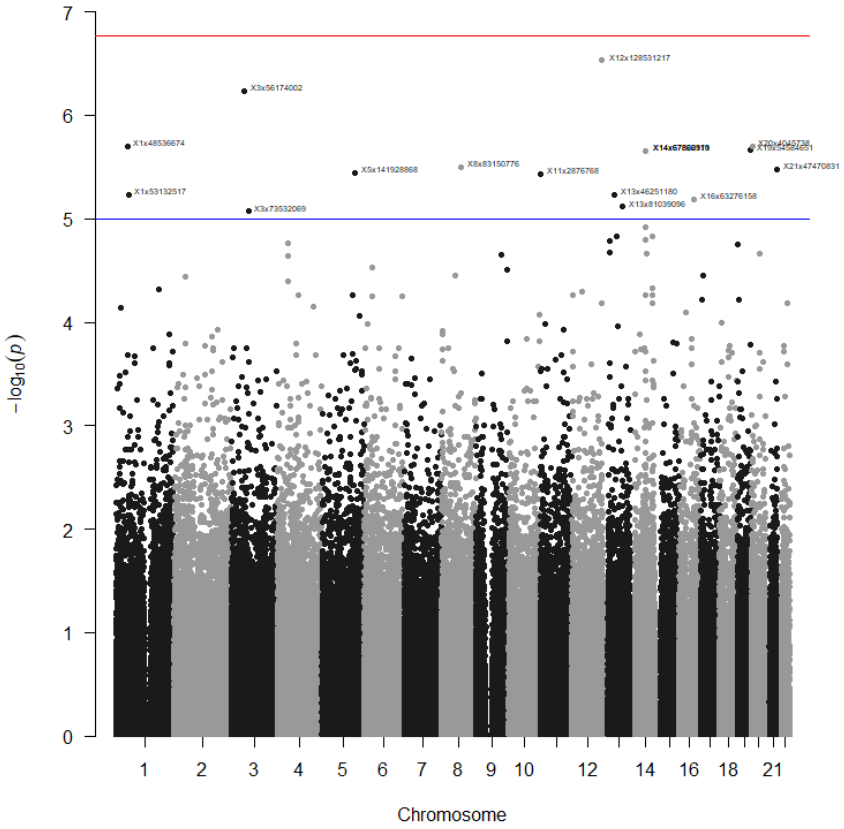

Figure K103: Manhattan plot of SNPs for whorls on the right little finger for the log-additive model

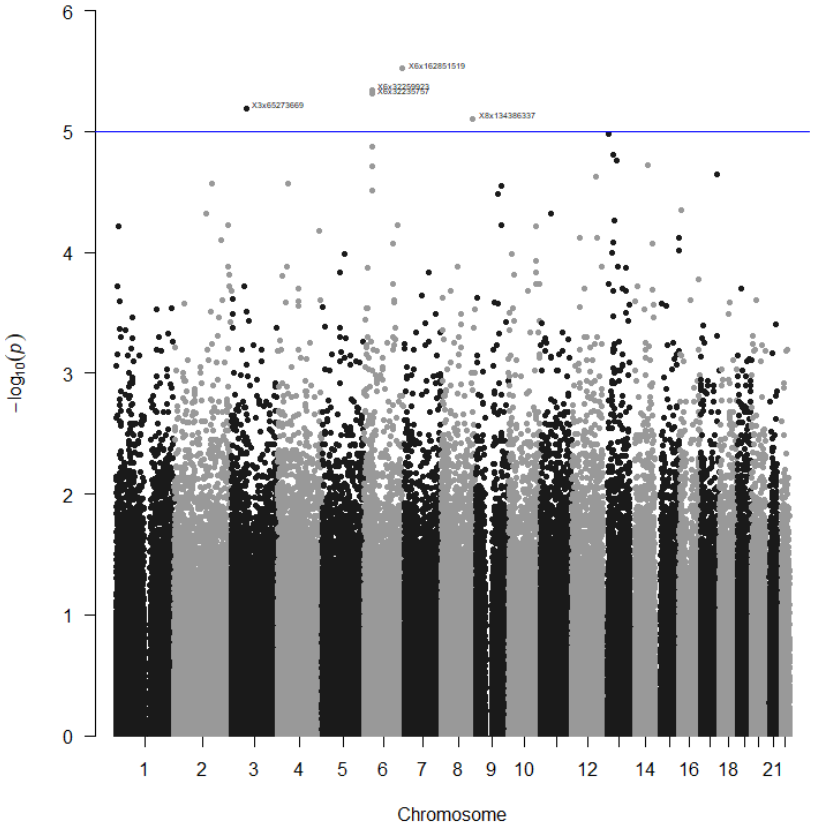

Figure K104: Manhattan plot of SNPs for whorls on the right little finger for the overdominant model

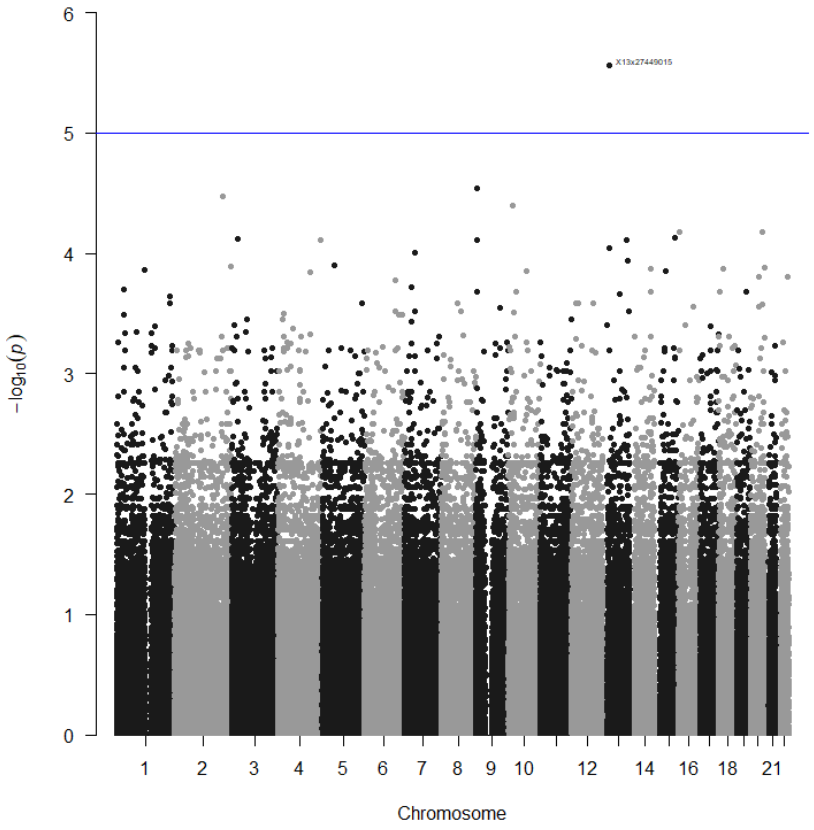

Figure K105: Manhattan plot of SNPs for whorls on the right little finger for the recessive model

Whorls on the left ring finger

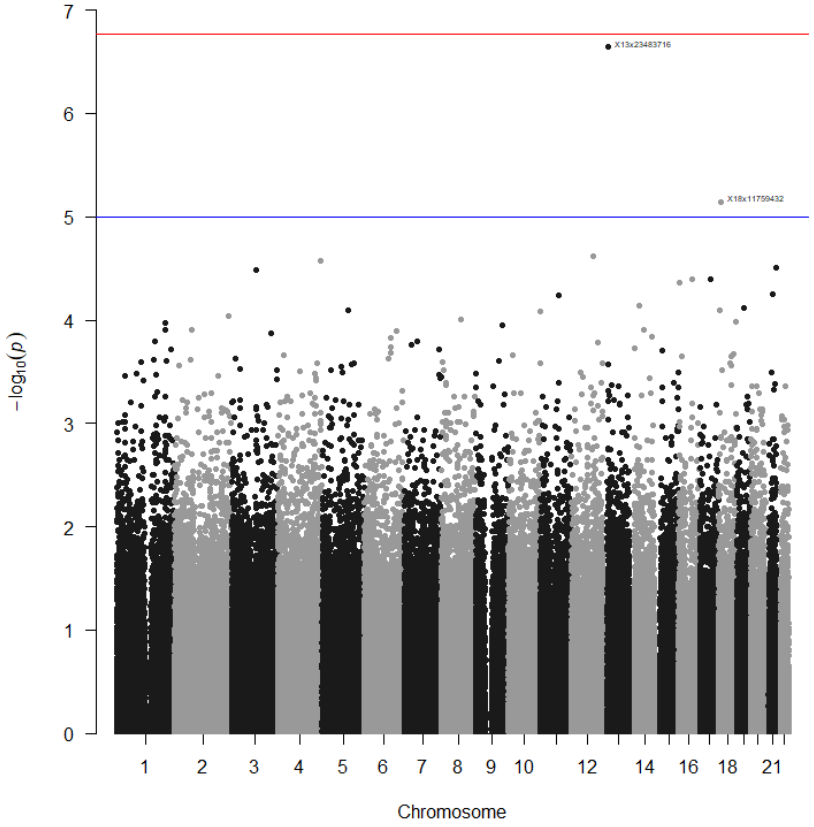

Figure K106: Manhattan plot of SNPs for whorls on the left ring finger for the codominant model

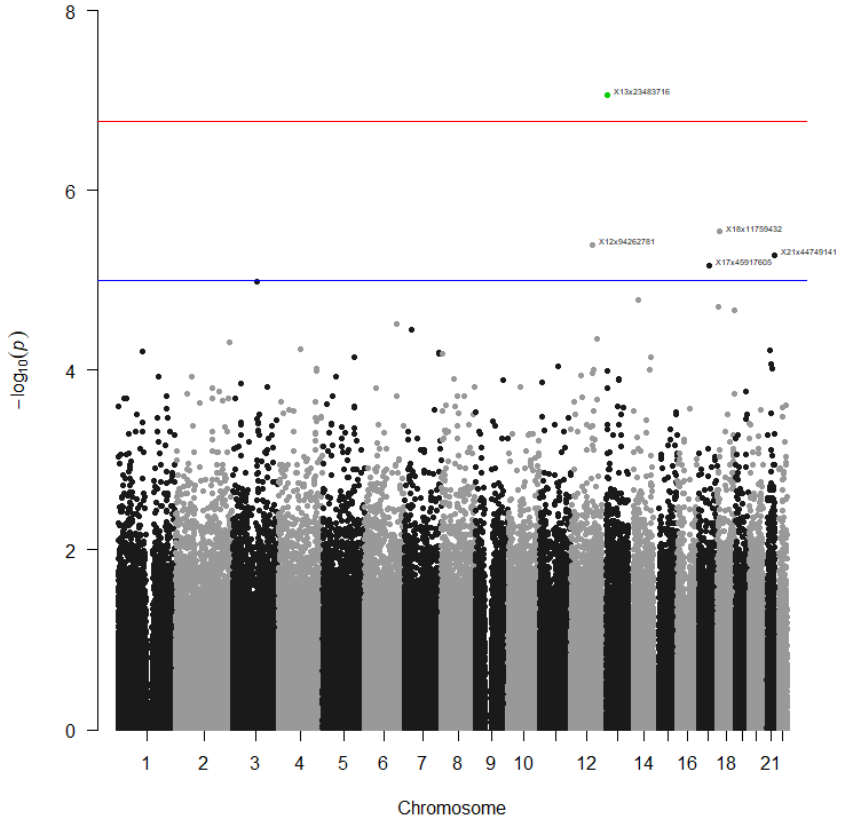

Figure K107: Manhattan plot of SNPs for whorls on the left ring finger for the dominant model

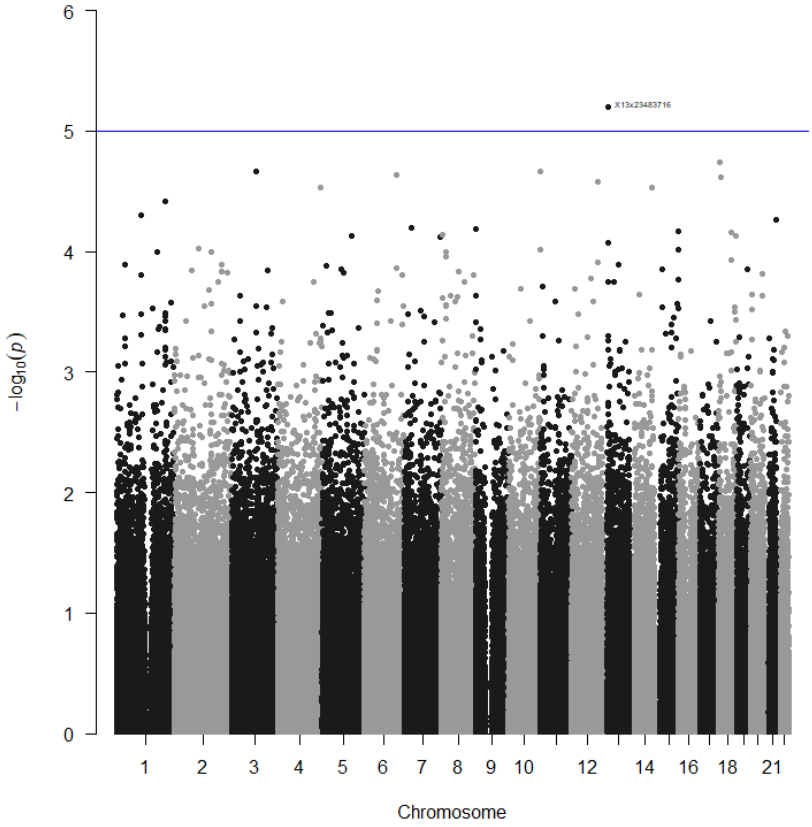

Figure K108: Manhattan plot of SNPs for whorls on the left ring finger for the log-additive model

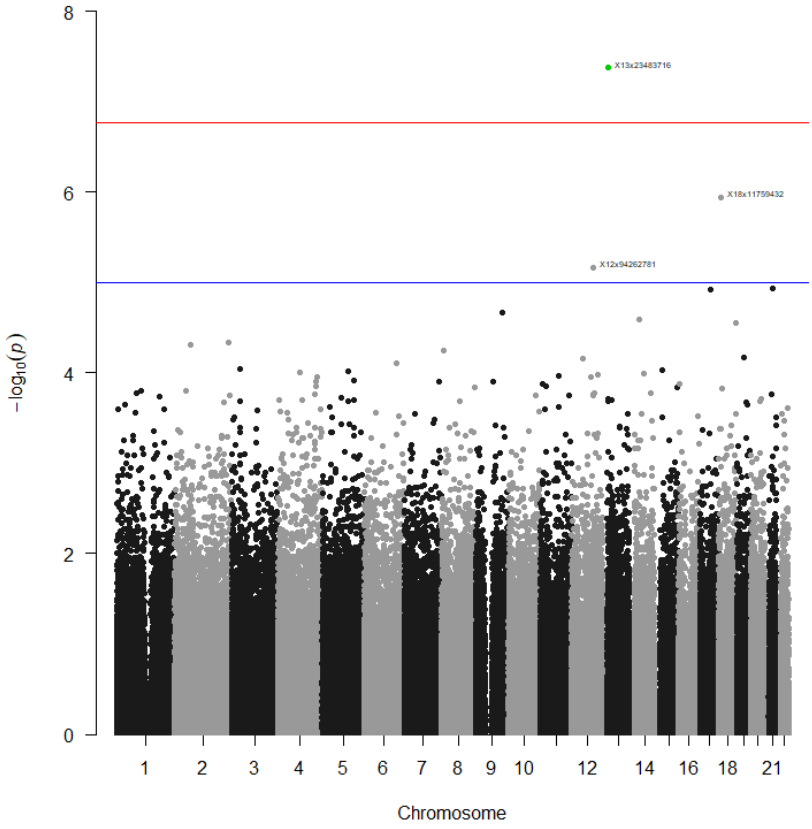

Figure K109: Manhattan plot of SNPs for whorls on the left ring finger for the overdominant model

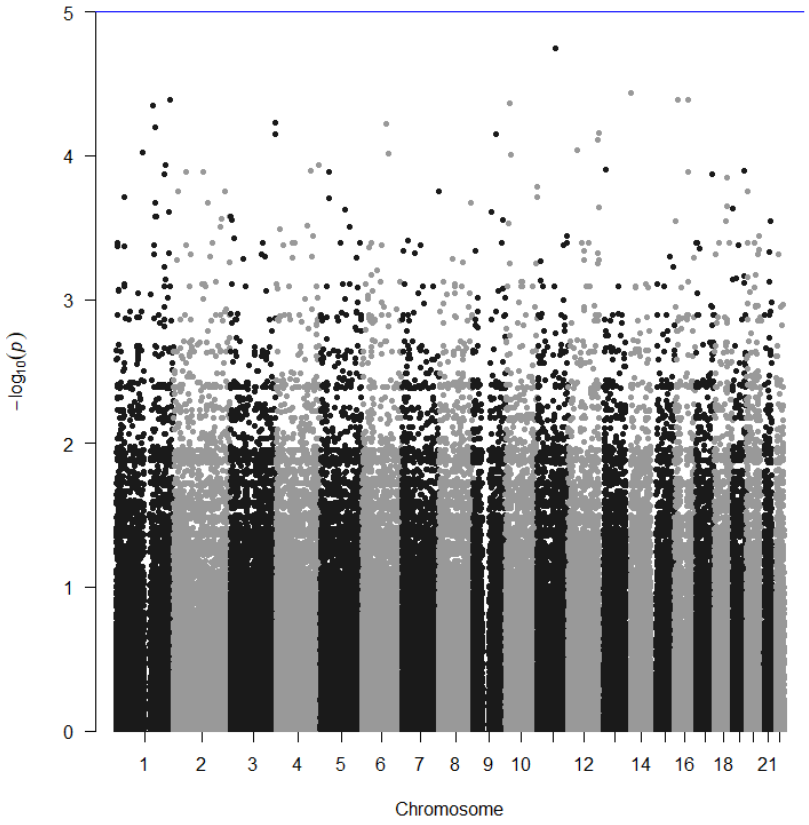

Figure K110: Manhattan plot of SNPs for whorls on the left ring finger for the recessive model

Whorls on the right ring finger

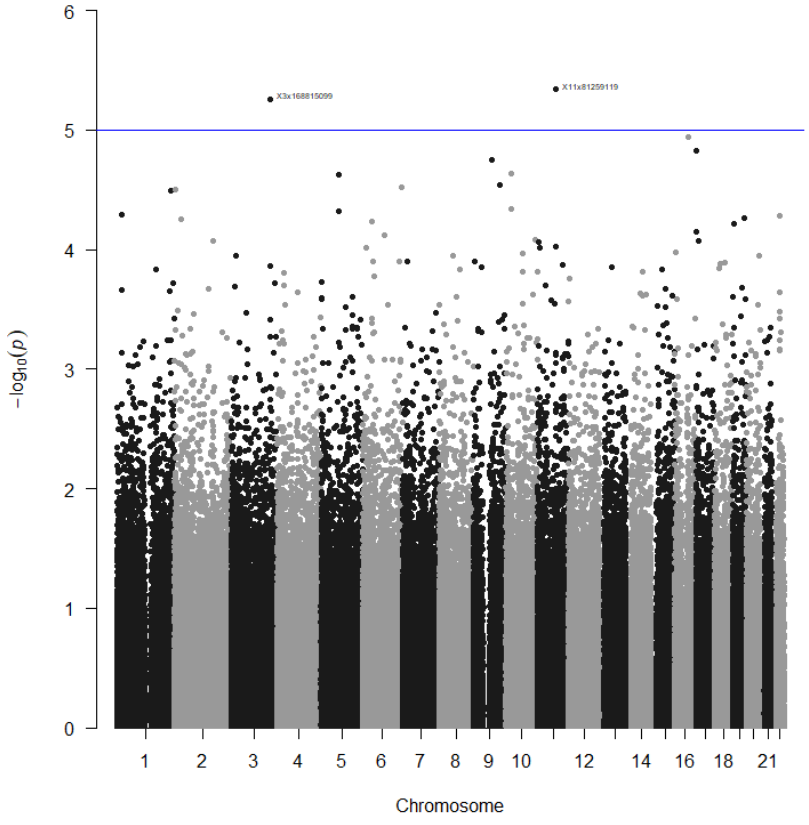

Figure K111: Manhattan plot of SNPs for whorls on the right ring finger for the codominant model

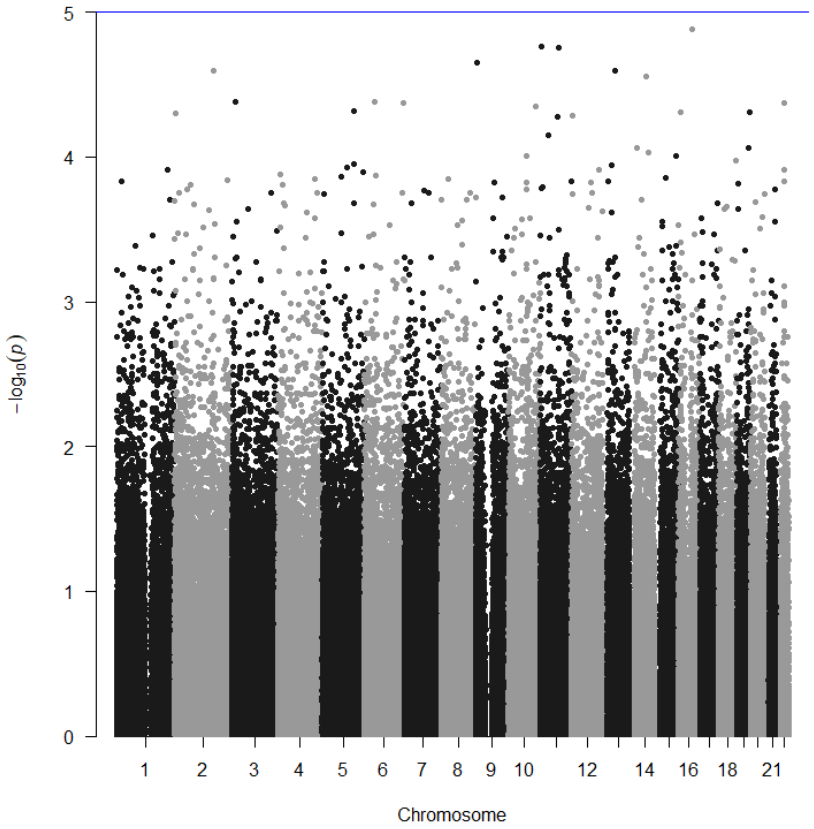

Figure K112: Manhattan plot of SNPs for whorls on the right ring finger for the dominant model

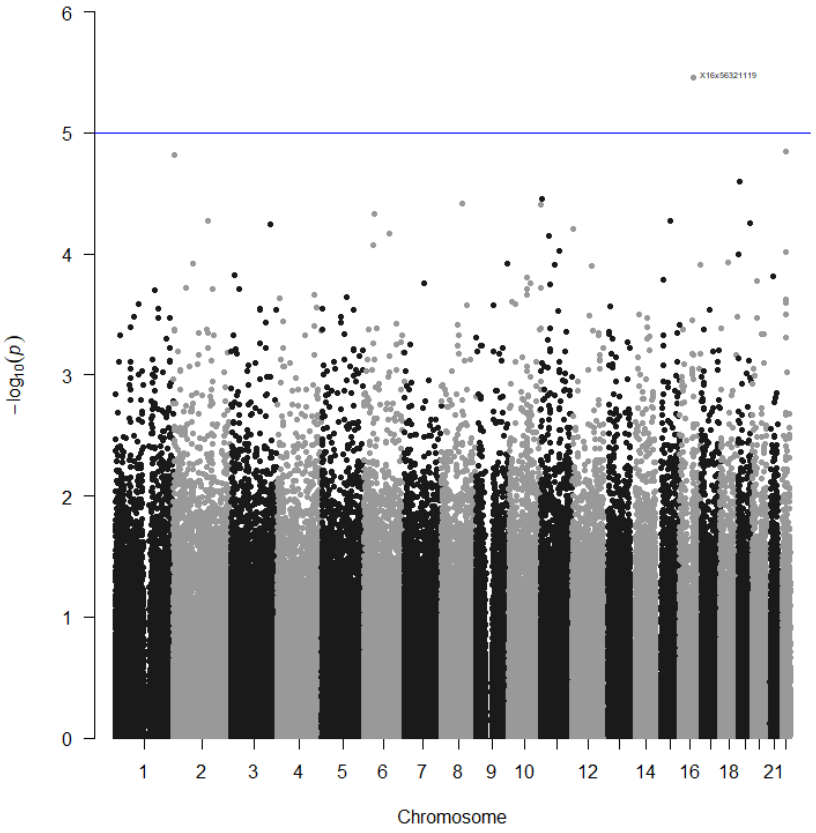

Figure K113: Manhattan plot of SNPs for whorls on the right ring finger for the log-additive model

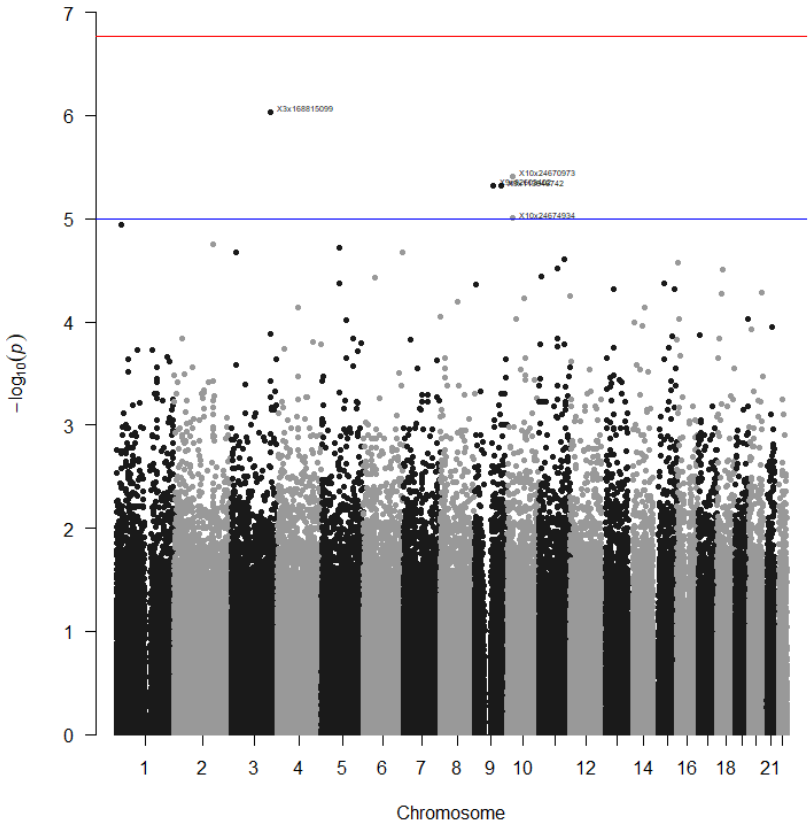

Figure K114: Manhattan plot of SNPs for whorls on the right ring finger for the overdominant model

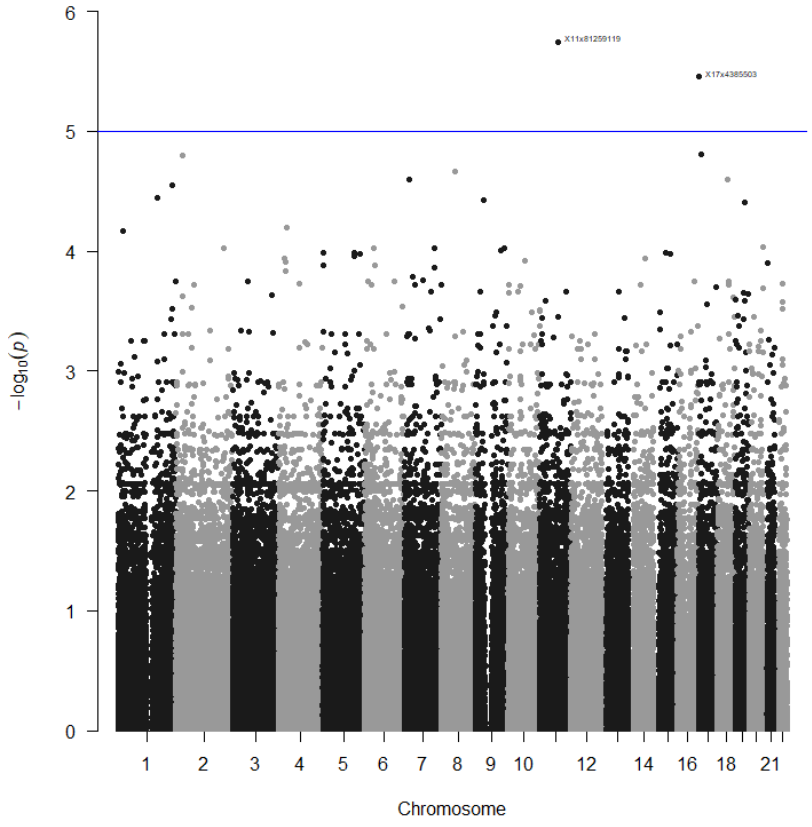

Figure K115: Manhattan plot of SNPs for whorls on the right ring finger for the recessive model

Whorls on the left middle finger

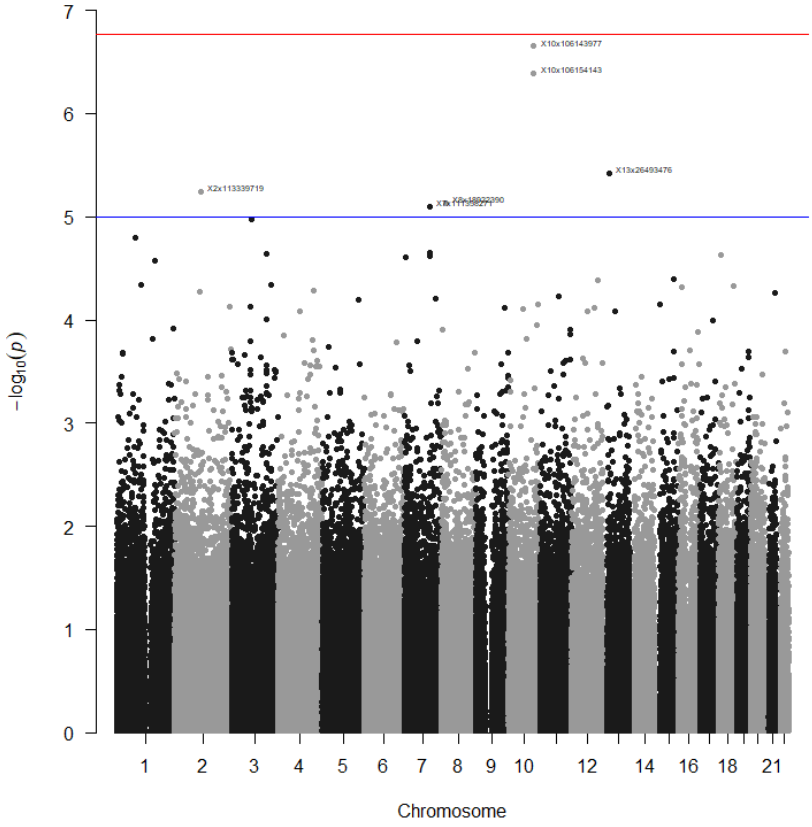

Figure K116: Manhattan plot of SNPs for whorls on the left middle finger for the codominant model

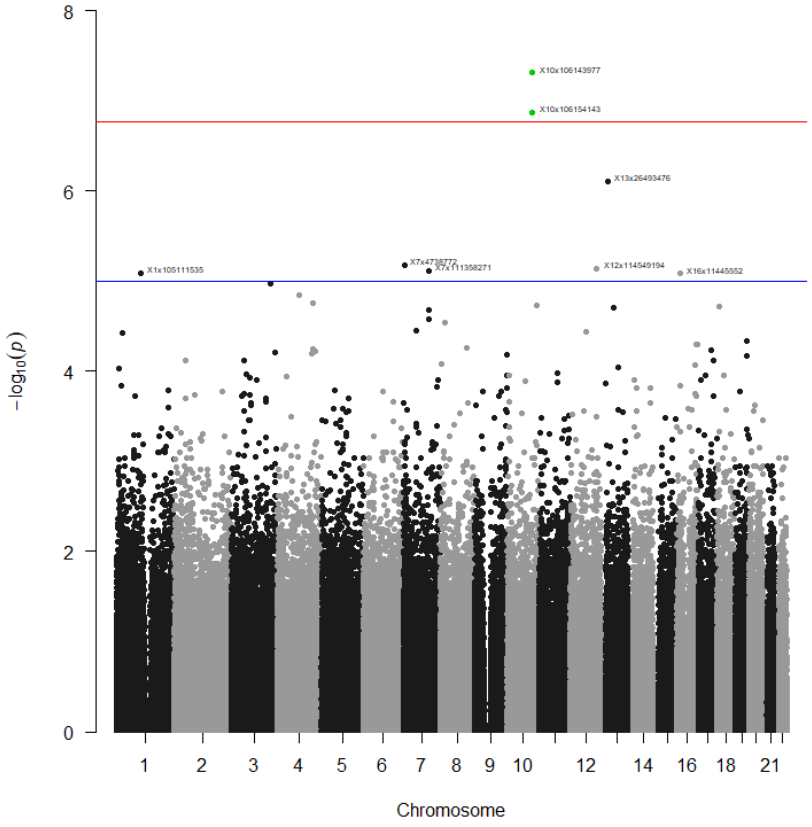

Figure K117: Manhattan plot of SNPs for whorls on the left middle finger for the dominant model

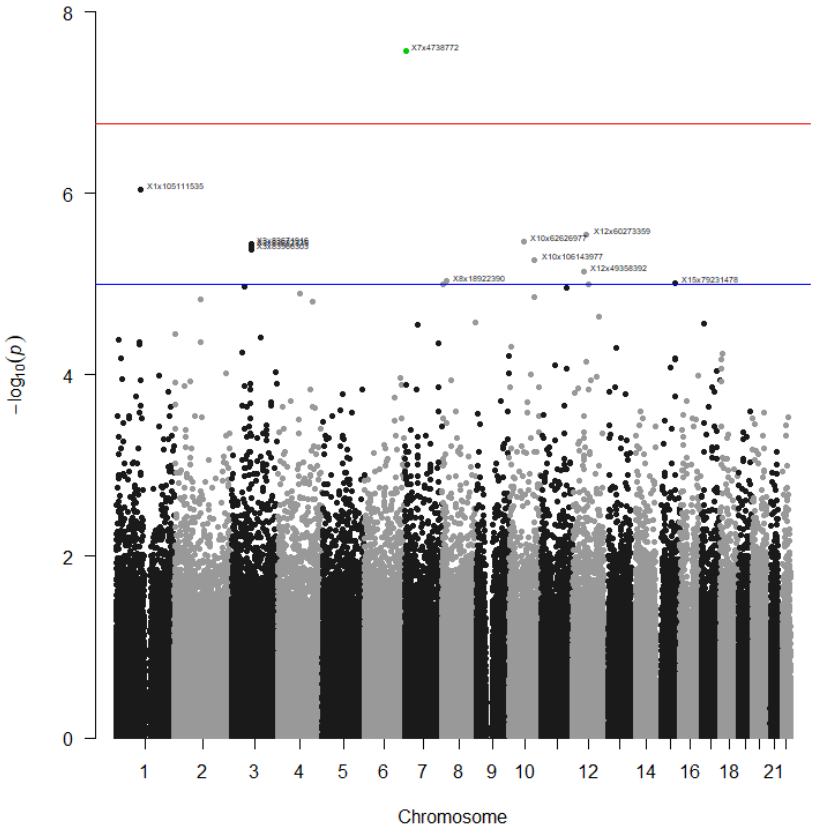

Figure K118: Manhattan plot of SNPs for whorls on the left middle finger for the log-additive model

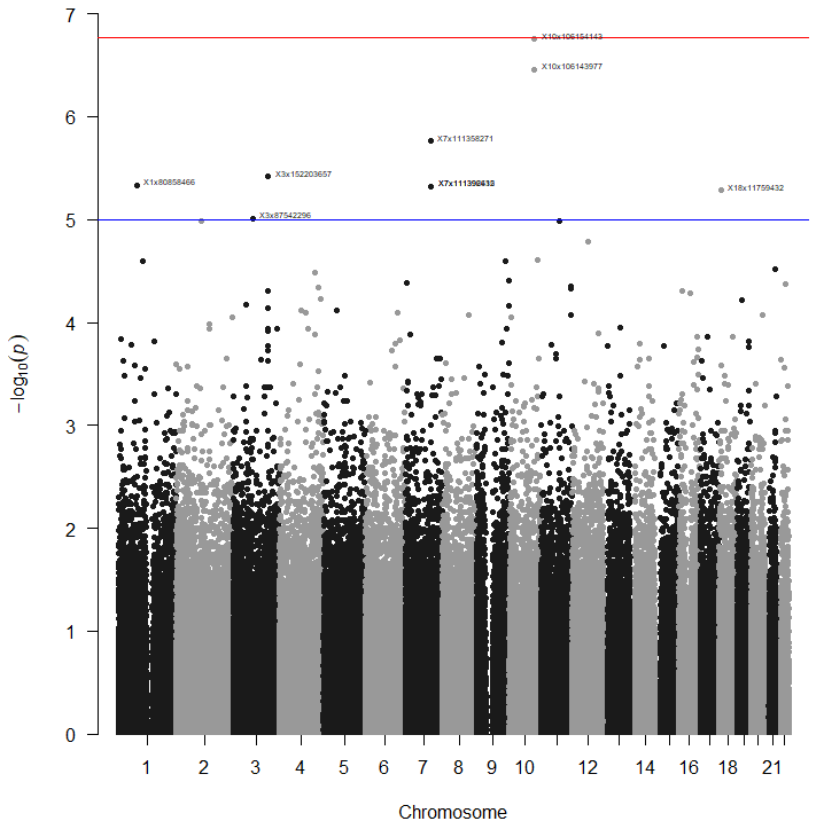

Figure K119: Manhattan plot of SNPs for whorls on the left middle finger for the overdominant model

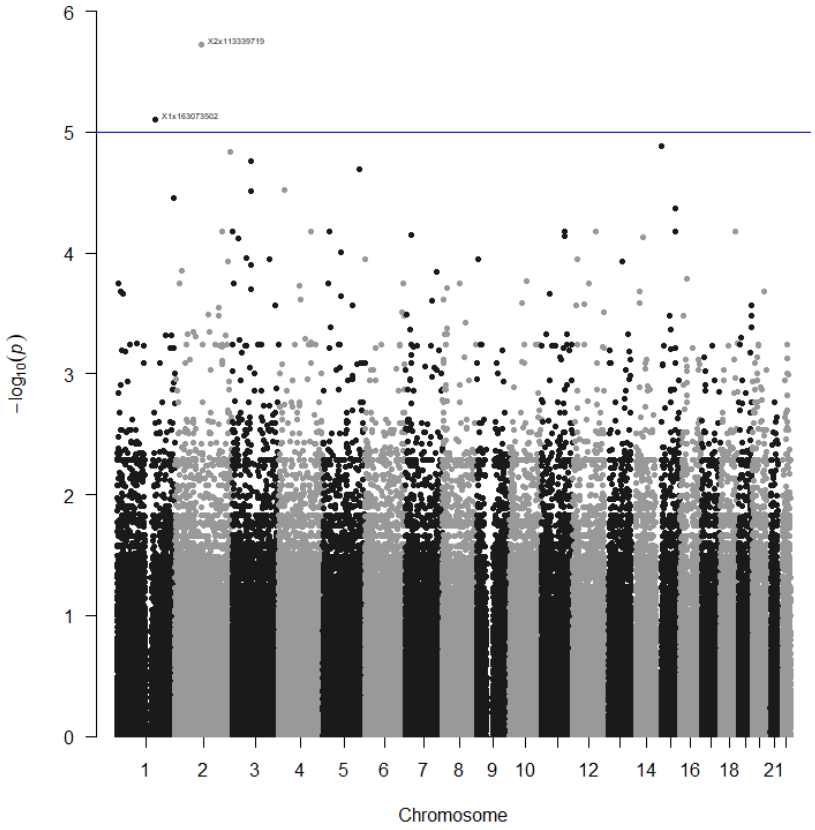

Figure K120: Manhattan plot of SNPs for whorls on the left middle finger for the recessive model

Whorls on the right middle finger

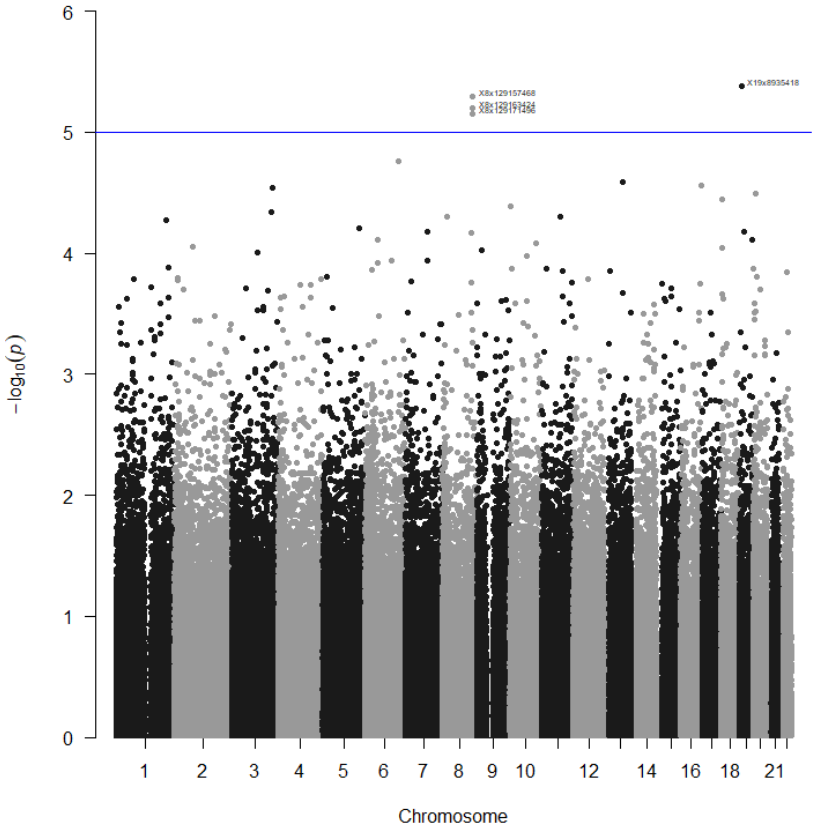

Figure K121: Manhattan plot of SNPs for whorls on the right middle finger for the codominant model

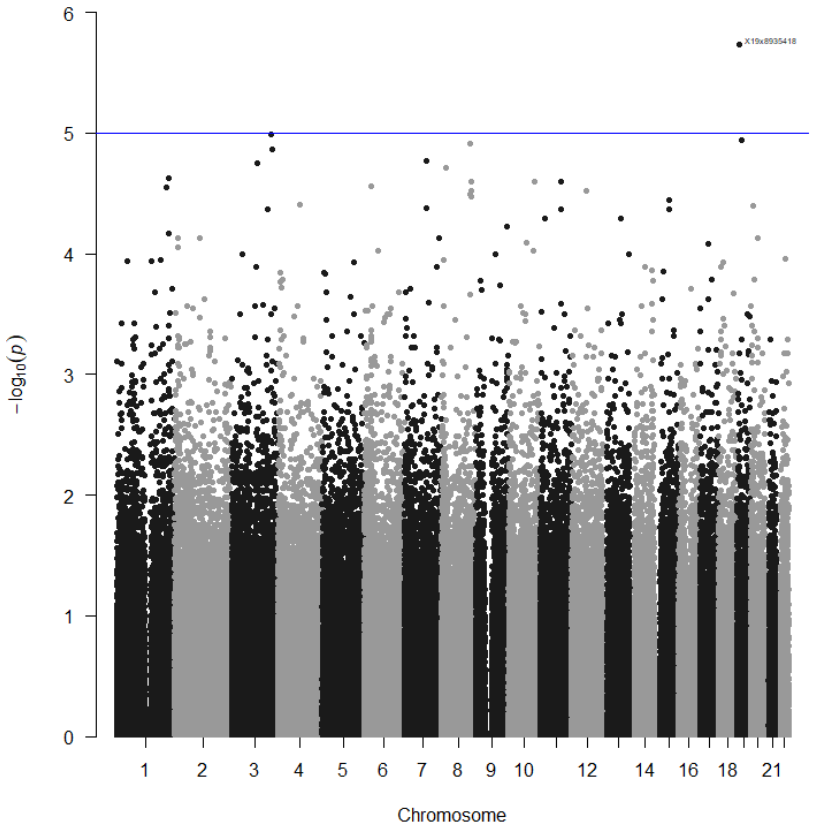

Figure K122: Manhattan plot of SNPs for whorls on the right middle finger for the dominant model

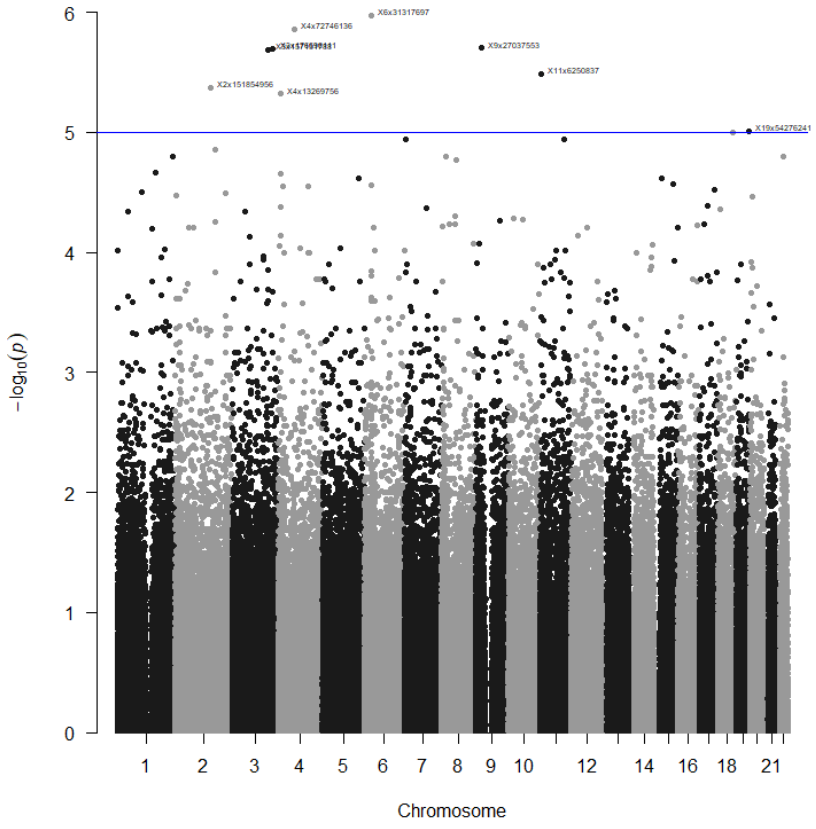

Figure K123: Manhattan plot of SNPs for whorls on the right middle finger for the log-additive model

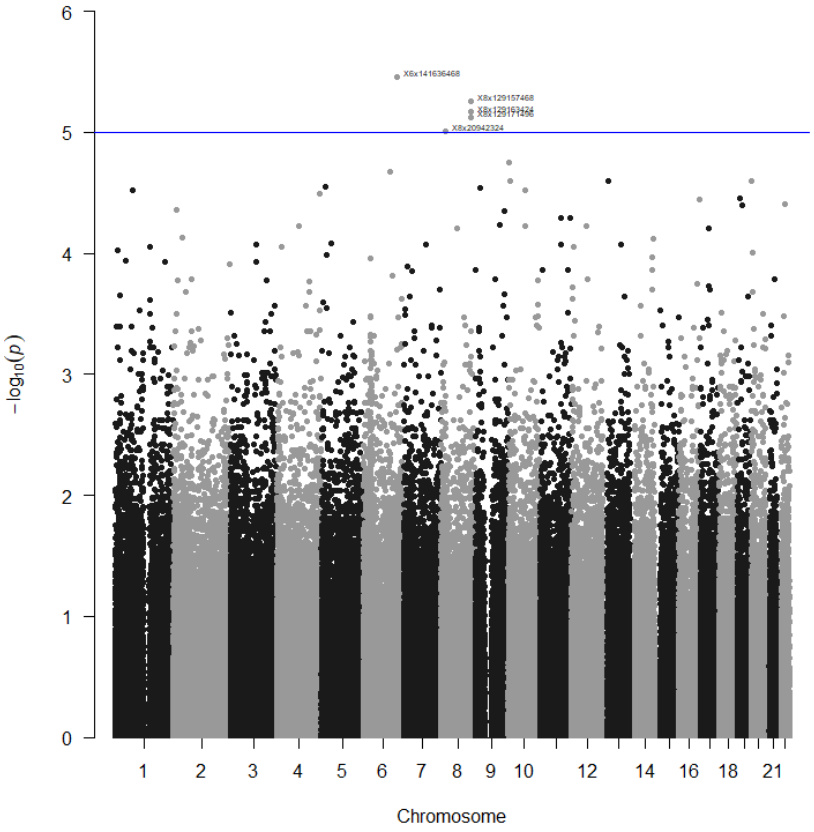

Figure K124: Manhattan plot of SNPs for whorls on the right middle finger for the overdominant model

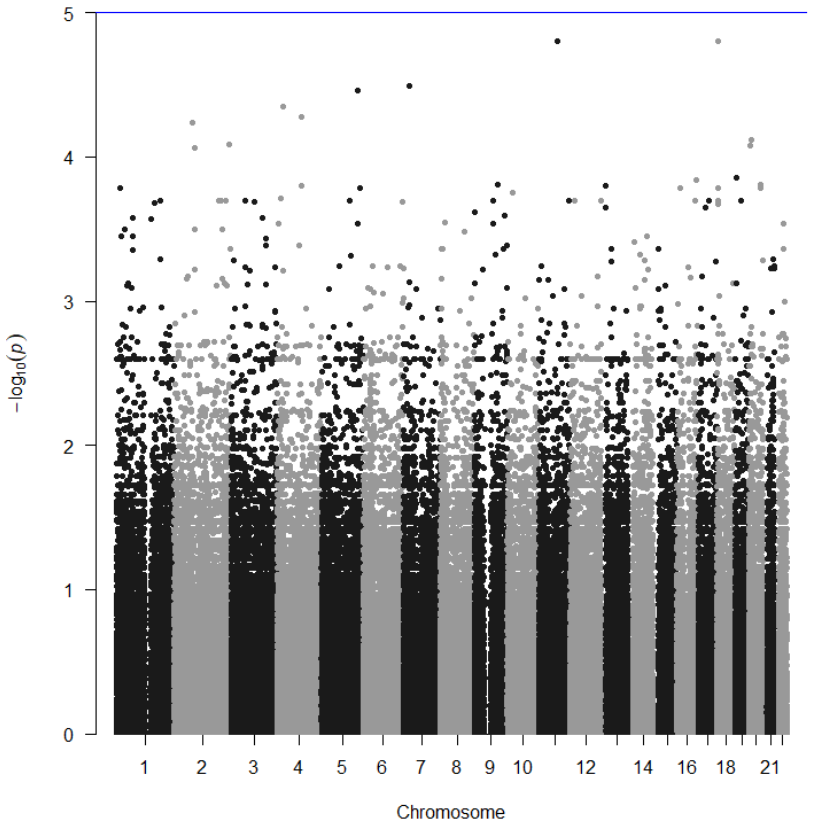

Figure K125: Manhattan plot of SNPs for whorls on the right middle finger for the recessive model

Whorls on the left index finger

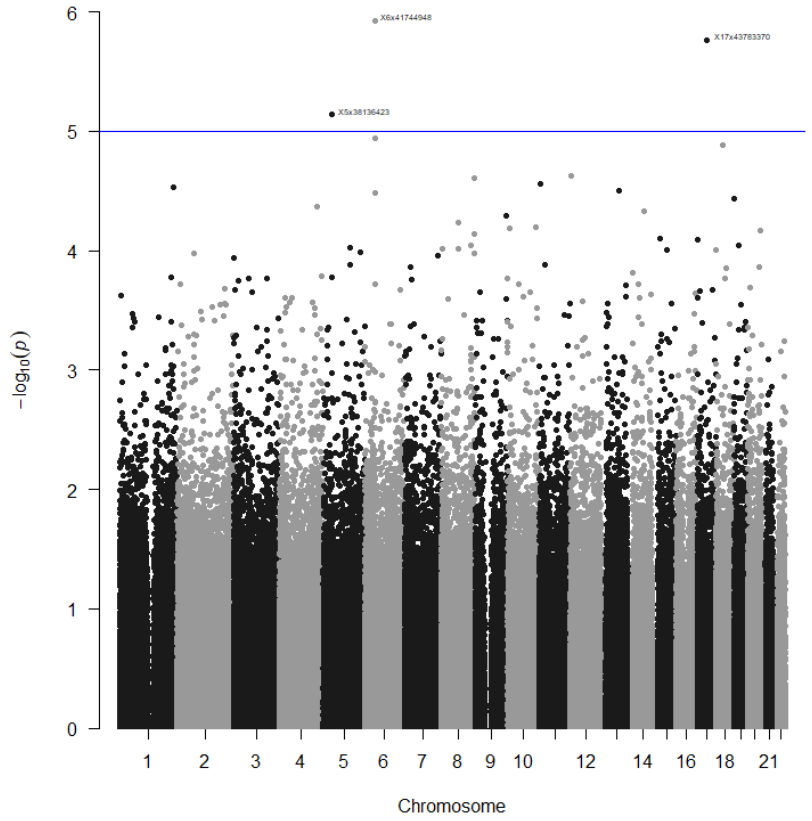

Figure K126: Manhattan plot of SNPs for whorls on the left index finger for the codominant model

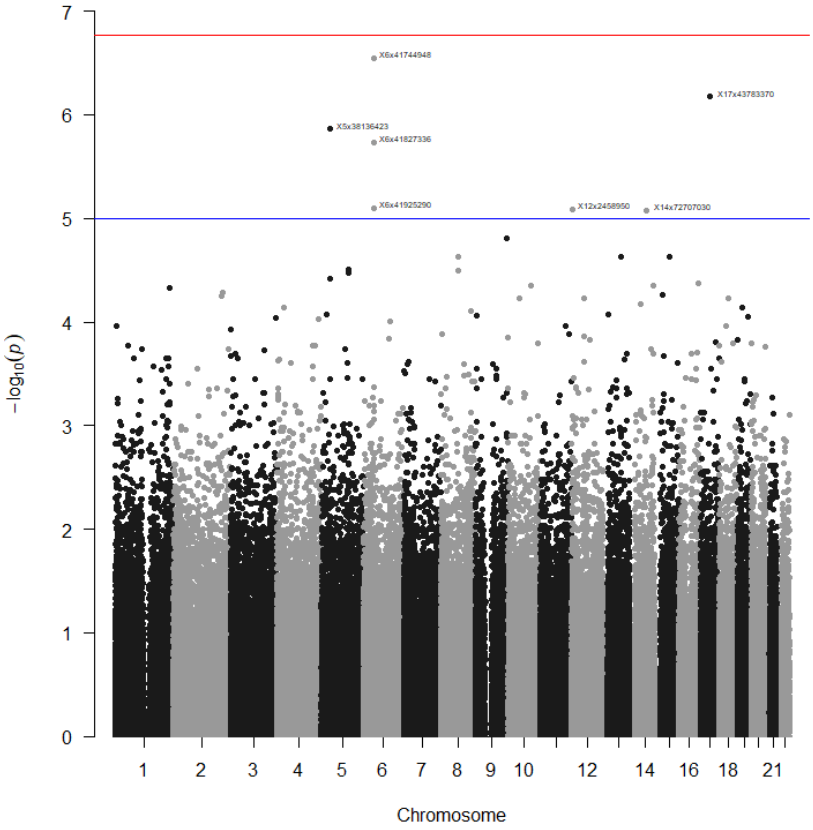

Figure K127: Manhattan plot of SNPs for whorls on the left index finger for the dominant model

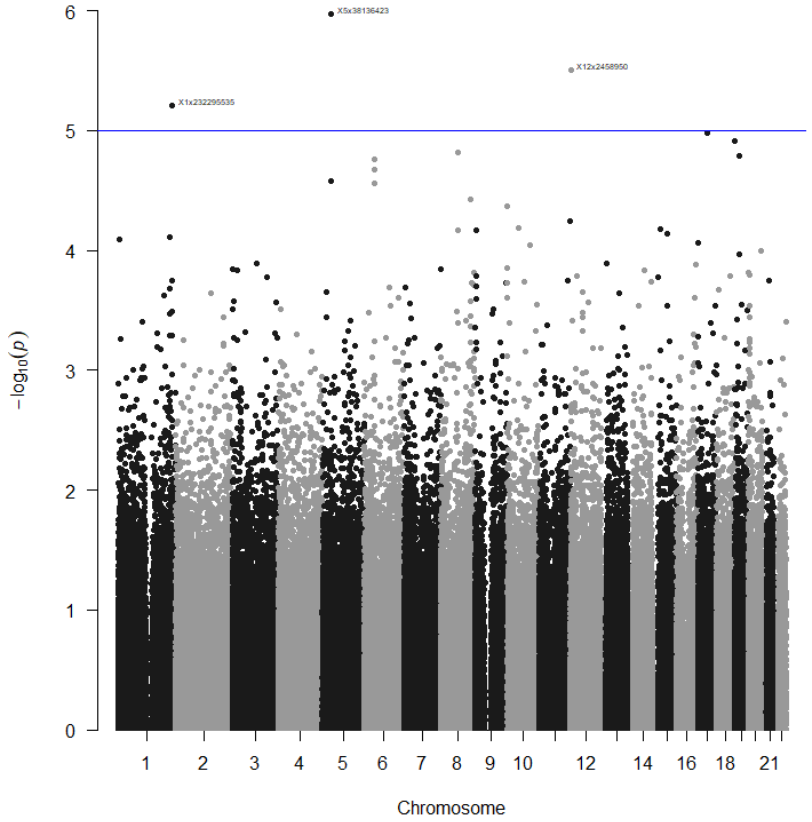

Figure K128: Manhattan plot of SNPs for whorls on the left index finger for the log-additive model

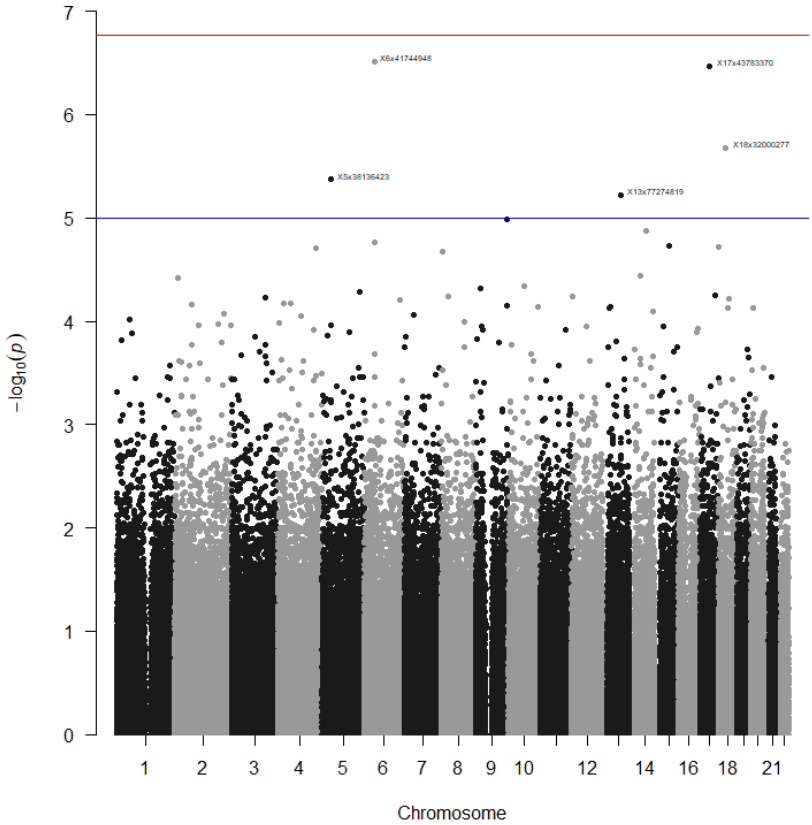

Figure K129: Manhattan plot of SNPs for whorls on the left index finger for the overdominant model

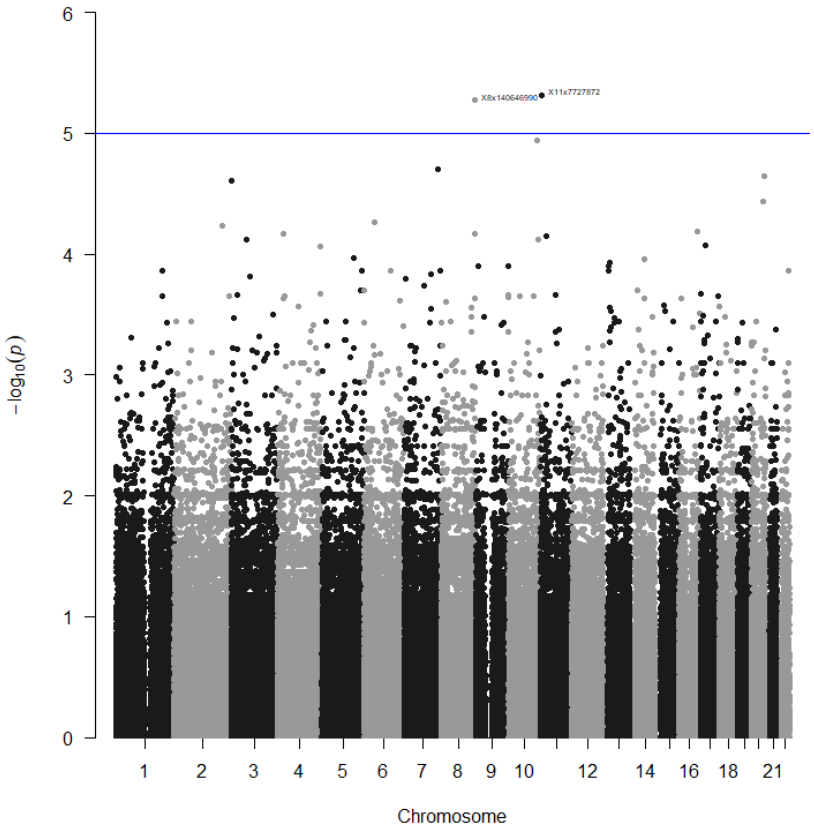

Figure K130: Manhattan plot of SNPs for whorls on the left index finger for the recessive model

Whorls on the right index finger

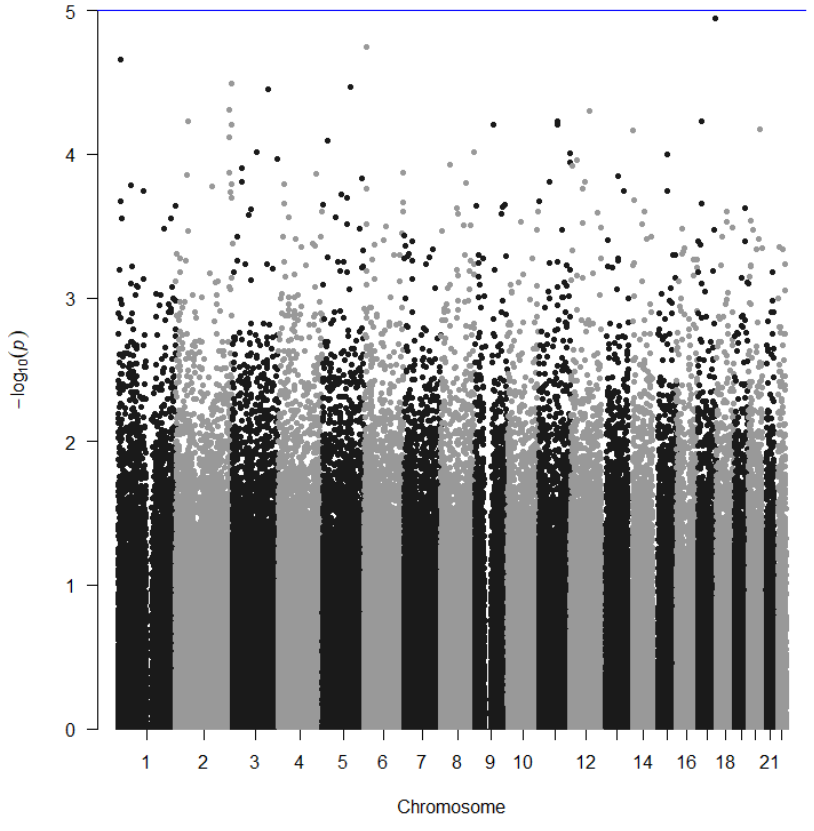

Figure K131: Manhattan plot of SNPs for whorls on the right index finger for the codominant model

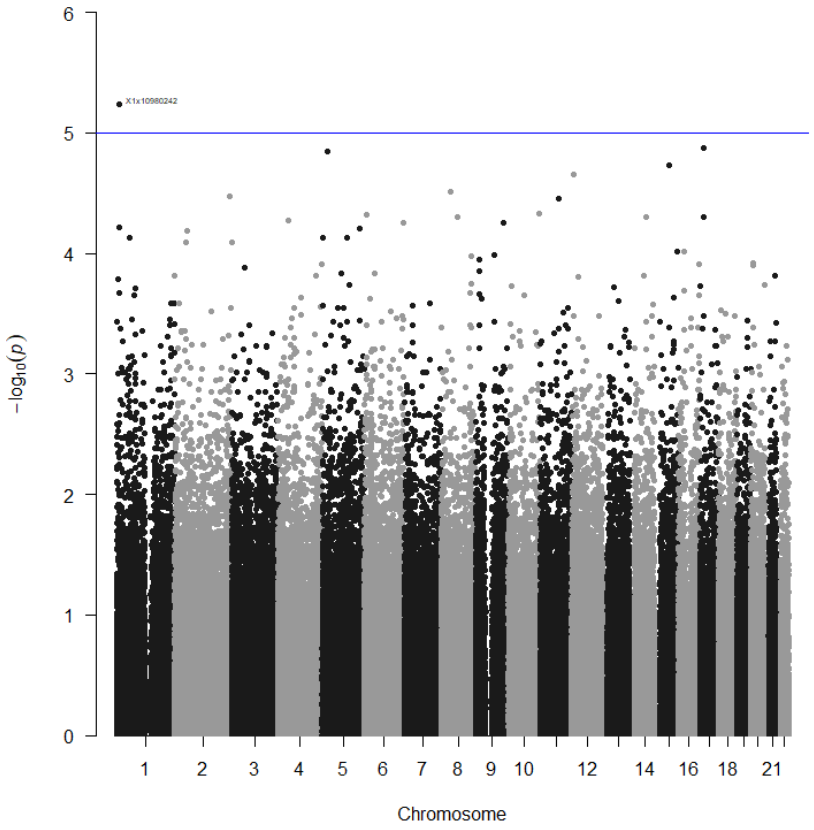

Figure K132: Manhattan plot of SNPs for whorls on the right index finger for the dominant model

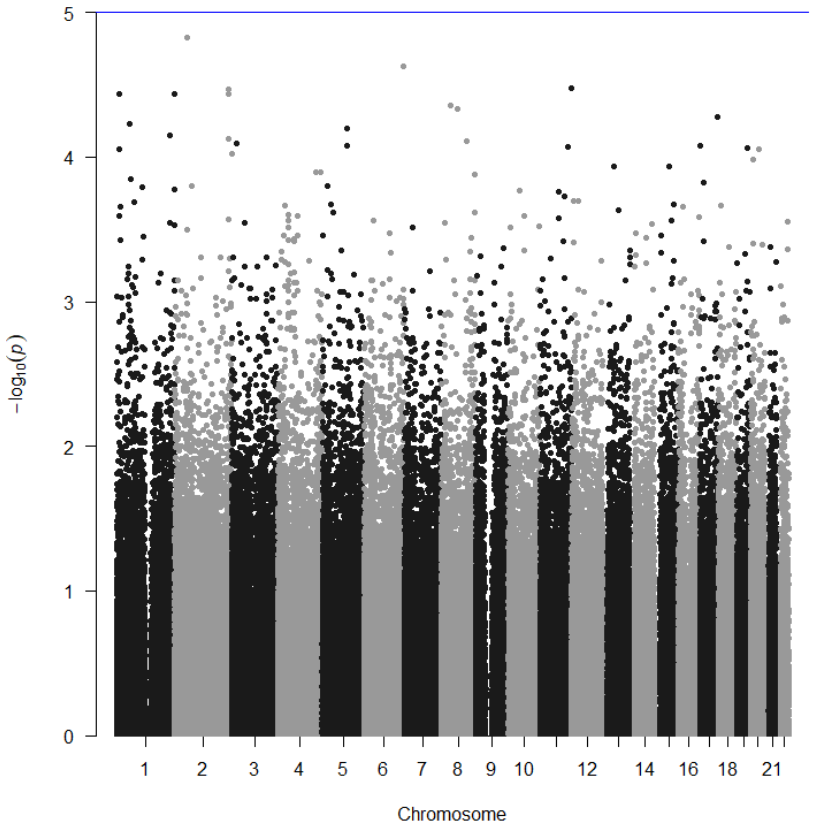

Figure K133: Manhattan plot of SNPs for whorls on the right index finger for the log-additive model

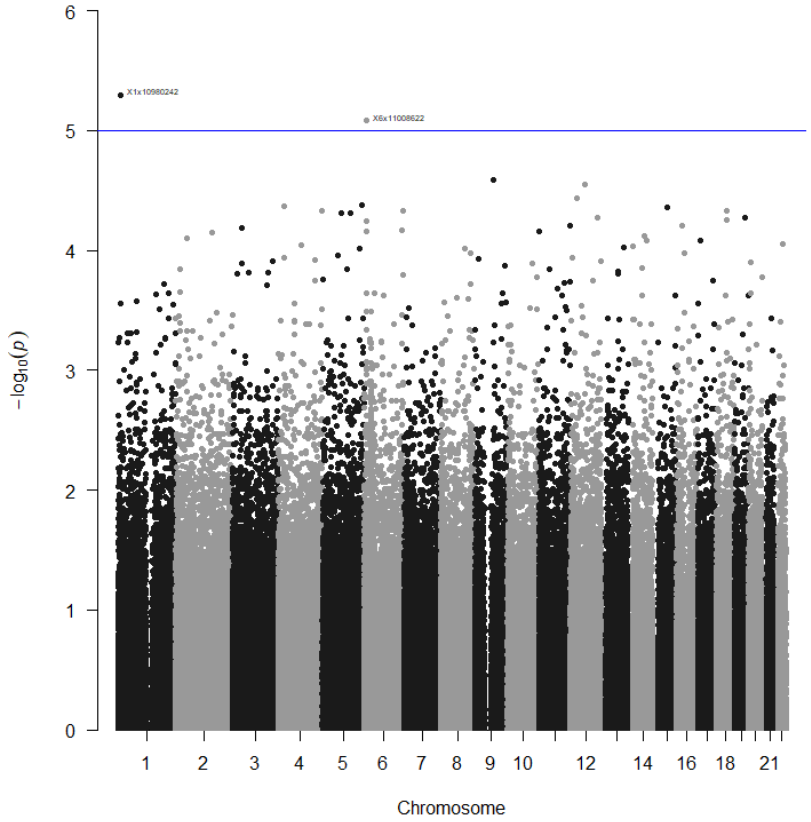

Figure K134: Manhattan plot of SNPs for whorls on the right index finger for the overdominant model

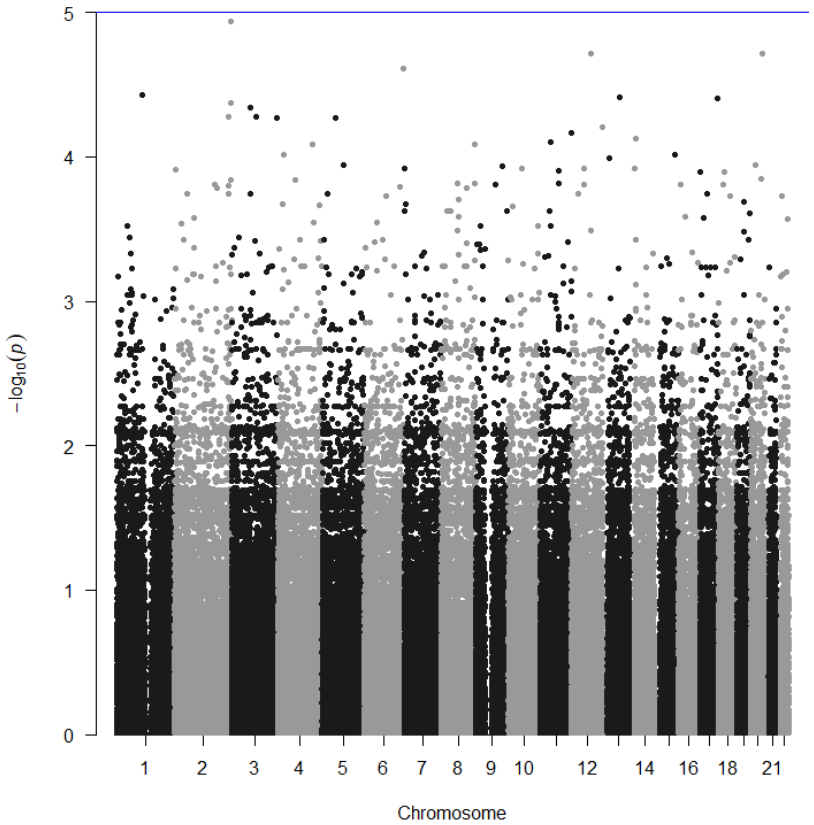

Figure K135: Manhattan plot of SNPs for whorls on the right index finger for the recessive model

Whorls on the left thumb

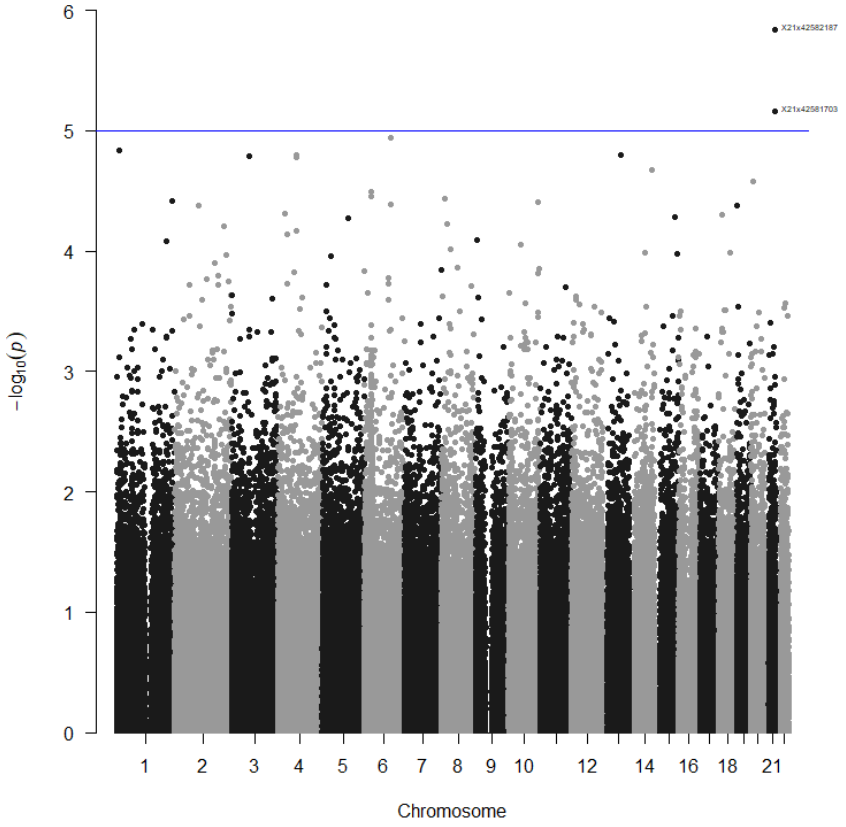

Figure K136: Manhattan plot of SNPs for whorls on the left thumb for the codominant model

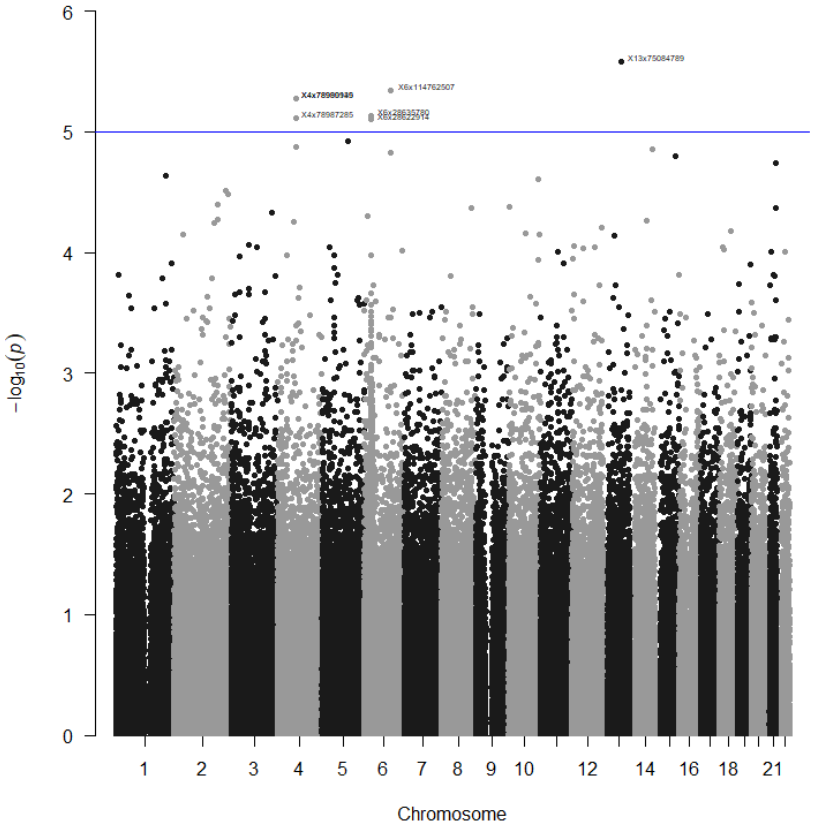

Figure K137: Manhattan plot of SNPs for whorls on the left thumb for the dominant model

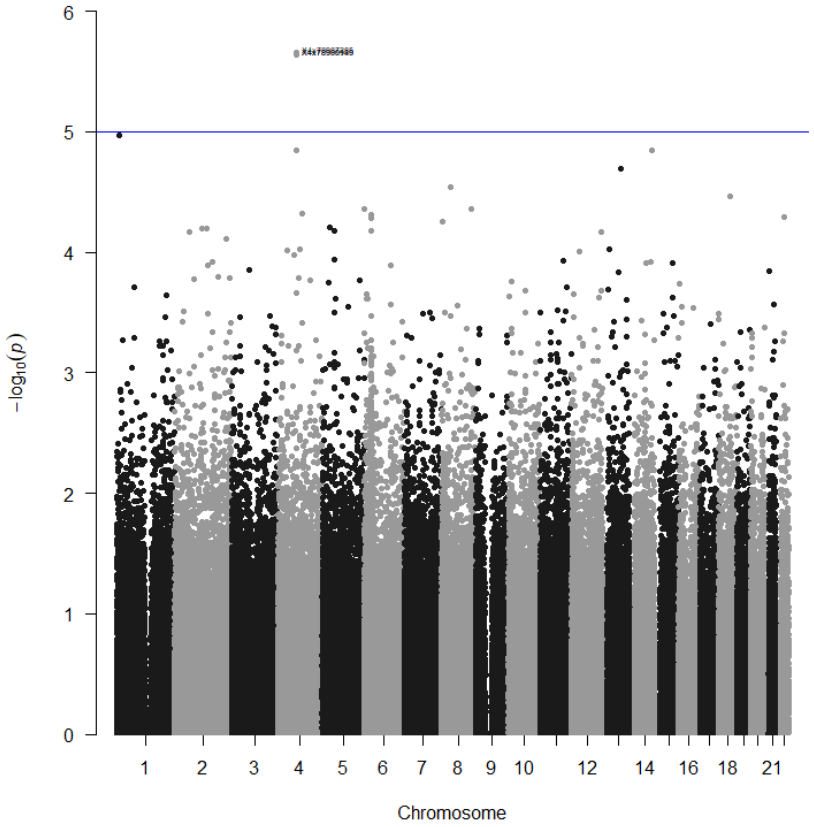

Figure K138: Manhattan plot of SNPs for whorls on the left thumb for the log-additive model

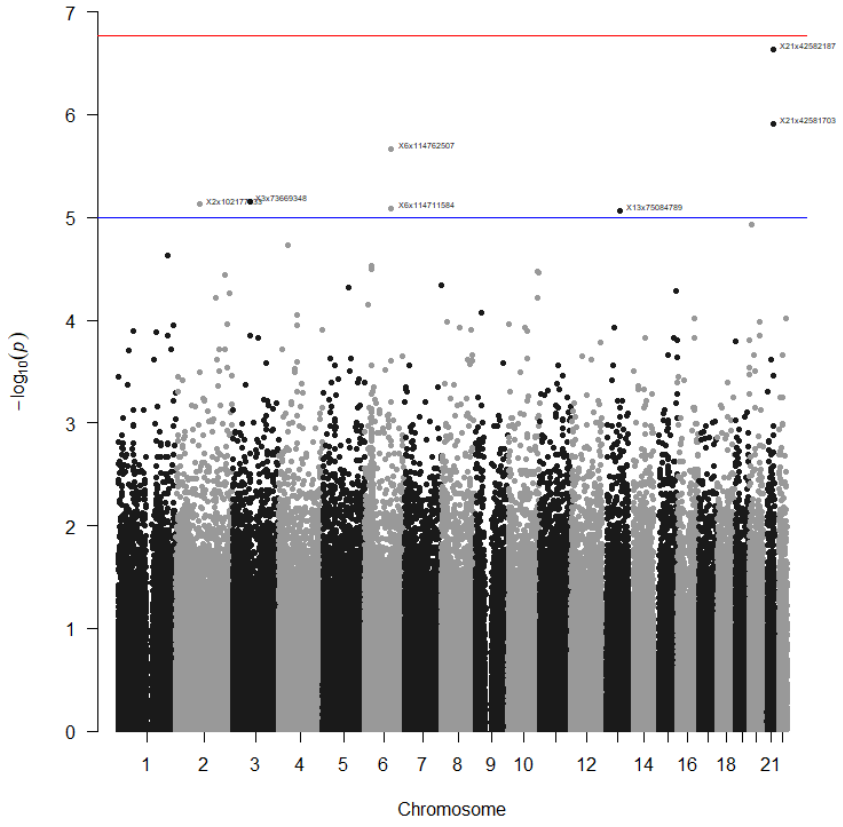

Figure K139: Manhattan plot of SNPs for whorls on the left thumb for the overdominant model

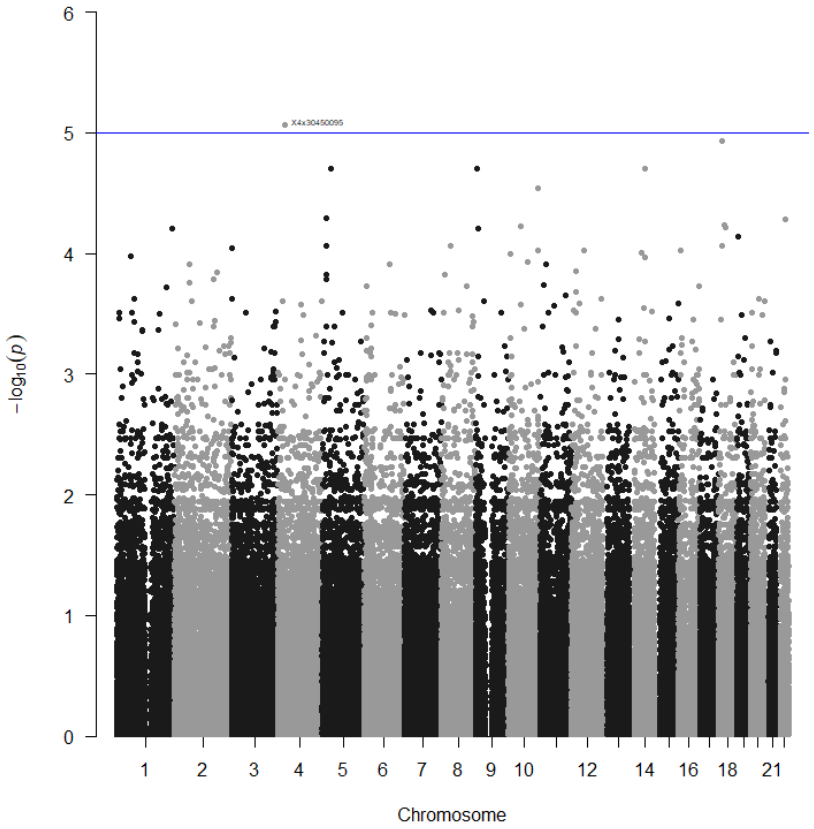

Figure K140: Manhattan plot of SNPs for whorls on the left thumb for the recessive model

Whorls on the right thumb

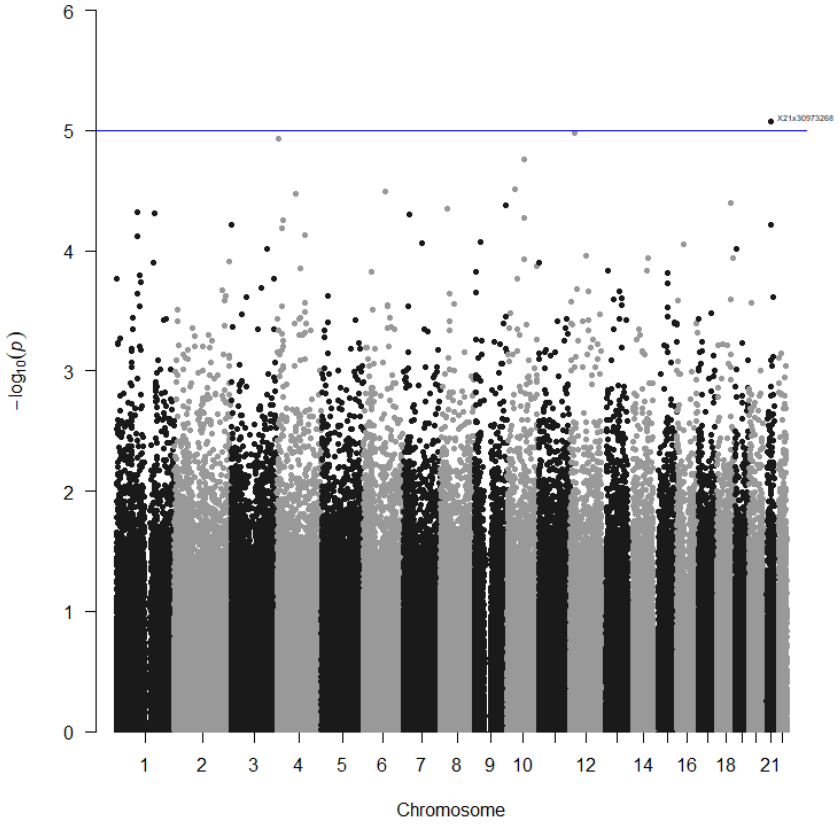

Figure K141: Manhattan plot of SNPs for whorls on the right thumb for the codominant model

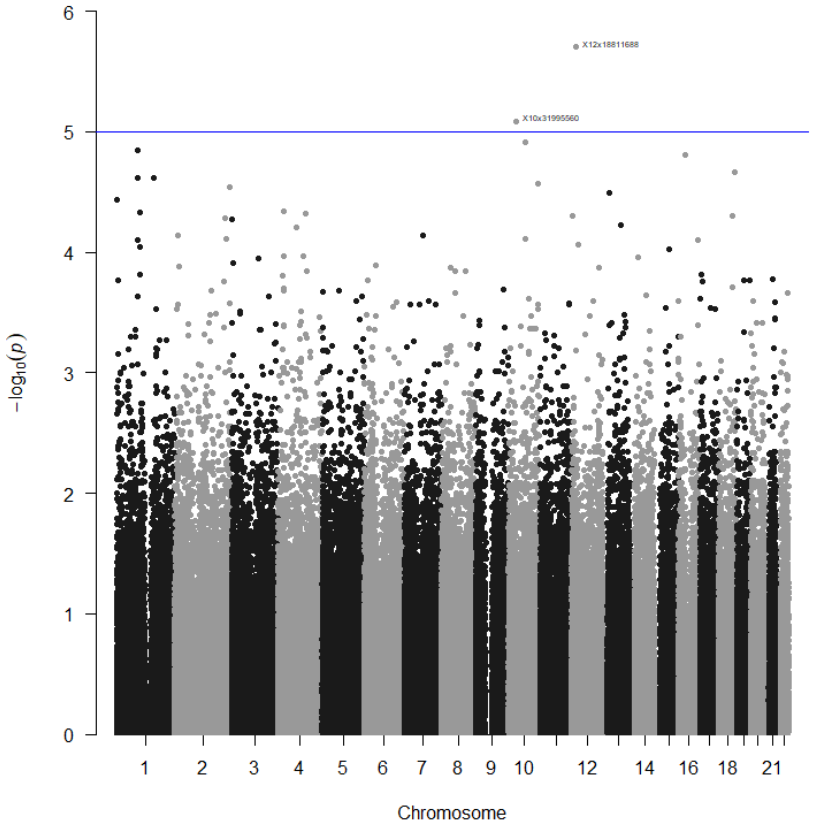

Figure K142: Manhattan plot of SNPs for whorls on the right thumb for the dominant model

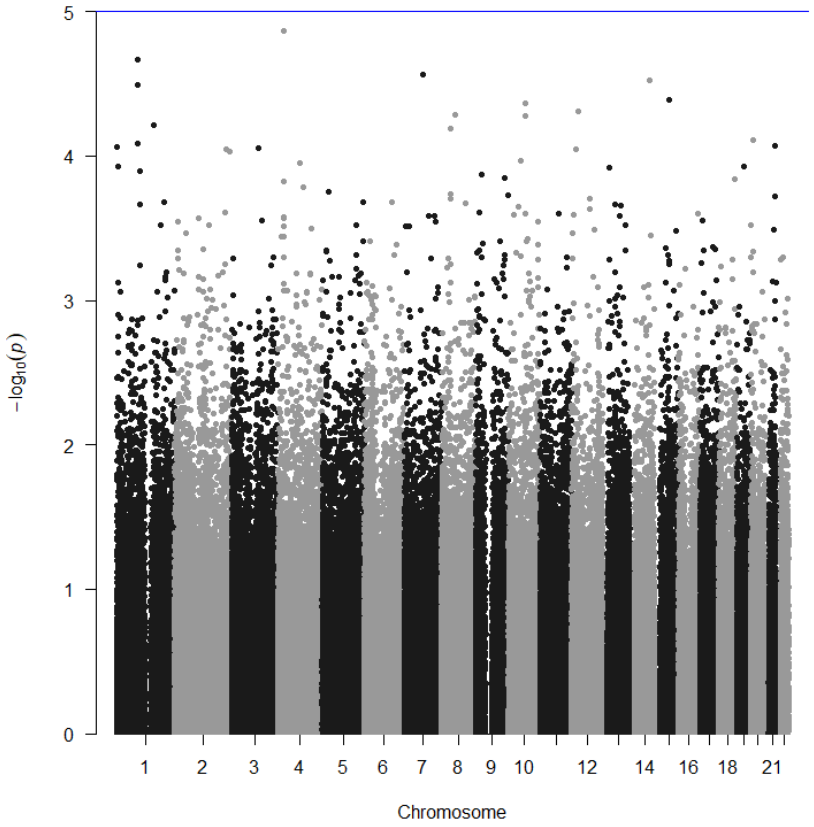

Figure K143: Manhattan plot of SNPs for whorls on the right thumb for the log-additive model

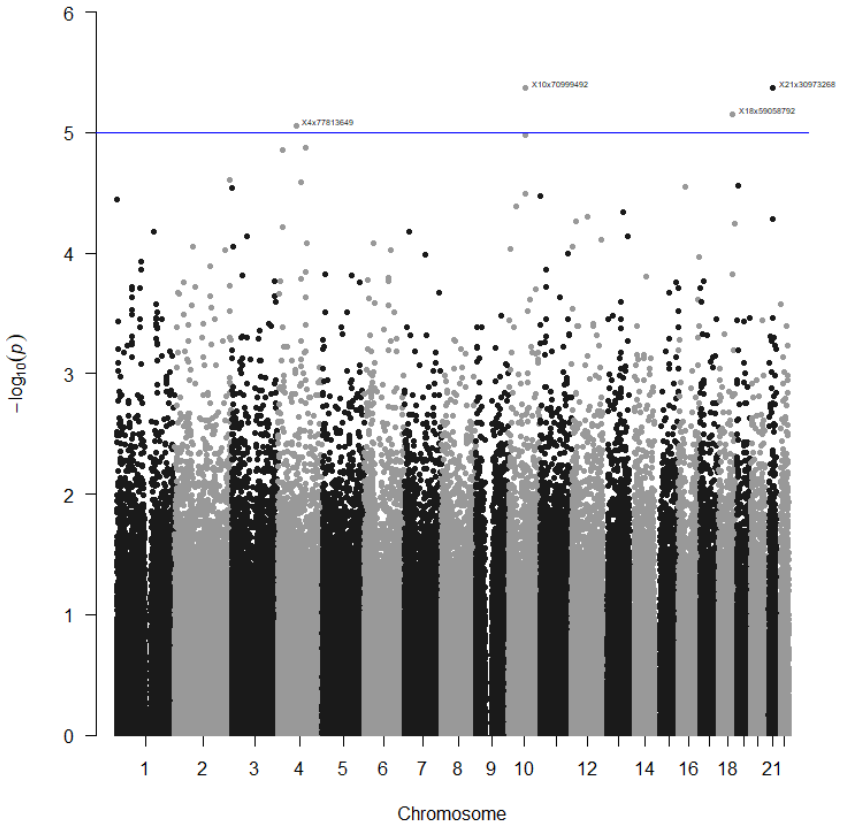

Figure K144: Manhattan plot of SNPs for whorls on the right thumb for the overdominant model

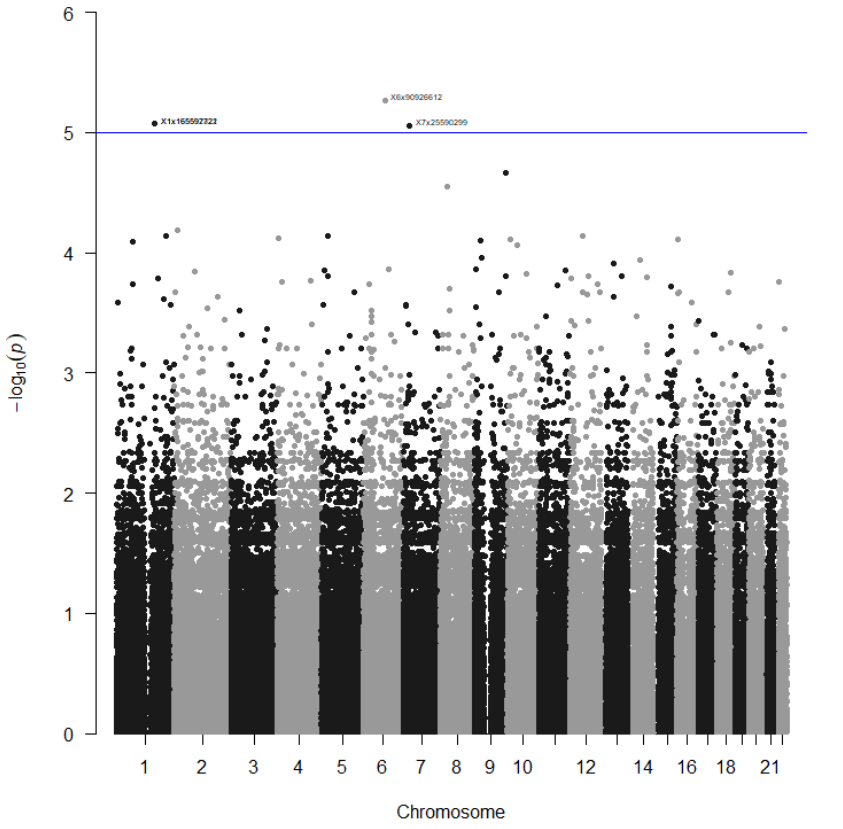

Figure K145: Manhattan plot of SNPs for whorls on the right thumb for the recessive model

Arches on the left little finger

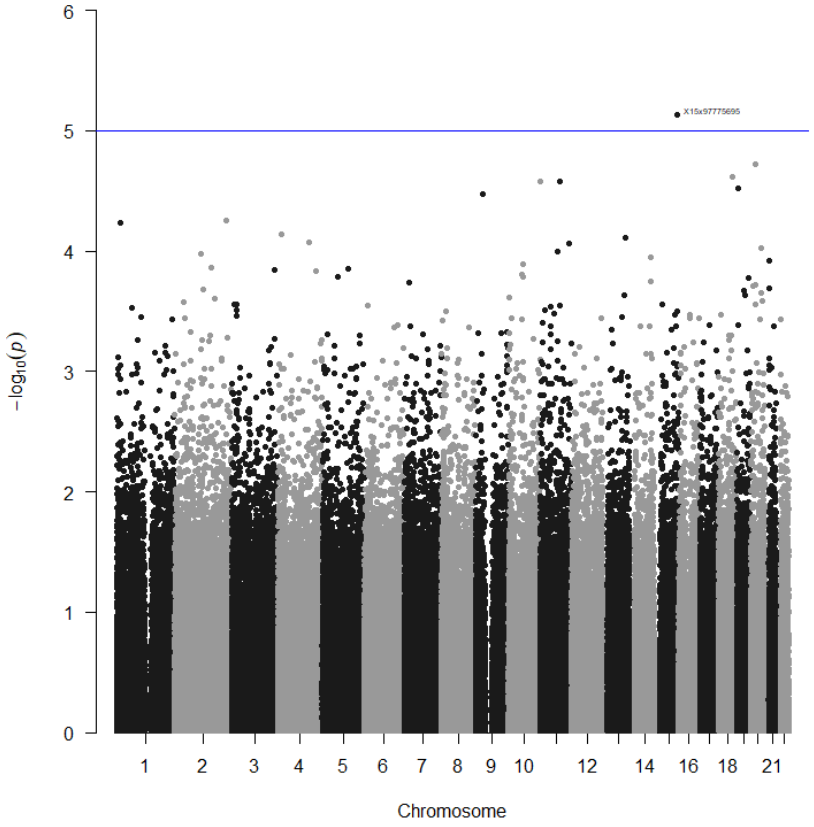

Figure K146: Manhattan plot of SNPs for arches on the left little finger for the codominant model

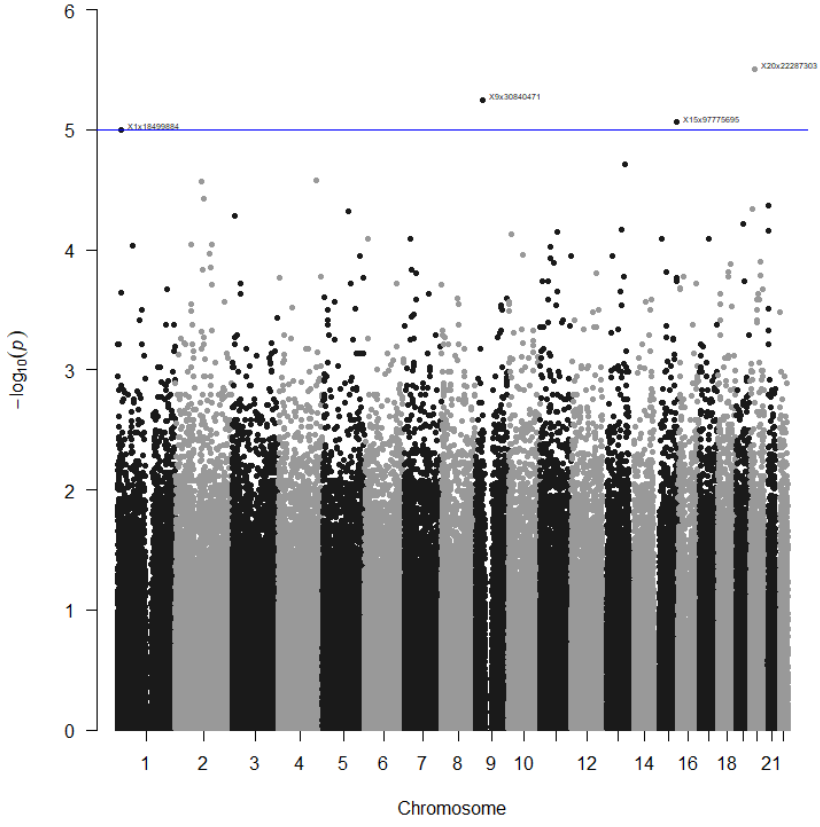

Figure K147: Manhattan plot of SNPs for arches on the left little finger for the dominant model

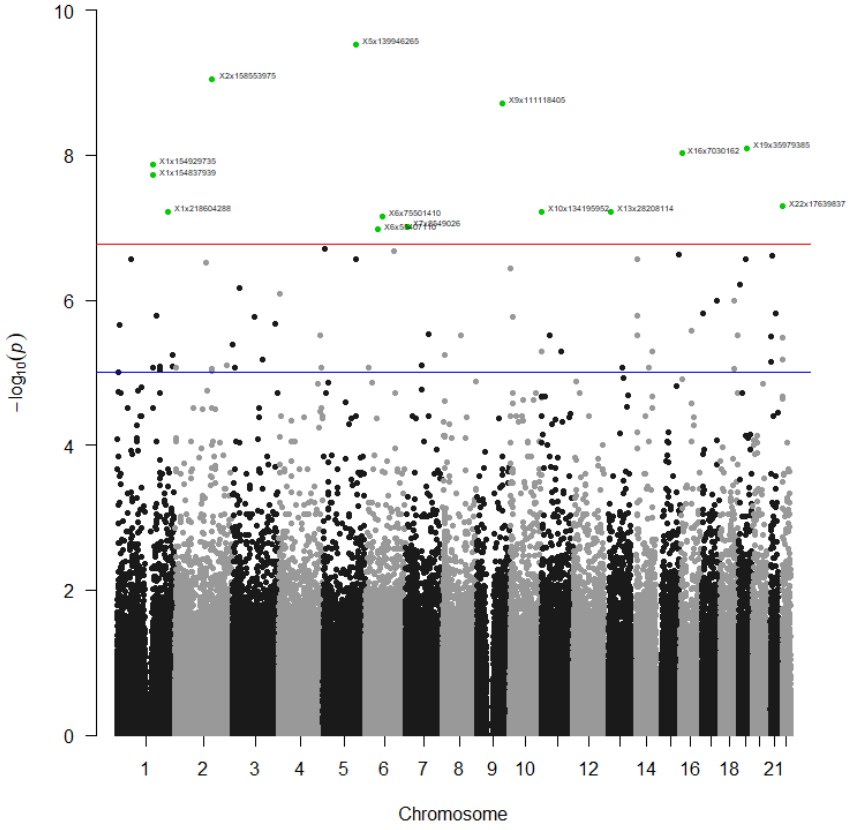

Figure K148: Manhattan plot of SNPs for arches on the left little finger for the log-additive model

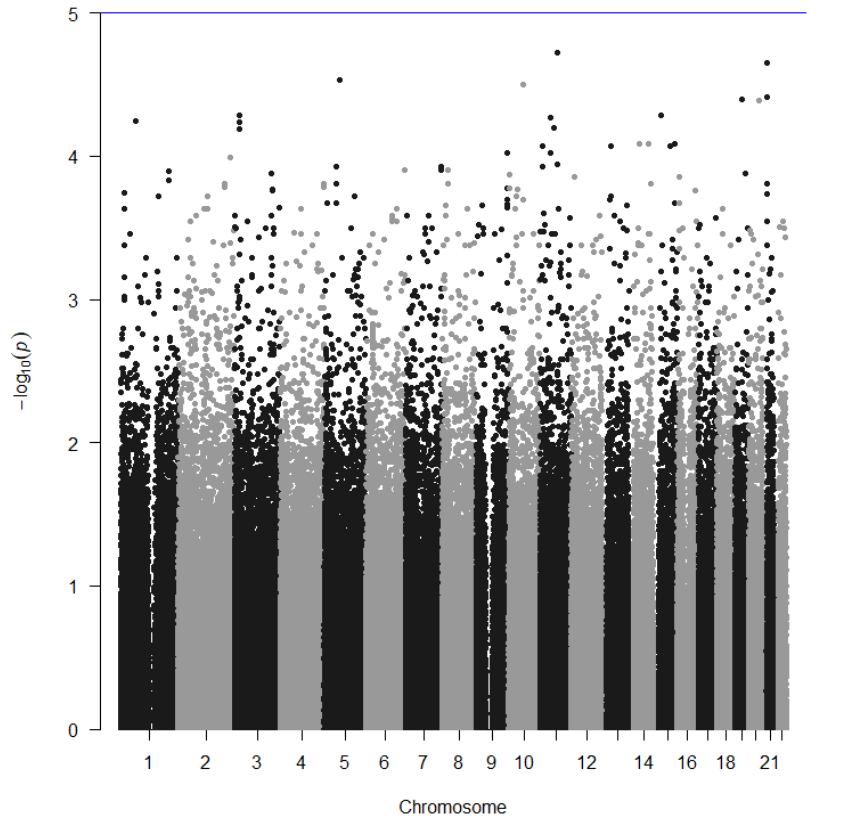

Figure K149: Manhattan plot of SNPs for arches on the left little finger for the overdominant model

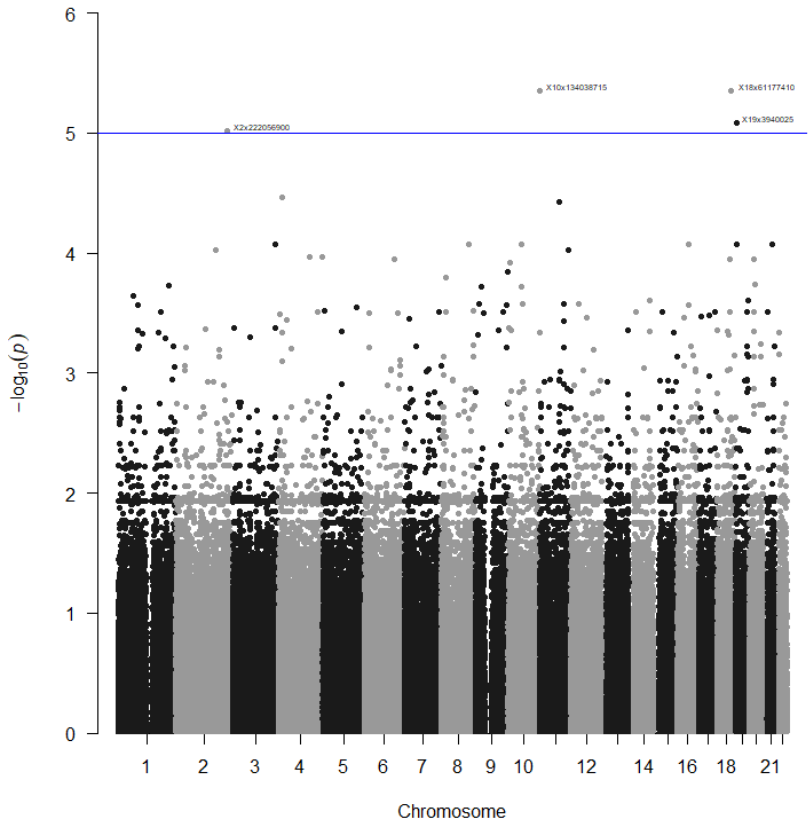

Figure K150: Manhattan plot of SNPs for arches on the left little finger for the recessive model

Arches on the right little finger

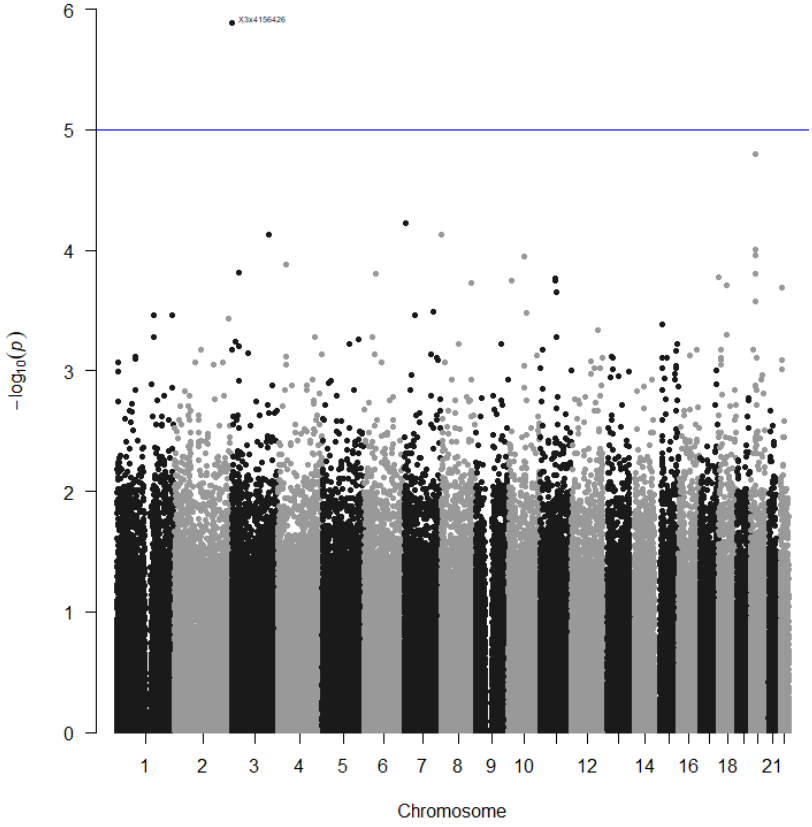

Figure K151: Manhattan plot of SNPs for arches on the right little finger for the codominant model

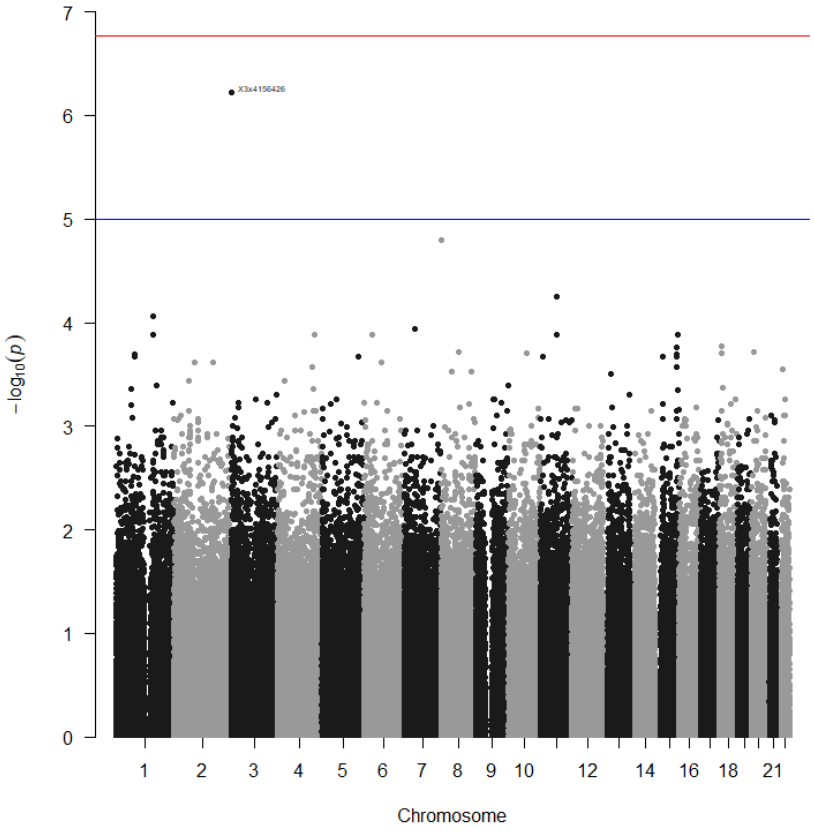

Figure K152: Manhattan plot of SNPs for arches on the right little finger for the dominant model

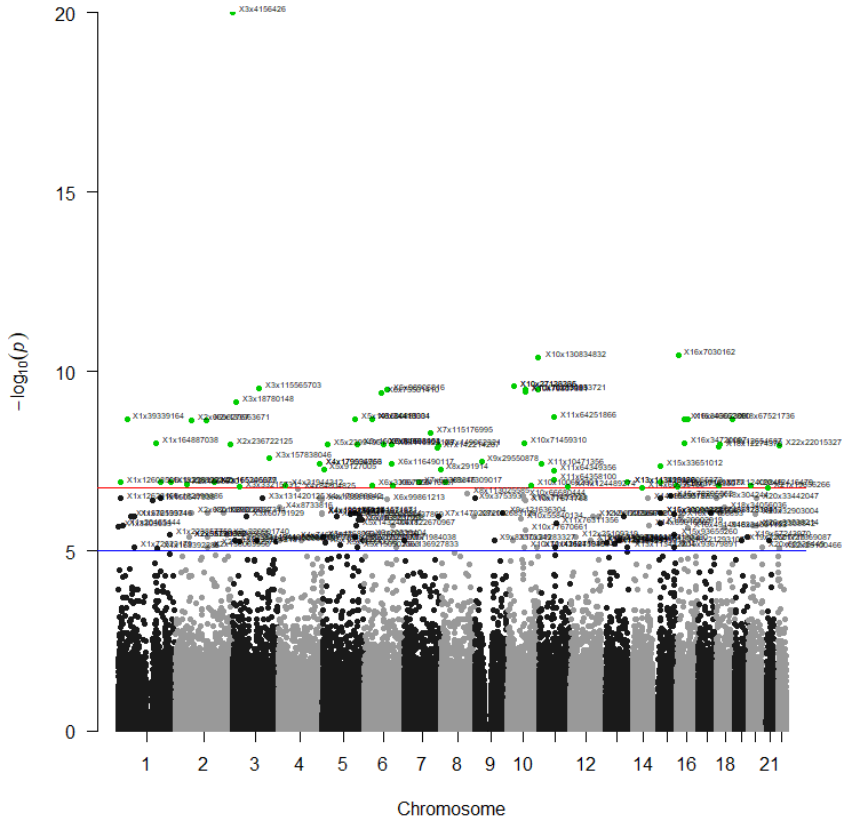

Figure K153: Manhattan plot of SNPs for arches on the right little finger for the log-additive model

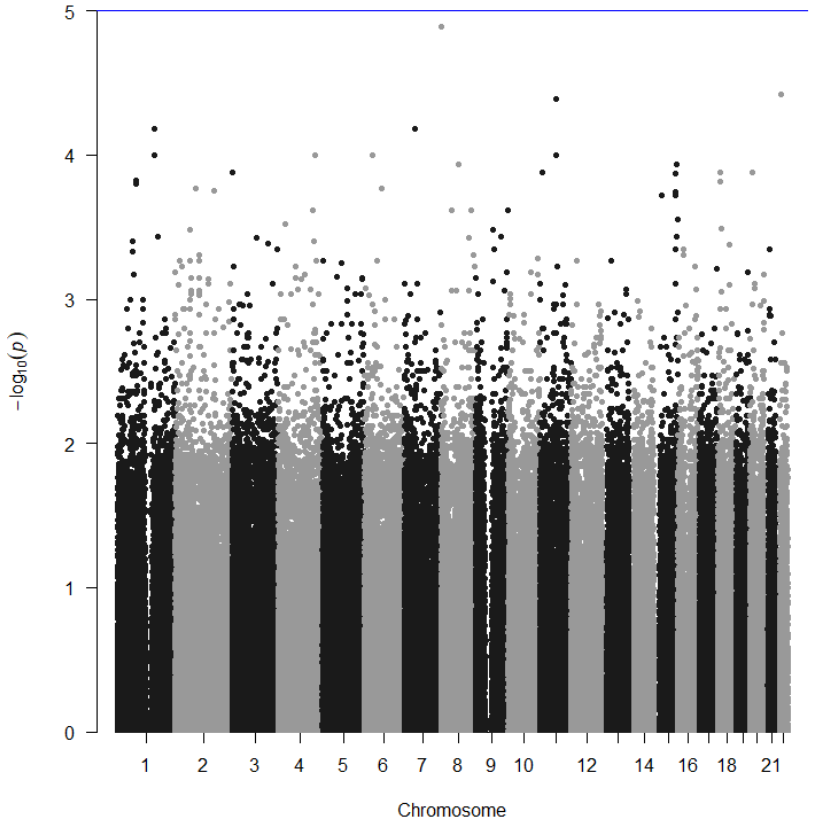

Figure K154: Manhattan plot of SNPs for arches on the right little finger for the overdominant model

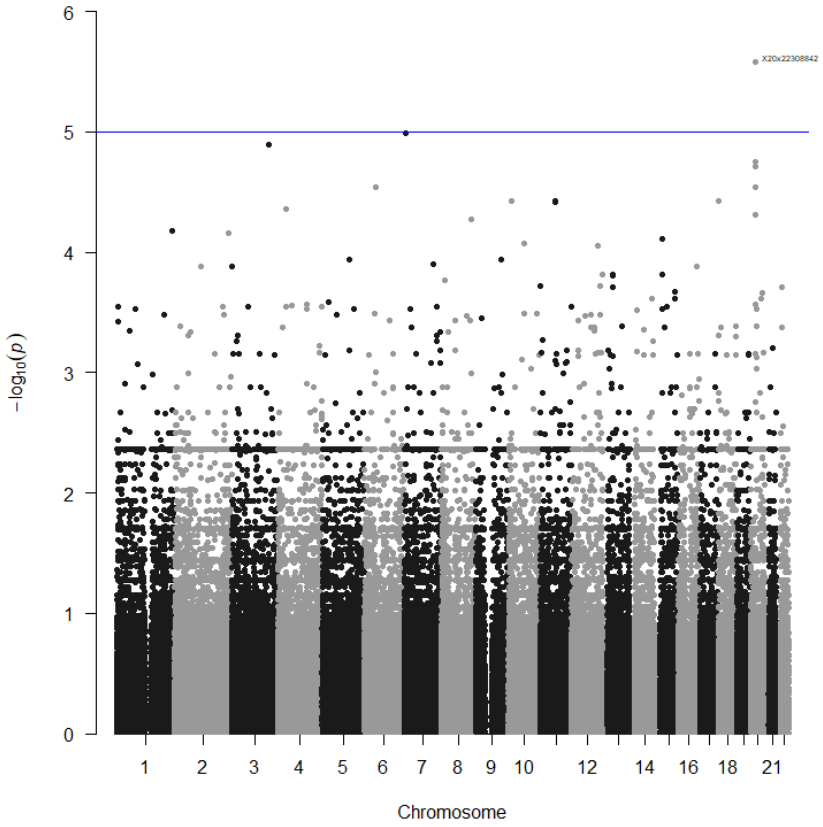

Figure K155: Manhattan plot of SNPs for arches on the right little finger for the recessive model

Arches on the left ring finger

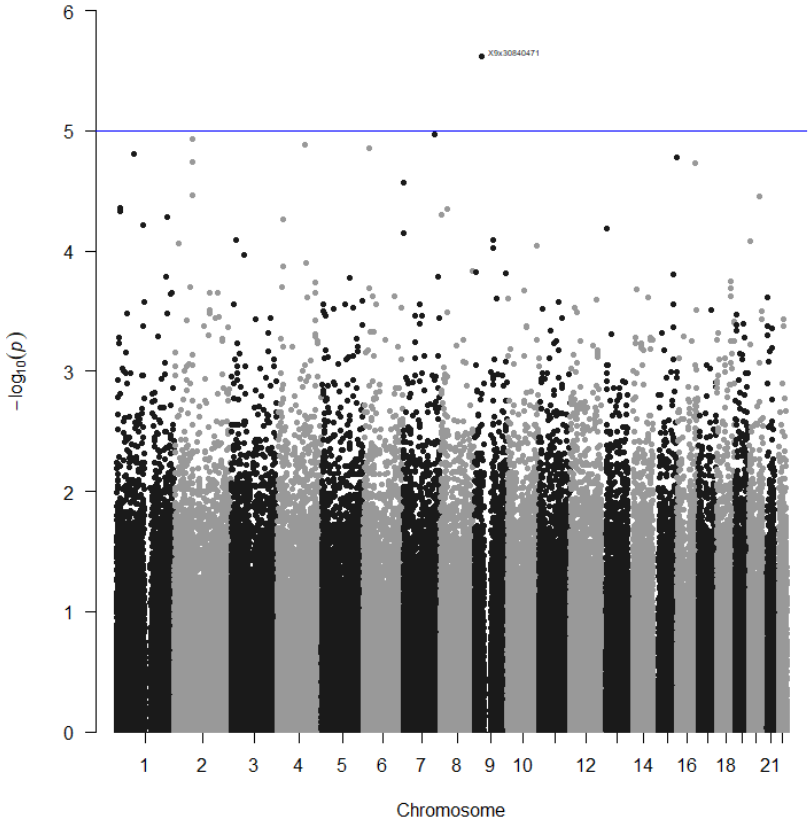

Figure K156: Manhattan plot of SNPs for arches on the left ring finger for the codominant model

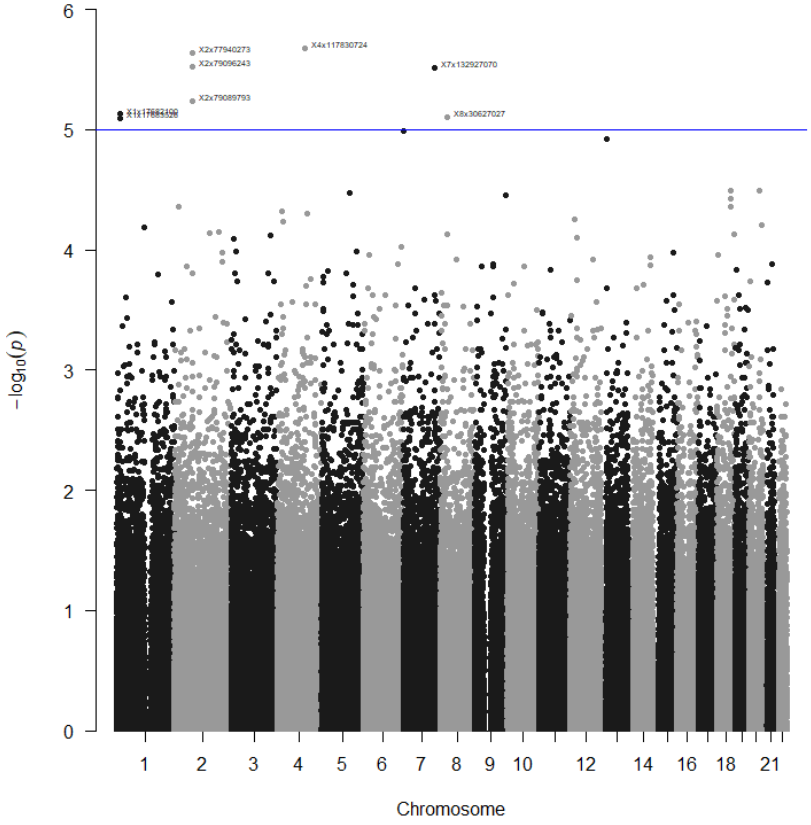

Figure K157: Manhattan plot of SNPs for arches on the left ring finger for the dominant model

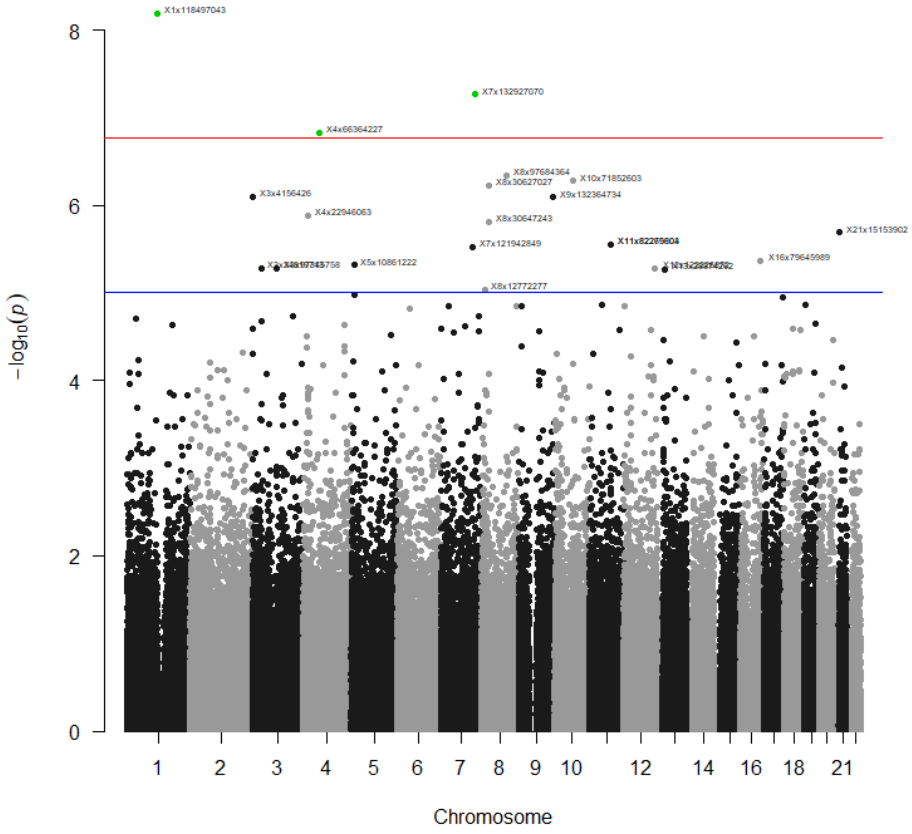

Figure K158: Manhattan plot of SNPs for arches on the left ring finger for the log-additive model

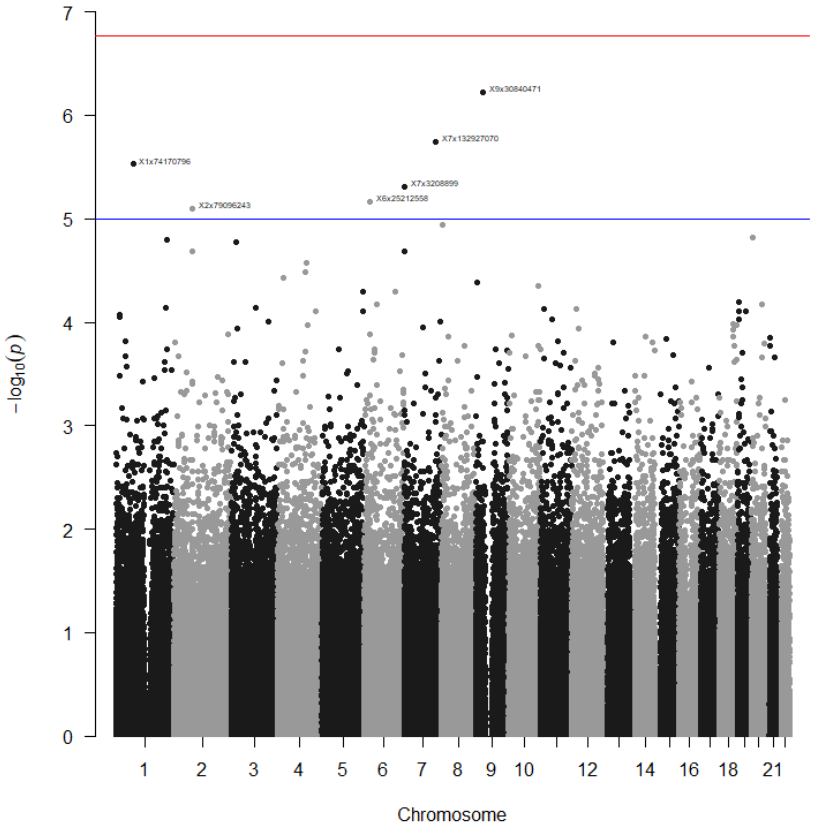

Figure K159: Manhattan plot of SNPs for arches on the left ring finger for the overdominant model

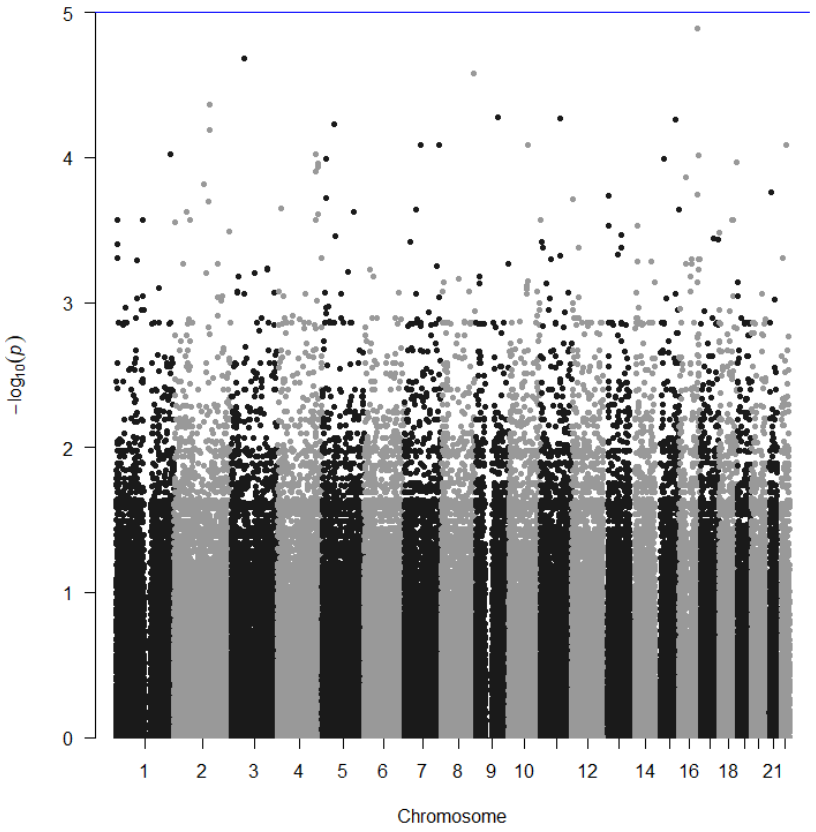

Figure K160: Manhattan plot of SNPs for arches on the left ring finger for the recessive model

Arches on the right ring finger

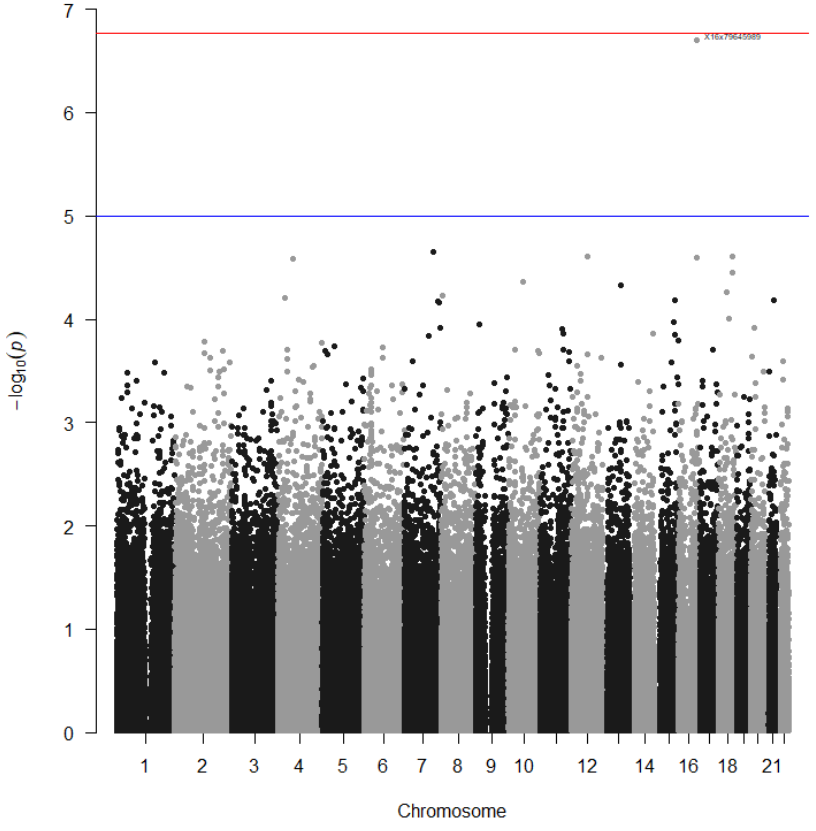

Figure K161: Manhattan plot of SNPs for arches on the right ring finger for the codominant model

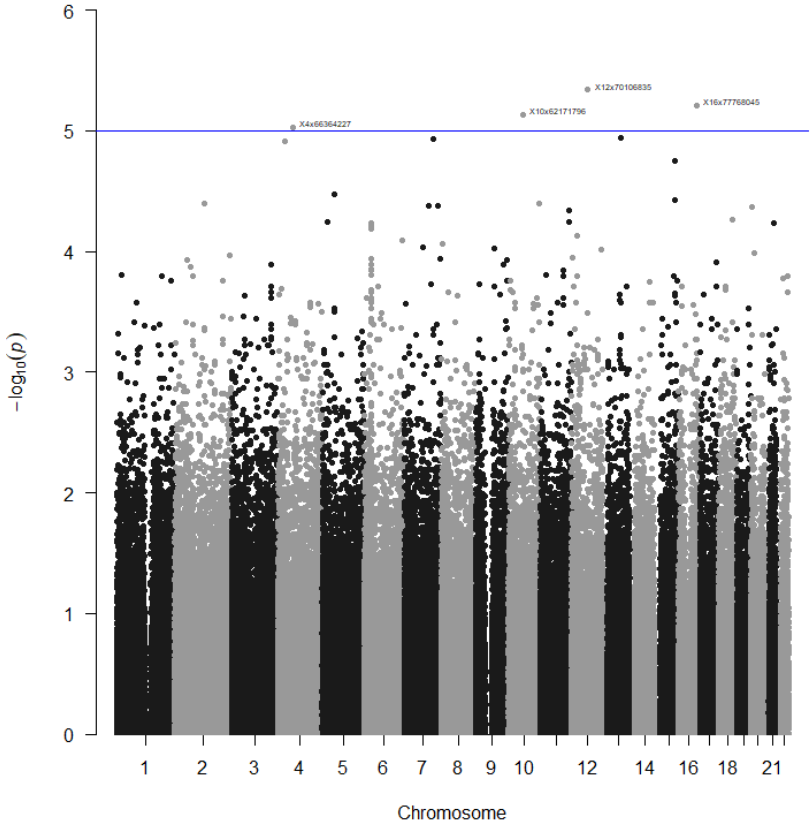

Figure K162: Manhattan plot of SNPs for arches on the right ring finger for the dominant model

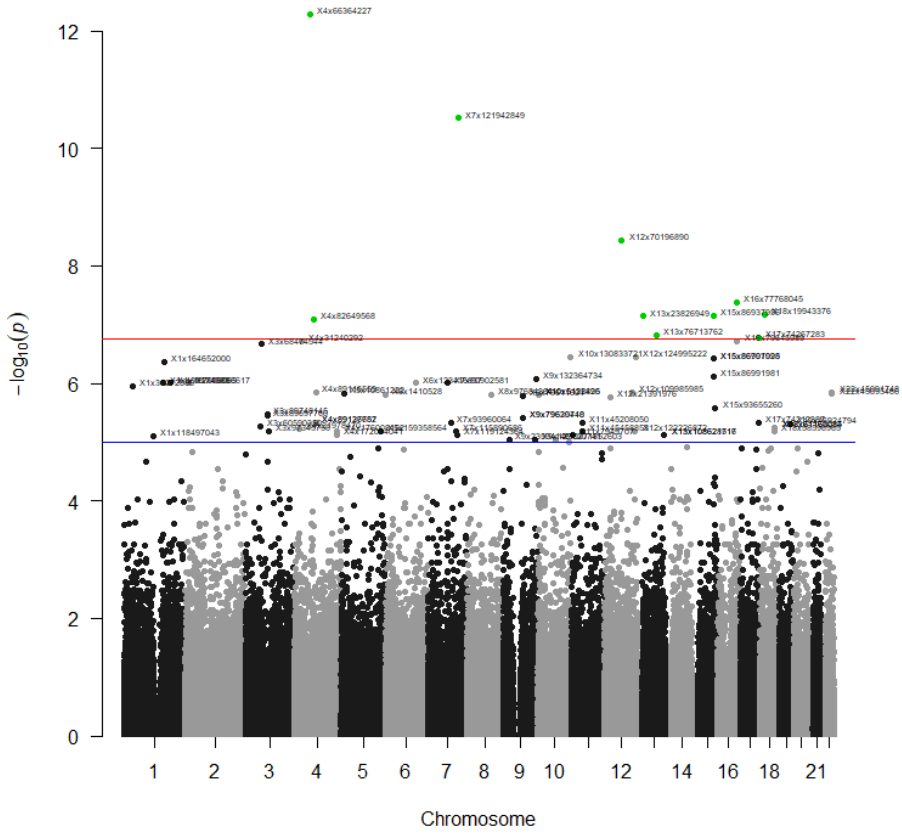

Figure K163: Manhattan plot of SNPs for arches on the right ring finger for the log-additive model

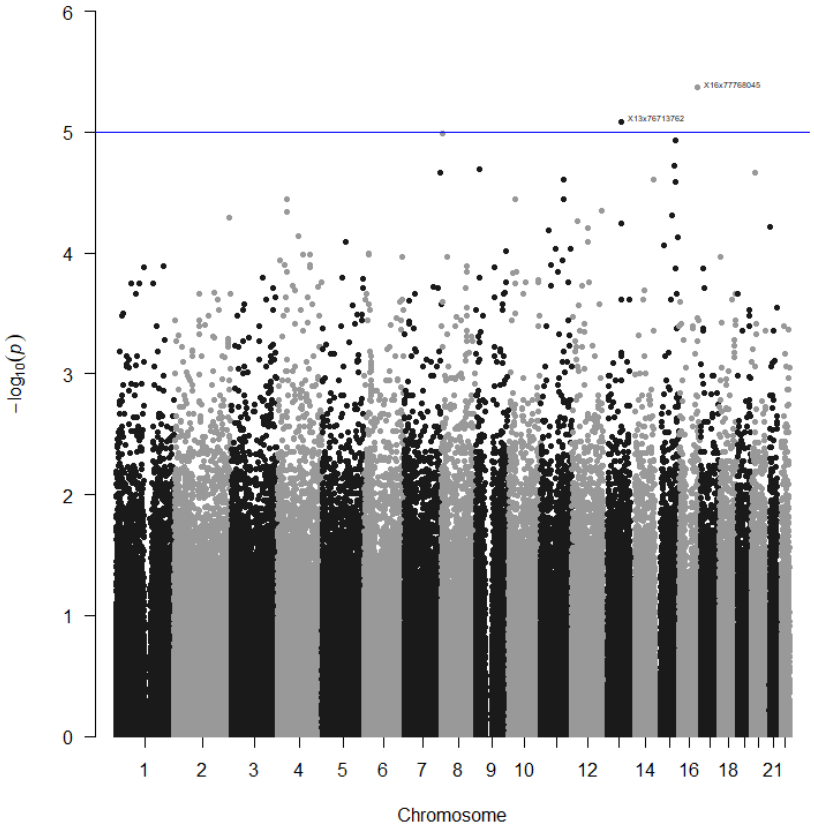

Figure K164: Manhattan plot of SNPs for arches on the right ring finger for the overdominant model

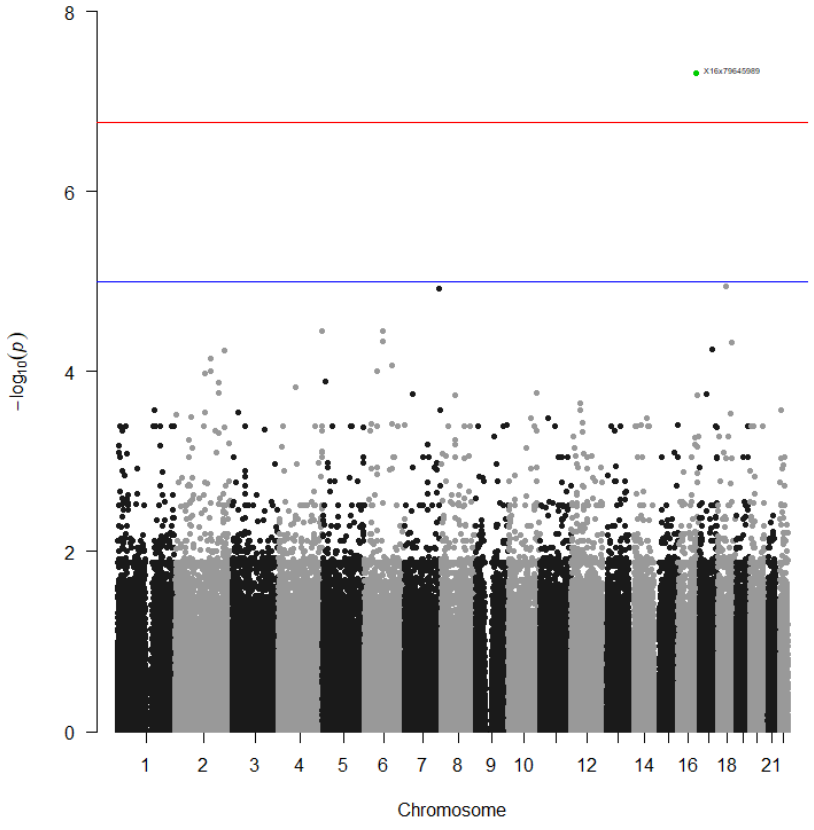

Figure K165: Manhattan plot of SNPs for arches on the right ring finger for the recessive model

Arches on the left middle finger

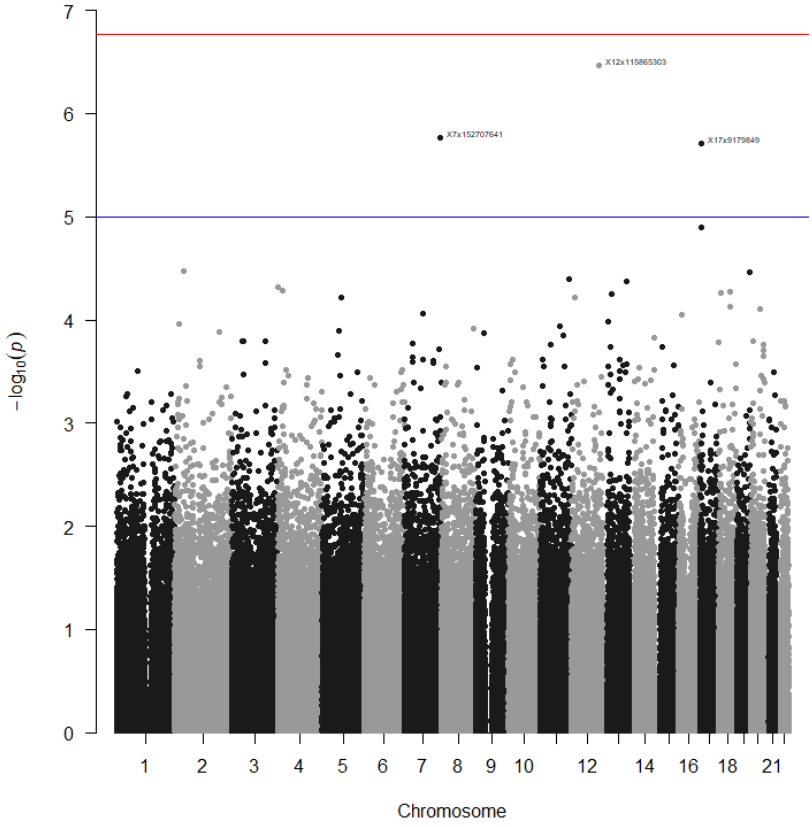

Figure K166: Manhattan plot of SNPs for arches on the left middle finger for the codominant model

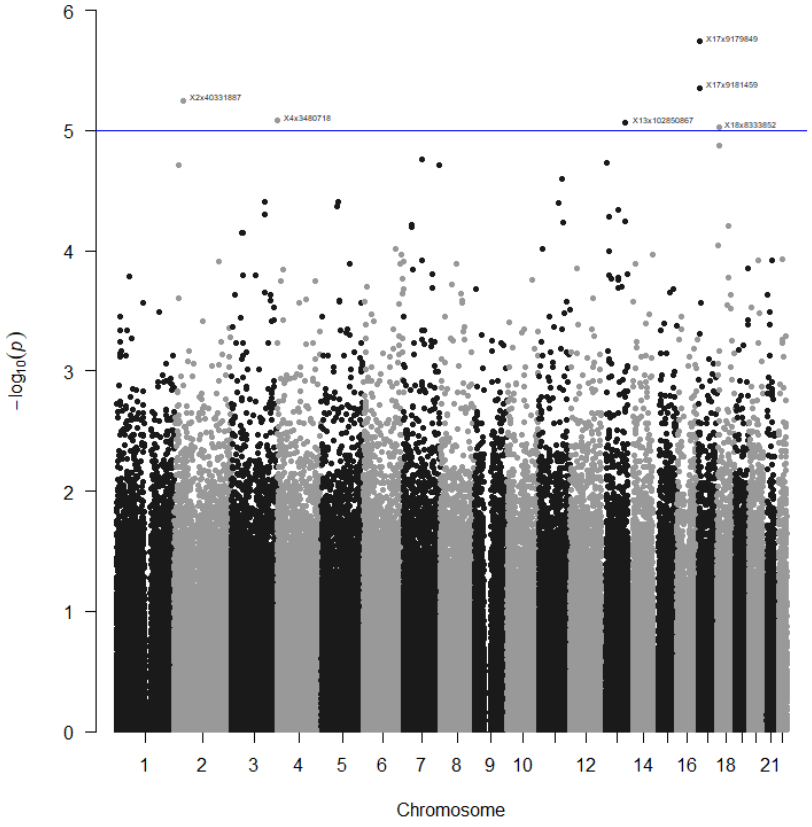

Figure K167: Manhattan plot of SNPs for arches on the left middle finger for the dominant model

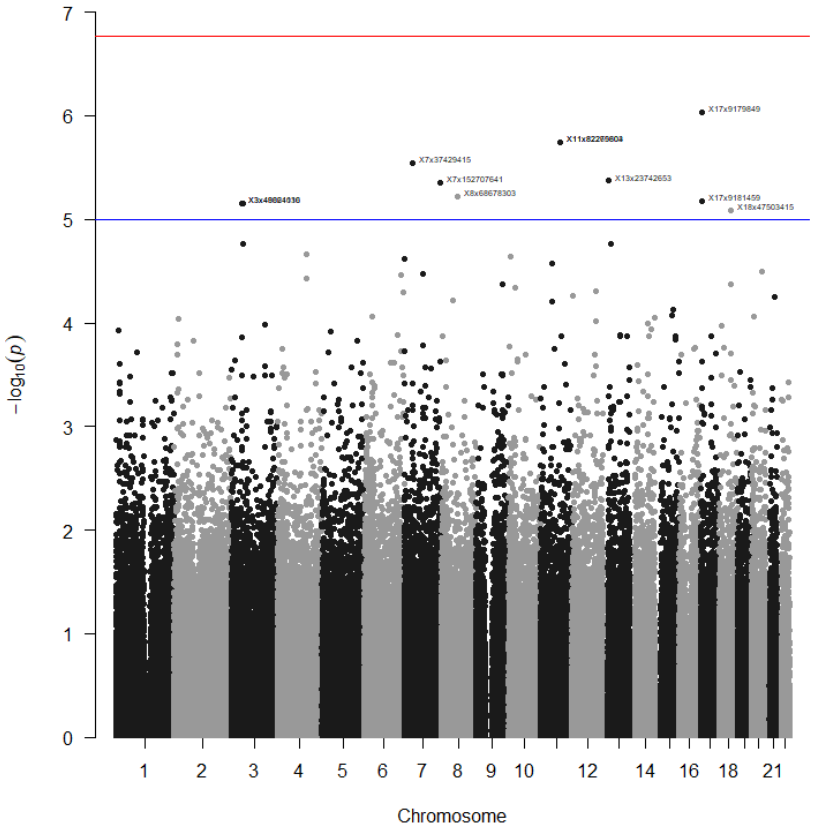

Figure K168: Manhattan plot of SNPs for arches on the left middle finger for the log-additive model

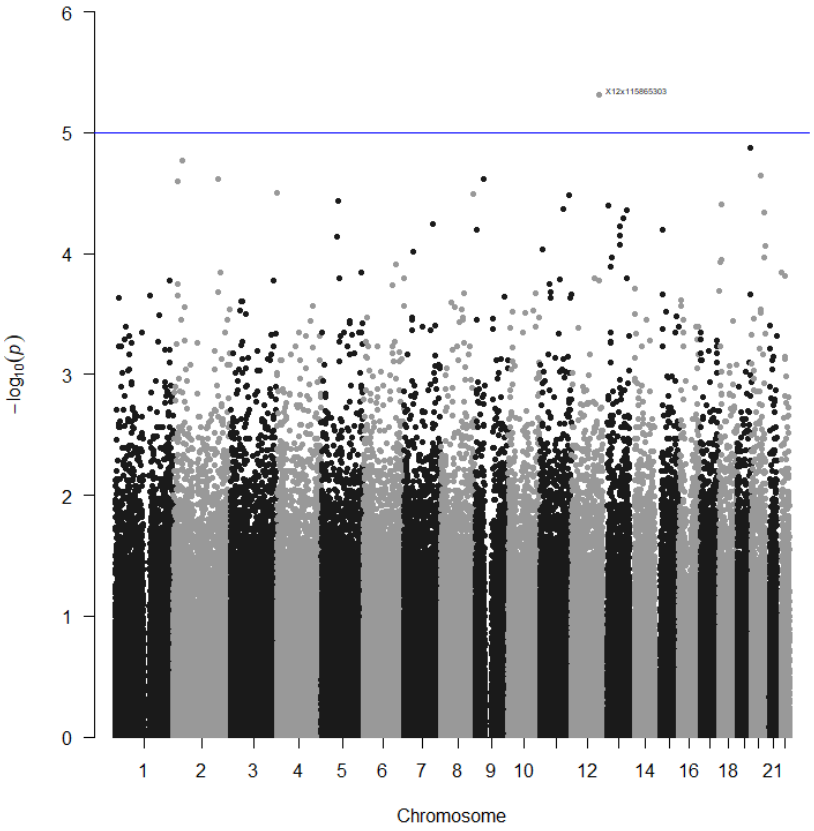

Figure K169: Manhattan plot of SNPs for arches on the left middle finger for the overdominant model

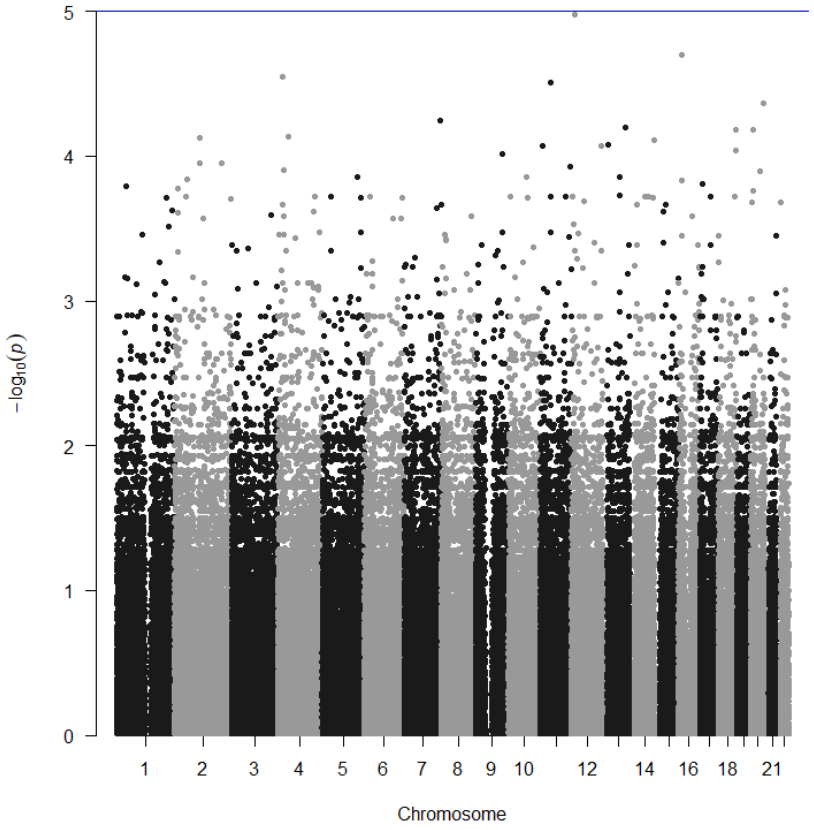

Figure K170: Manhattan plot of SNPs for arches on the left middle finger for the recessive model

Arches on the right middle finger

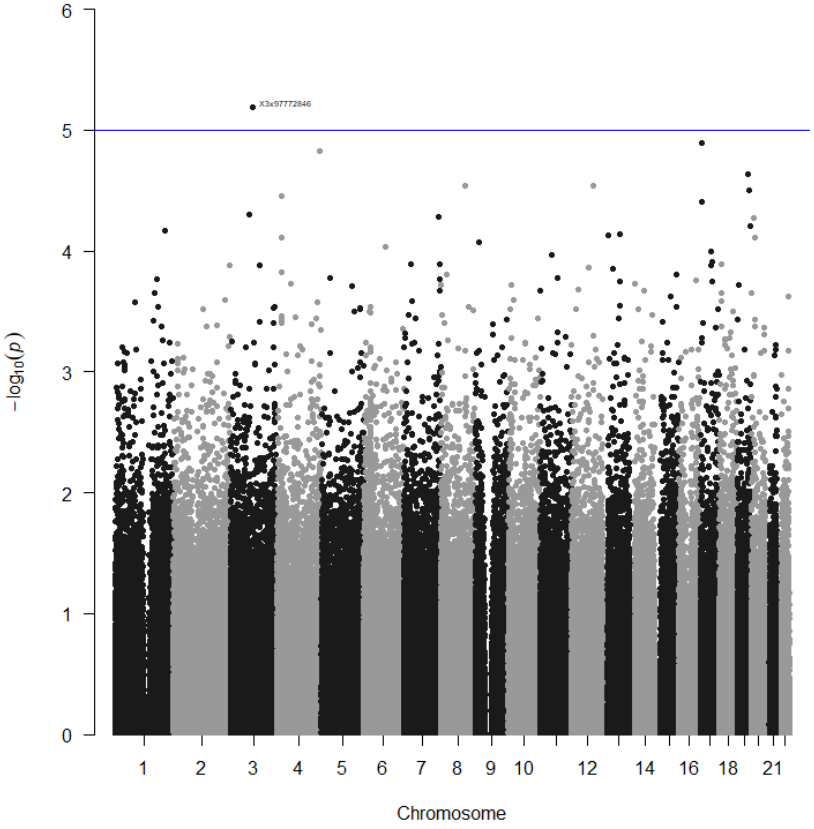

Figure K171: Manhattan plot of SNPs for arches on the right middle finger for the codominant model

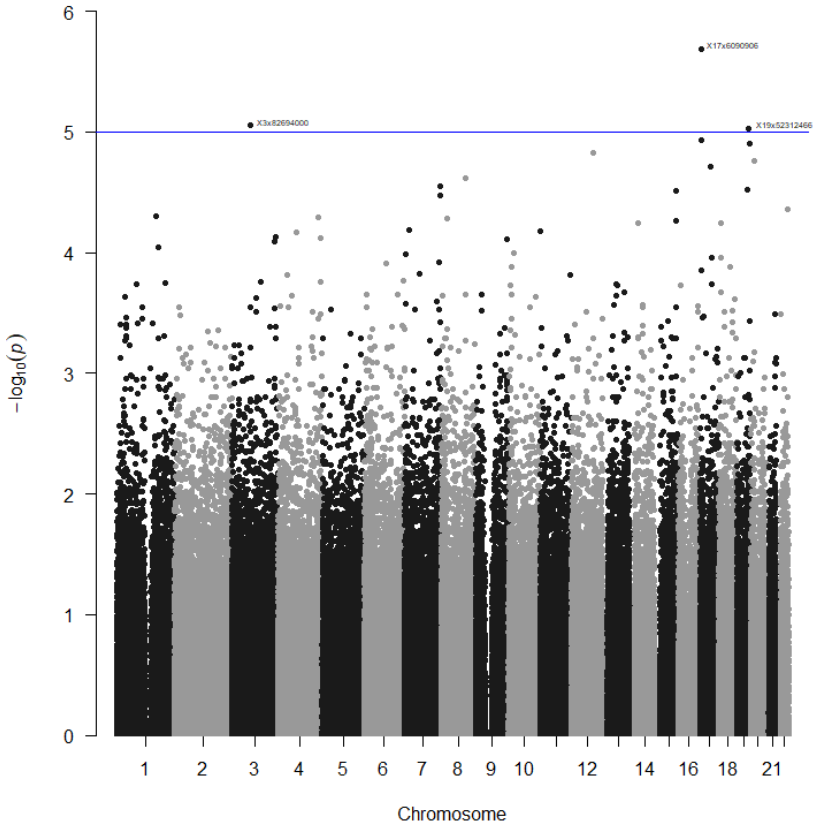

Figure K172: Manhattan plot of SNPs for arches on the right middle finger for the dominant model

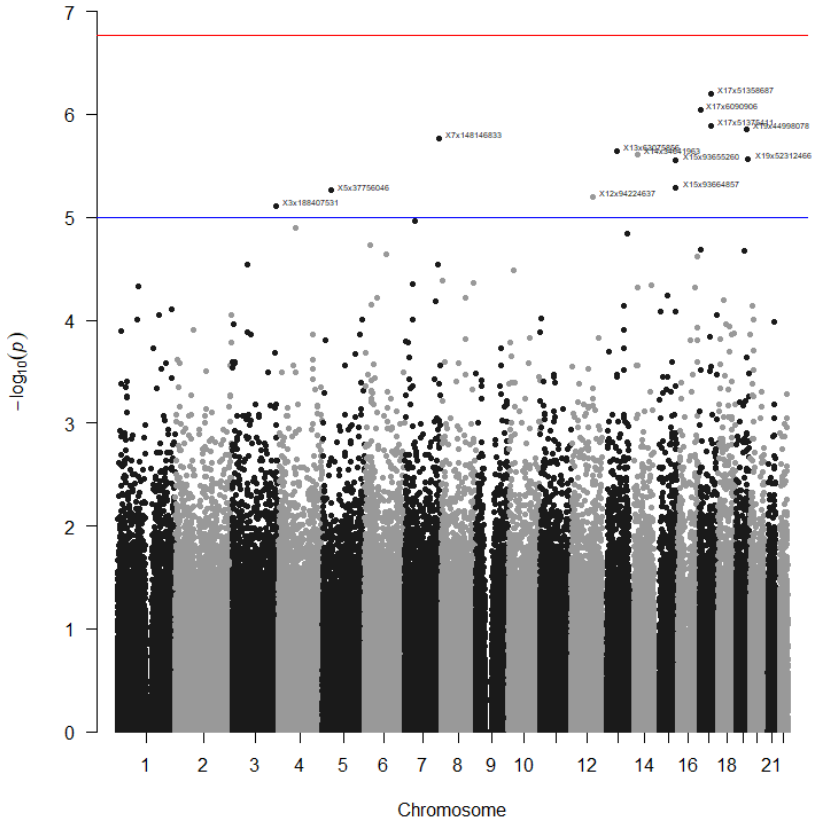

Figure K173: Manhattan plot of SNPs for arches on the right middle finger for the log-additive model

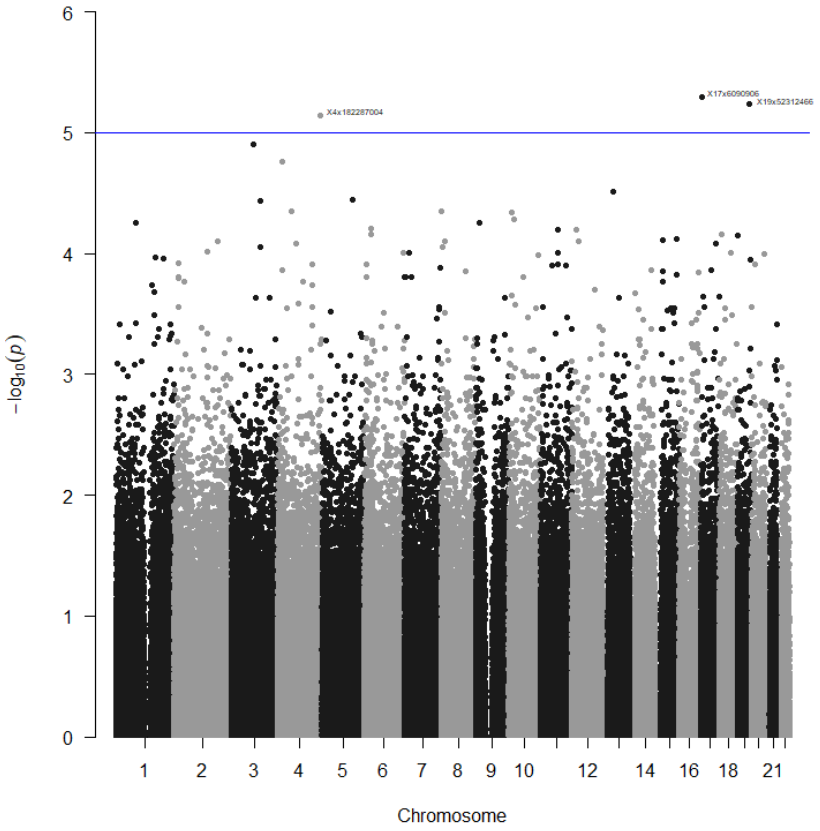

Figure K174: Manhattan plot of SNPs for arches on the right middle finger for the overdominant model

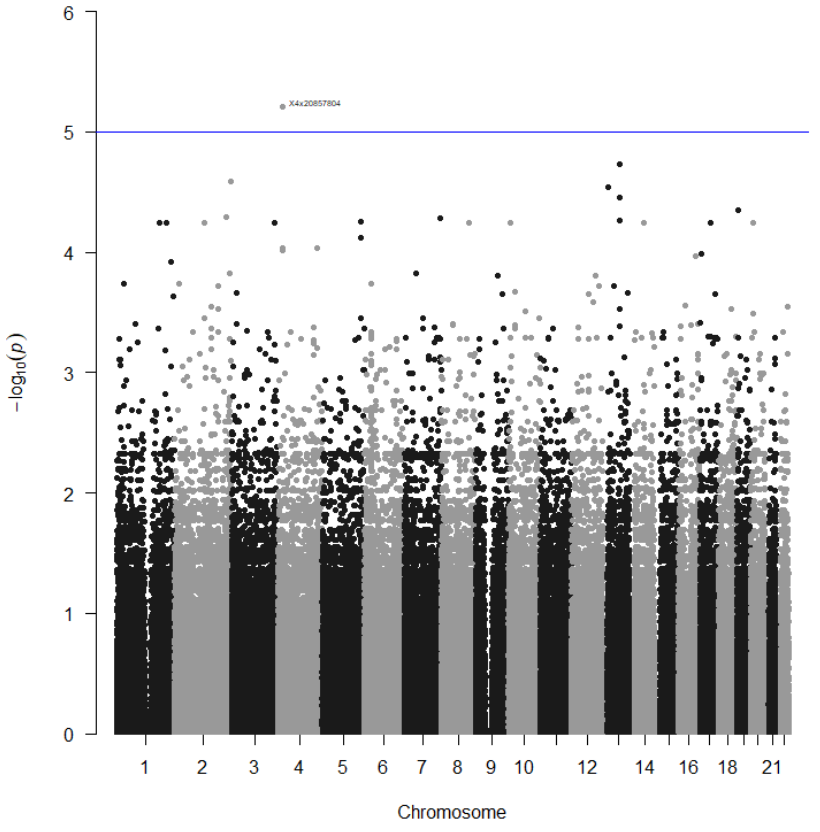

Figure K175: Manhattan plot of SNPs for arches on the right middle finger for the recessive model

Arches on the left index finger

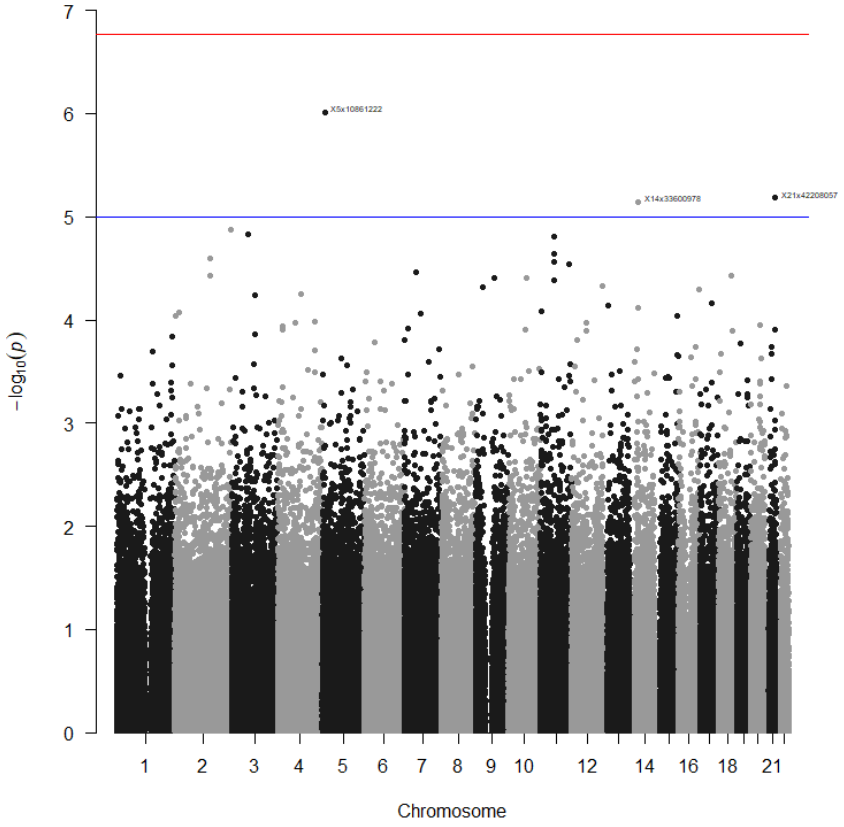

Figure K176: Manhattan plot of SNPs for arches on the left index finger for the codominant model

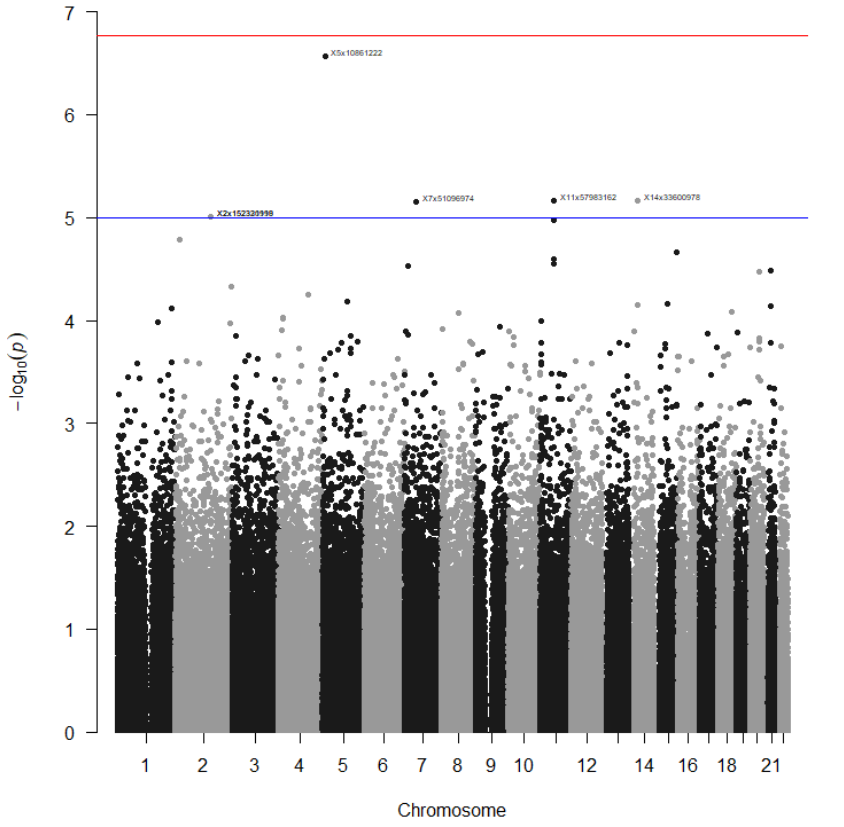

Figure K177: Manhattan plot of SNPs for arches on the left index finger for the dominant model

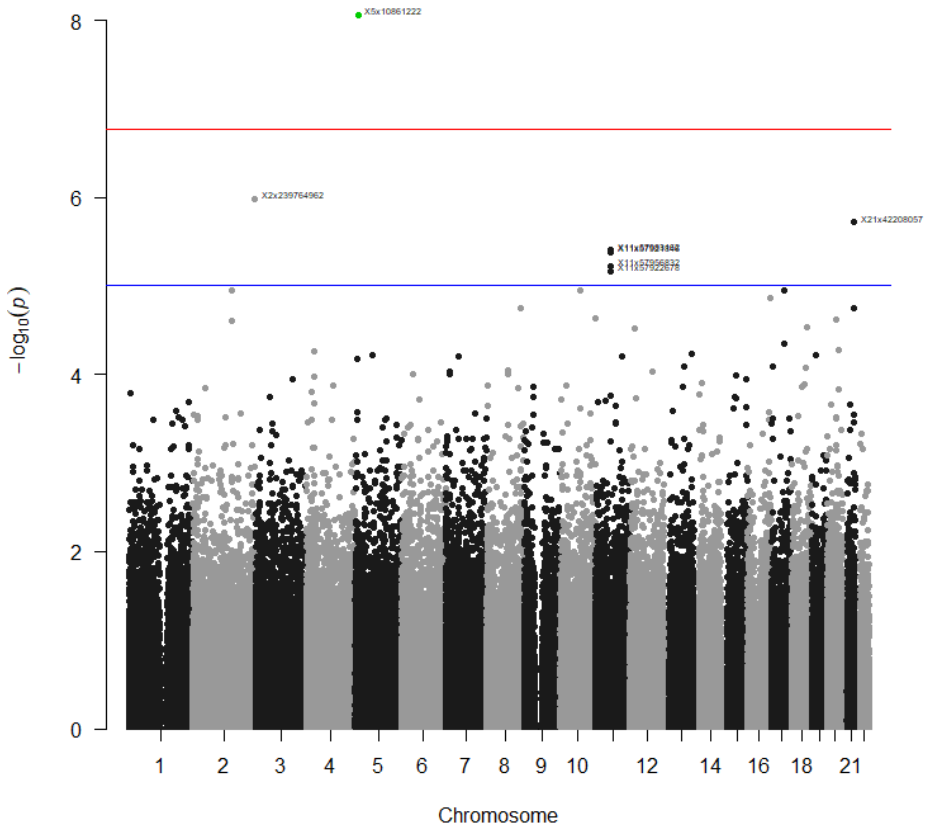

Figure K178: Manhattan plot of SNPs for arches on the left index finger for the log-additive model

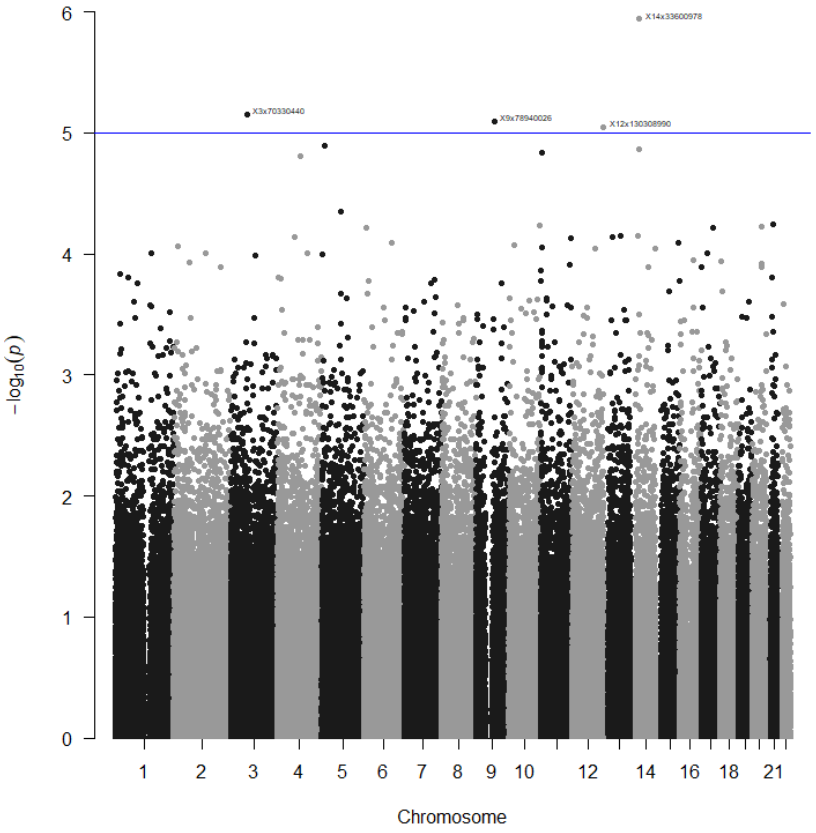

Figure K179: Manhattan plot of SNPs for arches on the left index finger for the overdominant model

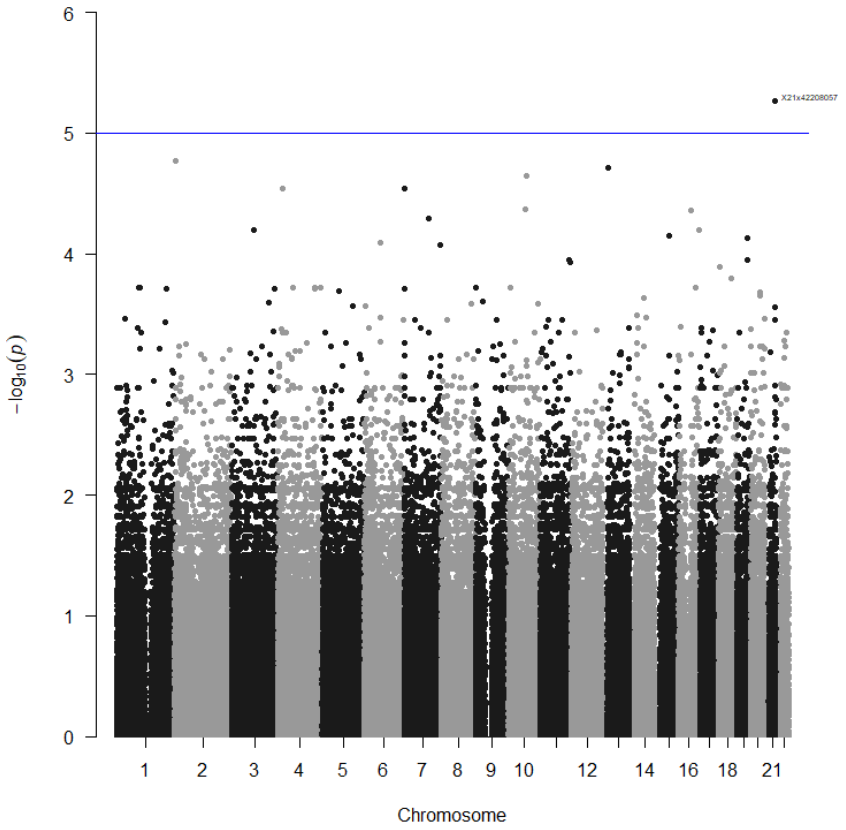

Figure K180: Manhattan plot of SNPs for arches on the left index finger for the recessive model

Arches on the right index finger

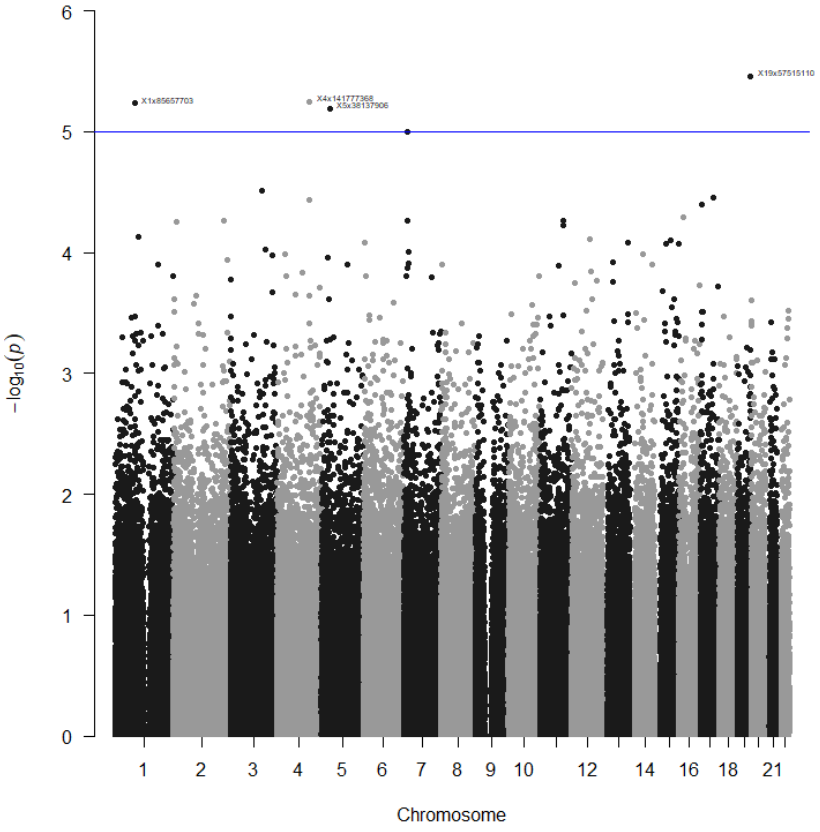

Figure K181: Manhattan plot of SNPs for arches on the right index finger for the codominant model

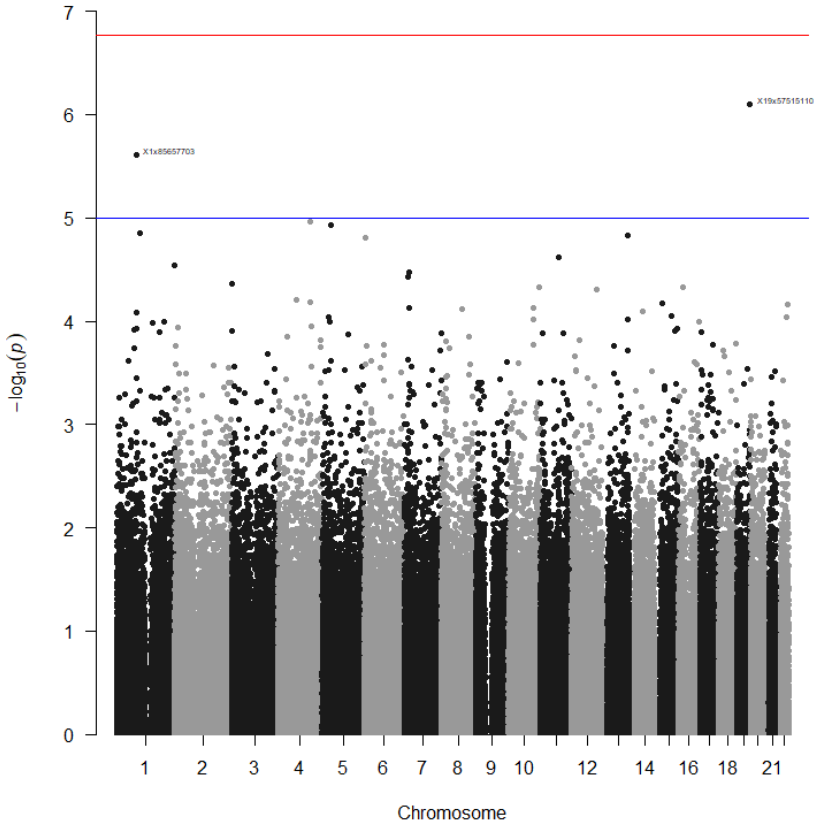

Figure K182: Manhattan plot of SNPs for arches on the right index finger for the dominant model

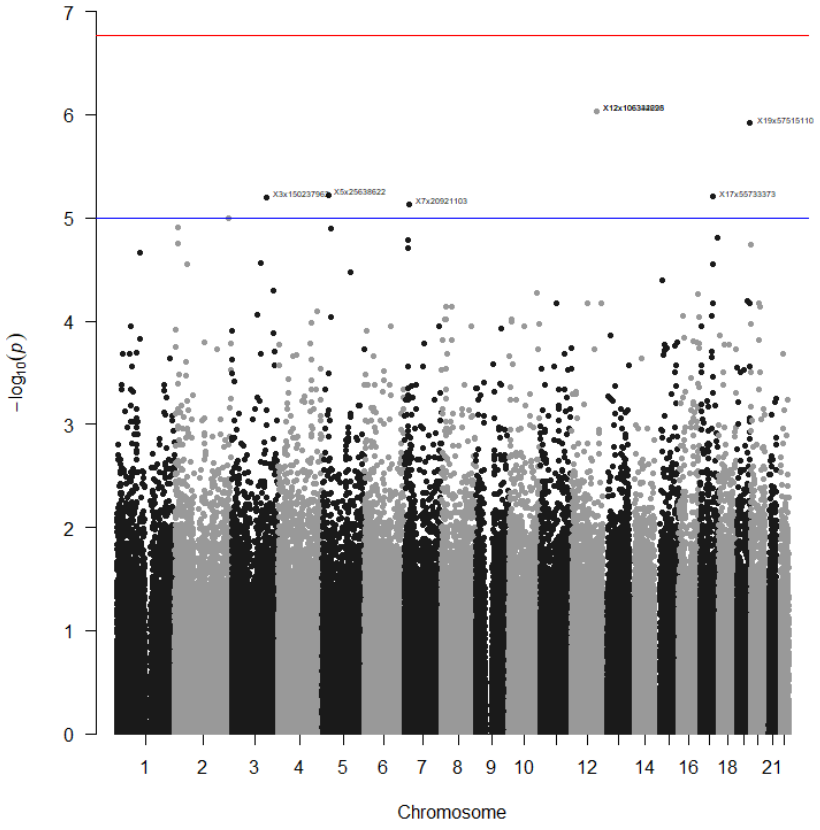

Figure K183: Manhattan plot of SNPs for arches on the right index finger for the log-additive model

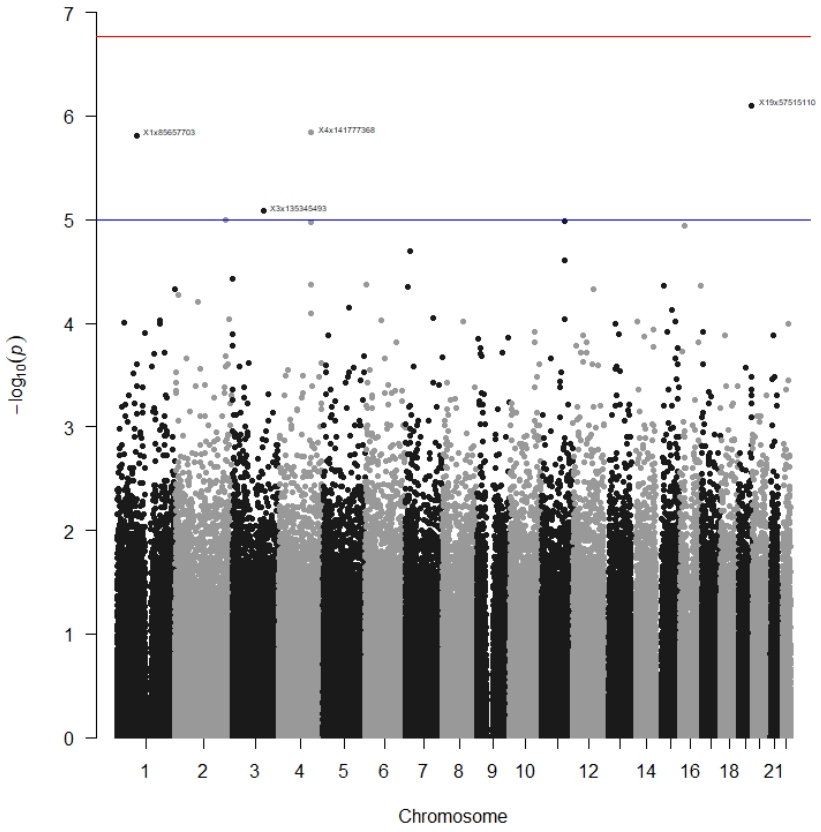

Figure K184: Manhattan plot of SNPs for arches on the right index finger for the overdominant model

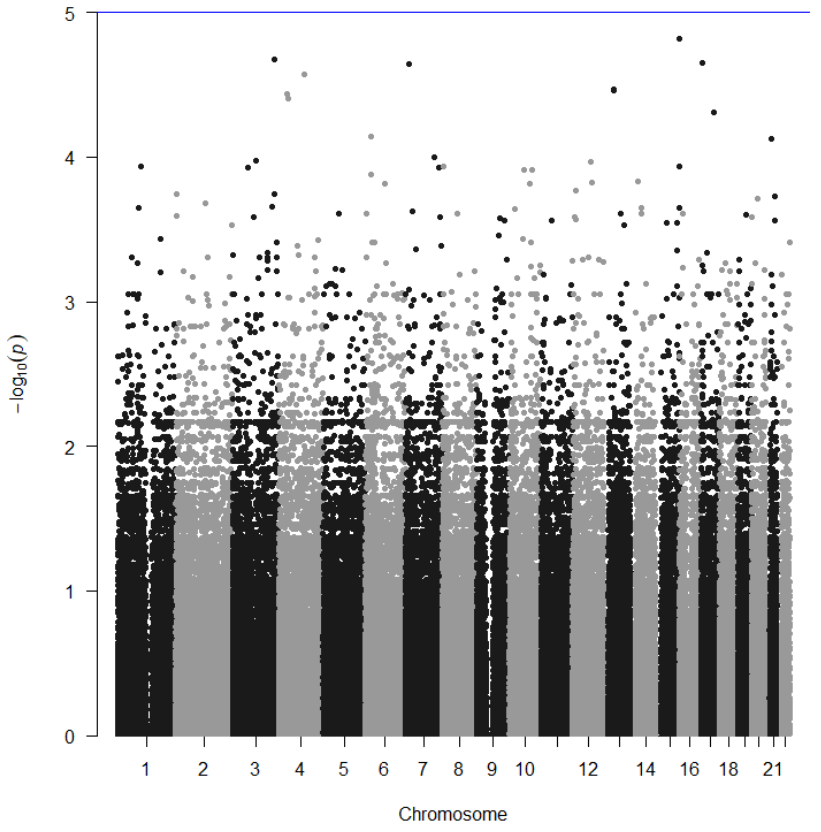

Figure K185: Manhattan plot of SNPs for arches on the right index finger for the recessive model

Arches on the left thumb

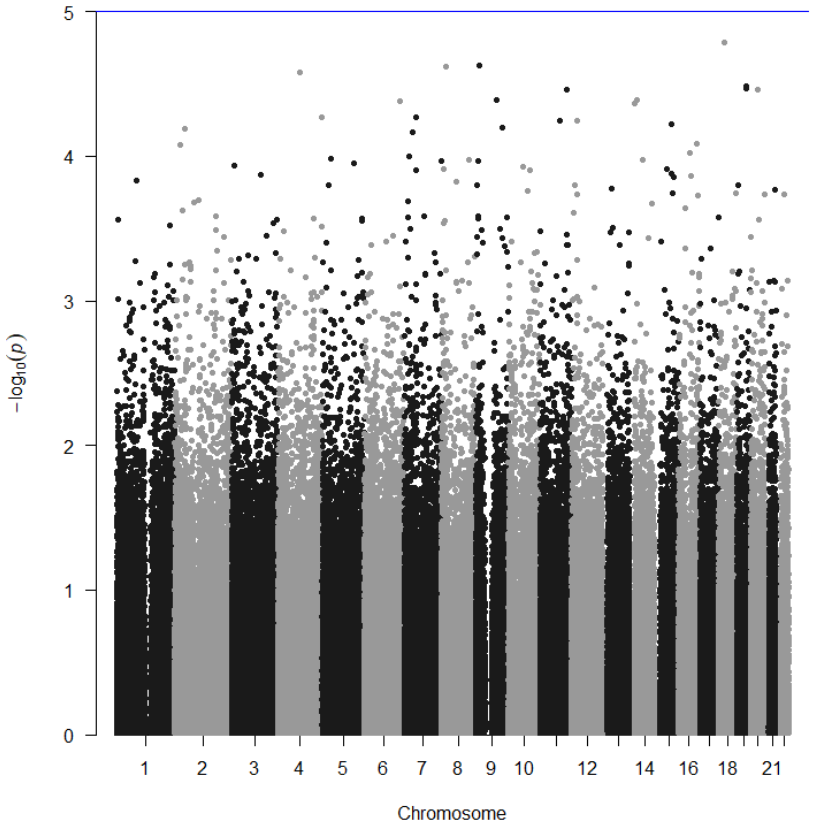

Figure K186: Manhattan plot of SNPs for arches on the left thumb for the codominant model

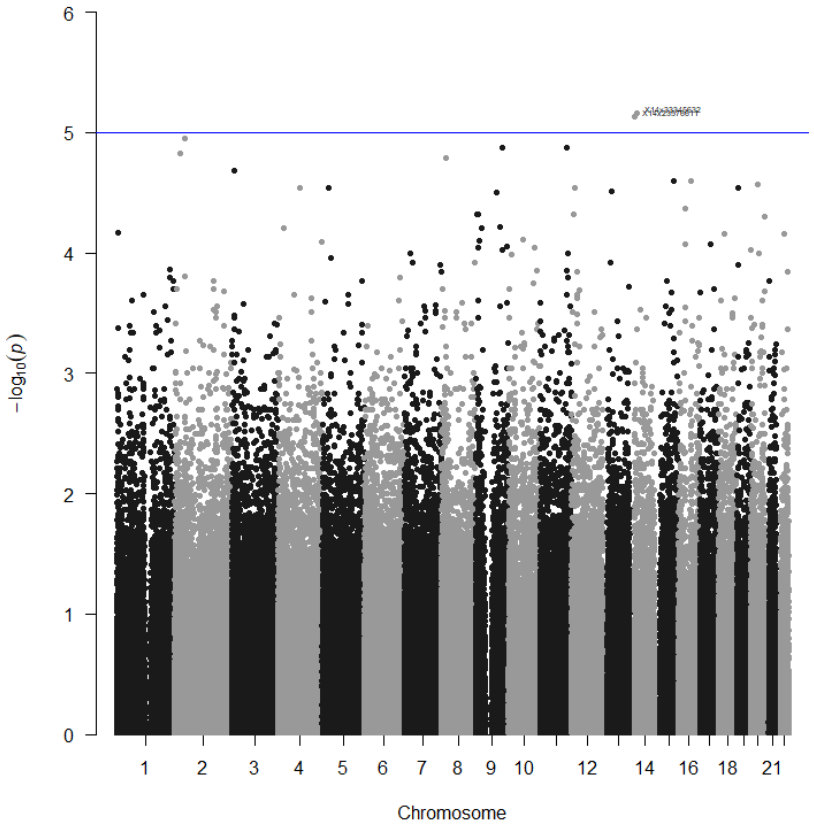

Figure K187: Manhattan plot of SNPs for arches on the left thumb for the dominant model

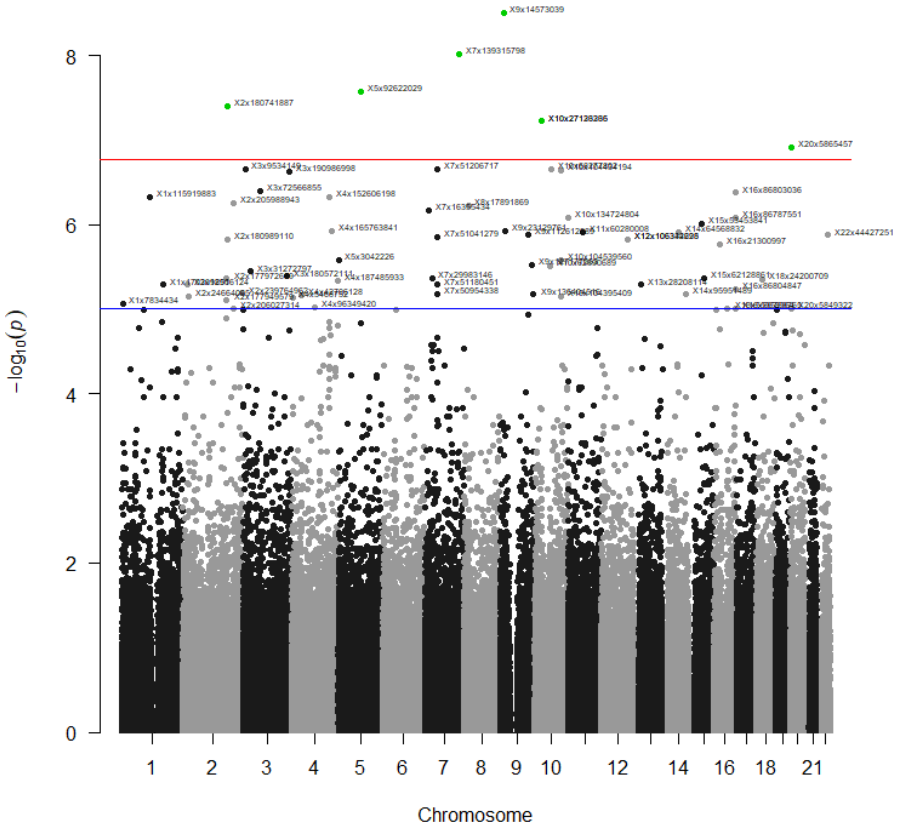

Figure K188: Manhattan plot of SNPs for arches on the left thumb for the log-additive model

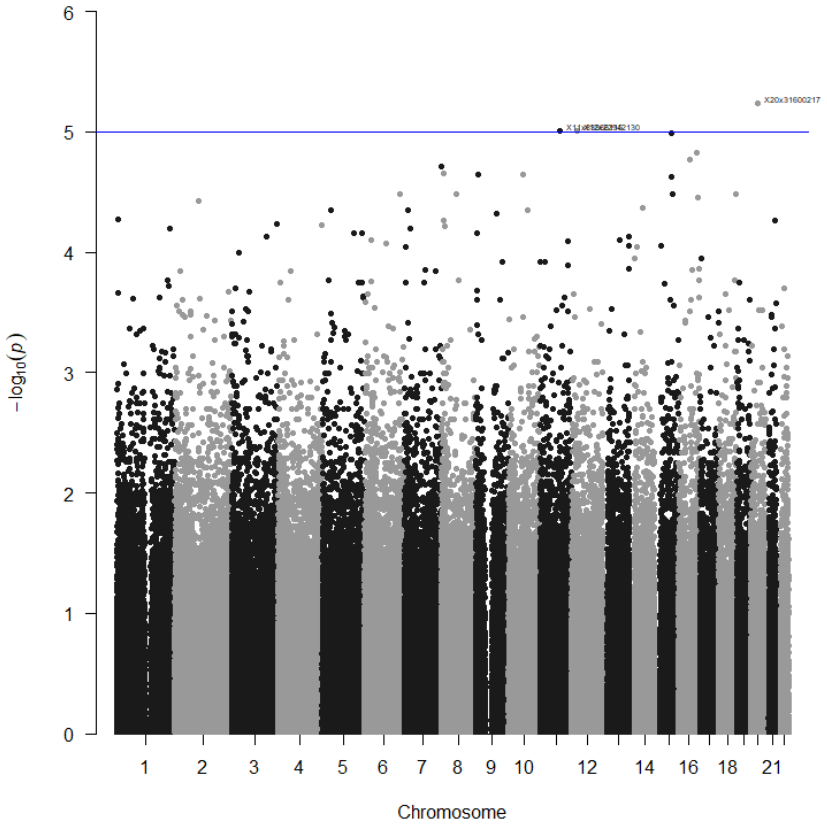

Figure K189: Manhattan plot of SNPs for arches on the left thumb for the overdominant model

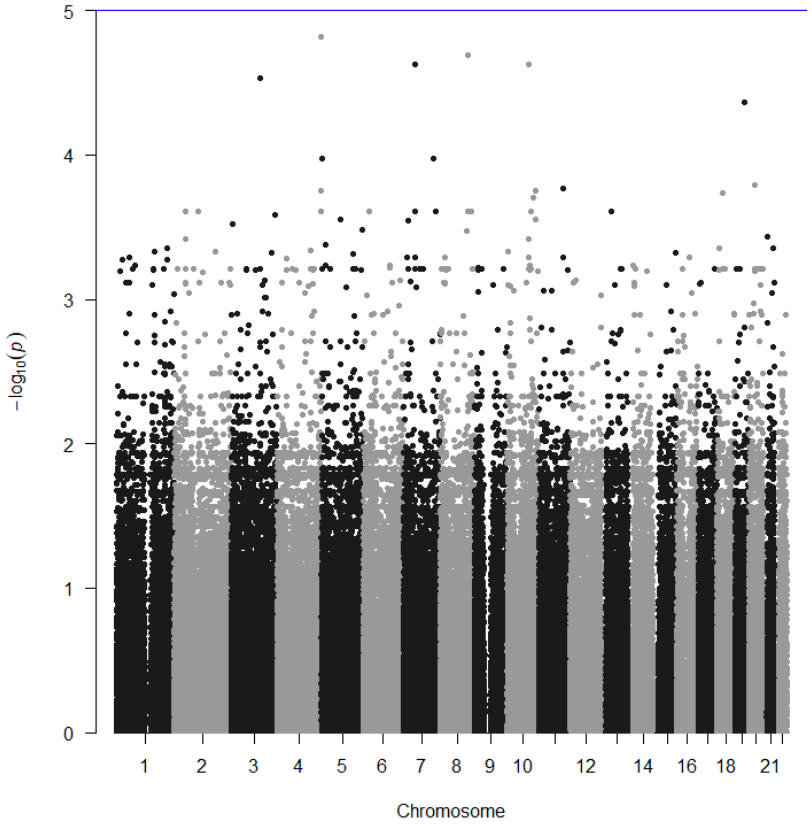

Figure K190: Manhattan plot of SNPs for arches on the left thumb for the recessive model

Arches on the right thumb

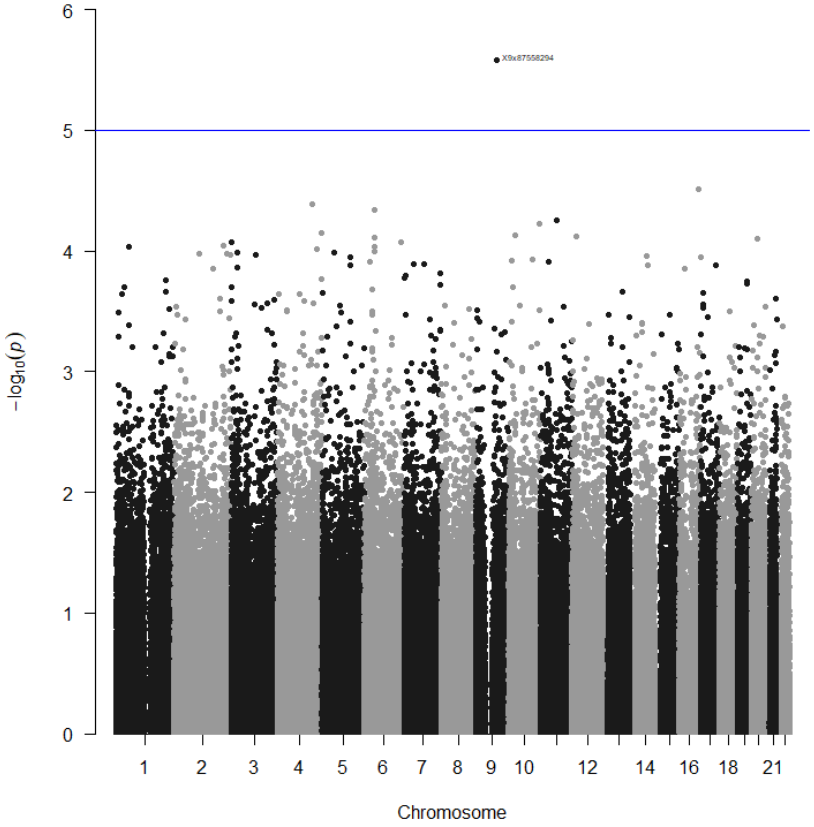

Figure K191: Manhattan plot of SNPs for arches on the right thumb for the codominant model

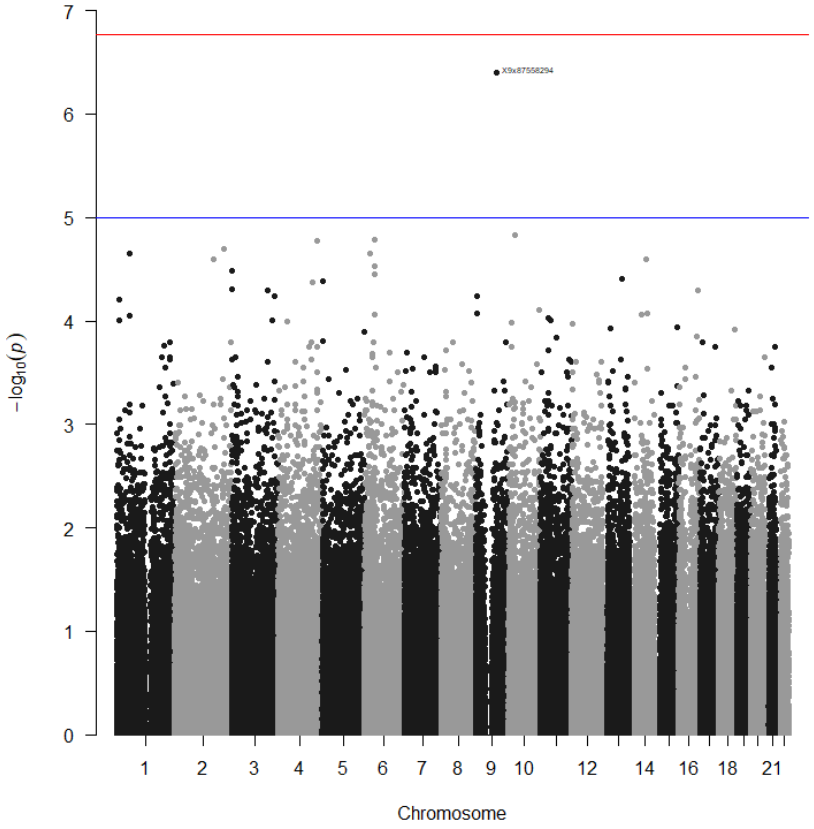

Figure K192: Manhattan plot of SNPs for arches on the right thumb for the dominant model

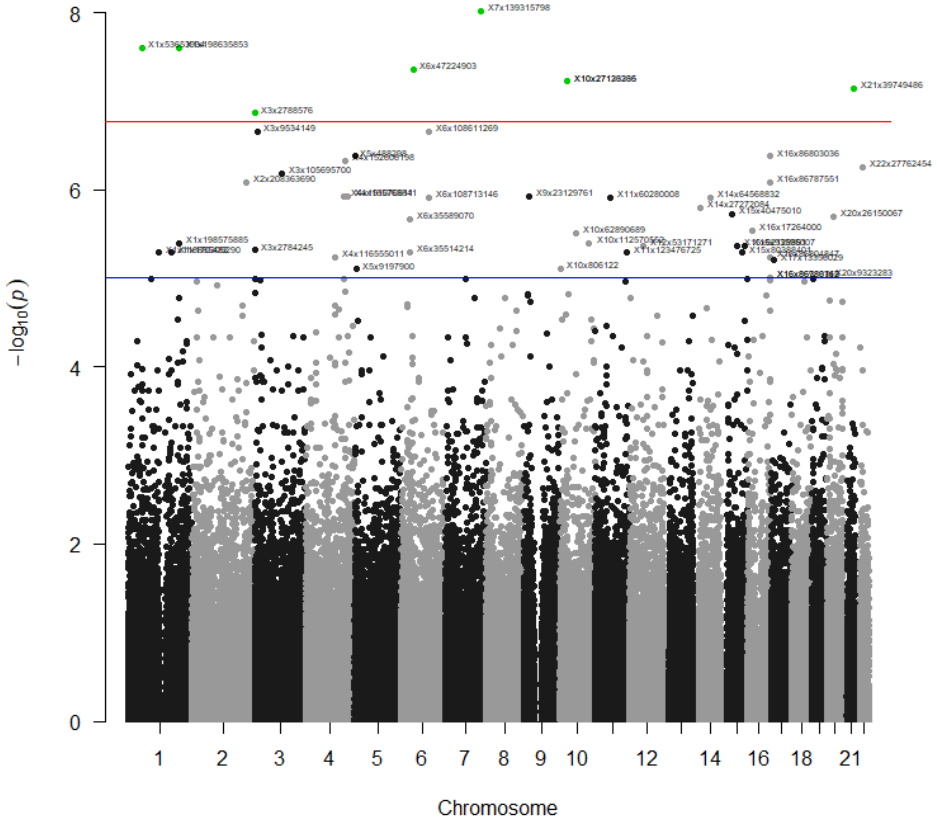

Figure K193: Manhattan plot of SNPs for arches on the right thumb for the log-additive model

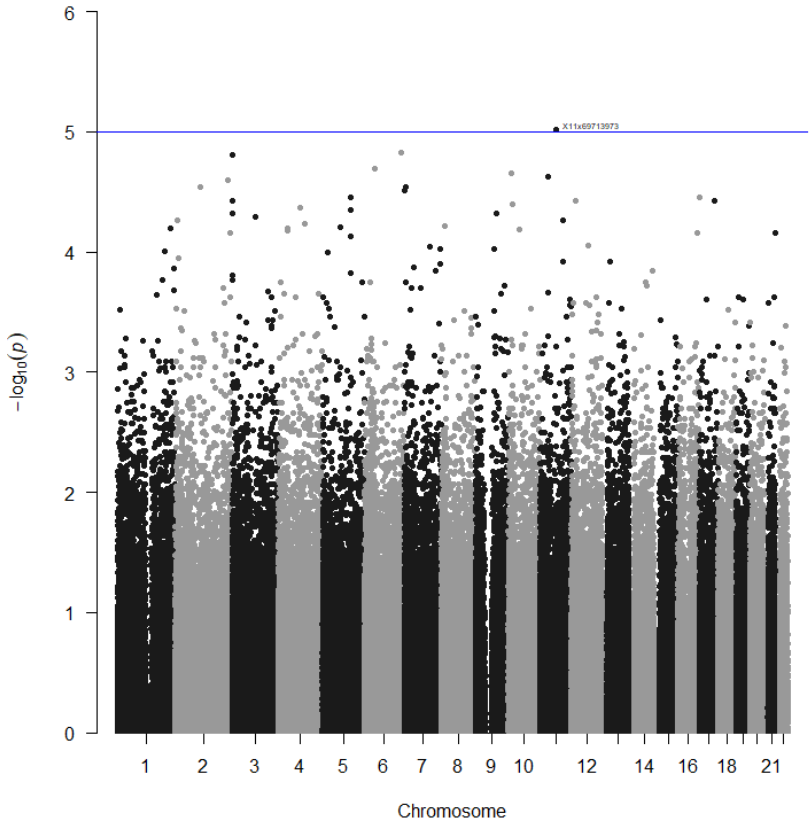

Figure K194: Manhattan plot of SNPs for arches on the right thumb for the overdominant model

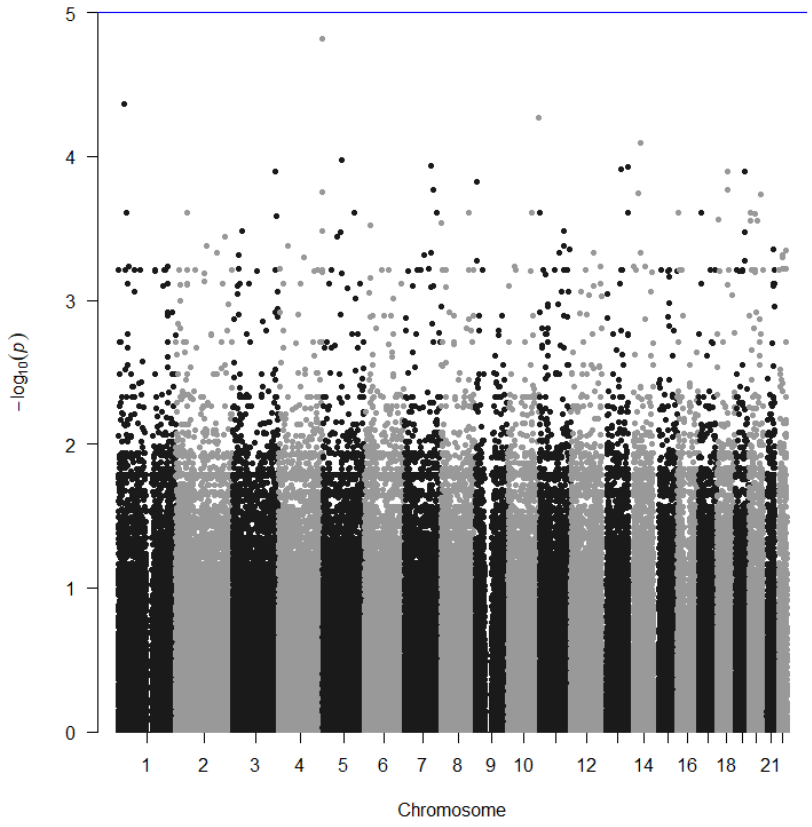

Figure K195: Manhattan plot of SNPs for arches on the right thumb for the recessive model

References

1. Wertheim, K. and Maceo, A., *The critical stage of friction ridge and pattern formation.* Journal of Forensic Identification, 2002. **52**(1): p. 35.
2. Kücken, M. and Newell, A.C., *Fingerprint Formation.* Journal of Theoretical Biology, 2005. **235**(1): p. 71-83.
3. Penrose, L. and Ohara, P., *The Development of the Epidermal Ridges.* Journal of Medical Genetics, 1973. **10**(3): p. 201.
4. Bonnevie, K., *Studies on papillary patterns of human fingers.* Journal of Genetics, 1924. **15**(1): p. 1-111.
5. Mardia, K., Li, Q., and Hainsworth, T., *On the Penrose hypothesis on fingerprint patterns.* Mathematical Medicine and Biology, 1992. **9**(4): p. 289-294.
6. Smith, C., *Note on the forms of dermatoglyphic patterns.* Birth Defects Original Article Series, 1979. **15**(6): p. 43-52.
7. Mulvihill, J.J. and Smith, D.W., *The genesis of dermatoglyphics.* The Journal of Pediatrics, 1969. **75**(4): p. 579-589.
8. Hirsch, W. and Schweighel, J., *Morphological evidence concerning the problem of skin ridge formation.* Journal of Intellectual Disability Research, 1973. **17**(1): p. 58-72.
9. Morohunfola, K.A., Jones, T.E., and Munger, B.L., *The differentiation of the skin and its appendages. II. Altered development of papillary ridges following neuralectomy.* The Anatomical Record, 1992. **232**(4): p. 599-611.
10. Champod, C., Lennard, C.J., Margot, P., and Stoilovic, M., *Fingerprints and other ridge skin impressions*. 2016, USA: CRC press.
11. Machado, J.F., Fernandes, P.R., Roquetti, R.W., and Filho, J.F., *Digital dermatoglyphic heritability differences as evidenced by a female twin study.* Twin Research and Human Genetics, 2010. **13**(5): p. 482-489.
12. Babler, W.J., *Embryologic development of epidermal ridges and their configurations.* Birth Defects Original Artical Series, 1991. **27**(2): p. 95-112.
13. Li, M., Wang, J., Li, Z., Zhang, J., Ni, C., Cheng, R., and Yao, Z., *Genome-wide linkage analysis and whole-genome sequencing identify a recurrent SMARCAD1 variant in a unique Chinese family with Basan syndrome.* European Journal of Human Genetics, 2016. **24**(9): p. 1367-1370.
14. Haber, R., Helou, J., Korkomaz, J., Habre, M., Ghanem, A., and Tomb, R., *Absence of fingertips with focus on dermatological etiologies; National Survey and Review.* Clinical Dermatology, 2015. **3**(1): p. 21-26.

15. Valentin, M.N., Solomon, B.D., Richard, G., Ferreira, C.R., and Kirkorian, A.Y., *Basan gets a new fingerprint: Mutations in the skin-specific isoform of SMARCAD1 cause ectodermal dysplasia syndromes with adermatoglyphia.* American Journal of Medical Genetics Part A, 2018. **176**(11): p. 2451-2455.
16. Ashbaugh, D.R., *The History of Friction Ridge Identification*, in *Quantitative-Qualitative Friction Ridge Analysis*. 1999, CRC Press: USA.
17. Hawthorne, M.R., *The History of Fingerprints*, in *Fingerprints*. 2008, CRC Press: USA. p. 3-13.
18. Hawthorne, M.R., *Fingerprint Pattern Types and Associated Terminology*, in *Fingerprints*. 2008, CRC Press: USA. p. 27-54.
19. Dale, C., *Fingerprint identification*, in *The Practice Of Crime Scene Investigation*. 2004, CRC Press: USA. p. 161-179.
20. Hawthorne, M.R., *Systematic Methods of Identification*, in *Fingerprints*. 2008, CRC Press: USA. p. 15-25.
21. Leo, W., *Fingerprint identification*. 2004, San Clemente, USA: LawTech Custom Publishing.
22. Walton, A., Moret, S., Barash, M., and Gunn, P., *The frequency of fingerprint patterns separated by ethnicity and sex in a general population from Sydney, Australia.* Australian Journal of Forensic Sciences, 2019: p. 1-6.
23. Temaj, G., Škarić-Jurić, T., Tomas, Ž., Behluli, I., Smolej Narančić, N., Sopi, R., Jakupi, M., and Miličić, J., *Qualitative dermatoglyphic traits in monozygotic and dizygotic twins of Albanian population in Kosovo.* HOMO - Journal of Comparative Human Biology, 2012. **63**(6): p. 459-467.
24. Ashbaugh, D.R., *The Friction Ridge Medium*, in *Quantitative-Qualitative Friction Ridge Analysis*. 1999, CRC Press: USA.
25. Holt, S.B., *Genetics of Dermal Ridges: Bilateral Asymmetry in Finger Ridge-Counts.* Annals of Human Eugenics, 1952. **17**(1): p. 211-231.
26. Fournier, N.A. and Ross, A.H., *Sex, Ancestral, and Pattern Type Variation of Fingerprint Minutiae: A Forensic Perspective on Anthropological Dermatoglyphics.* American Journal of Physical Anthropology, 2015. **160**(4): p. 625-632.
27. Holder, E.H., Robinson, L.O., Laub, J.H., and National Institute of, J., *The fingerprint sourcebook*. 2011, Washington, DC: U.S. Department. of Justice, Office of Justice Programs, National Institute of Justice.
28. Galton, F., *Finger Prints*. 1892, London, UK: McMillan & Co., New York.

29. Cummins, H., *Racial Differences in Finger-prints.* Journal of Criminal Law and Criminology, 1935. **25**(5): p. 829.
30. Acree, M.A., *Is there a gender difference in fingerprint ridge density?* Forensic Science International, 1999. **102**(1): p. 35-44.
31. Cummins, H., Waits, W.J., and McQuitty, J.T., *The breadths of epidermal ridges on the finger tips and palms: A study of variation.* American Journal of Anatomy, 1941. **68**(1): p. 127-150.
32. David, T., *Distribution, age and sex variation of the mean epidermal ridge breadth.* Human Heredity, 1981. **31**(5): p. 279-282.
33. Gutiérrez-Redomero, E., Alonso, C., Romero, E., and Galera, V., *Variability of fingerprint ridge density in a sample of Spanish Caucasians and its application to sex determination.* Forensic Science International, 2008. **180**(1): p. 17-22.
34. Joyner, J., *United States of America v Byron Mitchell*, U.S.D. COURT and F.T.E.D.O. PENNSYLVANIA, Editors. 2007: Pennsylvania, USA.
35. Kaye, D.H. *Questioning a Courtroom Proof of the Uniqueness of Fingerprints*. International Statistical Review, 2003. **71**, 521-533.
36. Pankanti, S., Prabhakar, S., and Jain, A.K., *On the individuality of fingerprints.* IEEE Transactions on pattern analysis and machine intelligence, 2002. **24**(8): p. 1010-1025.
37. Jiansheng, C. and Yiu-Sang, M. *The statistical modelling of fingerprint minutiae distribution with implications for fingerprint individuality studies*. in *2008 IEEE Conference on Computer Vision and Pattern Recognition*. 2008.
38. Han, Y., Ryu, C., Moon, J., Kim, H., and Choi, H. *A Study on Evaluating the Uniqueness of Fingerprints Using Statistical Analysis*. 2005. Berlin, Heidelberg: Springer Berlin Heidelberg.
39. Cole, S.A., *Forensics without uniqueness, conclusions without individualization: the new epistemology of forensic identification.* Law, probability and risk, 2009. **8**(3): p. 233-255.
40. Page, M., Taylor, J., and Blenkin, M., *Uniqueness in the forensic identification sciences—Fact or fiction?* Forensic Science International, 2011. **206**(1): p. 12-18.
41. Neumann, C., Evett, I.W., and Skerrett, J., *Quantifying the weight of evidence from a forensic fingerprint comparison: a new paradigm.* Journal of the Royal Statistical Society: Series A (Statistics in Society), 2012. **175**(2): p. 371-415.
42. Thompson, W.C. and Newman, E.J., *Lay understanding of forensic statistics: Evaluation of random match probabilities, likelihood ratios, and verbal equivalents.* Law and Human Behavior, 2015. **39**(4): p. 332-349.

43. Hendricks, J., Neumann, C., and Saunders, C.P., *Quantification of the weight of fingerprint evidence using a ROC-based Approximate Bayesian Computation algorithm for model selection.* Electronic Journal of Statistics, 2021. **15**(1): p. 1228-1262, 35.
44. Walker, J.F., *A Sex Linked Recessive Fingerprint Pattern.* Journal of Heredity, 1941. **32**(8): p. 279-280.
45. Wilder, H.H., *Physical Correspondences in Two Sets of Duplicate Twins: Striking Degree of Identity Shown in Bodily Measurements and Skin Patterns of Palms and Soles.* Journal of Heredity, 1919. **10**(9): p. 410-422.
46. McKusick, V.A. *Personal Communication in OMIM® Online Mendelian Inheritance in Man. MIM Number: 31220*. 1986 Last updated 28/2/1994. [Accessed 25/07/2016]; Available from: http://www.omim.org/entry/312200.
47. Holt, S., *The Genetics of Dermal Ridges*. 1968, Springfield, Illinois: Thomas.
48. Holt, S.B., *Genetics of Dermal Ridges: Inheritance of Total Finger Ridge-Count.* Annals of Human Eugenics, 1953. **18**(1): p. 140-161.
49. Holt, S.B., *Genetics of Dermal Ridges: Frequency Distributions of Total Finger Ridge-Count.* Annals of Human Eugenics, 1955. **20**(2): p. 159-70.
50. Holt, S.B., *Genetics of Dermal Ridges: Parent-Child Correlations For Total Finger Ridge-Count.* Annals of Human Eugenics, 1956. **20**(4): p. 270-81.
51. Holt, S.B., *Genetics of Dermal Ridges: Sib Pair Correlations For Total Finger Ridge-Count.* Annals of Human Eugenics, 1957. **21**(4): p. 352-362.
52. Holt, S.B., *Genetics of Dermal Ridges: Familial Correlations For (S/Check10), A Measurement of the Diversity of Ridgecounts From Finger to Finger.* Annals of Human Eugenics, 1960. **24**(3): p. 253-69.
53. Slatis, H.M., Katznelson, M.B., and Bonné-Tamir, B., *The inheritance of fingerprint patterns.* American Journal of Human Genetics, 1976. **28**(3): p. 280-289.
54. Medland, S.E., Loesch, D.Z., Mdzewski, B., Zhu, G., Montgomery, G.W., and Martin, N.G., *Linkage analysis of a model quantitative trait in humans: finger ridge count shows significant multivariate linkage to 5q14.1.* PLoS Genetics, 2007. **3**(9): p. 1736-44.
55. Ho, Y.Y., Evans, D.M., Montgomery, G.W., Henders, A.K., Kemp, J.P., Timpson, N.J., St Pourcain, B., Heath, A.C., Madden, P.A., Loesch, D.Z., McNevin, D., Daniel, R., Davey-Smith, G., Martin, N.G., and Medland, S.E., *Common Genetic Variants Influence Whorls in Fingerprint Patterns.* The Journal of Investigative Dermatology, 2016. **136**(4): p. 859-62.
56. Vecchi, D. and Hernández Aguirre, I., *The epistemological resilience of the concept of morphogenetic field*. 2014. p. 79-94.

57. Yao, J., Zhou, B., Zhang, J., Geng, P., Liu, K., Zhu, Y., and Zhu, W., *A new tumor suppressor LncRNA ADAMTS9-AS2 is regulated by DNMT1 and inhibits migration of glioma cells.* Tumor Biology, 2014. **35**(8): p. 7935-7944.
58. Zhang, J.-w., Rubio, V., Zheng, S., and Shi, Z.-z., *Knockdown of OLA1, a regulator of oxidative stress response, inhibits motility and invasion of breast cancer cells.* Journal of Zhejiang University SCIENCE B, 2009. **10**(11): p. 796-804.
59. Loyal, J. and Laub, D.R., *Ulnar-Mammary Syndrome: Clinical Presentation, Genetic Underpinnings, Diagnosis, and Treatment.* Eplasty, 2014. **14**: p. ic35.
60. Nousbeck, J., Burger, B., Fuchs-Telem, D., Pavlovsky, M., Fenig, S., Sarig, O., Itin, P., and Sprecher, E., *A Mutation in a Skin-Specific Isoform of SMARCAD1 Causes Autosomal-Dominant Adermatoglyphia.* The American Journal of Human Genetics, 2011. **89**(2): p. 302-307.
61. Nousbeck, J., Sarig, O., Magal, L., Warshauer, E., Burger, B., Itin, P., and Sprecher, E., *Mutations in SMARCAD1 cause autosomal dominant adermatoglyphia and perturb the expression of epidermal differentiation-associated genes.* The British Journal of Dermatology, 2014. **171**(6): p. 1521-4.
62. David, T.J., *'Ridges-off-the-End' – A Dermatoglyphic Syndrome.* Human Heredity, 1971. **21**(1): p. 39-53.
63. David, T.J., *Ridges-off-the-End Syndrome in Two Families, and a Third Family with a New Syndrome.* Human Heredity, 1973. **23**(1): p. 32-41.
64. David, T.J., *Congenital malformations of human dermatoglyphs.* Archives of disease in childhood, 1973. **48**(3): p. 191-198.
65. David, T.J., Darke, C., Bender, K., and Ray, B.D., *Linkage Study on the 'Ridges-off-the-End' and Nelson Syndromes.* Human Heredity, 1973. **23**(3): p. 280-287.
66. Dogramaci, A., Yenin, J., Bagriacik, M., and Savas, N., *Dermatoglyphs in patients with psoriasis.* Journal of the European Academy of Dermatology and Venereology, 2010. **24**(1): p. 88-89.
67. Grjibovski, A., Olsen, A., Magnus, P., and Harris, J., *Psoriasis in Norwegian twins: contribution of genetic and environmental effects.* Journal of the European Academy of Dermatology and Venereology, 2007. **21**(10): p. 1337-1343.
68. Wong, M., Choo, S.-P., and Tan, E.-H., *Travel warning with capecitabine.* Annals of Oncology, 2009. **20**(7): p. 1281-1281.
69. Yoon, S., Feng, J., and Jain, A.K., *Altered fingerprints: Analysis and detection.* Pattern Analysis and Machine Intelligence, IEEE Transactions on, 2012. **34**(3): p. 451-464.

70. Bush, N.J. and Hartkopf Smith, L., *Hand-Foot Syndrome.* Oncology Nursing Forum, 2001. **28**(10): p. 1519-1520.
71. Abbasi, S. and Rasouli, M., *Association between gastrointestinal cancers and fingerprint patterns in the Iranian population.* Genetics and molecular research: GMR, 2017. **16**(3).
72. Shakibaei, F., Asadollahi, G.A., and Tabibi, A., *Dermatoglyphics in patients with schizophrenia.* Journal of Research in Medical Sciences : The Official Journal of Isfahan University of Medical Sciences, 2011. **16**(8): p. 1055-1061.
73. Pahuja, K. and Agarwal, S., *Analysis of the Qualitative and Quantitative Dermatoglyphic Traits in Schizophrenia Patients.* Journal of Anatomical Society of India, 2012. **61**(2): p. 269-272.
74. Katznelson, M.B.-M., Bejerano, M., Yakovenko, K., and Kobyliansky, E., *Relationship between genetic anomalies of different levels and deviations in dermatoglyphic traits. Part 4: Dermatoglyphic peculiarities of males and females with Down syndrome. Family study.* Anthropologischer Anzeiger, 1999: p. 193-255.
75. Rajangam, S., Janakiram, S., and Thomas, I., *Dermatoglyphics in Down's syndrome.* Journal of the Indian Medical Association, 1995. **93**(1): p. 10-13.
76. Matsuyama, N. and Ito, Y., *The frequency of fingerprint type in parents of children with Trisomy 21 in Japan.* Journal of physiological anthropology, 2006. **25**(1): p. 15-21.
77. Alter, M., Gorlin, R., Yunis, J., Peagler, F., and Bruhl, H., *Dermatoglyphics in XXYY Klinefelter's syndrome.* American journal of human genetics, 1966. **18**(6): p. 507.
78. Komatz, Y. and Yoshida, O., *Finger patterns and ridge counts of patients with Klinefelter's syndrome (47, XXY) among the Japanese.* Human heredity, 1976. **26**(4): p. 290-297.
79. Reed, T., Reichmann, A., and Palmer, C., *Dermatoglyphic differences between 45, X and other chromosomal abnormalities of Turner syndrome.* Human genetics, 1977. **36**(1): p. 13-23.
80. Kashinathappa, B.S., *Study of palmar dermatoglyphics in carcinoma of cervix.* International Journal of Current Research and Review, 2013. **5**(4): p. 136.
81. Prabha, L.J. and Thenmozhi, R., *A short review on dermatoglyphics.* Journal of Pharmaceutical Sciences and Research, 2014. **6**(4): p. 200.
82. Lal, N. and Sureka, R., *A study of dermatoglyphic patterns in epileptic patients.* Journal of Anatomical Society of India, 2012. **61**(1): p. 26-29.

83. Jatti, D., Kantraj, Y.D.B., and Nagaraju, R., *Role of dermatoglyphics in malignant and potentially malignant disorders of the oral cavity: A cross-sectional study.* Journal of Indian Academy of Oral Medicine and Radiology, 2014. **26**(4): p. 379.
84. Abbasi, S., Einollahi, N., Dashti, N., and Vaez-Zadeh, F., *Study of dermatoglyphic patterns of hands in women with breast cancer.* Pakistan Journal of Medical Sciences, 2006. **22**(1): p. 18.
85. Chintamani, Khandelwal, R., Mittal, A., Saijanani, S., Tuteja, A., Bansal, A., Bhatnagar, D., and Saxena, S., *Qualitative and quantitative dermatoglyphic traits in patients with breast cancer: a prospective clinical study.* BMC Cancer, 2007. **7**(1): p. 44.
86. Raizada, A., Johri, V., Ramnath, T., Chowdhary, D., and Garg, R., *A cross-sectional study on the palmar dermatoglyphics in relation to carcinoma breast patients.* Journal of Clinical and Diagnostic Research: JCDR, 2013. **7**(4): p. 609.
87. Sariri, E., Kashanian, M., Vahdat, M., and Yari, S., *Comparison of the dermatoglyphic characteristics of women with and without breast cancer.* European Journal of Obstetrics & Gynecology and Reproductive Biology, 2012. **160**(2): p. 201-204.
88. Sridevi, N., Delphine Silvia, C., Kulkarni, R., and Seshagiri, C., *Palmar dermatoglyphics in carcinoma breast of Indian women.* Rom J Morphol Embryol, 2010. **51**(3): p. 547-50.
89. Wijerathne, B.T., Meier, R.J., Agampodi, T.C., and Agampodi, S.B., *Dermatoglyphics in hypertension: a review.* Journal of physiological anthropology, 2015. **34**(1): p. 29.
90. Rignell, A. and SJÖQVIST, K.E., *A Swedish method of fingerprint classification.* Hereditas, 1983. **98**(1): p. 115-125.
91. Ankel-Simons, F., *Primate Anatomy*. 2010, London, USA: Academic Press.
92. *Fingerprints of Koalas, Humans and chimpanzees*. 2011, Asian Dermatoglyphic Research Centre: Singapore.
93. Henneberg, M., Lambert, K.M., and Leigh, C. *Fingerprinting a chimpanzee and a koala: Animal dermatoglyphics can resemble human ones*. in *Proceedings of the Conference of the Australian and New Zealand International Symposium on the Forensic Sciences 1996*. 1998.
94. Henneberg, M., Lambert, K., and Leigh, C., *Fingerprint homoplasy: koalas and humans.* Natural Science, 1997. **1**: p. 4-6.
95. Jones, L.A. and Lederman, S.J., *Human hand function*. 2006, New York, USA: Oxford University Press.
96. Warman, P.H. and Ennos, A.R., *Fingerprints are unlikely to increase the friction of primate fingerpads.* Journal of Experimental Biology, 2009. **212**(13): p. 2016-2022.
97. Budrikis, Z., *Getting a grip on fingerprints.* Nature Reviews Physics, 2021. **3**(1): p. 5-5.

98. Yum, S.-M., Baek, I.-K., Hong, D., Kim, J., Jung, K., Kim, S., Eom, K., Jang, J., Kim, S., Sattorov, M., Lee, M.-G., Kim, S., Adams, M.J., and Park, G.-S., *Fingerprint ridges allow primates to regulate grip.* Proceedings of the National Academy of Sciences, 2020: p. 202001055.

99. Begum, F., Ghosh, D., Tseng, G.C., and Feingold, E., *Comprehensive literature review and statistical considerations for GWAS meta-analysis.* Nucleic acids research, 2012. **40**(9): p. 3777-3784.

100. Bush, W.S. and Moore, J.H. *Chapter 11: Genome-Wide Association Studies*. PLoS Computational Biology, 2012. **8**, e1002822 DOI: 10.1371/journal.pcbi.1002822.

101. Rees, J.L., *Genetics of hair and skin color.* Annual review of genetics, 2003. **37**(1): p. 67-90.

102. Shen, C., Gao, J., Sheng, Y., Dou, J., Zhou, F., Zheng, X., Ko, R., Tang, X., Zhu, C., and Yin, X., *Genetic susceptibility to vitiligo: GWAS approaches for identifying vitiligo susceptibility genes and loci.* Frontiers in genetics, 2016. **7**: p. 3.

103. de Jongh, A., Lubach, A.R., Lie, K.S.L., and Alberink, I., *Measuring the Rarity of Fingerprints Patterns in the Dutch Population Using an Extended Classification Set.* Journal of Forensic Sciences, 2018. **0**(0).

104. Stambouli, H., El Bouri, A., Tijani, N., El Baghdadi, M., and Rhazaf, A., *Occurrence of fingerprint patterns in the Moroccan population.* Canadian Society of Forensic Science Journal, 2015. **48**(4): p. 160-166.

105. Swofford, H.J., *Fingerprint patterns: a study on the finger and ethnicity prioritized order of occurrence.* Journal of Forensic Identification, 2005. **55**(4): p. 480.

106. Henn, B.M., Cavalli-Sforza, L.L., and Feldman, M.W., *The great human expansion.* Proceedings of the National Academy of Sciences, 2012. **109**(44): p. 17758.

107. Barreiro, L.B., Laval, G., Quach, H., Patin, E., and Quintana-Murci, L., *Natural selection has driven population differentiation in modern humans.* Nature genetics, 2008. **40**(3): p. 340.

108. Burke, D.F., Worth, C.L., Priego, E.-M., Cheng, T., Smink, L.J., Todd, J.A., and Blundell, T.L., *Genome bioinformatic analysis of nonsynonymous SNPs.* BMC bioinformatics, 2007. **8**: p. 301-301.

109. Capon, F., Allen, M.H., Ameen, M., Burden, A.D., Tillman, D., Barker, J.N., and Trembath, R.C., *A synonymous SNP of the corneodesmosin gene leads to increased mRNA stability and demonstrates association with psoriasis across diverse ethnic groups.* Hum Mol Genet, 2004. **13**(20): p. 2361-8.

110. Duan, J., Wainwright, M.S., Comeron, J.M., Saitou, N., Sanders, A.R., Gelernter, J., and Gejman, P.V., *Synonymous mutations in the human dopamine receptor D2 (DRD2) affect mRNA stability and synthesis of the receptor.* Human Molecular Genetics, 2003. **12**(3): p. 205-216.

111. Chamary, J.V. and Hurst, L.D., *Evidence for selection on synonymous mutations affecting stability of mRNA secondary structure in mammals.* Genome Biology, 2005. **6**(9): p. R75.

112. Wang, E.T., Sandberg, R., Luo, S., Khrebtukova, I., Zhang, L., Mayr, C., Kingsmore, S.F., Schroth, G.P., and Burge, C.B., *Alternative isoform regulation in human tissue transcriptomes.* Nature, 2008. **456**(7221): p. 470-476.

113. Pan, Q., Shai, O., Lee, L.J., Frey, B.J., and Blencowe, B.J., *Deep surveying of alternative splicing complexity in the human transcriptome by high-throughput sequencing.* Nature Genetics, 2008. **40**(12): p. 1413-1415.

114. González-Neira, A., Ke, X., Lao, O., Calafell, F., Navarro, A., Comas, D., Cann, H., Bumpstead, S., Ghori, J., Hunt, S., Deloukas, P., Dunham, I., Cardon, L.R., and Bertranpetit, J., *The portability of tagSNPs across populations: a worldwide survey.* Genome Res, 2006. **16**(3): p. 323-30.

115. *The International HapMap Project.* Nature, 2003. **426**(6968): p. 789-796.

116. Ellegren, H., *Microsatellites: simple sequences with complex evolution.* Nature Reviews Genetics, 2004. **5**(6): p. 435-445.

117. Senge, T., Madea, B., Junge, A., Rothschild, M.A., and Schneider, P.M., *STRs, mini STRs and SNPs – A comparative study for typing degraded DNA.* Legal Medicine, 2011. **13**(2): p. 68-74.

118. Westen, A.A., Kraaijenbrink, T., Robles de Medina, E.A., Harteveld, J., Willemse, P., Zuniga, S.B., van der Gaag, K.J., Weiler, N.E.C., Warnaar, J., Kayser, M., Sijen, T., and de Knijff, P., *Comparing six commercial autosomal STR kits in a large Dutch population sample.* Forensic Science International: Genetics, 2014. **10**: p. 55-63.

119. Buckleton, J.S., Bright, J.A., Gittelson, S., Moretti, T.R., Onorato, A.J., Bieber, F.R., Budowle, B., and Taylor, D.A., *The Probabilistic Genotyping Software STRmix: Utility and Evidence for its Validity.* J Forensic Sci, 2019. **64**(2): p. 393-405.

120. Alonso, A., Barrio, P.A., Müller, P., Köcher, S., Berger, B., Martin, P., Bodner, M., Willuweit, S., Parson, W., Roewer, L., and Budowle, B., *Current state-of-art of STR sequencing in forensic genetics.* Electrophoresis, 2018. **39**(21): p. 2655-2668.

121. Bornman, D.M., Hester, M.E., Schuetter, J.M., Kasoji, M.D., Minard-Smith, A., Barden, C.A., Nelson, S.C., Godbold, G.D., Baker, C.H., Yang, B., Walther, J.E., Tornes, I.E., Yan,

P.S., Rodriguez, B., Bundschuh, R., Dickens, M.L., Young, B.A., and Faith, S.A., *Short-read, high-throughput sequencing technology for STR genotyping.* BioTechniques. Rapid dispatches, 2012. **2012**: p. 1-6.

122. Kidd, K.K., Pakstis, A.J., Speed, W.C., Lagace, R., Chang, J., Wootton, S., and Ihuegbu, N., *Microhaplotype loci are a powerful new type of forensic marker.* Forensic Science International: Genetics Supplement Series, 2013. **4**(1): p. e123-e124.
123. Kidd, K.K. and Speed, W.C., *Criteria for selecting microhaplotypes: mixture detection and deconvolution.* Investigative Genetics, 2015. **6**(1): p. 1.
124. Chen, P., Deng, C., Li, Z., Pu, Y., Yang, J., Yu, Y., Li, K., Li, D., Liang, W., Zhang, L., and Chen, F., *A microhaplotypes panel for massively parallel sequencing analysis of DNA mixtures.* Forensic Sci Int Genet, 2019. **40**: p. 140-149.
125. Pang, J.-B., Rao, M., Chen, Q.-F., Ji, A.-Q., Zhang, C., Kang, K.-L., Wu, H., Ye, J., Nie, S.-J., and Wang, L., *A 124-plex Microhaplotype Panel Based on Next-generation Sequencing Developed for Forensic Applications.* Scientific Reports, 2020. **10**(1): p. 1945.
126. Standage, D.S. and Mitchell, R.N., *MicroHapDB: A Portable and Extensible Database of All Published Microhaplotype Marker and Frequency Data.* Front Genet, 2020. **11**: p. 781.
127. Kayser, M., *Forensic use of Y-chromosome DNA: a general overview.* Human genetics, 2017. **136**(5): p. 621-635.
128. Amorim, A., Fernandes, T., and Taveira, N., *Mitochondrial DNA in human identification: a review.* PeerJ, 2019. **7**: p. e7314-e7314.
129. Butler, J.M., Coble, M.D., and Vallone, P.M., *STRs vs. SNPs: thoughts on the future of forensic DNA testing.* Forensic science, medicine, and pathology, 2007. **3**(3): p. 200-205.
130. Gill, P., *An assessment of the utility of single nucleotide polymorphisms (SNPs) for forensic purposes.* Int J Legal Med, 2001. **114**(4-5): p. 204-10.
131. Ludeman, M.J., Zhong, C., Mulero, J.J., Lagacé, R.E., Hennessy, L.K., Short, M.L., and Wang, D.Y., *Developmental validation of GlobalFiler™ PCR amplification kit: a 6-dye multiplex assay designed for amplification of casework samples.* International Journal of Legal Medicine, 2018. **132**(6): p. 1555-1573.
132. Mehta, B., Daniel, R., Phillips, C., and McNevin, D., *Forensically relevant SNaPshot((R)) assays for human DNA SNP analysis: a review.* Int J Legal Med, 2017. **131**(1): p. 21-37.
133. Kidd, K.K., Pakstis, A.J., Speed, W.C., Grigorenko, E.L., Kajuna, S.L., Karoma, N.J., Kungulilo, S., Kim, J.J., Lu, R.B., Odunsi, A., Okonofua, F., Parnas, J., Schulz, L.O.,

Zhukova, O.V., and Kidd, J.R., *Developing a SNP panel for forensic identification of individuals.* Forensic Sci Int, 2006. **164**(1): p. 20-32.

134. Freire-Aradas, A., Fondevila, M., Kriegel, A.K., Phillips, C., Gill, P., Prieto, L., Schneider, P.M., Carracedo, A., and Lareu, M.V., *A new SNP assay for identification of highly degraded human DNA.* Forensic Sci Int Genet, 2012. **6**(3): p. 341-9.
135. Kling, D., Phillips, C., Kennett, D., and Tillmar, A., *Investigative genetic genealogy: Current methods, knowledge and practice.* Forensic Science International: Genetics, 2021. **52**.
136. Tillmar, A., Grandell, I., and Montelius, K., *DNA identification of compromised samples with massive parallel sequencing.* Forensic Sciences Research, 2019. **4**(4): p. 331-336.
137. Rosenberg, N.A., Mahajan, S., Ramachandran, S., Zhao, C., Pritchard, J.K., and Feldman, M.W., *Clines, clusters, and the effect of study design on the inference of human population structure.* PLoS Genet, 2005. **1**(6): p. e70.
138. Budowle, B. and Van Daal, A., *Forensically relevant SNP classes.* Biotechniques, 2008. **44**(5): p. 603-610.
139. Frudakis, T., Venkateswarlu, K., Thomas, M.J., Gaskin, Z., Ginjupalli, S., Gunturi, S., Ponnuswamy, V., Natarajan, S., and Nachimuthu, P.K., *A classifier for the SNP-based inference of ancestry.* J Forensic Sci, 2003. **48**(4): p. 771-82.
140. Pritchard, J.K. and Donnelly, P., *Case-control studies of association in structured or admixed populations.* Theor Popul Biol, 2001. **60**(3): p. 227-37.
141. Branicki, W., Liu, F., van Duijn, K., Draus-Barini, J., Pośpiech, E., Walsh, S., Kupiec, T., Wojas-Pelc, A., and Kayser, M., *Model-based prediction of human hair color using DNA variants.* Human Genetics, 2011. **129**(4): p. 443-454.
142. Kayser, M., *Forensic DNA Phenotyping: Predicting human appearance from crime scene material for investigative purposes.* Forensic Science International: Genetics, 2015. **18**: p. 33-48.
143. Kayser, M. and Schneider, P.M., *DNA-based prediction of human externally visible characteristics in forensics: motivations, scientific challenges, and ethical considerations.* Forensic Sci Int Genet, 2009. **3**(3): p. 154-61.
144. Liu, J.Z., Medland, S.E., Wright, M.J., Henders, A.K., Heath, A.C., Madden, P.A.F., Duncan, A., Montgomery, G.W., Martin, N.G., and McRae, A.F., *Genome-wide association study of height and body mass index in Australian twin families.* Twin research and human genetics : the official journal of the International Society for Twin Studies, 2010. **13**(2): p. 179-193.

145. Jiang, L., Willner, D., Danoy, P., Xu, H., and Brown, M.A., *Comparison of the performance of two commercial genome-wide association study genotyping platforms in Han Chinese samples.* G3 (Bethesda, Md.), 2013. **3**(1): p. 23-29.

146. Morelato, M., Baechler, S., Ribaux, O., Beavis, A., Tahtouh, M., Kirkbride, P., Roux, C., and Margot, P., *Forensic intelligence framework—Part I: Induction of a transversal model by comparing illicit drugs and false identity documents monitoring.* Forensic science international, 2014. **236**: p. 181-190.

147. Ratcliffe, J., *Intelligence-led Policing*. 2008, Collumpton: Willam Publishing.

148. Ratcliffe, J.H., *Integrated intelligence and crime analysis: Enhanced information management for law enforcement leaders.* 2007.

149. Peterson, M., *Intelligence-led policing: The new intelligence architecture*. 2005: Bureau of Justice Assistance Washington, DC.

150. Kirk, P.L., *Crime investigation; physical evidence and the police laboratory*. 1953, New York: Interscience Publishers.

151. Barash, M., Bayer, P.E., and van Daal, A. *Candidate gene scan for Single Nucleotide Polymorphisms involved in the determination of normal variability in human craniofacial morphology*. 2016. DOI: 10.1101/060814.

152. Sulem, P., Gudbjartsson, D.F., Stacey, S.N., Helgason, A., Rafnar, T., Magnusson, K.P., Manolescu, A., Karason, A., Palsson, A., Thorleifsson, G., Jakobsdottir, M., Steinberg, S., Pálsson, S., Jonasson, F., Sigurgeirsson, B., Thorisdottir, K., Ragnarsson, R., Benediktsdottir, K.R., Aben, K.K., Kiemeney, L.A., Olafsson, J.H., Gulcher, J., Kong, A., Thorsteinsdottir, U., and Stefansson, K., *Genetic determinants of hair, eye and skin pigmentation in Europeans.* Nature Genetics, 2007. **39**(12): p. 1443-1452.

153. Zhang, M., Song, F., Liang, L., Nan, H., Zhang, J., Liu, H., Wang, L.-E., Wei, Q., Lee, J.E., Amos, C.I., Kraft, P., Qureshi, A.A., and Han, J., *Genome-wide association studies identify several new loci associated with pigmentation traits and skin cancer risk in European Americans.* Human Molecular Genetics, 2013. **22**(14): p. 2948-2959.

154. Michailidou, K., Hall, P., Gonzalez-Neira, A., Ghoussaini, M., Dennis, J., Milne, R.L., Schmidt, M.K., Chang-Claude, J., Bojesen, S.E., Bolla, M.K., Wang, Q., Dicks, E., Lee, A., Turnbull, C., Rahman, N., Breast, Ovarian Cancer Susceptibility, C., Fletcher, O., Peto, J., Gibson, L., Dos Santos Silva, I., Nevanlinna, H., Muranen, T.A., Aittomäki, K., Blomqvist, C., Czene, K., Irwanto, A., Liu, J., Waisfisz, Q., Meijers-Heijboer, H., Adank, M., Hereditary, B., Ovarian Cancer Research Group, N., van der Luijt, R.B., Hein, R., Dahmen, N., Beckman, L., Meindl, A., Schmutzler, R.K., Müller-Myhsok, B., Lichtner, P., Hopper, J.L., Southey, M.C., Makalic, E., Schmidt, D.F., Uitterlinden, A.G., Hofman, A.,

Hunter, D.J., Chanock, S.J., Vincent, D., Bacot, F., Tessier, D.C., Canisius, S., Wessels, L.F.A., Haiman, C.A., Shah, M., Luben, R., Brown, J., Luccarini, C., Schoof, N., Humphreys, K., Li, J., Nordestgaard, B.G., Nielsen, S.F., Flyger, H., Couch, F.J., Wang, X., Vachon, C., Stevens, K.N., Lambrechts, D., Moisse, M., Paridaens, R., Christiaens, M.-R., Rudolph, A., Nickels, S., Flesch-Janys, D., Johnson, N., Aitken, Z., Aaltonen, K., Heikkinen, T., Broeks, A., Veer, L.J.V.t., van der Schoot, C.E., Guénel, P., Truong, T., Laurent-Puig, P., Menegaux, F., Marme, F., Schneeweiss, A., Sohn, C., Burwinkel, B., Zamora, M.P., Perez, J.I.A., Pita, G., Alonso, M.R., Cox, A., Brock, I.W., Cross, S.S., Reed, M.W.R., Sawyer, E.J., Tomlinson, I., Kerin, M.J., Miller, N., Henderson, B.E., Schumacher, F., Le Marchand, L., Andrulis, I.L., Knight, J.A., Glendon, G., Mulligan, A.M., kConFab, I., Australian Ovarian Cancer Study, G., Lindblom, A., Margolin, S., Hooning, M.J., Hollestelle, A., van den Ouweland, A.M.W., Jager, A., Bui, Q.M., Stone, J., Dite, G.S., Apicella, C., Tsimiklis, H., Giles, G.G., Severi, G., Baglietto, L., Fasching, P.A., Haeberle, L., Ekici, A.B., Beckmann, M.W., Brenner, H., Müller, H., Arndt, V., Stegmaier, C., Swerdlow, A., Ashworth, A., Orr, N., Jones, M., Figueroa, J., Lissowska, J., Brinton, L., Goldberg, M.S., Labrèche, F., Dumont, M., Winqvist, R., Pylkäs, K., Jukkola-Vuorinen, A., Grip, M., Brauch, H., Hamann, U., Brüning, T., Network, G., Radice, P., Peterlongo, P., Manoukian, S., Bonanni, B., Devilee, P., Tollenaar, R.A.E.M., Seynaeve, C., van Asperen, C.J., Jakubowska, A., Lubinski, J., Jaworska, K., Durda, K., Mannermaa, A., Kataja, V., Kosma, V.-M., Hartikainen, J.M., Bogdanova, N.V., Antonenkova, N.N., Dörk, T., Kristensen, V.N., Anton-Culver, H., Slager, S., Toland, A.E., Edge, S., Fostira, F., Kang, D., Yoo, K.-Y., Noh, D.-Y., Matsuo, K., Ito, H., Iwata, H., Sueta, A., Wu, A.H., Tseng, C.-C., Van Den Berg, D., Stram, D.O., Shu, X.-O., Lu, W., Gao, Y.-T., Cai, H., Teo, S.H., Yip, C.H., Phuah, S.Y., Cornes, B.K., Hartman, M., Miao, H., Lim, W.Y., Sng, J.-H., Muir, K., Lophatananon, A., Stewart-Brown, S., Siriwanarangsan, P., Shen, C.-Y., Hsiung, C.-N., Wu, P.-E., Ding, S.-L., Sangrajrang, S., Gaborieau, V., Brennan, P., McKay, J., Blot, W.J., Signorello, L.B., Cai, Q., Zheng, W., Deming-Halverson, S., Shrubsole, M., Long, J., Simard, J., Garcia-Closas, M., Pharoah, P.D.P., Chenevix-Trench, G., Dunning, A.M., Benitez, J. and Easton, D.F., *Large-scale genotyping identifies 41 new loci associated with breast cancer risk.* Nature Genetics, 2013. **45**(4): p. 353-361.

155. Hoffmann, T.J., Van Den Eeden, S.K., Sakoda, L.C., Jorgenson, E., Habel, L.A., Graff, R.E., Passarelli, M.N., Cario, C.L., Emami, N.C., Chao, C.R., Ghai, N.R., Shan, J., Ranatunga, D.K., Quesenberry, C.P., Aaronson, D., Presti, J., Wang, Z., Berndt, S.I., Chanock, S.J., McDonnell, S.K., French, A.J., Schaid, D.J., Thibodeau, S.N., Li, Q., Freedman, M.L., Penney, K.L., Mucci, L.A., Haiman, C.A., Henderson, B.E., Seminara, D., Kvale, M.N.,

Kwok, P.-Y., Schaefer, C., Risch, N., and Witte, J.S., *A large multiethnic genome-wide association study of prostate cancer identifies novel risk variants and substantial ethnic differences.* Cancer Discovery, 2015. **5**(8): p. 878-891.

156. Liu, J.Z., van Sommeren, S., Huang, H., Ng, S.C., Alberts, R., Takahashi, A., Ripke, S., Lee, J.C., Jostins, L., Shah, T., Abedian, S., Cheon, J.H., Cho, J., Daryani, N.E., Franke, L., Fuyuno, Y., Hart, A., Juyal, R.C., Juyal, G., Kim, W.H., Morris, A.P., Poustchi, H., Newman, W.G., Midha, V., Orchard, T.R., Vahedi, H., Sood, A., Sung, J.J.Y., Malekzadeh, R., Westra, H.-J., Yamazaki, K., Yang, S.-K., International Multiple Sclerosis Genetics, C., International, I.B.D.G.C., Barrett, J.C., Franke, A., Alizadeh, B.Z., Parkes, M., B K, T., Daly, M.J., Kubo, M., Anderson, C.A., and Weersma, R.K., *Association analyses identify 38 susceptibility loci for inflammatory bowel disease and highlight shared genetic risk across populations.* Nature genetics, 2015. **47**(9): p. 979-986.
157. Fotsing, S.F., Margoliash, J., Wang, C., Saini, S., Yanicky, R., Shleizer-Burko, S., Goren, A., and Gymrek, M., *The impact of short tandem repeat variation on gene expression.* Nature genetics, 2019. **51**(11): p. 1652-1659.
158. Quilez, J., Guilmatre, A., Garg, P., Highnam, G., Gymrek, M., Erlich, Y., Joshi, R.S., Mittelman, D., and Sharp, A.J., *Polymorphic tandem repeats within gene promoters act as modifiers of gene expression and DNA methylation in humans.* Nucleic acids research, 2016. **44**(8): p. 3750-3762.
159. Claes, P., Liberton, D.K., Daniels, K., Rosana, K.M., Quillen, E.E., Pearson, L.N., McEvoy, B., Bauchet, M., Zaidi, A.A., and Yao, W., *Modeling 3D facial shape from DNA.* PLoS genetics, 2014. **10**(3): p. e1004224.
160. Walsh, S., Wollstein, A., Liu, F., Chakravarthy, U., Rahu, M., Seland, J.H., Soubrane, G., Tomazzoli, L., Topouzis, F., Vingerling, J.R., Vioque, J., Fletcher, A.E., Ballantyne, K.N., and Kayser, M., *DNA-based eye colour prediction across Europe with the IrisPlex system.* Forensic Science International: Genetics, 2012. **6**(3): p. 330-340.
161. Walsh, S., Liu, F., Wollstein, A., Kovatsi, L., Ralf, A., Kosiniak-Kamysz, A., Branicki, W., and Kayser, M., *The HIrisPlex system for simultaneous prediction of hair and eye colour from DNA.* Forensic Science International: Genetics, 2013. **7**(1): p. 98-115.
162. Chaitanya, L., Breslin, K., Zuniga, S., Wirken, L., Pospiech, E., Kukla-Bartoszek, M., Sijen, T., Knijff, P., Liu, F., Branicki, W., Kayser, M., and Walsh, S., *The HIrisPlex-S system for eye, hair and skin colour prediction from DNA: Introduction and forensic developmental validation.* Forensic Sci Int Genet, 2018. **35**: p. 123-135.

163. Cheung, E.Y., Gahan, M.E., and McNevin, D., *Prediction of biogeographical ancestry from genotype: a comparison of classifiers.* International journal of legal medicine, 2017. **131**(4): p. 901-912.

164. Cheung, E.Y., Gahan, M.E., and McNevin, D., *Prediction of biogeographical ancestry in admixed individuals.* Forensic Science International: Genetics, 2018. **36**: p. 104-111.

165. Cheung, E.Y., Gahan, M.E., and McNevin, D., *Predictive DNA analysis for biogeographical ancestry.* Australian Journal of Forensic Sciences, 2018. **50**(6): p. 651-658.

166. Walsh, S., Pospiech, E., and Branicki, W., *Hot on the Trail of Genes that Shape Our Fingerprints.* The Journal of Investigative Dermatology, 2016. **136**(4): p. 740-2.

167. Walsh, S., Liu, F., Ballantyne, K.N., van Oven, M., Lao, O., and Kayser, M., *IrisPlex: A sensitive DNA tool for accurate prediction of blue and brown eye colour in the absence of ancestry information.* Forensic Science International: Genetics, 2011. **5**(3): p. 170-180.

168. Walsh, S., Chaitanya, L., Clarisse, L., Wirken, L., Draus-Barini, J., Kovatsi, L., Maeda, H., Ishikawa, T., Sijen, T., de Knijff, P., Branicki, W., Liu, F., and Kayser, M., *Developmental validation of the HIrisPlex system: DNA-based eye and hair colour prediction for forensic and anthropological usage.* Forensic Science International: Genetics, 2014. **9**: p. 150-161.

169. Kidd, K.K., Speed, W.C., Pakstis, A.J., Furtado, M.R., Fang, R., Madbouly, A., Maiers, M., Middha, M., Friedlaender, F.R., and Kidd, J.R., *Progress toward an efficient panel of SNPs for ancestry inference.* Forensic Science International: Genetics, 2014. **10**: p. 23-32.

170. Fairley, S., Lowy-Gallego, E., Perry, E., and Flicek, P., *The International Genome Sample Resource (IGSR) collection of open human genomic variation resources.* Nucleic Acids Research, 2019. **48**(D1): p. D941-D947.

171. Kosoy, R., Nassir, R., Tian, C., White, P.A., Butler, L.M., Silva, G., Kittles, R., Alarcon-Riquelme, M.E., Gregersen, P.K., and Belmont, J.W., *Ancestry informative marker sets for determining continental origin and admixture proportions in common populations in America.* Human mutation, 2009. **30**(1): p. 69-78.

172. Al-Asfi, M., McNevin, D., Mehta, B., Power, D., Gahan, M., and Daniel, R., *Assessment of the Precision ID Ancestry panel.* International Journal of Legal Medicine, 2018. **132**.

173. Porras-Hurtado, L., Ruiz, Y., Santos, C., Phillips, C., Carracedo, Á., and Lareu, M., *An overview of STRUCTURE: applications, parameter settings, and supporting software.* Frontiers in Genetics, 2013. **4**(98).

174. Liu, F., Wollstein, A., Hysi, P.G., Ankra-Badu, G.A., Spector, T.D., Park, D., Zhu, G., Larsson, M., Duffy, D.L., Montgomery, G.W., Mackey, D.A., Walsh, S., Lao, O., Hofman, A., Rivadeneira, F., Vingerling, J.R., Uitterlinden, A.G., Martin, N.G., Hammond, C.J., and Kayser, M., *Digital Quantification of Human Eye Color Highlights Genetic Association of Three New Loci.* PLOS Genetics, 2010. **6**(5): p. e1000934.

175. Grigore, M. and Avram, A., *Iris Colour Classification Scales - Then And Now.* Romanian journal of ophthalmology, 2015. **59**(1): p. 29.

176. *Australian Criminal Intelligence Commission Annual Report 2017–18*, A.C.I. Commission, Editor. 2018.

177. Greytak, E.M. and Armentrout, S. *DNA phenotyping: predicting ancestry and physical appearance from forensic DNA*. in *Proceedings of the 26th International Symposium on Human Identification*. 2015.

178. Wiley, R., Zeng, X., LaRue, B., Gill-King, H., and Budowle, B., *Evaluation of the Parabon® Snapshot™ DNA Phenotyping System.* 2017.

179. Davies, G.M. and Valentine, T., *Facial composites: Forensic utility and psychological research.* Handbook of eyewitness psychology, 2013. **2**: p. 59-83.

180. Claes, P., Hill, H., and Shriver, M.D., *Toward DNA-based facial composites: preliminary results and validation.* Forensic Science International: Genetics, 2014. **13**: p. 208-216.

181. Coussens, A.K. and Van Daal, A., *Linkage disequilibrium analysis identifies an FGFR1 haplotype-tag SNP associated with normal variation in craniofacial shape.* Genomics, 2005. **85**(5): p. 563-573.

182. Liu, F., Van Der Lijn, F., Schurmann, C., Zhu, G., Chakravarty, M.M., Hysi, P.G., Wollstein, A., Lao, O., De Bruijne, M., and Ikram, M.A., *A genome-wide association study identifies five loci influencing facial morphology in Europeans.* PLoS genetics, 2012. **8**(9): p. e1002932.

183. Cutler, B.L., Penrod, S.D., and Martens, T.K., *The reliability of eyewitness identification.* Law and Human Behavior, 1987. **11**(3): p. 233-258.

184. List, J.A., *Age and schematic differences in the reliability of eyewitness testimony.* Developmental Psychology, 1986. **22**(1): p. 50.

185. Penrod, S. and Bornstein, B.H., *Generalizing eyewitness reliability research.* 2007.

186. Shaw, J.I. and Skolnick, P., *Sex differences, weapon focus, and eyewitness reliability.* The Journal of Social Psychology, 1994. **134**(4): p. 413-420.

187. Neufeld, P. and Scheck, B. *Innocence Project*. 2021 [cited 2021 13/11/2021]; Available from: https://innocenceproject.org/.

188. Clifford, B.R. and Hollin, C.R., *Effects of the type of incident and the number of perpetrators on eyewitness memory.* Journal of Applied Psychology, 1981. **66**(3): p. 364-370.

189. Cohen, R.A., *Yerkes–Dodson Law.* Encyclopedia of clinical neuropsychology, 2011: p. 2737-2738.

190. Lindsay, R.C. and Wells, G.L., *Improving eyewitness identifications from lineups: Simultaneous versus sequential lineup presentation.* Journal of Applied Psychology, 1985. **70**(3): p. 556-564.

191. Wickenheiser, R., *Just Science Podcast*, in *Just Case Studies: Derrick Todd Lee - Baton Rouge Serial Killer*. 2017, National Institute of Justice (NIJ): United States of America.

192. Adda Neggaz, L., Meroufel, D.N., Deba, T., Bekada, A., Hammadi, M., Mediene Benchekor, S., Rosa, A., and Benhamamouch, S., *Digital dermatoglyphic study in three west Algerian populations: Reguibates, Zenata, Oran.* Canadian Society of Forensic Science Journal, 2017. **50**(4): p. 164-174.

193. Cho, C., *A finger dermatoglyphics of the new Zealand-Samoans.* Korean Journal of Biological Sciences, 1998. **2**(4): p. 507-511.

194. Cho, C., *A finger dermatoglyphic study of Maori.* Korean Journal of Biological Sciences, 1998. **2**(2): p. 277-280.

195. Cummins, H. and Setzler, F.M., *Dermatoglyphics in Australian Aborigines (Arnhem Land).* American journal of physical anthropology, 1951. **9**(4): p. 455-460.

196. Gangadhar, M. and Reddy, K.R., *Finger dermatoglyphics of Adikarnatakas: a scheduled caste population of Mysore City, Karnataka.* Man in India, 2003. **83**(1-2): p. 183-193.

197. Gutierrez-Redomero, E., Alonso-Rodríguez, C., Hernandez-Hurtado, L.E., and Rodríguez-Villalba, J.L., *Distribution of the minutiae in the fingerprints of a sample of the Spanish population.* Forensic science international, 2011. **208**(1-3): p. 79-90.

198. Heng, G., Ismail, N., Azreen, Z., and Anan, A., *Distribution of fingerprint patterns among young adults and siblings in Malaysia.* 2018. **3**: p. 11-17.

199. Igbigbi, P. and Msamati, B., *Palmar and digital dermatoglyphic patterns in Malawian subjects.* East African medical journal, 1999. **76**(12): p. 668-671.

200. Igbigbi, P.S. and Msamati, B.C., *Palmar and digital dermatoglyphics of indigenous black Zimbabweans.* Medical Science Monitor, 2002. **8**(11): p. CR757-CR761.

201. Igbigbi, P.S. and Msamati, B.C., *Palmer and digital dermatoglyphics traits of Kenyan & Tanzanian subjects.* West African Journal of Medicine, 2005. **24**(1): p. 26-30.

202. Jaja, B. and Igbigbi, P., *Digital and palmar dermatoglyphics of the Ijaw of Southern Nigeria.* Afr J Med Med Sci, 2008. **37**(1): p. 1-5.

203. Kapoor, N. and Badiye, A., *Digital dermatoglyphics: A study on Muslim population from India.* Egyptian Journal of Forensic Sciences, 2015. **5**(3): p. 90-95.

204. Meier, R.J., *Dermatoglyphics of Easter Islanders analyzed by pattern type, admixture effect, and ridge count variation.* American Journal of Physical Anthropology, 1975. **42**(2): p. 269-275.

205. Nithin, M.D., Balaraj, B.M., Manjunatha, B., and Mestri, S.C., *Study of fingerprint classification and their gender distribution among South Indian population.* Journal of Forensic and Legal Medicine, 2009. **16**(8): p. 460-463.

206. Plato, C. and Wertelecki, W. *Variation and distribution of dermatoglyphic features in different populations*. in *American Journal Of Human Genetics*. 1974. University of Chicago Press 5720 S Woodlawn Ave, Chicago, IL 60637.

207. Plato, C.C., Cereghino, J.J., and Steinberg, F.S., *The dermatoglyphics of American Caucasians.* Am J Phys Anthropol, 1975. **42**(2): p. 195-210.

208. Qazi, Q.H., Mapa, H.C., and Woods, J., *Dermatoglyphics of American blacks.* American journal of physical anthropology, 1977. **47**(3): p. 483-487.

209. Rao, P., *Finger prints of aborigines at Kalumburu mission in Western Australia.* Oceania, 1964. **34**(3): p. 225-233.

210. Rivaldería, N., Gutiérrez-Redomero, E., Alonso-Rodríguez, C., Dipierri, J.E., and Martín, L.M., *Study of fingerprints in Argentina population for application in personal identification.* Science and Justice, 2017. **57**(3): p. 199-208.

211. Singh, S., *Dermatoglyphics of Australian Aborigines living on Mornington Island, Gulf of Carpentaria.* Archaeology in Oceania, 1968. **3**(1): p. 41-48.

212. Sokal, R.R., Jantz, R.L., and Thomson, B.A. *Dermatoglyphic variation in Europe*. American journal of physical anthropology, 1996. **100**, 35-47.

213. Steinberg, F.S., Cereghino, J.J., and Plato, C.C., *The dermatoglyphics of American Negroes.* Am J Phys Anthropol, 1975. **42**(2): p. 183-93.

214. Temaj, G., Milicic, J., Skaric Juric, T., Behluli, I., Smolej Narancic, N., Hadziselimovic, R., and Nefic, H., *Comparative analysis of dermatoglyphic traits in Albanian and Turkish population living in Kosovo.* Coll Antropol, 2009. **33**(4): p. 1001-5.

215. Veale, A. and Adams, W., *Polynesian finger prints: Ellice Islanders.* Journal of the Anthropological Society of Nippon, 1968. **76**(5): p. 205-214.

216. Veale, A.M.O. and Adams, W.E., *Finger-prints of the New Zealand Maori.* Journal of the Anthropological Society of Nippon, 1965. **73**(2): p. 33-49.

217. Wijerathne, B.T.B., Rathnayake, G.K., Adikari, S.C., Amarasinghe, S., Abhayarathna, P.L., and Jayasena, A.S., *Sexual dimorphism in digital dermatoglyphic traits among*

Sinhalese people in Sri Lanka. Journal of physiological anthropology, 2013. **32**(1): p. 27-27.

218. Abdullah, S., Abdul Rahman, A.F.N., and Abas, Z., *Classification of gender by using fingerprint ridge density in northern part of Malaysia.* Journal of Engineering and Applied Sciences, 2015. **10**: p. 10722-10726.
219. Adamu, L.H., Ojo, S.A., Danborno, B., Adebisi, S.S., and Taura, M.G., *Sex prediction using ridge density and thickness among the Hausa ethnic group of Kano state, Nigeria.* Australian Journal of Forensic Sciences, 2018. **50**(5): p. 455-471.
220. Agnihotri, A.K., Jowaheer, V., and Allock, A., *An analysis of fingerprint ridge density in the Indo-Mauritian population and its application to gender determination.* Medicine, Science and the Law, 2012. **52**(3): p. 143-147.
221. Ahmed, A.A. and Osman, S., *Topological variability and sex differences in fingerprint ridge density in a sample of the Sudanese population.* Journal of Forensic and Legal Medicine, 2016. **42**(Supplement C): p. 25-32.
222. Aidid, M., Pravina, D., and Tan, E., *A preliminary study of age and sex in relation to fingerprint ridge density among Malaysian Indian population in management & science university (MSU).* International Journal of Medical Toxicology & Legal Medicine, 2018. **21**(3and4): p. 4-7.
223. Dhall, J.K. and Kapoor, A.K., *Fingerprint ridge density as a potential forensic anthropological tool for sex identification.* Journal of forensic sciences, 2016. **61**(2): p. 424-429.
224. Gutiérrez-Redomero, E., Alonso, M., and Dipierri, J., *Sex differences in fingerprint ridge density in the Mataco-Mataguayo population.* Homo, 2011. **62**(6): p. 487-499.
225. Gutiérrez-Redomero, E., Quirós, J.A., Rivaldería, N., and Alonso, M.C., *Topological Variability of Fingerprint Ridge Density in a Sub-Saharan Population Sample for Application in Personal Identification.* Journal of forensic sciences, 2013. **58**(3): p. 592-600.
226. Gutiérrez-Redomero, E., Sánchez-Andrés, Á., Rivaldería, N., Alonso-Rodríguez, C., Dipierri, J.E., and Martín, L.M., *A comparative study of topological and sex differences in fingerprint ridge density in Argentinian and Spanish population samples.* Journal of Forensic and Legal Medicine, 2013. **20**(5): p. 419-429.
227. Kapoor, N. and Badiye, A., *Sex differences in the thumbprint ridge density in a central Indian population.* Egyptian Journal of Forensic Sciences, 2015. **5**(1): p. 23-29.

228. Krishan, K., Kanchan, T., and Ngangom, C., *A study of sex differences in fingerprint ridge density in a North Indian young adult population.* Journal of Forensic and Legal Medicine, 2013. **20**(4): p. 217-222.

229. Moorthy, T.N. and MAK, H., *Sex determination from footprint ridge density in bidayuh population in Malaysian Borneo.* International Journal of Medical Toxicology & Legal Medicine, 2018. **21**(3and4): p. 158-161.

230. Nayak, V.C., Rastogi, P., Kanchan, T., Lobo, S.W., Yoganarasimha, K., Nayak, S., Rao, N.G., Kumar, G.P., Shetty, B.S.K., and Menezes, R.G., *Sex differences from fingerprint ridge density in the Indian population.* Journal of Forensic and Legal Medicine, 2010. **17**(2): p. 84-86.

231. Nayak, V.C., Rastogi, P., Kanchan, T., Yoganarasimha, K., Kumar, G.P., and Menezes, R.G., *Sex differences from fingerprint ridge density in Chinese and Malaysian population.* Forensic science international, 2010. **197**(1): p. 67-69.

232. Oktem, H., Kurkcuoglu, A., Pelin, I.C., Yazici, A.C., Aktaş, G., and Altunay, F., *Sex differences in fingerprint ridge density in a Turkish young adult population: A sample of Baskent University.* Journal of Forensic and Legal Medicine, 2015. **32**(Supplement C): p. 34-38.

233. R Siddapur, K., *Study on Sex Differences in Fingerprint Ridge Density of Patent Thumbprints by Ink Staining Method in Young Adult Indian Tamil Population.* 2018.

234. Rivaldería, N., Sánchez-Andrés, Á., Alonso-Rodríguez, C., Dipierri, J.E., and Gutiérrez-Redomero, E., *Fingerprint ridge density in the Argentinean population and its application to sex inference: A comparative study.* HOMO - Journal of Comparative Human Biology, 2016. **67**(1): p. 65-84.

235. Soanboon, P., Nanakorn, S., and Kutanan, W., *Determination of sex difference from fingerprint ridge density in northeastern Thai teenagers.* Egyptian Journal of Forensic Sciences, 2016. **6**(2): p. 185-193.

236. Sudesh Gungadin, M., *Sex determination from fingerprint ridge density.* Internet Journal of Medical Update, 2007. **2**(2).

237. Taduran, R.J.O., Tadeo, A.K.V., Escalona, N.A.C., and Townsend, G.C., *Sex determination from fingerprint ridge density and white line counts in Filipinos.* HOMO-Journal of Comparative Human Biology, 2016. **67**(2): p. 163-171.

238. *Instructions for Isohelix Buccal-Prep Plus DNA Isolation Kit: BPP-50/BPP-3*. 2017 15/4/2021]; Available from: https://isohelix.com/wp-content/uploads/2020/06/BPP-Buccal-Prep-Plus-Kit-22mg-PK-version-November-2017.pdf.

239. *NanoDrop One User Guide*. 2021 15/4/2021]; Available from: https://assets.thermofisher.com/TFS-Assets/MSD/manuals/nanodrop-one-user-guide-EN-309102.pdf.

240. *Qubit dsDNA HS Assay Kits*. 2015 15/4/2021]; Available from: https://www.thermofisher.com/document-connect/document-connect.html?url=https%3A%2F%2Fassets.thermofisher.com%2FTFS-Assets%2FLSG%2Fmanuals%2FQubit_dsDNA_HS_Assay_UG.pdf&title=VXNlciBHdWlkZTogUXViaXQgZHNETkEgSFMgQXNzYXkgS2l0cw==.

241. Kent, W.J., Sugnet, C.W., Furey, T.S., Roskin, K.M., Pringle, T.H., Zahler, A.M., and Haussler, D., *The human genome browser at UCSC.* Genome Res, 2002. **12**(6): p. 996-1006.

242. Lee, P.H. and Shatkay, H., *F-SNP: computationally predicted functional SNPs for disease association studies.* Nucleic Acids Res, 2008. **36**(Database issue): p. D820-4.

243. *Infinium HTS Assay Manual Workflow Checklist*. 2019 15/4/2021]; Available from: https://support.illumina.com/content/dam/illumina-support/documents/documentation/chemistry_documentation/infinium_assays/infinium-hts/infinium-hts-assay-manual-checklist-1000000074596-01.pdf.

244. Team, R.C., *R: A Language and Environment for Statistical Computing*. 2020, R Foundation for Statistical Computing: Vienna, Austria.

245. Team, R., *RStudio: Integrated Development for R*. 2020, RStudio, PBC.: Boston, MA.

246. Corp., I., *IBM SPSS Statistics for Windows, Version 25.0*. 2017, IBM Corp.: Armonk, NY.

247. McHugh, M.L., *The chi-square test of independence.* Biochemia medica, 2013. **23**(2): p. 143-149.

248. Kwak, C. and Clayton-Matthews, A., *Multinomial logistic regression.* Nursing research, 2002. **51**(6): p. 404-410.

249. Liang, K.-Y. and Zeger, S.L., *Longitudinal data analysis using generalized linear models.* Biometrika, 1986. **73**(1): p. 13-22.

250. McCullagh, P. and Nelder, J.A., *Generalized Linear Models, Second Edition*. 1989: Taylor & Francis.

251. Shapiro, S.S. and Wilk, M.B., *An Analysis of Variance Test for Normality (Complete Samples).* Biometrika, 1965. **52**(3/4): p. 591-611.

252. McKight, P.E. and Najab, J., *Kruskal-Wallis Test*, in *The Corsini Encyclopedia of Psychology*. p. 1-1.

253. Gonzalez, J.R. and Moreno, V., *SNPassoc: SNPs-based whole genome association studies*. 2019.

254. Turner, S., *qqman: Q-Q and Manhattan Plots for GWAS Data*. 2017.

255. Champod, C., Lennard, C.J., Margot, P., and Stoilovic, M., *Statistical Data For General Fingerprint Patterns*, in *Fingerprints and other ridge skin impressions*. 2016, CRC Press.

256. Babler, W.J., *The prenatal origins of populational differences in human dermatoglyphics*. 1977, University of Michigan: Michigan, USA.

257. García-pérez, M.A. and Núñez-antón, V., *Cellwise Residual Analysis in Two-Way Contingency Tables.* Educational and Psychological Measurement, 2003. **63**(5): p. 825-839.

258. Holm, S., *A simple sequentially rejective multiple test procedure.* Scandinavian journal of statistics, 1979: p. 65-70.

259. Beasley, T.M. and Schumacker, R.E., *Multiple regression approach to analyzing contingency tables: Post hoc and planned comparison procedures.* Journal of Experimental Education, 1995. **64**(1): p. 79-93.

260. MacDonald, P.L. and Gardner, R.C., *Type I error rate comparisons of post hoc procedures for I j Chi-Square tables.* Educational and psychological measurement, 2000. **60**(5): p. 735-754.

261. Eboh, D., *Digital dermatoglyphic patterns of Anioma and Urhobo stuaents in two tertiary institutions of Delta state, southern Nigeria.* Journal of Medicine and Biomedical Research, 2012. **11**: p. 90-96.

262. Hennessey, P., *Personal Communication*. 2019.

263. Ozcelik, D.S., *Analysis of the Crimean Tatars Situation During the Occupation of Crimea by Russia in 2014 with the Conflict and Peace Studies Approach.* E-Journal of Law, 2015. **1**: p. 10-19.

264. Karabacak, E., *The Emergence of the Volga Tatar National and Economic Consciousness*. 2019.

265. Malyarchuk, B., Derenko, M., Denisova, G., and Kravtsova, O., *Mitogenomic Diversity in Tatars from the Volga-Ural Region of Russia.* Molecular Biology and Evolution, 2010. **27**(10): p. 2220-2226.

266. Hecht, A.F., *Über das Hand- und Fußflächenrelief von Kindern.* Zeitschrift für die gesamte experimentelle Medizin, 1924. **39**(1): p. 56-66 (Cited in Cummins, H., Waits, W.J., and McQuitty, J.T., The breadths of epidermal ridges on the finger tips and palms: A study of variation. American Journal of Anatomy, 1941. 68(1): p. 127-150).

267. Lee, R., Comber, B., Abraham, J., Wagner, M., Lennard, C., Spindler, X., and Roux, C., *Supporting fingerprint identification assessments using a skin stretch model - A preliminary study.* Forensic Sci Int, 2017. **272**: p. 41-49.

268. Mil'shtein, S. and Doshi, U., *Scanning the pressure-induced distortion of fingerprints.* Scanning, 2004. **26**(6): p. 270-2.

269. Research, W., *Wolfram Mathematica*. 2021.

270. Nithin, M., Manjunatha, B., Preethi, D., and Balaraj, B., *Gender differentiation by finger ridge count among South Indian population.* Journal of forensic and legal medicine, 2011. **18**(2): p. 79-81.

271. Wang, M., *Generalized Estimating Equations in Longitudinal Data Analysis: A Review and Recent Developments.* Advances in Statistics, 2014. **2014**: p. 303728.

272. Penrose, L.S. and Loesch, D., *A study of dermal ridge width in the second (palmar) interdigital area with special reference to aneuploid states.* J Ment Defic Res, 1967. **11**(1): p. 36-42.

273. Kralik, M. and Novotný, V., *Epidermal ridge breadth: An indicator of age and sex in paleodermatoglyphics.* Variability and Evolution, 2003. **11**: p. 5-30.

274. Jamison, C.S., *Dermatoglyphics and the Geschwind Hypothesis. I. Theoretical Background and Palmar Results of Dyslexia*, in *Trends in Dermatoglyphic Research*, N.M. Durham and C.C. Plato, Editors. 1990, Springer Netherlands: Dordrecht. p. 99-113.

275. Martin, N.G., Jinks, J.L., Berry, H.S., and Loesch, D.Z., *A genetical analysis of diversity and asymmetry in finger ridge counts.* Heredity, 1982. **48**(3): p. 393-405.

276. United States Department of Justice and Federal Bureau of Investigation, *The science of fingerprints*. 1984, Washington DC: U.S. Government Printing Office.

277. Hoff, C., Plato, C.C., Garruto, R.M., and Dutt, J., *Dermatoglyphic assessment of the genetic relationships of native American populations.* American Journal of Physical Anthropology, 1981. **55**(4): p. 455-461.

278. Kamali, M.S., Mavalwala, J., Khaneqah, A.A., and Bhanu, B.V., *Qualitative dermatoglyphic traits as measures of population distance.* American Journal of Physical Anthropology, 1991. **85**(4): p. 429-450.

279. Weninger, M., Aue-Hauser, G., and Scheiber, V., *Total finger ridge-count and the polygenic hypothesis: a critique.* Hum Biol, 1976. **48**(4): p. 713-25.

280. Yang, X., Xiaojun, J., Yixuan, Z., and Hui, L., *Genetic rules for the dermatoglyphics of human fingertips and their role in spouse selection: a preliminary study.* SpringerPlus, 2016. **5**(1): p. 1396.

281. Keats, B.J.B. and Sherman, S.L., *Chapter 13 - Population Genetics*, in *Emery and Rimoin's Principles and Practice of Medical Genetics*, D. Rimoin, R. Pyeritz, and B. Korf, Editors. 2013, Academic Press: Oxford. p. 1-12.

282. International HapMap, C., Frazer, K.A., Ballinger, D.G., Cox, D.R., Hinds, D.A., Stuve, L.L., Gibbs, R.A., Belmont, J.W., Boudreau, A., Hardenbol, P., Leal, S.M., Pasternak, S., Wheeler, D.A., Willis, T.D., Yu, F., Yang, H., Zeng, C., Gao, Y., Hu, H., Hu, W., Li, C., Lin, W., Liu, S., Pan, H., Tang, X., Wang, J., Wang, W., Yu, J., Zhang, B., Zhang, Q., Zhao, H., Zhao, H., Zhou, J., Gabriel, S.B., Barry, R., Blumenstiel, B., Camargo, A., Defelice, M., Faggart, M., Goyette, M., Gupta, S., Moore, J., Nguyen, H., Onofrio, R.C., Parkin, M., Roy, J., Stahl, E., Winchester, E., Ziaugra, L., Altshuler, D., Shen, Y., Yao, Z., Huang, W., Chu, X., He, Y., Jin, L., Liu, Y., Shen, Y., Sun, W., Wang, H., Wang, Y., Wang, Y., Xiong, X., Xu, L., Waye, M.M.Y., Tsui, S.K.W., Xue, H., Wong, J.T.-F., Galver, L.M., Fan, J.-B., Gunderson, K., Murray, S.S., Oliphant, A.R., Chee, M.S., Montpetit, A., Chagnon, F., Ferretti, V., Leboeuf, M., Olivier, J.-F., Phillips, M.S., Roumy, S., Sallée, C., Verner, A., Hudson, T.J., Kwok, P.-Y., Cai, D., Koboldt, D.C., Miller, R.D., Pawlikowska, L., Taillon-Miller, P., Xiao, M., Tsui, L.-C., Mak, W., Song, Y.Q., Tam, P.K.H., Nakamura, Y., Kawaguchi, T., Kitamoto, T., Morizono, T., Nagashima, A., Ohnishi, Y., Sekine, A., Tanaka, T., Tsunoda, T., Deloukas, P., Bird, C.P., Delgado, M., Dermitzakis, E.T., Gwilliam, R., Hunt, S., Morrison, J., Powell, D., Stranger, B.E., Whittaker, P., Bentley, D.R., Daly, M.J., de Bakker, P.I.W., Barrett, J., Chretien, Y.R., Maller, J., McCarroll, S., Patterson, N., Pe'er, I., Price, A., Purcell, S., Richter, D.J., Sabeti, P., Saxena, R., Schaffner, S.F., Sham, P.C., Varilly, P., Altshuler, D., Stein, L.D., Krishnan, L., Smith, A.V., Tello-Ruiz, M.K., Thorisson, G.A., Chakravarti, A., Chen, P.E., Cutler, D.J., Kashuk, C.S., Lin, S., Abecasis, G.R., Guan, W., Li, Y., Munro, H.M., Qin, Z.S., Thomas, D.J., McVean, G., Auton, A., Bottolo, L., Cardin, N., Eyheramendy, S., Freeman, C., Marchini, J., Myers, S., Spencer, C., Stephens, M., Donnelly, P., Cardon, L.R., Clarke, G., Evans, D.M., Morris, A.P., Weir, B.S., Tsunoda, T., Mullikin, J.C., Sherry, S.T., Feolo, M., Skol, A., Zhang, H., Zeng, C., Zhao, H., Matsuda, I., Fukushima, Y., Macer, D.R., Suda, E., Rotimi, C.N., Adebamowo, C.A., Ajayi, I., Aniagwu, T., Marshall, P.A., Nkwodimmah, C., Royal, C.D.M., Leppert, M.F., Dixon, M., Peiffer, A., Qiu, R., Kent, A., Kato, K., Niikawa, N., Adewole, I.F., Knoppers, B.M., Foster, M.W., Clayton, E.W., Watkin, J., Gibbs, R.A., Belmont, J.W., Muzny, D., Nazareth, L., Sodergren, E., Weinstock, G.M., Wheeler, D.A., Yakub, I., Gabriel, S.B., Onofrio, R.C., Richter, D.J., Ziaugra, L., Birren, B.W., Daly, M.J., Altshuler, D., Wilson, R.K., Fulton, L.L., Rogers, J., Burton, J., Carter, N.P., Clee, C.M., Griffiths, M., Jones, M.C., McLay, K., Plumb, R.W., Ross, M.T., Sims, S.K., Willey, D.L., Chen, Z., Han, H., Kang, L., Godbout, M., Wallenburg, J.C., L'Archevêque, P., Bellemare, G., Saeki, K., Wang, H., An, D., Fu, H., Li, Q., Wang, Z., Wang, R., Holden, A.L., Brooks, L.D., McEwen, J.E., Guyer, M.S., Wang, V.O., Peterson, J.L., Shi, M., Spiegel, J., Sung,

L.M., Zacharia, L.F., Collins, F.S., Kennedy, K., Jamieson, R. and Stewart, J., *A second generation human haplotype map of over 3.1 million SNPs.* Nature, 2007. **449**(7164): p. 851-861.

283. Durbin, R.M., Altshuler, D., Durbin, R.M., Abecasis, G.R., Bentley, D.R., Chakravarti, A., Clark, A.G., Collins, F.S., De La Vega, F.M., Donnelly, P., Egholm, M., Flicek, P., Gabriel, S.B., Gibbs, R.A., Knoppers, B.M., Lander, E.S., Lehrach, H., Mardis, E.R., McVean, G.A., Nickerson, D.A., Peltonen, L., Schafer, A.J., Sherry, S.T., Wang, J., Wilson, R.K., Gibbs, R.A., Deiros, D., Metzker, M., Muzny, D., Reid, J., Wheeler, D., Wang, J., Li, J., Jian, M., Li, G., Li, R., Liang, H., Tian, G., Wang, B., Wang, J., Wang, W., Yang, H., Zhang, X., Zheng, H., Lander, E.S., Altshuler, D., Ambrogio, L., Bloom, T., Cibulskis, K., Fennell, T.J., Gabriel, S.B., Jaffe, D.B., Shefler, E., Sougnez, C.L., Bentley, D.R., Gormley, N., Humphray, S., Kingsbury, Z., Kokko-Gonzales, P., Stone, J., McKernan, K.J., Costa, G.L., Ichikawa, J.K., Lee, C.C., Sudbrak, R., Lehrach, H., Borodina, T.A., Dahl, A., Davydov, A.N., Marquardt, P., Mertes, F., Nietfeld, W., Rosenstiel, P., Schreiber, S., Soldatov, A.V., Timmermann, B., Tolzmann, M., Egholm, M., Affourtit, J., Ashworth, D., Attiya, S., Bachorski, M., Buglione, E., Burke, A., Caprio, A., Celone, C., Clark, S., Conners, D., Desany, B., Gu, L., Guccione, L., Kao, K., Kebbel, A., Knowlton, J., Labrecque, M., McDade, L., Mealmaker, C., Minderman, M., Nawrocki, A., Niazi, F., Pareja, K., Ramenani, R., Riches, D., Song, W., Turcotte, C., Wang, S., Mardis, E.R., Wilson, R.K., Dooling, D., Fulton, L., Fulton, R., Weinstock, G., Durbin, R.M., Burton, J., Carter, D.M., Churcher, C., Coffey, A., Cox, A., Palotie, A., Quail, M., Skelly, T., Stalker, J., Swerdlow, H.P., Turner, D., De Witte, A., Giles, S., Gibbs, R.A., Wheeler, D., Bainbridge, M., Challis, D., Sabo, A., Yu, F., Yu, J., Wang, J., Fang, X., Guo, X., Li, R., Li, Y., Luo, R., Tai, S., Wu, H., Zheng, H., Zheng, X., Zhou, Y., Li, G., Wang, J., Yang, H., Marth, G.T., Garrison, E.P., Huang, W., Indap, A., Kural, D., Lee, W.-P., Fung Leong, W., Quinlan, A.R., Stewart, C., Stromberg, M.P., Ward, A.N., Wu, J., Lee, C., Mills, R.E., Shi, X., Daly, M.J., DePristo, M.A., Altshuler, D., Ball, A.D., Banks, E., Bloom, T., Browning, B.L., Cibulskis, K., Fennell, T.J., Garimella, K.V., Grossman, S.R., Handsaker, R.E., Hanna, M., Hartl, C., Jaffe, D.B., Kernytsky, A.M., Korn, J.M., Li, H., Maguire, J.R., McCarroll, S.A., McKenna, A., Nemesh, J.C., Philippakis, A.A., Poplin, R.E., Price, A., Rivas, M.A., Sabeti, P.C., Schaffner, S.F., Shefler, E., Shlyakhter, I.A., Cooper, D.N., Ball, E.V., Mort, M., Phillips, A.D., Stenson, P.D., Sebat, J., Makarov, V., Ye, K., Yoon, S.C., Bustamante, C.D., Clarke, L., Flicek, P., Cunningham, F., Herrero, J., Keenen, S., Kulesha, E., Leinonen, R., McLaren, W.M., Radhakrishnan, R., Smith, R.E., Zalunin, V., Zheng-Bradley, X., Korbel, J.O., Stütz, A.M., Humphray, S., Bauer, M., Keira Cheetham, R., Cox, T., Eberle, M., James, T., Kahn, S.,

Murray, L., Chakravarti, A., Ye, K., De La Vega, F.M., Fu, Y., Hyland, F.C.L., Manning, J.M., McLaughlin, S.F., Peckham, H.E., Sakarya, O., Sun, Y.A., Tsung, E.F., Batzer, M.A., Konkel, M.K., Walker, J.A., Sudbrak, R., Albrecht, M.W., Amstislavskiy, V.S., Herwig, R., Parkhomchuk, D.V., Sherry, S.T., Agarwala, R., Khouri, H.M., Morgulis, A.O., Paschall, J.E., Phan, L.D., Rotmistrovsky, K.E., Sanders, R.D., Shumway, M.F., Xiao, C., McVean, G.A., Auton, A., Iqbal, Z., Lunter, G., Marchini, J.L., Moutsianas, L., Myers, S., Tumian, A., Desany, B., Knight, J., Winer, R., Craig, D.W., Beckstrom-Sternberg, S.M., Christoforides, A., The Genomes Project, C., Corresponding, a., Steering, c., Production group: Baylor College of, M., Shenzhen, B.G.I., Broad Institute of, M.I.T., Harvard, Illumina, Life, T., Max Planck Institute for Molecular, G., Roche Applied, S., Washington University in St, L., Wellcome Trust Sanger, I., Analysis group: Agilent, T., Baylor College of, M., Boston, C., Brigham, Women's, H., Cardiff University, T.H.G.M.D., Cold Spring Harbor, L., Cornell, Stanford, U., European Bioinformatics, I., European Molecular Biology, L., Johns Hopkins, U., Leiden University Medical, C., Louisiana State, U., Health, U.S.N.I.o., Oxford, U. and The Translational Genomics Research, I., *A map of human genome variation from population-scale sequencing.* Nature, 2010. **467**(7319): p. 1061-1073.

284. Kling, D., Phillips, C., Kennett, D., and Tillmar, A., *Investigative genetic genealogy: Current methods, knowledge and practice.* Forensic Science International: Genetics, 2021. **52**: p. 102474.

285. freire-aradas, A., Fondevila, M., Kriegel, A.K., Phillips, C., Gill, P., Prieto, L., Schneider, P.M., Carracedo, A., and Lareu, M., *A new SNP assay for identification of highly degraded human DNA.* Forensic science international. Genetics, 2011. **6**: p. 341-9.

286. González, J.R., Armengol, L., Solé, X., Guinó, E., Mercader, J.M., Estivill, X., and Moreno, V., *SNPassoc: an R package to perform whole genome association studies.* Bioinformatics, 2007. **23**(5): p. 654-655.

287. isglobal-brge. *SNPassoc*. GitHub repository 2021 15/01/2022]; Available from: https://github.com/isglobal-brge/SNPassoc.

288. Akaike, H., *Likelihood of a model and information criteria.* Journal of Econometrics, 1981. **16**(1): p. 3-14.

289. *ZNRD1ASP*. [cited 2021 24/4/21]; Available from: https://www.genecards.org/cgi-bin/carddisp.pl?gene=ZNRD1ASP.

290. *ZDHHC21*. [cited 2021 24/4/21]; Available from: https://www.genecards.org/cgi-bin/carddisp.pl?gene=ZDHHC21.

291. *NFIB*. [cited 2021 24/4/21]; Available from: https://www.genecards.org/cgi-bin/carddisp.pl?gene=ZDHHC21&keywords=NFIB.
292. *KYAT3*. 2/3/2021 [cited 2021 9/4]; Available from: https://www.ncbi.nlm.nih.gov/gene/56267.
293. *SNX7*. 2/3/2021 [cited 2021 9/4]; Available from: https://www.ncbi.nlm.nih.gov/gene/51375.
294. *LINC01776*. 2/3/2021 [cited 2021 9/4]; Available from: https://www.ncbi.nlm.nih.gov/gene/729987.
295. *CTD-2154B17.1*. [cited 2021 24/4/21]; Available from: https://www.genecards.org/cgi-bin/carddisp.pl?gene=CTD-2154B17.1.
296. *LOC105374654*. [cited 2021 24/4/21]; Available from: https://www.genecards.org/cgi-bin/carddisp.pl?gene=LOC105374654.
297. *CFAP58*. 2/3/2021 [cited 2021 9/4]; Available from: https://www.ncbi.nlm.nih.gov/gene/159686.
298. *NELL1*. 2/3/2021 [cited 2021 9/4]; Available from: https://www.ncbi.nlm.nih.gov/gene/4745.
299. *GLRA1*. [cited 2021 24/4/21]; Available from: https://www.genecards.org/cgi-bin/carddisp.pl?gene=GLRA1#summaries.
300. *LINC00621*. 2/3/2021 [cited 2021 9/4]; Available from: https://www.ncbi.nlm.nih.gov/gene/100996930.
301. *WDR3*. [cited 2021 24/4/21]; Available from: https://www.genecards.org/cgi-bin/carddisp.pl?gene=WDR3.
302. *EPHA5*. [cited 2021 24/4/21]; Available from: https://www.genecards.org/cgi-bin/carddisp.pl?gene=EPHA5.
303. *CASZ1*. [cited 2021 24/4/21]; Available from: https://www.genecards.org/cgi-bin/carddisp.pl?gene=CASZ1.
304. *SLC35A4*. [cited 2021 24/4/21]; Available from: https://www.genecards.org/cgi-bin/carddisp.pl?gene=SLC35A4.
305. *SUMF1*. [cited 2021 24/4/21]; Available from: https://www.genecards.org/cgi-bin/carddisp.pl?gene=SUMF1.
306. *LINC01427*. [cited 2021 24/4/21]; Available from: https://www.genecards.org/cgi-bin/carddisp.pl?gene=LINC01427.
307. *MECOM*. [cited 2021 24/4/21]; Available from: https://www.genecards.org/cgi-bin/carddisp.pl?gene=MECOM.
308. *rs62355044*. [cited 2021 9/4]; Available from: www.ncbi.nlm.nih.gov/snp/rs62355044.

309. *rs9793010*. [cited 2021 9/4]; Available from: https://www.ncbi.nlm.nih.gov/snp/rs9793010.

310. *SMARCAD1*. 2/3/2021 [cited 2021 9/4]; Available from: https://www.ncbi.nlm.nih.gov/gene/56916.

311. Kumar, V., Westra, H.-J., Karjalainen, J., Zhernakova, D.V., Esko, T., Hrdlickova, B., Almeida, R., Zhernakova, A., Reinmaa, E., Võsa, U., Hofker, M.H., Fehrmann, R.S.N., Fu, J., Withoff, S., Metspalu, A., Franke, L., and Wijmenga, C., *Human Disease-Associated Genetic Variation Impacts Large Intergenic Non-Coding RNA Expression.* PLOS Genetics, 2013. **9**(1): p. e1003201.

312. Manning, J.T., Scutt, D., Wilson, J., and Lewis-Jones, D.I., *The ratio of 2nd to 4th digit length: a predictor of sperm numbers and concentrations of testosterone, luteinizing hormone and oestrogen.* Hum Reprod, 1998. **13**(11): p. 3000-4.

313. Miao, L., Liu, H.Y., Zhou, C., and He, X., *LINC00612 enhances the proliferation and invasion ability of bladder cancer cells as ceRNA by sponging miR-590 to elevate expression of PHF14.* Journal of Experimental & Clinical Cancer Research, 2019. **38**(1): p. 143.

314. *PHF14*. [cited 2021 24/4/21]; Available from: https://www.genecards.org/cgi-bin/carddisp.pl?gene=PHF14.

315. Zhou, Y., Li, X., and Yang, H., *LINC00612 functions as a ceRNA for miR-214–5p to promote the proliferation and invasion of osteosarcoma in vitro and in vivo.* Experimental Cell Research, 2020. **392**(1): p. 112012.

316. Nakamura, M. and Tokura, Y., *Epithelial-mesenchymal transition in the skin.* J Dermatol Sci, 2011. **61**(1): p. 7-13.

317. Li, Z.-Z., Zhao, W.-L., Wang, G.-S., Gu, N.-H., and Sun, F., *The novel testicular enrichment protein Cfap58 is required for Notch-associated ciliogenesis.* Bioscience Reports, 2020. **40**(1).

318. Robles-Espinoza, C.D., Harland, M., Ramsay, A.J., Aoude, L.G., Quesada, V., Ding, Z., Pooley, K.A., Pritchard, A.L., Tiffen, J.C., and Petljak, M., *POT1 loss-of-function variants predispose to familial melanoma.* Nature genetics, 2014. **46**(5): p. 478-481.

319. Franceschini, N., van Rooij, Frank J.A., Prins, Bram P., Feitosa, Mary F., Karakas, M., Eckfeldt, John H., Folsom, Aaron R., Kopp, J., Vaez, A., Andrews, Jeanette S., Baumert, J., Boraska, V., Broer, L., Hayward, C., Ngwa, Julius S., Okada, Y., Polasek, O., Westra, H.-J., Wang, Ying A., Del Greco M, F., Glazer, Nicole L., Kapur, K., Kema, Ido P., Lopez, Lorna M., Schillert, A., Smith, Albert V., Winkler, Cheryl A., Zgaga, L., Bandinelli, S., Bergmann, S., Boban, M., Bochud, M., Chen, Y.D., Davies, G., Dehghan, A., Ding, J.,

Doering, A., Durda, J.P., Ferrucci, L., Franco, Oscar H., Franke, L., Gunjaca, G., Hofman, A., Hsu, F.-C., Kolcic, I., Kraja, A., Kubo, M., Lackner, Karl J., Launer, L., Loehr, Laura R., Li, G., Meisinger, C., Nakamura, Y., Schwienbacher, C., Starr, John M., Takahashi, A., Torlak, V., Uitterlinden, André G., Vitart, V., Waldenberger, M., Wild, Philipp S., Kirin, M., Zeller, T., Zemunik, T., Zhang, Q., Ziegler, A., Blankenberg, S., Boerwinkle, E., Borecki, Ingrid B., Campbell, H., Deary, Ian J., Frayling, Timothy M., Gieger, C., Harris, Tamara B., Hicks, Andrew A., Koenig, W., O'Donnell, Christopher J., Fox, Caroline S., Pramstaller, Peter P., Psaty, Bruce M., Reiner, Alex P., Rotter, Jerome I., Rudan, I., Snieder, H., Tanaka, T., van Duijn, Cornelia M., Vollenweider, P., Waeber, G., Wilson, James F., Witteman, Jacqueline C.M., Wolffenbuttel, Bruce H.R., Wright, Alan F., Wu, Q., Liu, Y., Jenny, Nancy S., North, Kari E., Felix, Janine F., Alizadeh, Behrooz Z., Cupples, L.A., Perry, John R.B. and Morris, Andrew P., *Discovery and Fine Mapping of Serum Protein Loci through Transethnic Meta-analysis.* The American Journal of Human Genetics, 2012. **91**(4): p. 744-753.

320. *FOXK1*. [cited 2021 24/4/21]; Available from: https://www.genecards.org/cgi-bin/carddisp.pl?gene=FOXK1.

321. Yang, X., Hu, F., Liu, J.A., Yu, S., Cheung, M.P.L., Liu, X., Ng, I.O.-L., Guan, X.-Y., Wong, K.K.W., Sharma, R., Lung, H.L., Jiao, Y., Lee, L.T.O., and Cheung, M., *Nuclear DLC1 exerts oncogenic function through association with FOXK1 for cooperative activation of MMP9 expression in melanoma.* Oncogene, 2020. **39**(20): p. 4061-4076.

322. Liu, Z., Yang, X., Li, Z., McMahon, C., Sizer, C., Barenboim-Stapleton, L., Bliskovsky, V., Mock, B., Ried, T., London, W.B., Maris, J., Khan, J., and Thiele, C.J., *CASZ1, a candidate tumor-suppressor gene, suppresses neuroblastoma tumor growth through reprogramming gene expression.* Cell Death Differ, 2011. **18**(7): p. 1174-83.

323. Yang, Z., Sun, G., Yao, F., Tao, D., and Zhu, B., *A novel compound mutation in GLRA1 cause hyperekplexia in a Chinese boy- a case report and review of the literature.* BMC Medical Genetics, 2017. **18**(1): p. 110.

324. Riess, C., Schneider, B., Kehnscherper, H., Gesche, J., Irmscher, N., Shokraie, F., Classen, C.F., Wirthgen, E., Domanska, G., Zimpfer, A., Strüder, D., Junghanss, C., and Maletzki, C., *Activation of the Kynurenine Pathway in Human Malignancies Can Be Suppressed by the Cyclin-Dependent Kinase Inhibitor Dinaciclib.* Frontiers in immunology, 2020. **11**: p. 55-55.

325. Tucci, A., Ciaccio, C., Scuvera, G., Esposito, S., and Milani, D., *MIR137 is the key gene mediator of the syndromic obesity phenotype of patients with 1p21.3 microdeletions.* Molecular Cytogenetics, 2016. **9**(1): p. 80.

326. Wu, Y., Cao, H., Baranova, A., Huang, H., Li, S., Cai, L., Rao, S., Dai, M., Xie, M., Dou, Y., Hao, Q., Zhu, L., Zhang, X., Yao, Y., Zhang, F., Xu, M., and Wang, Q., *Multi-trait analysis for genome-wide association study of five psychiatric disorders.* Translational Psychiatry, 2020. **10**(1): p. 209.

327. Chen, J., Calhoun, V.D., Lin, D., Perrone-Bizzozero, N.I., Bustillo, J.R., Pearlson, G.D., Potkin, S.G., van Erp, T.G.M., Macciardi, F., Ehrlich, S., Ho, B.C., Sponheim, S.R., Wang, L., Stephen, J.M., Mayer, A.R., Hanlon, F.M., Jung, R.E., Clementz, B.A., Keshavan, M.S., Gershon, E.S., Sweeney, J.A., Tamminga, C.A., Andreassen, O.A., Agartz, I., Westlye, L.T., Sui, J., Du, Y., Turner, J.A., and Liu, J., *Shared Genetic Risk of Schizophrenia and Gray Matter Reduction in 6p22.1.* Schizophr Bull, 2019. **45**(1): p. 222-232.

328. *TRA-AGC4-1*. [cited 2021 24/4/21]; Available from: https://www.genecards.org/cgi-bin/carddisp.pl?gene=TRA-AGC4-1.

329. *TRA-CGC2-1*. [cited 2021 24/4/21]; Available from: https://www.genecards.org/cgi-bin/carddisp.pl?gene=TRA-CGC2-1.

330. *FRS3*. [cited 2021 24/4/21]; Available from: https://www.genecards.org/cgi-bin/carddisp.pl?gene=FRS3.

331. Yao, J., Zhou, B., Zhang, J., Geng, P., Liu, K., Zhu, Y., and Zhu, W., *A new tumor suppressor LncRNA ADAMTS9-AS2 is regulated by DNMT1 and inhibits migration of glioma cells.* Tumour Biol, 2014. **35**(8): p. 7935-44.

332. Zhang, J.W., Rubio, V., Zheng, S., and Shi, Z.Z., *Knockdown of OLA1, a regulator of oxidative stress response, inhibits motility and invasion of breast cancer cells.* J Zhejiang Univ Sci B, 2009. **10**(11): p. 796-804.

333. Bai, L., Yu, Z., Zhang, J., Yuan, S., Liao, C., Jeyabal, P.V., Rubio, V., Chen, H., Li, Y., and Shi, Z.Z., *OLA1 contributes to epithelial-mesenchymal transition in lung cancer by modulating the GSK3β/snail/E-cadherin signaling.* Oncotarget, 2016. **7**(9): p. 10402-13.

334. Bamshad, M., Lin, R.C., Law, D.J., Watkins, W.S., Krakowiak, P.A., Moore, M.E., Franceschini, P., Lala, R., Holmes, L.B., Gebuhr, T.C., Bruneau, B.G., Schinzel, A., Seidman, J.G., Seidman, C.E., and Jorde, L.B., *Mutations in human TBX3 alter limb, apocrine and genital development in ulnar-mammary syndrome.* Nature Genetics, 1997. **16**(3): p. 311-315.

335. Krstic, M., Kolendowski, B., Cecchini, M.J., Postenka, C.O., Hassan, H.M., Andrews, J., MacMillan, C.D., Williams, K.C., Leong, H.S., Brackstone, M., Torchia, J., Chambers, A.F., and Tuck, A.B., *TBX3 promotes progression of pre-invasive breast cancer cells by inducing EMT and directly up-regulating SLUG.* The Journal of pathology, 2019. **248**(2): p. 191-203.

336. Willmer, T., Cooper, A., Peres, J., Omar, R., and Prince, S., *The T-Box transcription factor 3 in development and cancer.* Biosci Trends, 2017. **11**(3): p. 254-266.

337. Levin, M., *Morphogenetic fields in embryogenesis, regeneration, and cancer: non-local control of complex patterning.* Bio Systems, 2012. **109**(3): p. 243-261.

338. Levin, M. and Martyniuk, C.J., *The bioelectric code: An ancient computational medium for dynamic control of growth and form.* Biosystems, 2018. **164**: p. 76-93.

339. Herrera-Rincon, C. and Levin, M., *Booting up the organism during development: Pre-behavioral functions of the vertebrate brain in guiding body morphogenesis.* Communicative & Integrative Biology, 2018. **11**(1): p. e1433440.

340. Poretti, A., Meoded, A., Ceritoglu, E., Boltshauser, E., and Huisman, T.A.G.M., *Postnatal in-vivo MRI findings in Anencephaly.* Neuropediatrics, 2010. **41**(06): p. 264-266.

341. Cole, S.W., Nagaraja, A.S., Lutgendorf, S.K., Green, P.A., and Sood, A.K., *Sympathetic nervous system regulation of the tumour microenvironment.* Nature reviews. Cancer, 2015. **15**(9): p. 563-572.

342. Bushe, C.J., Bradley, A.J., Wildgust, H.J., and Hodgson, R.E., *Schizophrenia and breast cancer incidence: a systematic review of clinical studies.* Schizophr Res, 2009. **114**(1-3): p. 6-16.

343. Hodgson, R., Wildgust, H.J., and Bushe, C.J., *Cancer and schizophrenia: is there a paradox?* Journal of psychopharmacology (Oxford, England), 2010. **24**(4 Suppl): p. 51-60.

344. Jones, P.A. and Takai, D., *The role of DNA methylation in mammalian epigenetics.* Science, 2001. **293**(5532): p. 1068-1070.

345. Fraga, M.F., Ballestar, E., Paz, M.F., Ropero, S., Setien, F., Ballestar, M.L., Heine-Suñer, D., Cigudosa, J.C., Urioste, M., Benitez, J., Boix-Chornet, M., Sanchez-Aguilera, A., Ling, C., Carlsson, E., Poulsen, P., Vaag, A., Stephan, Z., Spector, T.D., Wu, Y.-Z., Plass, C., and Esteller, M., *Epigenetic differences arise during the lifetime of monozygotic twins.* Proceedings of the National Academy of Sciences of the United States of America, 2005. **102**(30): p. 10604.